LEABHARLANN CHOLÁISTE NA TRÍONÓIDE, BAILE ÁTHA CLIATH | TRINITY COLLEGE LIBRARY DUBLIN
Ollscoil Átha Cliath | The University of Dublin

Terms and Conditions of Use of Digitised Theses from Trinity College Library Dublin

Copyright statement

All material supplied by Trinity College Library is protected by copyright (under the Copyright and Related Rights Act, 2000 as amended) and other relevant Intellectual Property Rights. By accessing and using a Digitised Thesis from Trinity College Library you acknowledge that all Intellectual Property Rights in any Works supplied are the sole and exclusive property of the copyright and/or other IPR holder. Specific copyright holders may not be explicitly identified. Use of materials from other sources within a thesis should not be construed as a claim over them.

A non-exclusive, non-transferable licence is hereby granted to those using or reproducing, in whole or in part, the material for valid purposes, providing the copyright owners are acknowledged using the normal conventions. Where specific permission to use material is required, this is identified and such permission must be sought from the copyright holder or agency cited.

Liability statement

By using a Digitised Thesis, I accept that Trinity College Dublin bears no legal responsibility for the accuracy, legality or comprehensiveness of materials contained within the thesis, and that Trinity College Dublin accepts no liability for indirect, consequential, or incidental, damages or losses arising from use of the thesis for whatever reason. Information located in a thesis may be subject to specific use constraints, details of which may not be explicitly described. It is the responsibility of potential and actual users to be aware of such constraints and to abide by them. By making use of material from a digitised thesis, you accept these copyright and disclaimer provisions. Where it is brought to the attention of Trinity College Library that there may be a breach of copyright or other restraint, it is the policy to withdraw or take down access to a thesis while the issue is being resolved.

Access Agreement

By using a Digitised Thesis from Trinity College Library you are bound by the following Terms & Conditions. Please read them carefully.

I have read and I understand the following statement: All material supplied via a Digitised Thesis from Trinity College Library is protected by copyright and other intellectual property rights, and duplication or sale of all or part of any of a thesis is not permitted, except that material may be duplicated by you for your research use or for educational purposes in electronic or print form providing the copyright owners are acknowledged using the normal conventions. You must obtain permission for any other use. Electronic or print copies may not be offered, whether for sale or otherwise to anyone. This copy has been supplied on the understanding that it is copyright material and that no quotation from the thesis may be published without proper acknowledgement.

A Light and Electron Microscopical Study of the Regenerating Spinal Cord of the Eel

By

Adrian Gerard Niall Dervan

This thesis is submitted in fulfilment of requirements for the degree of Doctor of Philosophy to Trinity College, University of Dublin

Department of Zoology
University of Dublin
Trinity College

October 2000

Candidates Declaration

I hereby declare that this thesis consists of my own work, unless otherwise stated, and has not previously been submitted to Trinity College, University of Dublin or any other university.

I agree that the library may lend or copy this thesis upon request.



Adrian Gerard Niall Dervan

November 2000

Summary

The present study examined the regenerative capability of the European eel *Anguilla anguilla* following spinal cord transection injury using both light and electron microscopy. The primary aim of this investigation was to determine the role of the different cell types in the formation of a 'bridge' of regenerating tissue that facilitates the growth of axons back to their original targets. In addition, the chronological order for the appearance of the different cells was also investigated.

Both light and electron microscopical techniques were employed. Light microscopical methods included, axonal tracing, serial semithin sectioning with alternate thin sectioning for electron microscopy and an immunohistochemical investigation for a number of intermediate filament proteins, neurotransmitters and for cellular proliferation. The findings presented in this thesis show that the different cellular components of the eel spinal cord are capable of quickly restoring tissue integrity. The first event following transection injury, was the retraction of the cord to produce a gap of approximately 1mm, that was filled with blood. The resultant clot acted as a 'matrix bridge' between the rostral and caudal stumps of the injured cord. With time the clot changes such that some original blood-borne cells are lost and other cells such as fibroblasts, leucocytes and endothelial cells infiltrate and produce a scar-like structure. In the spinal stumps, extensive degeneration of the neural tissue occurred, particularly of axons and their myelin sheaths. Regrowth of the spinal cord occurred into this matrix at 6 days to produce the first connections or 'bridge' between the rostral and caudal cord by day 8. With time, this structure progressively increased in size such that 80% of the normal cross sectional area of the cord was restored 14 days following injury.

The first components of the regenerating bridge of neural tissue were unmyelinated axons closely followed by ependymocytes, which produced a new enlarged central canal in the bridge. DiI-tracer labelling of axons showed that they grew in relatively straight pathways from the rostral spinal cord into the caudal cord, where some could be traced for considerable distances (~1-2mm). Interestingly the number of axons continually increases, such that by day 54 approximately 137% were found in the bridge. A central canal developed quickly from migrating ependymocytes to form small 'plates' of cells that facilitated further growth and eventual closure of the canal lumen. Continuity of the central canal between both stumps was reestablished by

approximately day 10, although it remained open on the dorsal surface until approximately day 26. The size of the central canal in all cases was at least 200% greater than normal, eventually decreasing in size by day 54 but even at 200 days, it was still enlarged. A small population of neurons the liquor contacting neurons, immunoreactive to tyrosine hydroxylase (TH) and gamma amino butyric acid (GABA) appeared in the wall of the canal by approximately day 12. Tanycytes also developed from the cellular regions surrounding the canal and were evident by day 16; they extended long cellular processes to the periphery and labelled positively for the intermediate filament GFAP, a characteristic of mature astrocytes.

The meninges produced a new covering around portions of the developing bridge as early as day 8. In instances where the central canal remained open dorsally, this cell type failed to invade the exposed region, suggesting possible instructional events between this cell type and ependymocytes. To further investigate this notion, experiments involving meningeal denudation were carried out using mechanical removal in conjunction with 6-hydroxydopamine application. The findings from these studies suggest that meningeal tissue is necessary for correct bridge formation. The reactive radial astrocytic population expressed GFAP and S-100 but not vimentin and GFAP+ve processes could be traced entering the bridge approximately 12 days following injury. They extended immunopositive processes from cells in the stumps parallel to the direction of axonal growth. The complex hypertrophic entanglements of GFAP+ve fibres typical of the astrocytic reaction in amniotes were not found in the present study. Oligodendrocytes do not become apparent until much later, with 3% of axons myelinated by day 54, indicating a slow influx of this cell type into the bridge. Remyelination of axons was not size specific and may underline other factors such as successful pathfinding by axons to reach their original targets. The extent of myelination on axons was always suboptimal on the majority of axons analysed.

Taken together, the findings from the present study demonstrate that the milieu in which regrowing axons encounter as they regroe to their original targets is not inhibitory to regrowth. Furthermore, axons comprise some of the first regenerating elements to enter the lesion site and reestablish cord continuity. Other non-neuronal cell types appear in the bridge, but at different times during the regenerative event, providing evidence for a chronological regulation of the different cell types in the bridge. Such a regulation may have implications for reparative strategies in the mammalian central nervous system where neural recovery is abortive.

Acknowledgements

To those of you who read this little portion of my thesis after flicking through the rest of it very quickly, muttering something like 'nice pictures....err so what did you say you did then?' and decide to read this little piece of straight talking non jargon English, let me just say this has been by far the most difficult piece of the thesis to write for I have the difficult task of expressing in a few short words, an untold depth of thanks and gratitude to a great number of people, to which end I am probably going to fail.

First and foremost, I have to thank my supervisor Prof. Roberts, who has through the course of this work guided me through the exciting world that is regeneration research. Through your guidance my skills as a neuroscientist and all that it encompasses have been honed to a level I never thought possible, and more so the insightful conversations that brought science to life, Sir, I am indebted.

To Dr. Meredith who unfailingly answered my every question on immunohistochemistry and solved my innumerable problems, I thank you.

Special thanks must go to Peter, Alison, Martyn and Dick, for your ability to answer my every question and request, be it from printer paper to that little piece of piping needed to complete my masterpiece aquarium tanks greatly influenced by Dali, and the put right by Peter, my heartfelt thanks.

I must express my thanks to the staff of the electron microscope unit, to Dave and Colin and the two Neil's many thanks for the help and the good craic, when at times all I was ever sectioning were the dreaded purples in my quest for the perfect golds and silvers. In particular to 'The Ronan' a true friend and one who came to my rescue on numerous times, 'I'll see you after...'.

To my lab partners through the years many thanks for all the good times and in particular Louise who has lent her ear to my every moan, introduced me to some extreme-ish music tastes and those great nights out. To Ian, Niamh and Sarah , thanks guys for all the good times of which they always were. To Ramesh, Gerry, Declan and

Collette if you ever bring yourselves to read this a big thank you. And Dec, I am the tetris king!

To the thesis crew Dave, Gerry, Derek and Billy, many thanks guys you kept me sane when at times I felt I was just moving the deckchairs about on the titanic.

To Vicky, Helen, Colin, Jonathan and Steve, my fellow housemates, thanks guys!

To the old and the new postgrad crews you have been great and misled me on numerous occasions to receptions, ale houses, house parties, the 'vid' club or just the Lincoln, thanks guys!. In particular to 'my brothers in arms' Mike aka 'Bubba', Ciaran and Sossie I owe my sanity to you guys, your help and encouragement through it all has been a pillar I have often used, and have rarely expressed my gratitude. In the latter days Dave and Sarah, thanks for setting me to task, it helped, honestly!!. Moreover, thanks for the support and the constant laughs particularly when things appeared to be hitting terminal velocity in the wrong direction.

To the lads, Ger, Bill, Gary, Neil, Anto and Alan and the ladettes Rowena and Ed who bravely set out every other weekend to conquer the public houses of Dublin.

Finally I come to the people who above everyone else have provided me with the strength and encouragement to see this project to completion, to my family, I thank you and am forever in your debt (to my fellow siblings that does not equate to cash).

Table of Contents

Declaration 1

Summary 2

Acknowledgements 4

Abbreviations 8

Chapter 1 **General Introduction** 11

1.1 Regeneration in non-mammalian animals 12

1.2 Anamniote models 13

1.3 Types of spinal cord lesion 13

1.4 The requirements for regeneration 17

1.5 The present study 18

1.6 Organisation of the spinal cord of the eel 19

Chapter 2 **The organisation of the ependyma and glia in the uninjured spinal cord**

2.1 Introduction 23

2.2 Materials and Methods 26

2.3 Results 29

2.4 Discussion 51

Chapter 3 **The meninges of the uninjured brain and spinal cord**

3.1 Introduction 62

3.2 Materials and Methods 64

3.3 Results 65

3.4 Discussion 82

Chapter 4 **The injured spinal cord - the first stages of repair**

4.1 Introduction 93

4.2 Materials and Methods 95

4.3 Results 98

4.4 Discussion 112

Chapter 5 **The organisation of the regenerating central canal: I. The ependyma**

5.1 Introduction 129

5.2 Materials and Methods 131

5.3 Results 134

5.4 Discussion 162

Chapter 6 **The organisation of the regenerating central canal: II. Liquor contacting neurons**

6.1 Introduction 171

6.2 Materials and Methods 173

6.3 Results 175

6.4 Discussion 184

Chapter 7 **The meninges in the regenerating spinal cord**

7.1 Introduction 191

7.2 Materials and Methods 193

7.3 Results 196

7.4 Discussion 218

Chapter 8 **Radial astrocytes in the regenerating spinal cord**

8.1 Introduction 228

8.2 Materials and Methods 231

8.3 Results 233

8.4 Discussion 247

Chapter 9 **The regenerated axons**

9.1 Introduction 259

9.2 Materials and Methods 261

9.3 Results 265

9.4 Discussion 282

Chapter 10 **General Discussion** 300

Bibliography 314

Abbreviations

ABC	Avidin-biotin-peroxidase complex
APP	Apolipoprotein
Apo A-1	Apolipoprotein A-1
BrdU	5-Bromo-2-Deoxyuridine
Cau	Caudal
CNS	Central Nervous System
CPG	Central pattern generator
CSF	Cerebrospinal fluid
CSPG	Chondroitin sulphate proteoglycan
CK-8	Cytokeratin 8
CK-18	Cytokeratin 18
CK-19	Cytokeratin 19
DAB	3-3'-diaminobenzidine
DiI	1,1'–diotadecyl–3,3,3',3'-tetramethylindocarbocyanine perchlorate
DRG	Dorsal root ganglion
ECM	Extracellular matrix
GABA	γ-aminobutyric acid
GAP-43	Growth associated protein
GFAP	Glial Fibrillary Acidic Protein
HRP	Horse radish peroxidase
LCN	Liquor contacting neuron
MAG	Myelin associated glycoprotein
MF	Meningeal Fibroblasts
MS-222	3-aminobenzoic acid ethyl ester
NADPH	Nicotinamide adenine dinucleotide phosphate

-ve	Negative
N	Normal
OEC	Olfactory ensheathing cell
OsO_4	Osmium tetroxide
PB	Phosphate buffer
PMF	Perimeningeal fluid
PNS	Peripheral Nervous System
+ve	Positive
RBCs	Red blood cells
RGC	Retinal ganglion cell
Ros	Rostral
6-OHDA	6-Hydroxy-dopamine
TF	Tissue Fibroblasts
TH	Tyronsine hydroxylase
Tris	Tris(hydroxymethyl)methylamine
Vim	Vimentin
WBCs	White blood cells

Chapter 1

General Introduction

Following injury, the mammalian central nervous system (CNS) is unable to support tissue regrowth and some permanent loss of function results. Reaction to such injury to the spinal cord includes a temporarily induced spinal 'shock' that precedes a limited return (if any) of function. Damaged neurons soon die while, over longer periods, others not directly affected by the initial insult also succumb, a process known as 'secondary death'. The studies of such reactions are numerous and have grown in scope considerably since the early work on the injured nervous system, most notably that of Ramon-y-Cajal (1928). The inability of the mammalian CNS to regrow following injury contrasts with the behaviour of other components of the nervous system, such as peripheral nervous system (PNS) and the olfactory system (OS), which exhibit a strong regenerative capability. The developing CNS of juvenile mammals also possesses an intrinsic ability, within a certain time frame, to recover from injury, and regeneration is also seen in juvenile and adult non-mammalian animals.

1.1 Regeneration in non-mammalian animals

In the rest of the animal kingdom, recovery from nervous system damage has been demonstrated in a variety of invertebrate and vertebrate species. In the case of some invertebrates, such as annelids (Muller et al., 1987), crustaceans (Bittner, 1991), and insects (Smith et al., 1991), injured axons demonstrate a remarkable ability to regrow to their original targets (Muller et al., 1987; Margotta et al., 1989). Furthermore, this axonal regrowth is fully supported by glial cells (Smith et al., 1991).

Within the vertebrates, recovery from injury is also possible, in the cyclostomes, cartilaginous fishes, bony fishes, amphibians, reptiles and birds. In birds, however, recovery is limited to a small period during embryonic development (Hasan et al., 1993), while in the adult avian CNS the reaction to injury parallels that of mammals with the production of a glial scar and a failure of axons to regrow (e.g. Kestner, 1987). In the other vertebrate classes, collectively known as the anamniotes, numerous studies have shown that the CNS, upon injury, recovers to varying extents with the return of some functional control. In reptiles, a differential response of the spinal cord is found that has been termed the "Anolis paradox" (Simpson, 1983). The tail spinal cord is capable of full recovery following injury (Simpson, 1964; Duffy et al., 1992), but lumbar and more rostral portions of the cord do not recover and instead develop scar tissue similar to that found in amniotes (Simpson, 1970). In vertebrates, therefore, the cut-off point for successful regeneration appears to begin with reptiles.

1.2 Anamniote models

Because the CNS organisation of most anamniotes, both in neuronal and glial structure, resembles that of the mammalian CNS, several anamniote species have been utilised as experimental models of regeneration. As can be seen in Table 1.1, the range is extensive and there is no set model for regeneration research, unlike the rat for mammalian work. The lamprey has received much attention, with a number of investigations illustrating the ability of its axons to reform synaptic contacts on their original targets and so to facilitate functional recovery. While there appear to be have been few studies on cartilaginous fish regeneration, numerous researchers have reported on the regenerative capability of bony fish, including goldfish, zebrafish, carp, black ghost knife fish and the eel. Fewer species of amphibians have been utilised, but many studies have been carried out on these animals, most notably on *Triturus* and *Xenopus*. In reptiles, most work has been done with *Anolis*.

As with mammals, different regions of the anamniote nervous system have been used to determine the regenerative potential of axons and the ability of non-neuronal cells to support regrowth (Table 1.2), although most investigations have utilised either the optic nerve or the spinal cord. In the optic system, studies of the nerve predominate, although the optic tract and tectum have also been utilised.

1.3 Types of spinal cord lesion

In mammals, it is well recognised that the type and degree of injury inflicted greatly influences the extent of scarring and the regenerative potential of the axotomised neurons (e.g. Malhotra and Shnitka, 1994; Fawcett, 1997). The different lesioning paradigms that have been utilised (Table 1.2) involve chemical, stab and cold injuries, applied mainly to the brain, and transection, hemisection, compression, used mostly on the optic nerve and spinal cord; amputation has been exclusively used in relation to the spinal cord. Moreover, the different cellular reactions and interactions that occur are also injury dependent so that, for example, compression or microlesion injuries induce little meningeal/connective tissue-derived fibrotic scarring (e.g. Davies et al., 1996), whereas more traumatic injuries, such as transection, crush or ablation, evoke a much stronger response (Matthews et al., 1979; Fawcett and Asher, 1999). Other types of lesion such as crush or compression (e.g. Lowenger and Levine, 1988; Levine, 1991; Blaugrund et al., 1993; Rungger-Brandle et al, 1995), induce a different response from

Animals	Utilised References
Cyclostomes	
Lampetra	Wood and Cohen, (1981); Borgens et al. (1981); Yin et al. (1984); Lurie and Selzer, (1991); McClellan, (1992); Pijak et al. (1996); Curie and Ayers, (1983); Mackler and Selzer, (1987).
Petromyzon	
Icthyomyzon	
Elasmobranchs	
Scyliorhinus	Maron, (1963)
Gingylostoma	Gelderd, (1979)
Teleosts	
Carassius	Koppanyi and Weiss, (1922); Pearcy and Koppanyi, (1924-1925); Bernstein and Bernstein, (1967); Bignami et al. (1974); Coggeshall et al. (1982); Giulian and Iwanij, (1985); Giulian et al. (1985); Lowenger and Levine, (1988); Blaugrund et al. (1993); Nona and Stafford, (1995); Sharma et al. (1993).
Danio (Brachdanio)	Bernhardt et al. (1996); Becker et al. (1997).
Anguilla	Flight and Verheijen, (1993); Doyle et al. (2000); Bosch et al. (2000).
Phoxinus	Kirsche, (1951); Healey, (1967).
Lebistes	Hooker, (1932).
Sternarchus	Anderson et al. (1983); Anderson and Waxman, (1983a); Anderson et al. (1984); Anderson and Waxman, (1991); Anderson et al. (1986).
Apteronotus	Waxman and Anderson, (1986); Zupanc et al. (1998).
Sternopygus	Ungez and Zakon, (1997).
Amphibians	
Bufo	Skene and Willard, (1981).
Rana	Gruberg and Stirling, (1974); Scott and Foote, (1981).
Xenopus	Michel and Reier, (1979); Bohn et al. (1982); Nordlander and Singer, (1982); Reier and Webster, (1974); Reier, (1979).
Triturus	Singer et al. (1979); Egar and Singer, (1972); Nordlander and Singer, (1978); Benraiss et al. (1997); Philips and Turner, (1991).
Salamandra	Davis et al. (1989); Davis et al. (1990); Naujoks-Manteuffel, (1992).
Ambystoma (Axolotl)	O'Hara et al. (1992); Pietsch, (1993).

Animals Utilised	References
Reptiles	
Anolis	Simpson, (1968); Alibardi et al. (1992); Duffy et al. (1992).
Sphenodon	Alibardi and Meyer-Rochow (1990).
Lampropholis	Alibardi, (1994).
Ctenenophorus	Beazley et al. (1997).
Lygosoma	Simpson, (1964).
Birds	
Gallus (Juvenile)	Hassan et al. (1993).
Gallus (Adult)	Margotta et al. (1989); Park et al. (1998).
Mammals	
Didelphis (juvenile)	Wang et al. (1998a); Wang et al. (1998b).
Monodelphis (juvenile)	Nichols and Saunders, (1996).
Rattus (Juvenile)	Gilmore and Leiting, (1980); Goodlett et al. (1993); Maxwell et al. (1990); Varga et al. (1995); Wang et al. (1996); Dent et al. (1996).
Rattus (Adult)	Richardson et al. (1984); Bernstein et al. (1985); Bruni and Anderson, (1987); Schnell et al. (1994); Popovich et al. (1997); Beattie et al. (1997); Dryer et al. (1998); Keirstead et al. (1998a); Davies et al. (1999); Neumann and Woolf, (1999)
Mus	Wang et al. (1997).
Felis	Howland et al. (1995).
Canis	Shimizu, (1983); Ide et al. (1998).

Table 1.1. This figure highlights the different animal groups utilised for regeneration research but is not comprehensive, particularly for rats.

the more severe types such as transection, ablation or amputation (e.g. Simpson, 1968; Singer et al., 1979; Michel and Reier, 1979; Stensaas, 1983; Anderson and Waxman, 1983a). These differences appear to be dependent on a variety of factors, such as retention of the structural continuity and the presence or absence of a distal portion of target neural tissue. Amputation injuries deprive the regrowing cord axons of a target tissue, and instead they must grow into a blastema of newly developing tissue, thus

Type of Injury	Amniote/Anamniote	References
Ablation		
	Anamniote	Simpson (1964)
Amputation		
	Anamniote	Benraiss et al. (1997)
Chemically Induced		
	Amniote	Riva-Depaty et al. (1994)
Compression/Contusion		
	Amniote	Beattie et al. (1997)
Crush		
	Anamniote	Stafford et al. (1990)
	Amniote	Frank and Wolberg (1996)
Cold Injury		
	Amniote	Moore et al. (1987)
Laceration		
	Amniote	Malhotra et al. (1993)
Hemisection		
	Anamniote	Lurie and Selzer (1991)
	Amniote	Von Meyenburg et al (1998)
Transection		
	Anamniote	Bignami et al. (1974)
	Amniote	Krenz and Weaver (1998)
Stab		
	Amniote	Krushel et al. (1995)

Table 1.2. This table summarises some of the different lesioning methods used in regeneration research and provides some (representative) references.

conferring a different type of regenerative response (e.g. Anderson and Waxman, 1983a).

1.4 The requirements for regeneration

It is well known that the inability of the amniote CNS to support axonal regrowth is due to the formation of scar tissue at the site injury and other injury-associated events such

as the upregulation or release of numerous inhibitory molecules, many of which are cell derived (e.g. Malhotra and Shnitka, 1994; Powell et al., 1997; Fitch and silver, 1997). Since the anamniote CNS recovers, in these animals regrowing axons must be capable of entering, and traversing the injury site and reconnecting to original targets. This suggests that the different cellular events that occur in the lesion site are not inhibitory to regrowth and may even facilitate it.

From what we know of regenerative failure in adult amniotes (e.g.Matthews et al., 1979; Lotan and Schwartz, 1994; Schwab, 1996; Ridet et al., 1997; Raivich et al., 1999), and of the different restorative strategies utilised to promote limited axonal recovery (e.g. Krum and Rosenstein, 1998; Asada et al., 1998; Ramon-Cueto and Avila, 1998; Menei et al., 1998; Weibel et al., 1994), it seems that many component cells of the CNS fail to provide adequate support to regrowing axons and, therefore, contribute to the failure of regeneration. In part this failure results from the presence of inhibitory 'scar' tissue, the formation of which has been well documented (see Malhotra et al., 1990; Fawcett and Asher, 1999), but the intrinsic and extrinsic requirements of the resident cellular milieu to support axonal regrowth have been less well identified.

It is my view that a study of the different injury-related events in the anamniote CNS, with its intrinsic regenerative capability and successful axonal growth, could be revealing and, in particular, the sequence in which they occur may indicate key aspects of a successful restorative strategy.

From the numerous studies of different anamniote animal models (see fig. 1.1) it has been shown that some of the cellular components common to all vertebrate animals, such as astrocytes and ependymal cells, react in a manner so as to encourage regrowth. In the spinal cord, for example, ependymocytes which have been the most extensively studied non-neuronal cell type in the spinal cord play an integral part in re-establishing continuity between the spinal stumps following transection (e.g. Michel and Reier, 1979) and constructing new portions of caudal spinal cord following amputation (e.g. Egar and Singer, 1972). In the optic nerve, the role of astrocytes has received similar intensive study and the reactions of this cell type following crush have been well described (e.g. Levine, 1991; Rungger-Brandle et al., 1995). Furthermore, the role of both cell types has often been addressed in relation to the regrowth of axons through the lesion site in an effort to elucidate possible supportive functions and sequences of regrowth.

1.5 The present study

Our aim in the present study has been to determine the major events contributing to the successful regeneration of the spinal cord. We have done this by exploring the changes that occur, over time, following a specific injury at a defined location using the spinal cord of the European eel *Anguilla anguilla* L, as our model system. This species was selected for a number of reasons:

- it displays a strong regenerative capability following total cord transection (Flight and Verheijen, 1993; Bosch, 1994; Doyle et al., 2000) that results in an accurate restoration of swimming and startle responses (Bosch et al., 2000; Doyle et al., 2000);
- it is a hardy species and capable of enduring anaesthesia and surgical procedures well;
- transection injury in which the cord is completely cut to produce two stumps of cord separated by a small space is easily replicated with little variation from animal to animal;
- operated fish can swim and feed normally and recovery of swimming performance can be monitored, as the transection can be made in the caudal part of the body;
- the simple repetitive segmental organisation of the eel means that the different body segments, of essentially constant construction, can be used as replicates.

The study is divided into two major sections. The first section of the thesis examines in the uninjured spinal cord, the ependymal and glial organisation (Chapter 2) and the structure of the meninges that surround the brain and spinal cord (Chapter 3). This knowledge is necessary background to our work on regeneration, and little has been done on these spinal cord components in fish, and especially in eels.

The second section deals with the reactions of the spinal cord up to 200 days following a transection, and focuses on the new tissue that bridges the separated cord portions. Chapter 5 provides an overview of the organisation and development of the 'bridge' at set times following injury and the role of the blood clot that develops at the injury site because of haemorrhaging, is also explored. Chapters 6 and 7, together investigate the role of the central canal in the development of the bridge. The development and dynamics of central canal formation and the associated glial-type cells, the tanycytes, are investigated in chapter 6, while chapter 7 explores the role of a specialised neuronal cell type, the liquor contacting neuron, in the development of the canal. In chapter 8,

the meningeal reaction to injury is investigated and through experimental manipulation, its possible role in the development of the bridge is examined. The astrocytic reaction to injury is explored with immunohistochemical labelling for three common astroglial markers in chapter 9, while, finally, in chapter 10, the regenerative capability and the time scale for axonal growth through the bridge and the subsequent myelination by oligodendrocytes are investigated in the context of other developments in the forming bridge.

1.5 Organisation of the spinal cord of the eel

The spinal cord of the eel, as of other vertebrates, acts as a conduit for sensory and motor information between the brain and the peripheral nervous system and houses the generating circuits underlying locomotion. It is arranged into repeating segmental units containing similar neuronal circuitry. Numerous studies on a range of fishes have categorised these neuronal components as being (a) descending pathways from the brain, (b) interneurons or (c) local segmental neurons (Bosch et al., 2000). Interneurons project either from rostral cord segments caudally (descending interneurons) or from caudal portions to more rostral regions of the cord or targets in the brain, whereas local interneurons and motor neurons are intrinsic to each spinal segment. Within each spinal segment, groups of motor neurons project their axons through the ventral roots and into the peripheral nervous system to innervate the musculature.

In gross structure, the eel spinal cord is similar to that of other vertebrates. It is composed of the characteristic 'H' region of grey matter, containing neuronal cell bodies that surround a central canal. Outside the grey matter are the myelinated axonal tracts of the white matter which give the cord its shape; those concentrated near the ventral midline and in the ventrolateral margins of the spinal cord are probably descended from the brain (Kimmel, 1982; Kuwada et al., 1990).

In the dorsal horns, cell bodies of sensory interneurons receive inputs from the peripheral sensory neurons while the ventral horns contain the cell bodies of motor neurons in the motor column (see Fig. 2.1c), located according to the muscle compartments they innervate. The cell bodies of white muscle motor neurons occupy positions close to the central canal while the others are placed more ventrolaterally (van Raamsdonk et al., 1983a; 1983b; de Graaf et al., 1990). Localised injections of tracers into the segmental musculature of the eel have illustrated a repeating pattern of

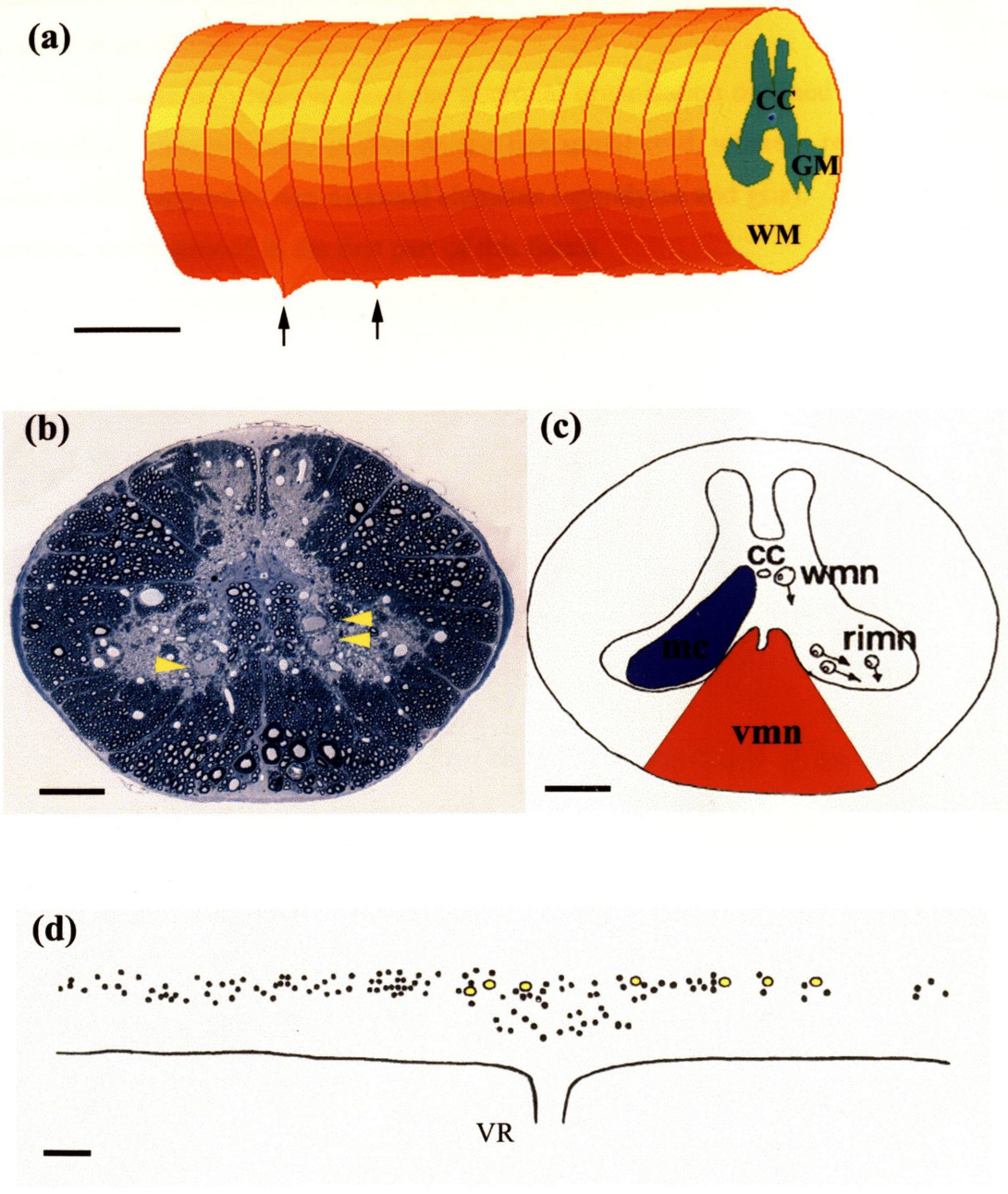


Figure 1.1a, b, c, d. The general organisation of the fish spinal cord can be seen from the reconstruction of a 1mm section of the cord in (a) and the photomicrograph of a toludine blue stained transverse section in (b). ventral roots (arrows), GM, grey matter, WM, white matter and cc, central canal. Men, demarcates the position of the meninges and the arrowheads highlight some of the motor neuronal cell bodies in the grey matter. In (c) the positions of identified descending tracts are marked in the ventral white matter (vwm, red) while the motor column (mc) containing white motor neurons (wmn) and red muscle neurons (rmn) is highlighted in the grey matter (blue). The segmental organisation of these neurons in longitudinal section is illustrated in (d). The yellow circles denote the large white matter neurons amid the labelled cell bodies of the intermediate and red muscle cell bodies on one side of one half segment of the cord (taken from Smit et al.,1991). VR, ventral root. Scale bar = 100 microns

motoneurons (Smit et al., 1991) including the 7-10 large identifiable cells that innervate the white musculature.

The basic information about the neuronal organisation outlined above has been derived from comprehensive studies on the fish spinal cord, whereas relatively little is known of the supportive non-neuronal elements (ependyma and glia). These structures, therefore, are examined in the first part of this thesis.

Chapter 2

The organisation of the ependyma and glia in the uninjured spinal cord

2.1 Introduction

Apart from a brief account of the cellular composition of the ependymal layer (Roberts et al., 1995), the cytoarchitecture of the glial components of the CNS of anguilliform fish remains undocumented. With respect to other anamniote vertebrates, many studies have concentrated upon the glial structures present in the brain, such as in the cerebellum (Dahl et al., 1985), the rhombencephalon (Rubio et al., 1992) and, more extensively the visual system (e.g. Nona et al., 1989; Rungger-Brandle et al., 1989), but few have described the glial cytoarchitecture of the spinal cord.

It is generally considered that the ependyma and astrocytes are major elements in the vertebrate CNS (Peters et al., 1991; Reichenbach and Robinson, 1995). The ependyma lines the ventricles of the brain and the central canal of the spinal cord and is arranged in two layers, an epithelial ependymal layer contacting the cerebrospinal fluid in the canal lumen, and a second layer, termed the subependyma or subependymal layer (Peters et al., 1991). Ependymal cells, or ependymocytes, are the main cell type in the epithelial ependymal layer and are simple cuboidal to columnar cells that are similar in all vertebrate classes (Roots 1986); little is known of the functions these cells perform in the nervous system (see Flament-Durand and Brion, 1985, for review). Interposed between the ependymal cells are the tanycytes which constitute a small population of cells that also contact the lumen of the canal but extend long cellular processes to the pial surface or to blood vessels where they end as club-shaped endfeet (Rafols, 1986).

Astrocytes comprise another type of non-neuronal cell in the vertebrate CNS. In mammals, where this cell type has been extensively studied, astrocytes possess a characterisitc 'stellate' or star-shaped morphology. Two groups, protoplasmic and fibrous astrocytes, are found in the grey and white matter respectively (Privat and Rataboul, 1986). Certain features are unique to astrocytes, such as membrane-associated orthogonal particle complexes (MOPC's) on the surface of the plasma membrane, glycogen granules, and large bundles of intermediate filaments in the cytoplasm composed primarily of glial fibrillary acidic protein (GFAP; for review see Privat and Rataboul, 1986; Roots, 1986). An astrocyte population is also present in anamniote vertebrates but with a different morphology; for example in the fish spinal cord each astrocyte extends a single, long cellular process into the surrounding grey matter in a radial manner, hence the term 'radial astrocyte' (Bodega et al., 1990). Their cell bodies are found in the grey matter close to the ependymal zone and they contain

numerous bundles of intermediate filaments containing glial fibrillary acidic protein characteristic of mammalian astrocytes.

In the eel spinal cord, the ependymal layer is known to contain ependymocytes and liquor contacting neurons (LCN's, Roberts et al., 1995); however, little is known of the tanycyte population interspersed between the ependymocytes of the ependymal layer or of the radial astrocyte structure in the grey and white matter. In light of the small number of studies that have described the glial structure and the use of a variety of analytical methods, such as HRP impregnation (Miller and Liuzzi, 1986), histochemical (Sarnat et al., 1975), immunohistochemical (Dahl et al., 1985) and ultrastructural analysis at the electron microscope level (Stevenson and Yoon, 1982), we have combined a light and electron microscopical study with an immunohistochemical analysis of GFAP, vimentin and S-100 to determine the glial structure of the eel spinal cord, as a background to our analysis of the regenerating structure.

GFAP is the major subunit of gliofilaments (Eng et al., 1971; Eng, 1980) and is considered to be a specific and reliable marker for mature cells of astrocytic origin (e.g. Eng, 1985). Labelling of glial cells with antibodies to this protein has been reported in all vertebrate classes: hagfish (Wicht et al., 1994), lamprey (Wasowicz et al., 1994), teleost fish (Anderson et al., 1984), amphibians (Miller and Liuzzi, 1986), reptiles (Yanes et al., 1990) and birds (Onteniente et al., 1983), suggesting a phylogenetic stability of this protein in vertebrates. In contrast to most other studies in teleost fish (e.g. Anderson et al., 1984; Onteniente et al., 1983; Bodega et al., 1990), where the antibodies used were specific to the mammalian form of GFAP, we have utilised an antibody raised to goldfish GFAP (Nona et al., 1989) that is proven to label specifically astrocytes in the CNS of teleost fish (Stafford et al., 1990) and hagfish (Wicht et al., 1994) and is also specific to a 51KDa band corresponding to GFAP isolated from rat and which labels astrocytes in the mammalian CNS (Shehab et al., 1989).

Vimentin is another major cytoskeletal protein that is present in immature cells of astroglial lineage in mammals (Voight, 1989; Elmquist et al., 1994), adult ependymal cells (Bignami et al., 1982) and is co-expressed with GFAP in mature Bergmann glia (Schnitzer et al., 1981; Bovolenta et al., 1984). Vimentin labelling has also been reported in reptiles (Monzon-Mayor et al., 1990), amphibians (Lazzari et al., 1997) and teleosts (Glasgow et al., 1994; Rubio et al., 1992).

The S-100 protein is specific to vertebrate glial cells, particularly astrocytes in mammals. It is part of a group of calcium-binding proteins that may play a role in the calcium-dependant regulation of the astrocyte cytoskeleton (Bianchi et al., 1993) and is found to label the astrocyte cell body more intensely than GFAP antibodies (e.g. Boyes et al., 1986). Few studies have utilised antibodies to this protein in the anamniote CNS. However, the results suggest that this protein is specific to glial cells (e.g. Nona et al., 1995).

In the present study, we demonstrate that the spinal cord contains an ependymal and radial astrocyte population similar to that of other teleost fish. We show that ependymal cells label GFAP-ve, and S-100+ve, the tanycytes and radial astrocytes are GFAP+ve and S-100+ve, while vimentin labelling is restricted to a small region containing the medial, ascending and descending glial tracts in the cord. We have also found evidence to suggest that a small population of cells, of non-ependymal or radial astrocytic origin, are present in the grey matter of the spinal cord.

2.2. Materials and Methods

This study is based on 34 European eels *Anguilla anguilla L.* in a non migratory immature stage of their lifecycle. These and all of the other animals used in this thesis came from a stock population maintained in aquaria within the Department that were obtained from two sources: captured wild glass eels (Salmon Research Agency, Newport) reared to the yellow eel stage and farmed yellow eels obtained from a commercial supplier (Aqua Arklow). All eels were housed in one of three specially constructed stock tanks with each served by its own biofiltration tank and separate aeration source. The filtration system was a scaled-down version of the latest commercial air-lift circulation systems using directed air flow to create water currents capable of carrying, and suspending, plastic "bio-balls", allowing for enhanced bacterial action. A 'top-up' of bacterial culture was added monthly and the system stripped and cleaned every 6 months. In each tank, the temperature was maintained at approximately 25°C. Both parameters were monitored daily and the animals were fed once daily using commercial eel feed.

Tissue preparation

For histological investigation, each fish was first anaesthetised by immersion in 0.3mg/l MS-222 (Methanesulphonate salt, Sigma) and further deep anaesthesia provided by a subcutaneous injection of 0.3ml alphaxalone ('Saffan', Pitman-Moore). In order to prevent blood clotting, 0.2ml heparin sodium (Leo Laboratories) was administered subcutaneously. Each animal underwent perfusion fixation, which necessitated the exposure of the heart and the insertion of a cannula through an opening in the ventricle and into the conus arteriosus. Using a peristaltic pump (Rabbit-Plus, Ranin) a primary flush of Ringer's solution, with 0.1% procaine (Sigma) for further anaesthesia, was given to remove the blood (through a second incision in the sinus venosus), and was then followed by the required fixative for approximately 30 minutes. Two fixative solutions were used (a) 4% paraformaldehyde in 0.1M phosphate buffer (PB) pH adjusted to 7.4 for immunohistochemical investigation and (b) 2% paraformaldehyde, 1.25% gluteraldehyde in 0.1M phosphate buffer (PB), pH adjusted to 7.4 for electron microscopy. Following perfusion, the spinal cord was immediately dissected from the spinal column and post-fixed in the same fixative for a maximum time of 3 hours at 4°C.

Immunohistochemistry

Following postfixation, the spinal cords were mounted in a medium consisting of 35% bovine serum albumin (Fraction V - Sigma) and 3% gelatin (Sigma). Using 25%w/v glutaraldehyde as denaturing agent, the protein was solidified to produce a strong gelatinous medium. The tissue was sectioned in one of three planes, transverse, horizontal or parasaggital, at 50 μm on a Vibratome (series 100). Cut sections were collected in 0.1M PB, pH 7.4 and processed for GFAP, S-100 or vimentin immunohistochemistry.

All sections were pre-treated in 1% sodium borohydride in distilled water to remove residual fixative and treated in 5% normal serum appropriate to the antibodies used to reduce background staining. Sections were rinsed for 5 x 5 minutes between each incubation.

For the primary antibody reaction, sections were incubated in (a) GFAP Rabbit anti-goldfish (generous gift by Dr. S. N. Nona), 1:20,000 in 0.1M PB, and 0.5% Triton X-100, or (b) S-100 rabbit anti-bovine (Dako) 1:20,000 in 0.1M Tris-HCl, 0.9% NaCl and 0.5% Triton X-100 or (c) vimentin mouse monoclonal (Dako), 1:1000 in 0.9% NaCl and 0.5% Triton X-100. Sections were incubated at 4°C for 48 hours and then treated respectively with (a) biotinylated goat anti-rabbit IgG (Vector), 1:200 in 0.1M PB and 0.5% Triton X-100 or (b) biotinylated goat anti rabbit IgG (Vector), 1:200 in 0.1M Tris-HCl and 0.5% Triton X-100 or (c) biotinylated horse anti mouse IgG (Vector), 1:200 in 0.1M Tris-HCl and 0.5% Triton X-100, and incubated overnight at 4°C or for 2 hours at room temperature. The avidin-biotin method (ABC kit, Vector) was used to treat the tissue at room temperature for 1.5 hours. Following the final treatment, sections were rinsed (x 3) in 0.1M Tris-HCl pH. 7.6 and treated with 0.05% 3,3′-diaminobenzidine (DAB, Sigma) as chromogen and 0.01% H_2O_2. Finally, sections were washed (x3) in 0.1M Tris-HCl, pH. 7.6, at room temperature and mounted onto clean slides using 0.2% gelatin in 0.1M Tris-HCl, pH. 7.6, as mountant, and left to dry for 48 hours, and thereafter dehydrated and coverslipped.

To determine the degree of non-specific binding, a series of experiments was run for each antibody that was used, and this involved omitting one of the reagents in the process. Non-specific labelling was minimal in all sections tested. In order to increase labelling specificity, both the primary and the secondary antibody for each

intermediate filament protein was preincubated for 24-48 hours at 4°C in sections of unused tissue to further reduce non-specific binding.

Electron microscopy

Following postfixation, the tissue was washed in 0.1M PB (x6) for 1 hour. Secondary fixation was completed in 2% OsO_4 in 0.1M PB for approximately 2 hours, and the tissue then dehydrated in a graded series of ethanol (10-100%) and embedded in resin (Agar 100 - medium mix) and left to solidify in an oven at 60°C for 24 hours.

Serial sections of the spinal cord were cut for both light (1.5µm) and electron microscopy (~500Å) on an LKB Ultramicrotome. Light sections were mounted on slides, stained with toludine blue and coverslipped. Thin sections were mounted onto copper-coated grids, post-stained with uranyl acetate, counterstained with lead citrate, and examined with a Hitachi H-7000 microscope. Images were either photographed on to plate film, or digitally acquired via a digital camera (Neuroimagor II).

Image analysis and reconstruction

Light microscopic images were acquired using an Optiphot -2 microscope (Nikon) with attached digital camera (Polaroid DMC) and downloaded to a Macintosh G3 computer. All images were analysed and formatted using Adobe 'PhotoShop 5'.

Using an Axiophot-2 microscope (Nikon) with attached camera lucida, serial sections (60µm apart) of the spinal cord and central canal were drawn, and then traced from a digitising tablet (Summagraphics) into a Macintosh Performa 630. Reconstructions were made using the 'MacStereology' program (version 1.01).

2.3. Results

Light Microscopy

Figure 2.1 provides a general view of the central canal region stained with toludine blue in the caudal spinal cord of an unoperated eel and illustrates the major glial elements examined in this chapter; the ependyma; the subependyma, and the radial glia.

Ependyma

As in other vertebrates, in the eel the cells surrounding the lumen of the central canal form two layers: a single layer of epithelial ependymal cells abutting the lumen of the canal and an outer layer of subependymal cells. These two layers comprise five cell groups: (a) ependymocytes; (b) subependymal cells; (c) tanycytes; (d) light staining cells, and (e) liquor contacting neurons (LCN's). The first four groups will be described here while the fifth, which is neuronal, is dealt with later (see chapter 6).

Analysis of toludine blue stained serial light microscopical sections of the two layers around the central canal shows that the cells stain heterogeneously with toludine blue; in particular the cell bodies of the ependymal layer stain more intensely than those in the subependymal layer. A small population of lightly staining cells with large cell bodies is seen on the dorsal surface of the canal and extends into the subependymal layer. Outside the subependymal layer, in the dorsal, ventral and lateral portions of the grey matter, are the soma of radial astrocytes which also stain heterogeneously. They are most conspicuous laterally where they produce two 'horns' of compact cells as revealed by GFAP labelling (Fig. 2.2). Occasionally oligodendrocytes are also found in this region and are identified by their dark staining soma and short processes. Long thin processes extend from this region into the grey and white matter where they appear to terminate at the meningeal surface.

Four large glial tracts are present in the cord that extend from around the central canal to the meningeal surface, in effect dividing the cord into four large sectors. Ventrally the tracts stain much more intensely than their dorsal counterparts and the point of origin of the processes is closer to the sub-ependyma. The processes terminate in the superficial regions (see Fig 2.1) placed dorsally and ventrally where there is a paucity of cell soma. Laterally, the glial tracts extend towards the periphery of the spinal cord in a slightly different way. A pair of large processes extends ventro-laterally curving gently to the ventro-lateral surface of the cord. Here, a small

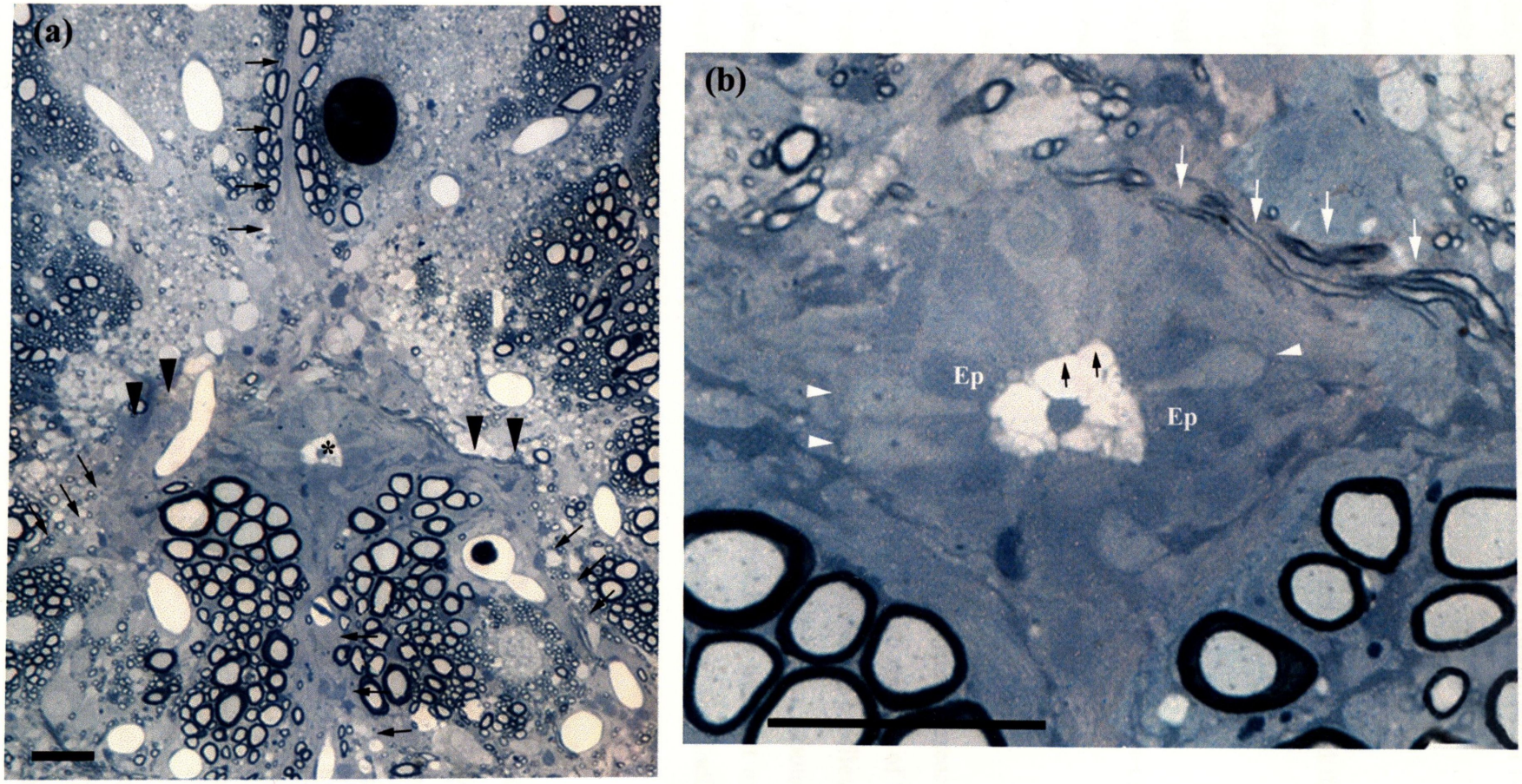


Figure 2.1a, b. (a) Photomontage of the central canal (*) and the glial horns (arrowheads) in the grey matter of the normal spinal cord. Note the radial processes (arrows) that extend from this region, particularly those that project dorsally, ventrally and ventrolaterally. In (b) note the heterogeneity of staining in the cells that surround the canal. LCN's (arrowheads) are conspicuous as are light staining cells placed dorsally (arrows) interspersed between the ependymocytes (Ep). Dorsal to the canal are small myelinated axonal tracts that cross between the two glial horns (white arrows). Scale bar = 25 microns.

submeningeal region is often present into which these processes project (Fig. 2.1).compact group of processes (Fig. 2.2c). Thinner processes also radiate from the glial horns and these extend to dorso-lateral, lateral and ventrolateral regions, while few project to the ventral cord.

Immunohistochemistry

In an examination of the ependymal and glial structures three different antibodies, GFAP, S-100 and vimentin were utilised.

Glial Fibrillary Acidic Protein (GFAP)

The radial astrocytes and the tanycytes in the cord labelled GFAP+ve including other elements in ventral portions of the grey matter (Fig. 2.2).

Ependymal Region

No ependymal cells surrounding the central canal immunoreacted for GFAP. Tanycytes, however, did label and were distributed in two regions of the canal, on the ventro-lateral and dorso-lateral surfaces (Fig. 2.2a,b). Labelled profiles were few, about four per section. The labelled cell body is elongate in shape, abuts the lumen, and extends a single large process laterally into the glial horns where it amalgamates with processes from the radial glia, making identification of the individual elements impossible beyond this point.

Radial Astrocytes

In the ventral tract, large thick immunopositive profiles extended towards the periphery of the cord. The origin of these fibres is twofold: the first source is the region close to the ventral subependyma while the second is the lateral glial horns (Fig 2.2c). Therefore two different groups of GFAP+ve glia extend into the ventral tract. The fibres are usually long and straight; although they deviate around blood vessels and branch extensively, close to the ventral surface, around the large myelinated axonal tracts. Occasionally the ventral processes bifurcate close to the sub-ependymal region to produce two or more large GFAP+ve branches.

Dorsally, immunopositive profiles also arise from two different locations to produce a thick projection that terminates at the periphery of the cord. The first set of fibres arises from the region dorsal to the subependymal zone of the central canal and

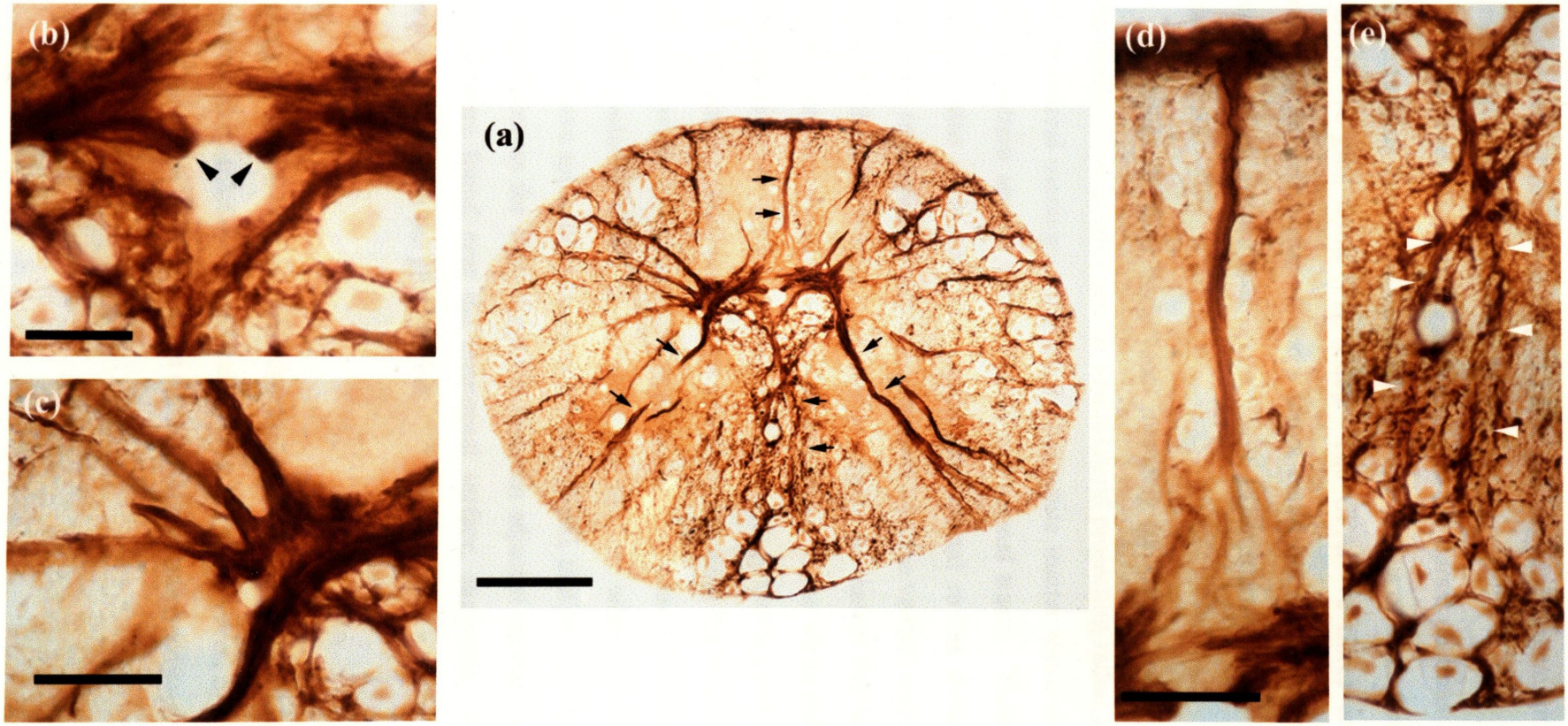


Figure 2.2. Photomicrographs of the spinal cord cut in transverse section and labelled for GFAP: (a) the whole cord, (b) the central canal region, (c) the glial 'horns', (d) the dorsal and (e) the ventral tracts. In (a) note the labelling for four major tracts (arrows) that extend dorsally (d), ventrally (e) and ventrolaterally. In (b) note that ependymocytes did not label for this marker and the intense labelling of tanycytes (arrowheads). In (c) the glial horns label intensely which is the origin of radial astrocyte cells and their immunopositive processes. In (d) the dorsal tract labels intensely as does the dorsal region into which this tract projects. In (e) note the ventral tract, which in this instance has split in two (arrowheads) and its extesion ventrally in which the processes divert (arrows) around the large myelinated tracts (*) to terminate at the pial surface. Scale bar = (a) 200 microns, (b), (c), (d) and (e) = 50 microns

the second set from fibres projecting from the lateral glial horns. In contrast to the ventral projections, the dorsal structure does not bifurcate and remains as a single compact group of processes (Fig. 2.2d). The large meningeal areas on the dorsal and ventral surfaces of the cord are GFAP+ve.

GFAP+ve filaments are also found in the dorsal portions of the subependymal zone surrounding the central canal where a thin plexus of these fibres traverses between the GFAP+ve glial horns (Fig. 2.2b). The GFAP+ve fibres are thin and intensely stained and the cell bodies of these fibres could not be discerned in the glial horns. These immunopositive fibres appear only intermittently along the cord in serially stained sections.

Laterally the glial horns label intensely for GFAP (see Fig. 2.2c). The most intensely stained structures are the ventrolateral projecting radial glia that terminate on the ventrolateral meningeal surface. In the white matter these processes deviate in a wave-like pattern around blood vessels and axonal tracts. Thinner GFAP+ve radial projections also arise from this region and extend to the dorso-lateral, lateral and ventrolateral region while only a few project into the ventral regions of the cord. The structure of these numerous processes is similar to that of the large descending glial projections and possesses the wave-like patterning in the white matter. Numerous side projections give rise to a highly branched morphology that is most common in the white matter. Ventrally, small projections also originate from the descending glial tracts and branch extensively to surround the large axonal tracts and blood vessels (Fig. 2.2e). At times their point of origin is unknown due to their wispy short processes. Smaller immunopositive spine-like processes are also found, that projected perpendicularly from each main process for short distances between adjacent axonal tracts. Few GFAP+ve processes were found near the meningeal surface, suggesting that this intermediate protein is absent from the glial endfeet.

S-100

Labeling for S-100 in the cord also highlighted the morphology of the radial glia characteristed by the GFAP+ve labeling (Fig. 2.3). However, S-100 also labeled somal structures that were GFAP-ve in the ependymal and subependymal layers.

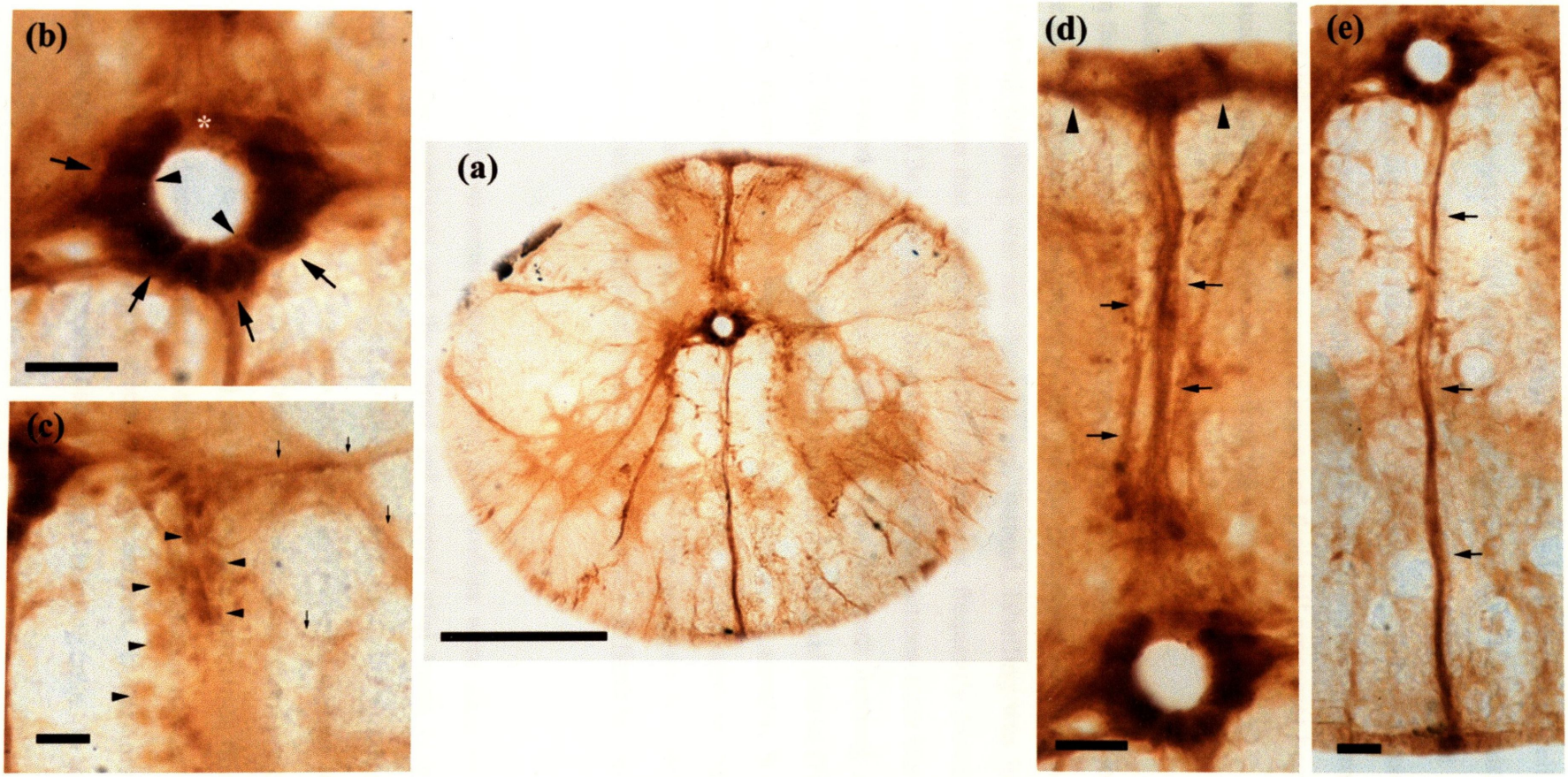


Figure 2.3. Photomicrographs of the spinal cord in transverse section and labelled for S-100. In (a) note the similar labelling pattern of the radial astrocytic network found for GFAP, but in contrast, cells surrounding central canal also labelled (b; arrows), however small portions (arrowheads) failed to label including the dorsal regions of the canal (*). In (c) labelling of cellular-type profiles can be seen (arrowheads) as well as the radial astrocytic network (arrows). In (d) and (e) corresponding to the dorsal and ventral tracts respectively, projecting glial tracts labelled for the antibody (arrows) and in the case of the dorsal surface the processes terminate into a region of intense labelling (arrowheads). Scale bar (a) = 200microns, (b), (c), (d) and (e) = 20 microns

Ependymal Region

Cell bodies surrounding the lumen of the canal have an intense, heterogeneous staining pattern. On the ventral and lateral surfaces densely labelled cell soma are visible abutting the lumen of the canal whereas dorsally, the 'light-staining' cells identified from toludine blue-stained sections are less intensely labelled (Fig. 2.3b). The subependymal layer also labels lightly. Occasionally, thin processes from this layer pass between the darker staining ependymal cells to contact the lumen of the canal. It proved difficult to identify tanycytic soma and their tail processes because of the intense staining intensity of the cells surrounding the central canal.

Radial Astrocytes

On the ventral surface of the canal, radial processes stain intensely for S-100; however, the highly branching morphology close to the meningeal surface characterised by the GFAP+ve labelling was not observed and, instead, labelling was isolated to a single straight process that terminated beneath the meninx, frequently forming a bugle-shaped endfoot (Fig. 2.3e). Dorsally, intensely labelled projections from the lateral glial horns could be traced from their point of origin into the tract forming a single group of processes that terminated in the densely labelled dorsal glial plexus (Fig. 2.3d); this area labelled more intensely than the ventral glial plexus. Laterally, S-100+ve processes radiate from the glial horns towards the periphery of the cord on the dorso-lateral and lateral surfaces (Fig. 2.3a, c), and small thin side branches frequently emanate from these larger structures, but label weakly and were often difficult to trace.

Vimentin

There was little vimentin labelling and few profiles were seen in the cord. These included the meninges and the dorsal and ventral glial tracts (Fig 2.4). Ventrally, immunopositive glial processes could be traced from the lumenal surface to the periphery of the cord. The positive profiles at the lumenal surface were very fine and difficult to discern; however, the intensity of labelling increased progressively closer to the meningeal surface (Fig. 2.4b, c). In these regions, numerous fine filaments branch from the main descending tract to surround the myelinated axonal tracts close to the meningeal surface. Labelling is absent from the endfeet. In the dorsal glial tracts, fine filaments originate from the area close to the light staining cells. In this region,

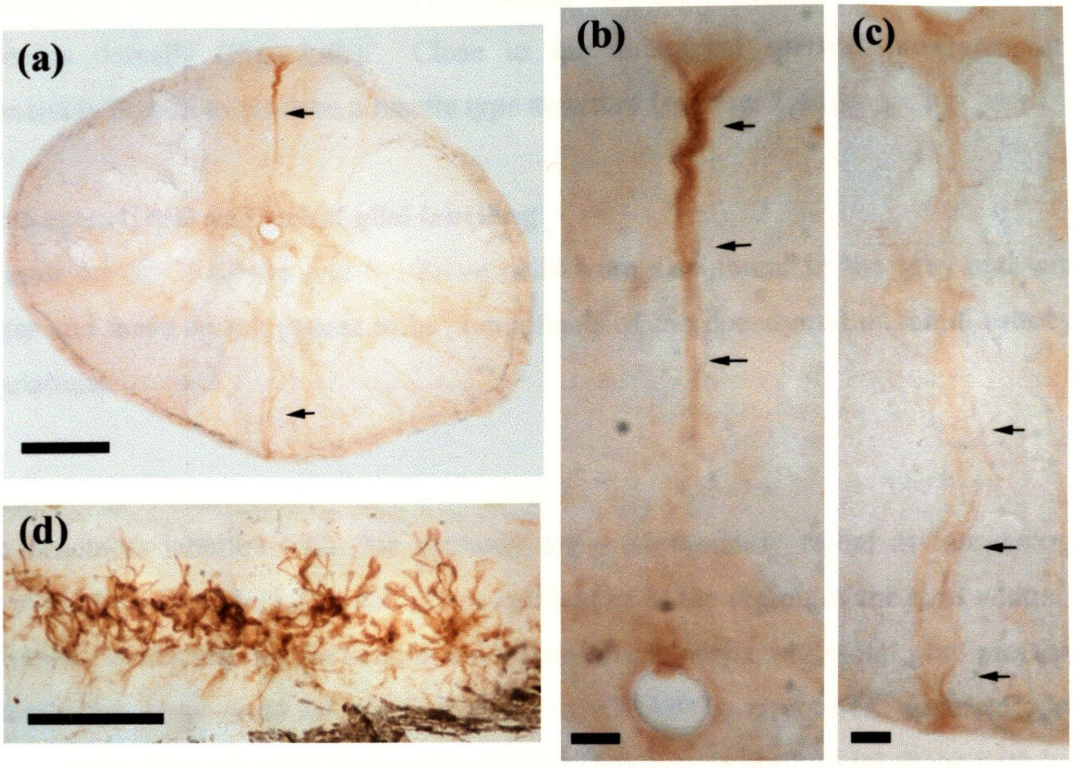


Figure 2.4. Vimentin labelling in the normal spinal cord in transverse section. Note the lack of labelling in the cord (a) save for the dorsal (b) and ventral (c) processes. In both immunopositive profiles there is a gradual increase in labelling intensity from the canal to the surface of the cord (small arrows). In (d), a horizontal section, the dorsal vimentin+ve profiles splay to form rosette -type profiles on the dorsal surface. Scale bar (a) = 50 microns and (c), (d), (d) = 20 microns.

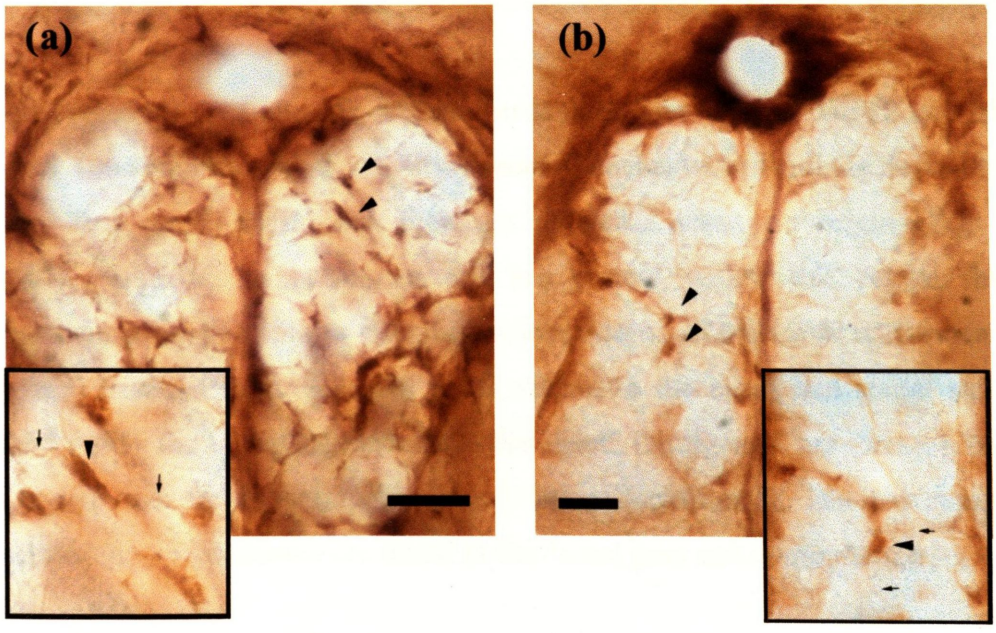


Figure 2.5. GFAP (a) and S-100 (b) labelling between the myelinated axons ventral to the central canal indicate the presence of cellular profiles. In both (a) and (b) structures resembling cell bodies (arrowheads) and fine cytoplasmic processes (arrows) are present. The insets highlight these immunopositive profiles. Scale bar = 20 microns.

labelling of vimentin+ve filaments is weak; however, labelling intensity steadily increases dorsally (Fig. 2.4b). Close to the meningeal surface, processes often extensively branch to produce a rosette type structure (see Fig. 2.4d).

Extra-ependymal and radial glial labelling

A small set of GFAP+ve and S-100+ve cells were also found in the grey and white matter and these do not appear to be components of the ependymal or radial astrocyte populations.

GFAP

The structures labelled with this antibody are predominantly radial in morphology; however, there is evidence for GFAP+ve cell bodies in the region of the cord ventral to the canal. In this region, the ventral and ventro-lateral projecting radial glial processes separate two large areas of myelinated axons; GFAP+ve structures, apparently cell bodies, nestle between these axons (Fig. 2.5a). They have a perikaryial shape with long thin cytoplasmic projections that appear to make contact with other cells, and the processes of radial astrocytes. These cells are seen only in this region and, occasionally, in portions of the grey matter close to the radial astrocytes situated ventrally.

S-100

Structures resembling cell bodies, and similar to those labelled with GFAP, are labelled with the S-100 antibody (Fig. 2.5b). They seem to be unattached and are devoid of long processes that may indicate that they are of radial astrocytic origin (Fig. 2.3c). Frequently, numerous somatal structures are present within this region that are heterogeneous in shape with few cytoplasmic extensions. In the dorsal white matter and interspersed between the myelinated tracts ventral to the canal, are somal structures situated outside the subependymal zone that label faintly and are present in close apposition to the dorsal radial glia (Fig. 2.5b). Occasionally, labelled somal type structures of unknown identity are found in the dorsal grey and white matter.

Glial Cytoarchitecture in the Spinal Cord

The light microscopical investigation has shown that the cord has a regular glial organisation that divides the cord into compartments. The analysis of the GFAP and S-100 immunoreacted material, cut in the horizontal, saggital and transverse planes,

reveals a repeating glial organisation in the spinal cord (Fig. 2.6a, b). This plan is best appreciated from 3-dimensional reconstructions made from serial immunoreacted and plastic sections, where the spinal cord is seen to be divided primarily into four compartments by the large dorsal, ventral and descending lateral processes (Fig 2.7a). Further sub-division is brought about by the smaller radiating glia, notably in the dorsal-lateral and lateral regions of the cord (Fig 2.7b). Ventrally, the glial division is augmented by a small population of radiating elements from the glial horns and by branching (sometimes quite extensive) of the ventral descending glial processes.

Electron Microscopy

The different glial components were investigated with the electron microscope to determine their ultrastructure and the organisation of the ependymal zone, the glial horns and the radial processes. The ultrastructure of the specialised liquor-contacting neurons is only briefly alluded to here as they are characterised further in chapter 6.

Ependymocytes

Ependymocytes are distributed on all surfaces of the central canal and make contact with its lumen. A typical ependymocyte can be considered as having two distinct parts, a large somal portion, and an apical non-ciliated region that contacts the lumen of the canal (Fig. 2.8). The nucleus is large and is placed centrally while its shape varies from elongate to highly irregular: in some cells there are deep invaginations in the nucleus created by cytoplasmic processes. The electron dense staining of the nucleus contains chromatin aggregates in the centre and along the nuclear membrane. The cytoplasm stains lightly and contains numerous organelles, including prominent mitochondria and a rough endoplasmic reticulum arranged in repeating lamellar units with abundant ribosomes. Large bundles of filaments, characteristic of other cell types in the cord, were absent from the ependymocytes. Occasionally small electron dense bodies are present in the cytoplasm, usually in the apical portion of the cell. Junctions between cells are common and consist primarily of *zonulae adherens* along the apical portions of the cell. Occasionally, short tail processes extend into the subependymal layer.

Tanycytes

Tanycytes are present on the ventro-lateral and dorso-lateral surfaces of the central canal and differ in morphology from their neighbouring ependymocytes. They

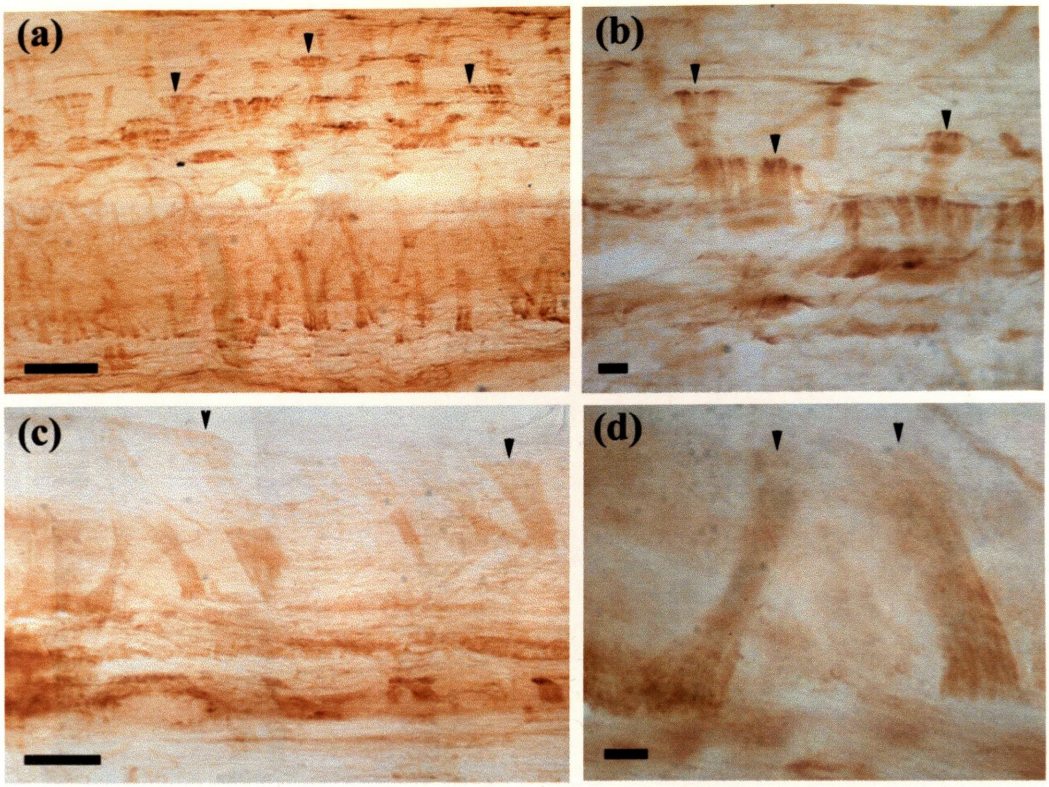


Figure 2.6a, b, c, d. Photomicrographs of the spinal cord labelled for (a, b) GFAP and (c, d) S-100. In (a) the plane of section is saggital and highlights portions of the radial astrocytic structure, seen at higher power in (b). Note the close apposition of processes (arrowheads). A similar pattern was found in horizontal section in (c) with wide bands of processes extending from the region close to central canal (d; arrowheads). Scale bar (a) and (b) = 100 microns, (c) and (d) = 20 microns.

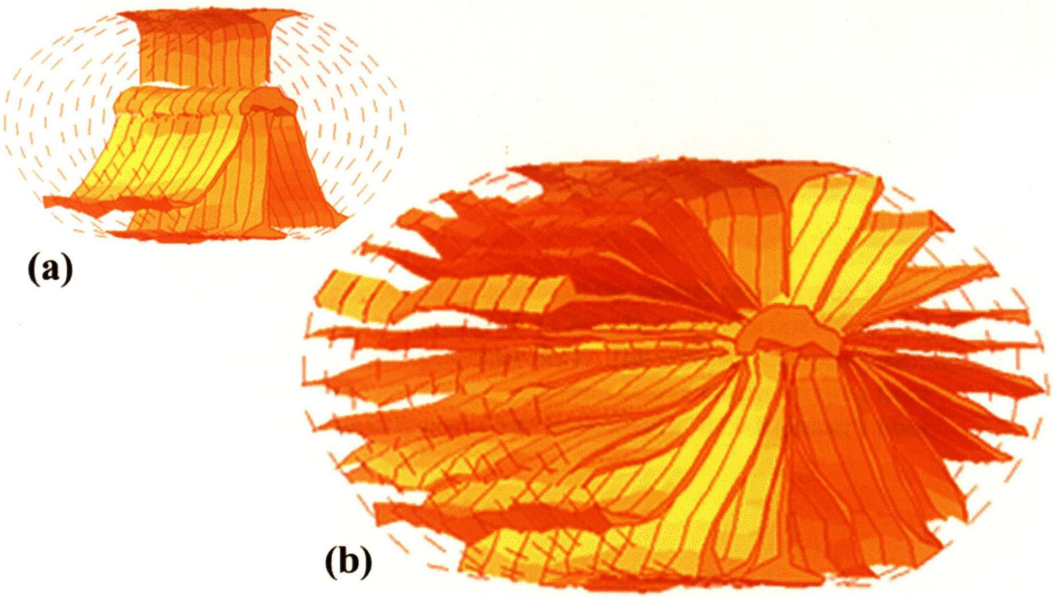


Figure 2.7a, b. Reconstructions of the radial glial structure in the normal spinal cord from serial transverse sections. In (a) the four large glial tracts are highlighted along with the central canal region while in (b) the smaller radial tracts are included. This representation does not include all of the smaller side branches.

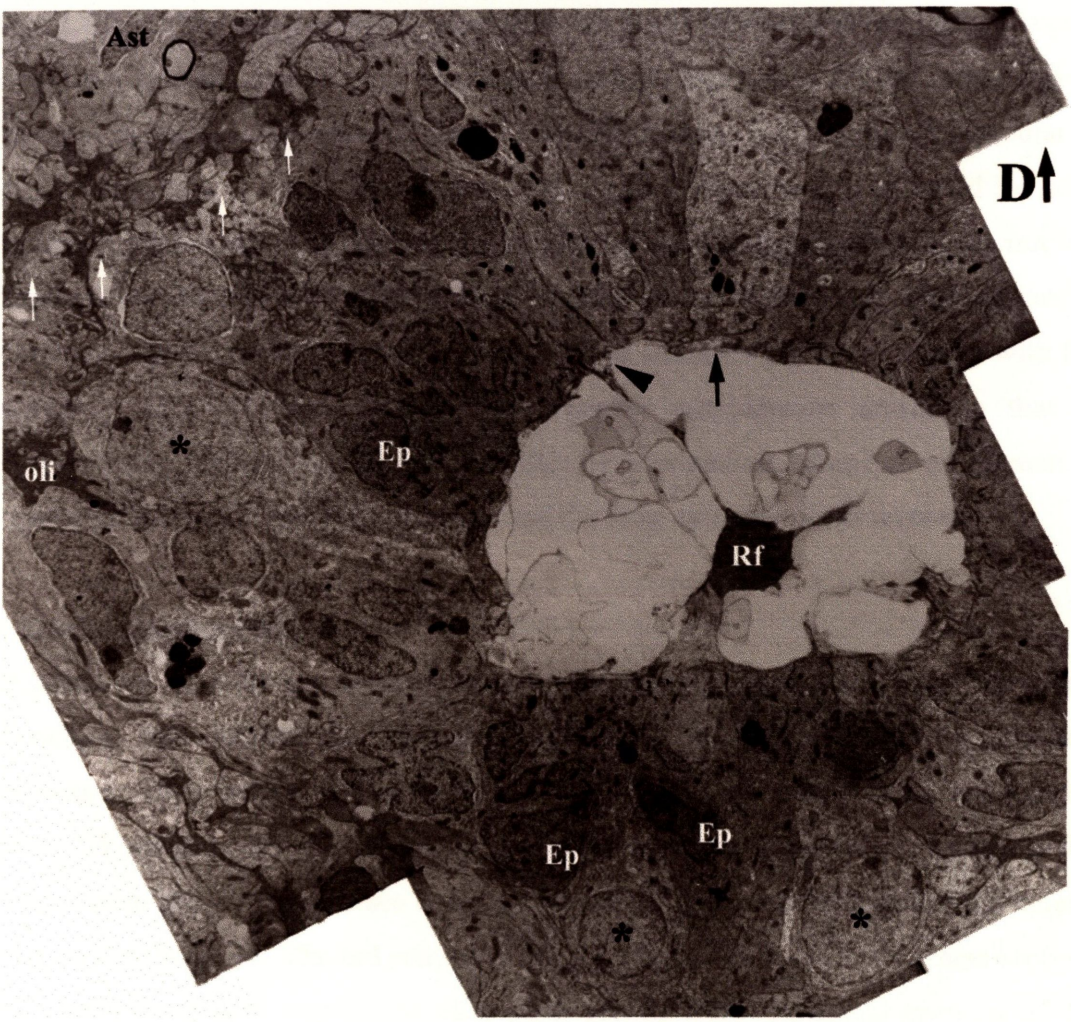


Figure 2.8. Photomontage of electron micrographs of the central canal region in the eel spinal cord. Note the conspicuous large cell bodies of LCN's (*), tanycytes (arerowheads), the dorsal light staining cells (arrows) and ependymocytes (Ep). The adjacent subependymal layer is composed primarily of dark and light staining processes (white arrows) arising from oligodendrocytes (oli) and radial astrocytes (Ast) respectively. Rf = Reissner's fibre. Dorsal surface = D. Scale bar = 5 microns.

comprise: (a) an apical region contacting the lumen of the canal, (b) a somal region containing the nucleus, and (c) a tail region that extends laterally into the glial horns (Fig. 2.9). These cells are generally bigger and more elongate than the surrounding ependymocytes and are slightly smaller and more darkly staining than the similarly shaped LCN's. The short apical portion connects to the slightly enlarged somal region to produce a 'goblet' shaped cell. The nucleus, which expands to fill the somal region, often close to the apical portion of the cell, varies in shape but is generally circular to elongate, possesses a 'rough' membrane surface and is occasionally indented by large cytoplasmic processes. It is electron dense with chromatin aggregations at the nuclear membrane. A nucleolus is often present, located to one side of the nucleus, and a discontinuous perinuclear space is frequently found demarcating the boundary with the cytoplasm. The cytoplasm contains an organelle complement similar to that of ependymocytes, although occasionally bundles of intermediate filaments are present in the cytosol close to the plasma membrane and the long cytoplasmic processes.

The 'Light' Staining Cells

This small set of cells has a characteristic light staining appearance under the light microscope, and retains this characteristic pattern at the level of the electron microscope. They are distributed on the dorsal surface of the central canal and usually number 2-5 profiles per section. Each cell body is large, and frequently extends into the subependymal layer. Its structure is similar to that of a tanycyte and comprises apical, somal, and tail regions. The tail processes are not always obvious in transverse section, being interspersed with axonal and glial tracts arising from the dorsal portions of the glial horns positioned laterally (Fig. 2.10). Occasionally a second layer of this cell type is present in the dorsal subependymal region in close association with the dorsal glial tracts that run horizontally between the glial horns. When present, tail processes extend dorsally into the ascending radial astrocyte tracts where they interpose with other glial profiles. In comparison to the liquor contacting neurons, which are the other type of lightly staining cell, this cell type contains fewer organelles and the cytosol is heterogeneous in staining density. The nucleus is slightly more electron dense than the cytoplasm and is generally large and circular in shape, with numerous indentations. Chromatin is condensed in the nucleus and also along the nuclear membrane. Nucleoli are occasionally found and a continuous perinuclear space is present. The cell contains a complement of organelles similar to that found in tanycytes and ependymocytes,

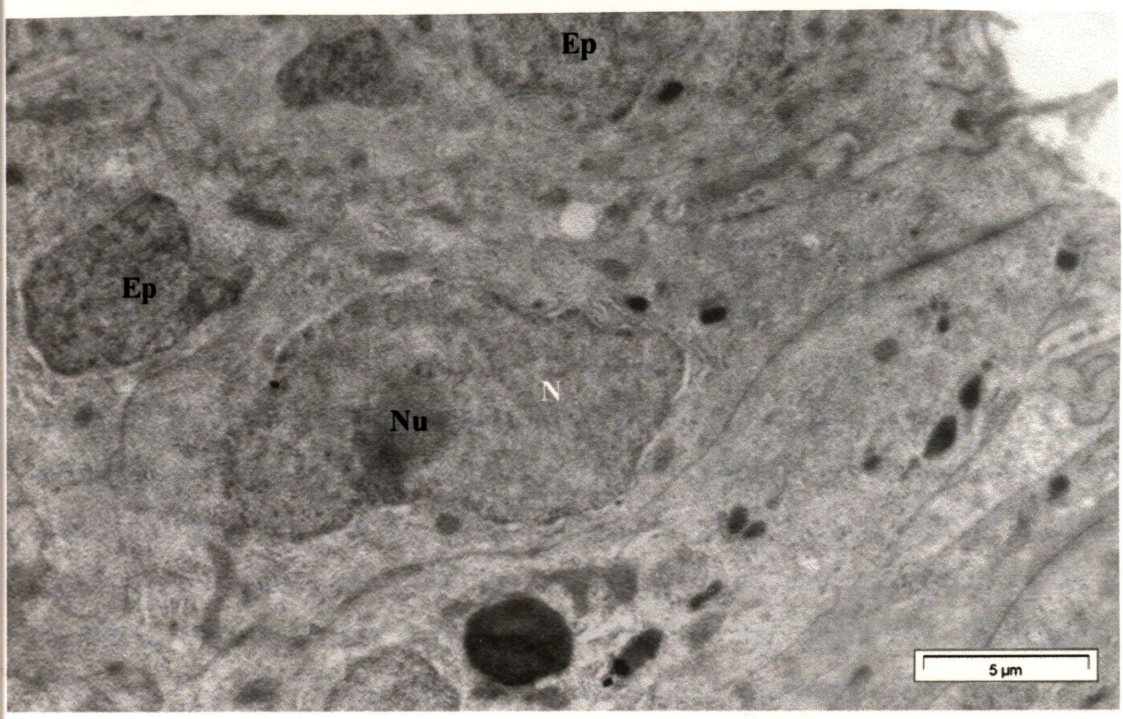
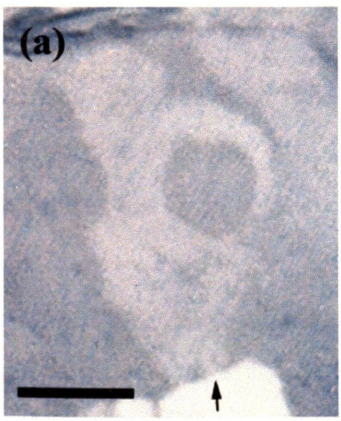


Figure 2.9. Electron micrograph of a tanycte cell body and a portion of the extending cellular process. Note the elonage shape and large nucleus (N) and nucleolus (Nu) compared to the surrounding ependymocytes (Ep).



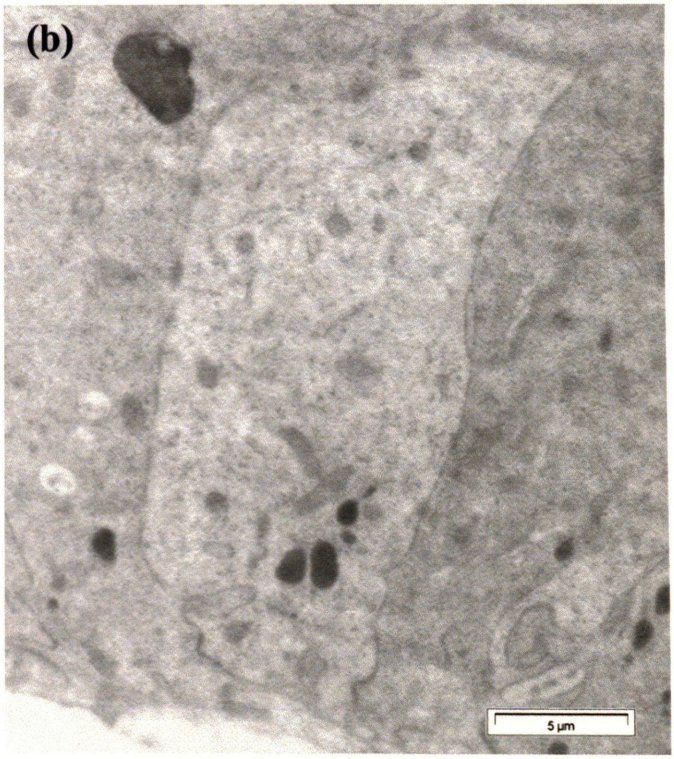


Figure 2.10a, b. Light staining cell on the dorsal surface of the canal. In (a) the light staining features of this cell type (arrows) can seen in the electron micrograph (b). Note the light staining cytoplasm, normal organelle complement and the inclusion of dark lipophilic-like structures. Scale bar = 10 um.

including densely staining structures that are absent from the LCN's. Close to the lumen of the canal, the apical portion of the light staining cells forms junctional complexes similar in appearance to *zonulae adherens*.

The subependymal region

The subependymal layer contains the processes of tanycytes, and the cell bodies and processes of LCN's, and, dorsally, the cell soma of the light staining glia and associated processes. A few cell bodies and a dense layer of light and dark staining processes are interspersed between these cellular structures. Cells that could be considered subependymal are infrequently found and they are similar to ependymocytes of the ependymal layer (Fig. 2.11). The cell body is irregular in shape and smaller than the adjoining ependymocytes while the nucleus is large and prominent in the cell. Numerous ribosomes and elongate mitochondria are distributed throughout the cytoplasm. A thin perinuclear space incompletely surrounds the darker staining nucleus, which contains a chromatin aggregation similar to that seen in ependymocytes. The main feature of this region is a thick layer of processes oriented parallel to the surface of the canal (Fig. 2.11, arrows). Many of the profiles follow tortuous pathways composed of at least two different cell types: characteristic long dark processes of medium oligodendrocytes close to the canal region intersperse between the second, lighter staining profiles that originate from radial astrocytes situated laterally and ventrally. Bundles of intermediate filaments are frequently found in these lighter staining profiles and characterise this cell type. Occasionally small groups of unmyelinated axonal profiles are present in this layer close to the ependymal cells, in particular the LCN's.

Glial Horns - Radial Astrocytes

Radial glial soma are found in the lateral and ventral portions of the grey matter close to the ependymal region in the cord and are of approximately similar size to ependymal cells. They vary in staining intensity and have irregular cellular profiles of different size. Interspersed occasionally between these cells are numerous darker staining cellular processes of oligodendrocytes. The irregular nucleus is large and prominent in the cell (Fig. 2.12), often with large cytoplasmic indentations. The cells are characterised by a light staining cytoplasm that contains numerous organelles, particularly rough endoplasmic reticulum, mitochondria and numerous ribosomes,

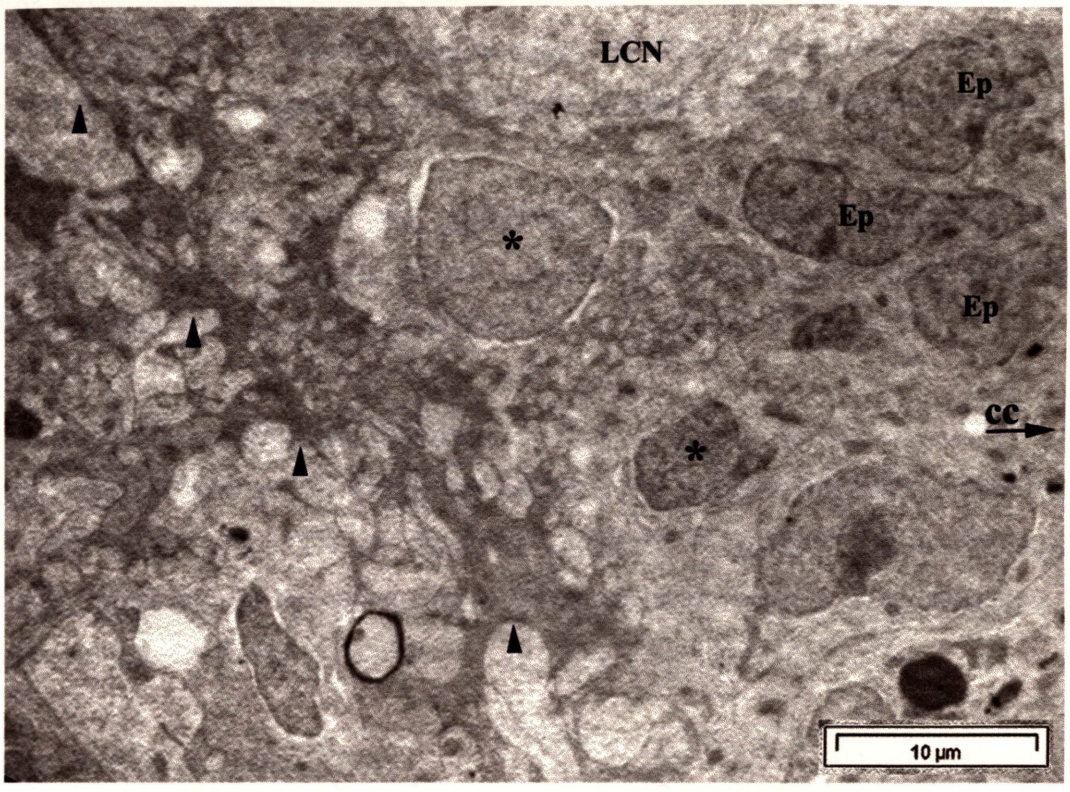


Figure 2.11. Electron micrograph montage of the subependymal region adjacent to the central canal. Note the presence of two cells (*) in this region and the large number of light and dark processes (arrowheads). The cell body of a liquor contacting neuron (LCN) and ependymocytes (Ep) can also be seen. C.C. denotes the position of the canal relative to the cells.

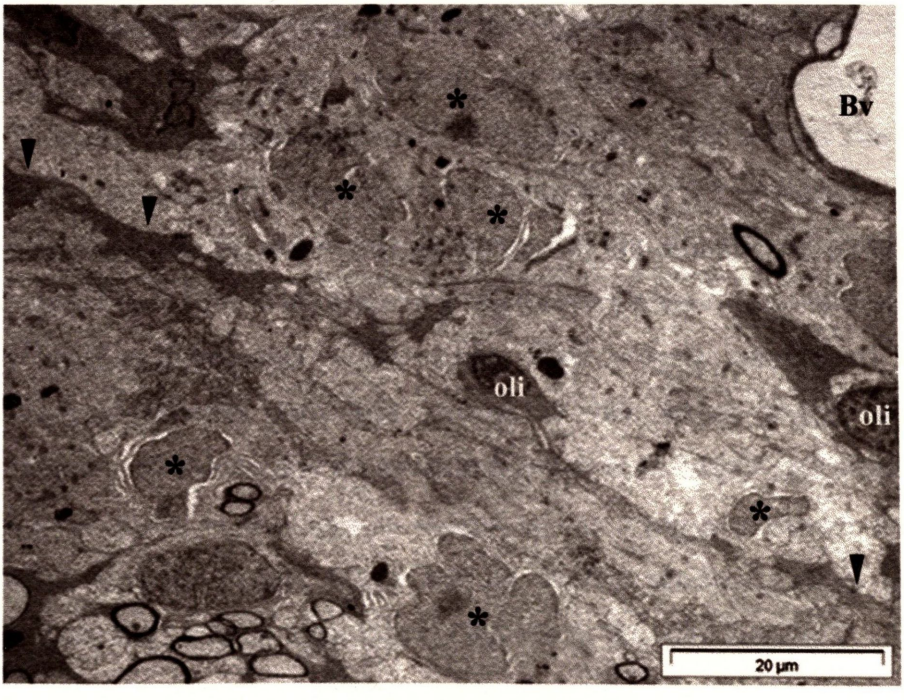


Figure 2.12. Radial astrocyte cell soma (*) in the glial horns. Note the irregualr shaped nuclei in the cells and the presence of oligodendrocytes (oli) and their processes (arrowheads). Bv = blood vessel.

while, occasionally, dark staining profiles similar to those found in the ependyma are present in the cytosol. Filaments are abundant and form dense bundles in the cytosol close to the plasma membrane in the cell soma and at the base of the long cytoplasmic process.

In the nucleus, chromatin aggregates along the nuclear membrane with a relatively homogenous staining density. A prominent perinuclear space continuous with the nuclear membrane is often present.

Radial Astrocyte and Tanycyte Processes

Since it proved difficult to distinguish between the cellular processes of the radial astrocytes and tanycytes, both are described together in this section. The descriptions of the glial tracts and the ascending dorsal tracts are separated into two sections as the structure of the latter differs considerably from the other tracts.

Ventral and Ventro-Lateral Tracts

The ventral and ventro-lateral glial tracts (which label GFAP+ve and S-100+ve) are free of cell bodies and composed of numerous closely apposed processes (~5-10) linked together by desmosomal-type junctional complexes. The processes periodically give off small side-branches that course between the surrounding axons (Fig. 2.13a). The most conspicuous and abundant structures are bundles of intermediate filaments arranged parallel to the longitudinal axis of the process. The smaller tracts, placed dorso-laterally, laterally and ventro-laterally, comprise only 2-5 processes. These are similar to the larger tracts and junctional complexes are periodically found between their processes (Fig. 2.13b). Side branching of processes is more frequent and can often be traced between myelinated axonal tracts. Each process consists of numerous intermediate-type filament structures similar to the larger tracts, along with mitochondria, free ribosomes and the occasional rough endoplasmic reticulum lamellae. Most processes appear to terminate as endfeet on the meningeal surface and contain large numbers of filaments that extend into the endfoot producing dense aggregates. Frequently these filaments are aligned perpendicular to the large bundles.

Dorsal Radial Astrocyte Tract

The processes in this tract appear to arise from at least two different sources: from radial astrocytes in the lateral glial horns (Figs. 2.2, 2.3), and periodically, lighter

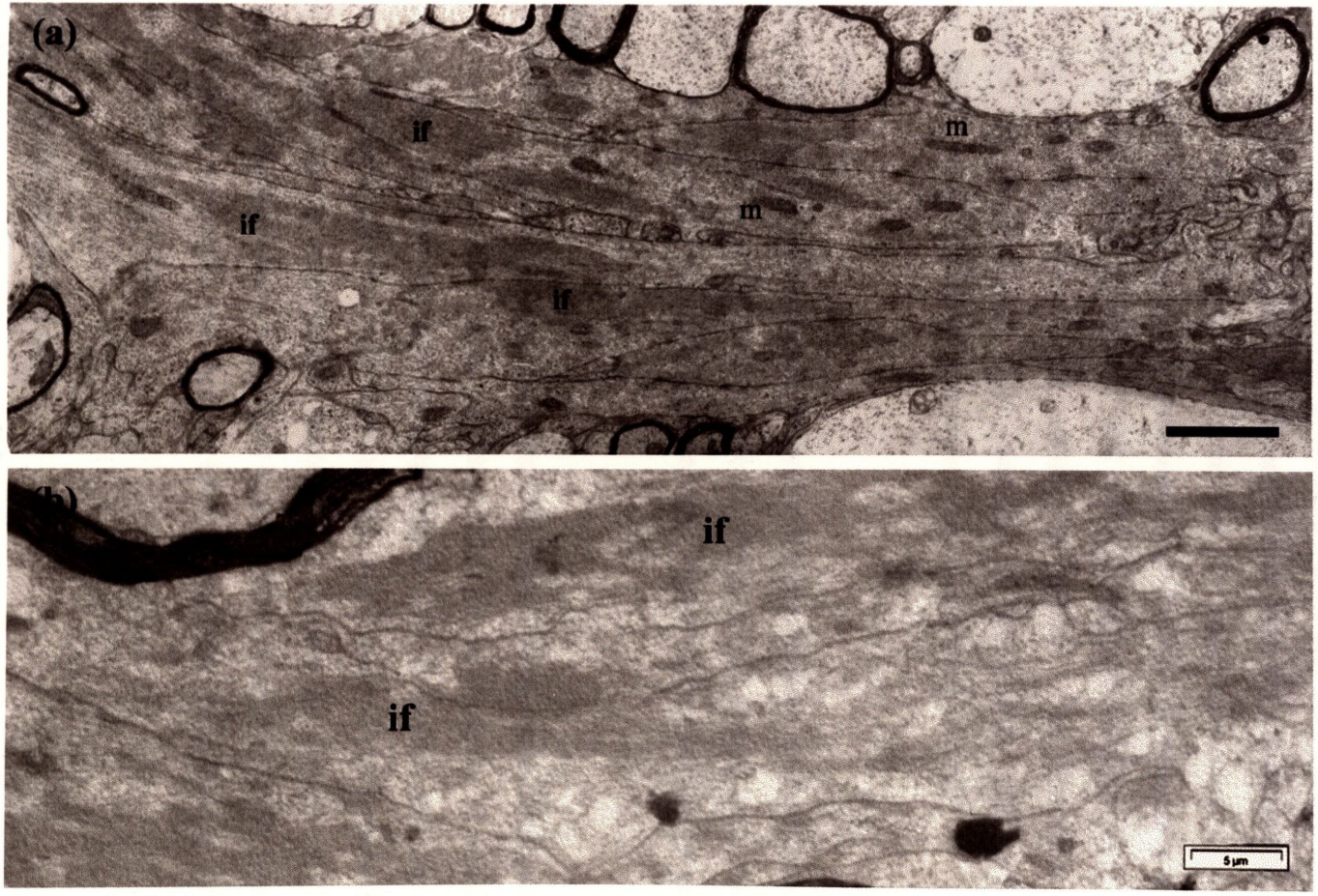


Figure 2.13a, b. Electron micrographs in transverse section of (a) the large and (b) the small radial glial processes. Note the complement of elongate mitochondria (m) and numerous bundles of intermediate filaments (if). In all cases the tracts are composed of numerous overlapping processes joined by junctional complexes, particularly in the large tracts. Scale bar = 10um.

staining processes from the light staining cells abutting the canal lumen (Fig. 2.14b, c).

The tract is composed of numerous (~10-15) short, ovoid to elongate processes in close apposition (Fig. 2.14d).

Along the periphery of the tract apposing the grey matter, processes are thinner and more elongate. The intensity of staining varies and they frequently contain small bundles of intermediate filaments, ribosomes and elongate mitochondria arrayed in the direction of the tract. All processes terminate in a large submeningeal region, which is compact and highly lamellar in structure (Fig. 2.14e). It possesses a homogenous staining pattern and occasionally cell bodies (oligodendrocytes and light staining astrocyte-type cells) are present within this region. The processes contain few organelles and, occasionally, small bundles of intermediate filaments are present. Desmosomal junctions between processes were occasionally found.

Other cell types

As part of this ultrastructural study several cell types, atypical of the normal ependymal and radial astrocytic complement, were identified in the spinal cord. Variants were found for oligodendrocytes and a light-staining astrocytic type cell in the grey matter.

Oligodendrocytes

Three different types of oligodendrocyte were found in the cord, dispersed throughout the grey and white matter. Each was identifiable by the intensity of staining and were classed as dark, medium or light staining (Fig. 2. 15). Both dark and medium staining types predominated and the light-staining type was found only occasionally, usually in close apposition to myelinated tracts. As shown in figures 2.11 and 2.12, oligodendrocytes are present in the grey matter where they intersperse between the cell bodies of radial astrocytes and form an intricate and extensive network of processes in the subependymal regions.

Light-staining astrocytic type cell

Cells that possess astrocytic type features are present in the regions surrounding the ependymal zone, the glial horns and the grey matter. In general these cells can be described as globular to elongate with occasional processes. The cell body stains

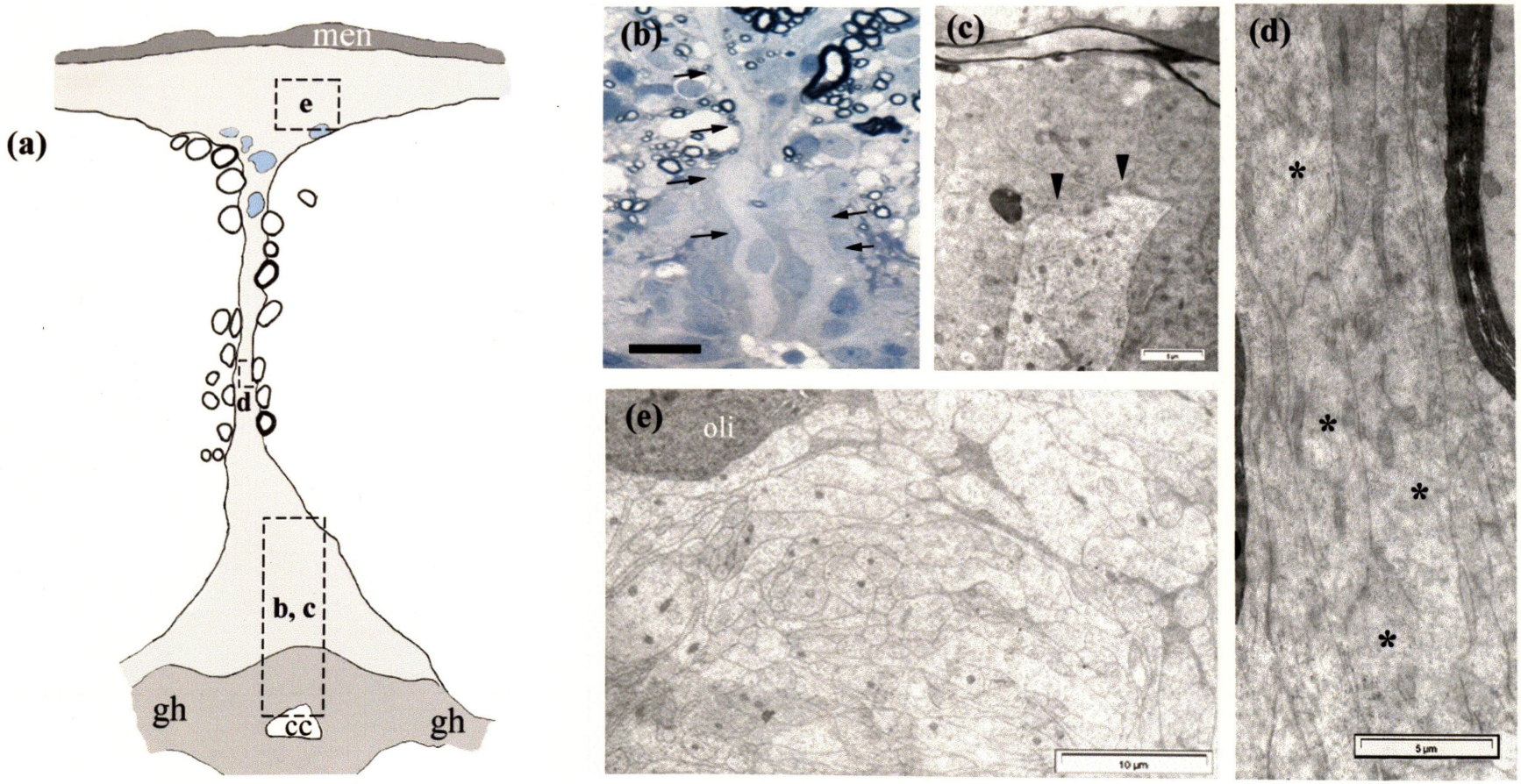


Figure 2.14 a, b , c, d, e. The dorsal glial tract. The diagrammatic representation in (a) illustrates its complex organisation. The tract contains the processes of the dorsal light-staining cells (arrowheads) surrounding the canal (b) and those of radial astrocytes. The processes of the dorsal light-staining cells however, are present intermittently (c; arrowheads). As can be seen in (d) the tract is composed of interlocking cellular processes (*) that terminate into a highly lamellar region (e) on dorsal surface. oli = oligodendrocyte, cc = central canal, men = meninges, gh = glial horns. Scale bar = 20 microns.

lightly while the nucleus stains slightly darker (Fig. 2.16). Small indentations in the irregularly shaped nucleus give a 'rough' outline and there is usually a single large indentation of the surrounding cytoplasm to produce a 'C' shaped nucleus. The cytoplasm appears 'watery' and contains few organelles. The cell membrane contains numerous indentations, indicating that these cells take their shape from the surrounding perikarya (Fig. 2.16a,b).

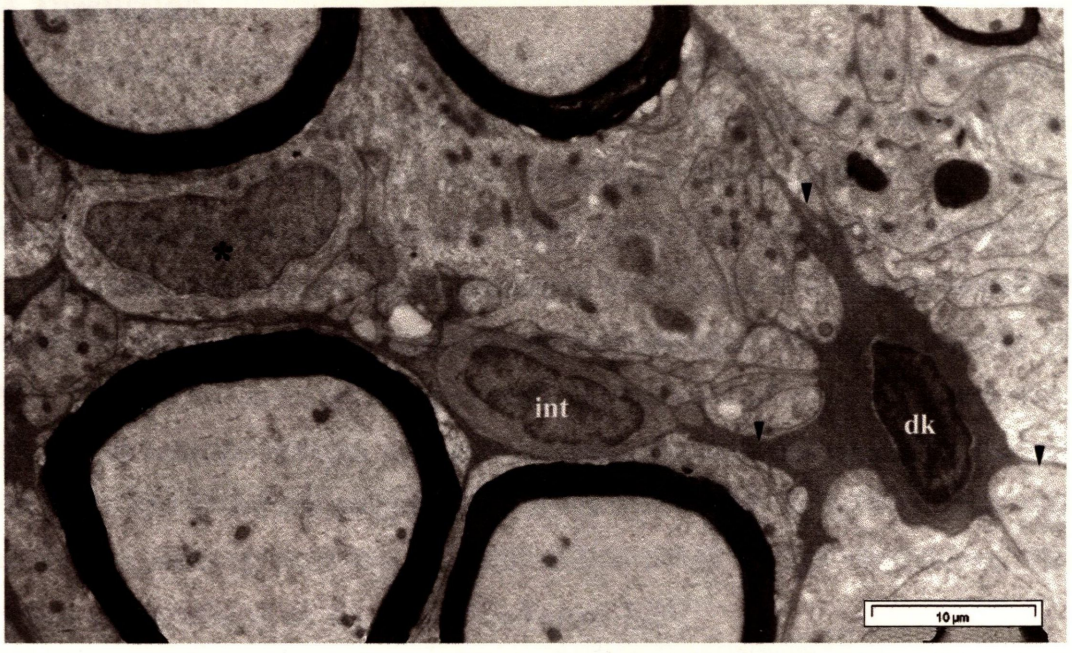


Figure 2.15. Electron micrograph of the different oligodendrocyte cell-types found in the eel cord seen here in the white matter region ventral to the central canal. Dark (dk) and intermediate (int) staining cells were the most common types found with occasional light staining types found, usually in close association to the myelinated tracts. In this figure a possible light-staining oligodendrocyte (*) is seen and numerous processes (arrowheads) extend from the dark staining oligodendrocyte.

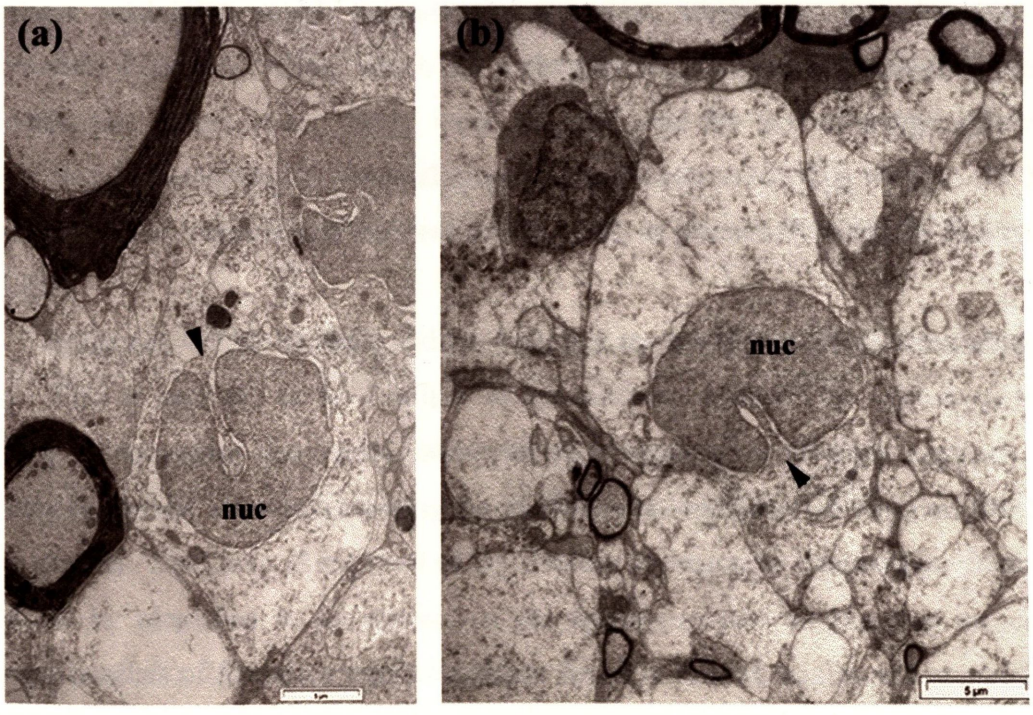


Figure 2.16. Electron micrographs of the light staining astrocytic-type cells in (a) interspersed between myelinated tracts ventral to the canal and (b) in the grey matter often in close proximity to blood vessels. Note the 'watery' cytoplasm, the light staining nucleus (nuc) with small aggregates of chromatin along the nuclear membrane and often with a cytoplasmic indentation producing a characteristic 'C' shape (arrowheads).

2.4 Discussion

The ependyma associated with the central canal has been found to be composed of the inner epithelial and the outer subependymal layers. The epithelial ependymal layer contains at least four different cell types, including columnar ependymocytes that are the most numerous cell type, tanycytes, which extend long cytoplasmic processes into the surrounding grey matter, liquor contacting neurons (LCN's) placed laterally and ventrally in the canal, and the light-staining tanycyte-type cells placed dorsally (Fig. 2.17). The second layer, the subependyma, is composed of rare ependymocyte-type cells and an intricate network of numerous processes arranged parallel to the canal. Most of the ependymal and subependymal layers were GFAP-ve, S-100+ve and weakly vimentin+ve, although some structures did label for GFAP+ve and vimentin+ve. These labelling characteristics are summarised in Figure 2.17.

Ependymocytes

Ependymocytes are common around the ventral and ventrolateral surfaces of the canal and display the cytoplasmic contents characteristic of this cell type; a densely populated cytoplasm containing rough endoplasmic reticulum, ribosomes, mitochondria and intermediate filaments. Cilia, which are a characteristic feature of ependymocytes in mammals (see Peters et al., 1991), were not seen, and the few cilia-type structures present could be attributed to the small population of liquor contacting neurons (LCN's) of the lateral and ventrolateral surfaces of the canal, as previously noted by Roberts et al. (1995).

In the eel, GFAP-labelling did not highlight the ependymocytes surrounding the canal. This is unlikely to be a failure of the antibody because the immunopositive labelling of tanycytes and radial astrocytes (discussed later) strongly suggests that labelling is specific to cells containing the gliofilaments composed of the glial fibrillary acidic protein. Similarly, at the level of the electron microscope, intermediate filaments could not be identified in the cytosol of the ependymocytes surrounding the canal, although bundles of filaments were commonly found in the cell bodies and processes of radial astrocytes. In other teleost fish, ependymocytes in the brain and spinal cord have been found to be GFAP+ve (Bodega et al., 1993; Anderson et al., 1984; Rubio et al., 1992; Cardone and Roots, 1990; Onteniente et al., 1983), and they have been reported as being GFAP+ve in other vertebrates such as the hagfish (Wicht et al., 1994), lamprey

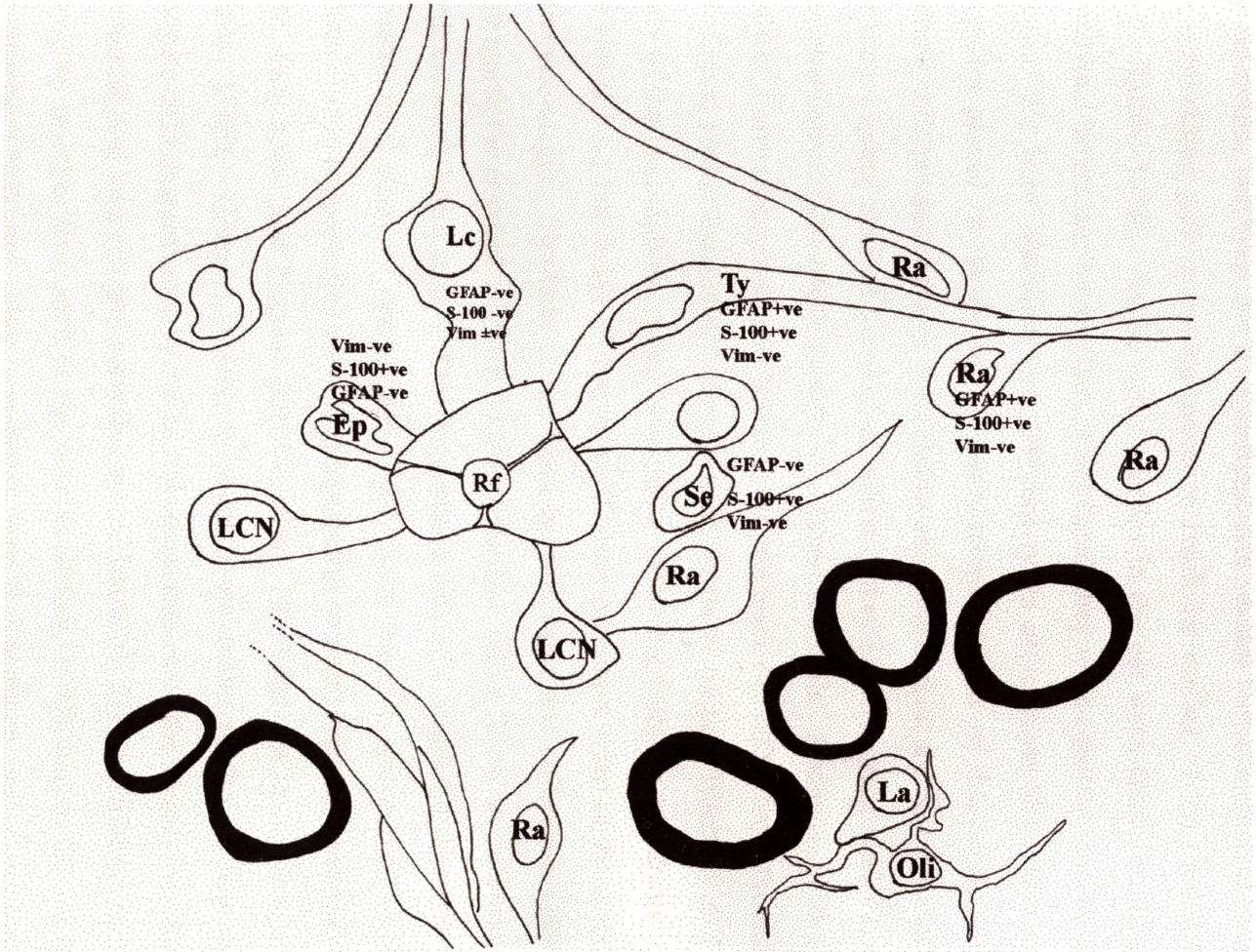


Figure 2.17. Diagrammatic representation of the different cell types surrounding the central canal in the eel spinal cord. The immunoreactivivty of each cell type to GFAP, S-100 and vimentin is also shown. Lc = light staining cell, Ep = ependymocyte, LCN = liquor contacting neuron, Ty = tanycyte, Ra = radial astrocyte, Se = subependymal cell, oli = oligodendrocyte and La = light astrocyte-like cell, Rf = Reissner's fibre, GFAP = glial fibrillary acidic protein, Vim = vimentin.

(Wasowicz et al., 1994), amphibians (Sasaki and Mannen, 1981; Miller and Liuzzi, 1986), see also Dahl et al. (1985) and Onteniente et al. (1983). Lazzari et al. (1997), in a study of two amphibian species, noted the presence of GFAP-labelling in the ependymal layer of *Ambystoma* spinal cord but its absence in *Triturus*.

Tanycyte-like cells

By definition, tanycytes are an ependymocyte variant that extend long processes into the surrounding grey and white matter to reach the surface of the cord (Peters et al., 1991; Rafols, 1986). As the radial profiles in the eel were shown to arise from the ependymal layers surrounding the central canal, they were considered to be of tanycytic origin. We have identified two different types of tanycyte-like cells: the 'normal' tanycytes placed in the dorso- or ventro-lateral regions of the canal, and the light staining cells present dorsally; both classes are not abundant and this matches a study of the rostral spinal cord of the sunfish, where Pokay (1993), using NADPH-diaphorase histochemistry to identify tanycytes, also found few cells. Anderson et al. (1984) in a study of *Carassius* spinal cord noted radial processes extending from the dark staining ependymal region but did not identify their points of origin. Wicht et al. (1994) in a study of the hagfish brain noted radial fibres extending from the ependymal region into the spinal cord but failed to determine if these processes were of tanycytic or radial astrocytic origin. Similarly in the lamprey, Wasowicz and colleagues (1994) did not distinguish the point of origin of what were termed 'radial fibres' in the brain and spinal cord, although Lurie et al. (1994) suggested a tanycytic origin for these fibres and the ultrastructural study of normal and regenerating lamprey spinal cord by Wood and Cohen (1981) supports this view. In amphibians, this cell type has been documented in both *Ambystoma* and *Triturus* (Lazzari et al., 1997) but not in the frog (Miller and Liuzzi, 1986). Ultrastructurally, tanycytes were found in the present study to be elongate cells characterised by apical and somal regions in the ependymal layer abutting the lumen, and long tail processes that extend laterally. Cilia have been reported for the tanycytes in other fish, such as the sunfish (Pokay, 1993), and in the rat (Rafols and Goshgarin, 1985) and other vertebrates (see Reichenbach and Robinson, 1995 for review), but they were not found in the present study.

Although there have been few studies in anamniotes of the glia in the spinal cord, structures in the brain have been more extensively studied. In the goldfish optic tectum (Cardone and Roots, 1991), the radial glial structure arises from the ependymal

and subependymal layers surrounding the ventricles. Onteniente et al. (1983) also noted an ependymal origin for GFAP+ve fibres from around the ventricles of the carp, while in the hagfish only a few tanycytic processes are labelled (Wicht et al., 1994). In an extensive study of the sunfish, Pokay (1993) noted tanycytes radiating from the ependymal layers surrounding the ventricles.

In reptiles, two populations of GFAP+ve cells are present in the adult brain (Monzon-Mayor, 1990; Yanes et al., 1990): astrocytes, typical of mammalian CNS, and radial glia which are strongly suggestive of tanycyte cells. In both studies, the transition of the intermediate filament protein structure in glial cells from GFAP-ve and vimentin+ve during development to GFAP+ve and vimentin-ve is indicative of glial cell maturation. In mammals, too, the labelling of tanycytes and astrocytes as GFAP+ve and vimentin-ve is commonly understood to indicate mature glial cells (Rafols 1986). In the present study we also find a similar labelling pattern in the tanycyte cells present around the canal (with the exception of the light staining cells). Therefore it is probable that the GFAP+ve and vimentin-ve tanycytic population surrounding the dorso-lateral and ventro-lateral surfaces of the canal in the eel are mature glial cells.

The dorsal light staining glia, noted previously by Roberts et al. (1995), labelled GFAP-ve and weakly vimentin+ve in the present study. More dorsally, labelling increases for both antibodies in the large glial tract but it proved impossible to determine if this cell type or the processes arising from the glial horns expressed these intermediate filaments.

The light staining population of cells in the eel have not been documented in any other study, although specialised cells have been found in many instances. In a study of the newt, *Triturus,* Schonbach (1969) noted the presence of a common light staining cell and a rarer dark staining cell in the ependyma that both extended processes to the surface of the spinal cord. Bodega et al. (1993) in an immunohistochemical study of the adult toad noted three different labelling patterns in the ependymal layer of the spinal cord, indicating the presence of at least three different cell types. Tennyson and Pappas (1964) in a study of the rabbit CNS identified three different forms of ependymal cell - normal ependymocytes, tanycytes and an ependymal cell they termed 'ependymal astrocyte' that extended a long cellular process that terminated in grey and white matter. In the mammalian third ventricle two different types of tanycyte, termed the α and β

tanycyte, have been identified by morphological criteria (Rodriguez et al., 1979; Rafols, 1986).

Other studies in anamniotes (e.g. Lazzari et al., 1997; Cardone and Roots, 1990; Pokay, 1993) and amniotes (de Vitry et al., 1981; Card and Rafols, 1978), labelled tanycytes that have been traced to the pial surface, but in the eel we could not trace the GFAP+ve or S-100+ve cytoplasmic processes of the tanycyte cells further than the large densely labelling radial glial structures placed laterally. However, we assume that these processes do reach the pial surface, probably ventro-laterally as part of the large glial tracts. This view is supported by the observation that tanycytes generally terminate as small endfeet directly on blood vessels or, more commonly, at the pial surface, where they form the glia limitans and are easily identified morphologically (Millhouse, 1972 quoted from Peters et al., 1991). In the eel, the few blood vessels present in the ventral part of the cord were frequently surrounded by *en passant* contacts of descending glial tracts; endfeet, however, were rarely found, suggesting that all processes terminate at the pial surface.

The Subependyma

In the eel, the subependyma is composed of ependymocyte-like cells and a thick network of long thin processes. Interspersed between these structures are the cell bodies and processes of the LCN's and tanycytes placed laterally and ventrally, while dorsally the cell soma and cellular projections of the light-staining cells also extend into this layer. On comparing our work with studies in other anamniote species we have found few reports that make reference to the structure of the subependymal layer and of those that do, they fail to describe the structures in any great detail. For example, Kruger and Maxwell (1967) in a combined study of teleost and reptile brain and spinal cord noted a thick subependymal region and a layer within this structure consisting of tightly packed nuclei. However, this description was made in general for all of the animals studied and failed to note the regions of the CNS where these cells were found. Similarly, Sarnat et al. (1975) in a representative histochemical study of vertebrate spinal cord, observed a subependymal region in shark, fish and lizard, but the ultrastructure of this region was not described. However the ultrastructure in mammals has been documented (Peters et al., 1991) and is similar to that in the eel. The organisation of astrocytic and oligodendrocytic processes into a large network in the present study is also found in the mammalian subependyma (Privat and LeBlond,

1972). Astrocytes are common to both, but in the eel the astrocytic (radial) soma are situated outside the subependymal layer whereas in the mammal this cell type forms an integral part of the subependymal layer.

A population of cells, termed subependymal cells, is found in the subependyma of the rat (Privat and Leblond, 1972). These cells are rare and little is known of their distribution (if any) in the spinal cord, although they can be up to 5 layers thick in some regions of the brain close to the corpus callosum (Privat and Leblond, 1972). Subependymal cells are smaller than the ependymocytes lining the ventricle and possess a darker staining nucleus. The discovery of cells in the present study that appear to be smaller in size to normal ependymal cells and of similar staining intensity may suggest the presence of a unique subependymal cell surrounding the central canal. Kruger and Maxwell (1967) also noted this difficulty in identifying subependymal cells because many are ultrastructurally similar to ependymocytes of the ependymal layers. In the teleost brain, however, subependymal cells have been identified, such as in the central posterior/prepacemaker nucleus (Zupanc and Zupanc, 1992). In mammals, a subependymal region, the subventricular zone, is identifiable in many areas of the brain (Peretto et al., 1999) and contains at least three different cell types (Doetsch et al., 1997), but it has been shown that this region is absent from many portions of the CNS, including the spinal cord (Momma et al., 2000). However, multipotent stem cells can be harvested from the spinal cord (Weiss et al., 1996a) which suggests that a specialised stem cell may reside within the ependymal layers (Johansson et al., 1999). Whether or not specialised subependymal cells are present in the spinal cord of teleost fish, with possible stem cell activity, still remains unclear, but the present *in vivo* results, and those of Kruger and Maxwell, (1967), may point to the possible presence of such a cell type. *In vitro* culturing of ependymal and subependymal cells aimed at identifying different sub-types, including possible stem cells, a common practice in mammalian research (e.g. Temple and Alvarez-Buylla, 1999), has, as yet, to be investigated in fishes.

Radial Astrocytes

It used to be thought that the glial structure of the anamniote spinal cord was similar to that of the brain and involved only one cell type, the tanycyte (see Roots, 1986 for review); however in recent times it has been shown that there are other cell types, most notably the radial astrocyte. The nomenclature for this cell type is diverse, although the

term radial astrocyte is the most commonly used (Lazzari et al., 1997). It is typified by a cell body in the grey matter displaced from the ependymal region and extending long cellular processes to the surface of the cord (Bodega et al., 1990). The presence of GFAP filaments in its cytosol, particularly in the cellular processes, is a common characteristic in all anamniote vertebrates (Roots, 1986; Bodega et al., 1994).

The structure of the four main glial tracts (dorsal, ventral and ventro-lateral) in the eel cord, comprising the long cellular processes of radial astrocytes, parallels reports of radial astrocytes in other anamniotes (e.g. Sasaki and Mannen, 1981). The GFAP+ve labelling found in these tracts in the present study matches those other GFAP studies of teleost fish - the barbel (Bodega et al., 1993), goldfish (Nona et al., 1995) and the black ghost knifefish (Anderson et al., 1984). In the lamprey spinal cord, however, radial astrocytes seem to be absent and tanyctes predominate (Wood and Cohen, 1981; Lurie et al., 1994). In amphibia, radial astrocytes have been described in the frog (Miller and Liuzzi, 1986), toad (Bodega et al., 1990) and newt (Lazzari et al., 1997).

Radial astrocytes appear to be limited to the spinal cord and are absent from the brain, although the Bergmann glia of the cerebellum are considered to be specialised astrocytes (Roots 1986; Dahl et al., 1985). Instead, in the brain the predominant glial type appears to be the tanycyte, with processes extending to the periphery from soma located in the ependymal and sub-ependymal layers. Occasionally, however, structures resembling radial astrocytes are found in portions of the brain displaced from the parent population at the ventricular surface. Pokay (1993) noted the presence of 'extra-ependymal' cells suggestive of a small radial astrocyte population in a study of the sunfish brain. Interestingly, the labelling of the glial structure in the hagfish brain for GFAP was considered by Wicht et al. (1994) to be similar to the astrocytes of mammals.

The visual system has also been extensively studied in anamniotes as a result of the considerable regenerative ability displayed by this region following injury (e.g. Nona et al., 1992, Blaugrund et al., 1993). The optic tectum and tract contain tanycytes and longitudinally orientated glial processes that label GFAP+ve, although the uninjured optic nerve fails to label for this protein (Nona et al., 1989). Cohen et al. (1993), in a similar study, but using cloned GFAP specific to carp CNS, labelled astrocytic profiles in the optic tract of the goldfish but did so at low levels. Rungger-Brandle et al. (1989) in a study of *Xenopus* demonstrated the presence of cytokeratins in the optic nerve and determined that this group of intermediate filaments constituted the

main glial intermediate filament protein. Levine (1989) characterised the astrocytic population in the optic nerve as a dense meshwork of processes through which optic fibres traversed. He called these 'reticular astrocytes' and later these were considered specialised glial cells (Maggs and Scholes, 1990). Since the optic nerve, brain and spinal cord possess different types of glial cells - reticular astrocytes, tanycytes and radial astrocytes respectively - it appears that each cell type is specific to a particular region of the CNS. In the case of fish spinal cord, this is the radial astrocyte. No comparative study that we are aware of has been completed in the same animal for these different cells, but such studies could help us to understand further the unique, and somewhat diverse glial structures that are present in anamniotes and shed light upon the surprising regenerative ability of the CNS.

The glial pathways

In the present study the radial astrocytic and tanycytic tracts in the cord comprised numerous cellular processes joined together periodically by junctional complexes. Each process contained abundant intermediate filament bundles presumably composed of GFAP, and numerous elongate mitochondria aligned on the long axis of the tracts. A distinction between the radial and tanycytic processes could not be made and all processes, including the smaller radiating processes in the dorsal, dorso-lateral and ventro-lateral regions of the cord, were similar in structure and cytoplasmic content. GFAP bundles are common in the radial astrocytes of other teleost fish (e.g. Bodega et al., 1993; Anderson et al., 1984). The structure of the cellular processes observed in the present study is similar to that reported for the processes of tanycytes present in the mammalian CNS (Flament-Durand, 1985; Rafols, 1986). However, unlike mammalian tanycytes where there is little side branching from the cytoplasmic processes, in the eel and other anamniotes radial glial processes frequently produce small thin GFAP+ve branches that extend into the surrounding perikarya and are interspersed between axonal bundles producing a loose mesh-like structure (the present study; Bodega et al., 1993).

Glial organisation in the spinal cord

The present study has shown that the glial elements in the spinal cord are arranged as longitudinal sheets. This interpretation is supported ultrastructurally by the presence of interlaced radial elements in the four large tracts joined together by junctional complexes. Using spinal cord labelled for GFAP+ve and S-100+ve, and cut in three

different planes of section (transversely, horizontal and saggital), the radial glial processes have been seen to extend from the cell bodies close to the canal, to produce continuous longitudinal sheets of glial processes. Although not shown, the structures of the smaller tracts also appear to be organised in the same longitudinal fashion producing smaller sheets further sub-dividing the spinal cord into distinct compartments. A similar structure has been noted in the lamprey spinal cord from ultrastructural (Wood and Cohen, 1981) and immunohistochemical analysis (Lurie et al., 1994); however, in this animal the cord is primarily composed of tanycytic processes linked together by desmosomes. Where the tanycytic processes are linked side-by-side in the lamprey, in the eel processes appear to overlap in the ventral and ventrolateral large glial tracts demonstrated by the irregular sizes of the processes in any one region.

Dorsally the glial structure is complex as it is composed of numerous projections from the light staining cells and smaller profiles from the lateral glial horns. The short structure of the processes suggests a much higher overlap rate compared to the other glial tracts producing a complex lacework pattern characterised by small ovoid to elongate processes. The smaller radial tracts in the other regions of the cord also possess an overlapping structure joined by junctional complexes, but they usually occur as a single process in the white matter close to the pial surface.

In the extensively studied optic nerve, the reticular astrocytes are arranged transversely as projecting fibres that merge periodically to produce a 3-dimensional structure. Astrocytes are evenly spaced 15μm apart to produce this structure, whereas in the spinal cord these processes are contiguous (present study, Wood and Cohen, 1981). The loose organisation of the astrocytes forms a zigzag pattern in the optic nerve that enhances structural integrity and flexibility (Maggs and Scholes, 1990; see Scholes, 1991 for review). The absence of such intricate three-dimensional radial architecture in the spinal cord is presumably because the vertebral column provides both mechanical and protective support and, therefore, an intrinsic tensile organisation would be redundant. Since the optic nerve lacks a protective bone covering, Maggs and Scholes (1991) suggest that this specialisation of the glial structure is necessary to confer stability and support.

The organisation of glia into repeating structural units is also found in mammals. For example, in the rat fimbria, the macroglial framework is organised as repeating units of oligodendrocytes and solitary astrocytes which produce a continuous network

of processes that develops from the radial glial framework (Suzuki and Raisman, 1992, 1994).

The glial framework in the present study appears to be composed primarily of tanycyte and radial astrocyte processes with no apparent interplay of oligodendrocytes, although cellular profiles do play an integral part in the organisation of the subependymal layer. The interplay of astrocytes and oligodendrocytes suggested by the structure of the rat fimbria may occur between the radial processes in the eel, as we have frequently found side projections from the radial tracts that are often closely apposed to oligodendrocytes and their processes. This, therefore, may suggest a secondary macroglial structure in the spinal cord of the eel.

Summary of main findings

- The spinal cord contains an ependymal and glial organisation that is arranged around the central canal region and associated areas.
- A heterogeneous cell population surrounds the central canal and comprises:

  Ependymocytes, which are GFAP-ve, S-100+ve and vimentin-ve

  Tanycytes, which are GFAP+ve, S-100+ve and vimentin-ve

  LCN's (see also chapter 6), which are GFAP-ve, S-100-ve and vimentin-ve

  Dorsal light staining cells, which are GFAP-ve, S-100-ve and weakly vimentin+ve
- The subependymal region is composed of the processess of dark oligodendrocytes and radial astrocytes. Included in this region are possible subependymal cells.
- Radial astrocytes reside in two regions, one on each side of the central canal, which we have termed the glial horns. The cell bodies of these GFAP+ve, S-100+ve but vimentin-ve cells reside here and extend long cell processes to the cord periphery.
- The interweaving long cell processess of radial astrocytes and tanycytes compartmentalise the spinal cord.
- Three different oligodendrocyte cell types have been identified; light, medium and dark staining cells.
- We have found GFAP+ve, S-100+ve cellular profiles and a light-staining cell-type in the grey and white matter, which may indicate another astrocyte-type cell in the eel spinal cord.

Chapter 3

The meninges of the uninjured brain and spinal cord

3.1. Introduction

Many aspects of anamniote CNS structure have been well described (e.g. Smeets et al., 1993; Butler and Hodos, 1996), but surprisingly little is known of the meningeal organisation surrounding the brain and spinal cord, which contrasts to the well characterised meninges of mammals (Peters et al., 1991; Haines, 1991).

Sterzi (1901; 1902) first reported on the meninges of anamniotes as part of a comprehensive study of vertebrate meningeal structure. He described this tissue in aquatic anamniotes as developing embryologically from mesoderm to form a single layer which he termed the *meninx primitiva* (Fig 3.1a), while he thought that those anamniotes that evolved for a more terrestrial form of living, such as amphibians and reptiles, possessed a two layered structure.

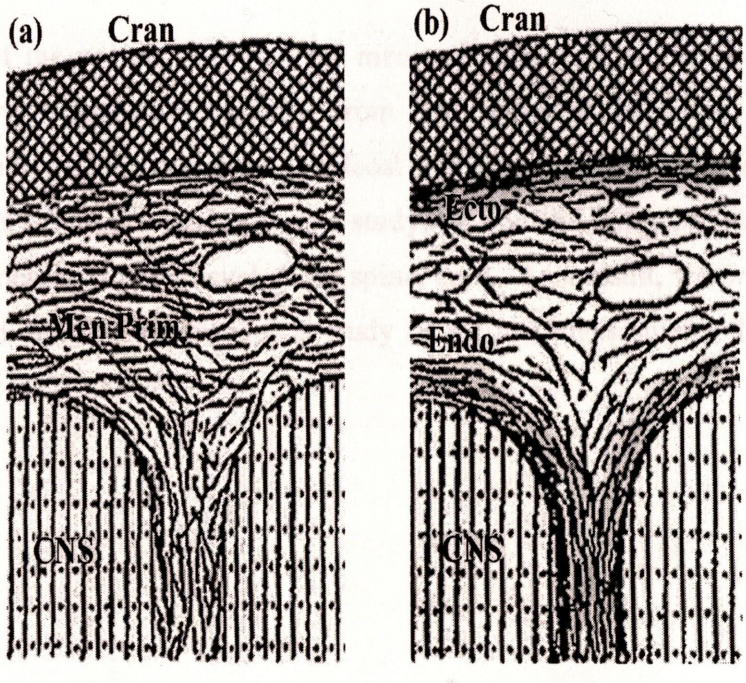


Figure 3.1a, b. Graphical representations of the development of the meninges in teleost fish according to (a) Sterzi (1901; 1902) and (b) Van Gelderen (1926). Both authors considered that the meninges arise from the perineural mesenchyme (PNM) during ontogenesis. Cran = cranium, endo = endomeninx, ecto = ectomeninx, CNS = central nervous system, Men prim = meninx primitiva. Modified from Van Gelderen, 1926.

In a later study, Van Gelderen (1926) using larvae of the European angler fish, *Lophius piscatorius,* proposed that the meninges of fish divided from a single layer during development into two separate layers which he termed the endomeninx (analogous to the meninx primitiva), covering the CNS, and an ectomeninx in close apposition to the endocranium (Fig. 3.1b).

Today, many textbooks of vertebrate anatomy describe the meninges of fish as being a single layer, the meninx or meninx primitiva (e.g. Andrew and Hickman, 1974; Hildebrand, 1995). However, it is evident from the few detailed light and electron microscopical studies, that the meninges possess a more intricate cellular organisation. Detailed electron microscopic studies of the meninx primitiva/endomeninx (and hereafter termed the endomeninx) in the lamprey (Rovainen et al., 1971; Nakao, 1979), goldfish (Momose et al., 1988; Caruncho et al., 1993; Wang et al., 1995) and trout (Schwarz et al., 1993) have shown that the meninges can be subdivided into distinct layers.

As part of the present study of the meninges surrounding the cord following transection injury it became apparent from an extensive literature search that ultrastructural studies of the meninges in teleost fish at the level of the spinal cord are lacking. In terms of anamniotes, only one study, that on the lamprey (Nakao, 1979), has detailed the meninges at the level of the spinal cord. As a result, we present here, a detailed light and electron microscopical study of the meninges surrounding both the brain and spinal cord of the eel.

3.2 Materials and Methods

This study is based on 5 European eels *Anguilla anguilla L.* in a non migratory immature stage of their lifecycle. Four different regions were used to examine the meningeal structure; at the level of the brain three areas were selected, the cerebellum, medulla oblongata and the adjacent rostral spinal cord while in the cord proper, tissue at the level of the anus was selected.

Histological Investigation

For histological investigation, each animal was treated according to the methodology described in the methods section in chapter 2. In brief, each animal was anaesthetised initially by immersion in 0.3mg/l MS-222 and further by a subcutaneous injection of 0.3ml alphaxalone (Saffan). To prevent blood clotting 0.2 ml heparin sodium (Leo Laboratories) was also given subcutaneously. The perfusion procedure consisted of a primary flush of Ringer's solution (with 0.1% procaine for added anaesthesia) through the heart followed by the fixative, 2% paraformaldehyde and 1.25% gluteraldehyde in 0.1M phosphate buffer (PB), pH adjusted to 7.4. Following perfusion, portions of the brain and spinal cord were immediately dissected from the spinal column and post-fixed in the same fixative at 4^0C for a maximum of 3 hours.

Electron Microscopy

The tissue was processed for electron microscopy according to the procedure described in chapter 2. Sections were cut for both light (1.5μm) and electron microscopy (500Å). All images were downloaded, analysed and formatted on a Macintosh G3 computer using Adobe PhotoShop 5.

3.3. Results

The meninges were examined in four regions of the CNS: the cerebellum, the medulla oblongata, the adjacent rostral spinal cord, and the spinal cord near to the anus. The meninges of the caudal spinal cord will be described separately.

The Endomeninx

At the level of the rostral spinal cord (approximately in the region of vertebrae 8-12) the endomeningeal layer abutting the CNS is evident as a thin band. Melanocytes are present, denoted by a dark staining band on the surface of the endomeninx; large blood vessels are found on all surfaces. At this level and the medulla oblongata, the endomeningeal layer appears as two bands that are strongly contrasted: an outer light-staining layer, and an inner dark staining layer (Fig. 3.2 c, d). Melanocytes are sparse in this region. The cerebellum also contains these two sharply contrasted layers and another lighter staining layer close to the glia limitans, particularly on the lateral surfaces; therefore at this level the meninges contain a light-dark-light staining pattern (Fig. 3.4).

Numerous blood vessels are present in the meninges at all three locations. On the rostral cord, blood vessels permeate the meningeal structure and can occur in large numbers (Fig. 3.2b), while on the lateral sides of the cord large blood vessels appear to be free from the meninges (Fig. 3.2a). At the level of the medulla, blood vessels are present in the meninges (Fig. 3.3) and in the perimeningeal fluid (PMF). Frequently these large vessels in the PMF appear to possess an outer layer of melanocytes. Blood vessels often permeate the barrier of the cerebellar meninges and the *glia limitans*. Here blood vessels are usually located within the meninges, interspersed between the inner, middle or outer layers, while vessels (capillaries) are rarely found on the outer surface of the meninges save for the large vessels in the PMF.

The Ectomeninx

An additional meningeal layer independent of the endomeninx is found closely apposed to the endocranium covering the brain and the vertebral arches overlying the rostral spinal cord. It is tightly apposed to the surfaces of the arches and is difficult to remove.

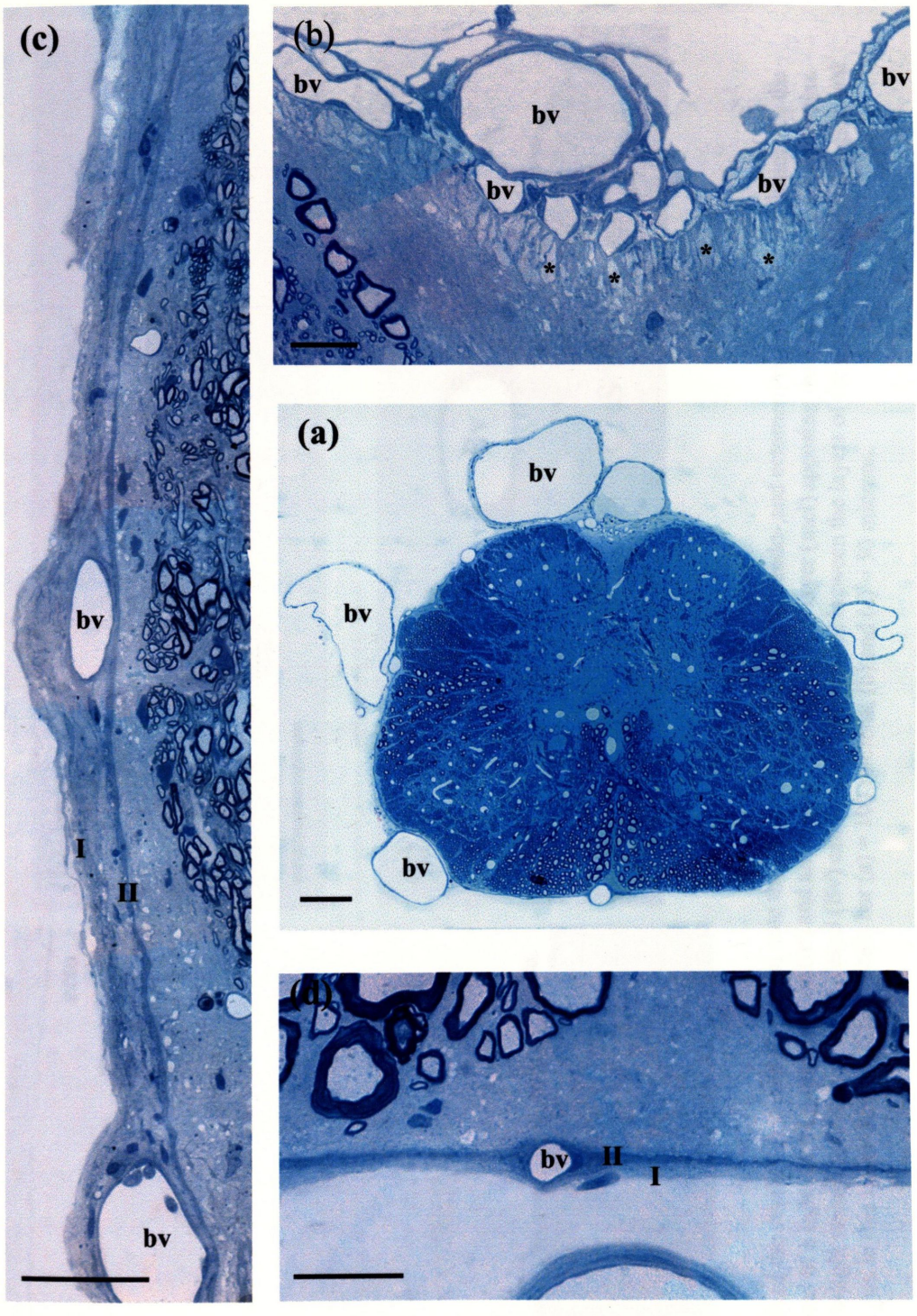


Figure 3.2a, b, c, d. Photomicrographs of toludine blue stained sections of the rostral spinal cord illustrating the endomeninx on the dorsal (b), lateral (c) and (d) ventral surfaces. Note the similar thickness of this layer on all surfaces. On the dorsal surface a plexus of blood vessels (bv) and extracellular spaces (*) are evident while more laterally (c) and ventrally (d) blood vessels permeate this layer. A subdivision of the meningeal layer can be seen ventrally with vessels are also present. On the lateral and ventral surfaces two layers are present, a light staining outer layer (I) and an inner darker staining layer (II). Scale bar (a) = 100 microns, (b), (c), (d) = 20 microns.

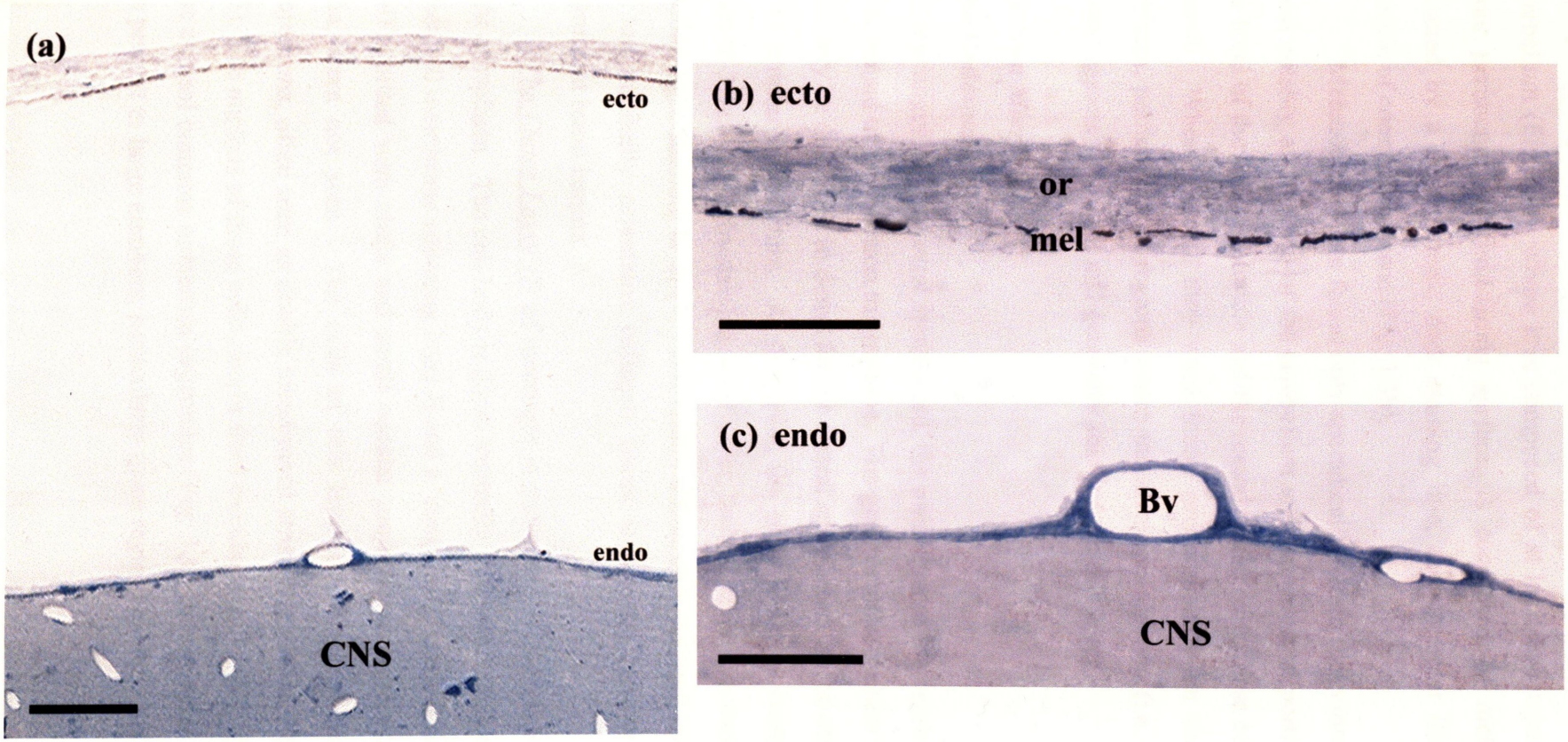


Figure 3.3. Photomicrograph of the cerebellar meninges. In (a) note the comparable thickness of the endo- and ectomeninx. At higher resolution (b) the ectomeninx (ecto) is composed of a light staining outer region (or) and an inner darker melanocyte layer (mel) apposing the PMF. In (c) the endomeninx (endo) comprises a light-dark-light staining pattern. A blood vessel (Bv) can be seen interspersed between the layers of the outer light staining region and note the absence of melanocytes in this layer. Brain = CNS. Scale bar (a) = 100 microns, (b) and (c) = 50 microns.

At the level of the rostral spinal cord this ectomeninx can be seen just as a thin line of lightly-staining connective tissue while it is much more pronounced overlying the cerebellum (Fig.3.2a), where it is composed of at least two layers. The first, on the inner perimeningeal fluid-facing surface, is composed of melanocytes which are denoted by a characteristic dark staining line, and an outer (thicker) light staining portion of connective tissue (Fig. 3.3b).

Melanocytes were found only sporadically within the ectomeninx, being present most notably at the level of the cerebellum and more rostral portions of the brain. At the level of the fourth ventricle and the rostral spinal cord, these cells are few and often absent. When present, they were found predominantly on the lateral and dorsal surfaces, particularly in regions where the meninges thicken (i.e. the lateral surfaces). Blood vessels are scarce and generally absent from this layer.

Electron Microscopy

The Endomeninx

The meninges of the rostral spinal cord, the medulla and the cerebellum were surveyed with the aid of the electron microscope. The general ultrastructure of the endomeninges will only be described in detail for the rostral spinal cord, as the other areas were found to be similar in structure. At this level, the endomeninx is composed of four layers (Figure 3.4a,b): a light-staining outer layer, termed layer I; a dark-staining layer (II); another light-staining layer (III) and finally a thin, dark-staining layer (IV). A thin band of longitudinally orientated collagen fibres is present between layer IV and the prominent basal lamina.

The Outer Layer (I) of meninges is composed of cells that possess an electron light cytoplasm. The cell body is dorso-ventrally flattened and elongate, with a smooth inner cell membrane apposing layer II and a 'rough' outer membrane (connecting to the PMF), pitted with clefts and small cellular projections; surface appendages, such as cilia, were not seen. The cells of this layer interdigitate via finger-like cellular projections, often seen as double membraned structures within the cytoplasm (see Fig. 3.5). The nucleus of these cells ranges from circular/ovoid to slightly elongate in shape. The cytosol contains numerous organelles (Fig. 3.5), in particular mitochondria, which are present in large numbers, particularly those regions close to the nucleus.

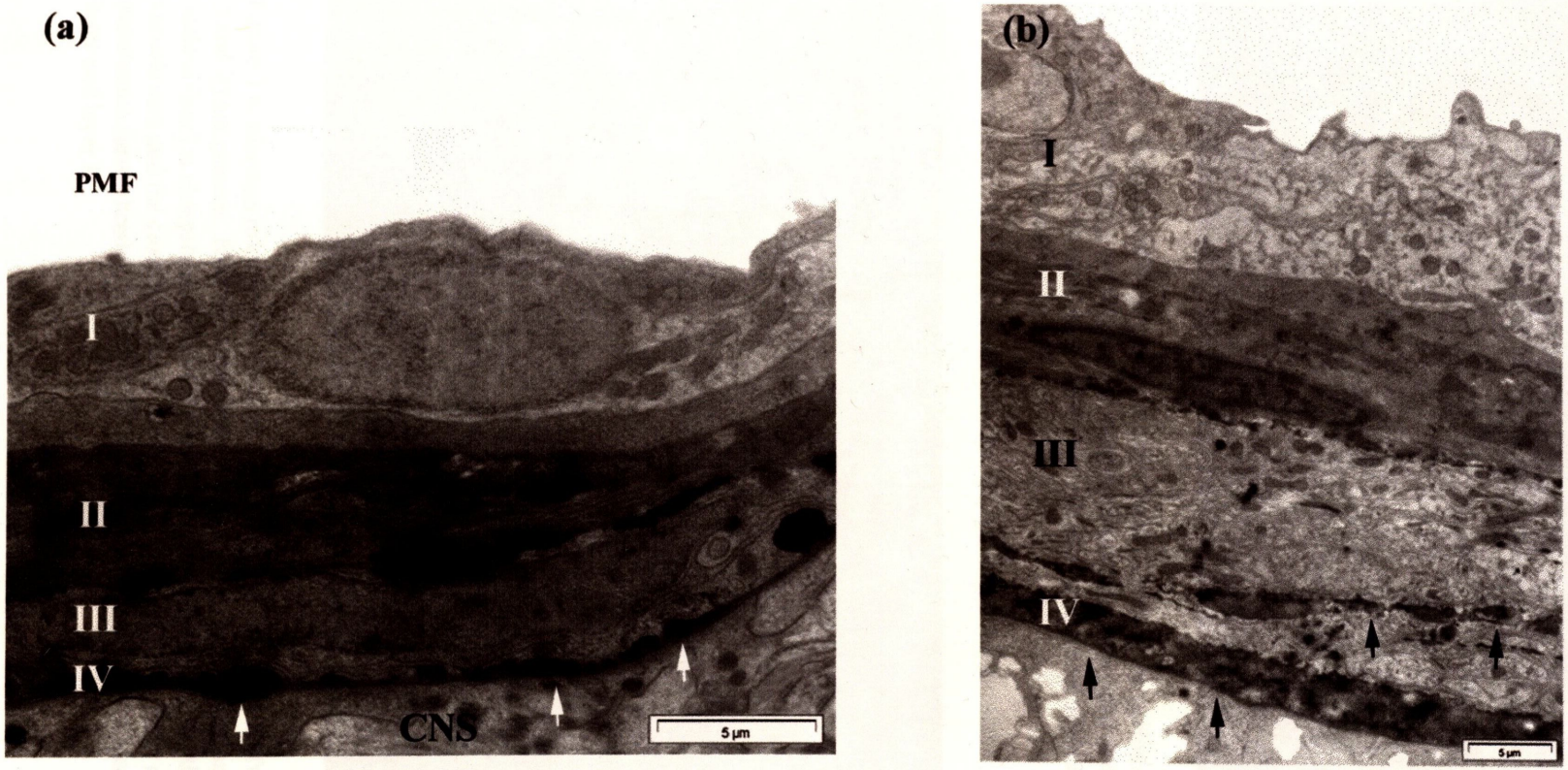


Figure 3.4a, b. Electron micrographs of the endomeninx covering the rostral spinal cord. In (a) the endomeninx present on the dorsal surface; note the the thin appearance of the layer III compared to the lateral surface. (b) Note the presence of abundant electron dense collagen in layer IV which appears as dark bands (arrowheads); no cells are present in this layer. In (b) note the presence of all four layers.

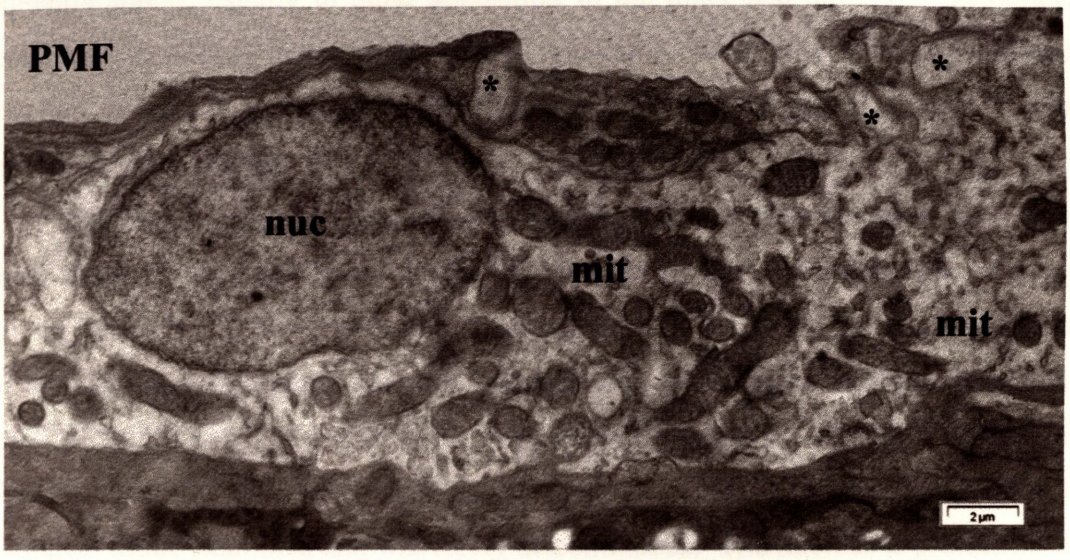


Figure 3.5. Electron micrograph of the outer layer I abutting the perimeningeal fluid (PMF). Note the light staining cytoplasm with numerous mitochondria (mit) and vacuoles, often in close apposition to the outer membrane (*). The generally ovoid nucleus (nuc) is light staining with dispersed chromatin.

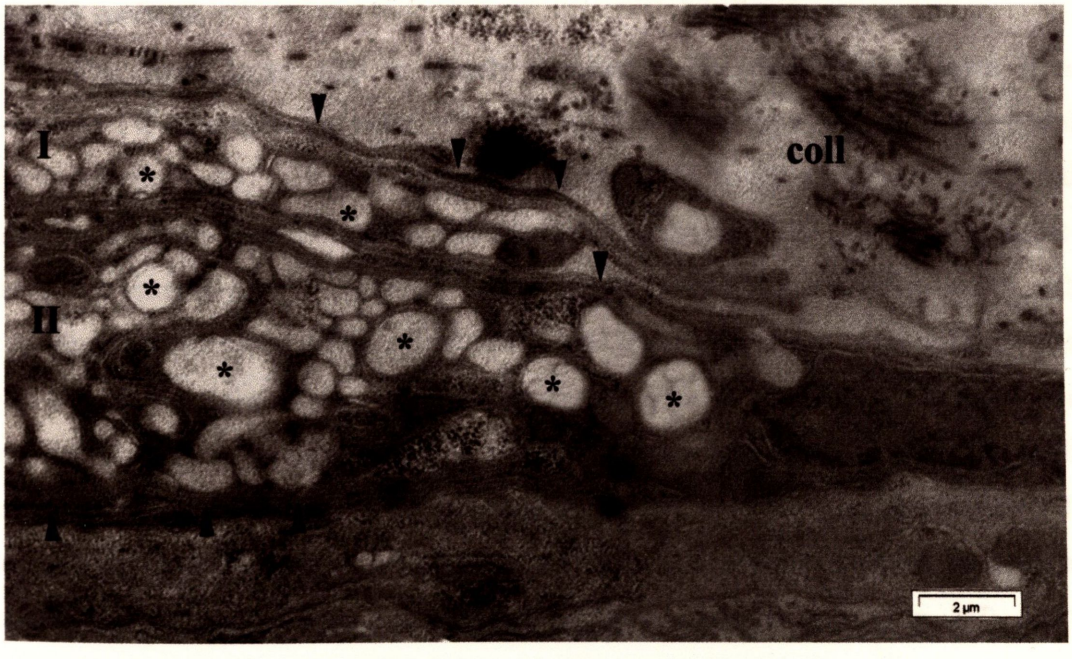


Figure 3.6. Electron micrograph montage of the dark staining layer II. Two overlapping cells (I and II) are present. Note the abundance of vacuoles (*) in the electron dense cytoplasm. The nucleus (nuc) is elongate and of similar density to the cytoplasm. Note the heterogeneity in vacuole size and the close position of many of the vacuoles to the inner and outer cell membranes (arrowheads). Collagen fibrils (coll) lay scattered in the space between the this layer and layer I.

These are usually ellipsoid to elongate with well-defined cristae. Vesicles are frequently found, usually in close apposition to the inner and outer cell membranes. Another organelle of note is the Golgi apparatus, while the rough endoplasmic reticulum is sparse and when present, occurs as single or paired strands in close association to the nucleus.

The Second Layer (II) comprises a thin band of 1-3 electron dense cells (much denser than the adjacent layers I and III); the nuclei and cytoplasm are of similar staining intensity and the latter is rich in organelles (Fig. 3.6). The cell body is elongate and cellular inter-digitations interlock adjacent cells at the apical surfaces where they meet. Cell-cell junctions are frequent, are composed primarily of tight junctions, and usually occur between these interlocking surfaces. This layer was present in all meningeal tissue examined and was rarely discontinuous. The nucleus is prominent and the shape is thin and elongate (very similar to the nuclei of spinal fibroblasts), with a slightly greater intensity of staining compared to the cytoplasm. Characteristic of this layer, the cytoplasm contains a large number of vacuole-like structures of differing size which are often found in close proximity to the inner layer III-facing and the outer layer II-facing surfaces.

The Inner Layer (III) is closely apposed to the dark-staining layer II and comprises 1-5 light-staining cells. The cell width varies, appearing as a thin cellular structure dorsally and ventrally, while thickening on the lateral surfaces. Occasionally this layer is absent from the dorsal and ventral endomeninx. Cell size is comparable to that in the outer layer (I); however, on the lateral surface it increases in width, often exceeding the combined width of the two outer layers (I and II). The nucleus of the layer III cell is a light staining structure appearing to be of similar if not at times equal electron density to the surrounding cytoplasm. The cytosol contains many organelles making this cell layer highly conspicuous compared to the other cell layers. The predominant organelle is the endoplasmic reticulum, the cisterns of which are long and close to the nucleus encircle it as singular, paired or multiple units (Fig. 3.7). In the surrounding cytoplasm, the cisterns form into large undulating whorls of multilayered units that surround vesicles and mitochondria. Ribosomes are found free in the cytoplasm and usually close to the reticulum. Mitochondria and Golgi apparatus are present and are surrounded by the large accumulations of these endoplasmic structures.

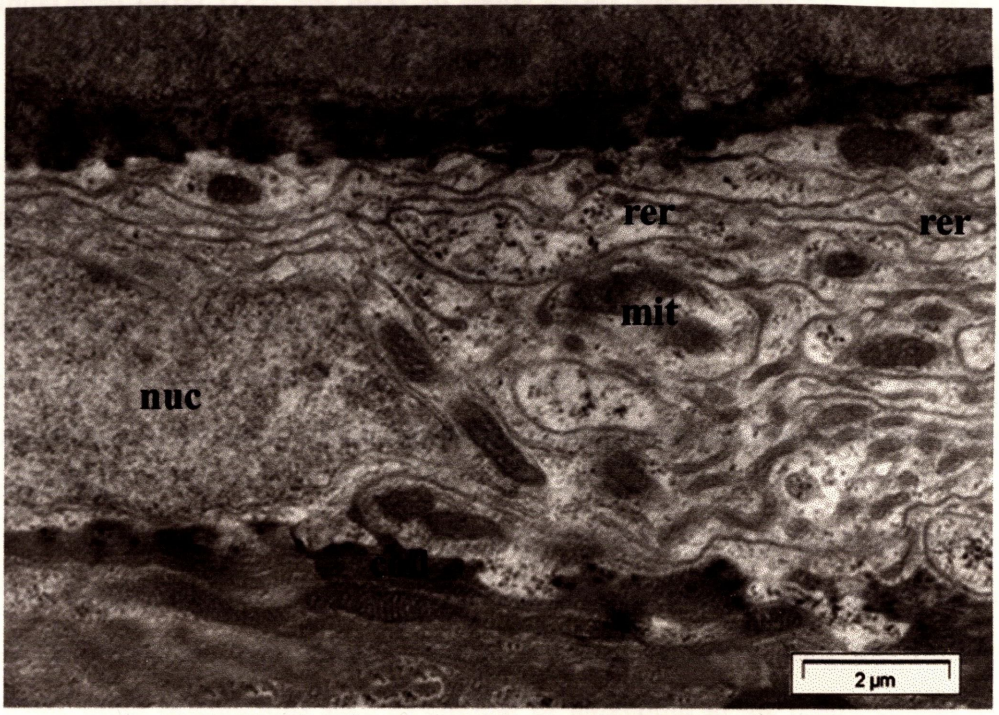


Figure 3.7. Montage of electron micrographs from layer III. Note the anundance of endoplasmic reticulum (er) in the cytosol with interspersed mitochondria (mit) and the light staining nucleus (nuc). Collagen (coll) bundles are present in the extracellular spaces created by this layer and layer IV.

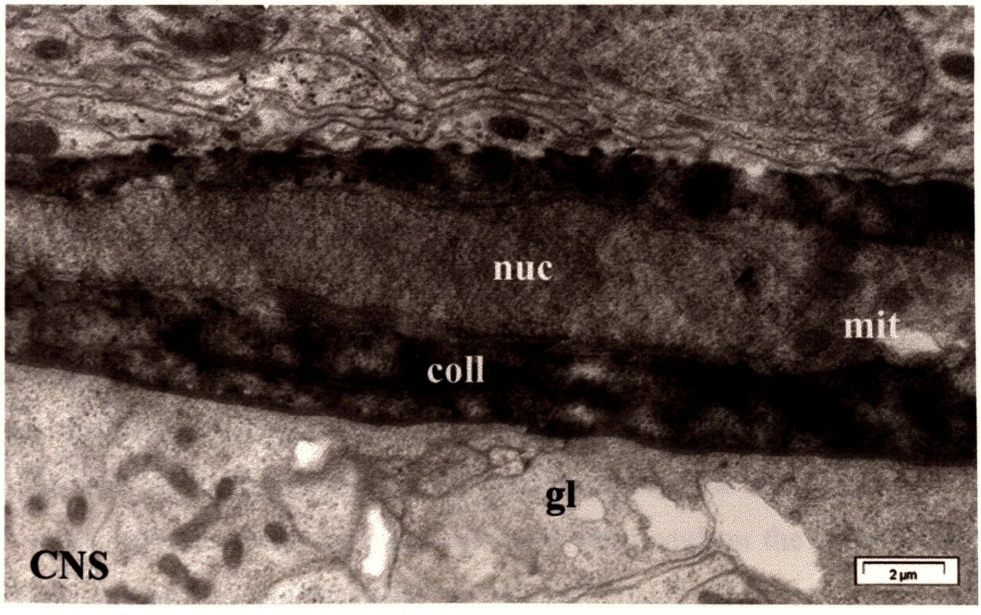


Figure 3.8. Electron micrograph of the layer IV. Note the electron dense cytoplasm and the similar homogenous staining elongate nucleus (nuc). Organelles are few, although mitochondria (mit) are found. Note the abundant electron dense collagen layers (coll) that permeate the spaces between this layer and the surface (glia limitans, gl) of the brain (CNS).

The Innermost Layer (IV), like layer II, stains darkly and contains cells in 1 or 2 layers with electron dense nuclei and cytoplasm (Fig. 3.8). Cell shape is usually elongate with long thin cytoplasmic processes that often form junctional complexes with other cells of the same layer. Occasionally spaces appear between this layer, layer III and the basal lamina often with interspersed collagen bundles. Occasionally collagen is absent from these spaces resulting in small unoccupied intercellular spaces that are presumably filled with fluid. Fewer organelles are seen in the cell bodies compared to the other cell layers. Rough endoplasmic reticulum is present in bundles of 3-5 cisterns distributed throughout the cytoplasm. Golgi apparatus, mitochondria and vacuoles are present in low densities.

Bundles of collagen are abundant between layer IV and the basal lamina (see Fig. 3.8) while collagen occasionally permeates the spaces between layers III and IV (Fig. 3.7). Fibres are longitudinally arrayed into finite bundles along the rostro-caudal axis while other orientations such as circular or tangential to the rostro-caudal axis are absent. As a result of the close packing of the meningeal cell layers, collagen fibres are confined to this particular region close to the well-defined basal lamina at the brain-endomeningeal interface (Fig.3.8).

Extra-meningeal Structures

Occasionally profiles were found on or near the outer layer I and interspersed between the meningeal layers that contain numerous vesicles (see Fig 3.9). In general, vesicle size was homogenous, smaller, and more regular in shape than the larger vesicle structures in adjacent meningeal cells.

The Ectomeninx

The ectomeninx covering the brain and rostral spinal cord is composed primarily of collagen fibres aligned longitudinally, circularly and tangentially. Fibroblasts are present between the collagen layers and constitute most of the small population of cells in this layer. Melanocytes, the other cell type, are found on the inner facing (PMF contacting) surface as a singular layer.

Fibroblasts

There are few cell bodies of fibroblasts in this layer, although their long cellular processes are more frequently found. The cell body is elongate and somewhat spindle

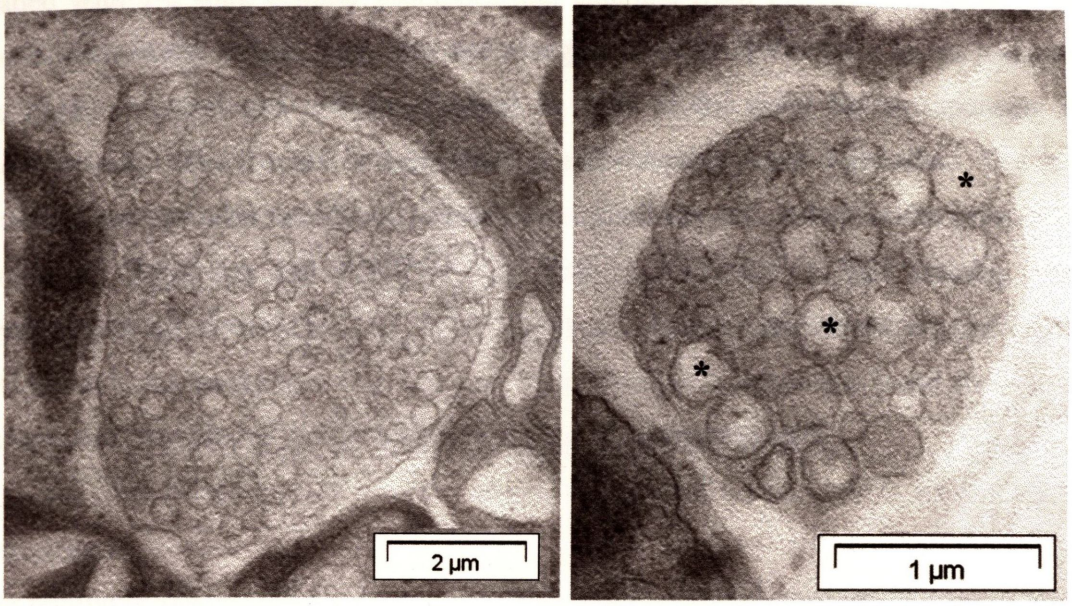


Figure 3.9. Extrameningeal structures were found interspersed between the cellular processes of layers I, II and III. They were also found in the PMF in close proximity to layer I cells. These structures (a, b) are atypical of the different cell layers and are densely packed with numerous small vesicles (*). Their structure is seen in (a) and at higher manification in (b).

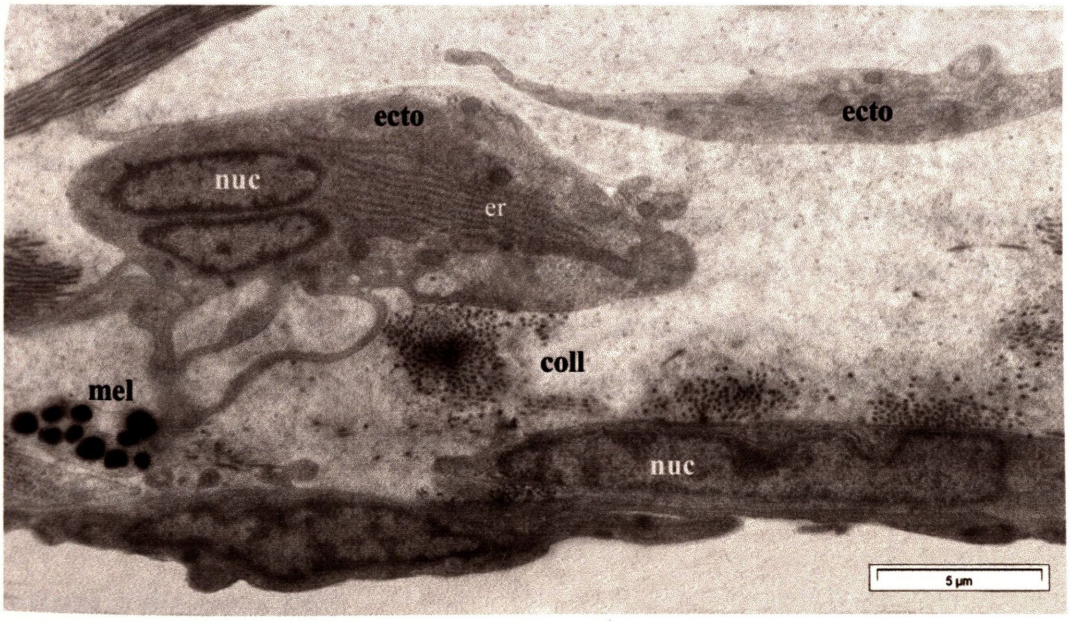


Figure 3.10. Electron micrograph of the fibroblast-like ectomeningeal layer with surrounding collagen bundles (coll). Note the close apposition of the ectomeningeal cells (ecto) and the presence of melanosomes (mel) in a small process which are part of a melanocyte cell. In all ectomeningeal cells the nucleus (nuc) is prominent in the cell and the cytoplasm often contains numerous lamellae of endoplasmic reticulum (er).

shaped with 1-2 long cellular processes that emanate from the cell body (Fig. 3.10). The nuclear shape ranges from thin and elongate in cells of the inner layers (apposing the PMF) to small and circular/ellipsoid in cells of the outer layers (apposing the endocranium). The cytosol is light staining and contains many organelles. The most abundant are vacuoles, which are present throughout the cell except in the cytoplasmic processes. Their size and structure is generally uniform with a light staining lumen containing small electron dense punctate structures. Another prominent organelle in the cytoplasm is the endoplasmic reticulum. Thin elongate cisterns are found close to the nucleus and vacuoles in the cytoplasm as single or multiple strands.

Melanocytes

The relatively few melanocytes were found primarily on the inner (PMF facing) layers of the ectomeninx. In general, the cytoplasmic extensions (containing melanosomes) were found in close proximity to the collagen layers and, occasionally, thin layers of collagen covered them.

Collagen

Large bundles of collagen fibres constitute the main component of the ectomeninges. They are aligned: (a) longitudinally, along the rostro-caudal axis of the brain; (b) in a circular fashion with the curvature of the underlying neural tissue, and (c) tangentially (angular orientated longitudinally fibres). Because of the different orientations of the collagen bundles, and the continuity of these structures in the meningeal tissue, the ectomeninx can be divided into 5 to 15 layers. In each layer, the orientation of fibre bundle is random. However, two layers of circularly aligned bundles are frequently found: one close to the innermost layers of collagen abutting the PMF, while the second is close to the outer layers of collagen in close proximity to the endocranium.

Meninges of the spinal cord

Because of the close apposition of the ectomeninx to the inner surface of the vertebral arches, we have been unable to provide a detailed description of this layer and so only the endomeninx is described at this level.

Endomeninx

As seen in plastic sections, the endomeninx encircles the spinal cord as a continuous sheath, which also envelops the dorsal and ventral roots. This membrane is very thin dorsally, somewhat thicker ventrally and is thickest at the lateral edges (Fig. 3.11c). It comprises an outer layer (I) consisting of melanocytes and an inner layer (II) comprising connective tissue. The melanocytes are particularly concentrated at the dorsal surface (Fig. 3.11b, c). Blood vessels are found interspersed between the two cell layers (see Fig. 3.11a); one vessel on the dorsal surface is particularly large.

The Outer Layer (I) at the level of the electron microscope was found to comprise only melanocytes, often overlapping and forming at times up to five layers. Melanocytes are characterised by melanosomes, specialised vesicular organelles that contain melanin. A typical melanocyte consists of a somal region (containing the nucleus and other cellular organelles), and numerous long cytoplasmic processes. Quite often, these dilate to form bulbous regions that contain melanosomes of varying sizes (Fig. 3.12). The vesicles are usually circular to ellipsoid with an enveloping membrane. The dorsal surface possesses most layers of melanocytes (2-5), whereas laterally there are only 1-3 layers and on the ventral surface, only one layer of melanocytes is present. Laterally, the nucleus is elongate and thinner than in dorsal melanocytes and melanosomes are confined to the long cytoplasmic processes that emanate from the cell, whereas dorsally they are found throughout the cytoplasm.

The Inner Layer (II) of the endomeninx is composed of fibroblasts and is not sharply differentiated from the outer layer (Fig. 3.13), whereas its inner limit is delineated by a basal lamina which provides a barrier between this layer and the glial processes of the spinal cord. Layer II comprises 2-4 layers dorsally, thickening to 8-10 layers laterally and decreasing to 2-6 layers on the ventral surface.

Generally fibroblasts are much smaller (~50%) than melanocytes. A typical fibroblast is an elongate spindle-shaped cell, with cytoplasmic processes that extend from the cell body (Fig 3.13). The terminal endings of these processes usually occur close to other fibroblasts where they were often found to form tight junctional complexes. The fibroblasts that are in close apposition to the basal lamina throughout the endomeninx possess a thinner and more elongate shape; the ventral inner layer is composed totally of these elongate fibroblasts.

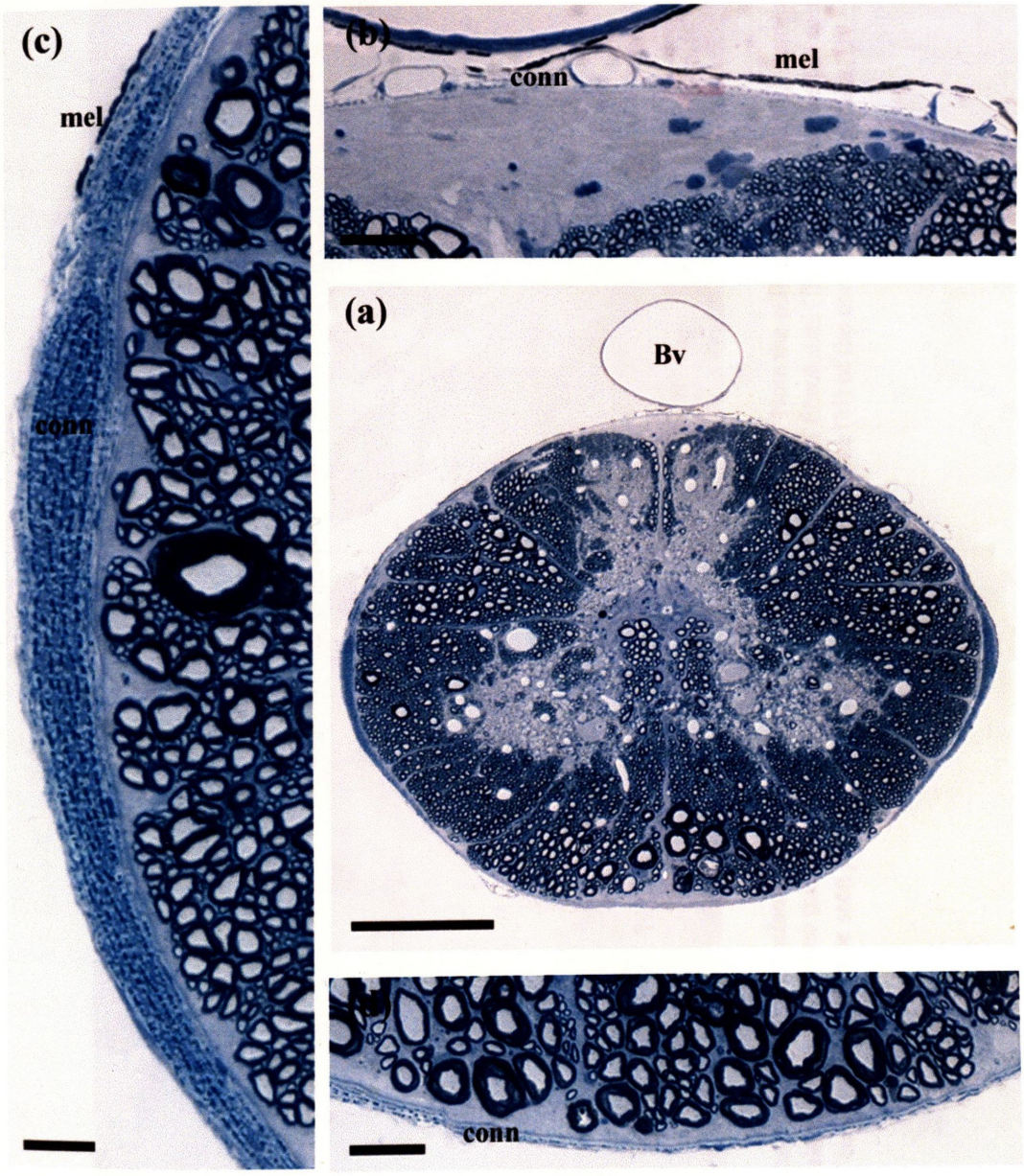


Figure 3.11a, b, c, d. Montage of the spinal meninx at the level of the fourth segment caudal to the anus. Two layers comprise the meninx; the outer melanocyte layer (mel) and an inner connective tissue layer (conn). A large blood vessel (bv) is placed dorsally. Note the change in thickness of the meninx in relation to position around the cord; the relatively thin covering on the dorsal (b) and ventral (d) surfaces compared to the much thicker structure situated on the lateral surfaces. Scale bar (a) = 200 microns, (b), (c) and (d) = 20 microns.

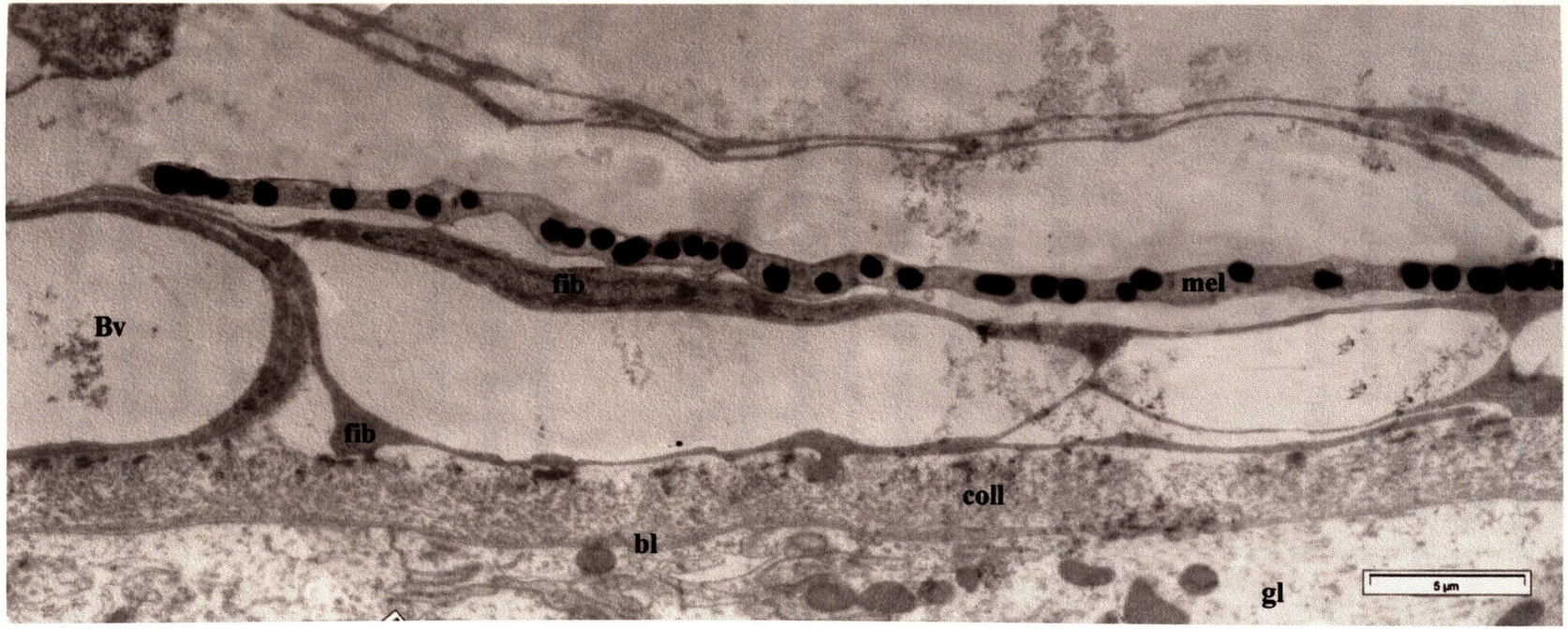


Figure 3.12. Electron micrograph montage of the outer melanocyte layer on the dorsal surface of the cord. Note the cell process containing numerous melanosomes (mel) indicative of melanocyte cells. Below this layer are the elonage cellular processes of fibroblasts (fib) which comprise the second layer in the spinal endomeninx. A layer of collagen (coll) can be seen just below this layer and the basal lamina (bl) of the cord. gl = glia limitans, Bv = blood vessel.

The fibroblast cytoplasm contains a normal organelle compliment, but the most prominent feature in the cytosol is the rough endoplasmic reticulum that allows for identification of this cell type (Figs 3.13). Its cisterns are elongate and have a slightly greater staining density compared to the surrounding cytosol; they are found in groups of 3-6 lamellae positioned close to the nucleus. The cisterns are more elongate in the cellular projections and occur singly or as groups of 5-6 layers. Other organelles such as the Golgi apparatus are also present in lower concentrations, often with associated vesicles. Mitochondria are distributed throughout the cell and possess a circular to elongate shape with prominent cisterns.

Collagen

Collagen was found to be the prominent extracellular component of layer II and with multidirectional fibres that were: (a) longitudinally oriented along the rostro-caudal axis of the spinal cord (in transverse section these fibres appear as small circular profiles); (b) circularly oriented with the curvature of the cord (thus in transverse section these fibres appear as dark lines), or (c) tangentially aligned with the cord. Although numerous orientations are present, a certain order is found in the placement of collagen fibres within the fibroblast layer (see Figure 3.13). A thin circular oriented layer of collagen is usually found close to the basal lamina while outside this layer collagen fibres are longitudinally and tangentially oriented, interspersed between fibroblasts.

Elastic Fibres

Elastic fibres are also found in the extracellular spaces between the fibroblasts of layer II while they are absent from the outer melanocyte layer. These structures are smaller and stain more darkly than collagen; they rarely exceed 20nm in diameter, but form large aggregates.

Blood Vessels

Numerous capillaries are present within the meninges and are in general usually localised to the outer layer of melanocytes. Rarely are blood vessels encompassed by the fibroblast layer; however, blood vessels frequently reside at the interface of these two layers. The large dorsal vein is covered in melanocytes.

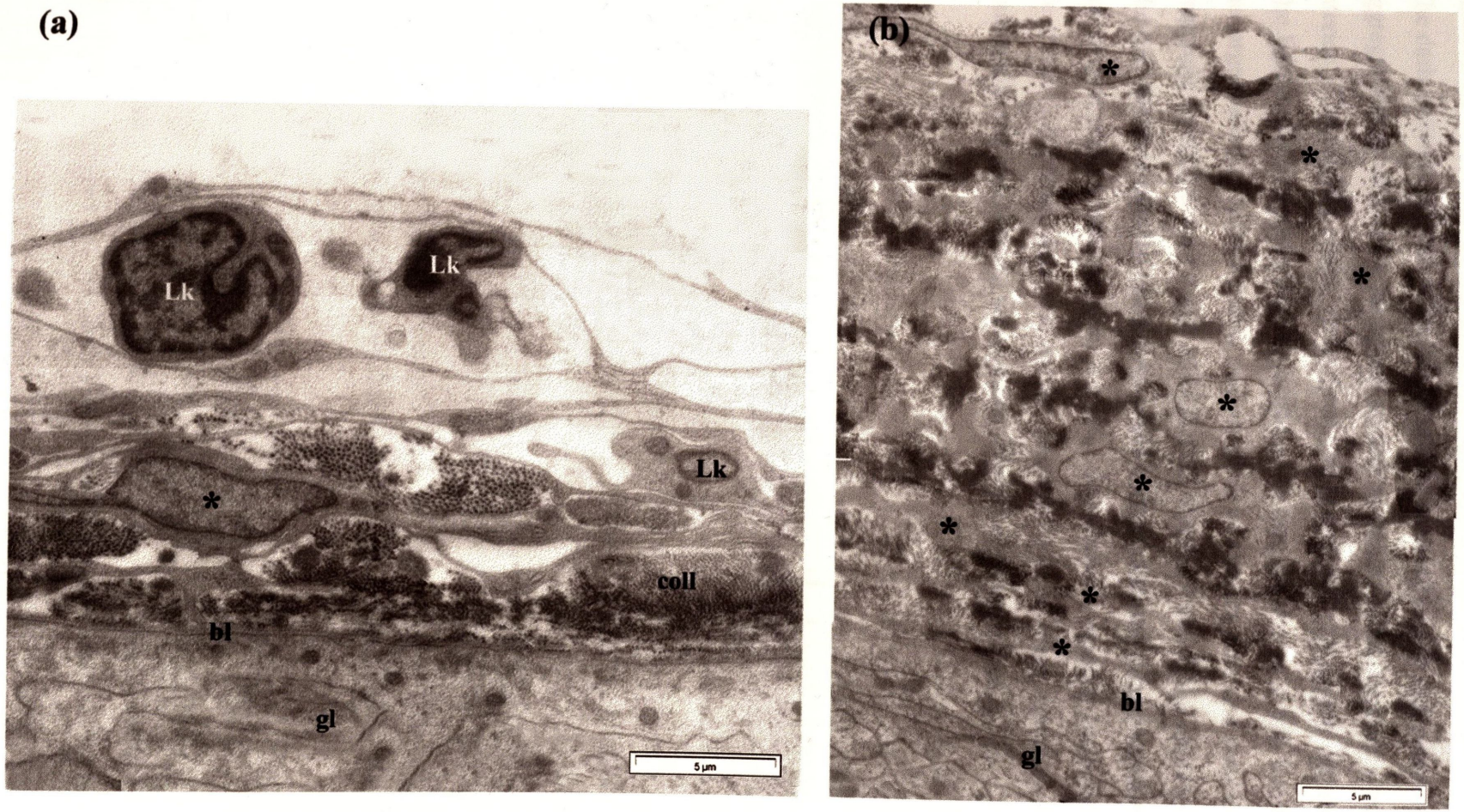


Figure 3.13. Electron micrographs of the dorsal (a) and lateral (b) endomeninx surrounding the spinal cord. In both regions the meninx comprises numerous layers of fibroblasts (*) with interspersed bundles of collagen (coll). Note the difference in thickness between both layers and the different cell shapes present: from predominantly elongate on the dorsal surface to a stellate-type on the lateral surfaces (b). Note the presence of elastic fibres (arrows) interspersed between the fibroblast layers. bl = basal lamina, gl = glia limitans, Lk = leukocyte.

Macrophages

Occasionally wandering cells of the immune system, namely macrophages and monocytes, are found interspersed between layers I and II and close to blood vessels. The dark staining nucleus of the macrophages is usually large and prominent with thick aggregations of chromatin along the nuclear membrane that frequently project into the interior. The nuclear shape varies from cell to cell and can appear circular or bilobed. The lighter staining cytoplasm is sparse and often appears as a thin band surrounding the large nucleus. Mitochondria and vacuoles of varying size and electron density are frequently found whereas rough endoplasmic reticulum and Golgi apparatus are sparse. The cell shape is usually circular to ovoid with occasional thin cytoplasmic processes that project small distances from the cell. Occasionally smaller irregular shaped cells are found. Electron dense vacuoles, characteristic of other immune cells such as neutrophils and eosinophils, were absent from all cells examined.

3.4 Discussion

The results of the present study show that the meninges surrounding the brain are composed of two component layers: an endomeninx, closely apposed to the surface of the brain, and an ectomeninx, in close proximity to the endocranium. This finding is in agreement with Van Gelderen (1926) but not Sterzi (1901, 1902) who believed there to be only a single meningeal covering, the *meninx primitiva*. Our view of the organisation of the meninges is summarised in figure 3.14.

The cranial endomeninx

We have found that the cranial endomeninx of the eel is composed of four layers and is similar, in part, to the endomeninx of other teleost fish. The outermost PMF-contacting layer I which is characterised by closely packed elongate cells with an electron light-staining cytoplasm is similar in structure to the outermost PMF-contacting layers of the goldfish (Momose et al., 1988; Wang et al., 1995), but differs from the report of Schwarz et al. (1993) in the trout where the staining was found to be extremely electron dense.

Layer II of the eel comprises a thin continuous band of 1-3 elongate cells just as has been found in the 'intermediate layer' of the goldfish (Momose et al., 1988) and trout (Schwarz et al., 1993), although in the trout the staining density is lighter. The presence of abundant mitochondria and vesicles has been noted in this layer in all species studied. Although vesicles were often observed in close apposition to the cell membrane, we were unable to find the active type which has been described in the trout (Schwarz et al., 1993) and goldfish (Momose et al., 1988). The interdigitating nature of the cells and the presence of numerous tight junctions suggests that this layer may play a similar role to the intermediate layer of the other teleosts, as a barrier to the PMF, and be functionally similar to the arachnoid layer of mammals (see Hoffmann and Schwarz, 1996, for review).

The compact layer we have termed layer III in the present study contains 1-5 elongate cells and is comparable to the inner 'fibroblast layer' of the trout endomeninx (Hoffmann and Schwarz, 1996; Schwarz et al., 1993) and to the inner 'reticular layer' of the goldfish (Momose et al., 1988), although the loose cellular configuration that has been reported in these fish was not observed in the present study; in fact we have found

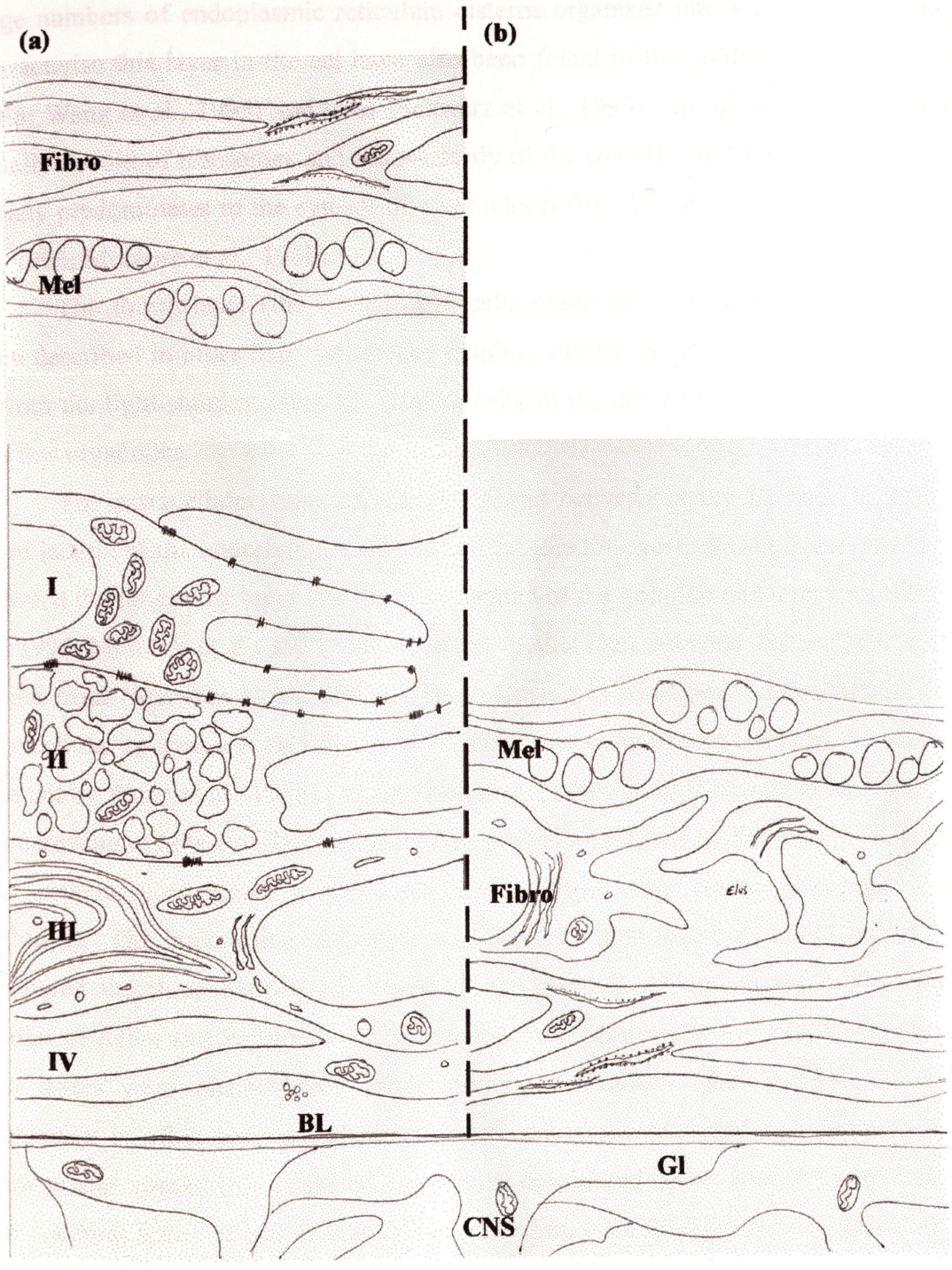


Figure 3.14. Diagrammatic representation of the meninges that surround the brain (a) and spinal cord (b) of the eel. In the brain, the meninges comprise the endo- and ectomeninx, which are divisible into four (I, II, III, IV) and two layers (mel, Fibro) respectively. Surrounding the spinal cord the endomeninx is composed of only two layers an outer melanocyte (mel) and an inner fibroblast layer (Fib).

that this is a compact layer that varies in thickness across the surface of the brain. The large numbers of endoplasmic reticulum cisterns organised into large lamellae which characterise this layer in the eel have also been found in the goldfish (Momose et al., 1988; Wang et al., 1995) and trout (Schwarz et al., 1993). In the eel, the cisterns are usually devoid of ribosomes and are primarily of the smooth variety whereas the rough variety predominates in the cytosol of other teleost fish (Wang et al., 1995; Schwarz et al., 1993; Momose et al., 1988).

The fourth layer (the layer IV) of cells observed in the present study has not been described in other fish. Its intense staining, similar to that of layer II, demarcates it from the light-staining layer III. Unlike cells in the other layers, the cell cytoplasm has few organelles.

The extracellular spaces frequently found between layers III and IV, and the basal lamina of the underlying neural tissue (the glia limitans), are similar to the spaces between the innermost layer and the basal lamina of the goldfish endomeninx (Wang et al., 1995; Momose et al., 1988) but are much smaller than the wide extracellular spaces of the trout (Schwarz et al., 1993). The inclusion of collagen bundles within these extracellular spaces was also found by Momose and co-workers (1988) in the goldfish (but not by Wang et al., 1995) and are also present in the trout (Schwarz et al., 1993). It is interesting to note that the type of fixation procedure utilised by Schwarz et al. (1993) was immersion compared to perfusion fixation for all other studies (the present one included). The importance of fixation was noted by Momose et al. (1988) when they compared the three defined cell layers of the goldfish endomeninges to the earlier studies of Klika and Zajikova, (1975) (quoted from Momose et al., 1988), where only two layers were characterised using immersion fixation. Eel material fixed by immersion is often severely disrupted - cell layers are fractured and produce wide extracellular spaces that could be mistakenly considered to be anatomically defined. The subdural space of mammalian spinal meninges, once thought to be an intercellular space, is now known to be an artefact of tissue preservation (Frederickson, 1991; Vandebeele et al., 1996). Perfusion fixation through the vasculature is essential for good preservation of CNS tissue (e.g. Palay et al., 1962).

The cranial ectomeninx

Few studies have characterised the structure of the ectomeninx and this is due, in part, to the difficulty of isolating this layer without damaging its structural integrity because

of the close association to the endocranium (Vandenabeele et al., 1996). Only the ectomeninges surrounding the lamprey spinal cord (Nakao, 1979), the brain of the skate (Bundgaard and Cserr, 1991), and the dura of mammals have been described ultrastructurally. Even in mammals, where the dura has been extensively described, few studies have characterised the ultrastructure of this layer at the spinal level (Vandenabeele et al., 1996).

The composition of this layer in the eel is similar to that of the lamprey (Nakao, 1979), and to the dura of mammals except for the inner, arachnoid-apposing, dural border which is composed primarily of elongate cells (Haines, 1991; Vandenabeele et al., 1996). The arrangement in the eel is different to that of the skate which possesses a highly cellular organisation that is devoid of collagen and comprises 10-12 cell layers that interdigitate with numerous desmosomal junctions between their membranes (Bundgaard and Cserr, 1991).

Melanocytes as observed in the inner, PMF-facing melanocyte layer of the eel were also reported by Rovainen et al. (1971) and Nakao (1979) for the lamprey but not by Bundgaard and Cserr (1991) in the skate. Meningeal melanocytes are usually considered to be absent in mammals in general; however, meningeal melanocytes have been found in C57 black mice and pigmented rats (Barden and Levine, 1983) and over the ventrolateral surfaces of the medulla oblongata in man (Goldgeier et al., 1984). Moreover, the formation of meningeal melanocytomas following compression of nerve roots (Sankhla et al., 1996), suggests that these cells may be present, but normally in very low numbers.

Vertebrate melanocytes are composed of two populations, cutaneous and extracutaneous (Prota, 1992). Extracutaneous melanocytes, which are present in all vertebrates, can be found at various internal sites such as the eye, inner ear, and oral mucosa (Breathnach, 1988) and, as in the present study, as part of the meninges. They synthesise melanin only during the early stages of their embryonic life and production appears to cease once a cell has attained a full complement of melanin packaged into vesicles termed melanosomes. Functionally, relatively little is known about these cells, although some functions have been attributed to them, such as: a sink for free radical species, as a reservoir for trace elements, and as an intercellular buffering system for calcium (see Prota, 1992) or, reflecting cutaneous functions, as camouflage; as bright colour warning predators; in the regulation of heat adsorption, or as a barrier to ultra-

violet light, although this last function is debatable and is considered to be of minor importance (Prota, 1992).

The abundance of this cell type surrounding the brain and spinal cord of the eel raises questions as to its function. This may be understood in the context of the life cycle of the eel. During the glass eel migratory stage, the body is unpigmented, and therefore transparent save for the meninges of the brain and spinal cord, which already possesses a covering of melanocytes. During this time eels frequent the upper levels of the water column, and therefore receive a greater intensity of sunlight and resultant heat along the body until reaching brackish waters, where cutaneous pigmentation begins to occur signifying the start of the next 'elver' stage. Therefore the function of the extracutaneous melanocyte population surrounding the CNS may simply reflect those of cutaneous melanocytes and serve to protect the still developing and growing neural tissue by regulating heat adsorption. In line with this, it is notable that the greatest densities are found the dorsal and dorso-lateral surfaces of the brain and spinal cord and few melanocytes are present ventrally.

Finally, melanocytes in the eel meninges are interesting not only because of their extensive distribution but also because of their ontogenetic origin. Their presence strongly suggests that migratory melanoblasts from the neural crest play a role in the development of the meninges surrounding the brain and the spinal cord. This interpretation would support the theory of a dioecious origin for this tissue first proposed by Le Douarin and Kalcheim (1999).

Spinal Meninges

Little is known of the meninges at the level of the spinal cord except for the lamprey (Rovainen, 1970; Nakao, 1979) and some mammalian species, such as rat (e.g. Morse and Lowe, 1972), mouse (Seitz et al., 1981) and man (e.g. Vandenabeele et al., 1996). The meninges in these studies have been divided into 4 layers in the case of the lamprey, and 3 layers for the mammals, including the ectomeningeal/dural layer closely apposed to the vertebral column. The present study on the eel focused solely on the endomeninx which was found to be a simplified version of the cranial endomeninx in comprising two layers, demarcated by cell type: an outer layer containing elongate melanocytes, 1-5 layers thick, and an inner layer, comprising fibroblasts, collagen and bundles of elastic fibres.

The composition of the endomeninges as two layers of closely apposing cells enwrapping the spinal cord contrasts with the lamprey spinal cord, where the meninges form a voluminous four-layered arrangement of cells. In the mammalian spinal cord too, the meninges span the distance between the surface of the cord and the inner portions of the vertebral column. The thin covering of meningeal tissue around the spinal cord (~ 10-20μm) in the present study is somewhat similar to the pia mater but, in contrast to mammals, the endomeninx is devoid of traberculae or equivalent structures extending into the PMF compartment.

One aspect of the spinal meninges that appears to be common to all species is the presence of fibroblasts and collagen. In the lamprey, collagen has been found in all four layers (Nakao, 1979), organised in a similar manner to the eel spinal cord, in close apposition to the basal lamina. In mammals, fibroblasts and collagen are found only as part of the dura (Frederickson, 1991), although Vandebeele and co workers (1996) have shown that the human spinal meninges contain a band of collagen fibres within the arachnoid layer. The pia in contrast, is devoid of collagen and is primarily a cellular layer. The different orientations of the collagen bundles (circular, longitudinal and tangential) to the rostro-caudal axis of the spinal cord confers tensile strength in two directions: circularly and longitudinally, and similar orientations are found in the mammalian dura, and in the endomeninx of the lamprey (Nakao, 1979).

The meninges as a barrier?

Tracer studies of the endomeninx in the goldfish using lanthanum in the fixative solution (Momose et al., 1988), and superfusion of the skate perimeningeal fluid compartment with HRP (Bundgaard and Cserr, 1991), have shown that the endomeninx in these animals functions as a barrier to the perimeningeal fluid in a manner similar to the arachnoid layer of mammals (Haines, 1991; Peters et al., 1991). Ultrastructurally, the organisation of the cell layers within the endomeninx has been shown to correlate with the stoppage of tracer and Momose and co-workers (1988) were able to identify the cells of the intermediate cell layer in the goldfish (corresponding to layer II of the present study) and, more specifically, the junctional complexes present between the cells of this layer, as acting as a barrier to the tracer. The similarity of the cranial meningeal ultrastructure in the present study to that of the goldfish (Momose et al., 1988; Wang et al., 1995) and trout (Schwarz et al., 1993; Hoffmann and Schwarz, 1996), and the presence of junctional complexes of the tight/desmosomal variety

between cells of all layers, but more so the intermediate and outer layers (which also possess numerous cellular interdigitations), would suggest that the cranial endomeninx of the eel also possibly acts as a barrier to the perimeningeal fluid. The spinal endomeninges in comparison possess a much 'looser' organisation particularly in the outer melanocyte layer, which contains only occasional tight junctions. The inner fibroblast layer, however, has a larger number of junctional complexes, usually on or close to the lateral surfaces. Consequently, it is our view that the spinal meninges possibly confer a barrier function to the PMF, but that this is achieved at deeper levels within the inner fibroblast layer. Only the future use of a tracer can decide the extent of this barrier.

Comparative structure of the cranial and spinal meninges

The meninges of teleost fish are usually considered to comprise three layers of cells (reviewed in Hoffmann and Schwarz, 1996). This simplification of the general structure fails to take into consideration the structure of the meninges at the level of the spinal cord. From the results of the present study, it is clear that a more cautious approach should be taken when describing the general structure of the meninges in fish. We have found that the organisation of the meninges changes from complex at the cranial level to a simpler arrangement at the level of the cord.

These structural differences most probably imply different functions for the meninges surrounding the brain and spinal cord. The organisation of the cranial endomeninx strongly suggests a secretory function for this tissue and the absence of fibroblast cells (typical of the ectomeninx and the spinal meninges) and the small collagen contribution – isolated to the regions between layers III and IV and the basal lamina - implies that this layer provides limited support to the underlying neural tissue. At this level of the CNS, the function of support and the provision of tensile strength is carried out by the ectomeninx, utilising its laminar organisation and collagen bundle orientation.

The endomeninx of the spinal cord resemble the cranial ectomeninx, in containing numerous fibroblasts and collagen bundles, but also elastic fibres. In this respect the spinal endomeninx resembles the mammalian dura which is thought to provide structural support to the cord within the manoeuvrable vertebral column. In the eel, the spinal column is also highly manoeuvrable – indeed more so than in mammals – and, therefore, the meninges must provide support to the spinal cord without hindering

the large range of movement. In mammals the organisation of interlaced bundles of collagen in different orientations, with elastic fibres, provides strength and elasticity to the dura when displaced during flexion and extension movements (e.g. Tencer et al., 1985). During limb movement this layer is tensed, due to the displacement of the spinal nerves and their dural cases (Sunderland, 1980). The inner layer of the eel spinal endomeninx, therefore, may also function in a similar manner and provide support to the cord during flexion and extension. It is interesting to note that all identifiable elastic fibres were found as part of the inner meningeal layer on the lateral surfaces of the cord, where they presumably confer flexibility to the endomeninx during sinusoidal swimming and during the large flexions of the body created by actions such as the startle response (Bosch, 1994; Doyle et al., 2000).

Secretory function for the cranial meninges?

Since the cellular organisation of the cranial endomeninx of the eel is similar to that of other teleost fish, and since it has been shown from ultrastructural (Momose et al., 1988), immunohistochemical (e.g. Konigstorfer et al., 1990) and freeze fracture studies (Caruncho et al., 1990a; 1990b; Caruncho and Silva, 1994) that this layer is capable of secretory activity, the question now arises as to what do the endomeninges of the brain and spinal cord secrete?

It is probable that the secretory products of the cranial meninges contribute to the overall composition of the perimeningeal fluid and the cerebrospinal fluid as found in other teleost fish (Hoffmann and Schwarz, 1996). Ependymins, for example, are major secretory products of the endomeninges of carp, such as the goldfish (Hoffmann, 1992) and have been isolated to the innermost endomeningeal layers. This glycoprotein is the predominant constituent of the CSF (Shashoua, 1981; Müller-Schmidt et al., 1993; Wang et al., 1995) and has been implicated in such aspects of neuronal function as memory and learning (Shashoua, 1991; Nelson and Alkon, 1989; Davis, 1988) and neural regeneration, where increased levels of synthesis are observed in the meninges following injury to the optic nerve (goldfish, Thormodsson et al., 1992).

Although ependymins have been localised to the cranial meninges of cypriniformes (e.g. Shashoua, 1981), salmoniformes (e.g. Schwarz et al., 1993) and clupeiformes (Müller-Schmidt et al., 1993), they have been reported to be absent from other orders of teleost fish (Hoffmann and Schwarz, 1996). Aside from ependymins, relatively little is known of the protein composition of the CSF and PMF in teleost fish

and relatively few studies have characterised the protein constituents. Recently Huang et al. (1995) identified a protease inhibitor of the serpin family that appears to be a major component of the PMF in some teleosts. It is possible therefore, that the meninges of the eel may secrete ependymins or another protein species and it cannot be ruled out that secretion of more than one type of protein may take place. It is interesting to note that secretory activity has recently been shown to occur in mammalian meninges where studies of the leptomeninges (pia and arachnoid) and of meningiomas have shown the secretion of a number proteins into the extracellular environment, such as laminin, various types of collagen, fibronectin, and heparin sulphate proteoglycan (Rutka et al., 1986; Ohe et al., 1996). Mammalian meninges are also known to secrete substances that appear to be the constituents of the CSF, such as prostaglandin-D-synthase (Urade et al., 1993), amyloid precursor protein (APP; LeBlanc et al., 1991), TGF β1 (Heine et al., 1987), IGF II and IGF-binding protein (de Pablo and de la Rosa, 1995; Ishikawa et al., 1995), Il-1 (Ban, 1994). Similarly parathyroid hormone-related activity (Struckoff and Turzynski, 1995), kinin activity (Takano et al., 1995), metabolism of epinephrine (Kern et al., 1995) and synthesis of retinoic acid at levels that exceed that of the liver (Dev et al., 1993) have been demonstrated in mammals while Ohe and colleagues (1996), in a comprehensive study of cultured leptomeningeal cells, found up to 18 different proteins to be secreted by these cells.

Since in the eel collagen and elastic fibres are generally absent from the melanocyte layers, it seems reasonable to suggest that this cell type contributes relatively little to the extracellular matrix (ECM), and that production of the different components of the ECM, such as collagen types I, III and IV and elastin, can be expected to be produced by the inner fibroblast layer of the endomeninges. In a similar fashion the scattered fibroblasts of the ectomeninges could also be expected to possess the same function. The small contribution of collagen to the overall structure of the cranial endomeninx – isolated between layers III, IV and the basal lamina – and the absence of elastic fibres, would suggest that upkeep of the ECM may not be the primary role of this tissue.

Comparison to mammalian meninges

Most studies on fish meninges (refs Nakao (1979), Momose et al. (1988); Schwarz et al., 1993) have attempted to equate the meningeal structure with that of mammals. For

example the three layered endomeninges of teleost fish are presumed to give rise through evolution to the leptomeninges (pia and arachnoid layers) Nakao (1979; Schwarz et al., 1993) and perhaps the dura (Hoffmann and Schwarz, 1996; Schwarz et al., 1993) but in light of the lack of embryological and comparative studies this correlation is probably premature.

Summary of main findings

- The meninges surrounding the brain comprise an endomeninx and ectomeninx, in agreement with the findings of Van Gelderen (1926). They contain: 4 layers in the endomeninx and 2 in the ectomeninx. In contrast, the spinal endomeninx has only 2 layers (the ectomeninx at this level was not examined).
- The cellular organisation of the layers I and II, and the presence of numerous cell-cell junctional complexes in the cranial endomeninx, suggests that this tissue acts as a barrier to the PMF. The spinal endomeninx does not possess such a defined layer; presumably at this level, the inner fibroblast-containing layer confers a barrier capability.
- Specialisation of the different cell layers in the cranial endomeninx, similar to those reported previously for other teleost fish, suggest that the endomeninx carries out secretory functions.
- The similar composition of the spinal endomeninx and the cranial ectomeninx suggest that both structures possess a similar function in providing mechanical stability and protection to the CNS.

Chapter 4

The injured spinal cord - the first stages of repair

4.1 Introduction

Although it is well known that the anamniote CNS possesses considerable regenerative potential and is capable of restoring functional behaviour following injury (e.g. McClellan, 1988; 1990; Bosch et al., 2000), relatively little is known of the early stages of regrowth when regenerating neural tissue extends into, and traverses, the lesion site. It has been shown from several studies, using light and electron microscopy, that neural tissue outgrowth may occur from different regions of the damaged CNS tissue, depending on the type of injury induced, and the region of the CNS that has been injured. The most extensively used models are the optic nerve and the spinal cord (e.g. Wood and Cohen, 1981; Bohn et al., 1982; Anderson et al., 1983; Stafford et al., 1990; Lurie and Selzer, 1991; Levine, 1991; Benraiss et al., 1997).

In the case of the optic nerve, regenerating tissue can arise from the nerve core (Scott and Foote, 1981) and periphery (Bohn et al., 1982; Lowenger and Levine, 1988); for the spinal cord, following amputation (fish, Anderson et al., 1986; amphibia, Nordlander and Singer, 1978; and reptiles Simpson 1968) and transection (*Xenopus* tadpole, Michel and Reier, 1979), regrowing tissue forms centrally. In contrast, following ablation injury the regrowing neural tissue arises from the periphery of the cord (the newt, *Triturus*, Stensaas, 1983).

The milieu, through which the regenerating neural tissue passes, both for the optic nerve and spinal cord, has also received little attention. The blastema formed following amputation provides a supportive structure for regrowing axons (Simpson and Duffy, 1994), but with injuries to more rostral regions of the cord this type of supportive tissue is absent and only the vertebral column provides mechanical support. Regrowth must occur through a medium of some type and therefore it may be presumed that a 'matrix' or 'ground substance' is present that facilitates growth of neural tissue into the lesion site. What comprises this matrix?

Most studies of the regenerating anamniote tissue variously describe this region as being composed of debris, degenerating neural elements, and elements from the haematological system (Reier and Webster, 1974; Bohn et al., 1982; Nona and Stafford, 1995) and often generally termed as a scar (e.g. Scott and Foote, 1981). The composition of the lesion site in amniotes has received more attention and some aspects, such as the extracellular matrix (e.g. Fitch and Silver, 1997) and the leucocyte infiltration, particularly the macrophage (e.g. Lawson et al., 1994) and lymphocyte (e.g.

Popovich et al., 1997) response, have been well documented. These, and other cell types of the immune system, are thought to stem from the widespread haemorrhaging and breakdown of the blood brain barrier, resulting in the leakage of blood into the lesion site, an infiltration that has been shown to play an important role in the development of scar tissue. The effects of this influx include myelin vesiculation and lipid peroxidation, among others, which are considered to be inhibitory to regrowth (Lotan and Schwartz, 1994; Perry et al., 1995). Moreover, astrocytes, which play a major determining role in the development and ultimate severity of the 'scarring' at the lesion site, are strongly influenced by macrophages and other components of the haematological system, such as T-cells and plasma cells, as well as numerous factors such as eicosands, interleukins, and interferons (Merrill and Benveniste, 1996). Since haemorrhaging is a common occurrence in the anamniote CNS following injury, a similar influx of haematogenous elements must also invade the lesion site.

In view of the limited literature concerning the response of neural tissue and immune system components and the unknown nature of a possible 'matrix' through which regenerating cord tissue may grow, the aims of the present study have been:

- to determine the regenerative behaviour of the spinal cord up to 200 days following the transection;
- to determine the initial origins and the cellular composition of the supportive milieu in the lesion site and,
- to determine the leucocytic response to injury.

We are particularly interested in the initial stages of regrowth and how the rostral and distal stumps reconnect, and we have used 3-D reconstructions of the bridge and adjacent cord in this analysis.

4.2 Materials and Methods

Animals

This study is based on 15 European eels *Anguilla anguilla L.* in a non migratory immature stage of their life-cycle. The times studied were days 4, 6, 8, 10, 14, 20, 26, 54, 144 and 200. For day 4 the results are based on data from two regenerates.

Transection of the spinal cord

For surgery, each eel was anaesthetised by immersion in 0.3g/l MS-222 (Sigma) to induce light anaesthesia and then administered 0.1ml alphaxalone ("Saffan" Pitman-Moore) subcutaneously. Cooling on ice provided additional anaesthesia. At all times while under anaesthesia, fresh water was continuously run over the gills.

A portion of the dorsal fin at a level around the thirteenth segment caudal to the anus was removed and the musculature cut down to the vertebral column. The opening was retracted, and the dorsal vertebral spines for 3 vertebral segments were removed and the roof of the underlying canal opened to expose the dorsal surface of the spinal cord. The spinal cord was then cut completely using fine micro-scissors, care being taken so as not to sever the dorsal blood vessels, if possible. The wound was fine stitched and the animal was allowed to recover before being placed in an individual holding tank with filtered recirculating water at 25^{o}C, and with constant aeration. Following each successful surgery a postural change was immediately noticeable in each animal as illustrated in figure 4.1.

Tissue Preparation

For histological investigation, each animal was treated according to the methods described in chapter 2. In brief, each animal was anaesthetised initially by immersion in 0.3mg/L MS-222 and then with a subcutaneous injection of 0.3ml alphaxalone (Saffan). To prevent blood clotting, 0.2ml heparin sodium (Leo Laboratories) was also given subcutaneously. The perfusion procedure consisted of a primary flush of Ringer's solution (with 0.1% Procaine (Sigma) for further anaesthesia) through the heart followed by the fixative, 2% paraformaldehyde and 1.25% gluteraldehyde in 0.1M phosphate buffer (PB), pH adjusted to 7.4. Following perfusion, the region of the spinal cord containing the injury and portions immediately rostral and caudal, were dissected

from the spinal column and post-fixed in the same fixative at 4°C for a maximum of 3 hours.

Electron Microscopy

The tissue was processed for electron microscopy and examined according to the procedures described in chapter 2. Sections were cut for both light (1.5μm) and electron microscopy (500Å). All images were downloaded, analysed and formatted on a Macintosh G3 computer using Adobe PhotoShop 5. Reconstructions from serial sections (60μm apart) of the regenerating spinal cord and blood clot/scar tissue were produced according to the methodology described in chapter 3.

Cell Counts

Counts were made from 1.5μm thick toludine blue-stained sections of identifiable nuclei of leucocytes in the lesion site at X1000 magnification. No correction was made for double counting as the distance between each section is 60μm whereas maximum leucocyte diameter was calculated as 40μm.



Figure 4.1a, b. Photographs illustrating the body posture of an uninjured eel (a) and that of an animal in which the spinal cord has been cut just caudal to the anus (b). In (a) note that the normal 'S' shape posture is lost in the body portion caudal to the injury (b). Normal posture eventually returns by approxmately day 50 as the system regenerates.

4.3 Results

A number of different events contribute to the regeneration of the transected cord of the eel. Initially, following transection, the cord retracts to produce a gap of approximately 0.5-1mm (see Fig. 4.2a, b), suggesting that normally the spinal cord is under a certain amount of tension. Almost immediately following the surgery, the wound site, including both the rostral and caudal stumps and adjoining undamaged spinal cord, is covered in blood (Fig. 4.2c), as a result of bleeding from the cord itself and from the surrounding meninges (particularly if the large blood vessels situated dorsally or laterally have been severed). This gap created by the transection is rapidly bridged, at first by components arising from the blood that are subsequently displaced by regenerating neural tissue.

Blood clot formation

Within a short period, the blood congeals to produce a 'bridge' that connects both stumps of the spinal cord. Morphological analysis of the clot during the early stages of recovery suggests that it is composed of plasma, nucleated red blood cells, macrophages and other cells of the immune system found within the blood, and fibroblast cells. During subsequent days the blood clot gradually reduces in size and is displaced by regenerating neural material until it has completely gone by approximately 15-20 days after transection.

The blood clot appears at first as a gelatinous mass, opaque and deep red in colour (indicating the presence of red blood cells) which gradually changes (days 4 and 6) to a more translucent and colourless structure (Days 10, 14, 20). At 4 days following surgery the blood clot is extensive and encompasses all of the wound region (Fig. 4.3), particularly in the dorsal and dorso-lateral direction, frequently spilling over the damaged vertebral column and coalescing with other regenerating material, such as bone and muscle tissue. So extensive is the scarring during the earliest stages of regeneration that a large proportion is inevitably removed mechanically during preparation of the material. Therefore it must be stressed that the reconstructions from the earliest stages of regrowth (days 4 and 6) only partially represent the extensive nature of the clot/scar tissue. At 6 days post-transection, the blood clot is still present, unreduced in size, but elements of the adjacent stumps have begun to grow into the

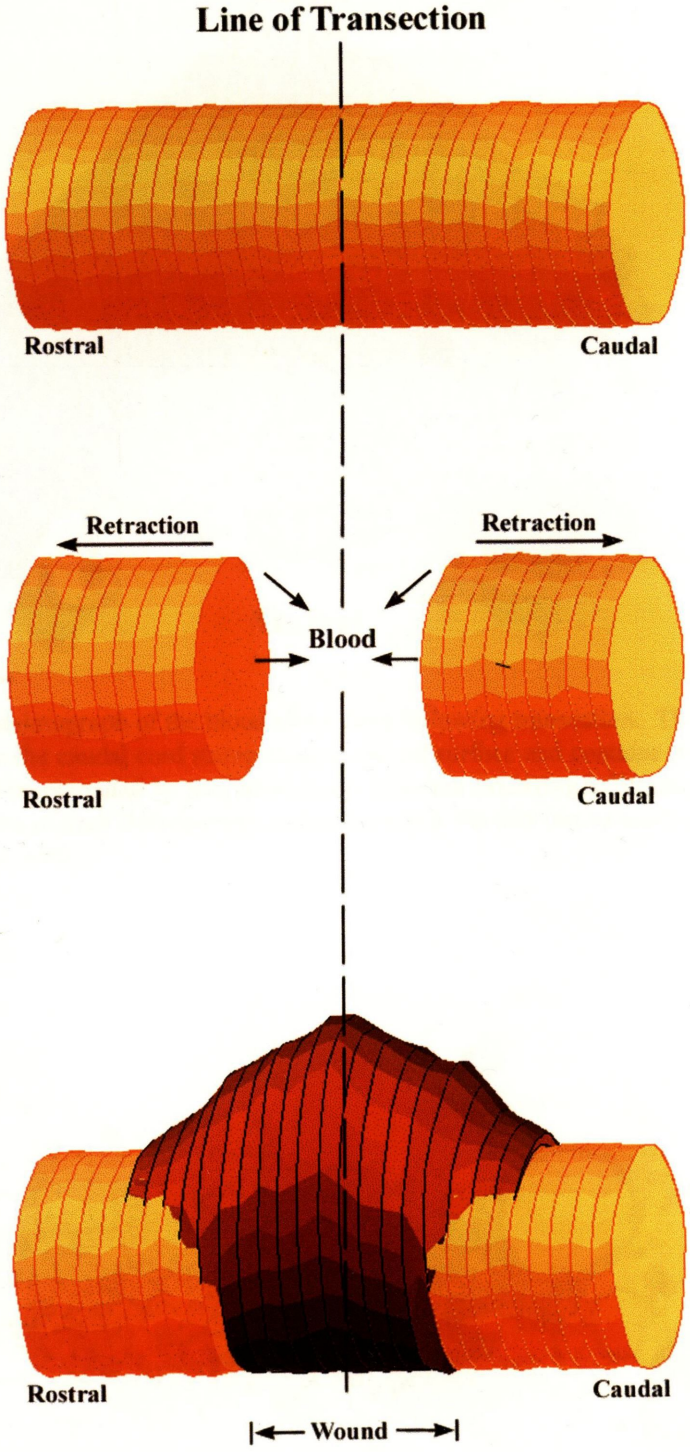


Figure 4.2. Diagramatic representation of the spinal cord following transection. The normal cord (represented in (a)) on transection, retracts to form a gap between the rostral and caudal stumps (b) that quickly fills with blood from severed blood vessels in the cord and meninges (c). The blood quickly congeals to form a blood clot (shaded portion) that covers the transection gap and portions of the stumps on both sides.

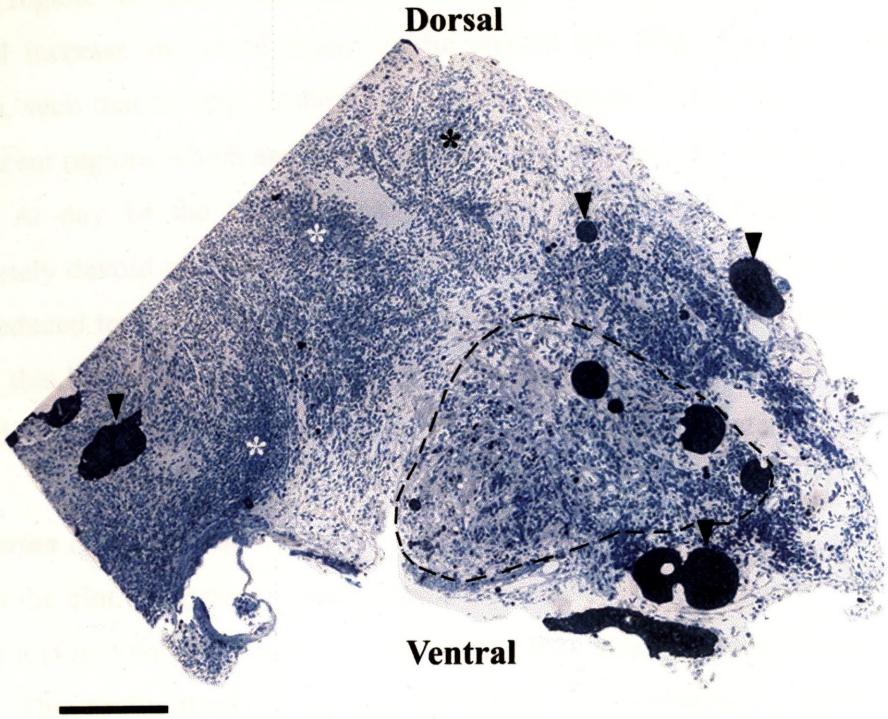


Figure 4.3. Photomicrograph of the blood clot 4 days following transection. This cross-sectional view is taken from the caudal cord stump close to the cut surface and contains remnants of the degenerating cord (demarcated by the dotted line). Note the extensive infiltration of erythrocytes (*) and the presence of dark homogenous structures within the clot (arrowheads).
Scale bar = 200 microns.

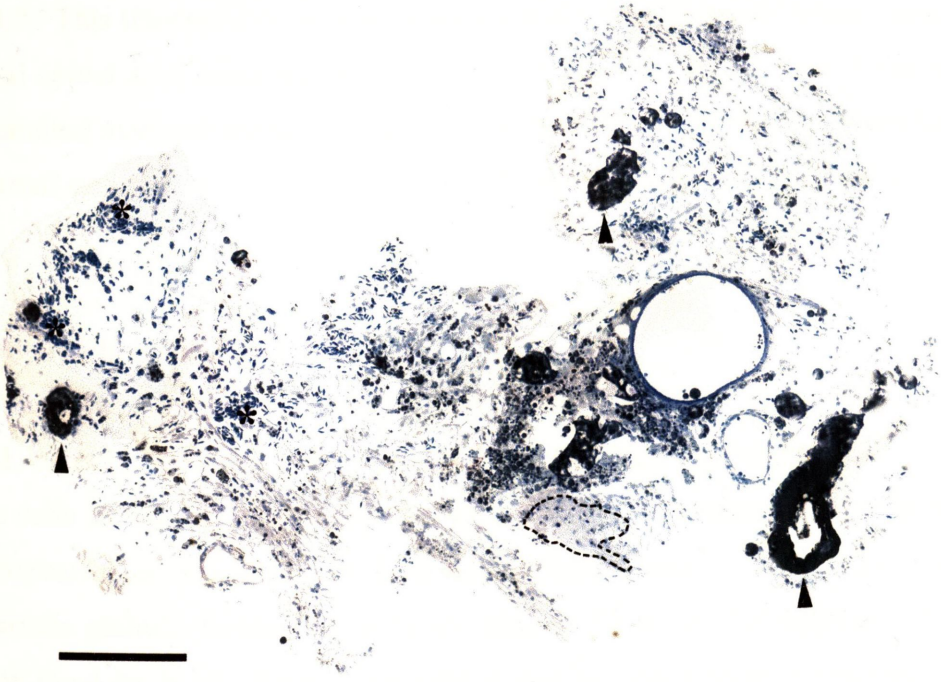


Figure 4.4. Photomicrographic montage of the blood clot at day 8. Note the presence of the blood clot in conjunction with the developing bridge (dotted line). Fewer red blood cells are present (*), however numerous macrophages/monocytes and fibroblasts are evident, as are large accumulations of dark staining debris (arrowheads) that are found close to the larg blood vessel.
Scale bar = 200 microns

wound region. By day 8 the blood clot has begun to reduce in size concurrent with the gradual increase in neural tissue in the wound site (Fig. 4.4), extending from the stumps, such that by day 10 there is a further reduction in the size of the clot, leaving translucent regions which are still present dorsally and laterally (see Fig. 4.5).

At day 14 the clot is greatly reduced and consists of clear regions and is completely devoid of blood-borne cells. The clot is either completely absent by day 20 or is reduced to small lateral thickenings located on top of the regenerating meningeal tissue; this has been seen as late as 200 days post transection. In all cases the bridge formed by the clot has been displaced by regenerating neural material by day 20.

Formation of the neural bridge

Within the clot, outgrowing neural tissue from the stumps, primarily ventrally, as seen by day 6 (Fig 4.6a) spans the gap and forms a very slim, tapering bridge by day 8 (Fig 4.6b). This bridge thickens by days 10 and 14 and continues to expand until day 26 (Fig. 4.6c, d) thereafter reducing to more normal proportions (Fig. 4.6e). However, the bridge is evident as a tapered zone as long as 144 days following surgery (Fig 4.6f).

The changes in size of the bridge and of the stumps are displayed graphically in Figure 4.7. This illustrates the initial formation at day 8 of the small bridge (around 5% of normal spinal cord area) and its subsequent expansion. By 14 days it has attained 80% of normal area and continues to expand by days 20 and 26. By day 54 the bridge is 40% normal size and even by day 200, it is still only 70% of the normal cross sectional area.

The components of the blood clot

Initially, such as at 4 days, the blood clot is composed mainly of the constituents found in blood, namely nucleated red blood cells, macrophages and other blood-associated immune cells in the serum. By approximately 6 days, fibroblasts are seen in the clot, which hereafter is considered to form a scar-type tissue. These cells possess a characteristic globular to elongate structure and can be easily distinguished from other cells (see Fig.4.8a, b, c). Elastic fibres are absent but small loosely arranged collagen fibrils were occasionally found, usually in close proximity to the fibroblasts, but large accumulations were never found. Blood vessels (capillaries) are present in the lesion site by day 6 dispersed throughout the scar. At day 8 the number of capillaries present in the scar increases (see Fig. 4.9) and they are often found close to the lead

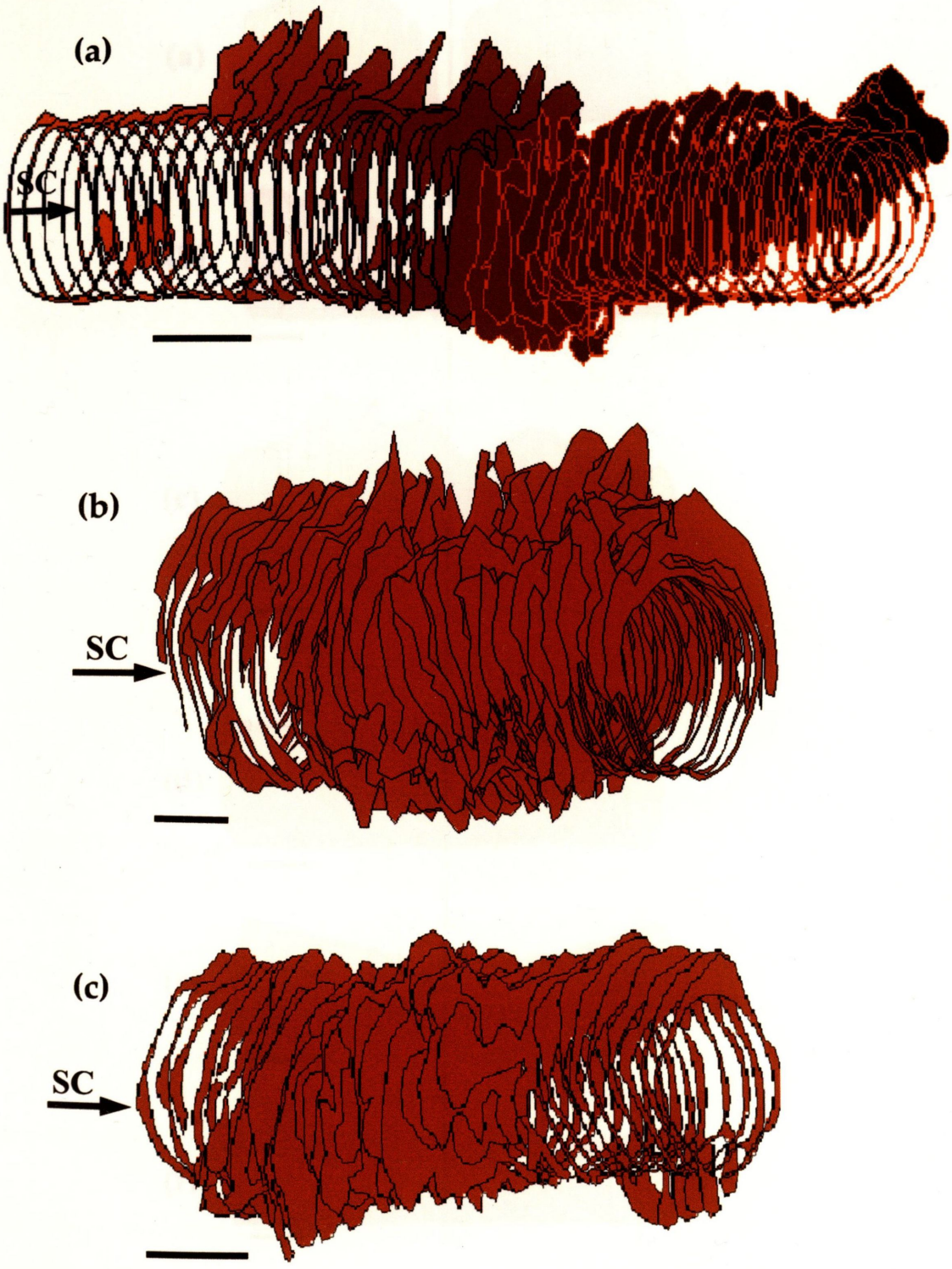


Figure 4.5. Reconstructions of the blood clot/scar at days 6 (a), 8 (b) and 10 (c). Note the profuse coverage of the clot over the transection gap and associated stumps by day 6. At later stages the clot is still present within the transection site but gradually reduces in size in conjunction with the appearance of regenerating neural tissue. Sc = spinal cord. Scale bar = 300 microns.

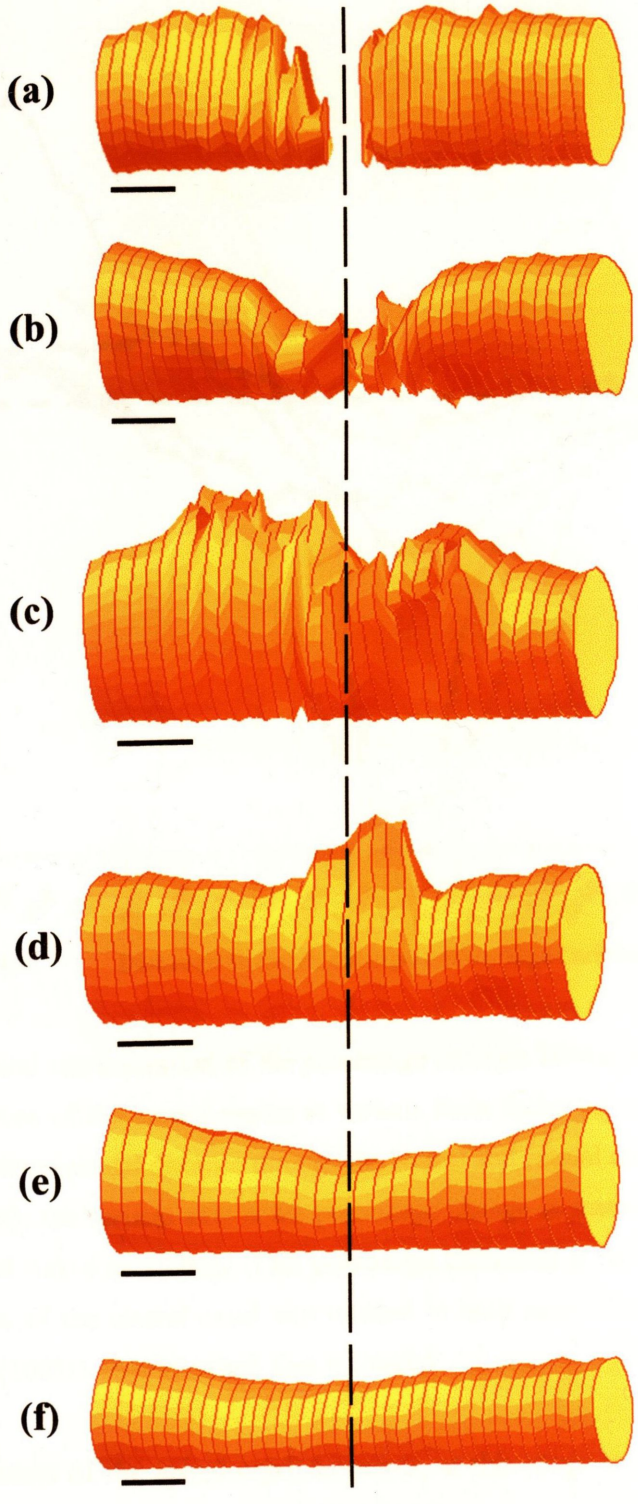


Figure 4.6. Reconstructions of regrowth through the wound site and stumps at 6 (a), 8 (b), 14 (c), 26 (d), 54 (e) and 144 (e) days. Note the extension of regenerating tissue at day 6 that produces the first reconnections of the stumps by day 8. With time the bridge of neural material increases in size (days 14 and 26) whereupon there is a reduction in size to produce a 'bottleneck' effect (day 54) that subsequently increases in size to more normal structure. Note that the offset of the reconstructions is in accordance with the approximate middle of each wound site. The dotted line represents the approximate centre of the lesion site/bridge. Scale bar = 300 microns.

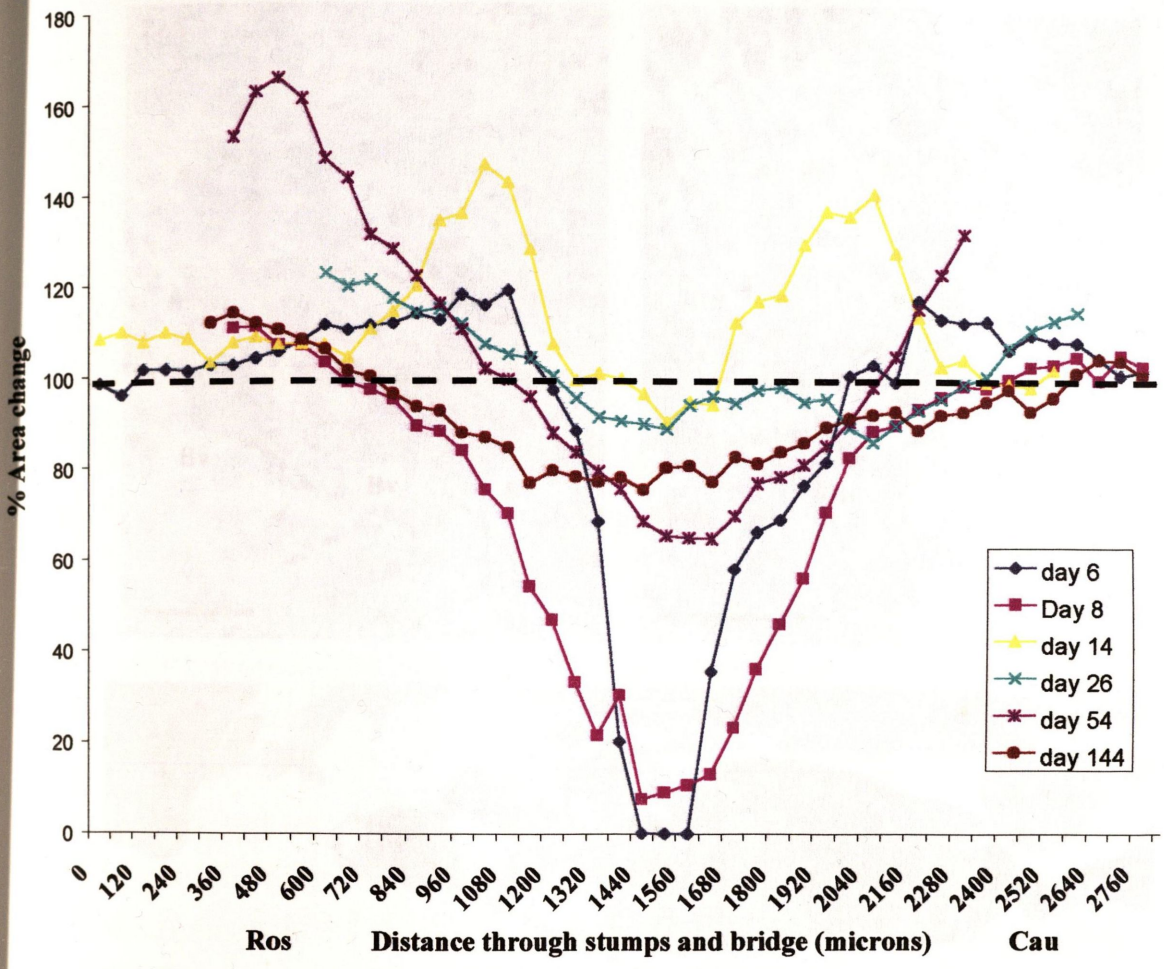


Figure 4.7. Graphical representation of the percentage changes in transectional area measured from semithin sections of the wound region at various times following spinal cord transection. The X-axis is the rostro-caudal distance through the rostral and caudal stumps and the wound in the middle (microns); the vertical axis is the percentage change in transectional area related to adjacent spinal cord (taken as 100%). This percentage difference is for neural tissue only, the cross sectional area of the central canal was omitted in each case. The dotted line represents normal cord tissue (100%). Ros= Rostral, Cau = Caudal.

regenerating elements of the spinal cord; however, at this stage relatively few capillaries are associated with the regrowing neural tissue. The components of the blood clot/scar disappear at different times: erythrocytes are removed first (around day 8), then the fibroblasts (around day 14) and finally the macrophages. The blood clot/scar 'matrix' produced by the extensive haemorrhaging is the last component to be removed, remaining for up to 20 days following injury. It was not determined whether the blood vessels in the scar are also removed or are incorporated into the forming neural bridge.

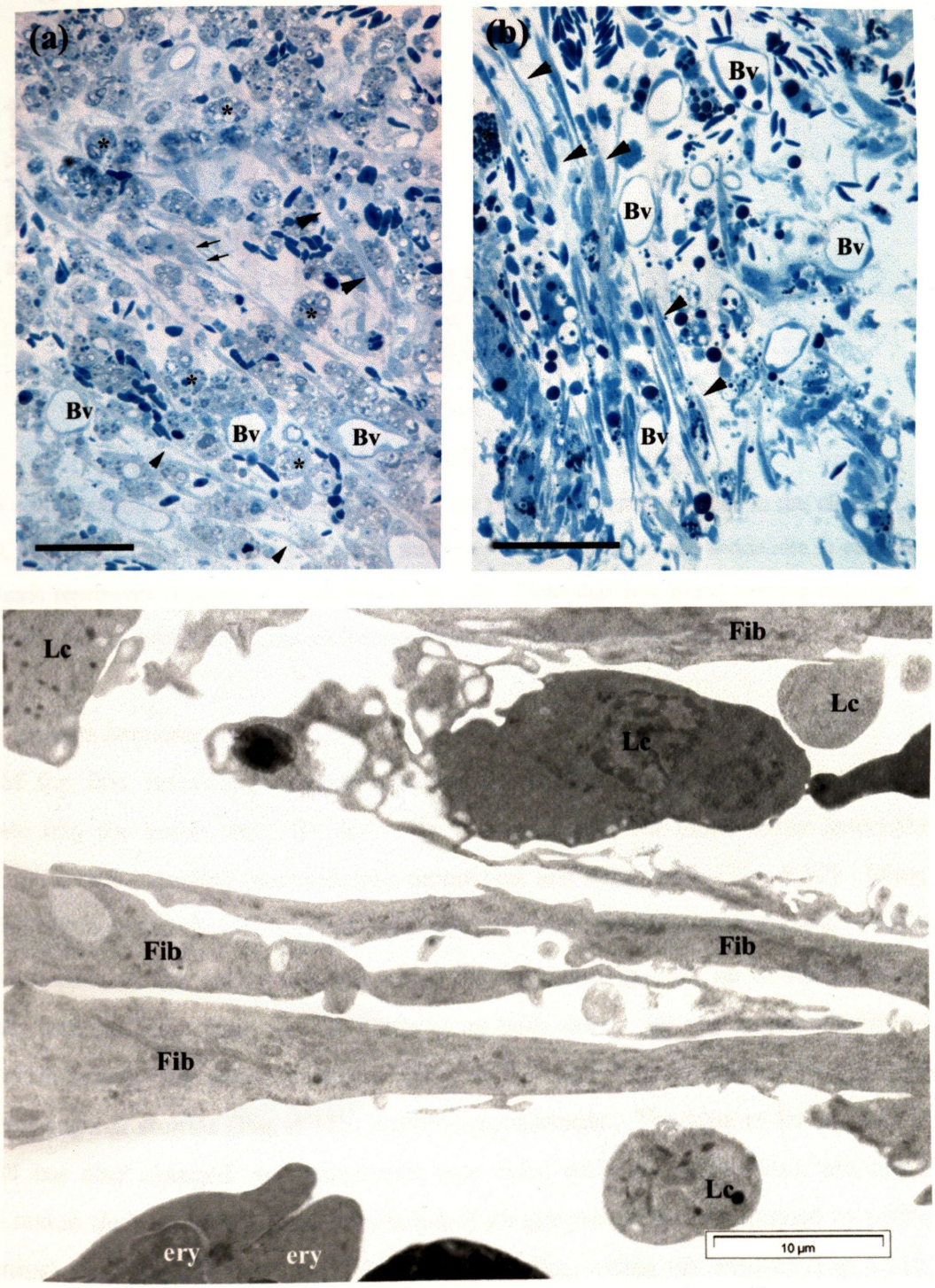


Figure 4.8. Photomicrographs of fibroblasts within the blood clot at days 6 (a) and 8 (b) (arrowheads). Cells are distinguished by their characteristic elongate morphology however other shapes are found based on an elipsoid morphology (arrows). Note the decrease in erythrocytes in the blood clot/scar by day 8. At the level of the electron microscope at day 8 in (c) the different cell types can be seen, fibroblasts (Fib), erythrocytes (ery) and different macrophagic leucocytes (Lc) that include fibroblasts. Note the presence of phagocytic leucocytes (*) and blood vessels (Bv) interspersed between the fibroblasts with an increase in number from day 6 and the absence collagen and elastic fibres. Scale bar = 50 microns.

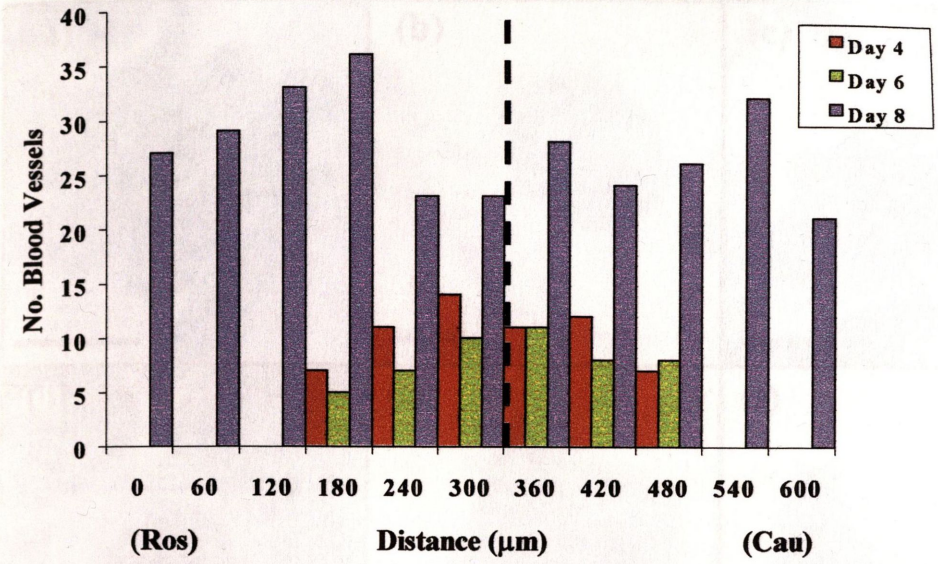


Figure 4.9. Graphical representation of the number of blood vessels present in the clot/scar at days 4, 6, and 8. The dotted line represents the approximate centre of the lesion site in each and the X-axis represents distance through the lesion site. Note that few blood vessels were found in the lesion site at days 4 and 6 but an increased number were found by day 8.

The leucocyte response to injury

One of the first reactive processes concerns the different leucocyte cell types that infiltrate into the lesion site. By day 4, for example, different blood-borne leucocyte types are found, including macrophages, monocytes and neutrophils (Fig. 4.10). Many of these cells are mostly interspersed between the profuse erythrocyte population within the blood clot. A few cells are found within the degenerating cord, up to some 900μm rostrally and caudally, from the cut surfaces on both sides. By day 6, the number of leucocytes within the blood clot/scar (Fig. 4.11a) and the developing bridge and associated spinal stumps (Fig. 4.11b) increase considerably. The type of leucocyte cell present has also changed: non-phagocytic type cells, such as lymphocytes, are rarely found and in their stead is a large population of phagocytic cells characterised by (often numerous) large vacuoles of material including myelin, within the cytosol (Fig 4.11d, e). Consequently, these cells are greatly increased in size due to the large intake of phagocytosed material. Cells in close association with degenerating myelin often possess numerous pseudopodal extensions and are often in close association with other phagocytic cells. A smaller set of these cells is interspersed between the degenerating (Fig 4.13a) and regenerating material within the spinal stumps (Fig 4.13b). Coupled with the change in the leucocyte cell-type is an apparent fluctuation in the numbers of

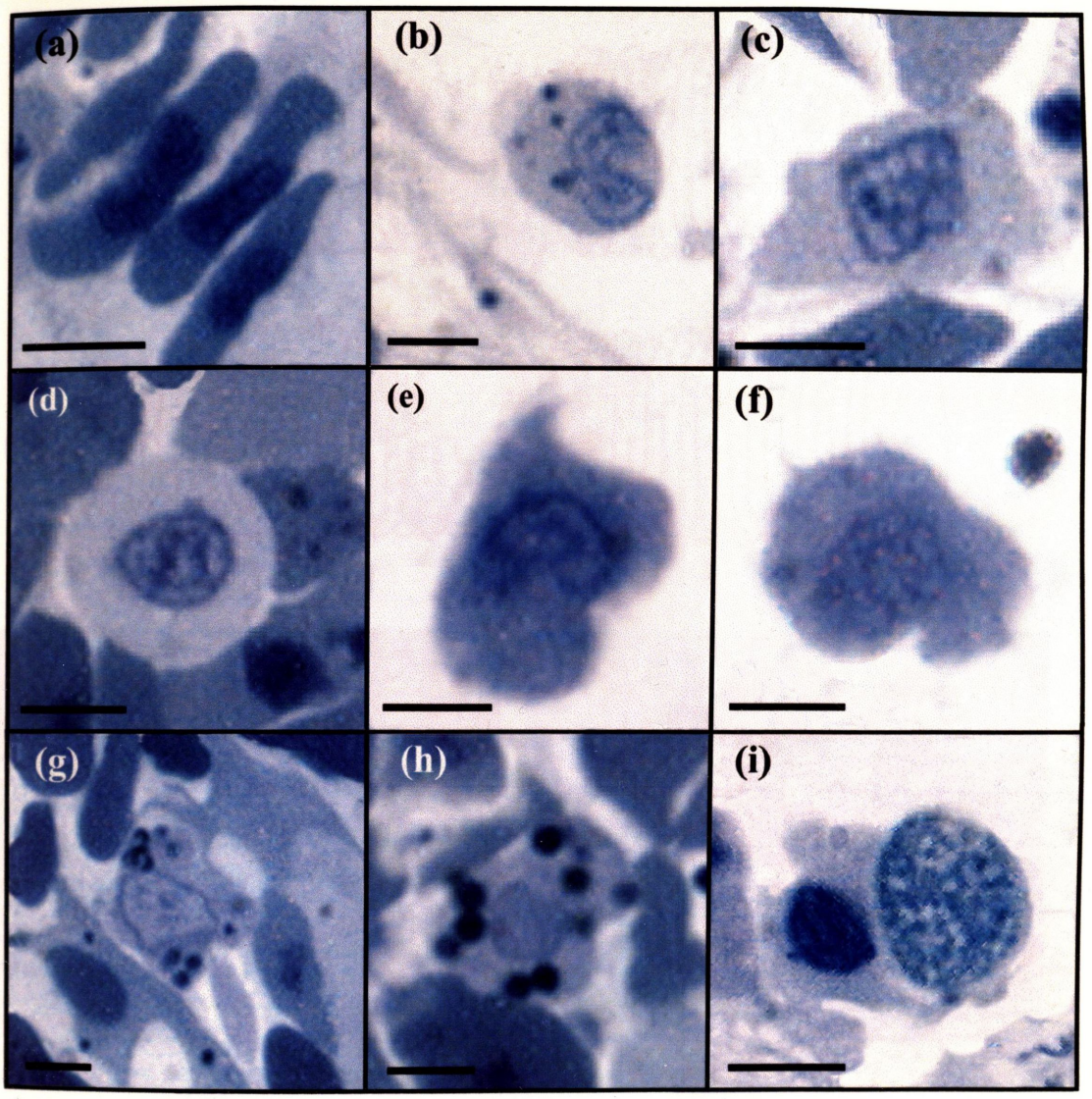


Figure 4.10. Montage of the different haematological cell types present in the blood clot by day 4. At this stage erythrocytes are the predominant cell type (a) and are characterised by an elongate to ovoid cell shape with a centrally placed nucleus. Note the intense staining of the nucleus and the cytoplasm. Thrombocytes are the other non-leucocyte type cell present, both (b) and (c) may represent the structure of this cell type in the eel, possess an ovoid to elongate structure are lighter staining than erythrocytes, possess an irregular shaped nucleus and cytoplasmic inclusions. Lymphocytes are frequently found in the clot and are characterised by an intense staining centrally placed circular to ovoid shaped nucleus in a light staining cytoplasm. The cell shape is circular to ovoid. Monocytes and macrophages are identified by their irregular cell shape and dark staining cytoplasm that is generally devoid of granules represented in (e) and (f). By far granulocytes are the predominant leucocyte within the clot and are represented by a light staining cytoplasm and slightly darker nucleus and with numerous dark staining granules within the cytoplasm. Typical granulocyte cells, of the neutrophil subtype are present in (g) and (h), while in (i) cells were occasionally found that resembled eosinophils with numerous small granules present in the cytoplasm.
Scale bar = 5 microns

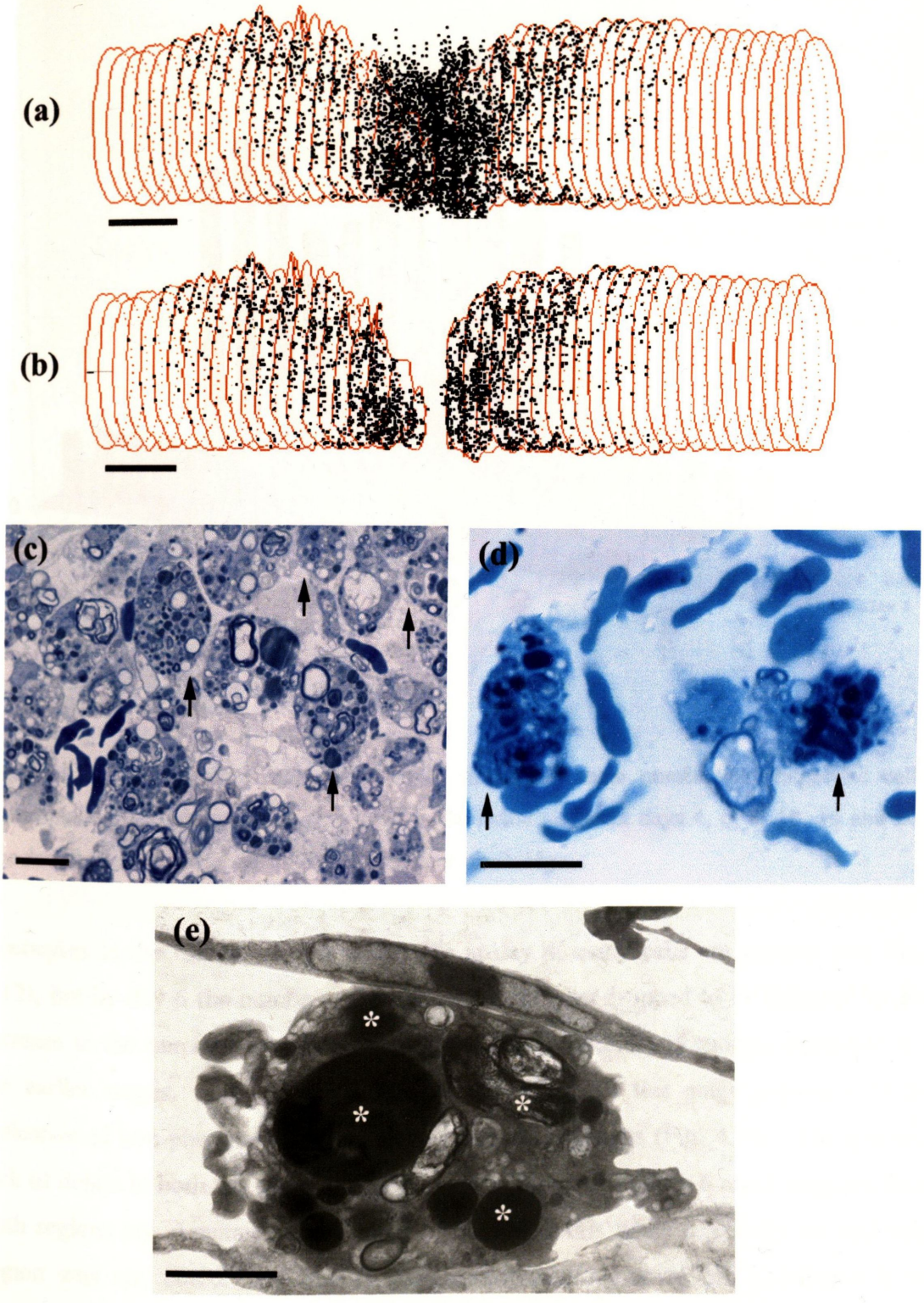


Figure 4.11a, b, c, d, e. In (a) and (b) reconstructions of the bridge at day 6, the distributions of leucocytes can be seen in (a) the spinal stumps and cord and (b) in the lesion site. Note the accumulation of cells close to the cut surface of the stumps. In the two photomicrographs (c) and (d) it can be seen that these cells are actively phagocytosing debris, particularly myelin sheath (arrows). At the level of the electron microscope (e) numerous dark cytoplasmic inclusions (*) can be seen indicating active phagocytosis. Scale bar = (a), (b) = 300 microns, (c), (d) = 10 microns, (e) = 5 microns.

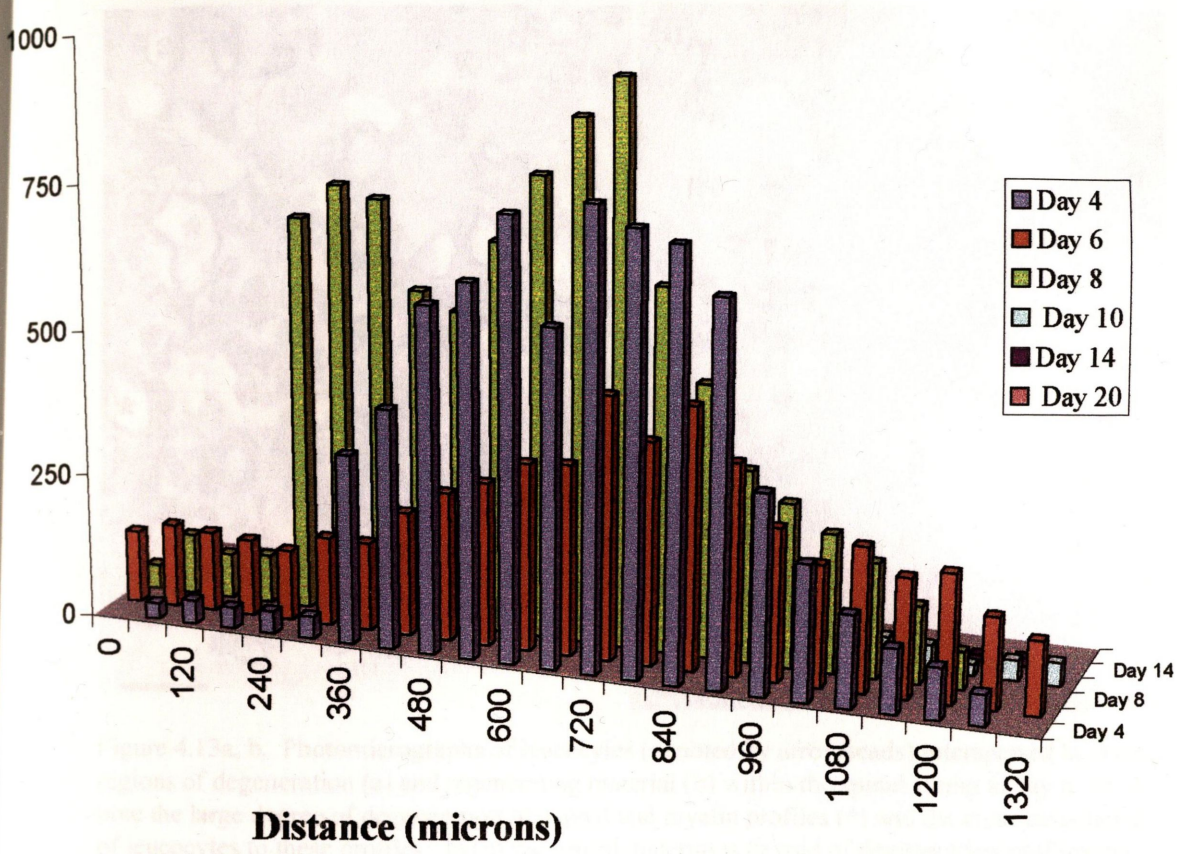


Figure 4.12. A graphical representation of the approximate number of phagocytic cells (neutrophils, macrophages and monocytes) in the lesion site from days 4, 6, 8, 10, 14 and 20. The dotted line represents the middle of the lesion site/bridge.

leucocytes in the bridge. In the lesion site at day 4, many cells are present (see Fig. 4.12), but by day 6 the numbers of phagocytic cells have dropped to be followed by an increase in the numbers by day 8, but they display a different phenotype compared to the earlier stages. Leucocytes in the blood clot/scar at this stage possess a form indicative of non-phagocytosing monocytes and macrophages (Fig. 4.14). The general lack of debris in both the spinal stumps and blood clot/scar at days 6 and 8 suggests that both regions are simultaneously cleared of cellular debris while selectivity for any one region was not noted. By day 10, the macrophage/monocyte cell population is in decline although cells are still evident within the remnants of the blood clot/scar tissue surrounding the developing bridge. No cells were found in the bridge. With further survival times (days 10, 14), the number associated with the regenerating bridge diminishes considerably (see Figure 4.15), such that by days 20 and later, reactive leucocytes are absent from the bridge neural tissue.

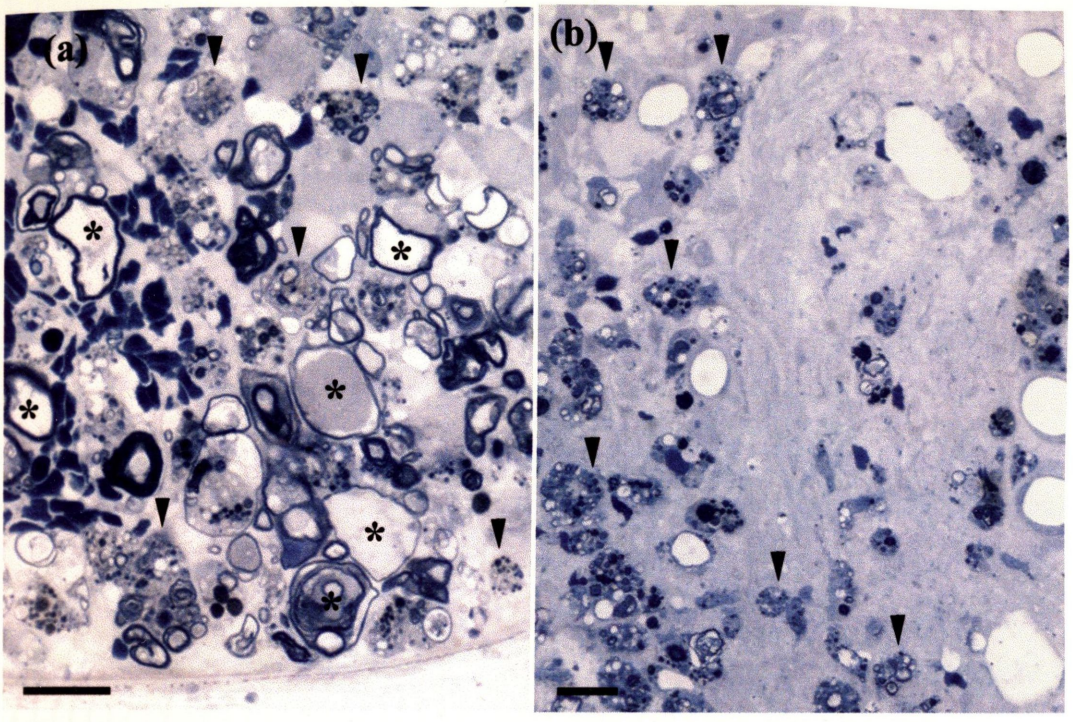


Figure 4.13a, b. Photomicrographs of leucocytes (denoted by arrowheads) interspersed between regions of degeneration (a) and regenerating material (b) within the spinal stump at day 6. In (b) note the large degree of degeneration of axonal and myelin profiles (*) and the close association of leucocytes to these profiles. In (b) the neural material is devoid of degenerating profiles but numerous leukocyte profiles can be seen intermixed with the regenerating tissue. bv = blood vessels, men = meninx. Scale bar = 20 microns.

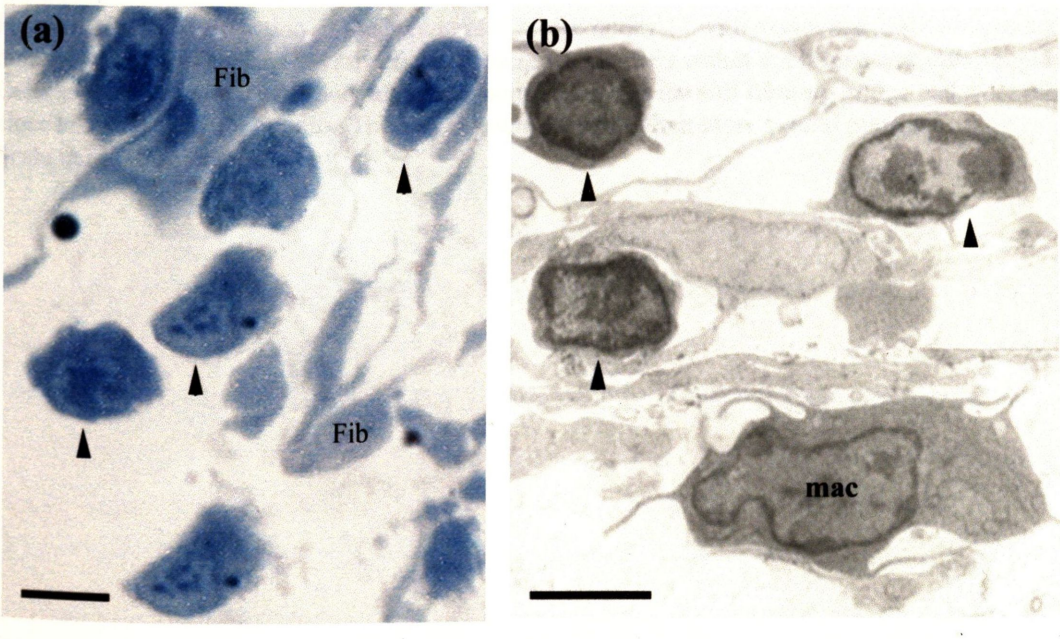


Figure 4.14a, b. Leucocytes (arrowheads) in the bridge 8 days following injury. In (a) note the lack of cytoplasmic inclusions and the small size of the cells that is also seen in the electron micrograph in (b). Note the macrophage (mac) in (b). At this stage many of the cells that infiltrate the blood clot/scar appear not to be phagocytosing debris. Fib = fibroblast. Scale bar = 5 microns.

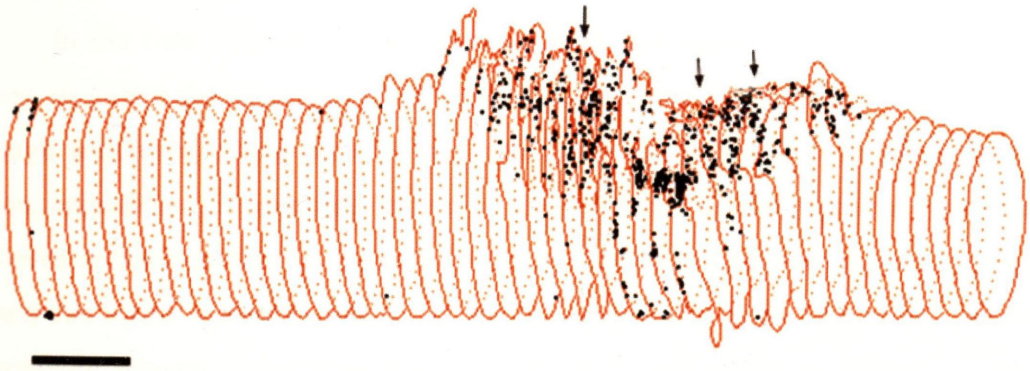


Figure 4.15. Reconstruction of the regenerated bridge at day 14 with associated macrophages and monocytes (arrows). Note the reduction of leucocyte numbers within the bridge and stump regions. Cells are isolated to the periphery along the 'horn' regions of the still forming bridge and were often close to the developing meninx. There is a general absence from more ventral portions.
Scale bar = 300 microns.

4.4 Discussion

The spinal cord of the eel reacts immediately to transection by retracting the cut ends, indicating that a certain degree of elastic tension exists within the cord. Whether this tension is created by the protective meningeal sheath which is known to possess elastic properties (see Chapter 3), by the blood vessels, by the neural tissue itself, or by a combination of all remains to be determined. But a similar gap has been observed in other studies. For example, cord separation of 1-2 mm was noted by Duffy et al. (1992) following tail transection in the lizard, *Anolis carolinensis*, and Hibbard (1963) found a gap of approximately 0.25mm in the transected lamprey spinal cord. In mammals the space created can often be large, as when Cheng and Olsen (1995) observed a gap of 4mm after cord transection in rats.

In the case of anamniotes, relatively little is known of the initial reactions to injury, including the structure of the material that fills the gap formed at transection and through which regrowing neural tissue must pass. In only one type of experimental lesion, amputation, is anything known of the behaviour of the regrowing cord tissue. But even in this experimental system the resultant blastema (self organising regrowth of tissue) that forms is poorly understood, and the relationship of the regrowing cord to the surrounding somatic tissue is unknown (see Anderson and Waxman, 1983a).

It is well acknowledged that the CNS of all vertebrates is endowed with a rich blood supply (e.g. Rowley et al., 1988; Peters et al., 1991) and it can be assumed that following all types of injury, haemorrhaging will occur as a natural consequence of blood vessel disruption. Obviously traumatic lesions such as transection and amputation will result in profuse bleeding (e.g. Hibbard, 1963), whereas it will be less following microlesion, contusion and compression injuries (e.g. Davies et al., 1996), but depending on the type and severity of the injury it can be assumed that a blood clot of varying size will occur. Nevertheless, Hibbard's (1963) note of the presence of 'a large mass of extravated blood filling the gap between the cut ends of the transected cord' is the only report that makes reference to a blood clot in the wound in any anamniote system. The presence of a 'scar' is better described and has been reported following cord (Bernstein and Bernstein, 1967) and optic nerve (Bohn et al., 1982; Hirsch et al., 1995) injury in anamniotes. In the amniotes, haemorrhaging has been frequently described (e.g. Matthews et al., 1979) and the ultimate effects in promoting

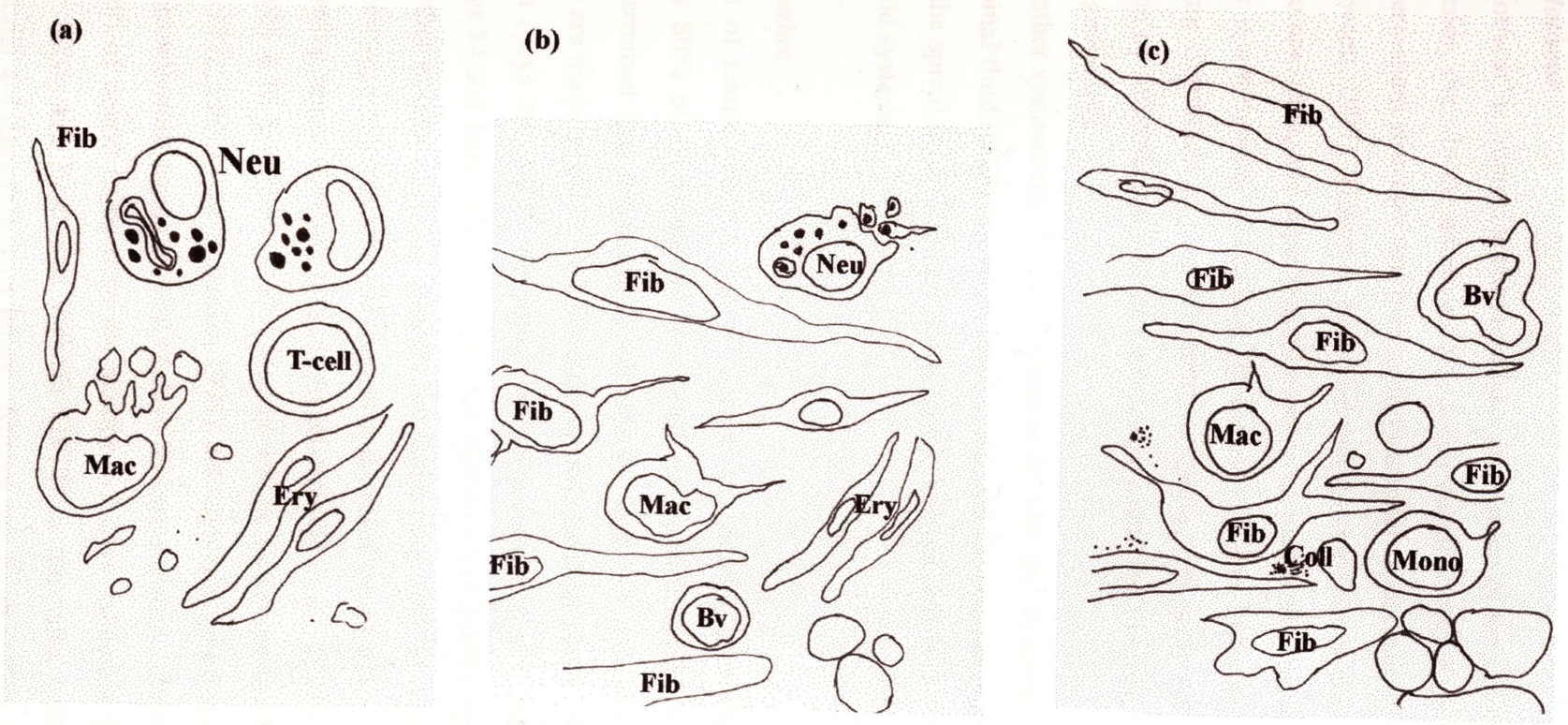


Figure 4.16. Diagrammatic representation of the different components of the scar tissue in the lesion site at days 4 (a), 6 (b), and 8 (c). Mac = Macrophages, Ery = erythrocytes, Bv = Blood vessels, Fib = Fibroblasts, Neu = Neutrophils, Mono = Monocytes, Coll = collagen.

scar formation are well known (e.g. Davies et al., 1996; Fawcett, 1997; Ridet et al., 1997).

The blood clot/scar

The term 'clot/scar' is imprecise but provides a description of the milieu that is present within the lesion site. In the amniote CNS, a scar develops and remains at the site of injury as a permanent structure that is thought to hamper regeneration (e.g. Malhotra et al., 1990; Fawcett, 1997). However, in the eel this structure changes dynamically, both in size and composition, and appears at all times to be permissive to neural regrowth so the term scar is a somewhat misleading. In the eel it begins to form congealed blood and infiltrating fibroblasts to give a supportive matrix, the composition of which is altered in time by infiltrating leucocytes, particularly those of the phagocytic type (see Fig. 4.16 for summary).

Two other systems may also contribute to the clot and eventual scar formation: the cerebrospinal fluid (CSF) from the central canal, and the perimeningeal fluid (PMF) surrounding the spinal cord. Because of the injury, leakage will inevitably occur from both these fluid systems.

Bridge Formation

The regrowth of neural tissue in the eel occurs very quickly such that by day 14 approximately 80% of the volume of the normal spinal cord has been reconstituted. We have determined that outgrowth is initiated by days 4-6 and that the tentative reconnections are made by day 8 with further outgrowth by days 10-14. With extended survival times (days 20 and 26) the bridge increases further in size but thereafter it decreases (days 54 and 144). This timeframe for regrowth is in general agreement with results from other studies when we compare the initial outgrowth of neural tissue. In goldfish optic nerve, regrowing material appears in the distal (eye-side) portion between 2-7 days following injury (Levine, 1991; Rungger-Brandle et al., 1995) and traverses the wound site by 8-12 days (Reier, 1979; Murray, 1982a; Lowenger and Levine, 1988; Paschke et al., 1992; Strobel and Stuermer, 1994), although Blaugrund et al. (1993) did not identify regrowth until approximately 14 days following injury. Bohn et al. (1982) noted outgrowth of neural tissue from the stumps 5-7 days following transection in *Xenopus* optic nerve and Reier and Webster (1974) in the same system observed regrowing material 4-8 days following injury. Michel and Reier (1979), in a study of

Xenopus spinal cord recorded regrowing cord tissue in the lesion site 5-7 days post-transection, while Stensaas (1983) reported outgrowth from the stumps approximately 4 days following ablation of the spinal cord in the newt *Triturus*, with both stumps reconnecting 14 days later.

In the amniote CNS, where regeneration is possible, namely in the immature CNS and adult PNS, similar times for the outgrowth of neural material are found. For example, neural tissue outgrowth occurs by 3-5 days following transection of the cord in neonatal *Monodelphis domestica* in culture (Nicholls and Saunders 1996; Varga et al., 1996). Regenerating peripheral nerve follows a similar pattern with a time lag of 2-3 days, after which neural tissue begins to grow into the lesion site (Bisby, 1995). Moreover where growth in the adult CNS is possible, using the conditioning lesion paradigm, regenerating elements begin to extend into the lesion site by day 4 (Jacob and Croes, 1998).

The similarity in regrowth times in response to injury throughout vertebrates (where regeneration is possible) is striking. It may be the case that this timeframe reflects a certain reorganisation within the damaged tissue at the cellular level, resulting in the alteration of the normal differentiated phenotype into a more migratory 'plastic' phenotype. Such a reorganisation has been suggested for some cell types following injury (O'Hara et al., 1992; Chernoff, 1996).

Source of regrowth

The medio-ventral outgrowth of neural tissue observed in the present study, along the dorsal surface of the vertebral centrum is similar to that found by Michel and Reier (1979) in their study of *Xenopus* tadpoles but contrasts with the situation following amputation in amphibians (Egar et al., 1970; Egar and Singer, 1972; Nordlander and Singer, 1978; Benraiss et al., 1997) and lizards (Simpson, 1968) where the outgrowth, in the form of an ependymal tube (see chapter 6), extends from central portions of the spinal cord. Singer et al. (1979) suggested that this centrally placed outgrowth following amputation reflected ontogenetic events and they proposed the 'blueprint hypothesis' in which outgrowth always occurs from central portions of the spinal cord. However, later studies showed that this is not always the case and that outgrowth can occur in more ventral regions of the cord, suggesting instead that there is a potential for regrowth that extends from central to ventral regions (see Anderson and Waxman, 1983a). Moreover, Simpson (1983) noted, in contrast to the earlier work of Butler and

Ward (1965, 1967), that neural regrowth did not necessarily extend from the regions surrounding the central canal after ablation injury in salamanders and found that neural tissue emanated from regions of the white matter. Stensaas (1983), using a set of ablation experiments that left the meninges intact in the spinal cord of the newt, *Triturus*, also found that regenerating neural tissue favoured the intact basal lamina at the cord periphery as a substrate.

In the regenerating anamniote optic nerve the method of regrowth is not well known as many of the reports have utilised crush rather than transection/ablation injuries (e.g. Lowenger and Levine, 1988; Levine, 1991; Blaugrund et al., 1993; Rungger-Brandle et al., 1995; Beazley et al., 1997). Since crush retains continuity of structure, neural regrowth occurs into the degenerating/regenerating neural tissue and not as a free, outgrowing entity, and so it is impossible to compare many of the optic nerve studies with the present research. However, a few have utilised transection (e.g. Scott and Foote, 1981; Bohn et al., 1982; Hirsch et al., 1995). Scott and Foote (1981) in the frog, *Rana pipiens*, noted regenerating material was central to the lesion by 3 weeks while Bohn and co-workers (1982), in a study of larval and adult *Xenopus,* reported a similar regrowth through a dense collagenous matrix in the centre of the lesion.

It would appear that regrowth of tissue following transection is different to that following amputation. The presence of a somewhat disorganised 'core' of tissue outgrowth from regions of the white and grey matter following transection/ablation in the cord differs considerably from the highly organised growth from the central canal region seen after amputation (Nordlander and Singer, 1978). Similarly, there may be a difference in the method by which the neural tissue of fish regrow compared to that of amphibians and reptiles. For instance, strong similarities in the method of tissue outgrowth exist between the transected and amputated spinal cord (the present study; Anderson and Waxman, 1983a) where outgrowth does not necessarily emanate from and around the central canal region, which is a strong feature of amphibian and reptile regrowth. In mammals where regrowth is possible, in neo/postnatal animals, the method of regrowth through the lesion site has not been documented in any detail (e.g. Nicholls and Saunders, 1996; Varga et al., 1996).

Composition of the blood clot/scar

The blood clot/scar tissue was found in the present study to consist of a variety of elements arising from different sources. In previous reports, in general the clot/scar in

general is described as comprising debris of neural and glial origin (e.g. Reier and Webster, 1974; Nona and Stafford, 1995) or being connective tissue of mesodermal origin (e.g. Bohn et al., 1982; Reier et al., 1983). Descriptions of cellular compositions are few: Michel and Reier (1979) noted macrophages and haematogenous elements within the lesion site along with debris in transected larval *Xenopus* spinal cord; Hirsch et al. (1995) noted fibroblasts within the lesion site of the goldfish optic nerve, as did Bohn et al. (1982) in the transected *Xenopus* optic nerve. We have found that the scar tissue that forms at the lesion site in the eel comprises fibroblasts, developing blood vessels, haematogenous elements (erythrocytes and leucocytes) and a ground substance (or matrix) in which the different cellular elements are embedded. Each component is discussed separately.

Fibroblasts

Fibroblasts have long been associated with the scar tissue that forms at the site of injury following spinal injury in mammals (Fawcett and Asher, 1999). Indeed the interaction of this cell type with 'reactive' astrocytes (see chapter 8) is considered to result in the formation of the inhibitory fibroglial scar (Krikorian et al., 1981; Fawcett and Asher, 1999), which forms when fibroblasts invade the lesion site. It is found following virtually all types of injury, save possibly microlesions, where only a small tract of injury is caused to the CNS (e.g. Davies et al., 1996). Conversely, in fishes, in those few studies that have described this cell type as a component of the scar tissue, regrowth of neural material has proceeded unhindered. Hirsch et al. (1995) demonstrated the presence of fibroblasts within the lesion site following transection or crush of the optic nerve. Similar observations were made following injury to the spinal cord (Michel and Reier, 1979) and the optic nerve of *Xenopus* (Bohn et al., 1982).

One noteworthy aspect of the fibroblast population noted in the present study, particularly at days 6 and 8, was the alignment of cells into loosely organised parallel 'sheets' that ran approximately dorso-ventrally and circularly. This was most pronounced close to regrowing neural material by day 8 and it may be argued that fibroblasts confer a cellular scaffold through which neural tissue can migrate, a hypothesis that is further strengthened by the fact that axons are frequently found in close apposition to fibroblasts by day 6 (see Chapter 7). Michel and Reier (1979) in regenerating *Xenopus* cord also noted that this cell type formed a complex trabercular meshwork of cells within the lesion. Bohn et al. (1982), following optic nerve

transection in the same animal, found that axons migrated through 'a cellular lattice of fibroblasts'; these authors further noted a graded appearance of fibroblasts within the lesion site with greater numbers being present closer to the middle of the lesion site. The origin of the fibroblast population within the vertebrate lesion site has often been attributed to meningeal cell infiltration, particularly in mammals (e.g. Wang et al., 1997; Krüger et al., 1986). In the present study, we have been unable to determine specifically a definitive origin for the infiltrating fibroblasts, although it is most likely that the majority of fibroblasts present within the lesion site possess a meningeal origin. Hirsch et al. (1995) concluded that the fibroblast population within the lesion site of the goldfish optic nerve arose from cells present in the interfasicular spaces and the surrounding 'nerve sheath'. Another possibility is that fibroblasts may originate from other sources, such as the connective tissue sheaths surrounding the damaged components of the overlying skeletal and muscular tissues.

Blood vessels

The presence of blood vessels in the wound, attaining maximum numbers by day 8 (see Fig. 4.17), is strongly indicative of angiogenesis. Angiogenesis is also a common feature in the CNS of other vertebrates following injury (Krum and Rosenstein, 1988; Rosenstein, 1996; from Krum and Rosenstein, 1998) and vascular endothelial growth factor (VEGF) which is known to be a potent stimulator of endothelial cells, has been shown to be expressed in the injured CNS. Krum and Rosenstein (1998), for example, have shown that levels of VEGF increased in the tissue surrounding the lesion site in the neocortex of rats following transplantation and stab injury. Therefore angiogenesis appears to a common reaction to injury in vertebrates and presumably increases the volume and flow of blood to the lesion site. Invariably in mammals, this has negative effects, as the increased blood flow carries with it large numbers of leucocytes (see next section).

The origin of the vasculature has not been settled in the present study, in part because of the complex organisation and frequent branching of vessels and also because of our inability to plot accurately the 3-D organisation of vessels using semithin sections collected every 10μm. However, two scenarios are possible: the vasculature could be an extension of blood vessels within the spinal stumps, or, it may arise from

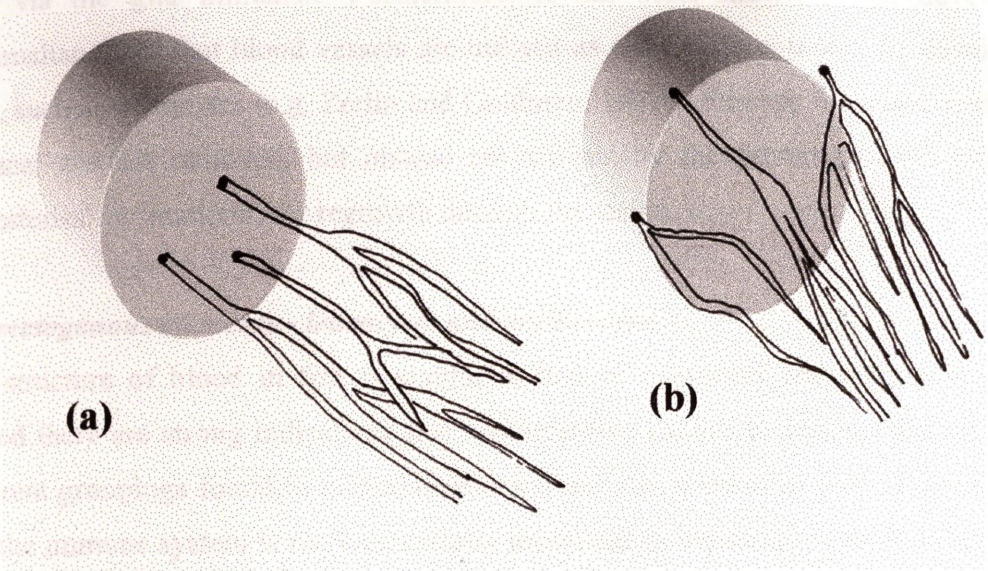


Figure 4.17. Possible origins for the blood vessel population within the lesion site. In (a) blood vessels arise from the vasculature within the spinal cord or (b) from the meninges.

vessels within the surrounding meningeal tissue (see Fig. 4.17). Simpson (1983) in one of the few reports that describe blood vessel formation in an anamniote model found little evidence of a capillary network in the regenerating cord and instead considered pial vessels to be the principal source. However, his report must be taken in the context of the animal model used, and the injury type - tail amputation in the lizard *Anolis*. Since the regenerating cord in this species does not grow into a lesion area but instead is a component of a blastema of newly forming tissue it is probable that different criteria govern vasculature formation around the forming spinal cord. Similarly, the developing cord within the blastema is composed of a small ependymal tube (see chapter 6) that may not be able to support any vasculature during this stage of development. Therefore, in so far as the eel is concerned, a neural origin for the blood vessels remains a possibility.

Within the constraints of the present study, the eventual fate of the scar blood vessels was not determined. Since virtually every other component of the scar tissue, such as fibroblasts, matrix and leucocytes are not components of normal neural tissue, it can be assumed that these elements are either removed from the bridge region or fail to be incorporated. However, neural tissue does contain blood vessels. Therefore, it is conceivable that those vessels in the path of neural outgrowth could be incorporated into the developing bridge. This is a particularly strong possibility since the meninges in the uninjured CNS contain numerous blood vessels that enter the brain and spinal

cord via the glia limitans. Furthermore, it has been shown in the developing mammalian CNS that blood vessels are utilised as early differentiators for developing cells, such as astrocytes (e.g. Zerlin and Goldman, 1997). Perhaps the blood vessels in the scar are not removed, but instead are utilised by the growing neural tissue as 'milestones' or 'markers' for regrowth through the lesion.

Haematogenous elements - leucocytes and erythrocytes

The structure of blood in fish is similar to that of mammals and other vertebrates. Indeed there are strong indications from comparative studies to suggest that all of the different groupings found in mammalian blood are also present in fish. This suggests that the immune system is phylogenetically preserved in vertebrates (see Rowley et al., 1988); we will assume, therefore, that *Anguilla* possesses the same variety of blood cell types as found in the goldfish and the carp (Rowley et al. 1988; Koumans-van Diepen et al., 1994; Rombout et al., 1997).

Erythrocytes are the largest population of circulating cells. In fish, as in mammals, these cells are flattened and biconcave, although in fish they are nucleated. Thrombocytes, which have almost identical functions to platelets in mammals, in that they are involved in the clotting of blood, have been shown in fish to possess phagocytic activity (Hill and Rowley, 1998). Leucocytes can be divided (as in mammals) into two groupings: granulocytes and agranulocytes. Granulocytes constitute the major group and can be divided into three different types: neutrophils/heterophils, eosinophils and basophils. There is considerable confusion in the literature relating to the structure and composition of the cells in this group in fish. It is generally agreed that neutrophils/heterophils are present in the blood; however the presence of eosinophils and, in particular, basophils, is still a matter of contention as they are found in some species, but not others (Rowley et al., 1988). A large literature exists concerning lymphocytes, B, T and NCC cells (fish equivalent of NK cells in mammals) and the reactions of these cells to different pathogens such as parasites (Evans and Gratzek, 1989; Leary et al., 1994; Lamas et al., 1994). Monocytes constitute the other agranulocyte population in the blood of vertebrates and are found free in the blood (monocytes) or within the body tissues as macrophages.

It can be assumed, therefore, that at least two different leucocyte-cell types possessing phagocytic activity may be present within the lesion site of the spinal cord. To what extent each contributes to 'mopping' up the debris is unknown. From the

morphology of cells at day 4 it appears that there is a general influx of cells due to the profuse bleeding into the lesion site. Therefore, all types are present and account for the large numbers of cells at this stage. The small cross sectional area of these cells suggests that only a few have begun to phagocytise debris within the wound site. At this stage it appears that most cells involved in this process are presumably neutrophils due to the presence of numerous distinct dark vesicles within the cytoplasm. By day 6 further recruitment of phagocytosing cells occurs and results in a large increase in cross sectional area due to often-large accumulations of debris-laden vesicles within the cytoplasm. At this stage there appears to be a loss in the number of cells and this is attributed to the removal of lymphocytes and thrombocytes from the lesion site. Specifying quantitatively the different types of phagocytically active cells at this stage is arduous, but it would suggest that there is a mixed group of neutrophils-macrophages within the lesion. In contrast to some studies in amniotes (Lawson et al., 1994; Avellino et al., 1995; Popovich et al., 1997) and anamniotes (Dowding et al., 1991; Battisti et al., 1995), where reference is made to the leucocyte response, the cells are generally considered to be macrophages with few references to the other cell types. It is interesting to note in the mammalian CNS, in many instances, neutrophils are reluctant to enter the CNS parenchyma (Perry et al., 1995). In the eel, cytoplasmic inclusions are evident within cells, some of which can be clearly identified as myelin while other, dark staining homogenous inclusions, that may possibly be compacted myelin debris, were also present; however these structures (often large) were also found extracellularly and so are not exclusive to the phagocytes. Phagocytosis of myelin debris is a well-known function of invading inflammatory cells such as neutrophils and macrophages in the mammalian CNS (Lotan and Schwartz, 1994). Similar activity has been described in the anamniote CNS (Reier et al., 1983) and phagocytic cells have been reported in regenerating *Xenopus* optic nerve (Bohn et al., 1982) and goldfish spinal cord (Bernstein and Bernstein, 1969).

At day 8 the number of cells within the lesion site increases in conjunction with a decrease in their size; phagocytes are still present, but in lower numbers. It is likely that a biphasic response occurs in which there is an initial infiltration of cells that with time is refined to a smaller population specific to wound repair. The second influx can be seen as the large increase at day 8 of smaller, irregular shaped cells often in close association with blood vessels that are considered to be moncytes/macrophages that have been recruited to the lesion site (see Fig. 4.12). The present results would suggest

Animal	Tissue	Lesion Type	Initiation (Day)	Max Numbers (Day)	Clearance (Day)	Reference
Rat	Brain	Microlesion	-	1-2	3-4	Davies et al. (1996)
Rat	Optic Nerve	Crush	-	7	21	Frank and Wolburg (1996)
Rat	Spinal Cord	Contusion	-	3-7	-	Popovich et al. (1997)
Rat	Brain	Needle Stab	1-3	3-12	-	Riva-Depaty et al., 1994
Mice	Brain	Ablation	-	2-6	12	Schauwecker and Steward (1997)
Amphibian	Optic Nerve	Transection	1	3-7	-	Bohn et al., 1982
Fish	Spinal Cord	Transection	-	2	-	Bernstein and Bernstein, (1969)
Fish	Spinal Cord	Transection	1-4	8	10-14	The present study

Table 4.1. Table summarising some of the different reports of leucocyte infiltration, maximum numbers and the time taken to clear from lesion site.

that at least neutrophils and monocyte/macrophage cells are involved in the response. The chronological order of the leucocyte response in the eel is summarised in the above table (Table. 4.1) along with comparisons with other studies. Concurrent with the infiltration of phagocytes within the lesion site, it would appear from the present study that maximum phagocytic activity occurs approximately by day 6, while the maximum number of cells is found by day 8. Thereafter the numbers decrease rapidly with the formation of the bridge, at around the 6-7 day mark.

A smaller population was found within the spinal stumps close to the cut surfaces, with a small number of cells penetrating the spinal cord for considerable distances. Whether these cells travelled into the cord from the cut surfaces, gained

entry through a breach in the glia limitans or the blood brain barrier, or are activated microglia could not be determined from the present study. It is well known particularly in mammals that any breach of these barriers results in the infiltration of monocytes-macrophages (e.g. Lotan and Schwartz, 1994; Merrill and Benveniste, 1996). It would appear that many if not all of the infiltrating inflammatory cells in the eel were involved in phagocytosing myelin debris that was found within the cytoplasm. Similar findings have been reported in the regenerating goldfish spinal cord (Bernstein and Bernstein, 1969) and the mammalian CNS (e.g. Lazarov-Spiegler et al., 1996). The limited distances travelled through the spinal cord is similar to that found in mammals, with most cells isolated to the lesion site (e.g. Popovich et al., 1997). At the onset of the formation of the bridge in the eel phagocytic cells were found within the regenerating neural tissue and comprised a small population of easily identifiable cells in the bridge once fully formed. What are the origins of these cells? It is possible that they may be of microglial origin as this cell type is well described in the amniote CNS (e.g. Raivich et al., 1999) and also in some anamniote species (Dowding et al., 1991) but in the present study we have been unable to identify cells that could be described as microglia. Alternatively a haematological origin may explain their presence, with cells becoming incorporated into the bridge during its formation. Since it is well known that microglia originate from haemopoietic origins (e.g. Eglitis and Mezey, 1997) and are considered to be of a quiescent macrophage phenotype it is possible that these cells constitute a small 'microglial' population in the bridge. At later stages of recovery (days 26+), identification of cells becomes difficult within the bridge, indicating that these cells are either lost or quiescent.

Since invading leucocytes contribute to the removal of debris within the scar tissue we may ask whether this infiltration is beneficial for regrowth? In mammals inflammatory cells are present in the lesion site within a short time after injury and remain there a further 21 days or so before declining (Avellino et al., 1995; Bisby, 1995). The beneficial roles attributed to these cells include the removal of dead tissue and debris (e.g. Friede and Beuche, 1993) and lipid recycling (e.g. Stoll and Muller, 1988). In fish, an upregulation of apolipoprotein A-I (Apo A-I) in the regenerating carp optic nerve (Harel et al., 1989) has been localised to macrophages suggesting that these cells recycle phospholipids and cholesterol in a manner similar to that of mammals. Other studies have shown that macrophages can be beneficial for axon regrowth (Lazarov-Spiegler et al., 1996). However, inflammatory cells seem also to modulate

inhibitory effects that contribute to the production of scar tissue. As part of the inflammatory response in the lesion site in mammals cytokines are released primarily by infiltrating macrophages and these are responsible, in part, for inducing astrocytes to become reactive (Campbell et al., 1993; see Merrill and Benveniste, 1996 for review). The extent of leucocyte-macrophage involvement in the development of the scar tissue may be dependent on the type of lesion. Davies et al. (1996) found that microlesions of the rat CNS induced only a transient influx of macrophages (inflammatory cells) that also triggered a transient stimulation of resident tract ramified microglia and astrocytes. The blood brain barrier was considered to remain intact and the leakage of blood into the lesion site was rarely found. Following larger lesions that induce extensive necrosis, bleeding and exudation, infiltrating macrophages/microglia remain in an activated state, continue to phagocytose necrotic material and debris, and become resident. Consequently, Davies and co-workers (1996) suggested that larger lesions induce a continuous stimulus to activate astrocytes and microglia and lead to the formation of an astroglial scar.

It appears that at least some of the many functions performed by mammalian macrophages are carried out by fish macrophages, such as phagocytosis (the present study) and upregulation of Apo-A-I (Harel et al., 1989), indicating a certain degree of homology between fish and mammalian inflammatory cells. Whether this extends to other aspects, such as the release of cytokines, remains to be seen.

Matrix

The origins of the component we have termed the 'matrix' (or ground substance) in the present study presumably stems from the clotting of blood to produce the gelatinous mass in which the different infiltrating blood-borne, meningeal/fibroblast and neural tissue components reside. Therefore, the components of the matrix initially, will be the different proteins involved in blood clotting. Although the blood protein content in fish is lower than in mammals (see Rowley et al., 1988), and relatively little is known of the different plasma components, it is known that fibrinogen and thrombin are present in some fish species, such as the lamprey (Doolittle, 1965). Blood coagulation in fishes is considered to occur in a similar manner to the mammalian process, producing a clot in a matter of minutes. Therefore the processes of thrombin conversion from prothrombin, which in turn results in the conversion of soluble plasma fibrinogen to fibrin, is considered to be conserved and indeed this process has been demonstrated in the

lamprey (Laudano and Doolittle, 1980). The formation of the fibrin-based matrix is termed the *provisional matrix* in mammals (Clark et al., 1982). At later stages this fibrin-based matrix is lysed by infiltrating fibroblasts, which then proceed to lay down a fibronectin and hyaluronan rich matrix (Clark, 1996). In the present study, fibroblast infiltration into the lesion site occurs by day 6 thus indicating that this movement of cells may effect a turnover of the matrix. Evidence to support such a turnover in fish comes from the study of Hirsch and co-workers (1995) where strong fibronectin labelling was noted in the lesion site. In mammals it has been shown that fibronectin is one of a small number of ECM components that is permissible to neural growth (see Fawcett, 1997) and will support neurite extension *in vitro* (Rogers et al., 1983). It can be concluded then that the fibrin and/or fibronectin based matrix within the lesion site of the eel is a permissible substrate for neural growth. However, fibrin and fibronectin are not the only matrix proteins present; others, such as vitronectin, thrombospondin, and tenascin are common components (see Yamada and Clark, 1996 for review). Two of these proteins have received particular attention since they are upregulated following injury. Tenascin and the chondroitin sulphate proteoglycan family (CSPG's) have been shown to possess growth inhibitory properties in adult tissue (see Fawcett, 1997), and are considered to act as inhibitory boundary molecules, having been demonstrated to be involved in axon guidance during development (see Fitch and Silver, 1997). It has also been shown that CSPG production is associated with the breakdown of the blood-brain barrier and infiltration of macrophages into the lesion site (Fitch and Silver, 1997). In this respect, the lesion site in the eel, with the obvious quite extensive damage to the blood-brain barrier displays all the hallmarks necessary for the production of such molecules. Whether tenascin or members of the CSPG family are present at the lesion site of the spinal cord in fish and other anamniotes remains, as far as we can ascertain, unknown. Battisti and co-workers (1992), however, have shown CSPG immunoreactivity at the lesion site of the goldfish optic nerve following crush, with increased levels between 1-3 weeks after injury. The well-recognised ability of the goldfish optic nerve to regenerate following injury (as with the spinal cord) suggests that in fish CSPG's may not be inhibitory to regrowth.

With the formation of a bridge of regenerating neural tissue in the eel from day 6 onwards, the clot/scar begins to reduce in size such that by day 14 it is almost absent. Therefore, a regulatory mechanism must be present that is set in motion to remove the matrix components. In mammals, this is achieved through the use of the proteolytic

enzymes, plasminogen activators and plasmin, and the whole process is rigorously controlled (see Clark, 1996 for review). Whether these specific enzymes are utilised to lyse the matrix in the eel and other fish regenerates or is carried out by another family of proteolytic enzymes is unknown. However, it is probable that a regulatory control similar to the plasminogen activator/plasmin pathway found in mammals is present.

Fibres

The presence of small amounts of collagen but not elastic fibres in the lesion site, particularly at day 8, has been described in the lesion site of the regenerating goldfish (Hirsch et al., 1995) and *Xenopus* (Bohn et al., 1982) optic nerve. Interestingly Bohn and co-workers (1982) noted that this extracellular fibre was abundant in the lesion site of the adult regenerates but scarce in juvenile tadpoles. In this context it is interesting to note that the authors found that regrowth in the adult was not as accurate as in the juvenile and attributed this inaccuracy, in part, to the presence of dense collagen bundles in the lesion site. In the present study, we did not find such dense aggregations of collagen bundles and instead fibres were distributed in small loose bundles close to, and interspersed between, the fibroblasts. Although not stated by Hirsch and colleagues (1995) in their study, the collagen distribution in their electron micrographs bears strong resemblance to the present study. Therefore, the lesion site in the present study and in the goldfish optic nerve (Hirsch et al., 1995) display characteristics closer to juvenile *Xenopus* than the adult regenerate. Although often associated as a component of the inhibitory scar that forms following CNS injury in anamniotes, collagen has been shown to be capable of supporting the regrowth of motor axons in the spinal cord (Risling et al., 1993). It is possible, therefore, that as suggested by Bohn and colleagues (1982) the collagen bundles within the lesion site of the eel may act as a substrate along which neural tissue can migrate.

Summary of main findings

- The first event following transection injury is the extravasation of blood into the lesion site that congeals to produce a blood clot that provides continuity between both spinal stumps.
- Regenerating neural tissue infiltrates the blood clot to produce the first connections between both stumps by approximately day 8. We have termed this regrowth the

'bridge' and it continues to develop and increase in size until approximately day 20, whereafter a gradual reduction in size takes place.

- Fibroblasts colonise the blood clot by day 6 and produce parallel arrays of elongate cells
- Angiogenesis of undetermined origin is evident in the bridge by days 4 and 6 the numbers sharply increase by day 8, indicating an increased metabolic demand in the lesion site/developing bridge.
- A biphasic influx of blood cells occurs in the bridge. Large numbers are present at day 4 which fall by day 6 but increase again by day 8. We attribute this to the removal of inappropriate cell types and the influx of wound specific leucocytes.

Chapter 5

The organisation of the regenerating central canal:

I. The ependyma

5.1 Introduction

It is usually thought that once injured the ependyma surrounding the ventricles of the brain and spinal cord of amniotes fail to contribute to the repair and regrowth of the injured region (e.g. Matthews et al., 1979). More recently, however, evidence suggests that this may not always be the case, and that under certain conditions, the ependyma is capable of mounting a successful response to injury (e.g. Bruni and Anderson, 1987). The discovery of neural stem cells in the adult amniote CNS indicates that the ependyma and subependyma may retain a degree of exploitable plasticity that has already been shown to produce, under correct conditions, new neurons and glia *in vivo* (Morshead et al., 1994; Temple and Alvarez-Buylla, 1999). Indeed, following injury to regions of the rat brain there is an increase in the development and survival of stem cells (Johansson et al., 1999).

Whatever the situation in higher vertebrates, the ependyma in the CNS of some anamniote species retains considerable regenerative ability (e.g. Egar and Singer, 1972; Anderson et al., 1983) and appears to play an integral part in the regenerative event, suggesting possible stem cell ability. For example, Simpson (1964; 1968) found that regeneration of the amputated tail of the lizard *Lygosoma* is prevented if ependymal cells are destroyed. Certainly, the ependymal reaction to injury appears to lead to the production of a new central canal (see Anderson and Waxman, 1983a for review), but it remains uncertain whether it plays a role in facilitating the extension of regrowing axons.

The possible role of the ependyma in the eel spinal cord was examined in the present study. The objectives were twofold:

(1) To chart the distribution of ependymal cells in the regenerated bridge by the use of serial sections of light and electron microscopic material. In doing so, it was hoped to determine the role of ependymal cells in the formation of bridge and to see if they were the primary cell type facilitating axon regrowth (Nordlander and Singer, 1978) or if their growth was synchronous with the regrowing axons as found by Michel and Reier, (1979) in the regenerating *Xenopus* spinal cord. In all previous studies of central canal and ependymal proliferation, interest has been directed towards the proximal stumps and the wound site (e.g. Egar and Singer, 1972; Anderson et al., 1986). Therefore, in order to determine if there is a canal and ependymal reaction in

more distal portions of the cord away from the wound, the central canal in both the rostral and caudal cord up to 1mm away from the transection was also examined.

(2) Following transection, the ultrastructural and immunohistochemical changes to the cell population surrounding the central canal - ependymal cells (ependymocytes), tanycytes and light staining cells (see chapter 6) - were documented. The immunoreactivity to the common intermediate filaments GFAP, S-100 and vimentin was determined for cells in the stumps and for cells migrating into the bridge region. In particular, we wanted to determine the role of tanycytes in the developing bridge as these cells correspond to the radial glia of the developing vertebrate nervous system (e.g. Levitt and Rakic, 1980; Pixley and deVellis, 1984; Voigt, 1989; Soriano et al., 1997) and are found in the regenerating cord following amputation (Nordlander and Singer. 1978; Anderson et al., 1983).

5.2 Materials and Methods

Animals

This study is based on 34 European eels *Anguilla anguilla L.* in a non migratory immature stage of the lifecycle. For some of the time dates studied replicates were performed, however in all cases the differences in staining and structural organisation were negligible.

Surgery

For surgery, each eel was treated according to the operational procedures outlined in chapter 4. In brief, each animal was anaesthetised by immersion in 0.3g/l MS-222 (Sigma) and further by a subcutaneous injection of 0.1ml alphaxalone ("Saffan" Pitman-Moore) subcutaneously. Cooling on ice provided additional anaesthesia. The spinal cord was exposed and transected using fine micro-scissors at the region of the fourth segment caudal to the anus. Following surgery, animals were placed in separate holding tanks.

Tissue Preparation

For histological investigation, each animal was treated according to the methods described in chapter 2. In brief, each animal was anaesthetised initially by immersion in 0.3mg/L MS-222 and further by a subcutaneous injection of 0.3ml alphaxalone ('Saffan' Pitman-Moore). To prevent blood clotting, 0.2ml heparin sodium (Leo Laboratories) was also given subcutaneously. The perfusion procedure consisted of a primary flush of Ringer's solution (with 0.1% procaine (Sigma) for further anaesthesia) through the heart followed by the fixative. Two fixative solutions were used (a) 4% paraformaldehyde in 0.1M phosphate buffer (PB), pH adjusted to 7.4, for immunohistochemical investigation and (b) 2% paraformaldehyde, 1.25% glutaraldehyde in 0.1M phosphate buffer (PB), pH adjusted to 7.4, for electron microscopy. Following perfusion, the region of the spinal cord containing the injury and portions immediately rostral and caudal, were dissected from the spinal column and post-fixed in the same fixative at 4°C for a maximum of 3 hours.

Light Microscopy

Following postfixation, the spinal cords were treated according to the methods laid out in chapter 2. However, tissue from two days, 16 and 20 after surgery was cryosectioned to produce 20μm thick transverse sections. All procedures remained the same but the tissue was cryoprotected in 30% sucrose solution overnight at 4°C prior to sectioning. All tissue was processed for rabbit anti-goldfish GFAP (generous gift from Dr. S. N. Nona), S-100 rabbit anti-bovine (Dako) and vimentin mouse monoclonal (Dako) antibodies. For visualisation the avidin-biotin method (ABC kit, Vector) was used with (0.05%) 3,3'-diaminobenzidine (DAB, Sigma) as chromogen.

BrdU immunohistochemistry

For BrdU immunohistochemistry, animals that had received a transection injury were administered a pulse dosage of 5-Bromo-2′-Deoxyuridine (Sigma; hereafter BrdU) approximately 12 hours prior to surgery. It was estimated that this pulse would provide a period of approximately 4-6 hours during which all dividing cells within the bridge would be labelled. Each animal was first anaesthetised by immersion in 0.3mg/l MS-222 and then administered 20mg/kg of BrdU dissolved in Ringer's solution (without added procaine anaesthetic) intraperitoneally. When allowed to recover from the mild anaesthesia each animal was returned to a separate holding tank.

The same procedures were used for histological investigation as stated in chapter 2. Collected sections were pre-treated in 1% sodium borohydride in distilled water to remove residual fixative, in 1% H_2O_2 in appropriate buffer to reduce any existing endogenous peroxidases due to the presence of the blood clot, in 0.01% protease (Type 1, Sigma) for 2 minutes to disrupt mildly the cellular integrity, in 4N HCl in 0.1M PB, and 0.5% Triton X-100 to cause further cellular disruption, and finally, treated in 5% normal serum appropriate to the antibodies used to reduce background staining. Sections were rinsed for 5 x 5 minutes between each incubation.

For the primary antibody reaction, sections were incubated in BrdU mouse monoclonal (Dako) 1:2,000 in 0.1M PB, and 0.5% Triton X-100I for 48 hours at 4°C and then treated with biotinylated horse anti-mouse IgG (Vector), 1:200 in 0.1M Tris-HCl and 0.5% Triton X-100, and incubated overnight at 4°C, or for 2 hours at room temperature. Following secondary antibody incubation, sections were treated in

accordance to the procedures outlined for all other antibodies, which is detailed in chapter 2.

Electron Microscopy

The tissue was processed for electron microscopy according to the procedure described in chapter 2. Sections were cut for both light (1.5μm) and electron microscopy (~500Å). All images were downloaded, analysed and formatted on a Macintosh G3 computer using Adobe PhotoShop 5. Reconstructions from serial sections (60μm apart) of the regenerating spinal cord and central canal were produced according to the procedure described in chapter 3.

Cell Counts

Cell counts were derived from the numbers of identifiable ependymal nuclei abutting the lumen of the canal. Counts were made at the level of the light microscope from toludine-blue stained sections 1.5μm thick using x1000 magnification. Correction of the obtained values to rule out double counting was deemed unnecessary as the distance between each section was 60μm and the average width of the ependymal cells in the wound was calculated as approximately 20μm.

5.3 Results

The results are divided into three sections: the first will describe the initial reactions of the canal to injury and the subsequent formation of a new central canal in the bridge region; the second section deals with the mechanisms underlying canal formation and, finally, the ultrastructural and immunohistochemical changes of ependymal cells to injury will be documented.

Central canal formation

As a result of extensive degeneration, the central canal is absent from portions of the stumps close to the cut surface four days following transection. By day six, however, marked changes have taken place in the central canal in the adjacent rostral and caudal stumps (as shown in Fig 5.1a). The lumenal area of the central canal in the stumps increases significantly, being larger than normal for as much as 1.0 mm on each side of the wound. In regions devoid of a complete central canal at the stump ends, ependymal cells begin to group both rostrally and caudally in the stumps, but appear to form at a faster rate rostrally. Although regenerating tissue begins to produce the first elements of a bridge by day 8 (Fig. 5.1.b), the rostral and caudal canals do not reconnect within this region until around day 10 (Figure 5.1c). As the bridge begins to expand in a dorso-ventral direction at this stage with the dorsal expansion creating the distinct 'horns' of neural tissue, it results in the formation of a canal that is open dorsally. Fourteen days following injury the dorsal expansion continues (Fig. 5.1d) the canal begins to close, as a result of the fusion of the dorsal-most regions of the horns. This closure is first seen in the rostral and caudal portions of the bridge by day 20 (Fig. 5.2a) producing an almost zipper-like appearance and is not completed in central portions of the bridge until approximately day 26 (Fig. 5.2b). By day 54 (Fig. 5.2c) the canal has begun to reduce in size and continues to do so by day 144 (Fig. 5.2d). In the regenerated bridge, the enlarged central canal is the most conspicuous structure, at times occupying as much as 50% of the total cord, whereas in normal undamaged cord it constitutes as little as 0.02-0.05% of the total cross sectional area (see Fig. 5.3). As we have seen, this enlargement of the canal is not restricted to the bridge but is also evident in the adjacent rostral and caudal stumps. Even by day four, the canal in the caudal and, particularly, the rostral stumps has already enlarged 2-8 times normal size. This expansion of the lumenal area is common for all dates studied and continues to be seen

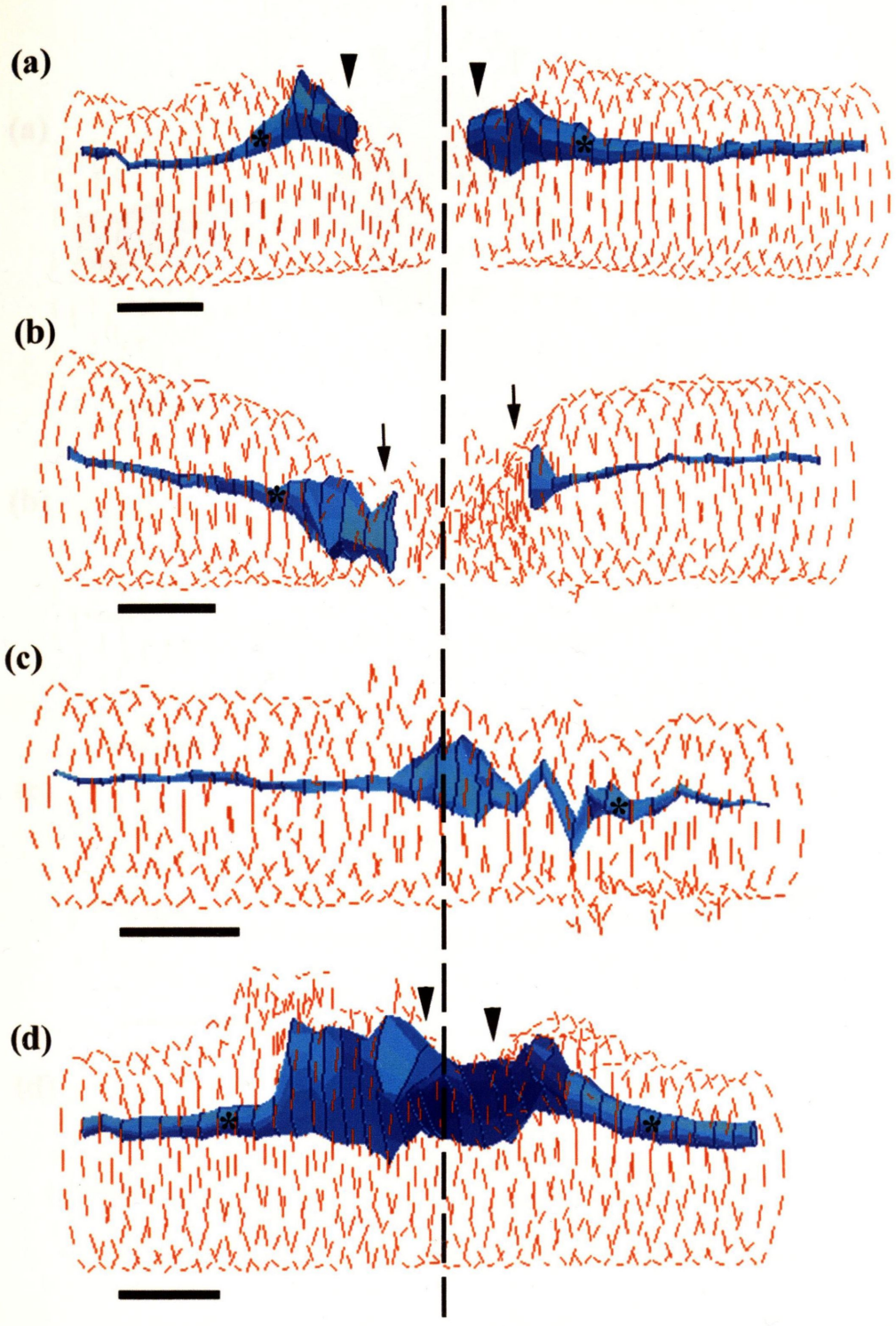


Figure 5.1. Reconstructions of the developing central canal at days 6 (a), 8 (b), 10 (c), 14 (d). At day 6 (a) the central canal has already enlarged in the rostral and caudal spinal stumps (arrowheads) and by day 8 (b) a new central canal begins to develop in the bridge (arrows). 10 days following injury this canal has reconnected to produce a continuous canal although by day 14 it has not completely sealed over and is open dorsally (arrowheads). At all days note the enlargement of the canal in the spinal stumps adjacent to the lesion site (*). The dotted line represents the approximate centre of the lesion site/bridge. Scale bar = 300 microns.

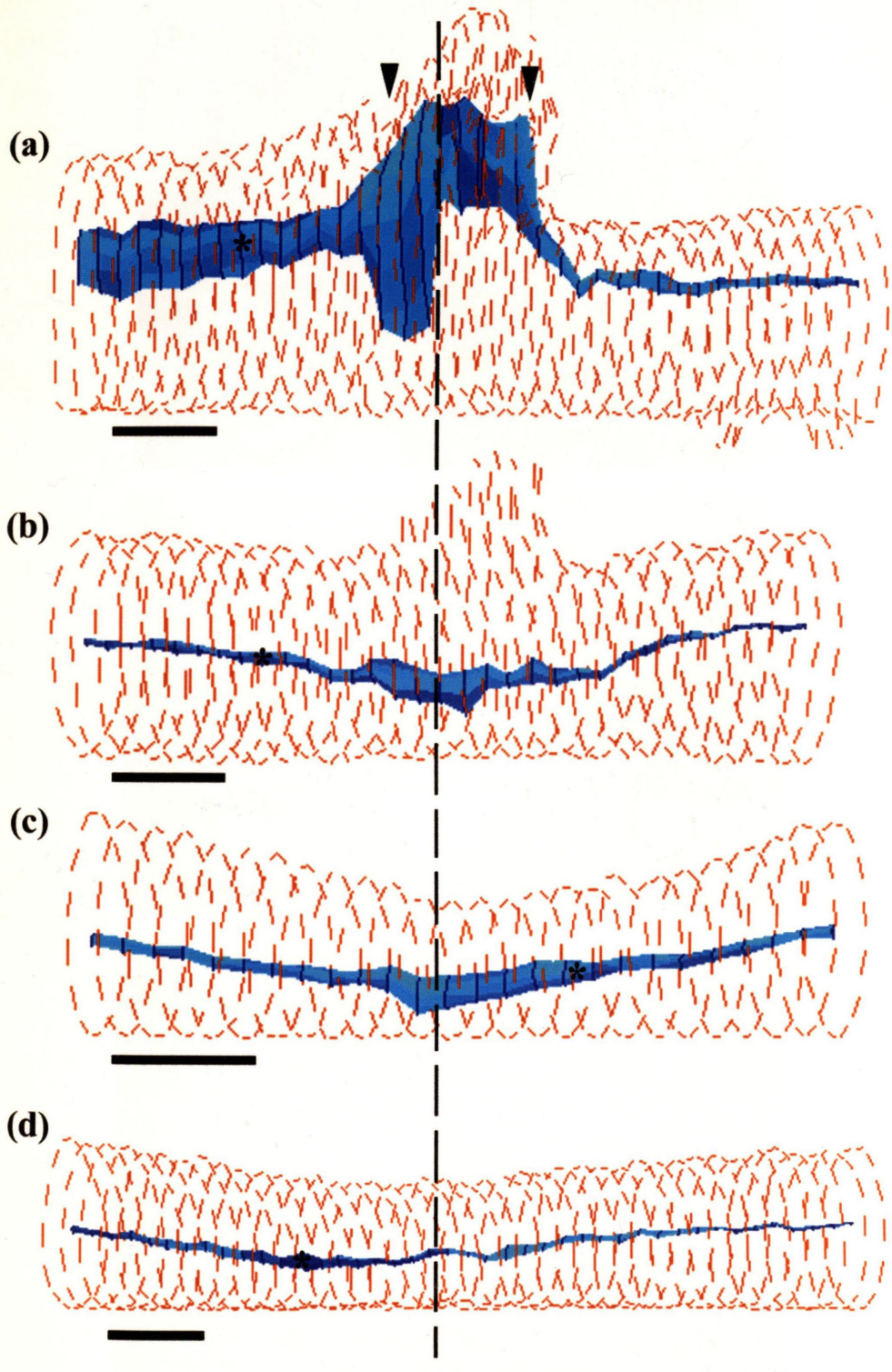


Figure 5.2. Reconstructions of the bridge at days 20 (a), 26 (b), 54 (c), and 144 (d). In (a) note the dorsally enlarged canal in the bridge (arrowheads) which is closed by approximately day 26 (b). By day 54 (c) the canal has reduced considerably in the bridge although it is still enlarged and in this instance it is ventrally placed. At later stages of recovery, at days 144 (d) the canal continues to reduce in size. Note the enlarged size of the canal in both the rostral and caudal stumps (*). The dashed line represents the approximate centre of the lesion site. Scale bar = 300 microns.

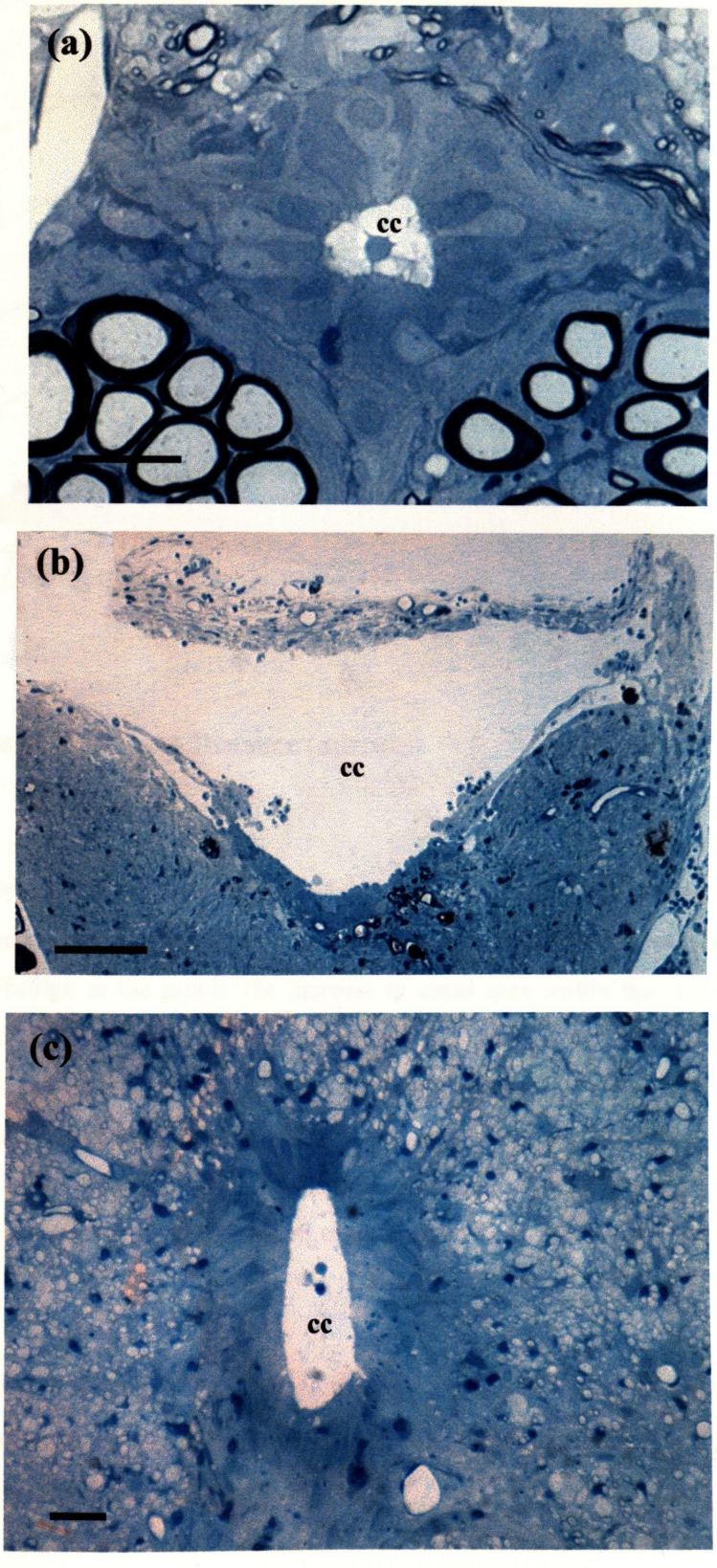


Figure 5.3. Comparison of central canal size between (a) uninjured cord and days 14 (b) and 54 (c). Note the extensive increase in lumenal area for day 14 and even though it is reduced by day 54 the canal is larger than normal. cc = central canal. Scale bar (a) and (c) = 20 microns, (b) = 100 microns.

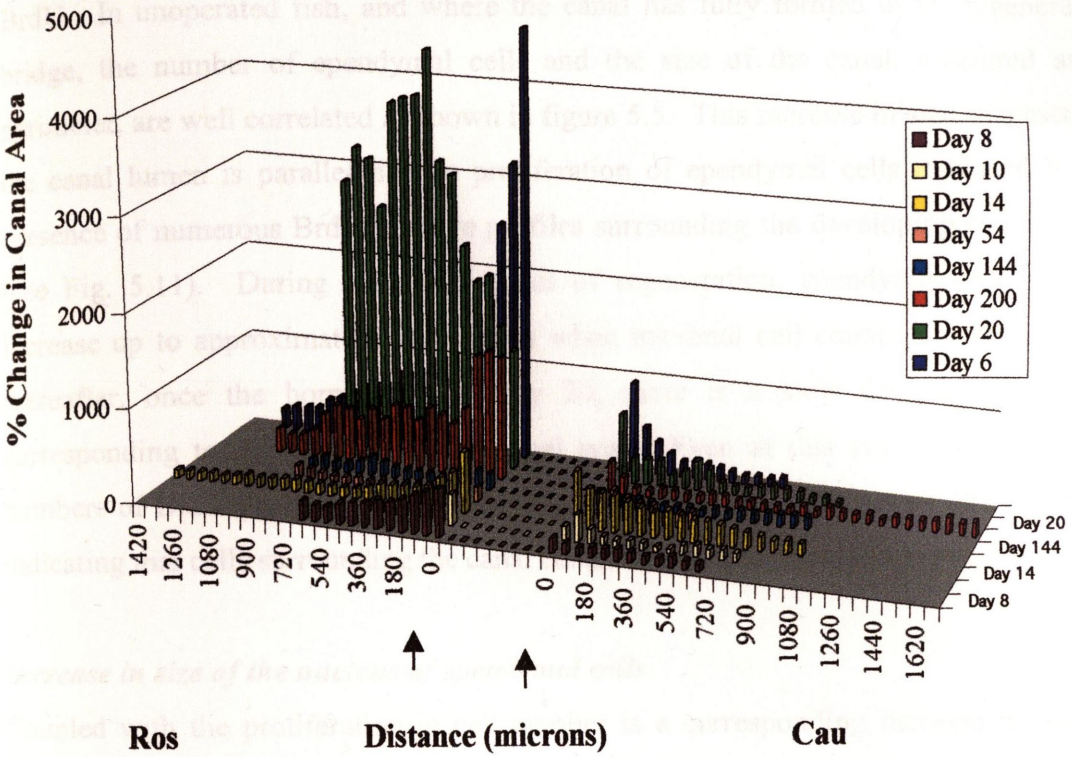


Figure 5.4. Graphical representation(s) of the percentage change in central canal size in the rostral (ros) and caudal (cau) stumps up to approximately 1mm. The arrows denote the extent of the lesion site/bridge in the graph (the increase in canal area within the bridge, denoted as the region between both arrows is not shown here) and the x-axis is the distance from the transition of the rostral/caudal cord (for day 6) and the lesion site/bridge (days 8-200) into the spinal stumps, thus all values start at zero. The y-axis represents the percentage increase in cross sectional area of the canal, determined from an uninjured area of the cord. Note that there is often a greater enlargement of the rostral canal compared to the caudal canal. Ros = Rostral, Cau = Caudal

even at day 200, the longest time studied (Fig. 5.4). The canal enlargement appears to occur predominantly in the rostral cord extending further into the uninjured stump cord compared to the caudal canal.

Ependymal proliferation

In the present study an increase (and eventually a decrease) in ependymal cell number was found to accompany the striking changes in canal size. This was determined from

cell counts in toludine blue-stained semithin sections and from material labelled with BrdU. In unoperated fish, and where the canal has fully formed in the regenerating bridge, the number of ependymal cells and the size of the canal, measured as its perimeter, are well correlated as shown in figure 5.5. This increase in size suggests that the canal lumen is paralleled by a proliferation of ependymal cells indicated by the presence of numerous BrdU-positive profiles surrounding the developing central canal (see Fig. 5.11). During the early stages of regeneration, ependymal cell numbers increase up to approximately 10-14 days when maximal cell counts are attained and, thereafter, once the horns fuse by day 20, there is a slow decrease (Fig. 5.6), corresponding to the reduction in lumenal area. Even at this stage however, small numbers of BrdU-positive profiles can still be found within this layer even by day 30 indicating that cells surrounding the canal continue to undergo cell division.

Increase in size of the nucleus of ependymal cells

Coupled with the proliferation in cell number is a corresponding increase in nuclear area of ependymal cells in both the stumps and the bridge and this is seen in both (see Fig. 5.7) toludine blue stained semithin sections and immunopositive BrdU labelled material. Values (with standard deviation) increase from $14.6 \pm 4.6\ \mu m^2$ in uninjured spinal cord to $27.3 \pm 10.7\ \mu m^2$ by day 14 for toludine blue stained semithin sections and $36 \pm 12.9 \mu m^2$ by day 15 for BrdU-labelled tissue indicating an increase in nuclear area following injury.

Ependymal cell migration

It is our view that the central canal forms through the proliferation, migration and settlement of ependymal cells in the rostral and caudal stumps. As already described, by day 4 the canal enlarges in the stumps rostral and caudal to the wound (Fig. 5.8a), in line with an increase in ependymal cell number. Progressing towards the lesion site in the stumps on both sides (~2-300μm), the enlarged lumen is seen to be surrounded by loosely arranged ependymal cells indicating expansion of the canal in these regions (Fig. 5.8b). In regions of the stumps closer to cut surface of the cord (~100μm) ependymal cells are absent from portions of the proximal cord; however, just in front of the enlarging canal (Fig. 5.8c), small groups of ependymal cells clustered as 'plates' can be found interspersed between the debris and invading elements of the blood clot. At

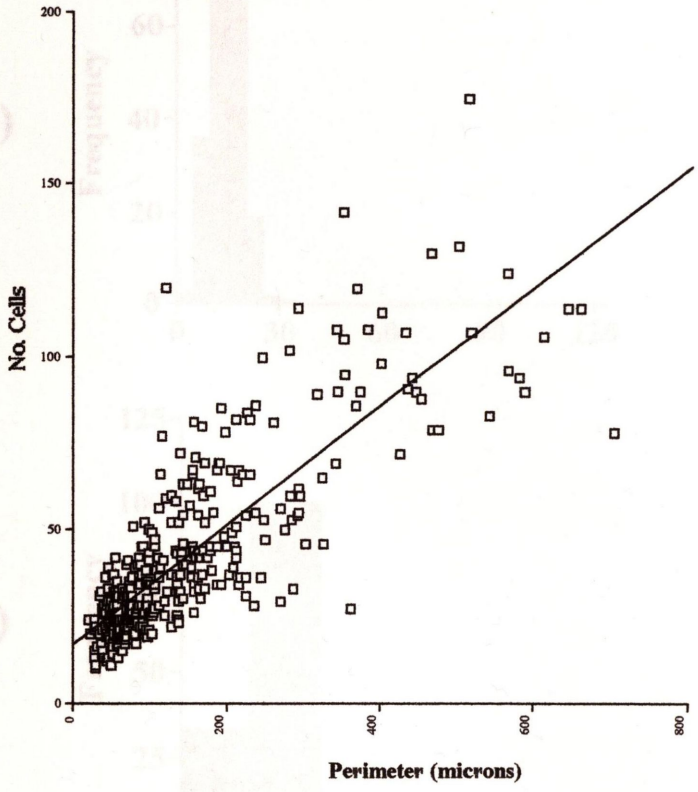


Figure 5.5. Graph of the lumenal perimeter against ependymal cell number for the central canal of normal cord and in the bridge at 4, 6, 8, 10, 14, 20, 54, 144 and 200 days following transection. The x-axis is the perimeter of the canal in microns and the y-axis is the number of cells in each case. The linear regression gives an r^2 value of 0.67.

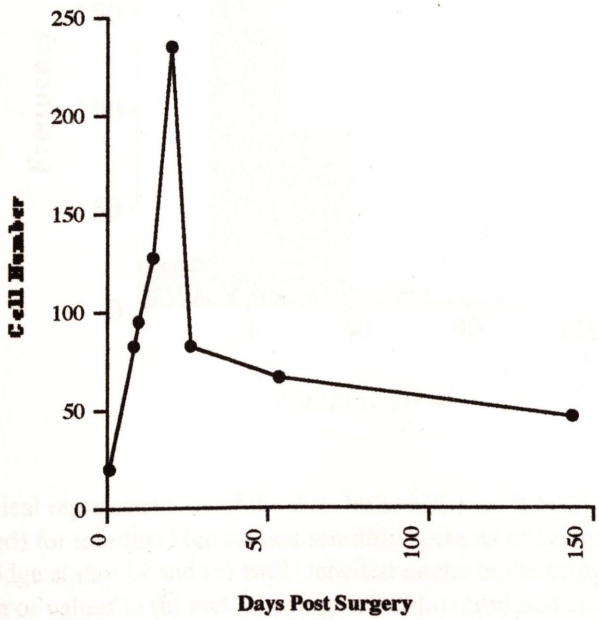


Figure 5.6. Graphical representation of the maximum number of cells surrounding the enlarged canal at each time studied. Note the rapid proliferation before the slow reduction following day 20.

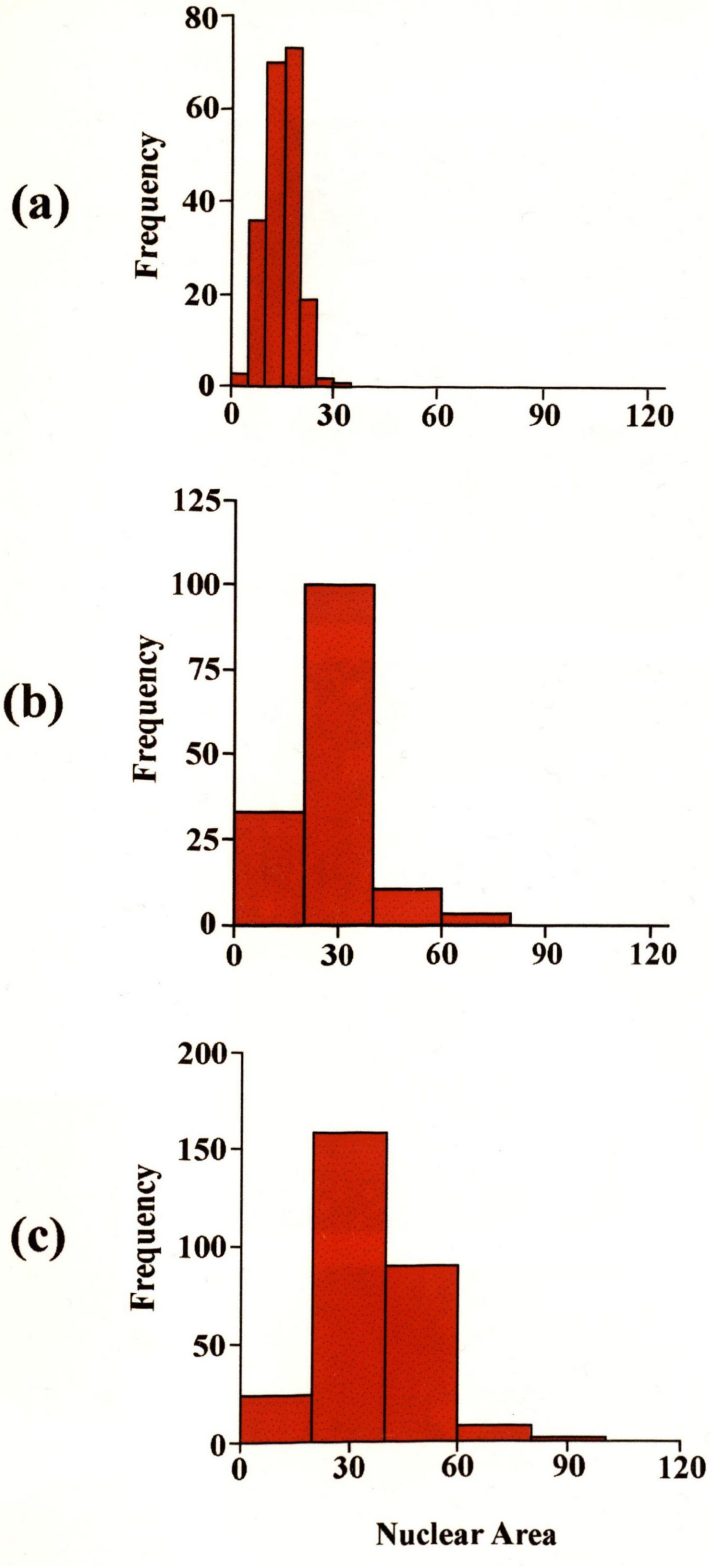


Figure 5.7. Graphical representations of the distribution of ependymal nuclear area expressed as (microns squared) for toludine blue stained semithin sections of (a) the uninjured canal, (b) the canal in the bridge at day 14 and (c) BrdU labelled nuclei in the bridge at day 15. Note the similar distribution of values in (b) and (c) compared to (a) uninjured ependymal cells.

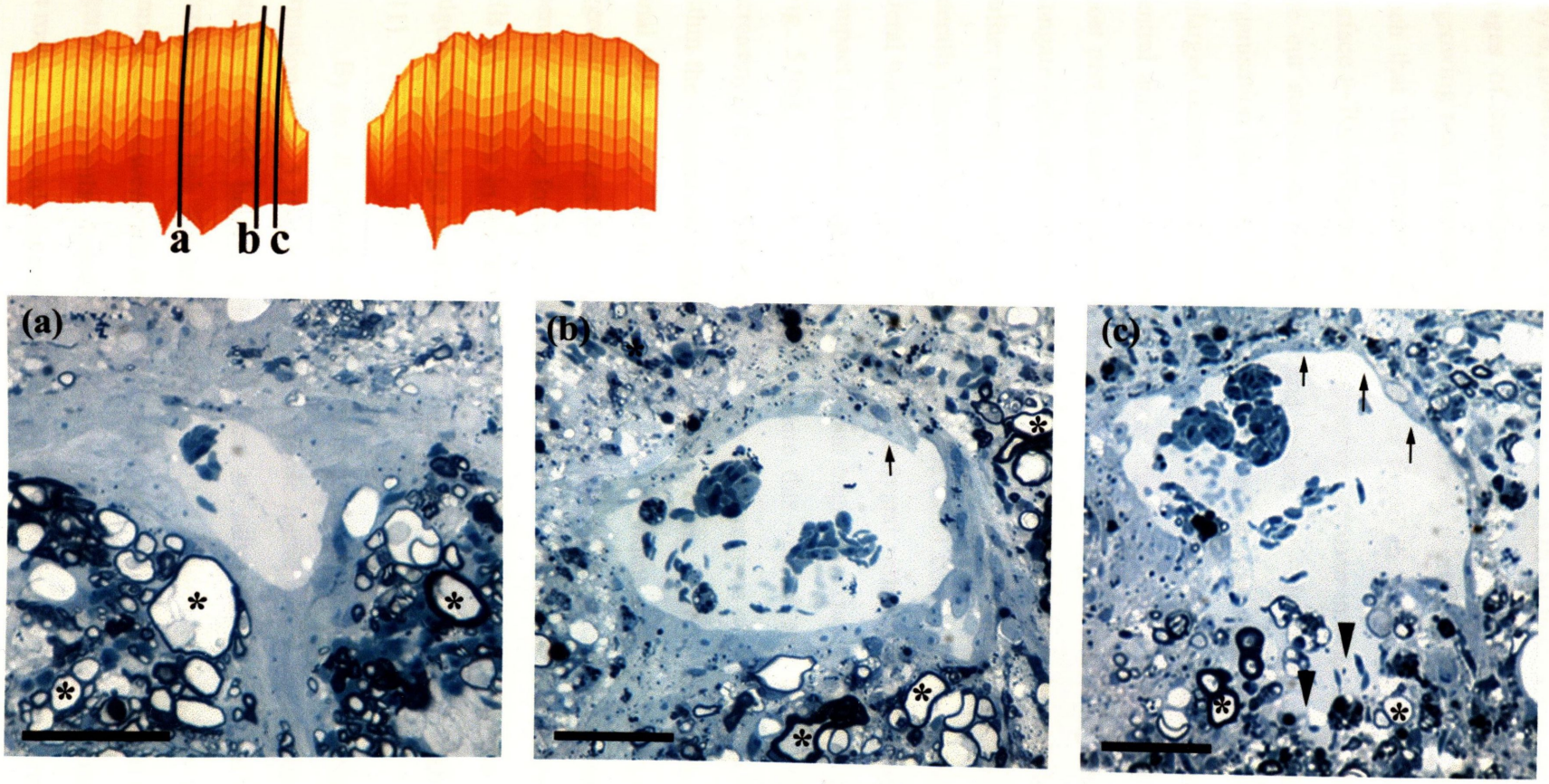


Figure 5.8. The central canal in the rostral spinal stump 4 days following injury. Note that the central canal has already begun to enlarge in the rostral cord (a) and this elargement increases closer to the cut surfaces (b). In the regions close to the cut surface the canal takes on a very loose organisation (c) with some elongate cells present dorsally (arrows) and the absence of cells ventrally (arrowheads). In all regions note the extensive degeneration that is taking place, particularly in the myelinated axons close to the canal (*). Scale bar = 50 microns.

this early stage of regrowth, it is difficult to determine whether these cells are the last cellular remnants of the degenerating canal or the initiation of new canal formation. By day 6, however, ependymal cells can be found in all portions of the stumps at different stages of canal reformation and a few are also found in the lesion site with the regrowing neural tissue. Within the stumps, a gradient of canal formation is evident, such that the greatest development is found in those regions furthest from the cut surface (~700-900μm) with a progressive decrease in organisation in regions closer to the cut surface of the stumps and lesion site. In those regions with the greatest organisation (see Fig 5.9a) proliferating and/or migrating ependymal cells produce an enlarged central canal composed of compact cuboidal to columnar plates of cells on the ventral and lateral surfaces, with more disorganised elongate cells dorsally. For the most part the canal remains open dorsally, although in some regions, loosely arranged elongate cells are present in this region that are indicative of canal closure. Progressing further towards the cut surface of the stumps on both sides (~100μm), dorsal and dorso-laterally placed cells become rare and the canal comprises the developing ventral and lateral walls. Even at this level the ependymal cells are well organised and consist of compact columnar ependymal cells that begin to expand laterally and dorso-laterally (Fig. 5.9b). Closer to the lesion site this ventral and lateral formation becomes increasingly disorganised such that only small regions of developing 'plates' are present within the regenerating tissue, usually producing the ventral aspects of the developing canal (Fig. 5.9c). At the cut surface and extending into the lesion site, small loosely aggregated clusters of cells were found that might indicate the initiation of possible ependymal plate formation in the lesion site. Around day 6, therefore, few ependymal cells are present in the bridge, although cells close to the lesion site in both stumps as judged by the large numbers of BrdU-positive nuclei possess a high mitotic rate (Fig. 5.11).

By day 8, ependymal cells can be found in the bridge at various stages of canal formation (Fig. 5.10a, b, c), similar to those found in the spinal stumps at day 6. This outgrowth trails behind a leading front of other non-ependymal material (situated laterally) that has extended further into the bridge to produce the first tentative connections between the rostral and caudal cord. Hence, in relation to the sequence of regenerative events, ependymal cells are not responsible for the first reconnections of the rostral and caudal spinal cord. Further development by day ten, results in

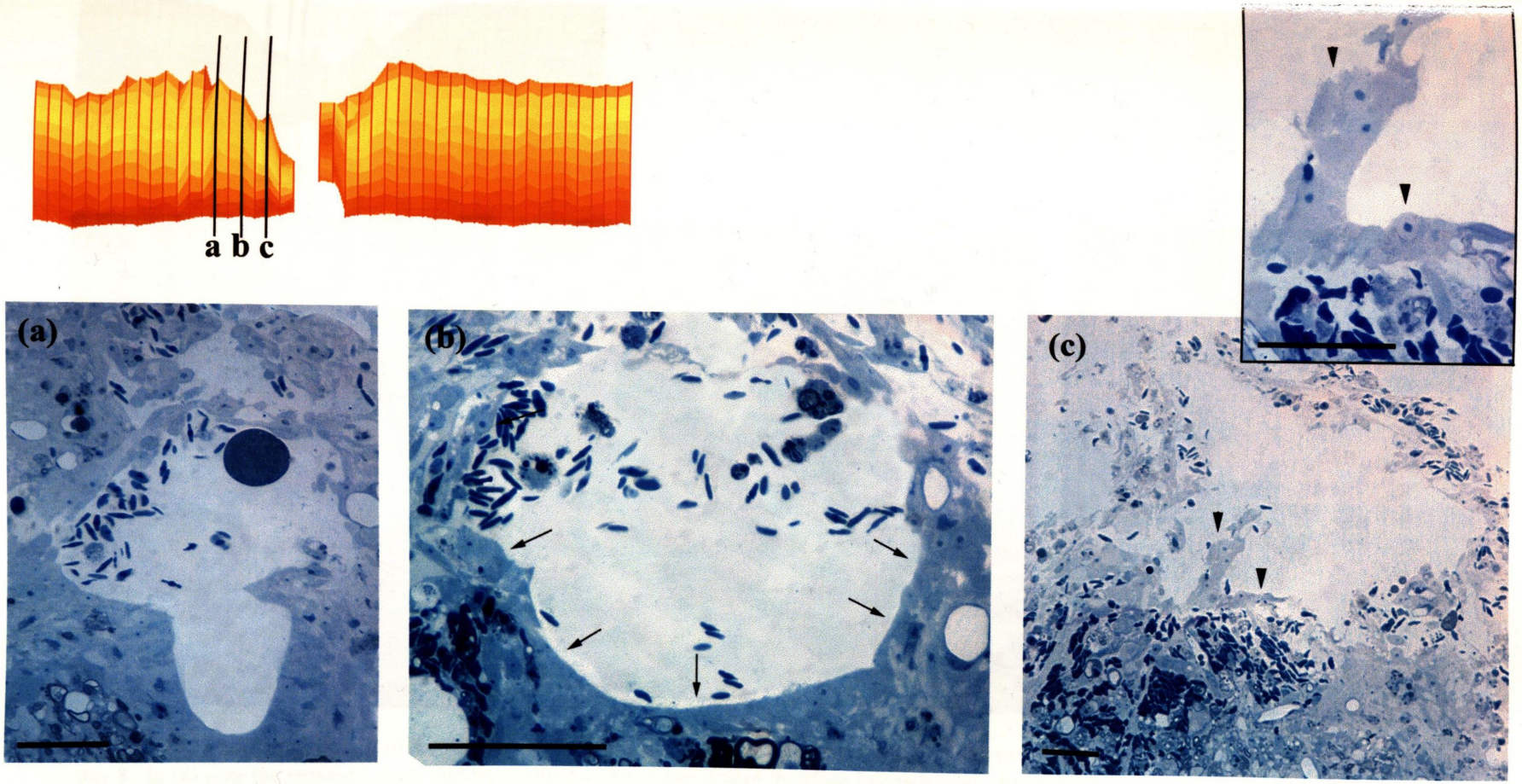


Figure 5.9. Organisation of the regenerating central canal in the rostral stump at day 6. The photomicrographs show the organisation of the developing canal in regions (a) furthest from the cut surface of the stump and in (b) and (c) regions progressively closer to the cut surface. Note the enlarged canal in (a) while in (b) note the presence of only the lateral and ventral aspects (arrows) and in (c) only ventral portions of the canal that indicate a graded development of the canal (arreowheads; see inset). Scale bar = 50 microns.

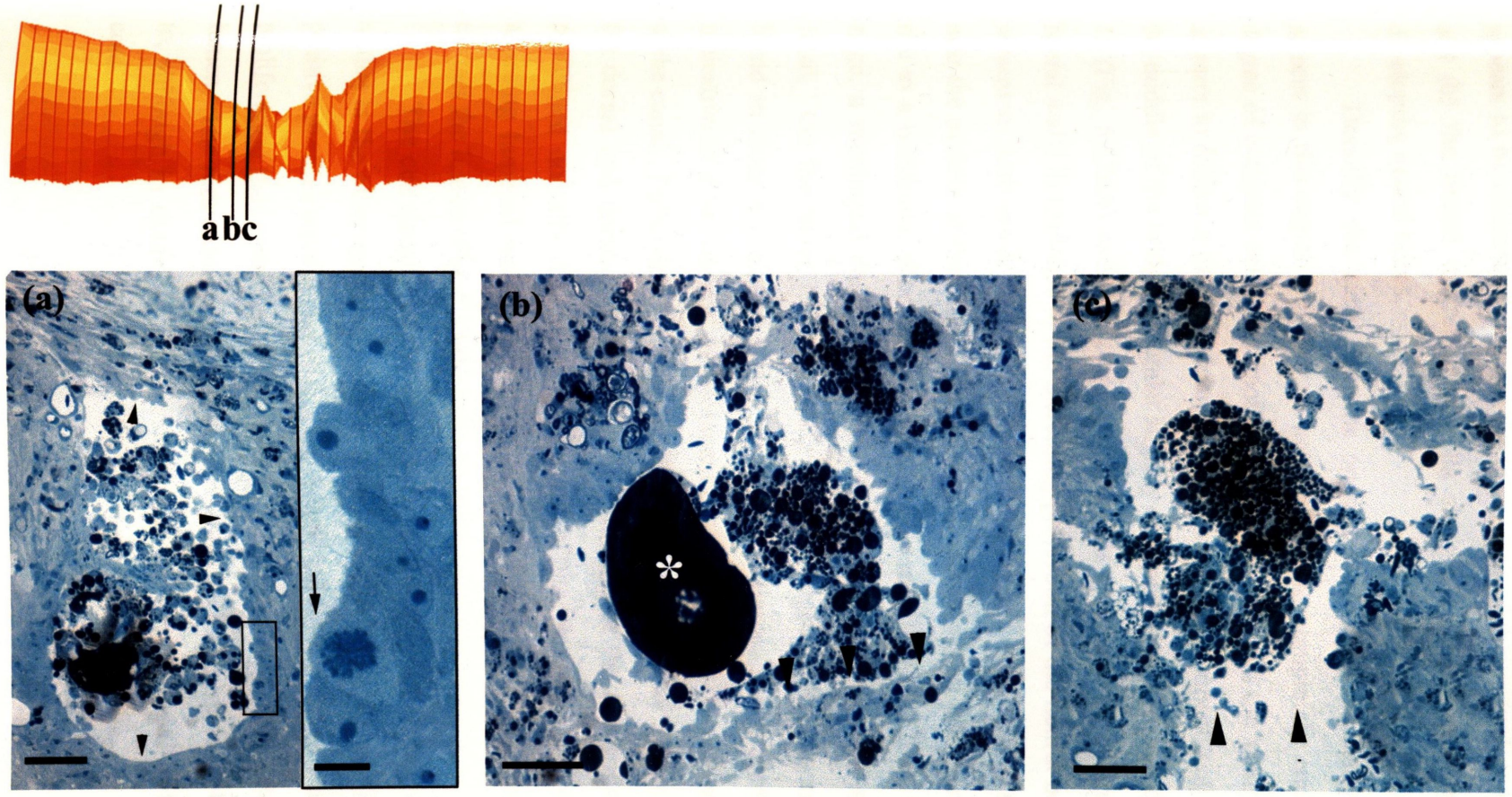


Figure 5.10. Photomicrographs of the developing bridge in (a) the rostral cord-bridge region and two successive regions within the bridge (b) and (c) at day 8. In (a) note the enlarged canal that has formed at the stump-bridge interface (arrowheads), the inset illustrates the close arrangement of the cells and note the cell undergoing mitotic division (arrow). In the bridge proper, (b) and (c), ependymal cells line the inner surfaces of the large blocks of regenerating tissue, thus forming the basis of a rudimentary canal. However, as can be seen in both (b) and (c) portions of the canal have not yet formed (arrowheads). Note the elongate cells (arrows) in (c) that line this canal-like structure. The dark staining debris (*) was found in all regions of the developing canal and was often associated with numerous leucocytes. Scale bar (a), (b) and (c) = 50 microns, inset = 10 microns.

ependymal cells from both sides of the bridge rejoining to bring about continuity between the rostral and caudal central canals. Formation of the new canal at this stage appears to be concentrated to (a) the thickening of the ventral and ventro-lateral walls and (b) the dorsal migration of cells along the inner (endothelial) surface of the developing neural horns.

Dorsally the canal remains open; however, occasionally elongate cells are present in this region but they do not associate to completely enclose the canal. The degree of compact cellular organisation on the lateral and the ventral walls of the canal appears to follow a gradient from the proximal cord (compact, columnar cells) towards the middle of the bridge (irregular slightly elongate cells). Further development by days 14 (Fig. 5.12a,b) and day 20 (Fig. 5.13a,b) is concentrated on the lateral and dorso-lateral walls in response to the increasing projection of the neural horns dorsally. While present in portions of the bridge close to the stumps (Fig 5.12a), the horns are absent near the middle of the bridge, save for small elevations on the lateral sides, thus giving rise to a horizontal sheet of ependymal cells (see Figure 5.12b). Interestingly, at this stage, a meningeal sheath was found to grow over but not infiltrate the developing canal. On the inner lumenal-facing surface, migratory ependymal cells were often found in close association with this meningeal tissue. The graded canal formation is indicative of a 'wave-like' development of the horns and consequently the lateral sides of the canal. Following the fusion of the dorsal horns by day 20, the ependymal cells on the dorsal and dorso-lateral surfaces join to enclose the canal. Frequently the lumen positioned dorsally disappears as a result of the close contact between cells of the apposing lumenal walls, giving rise to small islands of ependymal cells that do not contact the lumen (Fig. 5.13a).

The cell density on the dorsal surface of the newly formed canal is comparable to that at the other surfaces. At this stage, and later (day 30), small numbers of BrdU-positive profiles were found within the ependymal layer indicating a decrease in cellular proliferation that parallels the decrease in ependymocyte number surrounding the canal lumen. The reduction in cell number continues such that by day 144 values are similar to, although in excess of, those surrounding the central canal in the uninjured spinal cord.

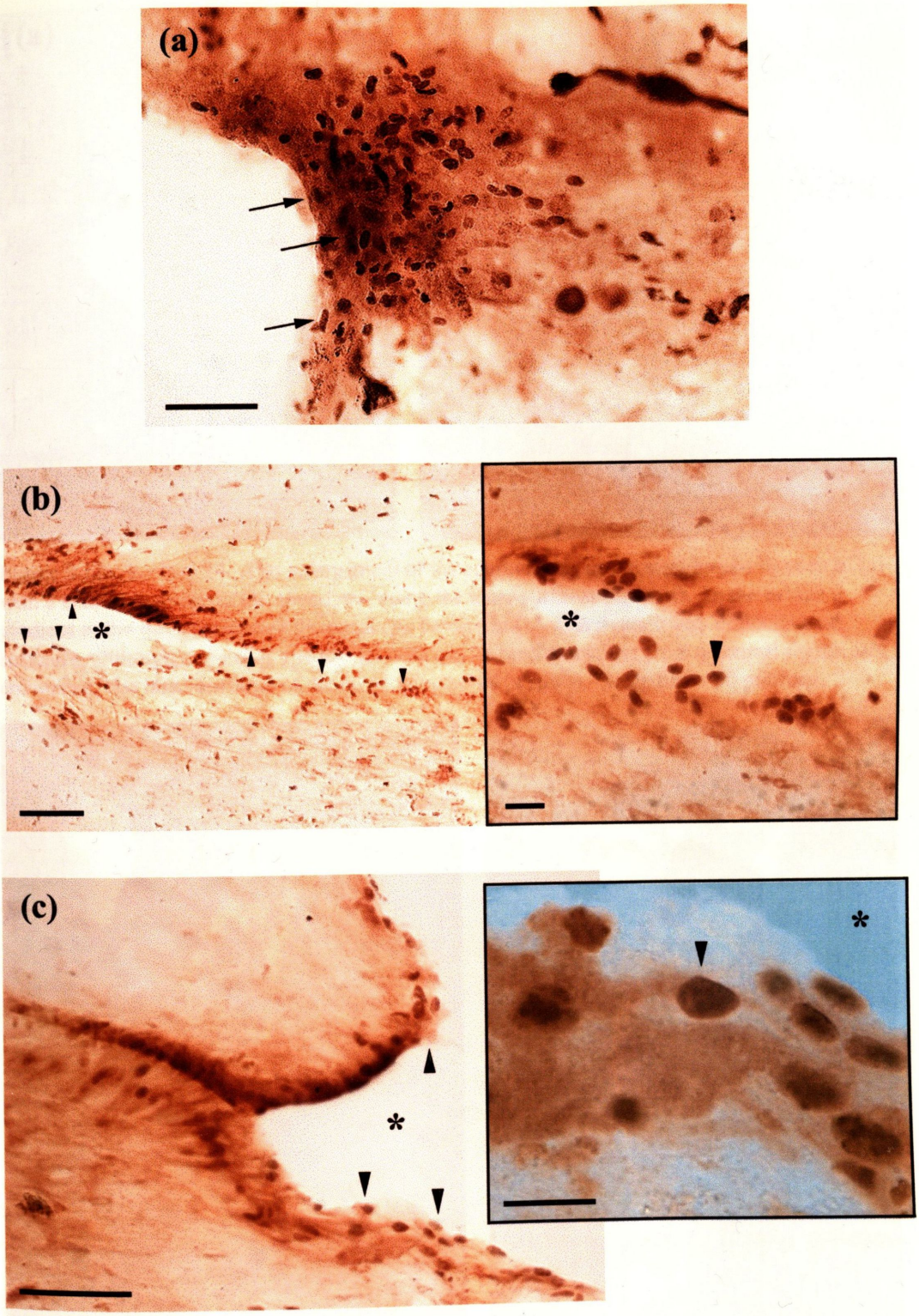


Figure 5.11a, b, c. BrdU-immunopositive profiles surrounding the enlarging central canal at days 7 (a), 11 (b) and 15 (c). In (a) note the presence of numerous immunopositive profiles at the cut surface of the stump (arrows) while at later stages numerous BrdU+ve profiles are found as part of the ependymal layers (arrowheads) surrounding the central canal (*) in the bridge at days 11 (b; see inset) and 15 (c; see inset). In (b) note the presence of numerous profiles in the caudal canal (arrows). Scale bar (a), (b) and (c) = 50 microns, insets = 10 microns.

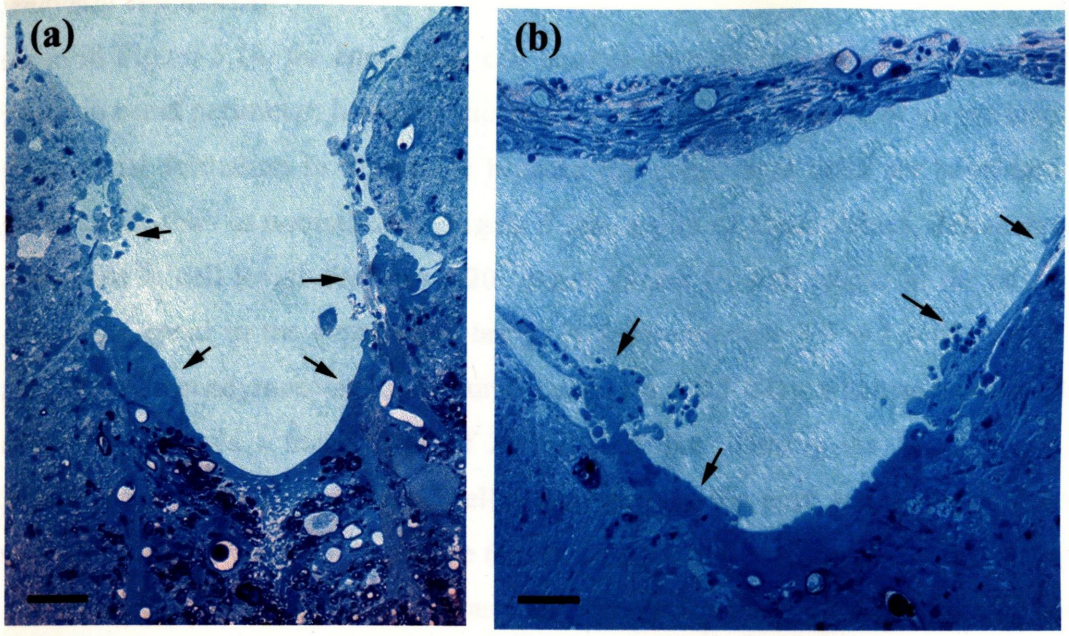
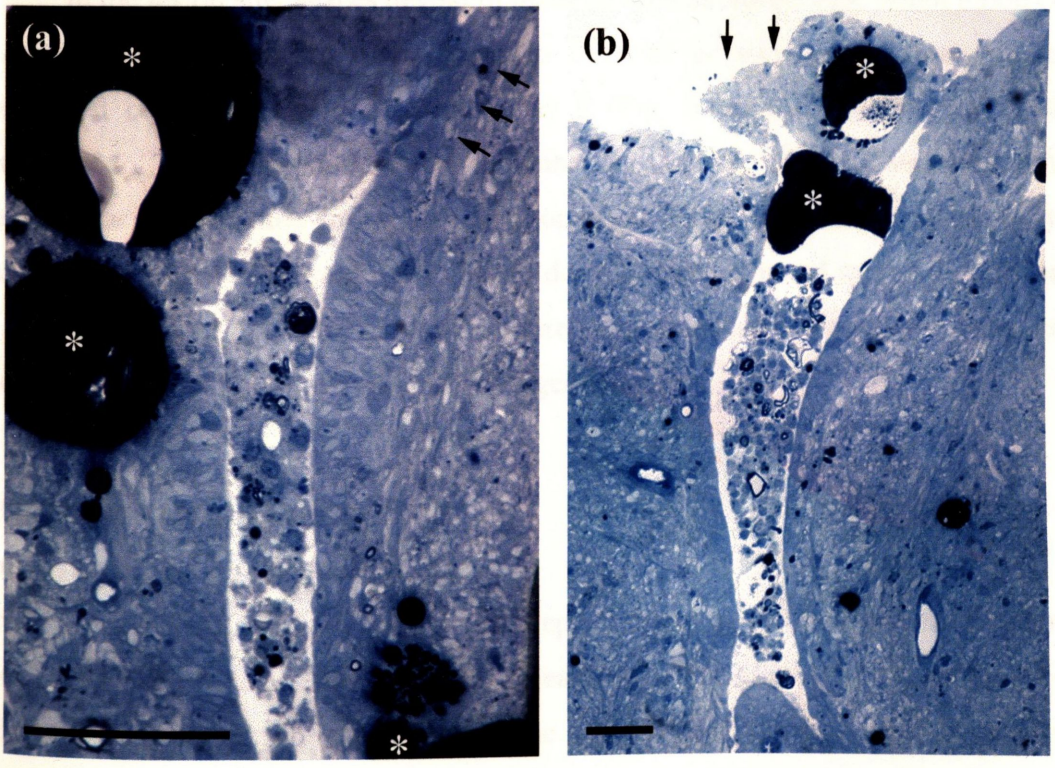


Figure 5.12a, b. Day 14. The enlargement of the neural horns in the stumps can be seen in (a) with a similar increase in the ependyma lining the inner surfaces (arrows). In the bridge a gradient in the development of the canal can be seen in (b) with a much less defined canal structure, although numerous ependymal cells can be seen extending from a central region and colonising the inner surfaces of the developing horns (arrows). Scale bar = 50 microns.



Fgiure 5.13. Day 20 a, b. Enclosure of the canal at this stage occurs through the fusion of the horns dorsally to enclose the canal and often isolating ependymal cells from the main canal (arrows). Further into the bridge (b) this dorsal development is much less organised (arrows) indicating that the gradient of development is still present at this stage. Note the large dark staining processes close to the canal (*). Scale bar = 50 microns.

Ependymal cell density

As seen in Figure 5.14, the ependymal cell number surrounding the canal parallels the increase in canal perimeter; however, this relationship differs close to, or at, the leading edge of canal formation in the bridge because the ependymal cells are considerably more elongate than in normal cord. Figure 5.14a, a plot of these values, demonstrates this increase in cell length for days 4-20. Mean values for cell length in the enlarged but enclosed canal in the stumps and bridge is approximately 3.3 ± 1.5 SD which is comparable to ependymocytes in uninjured canal (3.4 ± 0.5 SD), whereas leading edge ependymocytes have a mean value of 21.1 ± 18.8 SD. During the initial phase of regrowth (days 4-10), as ependymal cells begin to form the new and enlarged central canal, there are fewer cells in the bridge than in the enlarged central canal of the stumps. At later stages of recovery (days 14 and 20), when the canal in the bridge is open dorsally, values remain high, although by day 26 when the canal is fully enclosed, they return to more normal values. It is interesting to note that this occurs almost immediately following closure of the canal.

In the lesion site, spaces devoid of material such as fibroblasts, white blood cells and red blood cells, were often found in front of or surrounding the migrating ependymal cells such as those seen at day 6 (Fig. 5.9c) and day 8 (Fig. 5.10c). Similarly, following reconnection of the canal by day 10, this characteristic debris clearing was further noted during the formation of the dorsal horns leading eventually to closure of the canal. For example, the large dorsally-open lumenal spaces that are seen at days 14 (Fig. 5.12) and 20 (Fig. 5.13) were always devoid of debris and other cells such as meningeal-fibroblasts and macrophage/monocytes.

GFAP immunohistochemistry

Tanycytes in the regenerating bridge

Goldfish anti-GFAP antibody did not label ependymocytes in the regenerating central canal; however, tanycytes did label. At the earliest time studied (day 4), no GFAP+ve cellular processes indicative of this cell type were evident in regions of the proximal stumps. Immunopositive profiles were first noted in the bridge at day 8, as long cytoplasmic extensions that could be traced into the adjacent spinal cord but not to their originating cell bodies (see also chapter 8). Staining of GFAP+ve tanycytic perikaryal-type profiles was first noted in the bridge at day 14 where a few weakly staining cell

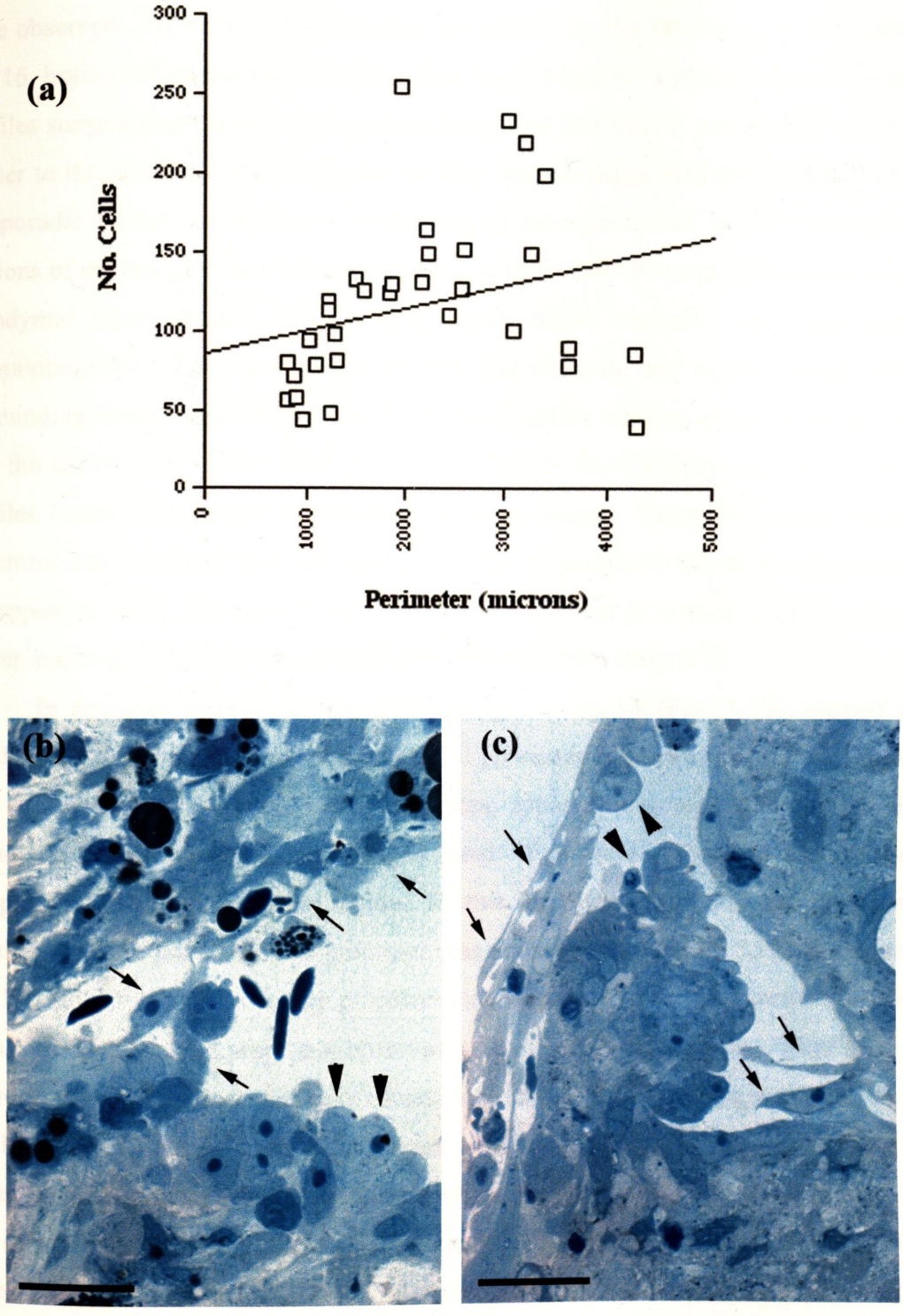


Figure 5.14a, b, c. Graphical representation of ependymal cell number in relation to the perimeter of the developing central canal at the leading edge of regrowth is seen in (a). Note the spread of the data and the large perimeter values to cell number reflecting their more elongate structure. In (b) and (c) at days 8 and 14 respectively, note the elongate nature of the cells (arrows); columnar ependymal cells can also be seen (arrowheads). Scale bar = 20 microns.

body-type profiles in the ependymal layer contacting the lumen of the forming canal were observed. However the ncleus was not defined by the labelling. A little later, at day 16, horizontal sections of the bridge (see Fig. 5.15) show abundant immunopositive profiles surrounding the enlarged canal in the rostral and caudal portions of the bridge. Closer to the middle of the bridge, the profiles are less dense and only a small number of sporadic GFAP+ve structures are present in the ependymal layer. In transverse sections of the bridge it can be seen that some of these GFAP+ve profiles arise from the ependymal layer situated laterally (Fig. 5.16), while ventrally, this cell layer is immunonegative. Labelled profiles are thin and elongate and rarely extend into the surrounding tissue; however, by day 20, immunopositive profiles extend short distances into the lateral and ventral cord (Fig. 5.17). By 26 days, lightly staining GFAP+ve profiles contact the lumen of the canal on all surfaces. Ventrally, immunopositive structures can be traced from the canal lumen to the periphery of the cord but they do not appear to reach the subpial layer; the staining of these processes is lighter than the darker-staining regrowing longitudinal glial processes (see chapter 8).

In semithin plastic sections of the bridge at day 54 (Fig. 5.18), stained with toludine blue, a population of long thin radial processes is seen to extend well into the cord and a network of smaller thin processes, apparently emanating from the thick ependymal region surround the enlarged canal. Few radial processes can be traced completely to the submeningeal region. Further increases in the size and intensity of staining of the radial GFAP+ve processes was noted at day 70 (fig. 5.19) and again at day 175 (Fig. 5.19b) when many processes extended fully to the pial surface, although GFAP-positive endfeet were not observed at the meningeal surface. Similarly, the network of fine processes that were found close to the ependymal region at day 54 did not label for GFAP at these later stages. At these extended periods of recovery, tanycytes in the bridge possess an intensity of staining that is equal to if not greater than that of surrounding longitudinal glial processes. These labelled profiles continue to increase in density by day 200 (Fig. 5.21) and project into the cord, often reaching the pial surface, particularly in the lateral regions, although endfeet do not label for this intermediate filament.

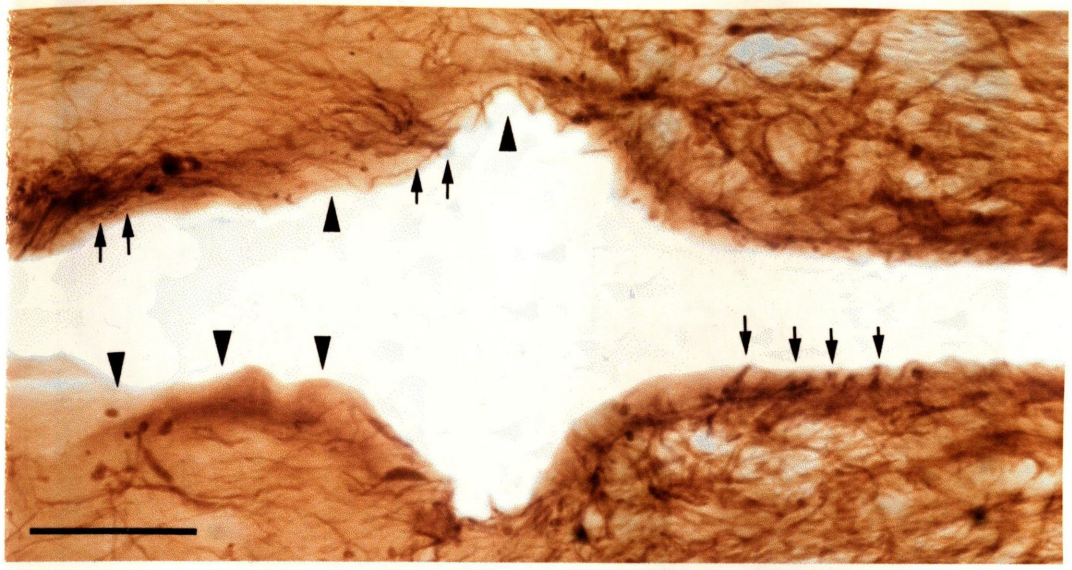


Figure 5.15. Photomicrographic montage of a horizontal section through the enlarged central canal in the bridge at day 16. Note the numerous long GFAP+ve processes that extend into the bridge from the stump regions. Tanycytic profiles surround the enlarged canal (arrows) but are rare in the middle of the bridge (arrowheads). Note the absence of particulate matter in the lumen of the canal. Scale bar = 100 microns.

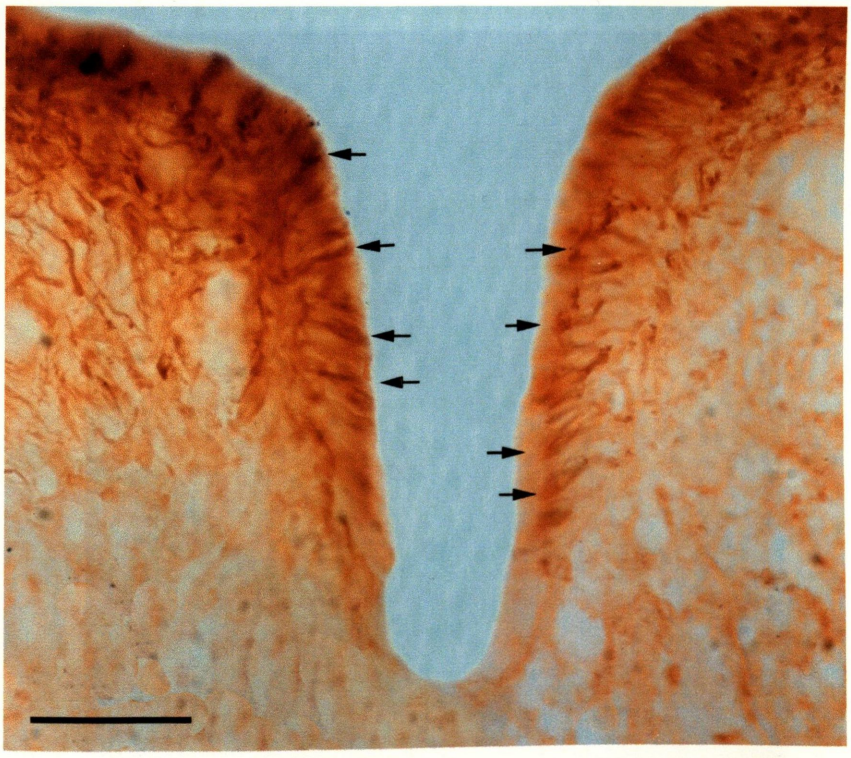


Figure 5.16. Photomicrograph of a transverse section of the central canal in the bridge 16 days post injury. Note the presence of GFAP+ve profiles in the ependymal layer at the lateral surface of the canal (arrows) and the short projections. Scale bar = 50 microns.

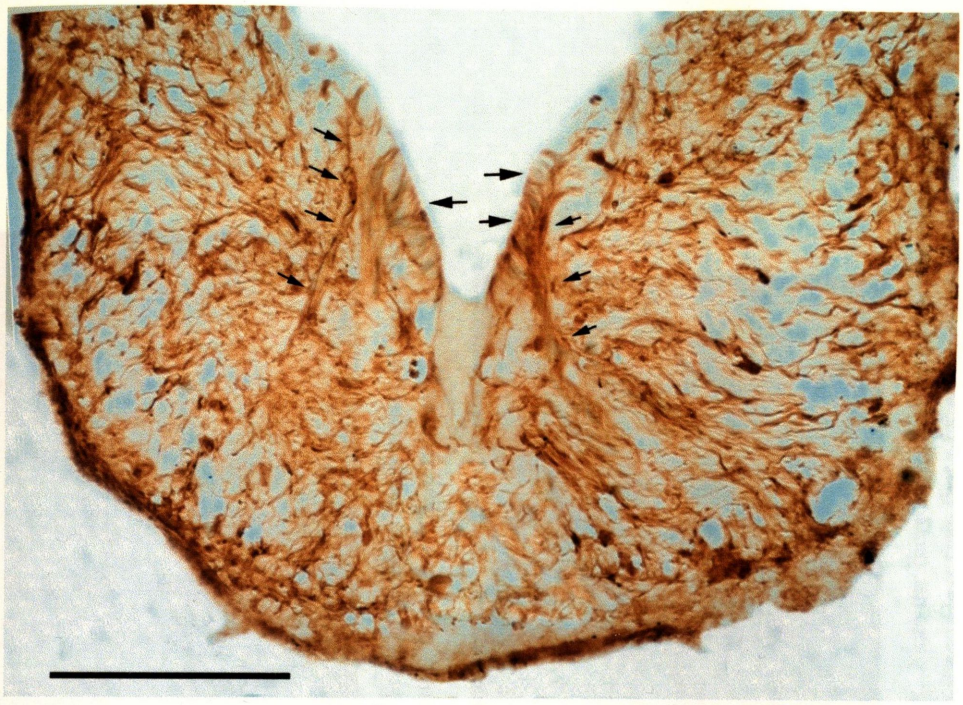


Figure 5.17. Photomicrograph of the central canal in transverse section at day 20 with GFAP labelling. Note the increase of tanycytic profiles and the extension of these structures into the surrounding cord (arrows). Scale bar = 200 microns.

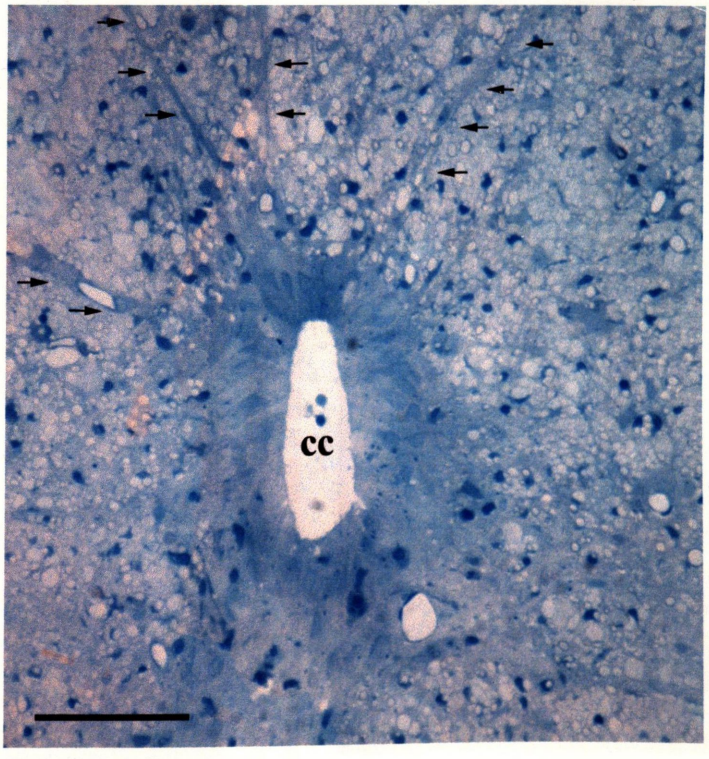


Figure 5.18. Photomicrograph of a toludine blue stained section of the central canal 54 days following injury. Note the presence of numerous processes that extend away from the large ependymal region (arrows). cc = central canal. Scale bar = 50 microns.

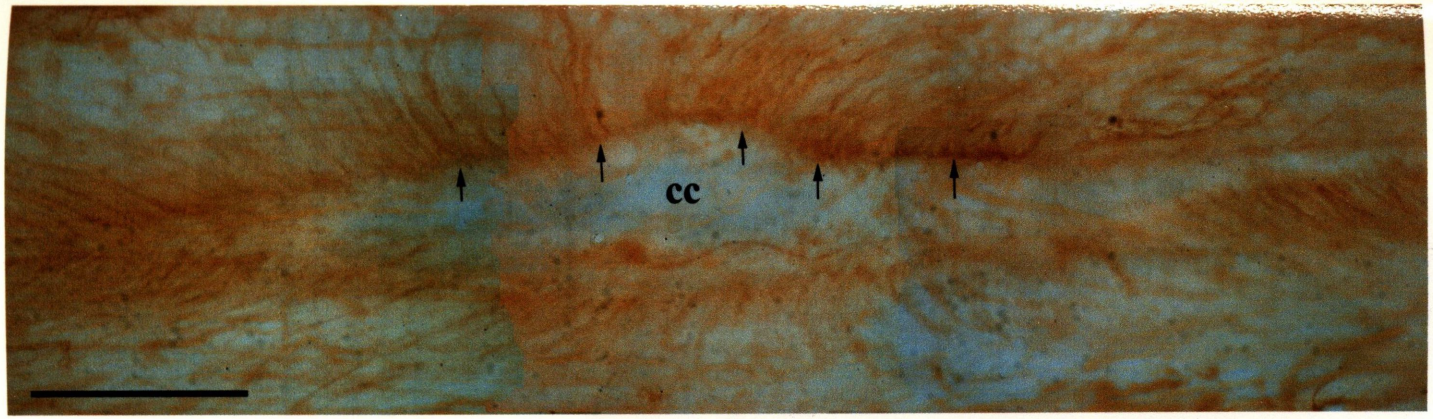


Figure 5.19. Photomicrograph of the bridge 70 days following injury cut horizontally and labelled for GFAP. Note the presence of tanycytic processes (arrows) that extend from the lumenal area of the canal to the periphery of the cord. cc = central canal. Scale bar = 100 microns.

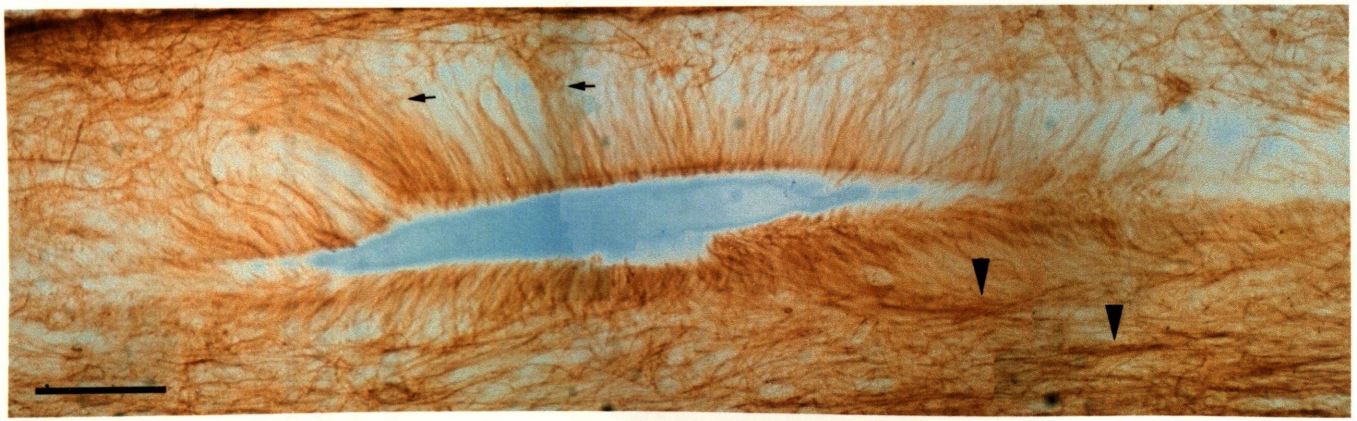


Figure 5.20. Photomicrograph of the GFAP-stained bridge region 175 days following cord transection. Note the increase in density of the processes that extend from the lumen to the periphery of the cord (arrows). The intensity of labelling of these projections is less than that of the longitudinally orientated processes that are found closer to the periphery of the cord (arrowheads). Scale bar = 100 microns.

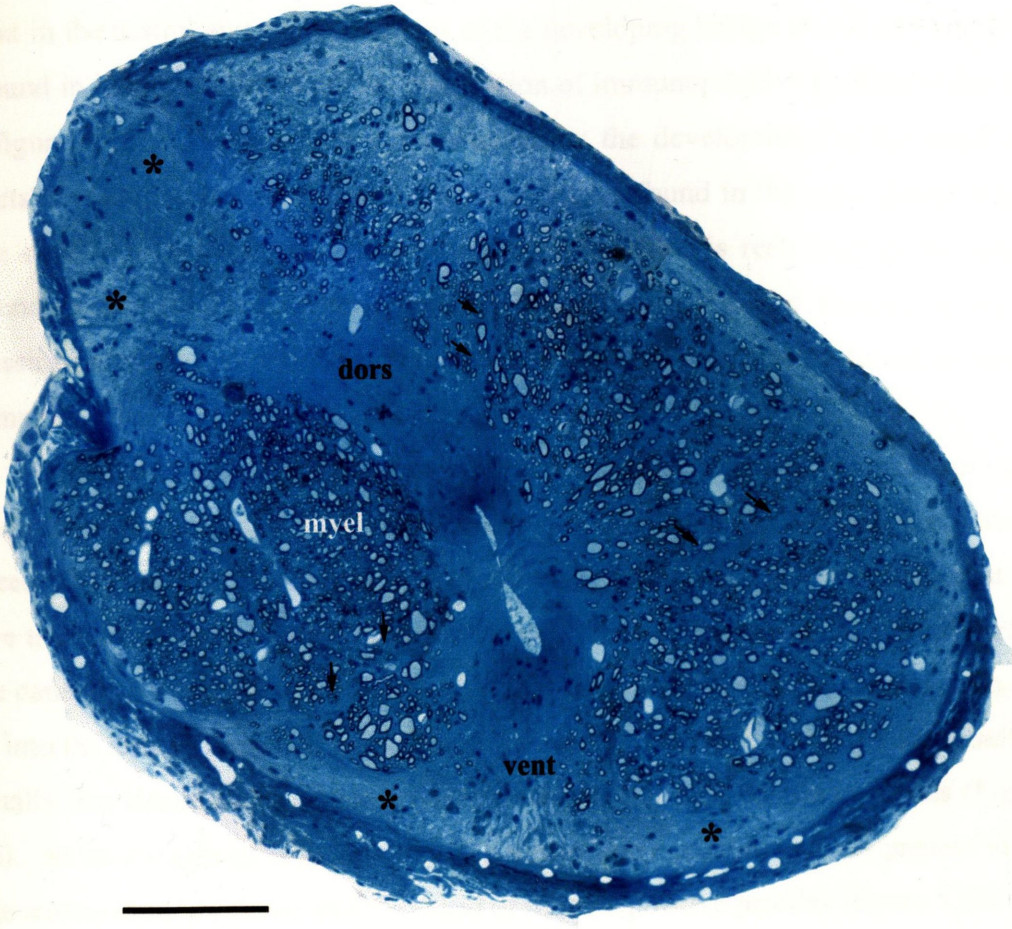


Figure 5.21. Photomicrograph of toludine blue stained semithin section of the bridge at 200 days. Note the increased thickness of the tracts emanating from around the canal (arrows) and extending into the bridge to terminate into a large sub pial region (*). Note the extensive projections both dorsally (dors) and ventrally (vent). A large portion of the axons present in the cord contain some degree of myelination (myel). Scale bar = 200 microns.

Vimentin Immunohistochemistry

In contrast to the weak labelling for this intermediate filament in uninjured spinal cord, by four days following injury, cells surrounding the enlarged canal on both sides of the wound labelled intensely for this protein. By day six immunopositive profiles are present in the rostral and caudal portions of the developing bridge and at day eight they are found in its middle, although the distribution of immunopositive profiles is not even (see figure 5.22). The labelling appears to follow the development of the canal as it projects dorsally; at day 10 vimentin+ve profiles were found in the most dorsal regions of the canal. In general, the intense labelling of profiles is restricted to the regions surrounding the enlarged central canal in the bridge and in the stumps, while the expression in uninjured regions is comparable to the staining pattern found in normal undamaged canal.

Within the bridge the immunopositive structures are thin and elongate but rarely extend into the surrounding cord. Differences were also noted in the staining intensity between the dorsal and ventral surfaces of the canal in the bridge. For example, at day twelve the most intense staining occurs in the cell layers surrounding the ventral surface of the canal as a dense network of processes (Figure 5.23b). Cells that extend from this layer into the ventral cord also label intensely (Figure 5.23c) while dorsally the labelling is usually less dense and contains a mixture of light and dark staining profiles (Figure 5.23a). At later stages of recovery (day 26), vimentin+ve profiles are still present in the bridge surrounding the canal as a thin band of immunopositive profiles (figure 5.24).

Electron Microscopy

Electron microscopy confirmed the characteristic migratory ependymal cell structure; the nucleus is generally elongate, with a light staining nucleus and cytoplasm. The cytoplasm often contains abundant endoplasmic reticulum and mitochondria that are usually in close association to the nucleus (see Fig. 5.25). At later stages of regeneration, tanycyte cells and their long processes become increasingly evident in the ependymal layers surrounding the enlarged canal (day 144) such that some were traceable for short distances as they project towards the bridge periphery (Fig. 5.26). These cells are of varying electron density although all project long tail processes that often contain small-dispersed bundles reminiscent of intermediate fibres.

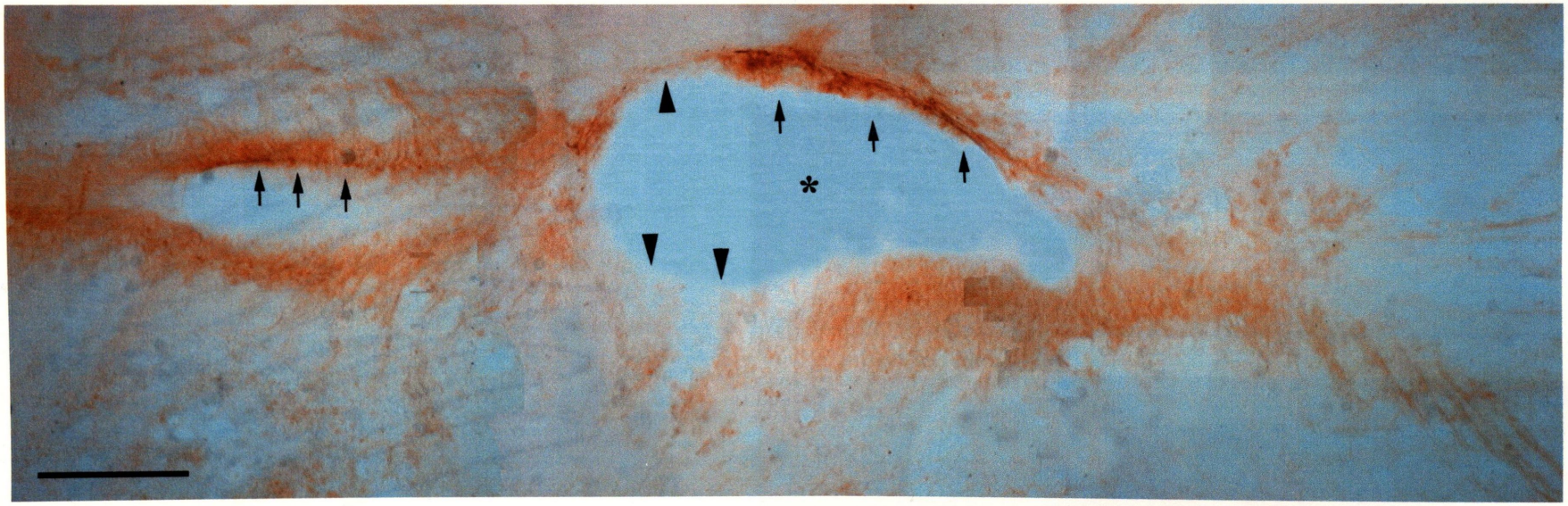


Figure 5.22. Day 8. Horizontal section of the bridge and stumps reacted for vimentin. Note that the developing canal (*) is surrounded by a band of vimentin positive profiles (arrows) with an absence of labelling in other regions of the canal (arrowheads) that probably indicates the absence of ependymocytes in this region. Note the similar labelling in the adjacent canal of the rostral stump which is also enlarged. Scale bar = 100 microns.

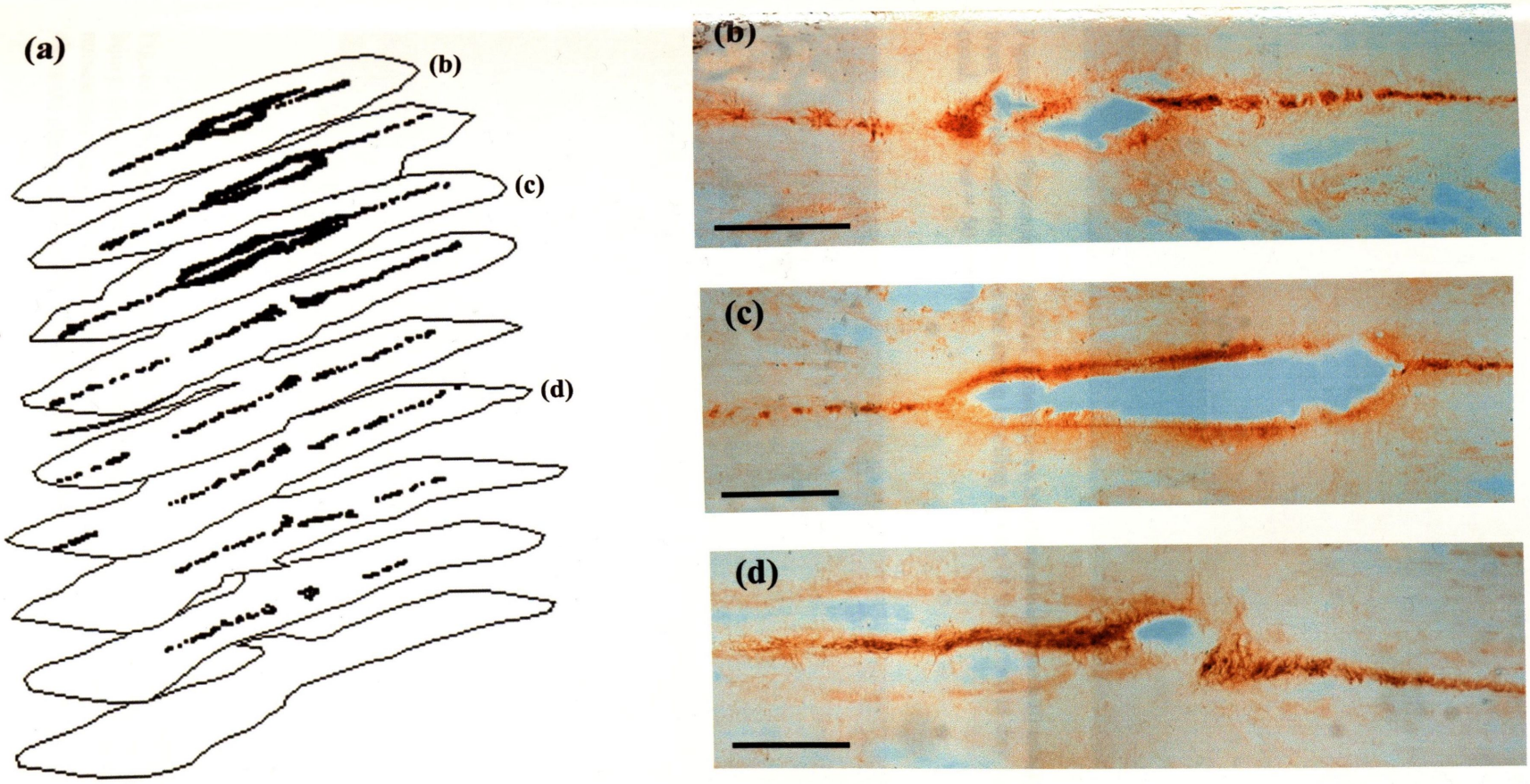


Figure 5.23. Day 12a, b, c, d. (a) Reconstruction from horizontal sections of vimentin+ve profiles in the bridge and rostral and caudal cord. Photomicrographs of the different regions are highlighted in (b), (c) and (d). In (b) labelling around the enlarged central canal is shown, while in (c) the ventral portion of the canal is illustrated and finally in (d) the level of staining is highlighted in the ventral ependymal region. Note that the intensity of labelling in the ventral portions is greater than more dorsal regions. Scale bar = 50 microns.

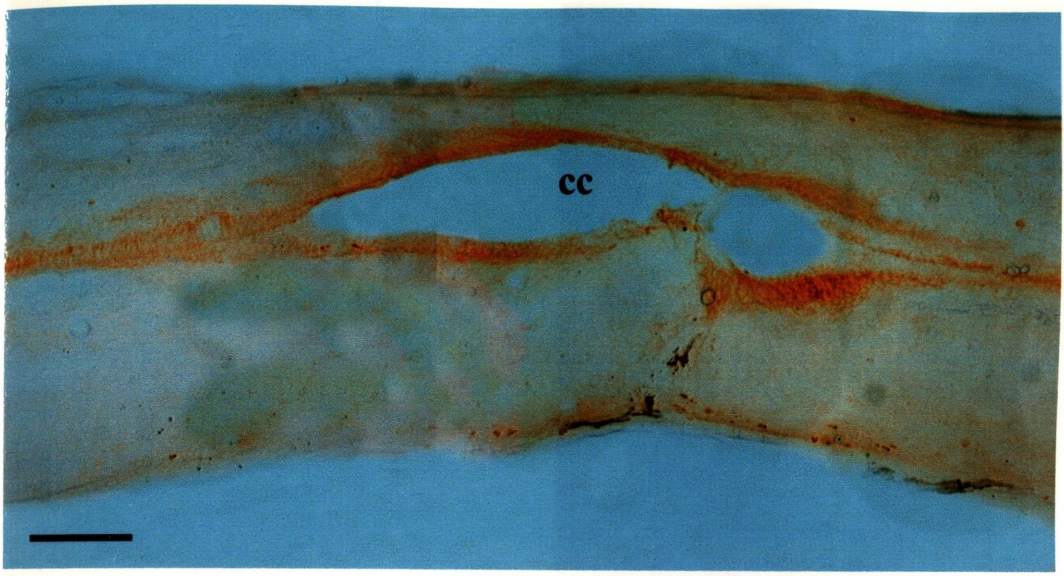


Figure 5.24. Photomicrograph of vimentin+ve labelling around the still enlarged central canal from saggital section. Note the strong labelling similar to that found at day 12. cc = central canal. Scale bar = 50 microns.

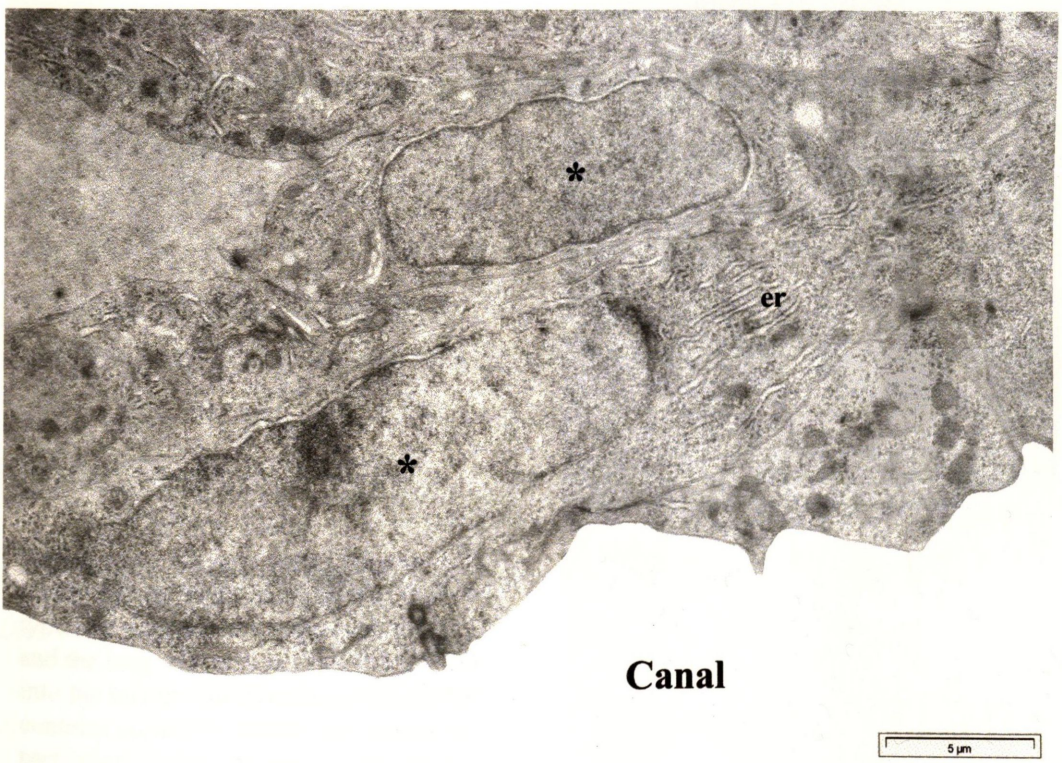


Figure 5.25. Electron micrograph of migratory ependymocytyes in the bridge 10 days following injury. Note the lightly stained and enlarged nucleus which fills the cell (*). In the cytoplasm are numerous cisterns of endoplasmic reticulum (er) in close association to the nucleus. Note the elongate shape of the cells. Canal = central canal lumen.



Figure 5.26. A light staining tanycyte in the bridge 144 days following injury. Note the typically elongate and large nucleus (nuc) and the long tail process (Tp) that extends into the bridge. The cytoplasm is light and contains numerous bundle-like structures particularly in the tail process which may be of intermediate filament origin (if). Note the presence of myelinated axons at this stage (Ax) between which the long processes course. The darker staining elongate processes (*) in close proximity are also of possible tanycyte origin.

5.4 Discussion

The results of the present study show that following transection of the spinal cord the central canal increases in lumenal area both in the newly formed bridge, in the adjacent portions of the rostral and caudal cord (<200μm), and also in the spinal cord some distance (200-1000μm) from the wound. This increase is coupled with the proliferation, migration and settlement of ependymal cells. Vimentin staining was limited exclusively to the proliferating ependymal cells in the bridge while GFAP labelling was seen only in forming tanycyte processes. Labelling of S-100 was negligible and, when present, mirrored that seen for GFAP.

Central Canal Enlargement

Soon after transection (day 4) the central canal is not seen in the proximal portions of the rostral and caudal stumps, presumably because ependymal cells in those regions have been injured and have degenerated. Therefore, the initial stage of central canal reformation occurs in these degenerated portions of the extant spinal cord. Adjacent to the cut surfaces three repair stages can be recognised:

(a) Dorso-ventral enlargement and formation of the canal in the stumps (days 4-6). A similar enlargement of the canal in the rostral and caudal stumps was noted in the spinal cord of *Xenopus* tadpoles (Michel and Reier, 1979) and the larval lamprey, *Petromyzon* (Wood and Cohen, 1981), following transection. The urodele central canal, following tail amputation, enlarges to form a bulb region surrounded by ependymal cells at the caudal-most point of growth (Egar and Singer, 1972; Nordlander and Singer, 1978); however, in the teleost, *Apteronotus* (Anderson et al., 1983), the bulb region is absent following similar injury.

(b) The canal forms in the bridge by extending dorsally as a result of ependymal cell outgrowth (see next section). The development is initiated from the rostral and caudal portions of the bridge eventually establishing a gradient of canal development (see Fig. 5.27). The dorsal portions of the canal do not close for some time and remains open even when the bridge is well formed. The studies of regeneration in the lamprey (Lurie and Selzer, 1991; Lurie et al., 1994) and fish (e.g. Anderson et al., 1983) provide little insight into the mechanism by which the canal forms, although interestingly, the opening of the central canal to the lesion cavity has been reported in amniotes (Beattie et al., 1997). Following amputation of the urodele tail, however, the canal appears to

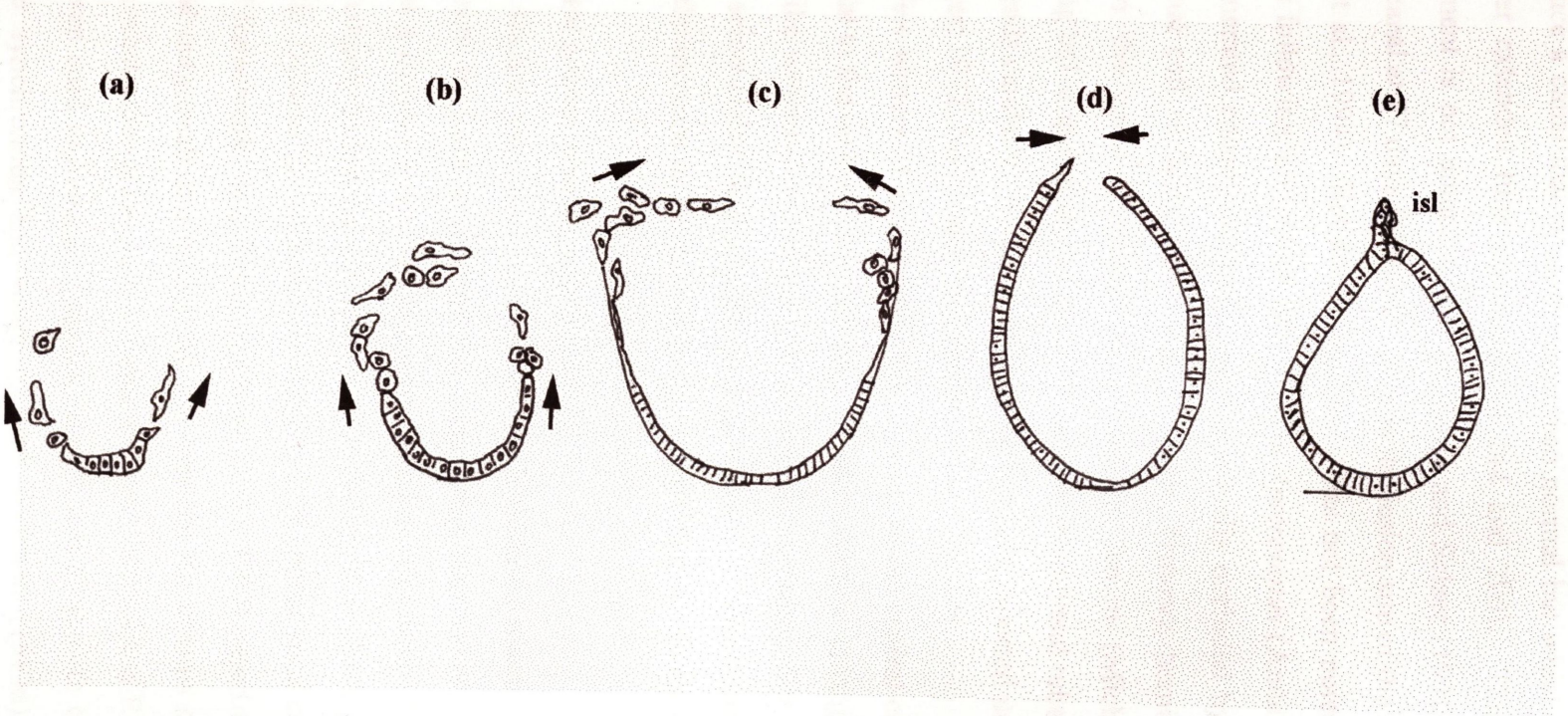


Figure 5.27. Diagrammatic representation of central canal development at days 6 (a), 8 (b), 14 (c), 20 (d) and 26 (e). The intial formation occurs through the development of what we have termed as 'plates' of columnar cells that serve as the basis for further development of the lateral and dorsal aspects of the canal. Canal closure begins by day 20 and is complete by day 26 often creating small islets of cells dorsally (isl). Arrows denote the direction of growth.

develop from the elongation of the enlarged bulb region in unison with the regeneration of the tail (Nordlander and Singer, 1978).

(c) Closure of the canal occurs by the fusion, at the dorsal surface, of the horns to produce a canal that is much larger than normal but which eventually decreases in size over extended time periods (days 144 and 200). This long period of canal enlargement is not unique to the eel; Lurie and Selzer (1991) described an enlarged central canal at 77 days following injury in the lesion site of the transected lamprey cord (Lurie et al., 1994). But an enlarged canal has not been noted in other reports. For example following amputation of the tail in *Apteronotus* (Anderson et al., 1983; 1986) the regenerated ependymal tube/canal was actually occluded by apical processes from ependymal cell surfaces, while in the urodele, *Triturus*, herniated white matter was found in the canal, frequently occluding the lumen (Michel and Reier, 1979). Following tail amputation, the canal forms as an ependymal tube behind the initial bulb as it extends caudally. No lumenal increase has been reported in this preparation (Egar and Singer, 1972; Nordlander and Singer, 1978).

Few writers, if any, refer to the reactions of the central canal in the cord rostral and caudal to the lesion site yet we have found the canal to enlarge considerably on both sides of the wound very early in the regenerative process. For example, at day 4 the canal is some eight times normal size. Increases in ependymal cell number closely matches the increase in lumenal area suggesting that cells are dividing rapidly.

Ependymal guided neurite outgrowth?

Previous studies have tried to establish the hypothesis that the ependyma following injury reacts to form a scaffold for outgrowing neurites (Anderson and Waxman, 1983a), in a manner similar to that seen during development (Nordlander and Singer, 1982). Certainly following tail amputation in the lizard *Anolis* (e.g. Simpson, 1968) and the urodele *Triturus* (Nordlander and Singer, 1978) ependymal cells produce a loosely organised framework. But Butler and Ward (1965; 1967) report that the axons precede ependymal outgrowth and bridge the gap between the stumps of ablated spinal cord through a substratum of connective tissue elements. Michel and Reier (1979), in a study of transected cord in *Xenopus* tadpoles, suggest that outgrowth of both ependyma and axons are synchronous and Anderson and Waxman (1983a) found the same in *Apteronotus*.

The present study offers strong evidence to propose that ependymal cells lag behind an initial wave of regeneration (days 6 and 8), although they span the bridge by day 10 suggesting that their regrowth is only marginally slower than that of other elements. A similar delayed appearance of ependymal cells has also been noted in the lamprey (Hibbard, 1963; Lurie et al., 1994).

The finding in the present study of rapidly dividing ependymal cells has been made elsewhere (see Wood and Cohen, 1981; Simpson, 1983; Stensaas, 1983; Anderson and Waxman, 1983a; Lurie and Selzer, 1991) although in the regenerating tail cord of amphibians (Stensaas, 1983) and lizards (Simpson, 1968; Alibardi et al., 1993) it does not result in an enlarged central canal. Interestingly, it seems that a greatly enlarged central canal appears to follow transection but not amputation injury, although ependymal outgrowth in the form of an end bulb has been described following some amputation injuries (Egar and Singer, 1972; Nordlander and Singer, 1978). In the present study development of the bridge occurred through the migration of ependymal cells and their coalescence into plates of columnar cells. These, we propose, act as templates for the further development of the canal, usually in a ventral to dorsal direction. Spindle-like ependymocytes have been described in the regenerating amphibian cord (Michel and Reier, 1979). In *Anguilla*, they are located dorsally in the stumps, and often act as a loose 'cap' of cells that occasionally seals the canal but more often provides a link between the dispersed 'plates' of cells placed more ventrally.

Not all portions of the inner lumenal-facing surface of the canal possess an ependymal coverage by day 14 indicating that the cells follow, rather than lead, the dorsal growth. Elsewhere, as in the regenerating amphibian tail, ependymal cells migrate out of the cord into the surrounding mesenchyme (Benraiss et al., 1997), but as this did not appear to happen in *Anguilla* it seems that they are encouraged to remain within the environs of the developing canal. Further evidence of such a regulatory mechanism is the absence of abnormal ependymal structures in the lumen of the enlarged canal further suggesting at a strict pattern of growth and migration. Similar methods of organised ependymal outgrowth have been demonstrated in the regenerating amphibian (e.g. Nordlander and Singer, 1978) and reptile (e.g. Simpson, 1983) tail, where the terminal portion of the regenerating ependymal tube consists of a bulb-type structure that organises and produces, through elongation, a new ependymal-lined central canal of similar size and organisation to that of the normal uninjured canal (e.g. Anderson et al., 1983; Stensaas, 1983)

At all times, the canal was more advanced in its formation in the stumps than in the bridge, effectively forming a gradient of canal development. Such gradients of outgrowth have been observed in the tail regenerate, with the ependymal based cord developing through a gradient of organisation that again begins at the terminal bulb (Nordlander and Singer, 1978) and eventually, with time, to produce a cellular organisation in the central canal in more rostral portions that was indistinguishable from normal (Anderson et al., 1983). It is noteworthy that the filum terminalum of normal uninjured spinal cord is similar to that of the regenerating cord (Anderson and Waxman, 1983a) suggesting that the cellular structures and organisation attained may reflect the normal development of this region of the cord. Such is the similarity that a 'blueprint hypothesis' for growth has been proposed by Singer and colleagues (1979). The nature of the lesion in the present study coupled with the position mid way along the body, affected a different ependymal response to those influenced by such specialised regions in the cord, and thus may serve to explain the obvious differences in ependymal outgrowth and subsequent formation of the enlarged central canal.

Migratory ependymal cells and those in the developing bridge expressed a cellular phenotype atypical of normal ependymocytes. Whereas the cells in uninjured cord possessed a columnar, electron dense appearance with an irregular shaped nucleus, these cells in general possessed a circular to elongate structure with a medium to light staining cytoplasm and nucleus with dispersed chromatin. Nuclear shape also changed from irregular to ellipsoid, with an increase in size evidenced from electron micrographs and the numerous large BrdU labelled nuclear profiles found at days 7, 11 and 15 (as seen in Fig's. 5.6 and 5.10). An increase in nuclear size is common in cells undergoing mitotic division and a similar intense mitotic rate has been shown in the regenerating ependymal cells of the newt *Pleurodeles* (Benraiss et al., 1997). Indeed in many different anamniote studies, ependymal cells have been described undergoing mitosis *in vivo* (e.g. Michel and Reier, 1979; Simpson, 1983; Anderson et al., 1986; Anderson and Waxman, 1991) and *in vitro* (O'Hara et al., 1994) while ependymal cell division has been noted in amniotes (Gilmore and Leiting, 1980; Beattie et al., 1997). The finding in the present study of an elevated mitotic rate until approximately day 26 corresponds with the complete internalisation of the central canal in the bridge. This suggests that (a) the ependymal cell proliferation is controlled by some unknown mechanism that is triggered by complete formation of the new canal and (b) the

ependymal cells themselves have begun to change from their migratory and proliferative phenotype.

The alterations in cellular structure to produce a migratory phenotype has been described in some studies (e.g. Wood and Cohen, 1981; Anderson et al., 1983a) but not all, as in some studies few differences were noted (e.g. Simpson, 1968). Interestingly proliferating ependymal cells in injured amniote spinal cord were also found not to differ considerably from cells of uninjured cord (Matthews et al., 1979; Bruni and Anderson, 1987) although different shaped ependymal cells with varying nuclear staining was noted by Bernstein (1986).

Vimentin labelling illustrated an alteration of the intermediate filament fibre content in the ependymocytes surrounding the enlarged canal in the bridge. Vimentin labelling in the uninjured cord is negligible and confined specifically to small portions of the dorsal and ventral tracts (see chapter 2) but in the regenerating cord, the ependymal layer strongly labels for this antibody indicating an alteration of the intermediate filament content in these cells. Similar increases in vimentin have been noted in the regenerating tail ependymocytes of the axolotl *Ambystoma* (O'Hara et al., 1992). It has been proposed that this upregulation of vimentin is an indicator of change from an epithelial (normal ependymocytes, Kettenmann and Ransom, 1995) to a mesenchymal phenotype during formation of the central canal when ependymocytes are actively migrating (Chernoff, 1996). The present study lends support to such a hypothesis. An alternative viewpoint is that these ependymal cells may re-enact a developmental program which imbues a migratory phenotype such as that found during the formation of the different CNS structures from the primitive neuroepithelium (e.g. Levitt and Rakic, 1980; Raamsdonk et al., 1984).

Fate of cells?

The reduction in the number of ependymal cells following closure of the canal by day 26, also seen with the reduction in BrdU labelling, suggests that the ependymocytes surrounding central canal are changing their behaviour at this time, perhaps they cease or enter a period of relatively low mitotic division, such that more cells are lost than are replaced or else they undergo apoptosis or programmed cell death similar to that found during development (e.g. Kuan et al., 2000) so as to reduce cell numbers. Alternatively, of course, they could migrate from around the central canal, perhaps differentiating into other cell types. The finding of small numbers of tanycytic processes extending from

the ependymal regions of the canal by day 16 suggests that some ependymal cells are differentiating into this cell type. Benraiss and colleagues (1997) have demonstrated that ependymal cells migrate to produce melanocyte and Schwann cells. Furthermore, the production of new neurons in the regenerated portion of the cord of two weakly electric fish species, *Sternachus* (Anderson and Waxman, 1991) and *Sternopygus* (Ungez and Zakon, 1997) has been attributed to the migration and differentiation of ependymal layers cells.

Tanycytes

The presence of tanycyte cells in the bridge is an unusual finding but one that suggests that they are an integral component of the regenerating cord. Its morphology, association with the central canal and immunoreactivity to GFAP identified this cell type (Flament-Durand and Brion, 1985; Rafols 1986). Their tail processes extend to the periphery and compartmentalise the regenerating cord; moreover, they are often adjacent to regrowing axons (e.g. Nordlander and Singer, 1978; Singer et al., 1979). Nevertheless, they are not seen in the early stages of bridge formation and their numbers are generally low even by day 26 when a large proportion of bridge material, including the axons, has been reconstituted. Thus, it appears that this cell type in the eel may play a greater role in reconstituting the long-term glial organisation in the bridge. This resembles the glial structure found in the fish brain which is considered to be primarily of tanycytic origin (e.g. Pokay, 1993) and the radial glia found in the developing amniote spinal cord (Pixley and de Vellis, 1984; Voigt, 1989). Interestingly, radially orientated ependymal processes have been found in the reactive ependymal population of the injured rat spinal cord (Bruni and Anderson, 1987). In anamniotes the major glial structure is the radial astrocyte (e.g. Bodega et al., 1993) however, in the regenerating bridge no such structure was found although it is known that radial astrocytes develop through the displacement of cells from the ependymal region, but since we have looked only to day 175, it is possible that the radial astrocytic structure is also reconstituted. Nonetheless, the slow formation of the tanycytes in the bridge points to a very slow reorganisation of the bridge that occurs over a longer period of time.

Summary of main findings

- As a result of degenerative events a central canal is absent from portions of the spinal stumps during the initial stages of regeneration
- Reformation of a new central canal begins in the stumps by approximately day 6 through the outgrowth of ependymal cells to produce plates of columnar cells, usually placed ventrally that provide the basis for further canal formation.
- Portions of the new central canal have formed in the bridge by day 8, but continuity is not achieved until approximately day 10.
- BrdU labelling indicates that ependymal cells involved in the formation of the bridge and in the associated stumps are highly mitotic, with enlarged generally oval to ellipsoid nuclei.
- The strong correlation between cell number and perimeter, indicative of a uniform cell density suggests that cells quickly acquire a columnar organisation in the bridge. At the leading edge of canal formation however, cells possess a more elongate spindle shaped form.
- Canal development is characterised by the formation of dorsally projecting glial horns in the bridge that is colonised by ependymocytes along the inner surface to produce the lateral walls of the enlarged canal.
- Canal formation is characterised by a specific and intense labelling for vimentin in the ependymal layers.
- Canal closure is initiated by the fusion of the horns along the dorsal surface, resulting in the fusion of the ependymal cells dorsally, often creating small islets of ependymal cells.
- With time, the canal size decreases and is characterised by a parallel reduction in ependymal cell number. BrdU+ve profiles in the ependymal layers during this time is also reduced.
- Tanycytes differentiate from the ependymal layers and produce long GFAP+ve cellular processes that extend to the periphery of the bridge. With time this cell type becomes the predominant glial cell in the bridge.

Chapter 6

The organisation of the regenerating central canal: II. Liquor contacting neurons

6.1 Introduction

In chapter 6, we have reported on the contribution made by ependymocytes to the formation of a new central canal following injury and we have also shown that tanycytes, a specialised cell type of ependyma surrounding the uninjured central canal (see chapter 4), are also involved in the reparative process. Since other cell-types have also been described as components of the uninjured ependyma in several vertebrates (e.g. Mugnaini and Walberg, 1965; Schonbach, 1969; Stevenson and Yoon, 1982) it is possible that following injury some of these cells could play a role in the regenerative event. One such group is a population of highly specialised neurons that have been described as a component of the ependyma surrounding the central canal in the cord and ventricles of the brain in most vertebrate group. The terminology used to describe these cells is extensive: in the developing embryo they are often designated as Kolmer-Agduhr cells (Dale et al., 1987a; 1987b; Nordlander and Liu, 1996; Martin et al., 1998), while in the adult they are called cerebrospinal fluid-contacting neurons, CFCN's (Alibardi et al., 1992), or liquor contacting neurons, LCN's (Vigh-Teichmann et al., 1973; Roberts et al., 1995); hereafter we term these neurons as LCN's. The cell is generally bipolar in form, comprising an amphora-shaped perikaryon (Roberts et al., 1995) with processes that extend to the lumenal surface of the canal and into the surrounding grey matter (Vigh-Teichmann et al., 1973; but see Roberts et al., 1995). Functionally, relatively little is known of these neurons which constitute a large proportion of the dopaminergic population in the fish spinal cord (Roberts et al., 1995), but it is known that they immunoreact for numerous neurotransmitters, including GABA (Uematsu et al., 1993), dopamine (Roberts and Meredith, 1987; Roberts et al., 1989) and tyrosine hydroxylase (Roberts et al., 1995). Furthermore, LCN's surrounding the central canal of the cord label heterogeneously for different neurotransmitters (Roberts et al., 1995) with some labelling for two or more (Silver et al., 1988) suggesting that functional differences may exist between different groups.

Little is known of the regenerative capacity, if any, of this neuron. Studies of the regenerating amphibian (Alibardi, 1989) and lizard (Alibardi and Meyer-Rochow, 1990) spinal cord following amputation injury have shown that LCN's are a component of the developing ependymal tube in the regenerating tail and in the lizard immunoreact for GABA (Alibardi et al., 1993). But it remains unclear whether LCN's play a central

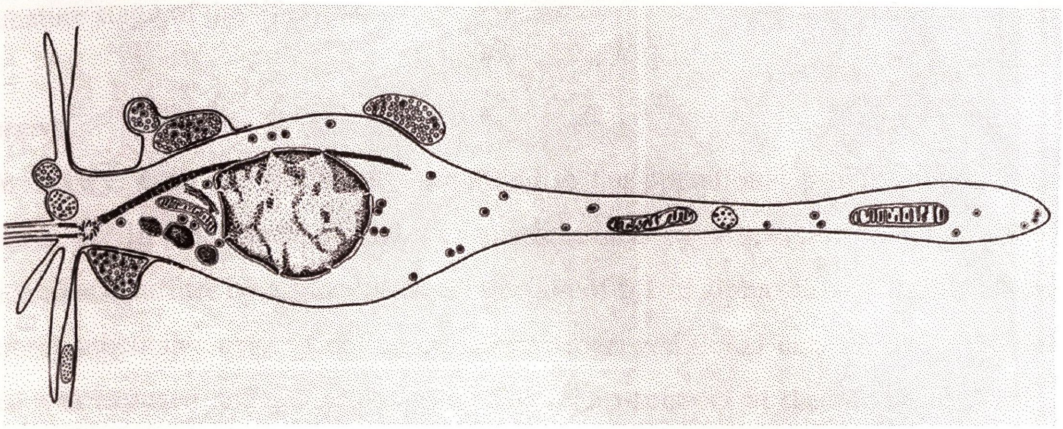


Figure 6.1. LCN's of fish can be divided into three parts: a central somal region containing the nucleus; a 'head' region that contacts the cerebrospinal fluid, forming a rosette of cellular processes with a single cilium attached, and a tail region that extends into the grey matter of the cord. Synaptic junctions are common on the cell body and tail process (taken from Roberts et al., 1995).

role in the development of the regenerating cord or appear at later stages following injury.

In the present study, we have attempted to determine the effects of spinal injury on the LCN population in the spinal cord of the eel. A previous study by Roberts and colleagues (1995) has shown that the LCN population surrounding the central canal of the eel is immunoreactive for the neurotransmitter gamma-aminobutyric acid (GABA) and the enzyme tyrosine hydroxylase (TH), involved in dopamine synthesis. Furthermore, LCN's immunoreactive for each antibody hold distinct positions around the canal lumen (Roberts et al., 1995). Using both TH and GABA immunohistochemistry, in combination with light and electron microscopy, we have attempted to chart the effects of a transection injury on the LCN population in the spinal cord and their role, if any, in the development of the bridge at set times following injury.

6.2 Materials and Methods

Animals

This study is based on 20 European eels *Anguilla anguilla L.* in a non migratory immature stage of the lifecycle.

Surgery

For surgery, each eel was treated according to the operational procedures outlined in chapter 4. In brief each animal was anaesthetised by immersion in 0.3g/l MS-222 (Sigma) and further by a subcutaneous injection of 0.1ml alphaxalone ("Saffan" Pitman-Moore) subcutaneously. Cooling on ice provided additional anaesthesia. The spinal cord was exposed and transected using fine micro-scissors at the region of the fourth segment caudal to the anus. Following surgery, animals were placed in separate holding tanks.

Tissue Preparation

For histological investigation, each animal was treated according to the methods described in chapter 2. In brief, each animal was anaesthetised initially by immersion in 0.3mg/L MS-222 and further by a subcutaneous injection of 0.3ml alphaxalone ('Saffan' Pitman-Moore). To prevent blood clotting, 0.2ml heparin sodium (Leo Laboratories) was also given subcutaneously. The perfusion procedure consisted of a primary flush of Ringer's solution (with 0.1% procaine (Sigma) for further anaesthesia) through the heart followed by the fixative. Two fixative solutions were used (a) 4% paraformaldehyde in 0.1M phosphate buffer (PB), pH adjusted to 7.4, for immunohistochemical investigation and (b) 2% paraformaldehyde, 1.25% gluteraldehyde in 0.1M phosphate buffer (PB), pH adjusted to 7.4, for electron microscopy. Following perfusion, the region of the spinal cord containing the injury and portions immediately rostral and caudal, were dissected from the spinal column and post-fixed in the same fixative at $4^{o}C$ for a maximum of 3 hours.

Light Microscopy

Following postfixation, all sections were pre-treated in 1% sodium borohydride in distilled water to remove residual fixative, 1% H_2O_2 in appropriate buffer to reduce any existing endogenous peroxidases due to the presence of the blood clot and finally

treated in 5% normal serum appropriate to the antibodies used to reduce background staining. Sections were rinsed for 5 x 5 minutes between each incubation.

For the primary antibody reaction, sections were incubated in (a) tyrosine hydroxylase (TH) mouse monoclonal (Incstar), 1:3,000 in 0.1M Tris-HCl, 0.9% NaCl and 0.5% Triton X-100, or (b) rabbit antisera raised to GABA (generous gift by Dr. R. Buijs), 1:10,000 in 0.1M PB, 0.9% NaCl and 0.5% Triton X-100. Sections were incubated at 4°C for 48 hours and then treated respectively with (a) biotinylated horse anti mouse IgG (Vector), 1:200 in 0.1M Tris-HCl, 0.9% NaCl and 0.5% Triton X-100 (b) biotinylated goat anti rabbit IgG (Vector), 1:200 in 0.1M PB, 0.9% NaCl and 0.5% Triton X-100 and incubated overnight at 4°C or for 2 hours at room temperature.

All other procedures were carried out as described in chapter 2 using the avidin-biotin method (ABC kit, Vector) and (0.05%) 3,3'-diaminobenzidine (DAB, Sigma) as chromogen.

Electron Microscopy

The tissue was processed for electron microscopy according to the procedure described in chapter 2. Sections were cut for both light (1.5μm) and electron microscopy (~500Å). All images were downloaded, analysed and formatted on a Macintosh G3 computer using Adobe PhotoShop 5.

6.3 Results

Normal Cord

In the uninjured spinal cord, liquor-contacting neurons (LCN's) are easily distinguished because they contact the cerebrospinal fluid of the canal and have a characteristic shape (Fig 6.2). The bipolar shape and their cellular ultrastructure, as seen with the electron microscope (Fig. 6.3), distinguishes them from the other cells of the canal such as ependymocytes, tanycytes and light-staining cells (see also chapter 2).

These cells label with the antibodies for tyrosine hydroxylase (TH) and gamma-aminobutyric acid (GABA), but TH+ve profiles are confined to the ventral portions of the canal while GABA+ve profiles mostly line the lateral regions of the canal although, occasionally, profiles immunopositive for this neurotransmitter are also found ventrally (Fig. 6.4a,c). In longitudinal section of the cord, these neurons are seen to be densely packed with an approximate density of 10 neurons per 100μm of the cord.

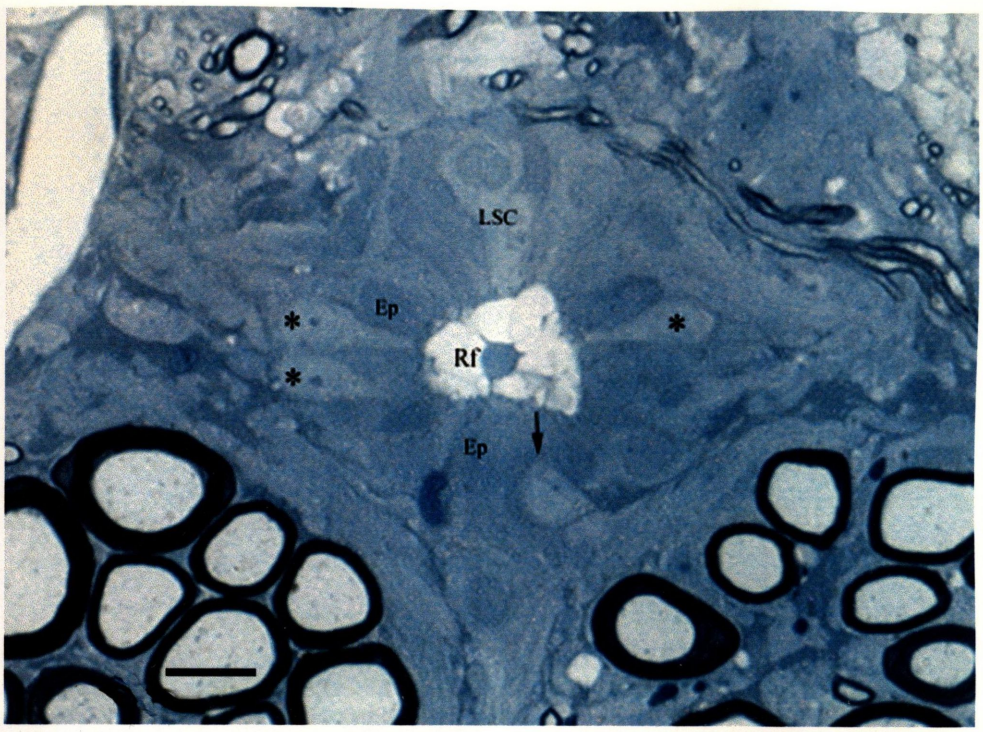


Figure 6.2. Photomicrograph of LCN's surrounding the central canal of the uninjured spinal cord. Note the distinctive structure and positions of these neurons on the lateral (*) and ventral (arrowheads) sides of the canal. Scale bar = 10 microns.

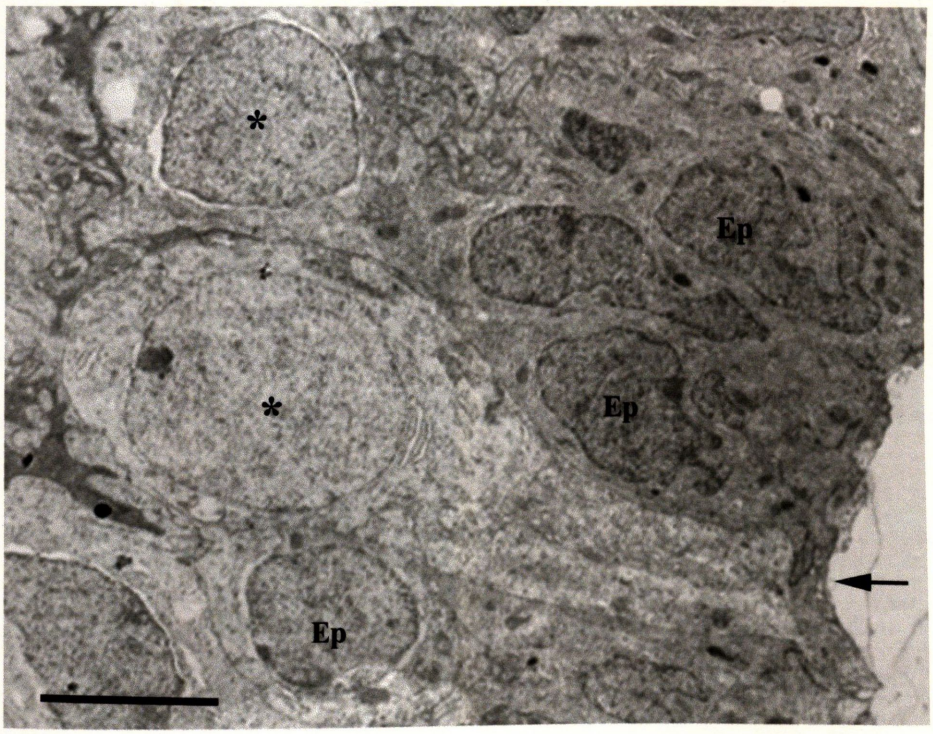


Figure 6.3. Electron micrograph of two LCN's on the lateral surface of the canal. Note the prominent light staining nucleus which is characteristically circular in shape (*). Other features include a cytoplasmic process that contacts the lumen of the canal (arrow). Note the difference in staining compared to the surrounding ependymocytes (Ep).
Scale bar = 3 microns.

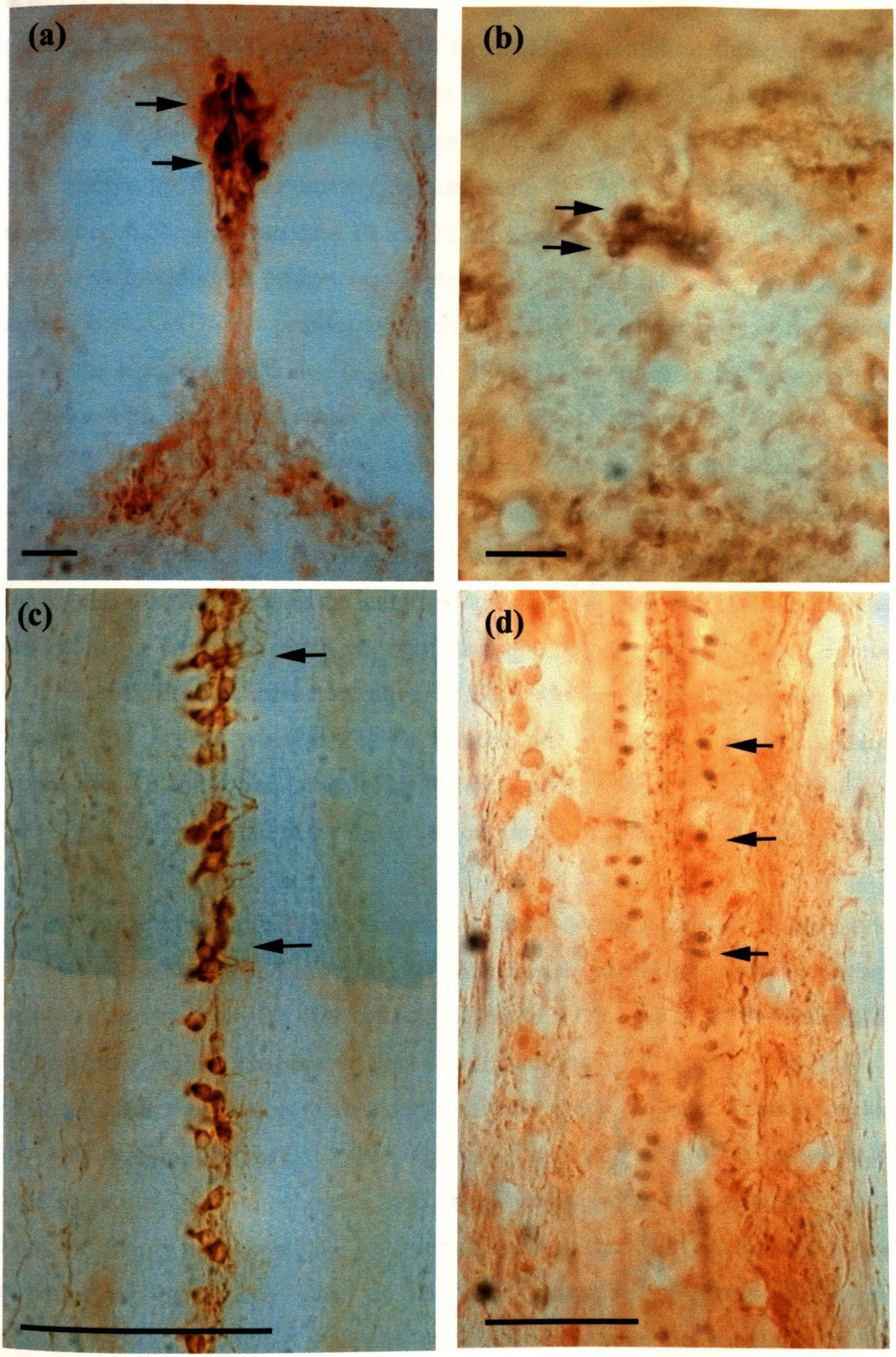


Figure 6.4. Photoicrographs of TH+ve (a, c) and GABA+ve (b, d) profiles seen in transverse (a, b) and horizontal (c, d) section (arrows). Note the distinctive positions of the the TH+ve and GABA+ve profiles and the relatively homogeneous distribution of both along the rostro-caudal axis of the cord. Scale bar (a) and (b) = 20 microns, (c) and (d) = 100 microns.

The Regenerating Cord

Immunopositive structures (for either GABA or TH) resembling those found in the uninjured cord were not found in the bridge until approximately 11 days following the transection. However, at earlier stages, days 5-10, LCN profiles in both the rostral and caudal stumps up to approximately 300μm from the developing bridge decline in number (Fig. 6.5). Between days 10 and 11, small numbers of TH+ve and GABA+ve profiles were found in the bridge close to the developing central canal. As found in the uninjured cord, GABA+ve profiles were located along the lateral sides of the enlarged canal in the regenerating bridge (Fig. 6.6), while TH+ve profiles lay more ventrally (Fig. 6.7). With time, the numbers of TH+ve and GABA+ve profiles increased in the bridge (Fig. 6.8) but their densities were always lower than in the uninjured cord. Furthermore, the intensity of labelling in the bridge was often lower compared to the stumps (see Figs 6.8a). The GABA+ve profiles are generally aligned around the canal of the regenerating bridge as in the uninjured cord (see Fig. 6.9) but TH+ve profiles are somewhat more erratically arranged, particularly during the early stages of recovery (Fig. 6.10a, b). Profiles immunopositive for GABA have a flask shape, with few tail processes (Fig 6.11a), whereas TH+ve neurons are bipolar and possess elaborate processes that extend to the lumen of the enlarged canal as well as the bridge (Fig. 6. 11b). These TH+ve tails often form a ventral plexus of thin TH+ve processes (Fig. 6.12a, b).

At the level of the electron microscope, light staining cells with large circular-like nuclei, atypical of ependymocytes, were found on the lateral and ventral surfaces of the central canal by at day 20. The cells on the lateral surface are ovoid to amphora-like in shape with a large homogeneous light-staining nucleus (Fig. 6.13a), while those on the ventral surface possess a more elongate bipolar shape but with a similar nuclear shape and staining intensity. The light-staining cytoplasm contains numerous organelles particularly mitochondria and rough endoplasmic reticulum. Junctional complexes, mainly tight junctions, are common between this cell type and the adjacent ependymocytes, particularly close to the canal lumen (Fig. 6.13b). Evidence of complex rosettes of cellular processes and cilia contacting the canal lumen were occasionally found but many of the cells lacked these elaborate structures. Few synaptic junctions were found on the perikaryon or the tail processes and Reissner's fibre was absent from the enlarged canal in the bridge at all days studied.

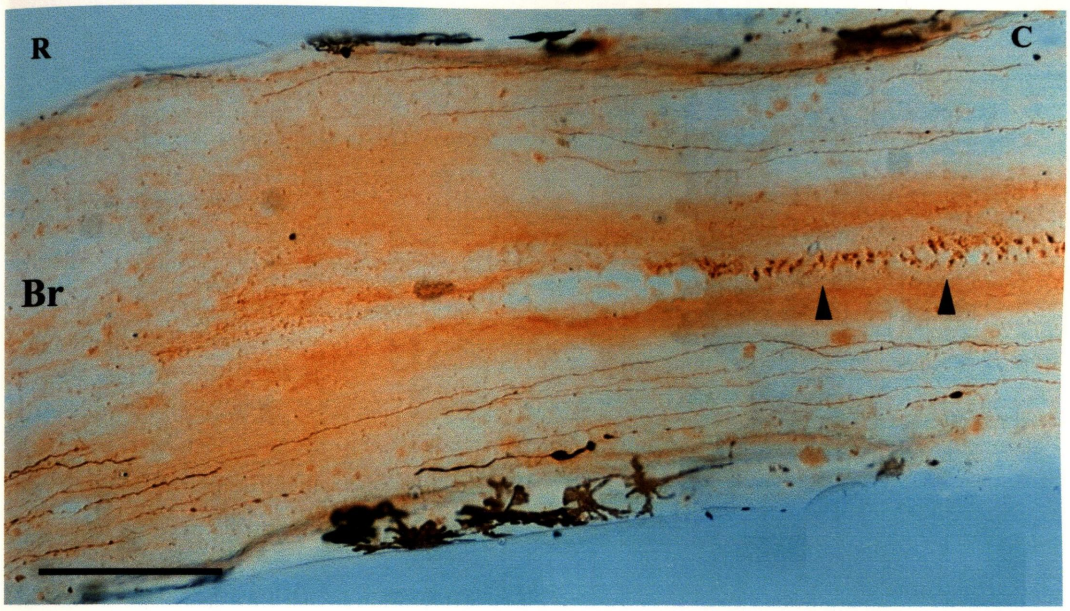


Figure 6.5. Photomicrograph of TH+ve profiles in the caudal stump 8 days following injury (arrowheads). Note the absence of immunopositive profiles from regions close to the developing bridge. R = rostral, C = caudal, Br = the developing bridge.
Scale bar = 50 microns.

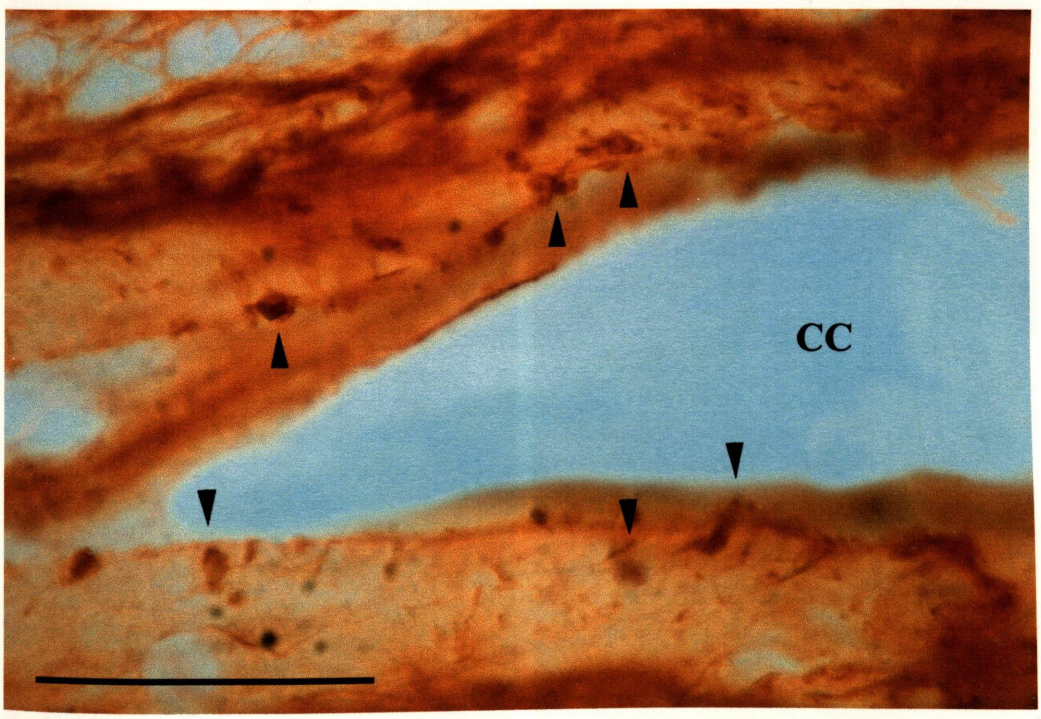


Figure 6.6. GABA+ve profiles in the bridge 11 days following injury. Note the immunopositive profiles apposing the lumen of the enlarged central canal (arrowheads). CC = central canal. Scale bar = 50 microns.

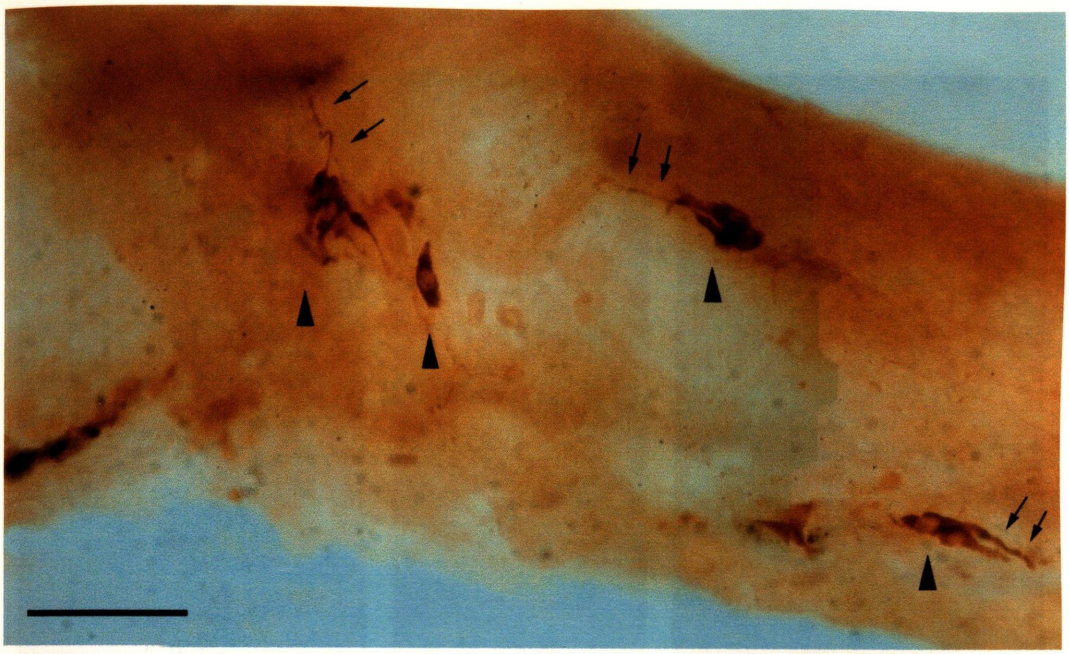


Figure 6.7. Phtotmicrograph of TH+ve profiles in the bridge at day 10. Note their loose organisation (arrowheads), and the absence of a central canal in this section. Long tail processes extend in apparently random directions from the cell body (arrows). Scale bar = 50 microns.

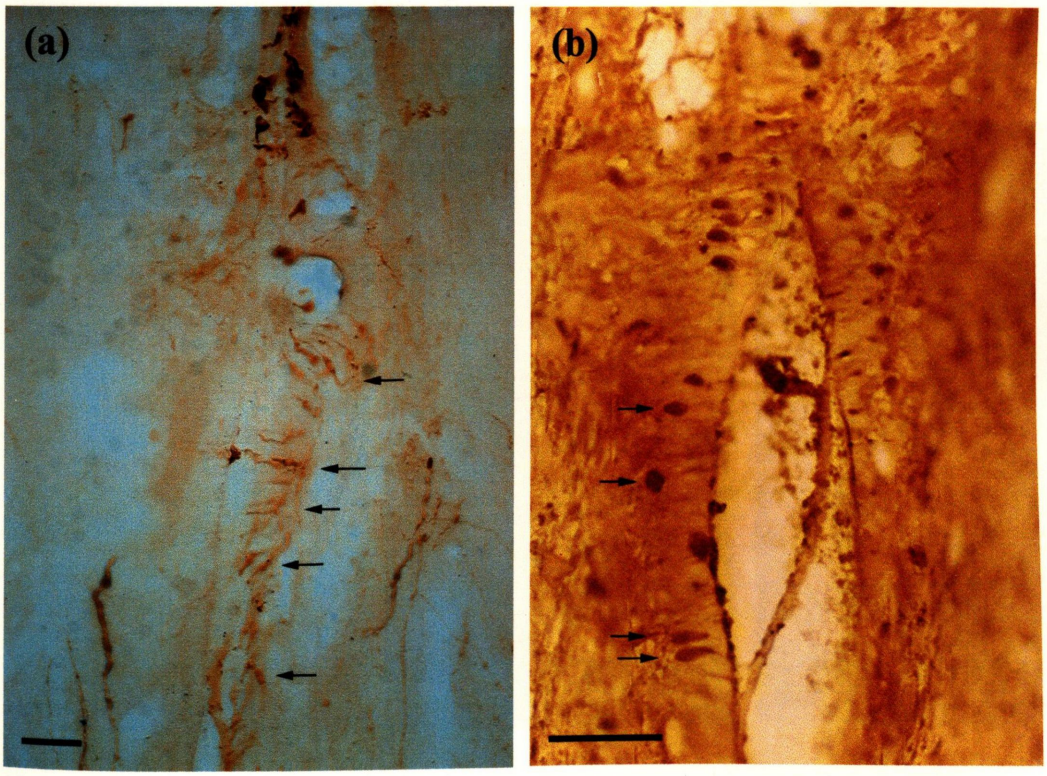


Figure 6.8a, b. Phtotmicrographs of (a) TH+ve and (b) GABA+ve profiles in the bridge at days 13 and 21 respectively. Note the increase in the number of immunopositive profiles (arrows) in the bridge compared to earlier stages of recovery. Scale bar = 50 microns.

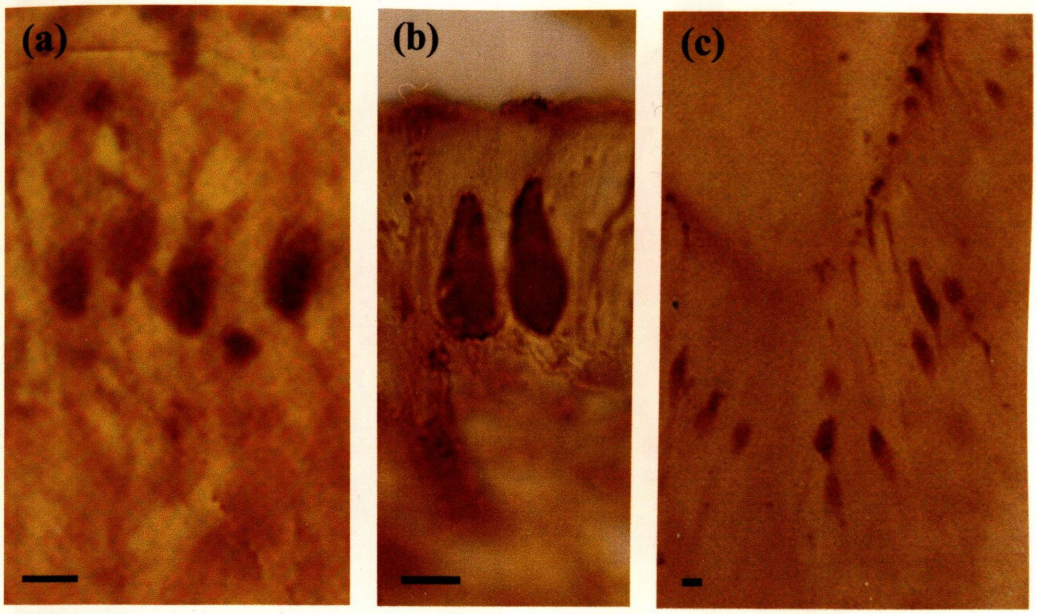


Figure 6.9. Orientation of GABA+ve profiles apposing the canal in (a) uninjured cord, and the regenerated bridge at days 21 (b) and 34 (c). Note the regular organisation of the immunopositive profiles. Scale bar = 20 microns.

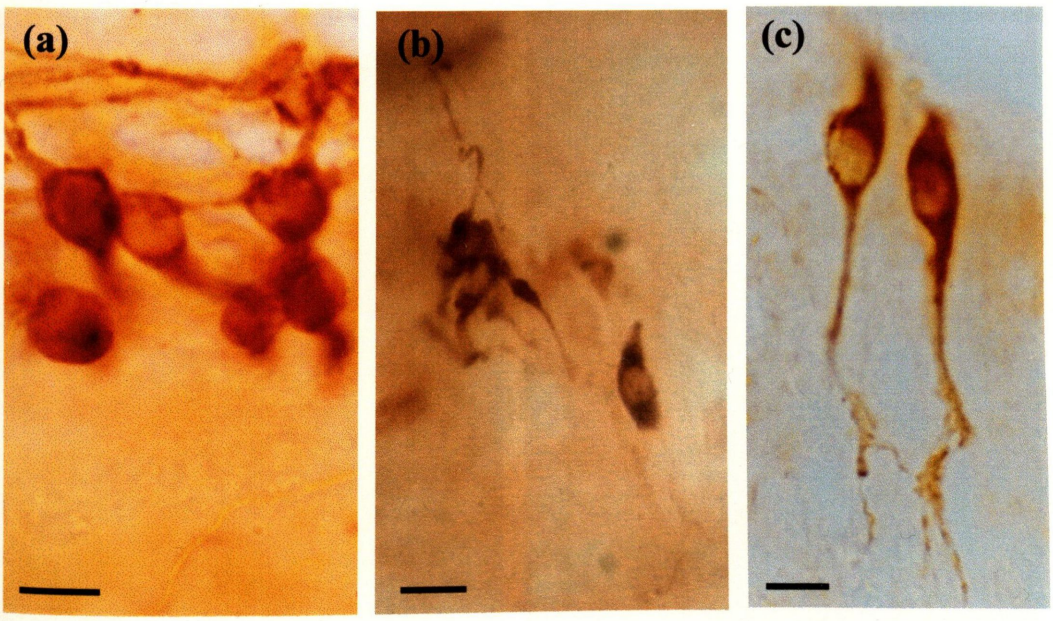


Figure 6.10. Photomicrographs of TH+ve profiles in (a) the normal cord and in the bridge at days 11 (a) and 30 (c) following transection. Note the erratic orientation of the immunopositive profiles and the long tail processes as they project into the ventral cord. Scale bar = 10 microns.

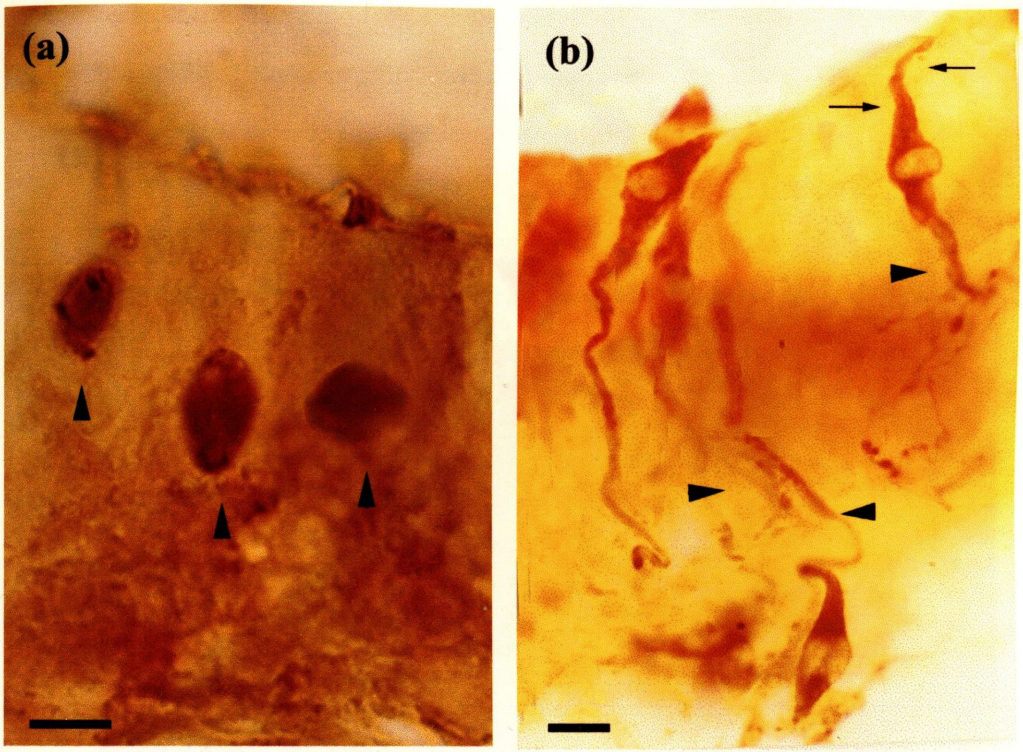


Figure 6.11a, b. Phtotmicrographs of (a) GABA+ve and (b) TH+ve profiles in the bridge. Note the absence of tail processes in the GABA+ve profiles (arrowheads). When present, short projections, extend to the lumenal surfaces. In (b), TH+ve profiles possess a more elaborate form, with long processes that extend considerable distances to the lumenal surface (arrows) and long tail processes (arrowheads) that project into the ventral aspects of the bridge. The cell bodies were often displaced from around the canal, but in all instances contacted the lumenal of the canal. Scale bar = 10 microns.

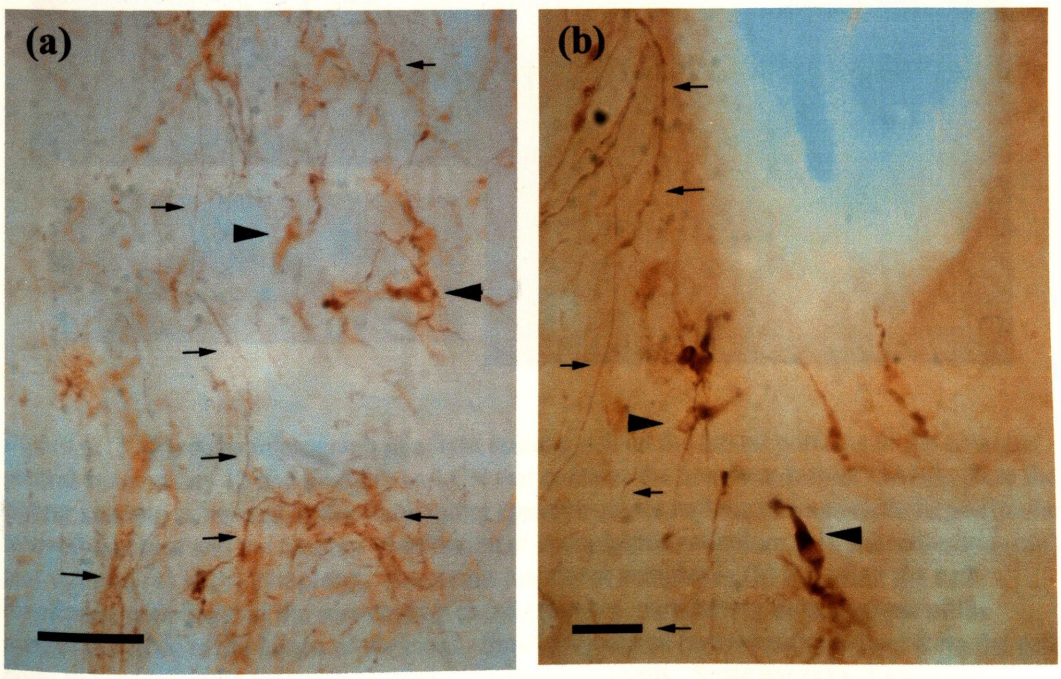


Figure 6.12a, b. Photomicrographs of the ventral portions of the bridge at days 13 (a) and 30 (b) that contained numerous thin TH+ve processes of undetermined origin (arrows). Note the erratic organisation of the profiles and the presence of TH+ve cell profiles (arrowheads). Scale bar = 50 microns.

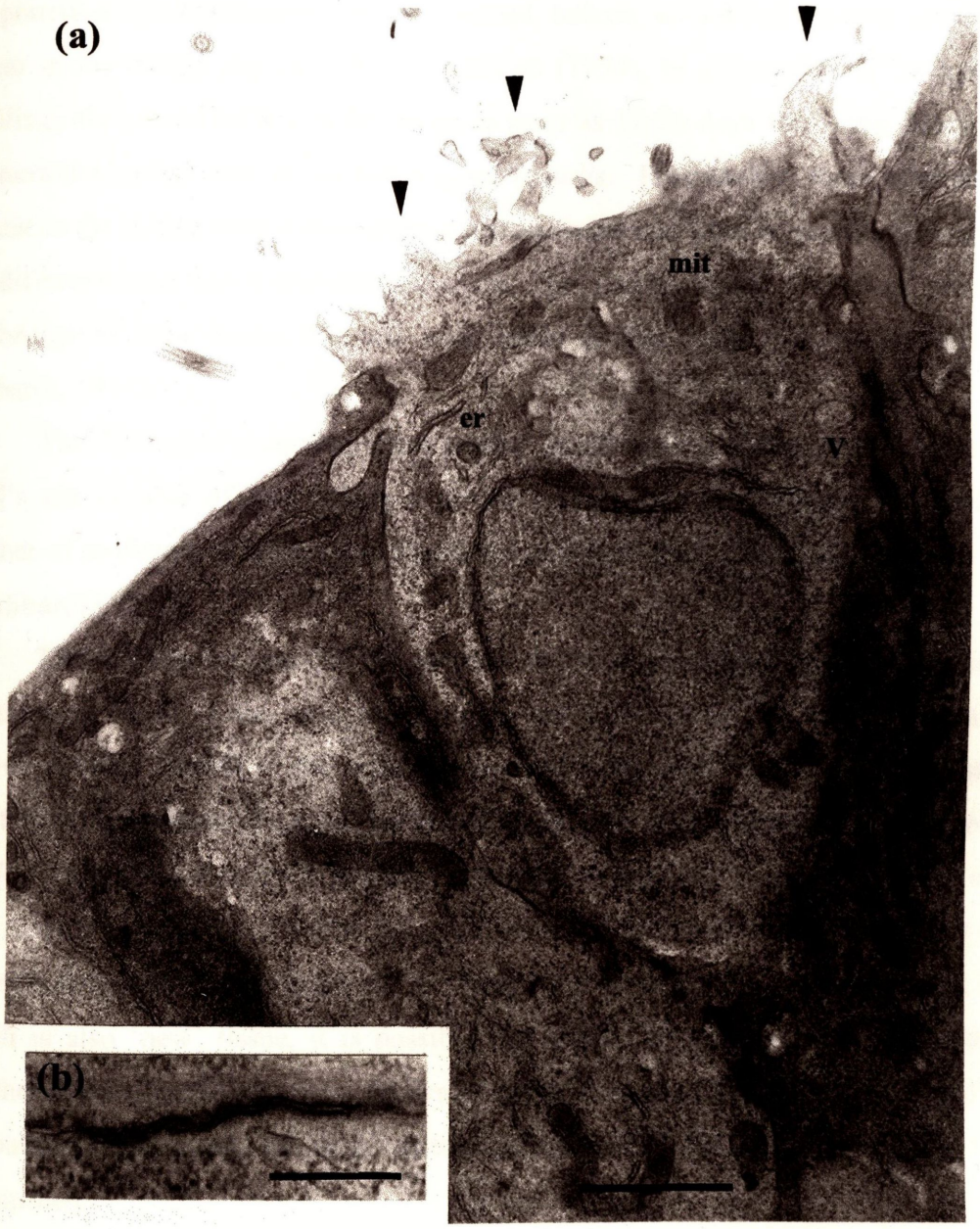


Figure 6.13. Electron micrograph of a light staining cell on the lateral portions of the enlarged central canal at day 12 and possibly an LCN that contains the neurotransmitter GABA. Note the lighter staining compared to the surrounding ependymocytes and the characteristic large circular to ovoid nucleus and the random distribution of endoplasmic reticulum (er), mitochondria (mit) and vesicles (v) in the cytoplasm. Numerous junctional complexes (b) inter-link the cell membrane with those of the surrounding ependymocytes, particularly those regions of the membrane close to the lumen of the canal. Small projections (arrowheads) extend from the cell body to produce indentations in the apposing ependymocytes. Scale bar (a) = 3 microns, (b) = 1 micron.

6.4 Discussion

The present results demonstrate that liquor-contacting neurons (LCN's) are a component of the regenerating spinal cord and, indeed, are one of the first cell types to appear in the bridge (by day 10-11). Alibardi (1994), in a study using ^{3}H-thymidine labelling, also noted LCN's in the bridge as early as 12-20 days following injury of the regenerating spinal cord of the lizard *Lampropholis*. Presumably, these cells must be present in the bridge even earlier since a certain amount of time is necessary for genesis and differentiation into a neuronal phenotype. The increase in the number of neurons in the bridge as time passes has also been noted in the study of *Lampropholis* cord (Alibardi, 1994).

The finding of immunopositive profiles in all regions of the canal indicates that LCN's are capable of establishing a presence throughout the bridge. However, the number of profiles was always less than in the uninjured cord, as has already been noted by Alibardi (1994).

The GABA+ve and TH+ve neurons in the regenerating bridge have similar positions to those of the uninjured cord in that GABA+ve neurons are lateral and TH+ve neurons ventral to the canal lumen. Nordlander and Liu (1996) demonstrated that following rotation of a small portion of neural tube in developing *Xenopus* embryo, LCN's close to the host/graft interface reoriented to conform to the neural tube of the host embryo, while those within the graft remained unchanged, suggesting that local intrinsic factors are responsible for the directional growth. In the regenerating cord, which is also 'new' tissue, it is possible that similar signalling may also occur, but whether these signals arise from factors in the cerebrospinal fluid, the ependymal cells surrounding the canal, or from particular regions of the bridge, remains to be determined.

The orientations of the immunopositive neurons in the bridge even at the earliest stages (days 10-11) indicates an ordered alignment with the central canal. Similar findings in the developing CNS (Dale et al., 1987) and regenerating cord (Alibardi et al., 1993) indicate that this cell type quickly assumes an ordered orientation in the developing canal similar to that of the uninjured cord (see Fig. 6.14).

Although neurons immunoreactive for both antibodies were detected in the bridge at approximately the same time following injury, they differ in size and shape.

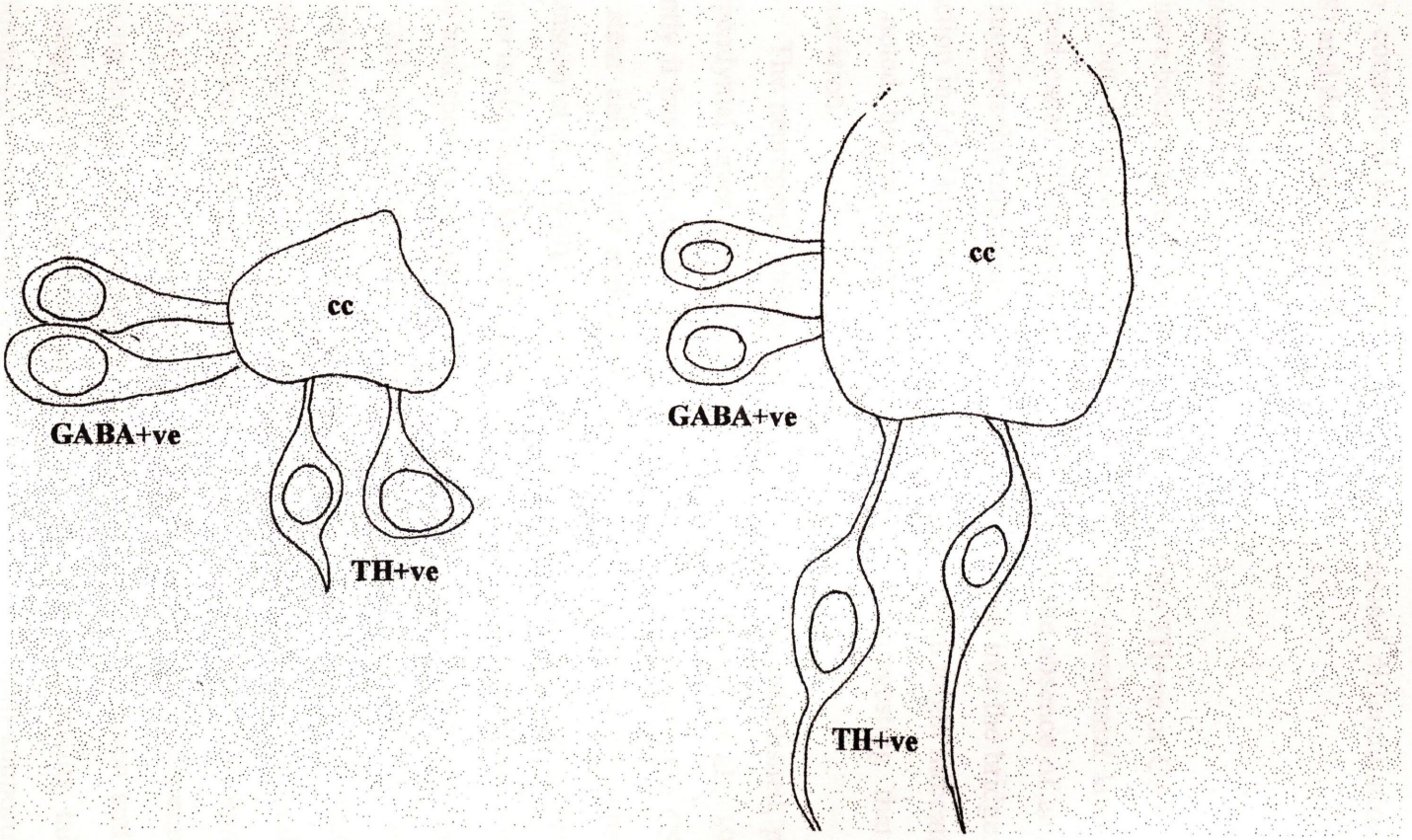


Figure 6.14a, b. Diagrammatic representation of LCN's immunoreactive for GABA and TH in (a) the uninjured cord and (b) the regenerating bridge. Note the similar positions and orientations of the neurons in the bridge compared to those surrounding the canal in the uninjured cord. TH+ve LCN's however display a more elongate form and a greater disorganisation in the bridge compared to the GABA+ve neurons situated in the lateral walls of the canal.

In general, both types resemble those of the uninjured cord (see Fig. 6.14), although for some GABA+ve cells the cellular processes that extend towards the lumen of the canal are absent and the cell body appears to make direct contact with the lumen. Such neurons close to the ependymal layers in some regions of the developing CNS have been considered to represent early stages of neuronal differentiation (e.g. Supèr et al., 1998) and that may also be the case here.

Neurogenesis

We have been unable to determine the origins of the TH+ve or GABA+ve LCN's in the bridge but the most obvious source would be the ependymal layers surrounding the enlarged canal. This assumption is supported by the absence of any labelling pattern that suggests the migration of LCN's from the stumps into the bridge. Furthermore, the reduction in LCN number in the adjacent stumps, which might indicate some migration, was noted before bridge formation (days 5-8), suggesting that it results from degeneration.

The neurogenic ability of the ependyma is well-established, particularly of the subependymal layer (see Morshead et al., 1994; Peretto et al., 1999), while more recently it has been shown that the ependymal layer apposing the CSF also possesses true stem cell ability and contributes progenitor cells to the subependymal layers (Johansson et al., 1999). In fish, the ability of the ependymal layers to produce new neurons is also well known (Zupanc and Zupanc, 1992; Huang and Sato, 1998; Zupanc, 1999) and there is evidence to suggest that the regenerating ependyma may possess stem cell capability. For example, Benraiss et al. (1997) in an elegant set of experiments demonstrated that the ependyma surrounding the central canal in the regenerating tail of two urodeles was capable of generating neural crest-like cells, indicating true stem cell ability. In the weakly electric teleost fish *Apternotous,* Zupanc and Ott (1999) have shown that the cerebellum is capable of generating new neurons following injury while in the regenerating spinal cord Anderson and Waxman (1991) have proposed that the electromotoneurons in the regenerating tail arise from the ependyma surrounding the central canal, and this has been supported by findings in *Sternopygus* (Ungez and Zakon, 1997). Alibardi (1989) in a detailed electron microscopic study of LCN development in the regenerating cord of the newt *Triturus* proposed that the new neurons arose from ependymal cells that undergo neural differentiation. In light of these findings, it is probable that the LCN's found in the

bridge arise from a neural progenitor cell type associated with the ependymal layers surrounding the central canal.

Functional Aspects

The possible role of LCN's in the developing and uninjured spinal cord remains unknown, although dopamine and GABA are known to modulate the activity of spinal cord CPG's (e.g. Grillner et al., 1995; Arshavsky et al., 1997; Kemnitz, 1997). However at no time have we seen neurons other than the TH+ve and GABA+ve profiles in the regenerating bridge, which consists solely of blood vessels, glia and regrowing axons. The axons of LCN's have, therefore, either to seek out targets in the adjacent stumps or to liberate their transmitters into the volume of the bridge. Should this be the case, the appearance of these neurons at a time when regenerating axons have yet to find their targets raises the possibility that these neurotransmitters are contributing in some way to the formation of the bridge.

It is known that alteration of the ventral midline region of the developing spinal cord of fish results in abnormal formation of neuronal structures. For example, there are fewer than normal Kolmer-Agduhr cells (LCN's) along the ventral midline in cyc-1 mutant zebrafish (Bernhardt et al., 1992) from which midline floor plate cells have been depleted. Furthermore, the axonal trajectories of these cells are often altered. Clarke et al. (1991) in a study of notochordless *Xenopus* embryos produced by UV irradiation also noted an alteration in the floor plate organisation and a subsequent reduction (85%) in the number of motor neurons. Since LCN's are interspersed between ventral midline cells it is possible that LCN's may be playing a role in some of these instructional events. Since the bridge of regenerating tissue in the present study is composed of 'new' tissue, the presence of LCN's surrounding the central canal could reflect a recapitulation of embryonic events. The following sections explore such a possibility in relation to the presence of GABAergic and catecholaminergic neurons in the bridge.

TH+ve neurons in the bridge

The presence of TH+ve immunolabelling of neurons in the bridge by day 10 demonstrates that the ventrally placed LCN's are actively involved in catecholamine production. In some locations in the CNS, LCN's immunoreact negatively for TH yet positively for dopamine (Ekström et al., 1992; Gugielmone, 1995) indicating an uptake of dopamine from an external source, rather than actual synthesis in the cytoplasm.

However it has been shown by Roberts and co-workers (1995) that the ventrally placed LCN's in the uninjured eel cord immunoreact for both TH and dopamine antibodies (Roberts et al., 1989), and so it is probable that the TH+ve neurons observed in the present study are truly dopaminergic.

During development dopaminergic neurons - including LCN's - are some of the first neurons to differentiate from the primitive neuroepithelium, and appear to develop in advance of GABAergic neurons (Casper, 1996).

GABA+ve neurons in the bridge

The finding of GABAergic LCN's in the bridge at approximately the same time as the TH+ve LCN's indicates that this type of LCN may also be critical for the formation of the bridge. In the developing CNS, GABAergic neurons, including LCN's (Dale et al., 1987a; 1987b; Bernhardt et al., 1992), are among the first to differentiate. While GABAergic neurons are traditionally associated with inhibitory control of neural function in the adult CNS (see Deutch and Roth, 1999), in the developing CNS it has been shown that this neurotransmitter behaves as a trophic substance (Lauder et al., 1998; Waagepetersen et al., 1999). It has been shown, for example, that GABA directs the migration of postmitotic neuroblasts in the developing cord and stimulates their motility (Barker et al., 1998). In the developing hippocampus, the activity of GABAergic neurons facilitates maturation of other receptor systems (Davies et al., 1998). The differing effects of GABA seem to involve two forms of the enzyme glutamic acid decarboxylase – GAD65 and GAD67 - and two differentially expressed genes (see Pinal and Tobin, 1998). In late development and in the adult, GAD65 predominates while, in the developing CNS, GAD67 is the major GABA-producing enzyme. In the developing fish CNS, both GAD genes have been isolated and localised to a variety of different neuronal populations in the CNS including the LCN's of the spinal cord (Martin et al., 1998). It is therefore possible that the function of LCN's during regeneration may be a reflection of their developmental role.

The close parallels between the regenerating bridge in the present study and the developing vertebrate CNS in relation to the early appearance and distribution of LCN's suggests that these neurons in the bridge may recapitulate earlier embryonic events such as neuronal differentiation and axonal guidance (Casper, 1996; Barker et al., 1998; Belhage et al., 1998; Fairén et al., 1998; Waagepetersen et al., 1999)

Summary of main findings

- Both TH+ve and GABA+ve liquor contacting neurons are present in the bridge by approximately day 12.
- These specialised neurons are found interspersed between ependymocytes and contact the lumen of the canal.
- The spatial organisation of cells around the uninjured canal is preserved in the developing bridge with TH+ve cells found ventrally and GABA+ve cells laterally.
- The presence of neurons amidst the mitotically active ependymocytes in the bridge points to possible neurogenesic events in the regenerating bridge.

Chapter 7

The meninges in the regenerating spinal cord

7.1 Introduction

Following most types of injury to the vertebrate central nervous system, the basal lamina and the glia limitans at the periphery are disrupted and frequently breached, exposing the underlying neural tissue (Reier et al., 1983; Lindsay, 1986). In mammals, this breach usually results in the formation of an astrocytic glial scar, characterised by hypertrophy and hyperplasia of reactive cells (see chapter 8; Ridet et al.1997). In addition, reactive astrocytes form a glia limitans and basal lamina within the lesion site which contributes to the inhibition of axonal regrowth (e.g. Abnet et al., 1991). These formations, however, occur only when there is an infiltration of meningeal tissue and/or fibroblasts into the wound site (Franklin et al., 1992), as happens, for example, following stab (Carbonell and Boya, 1988) or laceration/transection type injuries (e.g. Wang et al., 1997). Where meningeal infiltration is largely prevented, such as following microlesion (e.g. Davies et al., 1996), a glia limitans does not develop within the lesion site. Similarly, in neonatal mammals (Moore et al., 1987; Balasingam et al., 1996), where successful regeneration is possible, astrocytes do not form a glia limitans within the lesion site and meningeal cell infiltration into the lesion site is not seen until the juveniles are over 1 week old (see Nichols and Saunders, 1996), when scar tissue, typical of that of adults, develops (Varga et al., 1995).

Since it is well known that the CNS of anamniotes is capable of extensive recovery following numerous types of injury, the effects of meningeal cell infiltration, and their subsequent reactions with exposed elements of the CNS, may not in these species be inhibitory to the regenerative event. But whether meningeal cells interact in a positive manner with the regenerating neural tissue, fail to interact, or are actively excluded from the wound site, is unknown. As far as it is known, relatively few studies of the anamniote regenerate have documented the meningeal reaction during the regenerative event, although a meningeal covering has been noted at later stages of recovery (Bernstein and Bernstein, 1967; Michel and Reier, 1979). As a result, the primary aim of the present study has been to determine the behaviour of meningeal cells (melanocytes and meningeal fibroblasts, see chapter 3) surrounding the spinal cord following cord transection and their role during the initial regrowth and during the subsequent development of the bridge.

In the second part of this study, we have endeavoured to determine the effects of removing meningeal cells during the initial stages of regrowth. Selective destruction of

meningeal cells using chemical application of 6-hydroxydopamine (6-OHDA) in neonatal rats (Sievers et al.1994b) and hamsters (Sievers et al., 1994a) has been shown to result in the altered development of the brain, such as incomplete foliation of the cerebellar cortex (Sievers et al., 1994a). However, this disruption is not seen once meningeal ensheathment of the brain has been completed (Sievers et al., 1985), suggesting that it is only when cells are in a proliferative and/or migratory stage, that they can be affected. Since meningeal cells proliferate and migrate following CNS injury in all vertebrates, it can be inferred that they exhibit plasticity similar to that seen during development. Therefore, these cells may be susceptible to similar manipulation during recovery following CNS injury. It has also been shown that the basal lamina, formed at the interface between the glia limitans and the meninges (Krisch et al., 1983; Pehlemann et al., 1985), may also play a contributory role to CNS development, since selective disruption of this structure using the enzyme collagenase in developing chick results in CNS malformation (Halfter, 1998; Halfter and Schurer, 1998).

In an attempt to determine the possible effects of inhibiting meningeal and basal lamina formation, three different methods were employed; these were: (a) mechanical removal of the meninges, (b) mechanical removal followed by application of 6-OHDA to inhibit meningeal infiltration (Sievers et al., 1994a), and (c), mechanical removal followed by treatment with collagenase type VII to disrupt formation of the basal lamina (Halfter, 1998).

7.2 Materials and Methods

Animals

This study is based on 25 European eels, *Anguilla anguilla L.,* in a non-migratory immature stage of their lifecycle.

Transection of the spinal cord

For surgery, each eel was anaesthetised according to the protocol outlined in chapter 4. In brief, each animal following immersion in 0.3g/l MS-222 (Sigma) to induce light anaesthesia was administered 0.1ml alphaxalone ("Saffan" Pitman-Moore) subcutaneously. Cooling on ice provided additional anaesthesia. The transection procedure followed a similar protocol to that outlined in chapter 4, with laminectomy of the spinal column over three vertebral segments. However, the lateral portions of the cord and overlying meningeal sheath were also exposed by further removal of the column on both sides. Removal of the meningeal sheath was accomplished by gently heating the dorsal surface of the cord using a small lamp and the tissue gently teased away and removed using fine forceps. However, in all cases it proved impossible to remove the ventral meninges without causing unnecessary damage to the cord and therefore these were left *in situ.*

The spinal cord was then cut completely using fine micro-scissors, care being taken so as not to sever the dorsal blood vessels. Sections of gelfoam acting as the carrier medium, was soaked in either 6-OHDA or collagenase type VII (see next section) was placed on the vertebral column over the stump on each side of the wound (see Fig. 7.1). In all cases, gelfoam placement did not infringe upon the lesion site. Finally the wound was fine stitched and the animal allowed to resuscitate before being placed in an individual holding tank.

6-hydroxydopamine (6-OHDA)

To inhibit meningeal cell migration 6-hydroxydopamine (Sigma), with 0.1% ascorbic acid (Sigma) to prevent degradation, was made up in distilled water to a final concentration of 6μg/μl. The solution was freshly made to ensure optimal activity of 6-OHDA. For application, small pieces of gelfoam were soaked in the solution immediately prior to application and one piece placed on each side of the wound.

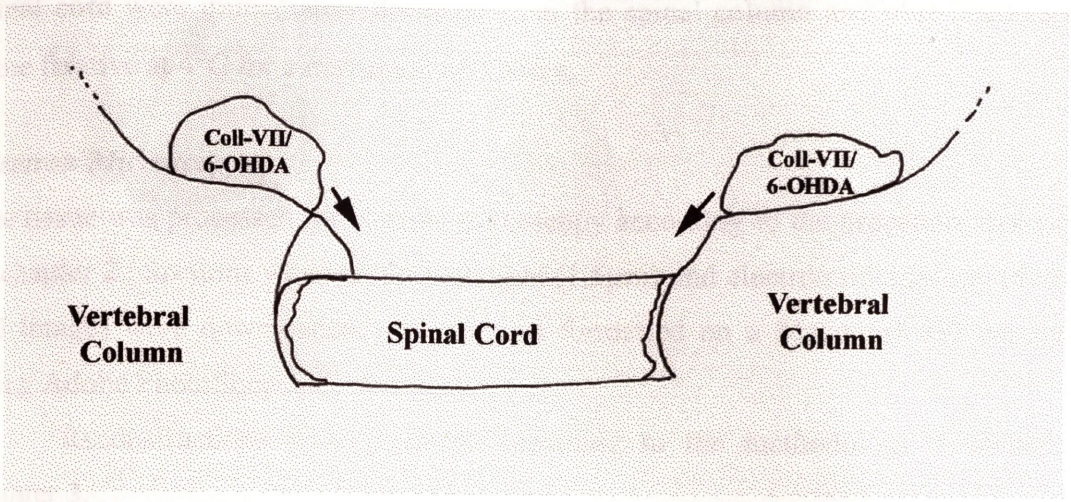


Figure 7.1. Outline of the surgical procedure and the application of 6-OHDA/collagenase type VII soaked gelfoam to the vertebral column overlying the spinal stumps.

Collagenase type VII

To inhibit basal lamina formation, collagenase type VII (Sigma) was dissolved in distilled water to a concentration of 50μg/μl. In a similar manner to 6-OHDA application, small pieces of gelfoam were soaked in a fresh preparation and applied to the vertebral columns overlying the transected spinal cord.

Histological Investigation

For histological investigation, each animal was treated according to the methodology described in the methods section in chapter 2. In brief, each animal was anaesthetised initially by immersion in 0.3mg/l MS-222 and a subcutaneous injection of 0.3ml alphaxalone (Saffan). To prevent blood clotting 0.2 ml heparin sodium (Leo Laboratories) was also given subcutaneously. The perfusion procedure consisted of a primary flush of Ringer's solution (with 0.1% procaine for added anaesthesia) through the heart followed by the fixative, 2% paraformaldehyde and 1.25% gluteraldehyde in

0.1M phosphate buffer (PB), pH adjusted to 7.4. Following perfusion, portions of the spinal cord were immediately dissected from the spinal column and post-fixed in the same fixative at 4°C for a maximum of 3 hours.

Electron Microscopy

The tissue was processed for electron microscopy according to the procedure described in chapter 2. Sections were cut for both light (1.5μm) and electron microscopy (500Å). All images were downloaded, analysed and formatted on a Macintosh G3 computer using Adobe PhotoShop 5.

Reconstructions were produced according to the methodology described in chapter 3.

7.3 Results

Four days following spinal cord transection, the meninx surrounding the spinal stumps adjacent to the cut degenerate and expose the underlying neural tissue, such that it often extrudes through the breaches in the meninx (Fig. 7.2). The breakdown in structure occurs first dorsally and proceeds in a ventral direction. The basal lamina is also lost from these regions. Where the meninx (and presumably the basal lamina) persist, the structural integrity of the cord remains, even when large spaces devoid of any neural tissue appear within the cord. When present in the stump regions, the meninx differ little from normal, although some 'loosening' of the structure is seen, resulting from the infiltration of erythrocytes and leucocytes between the cellular layers. The blood clot, when present over the stumps, is closely associated with the meninx. Blood vessels are numerous and were often found close to the outer layers of the meninx; numerous infiltrating erythrocytes and leucocytes were also observed.

By day 6, further denudation of the meninx in the spinal stumps results in greater exposure of the cord, usually on the dorsal surface, up to 1 mm from the cut on both sides (Fig. 7.3); however a ventral covering is always present. In those regions without a meningeal covering, particularly laterally, a loose grouping of elongate fibroblast-like cells is interspersed with infiltrating leucocytes of neutrophil/macrophage origin. The dorsal surface, in contrast, is usually devoid of this cellular covering, particularly in those regions where an open central canal is present. Close to the lesion site, a similar covering of loosely organised cells is found in close association with the leading edge of neural regrowth (Figs 7.3).

The loose organisation of cells described for day 6 becomes increasingly ordered and prominent around the stumps and the forming bridge by day 8, although towards the middle of the bridge the looser configuration is still evident. Hence by day 6 and thereafter a gradient of organisation is evident within the meninx from the stumps (greatest) to the middle of the bridge (lowest) until approximately day 26 when the organisation is homogeneous. Within the bridge, the fibroblast-like cells that cover the regenerating neural tissue are often closely associated with the fibroblasts of the scar, such that it is often impossible to distinguish between both cell types and to demarcate a boundary between them; ultrastructurally, there appears to be no significant difference between the cells (Fig.7.4). Where the bridge is thinnest, the fibroblast-like cells show little association to the neural tissue; however ventrally, a somewhat more organised but

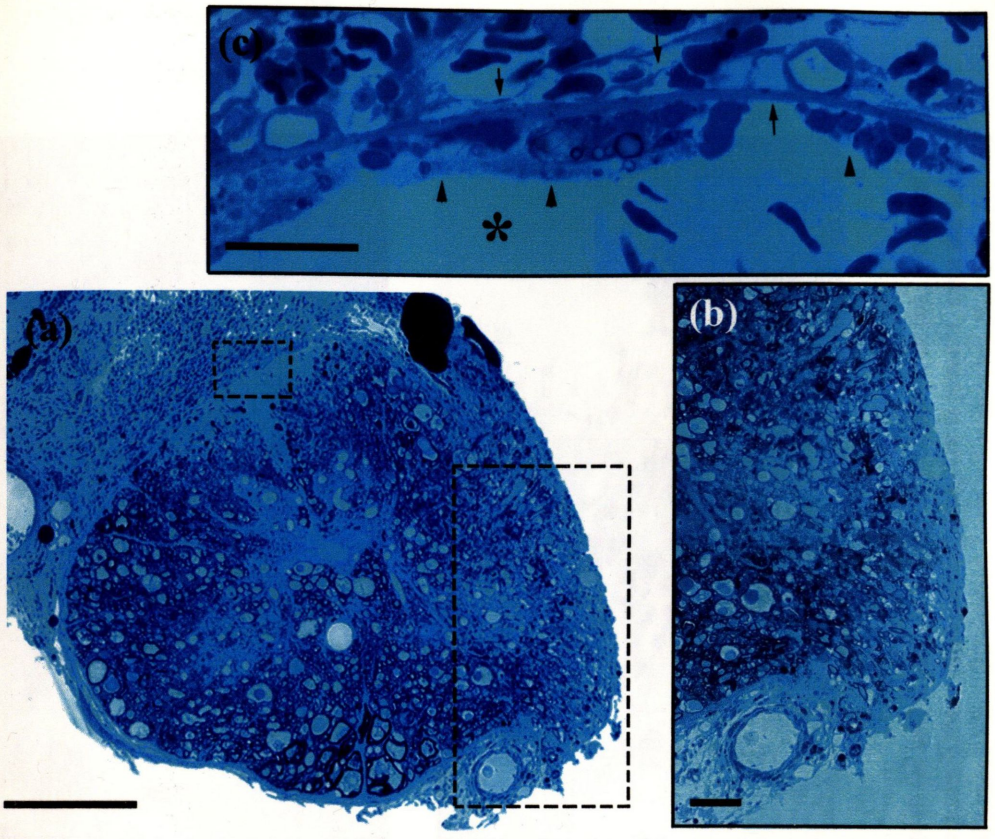


Figure 7.2a, b, c. Degeneration in the spinal stumps at day 4. In (a) note the extrusion of the neural tissue laterally, seen at higher magnification in (b; arrowheads). In (c) note the large space (*) created by the degeneration within the cord and the presence of a meningeal sheath (arrows). Arrowheads denote the the basal lamina and the remnants of the glia limitans. Scale bar (a) = 100 microns, (b) = 50 microns, (c) = 20 microns.

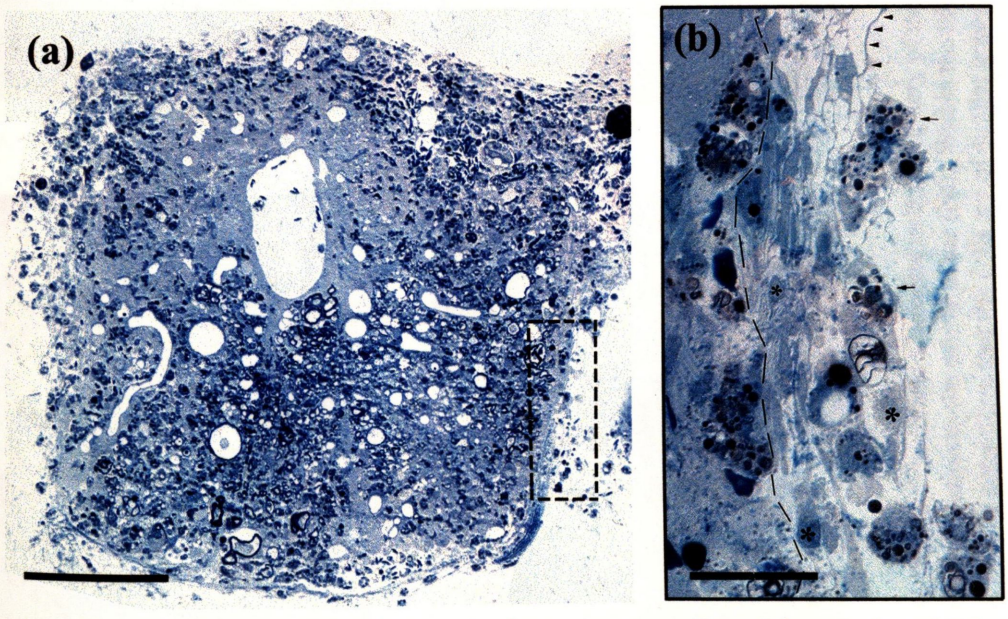


Figure 7.3a, b. Day 6. In the photomicrograph of a transverse section of the spinal cord 0.3mm from the cut surface. Note the presence of a meningeal covering ventrally and a loose disorganised covering of elongate cells on the lateral surfaces (outlined) and seen at higher magnification in (b). Scale bar (a) = 100 microns, (b) = 20 microns.

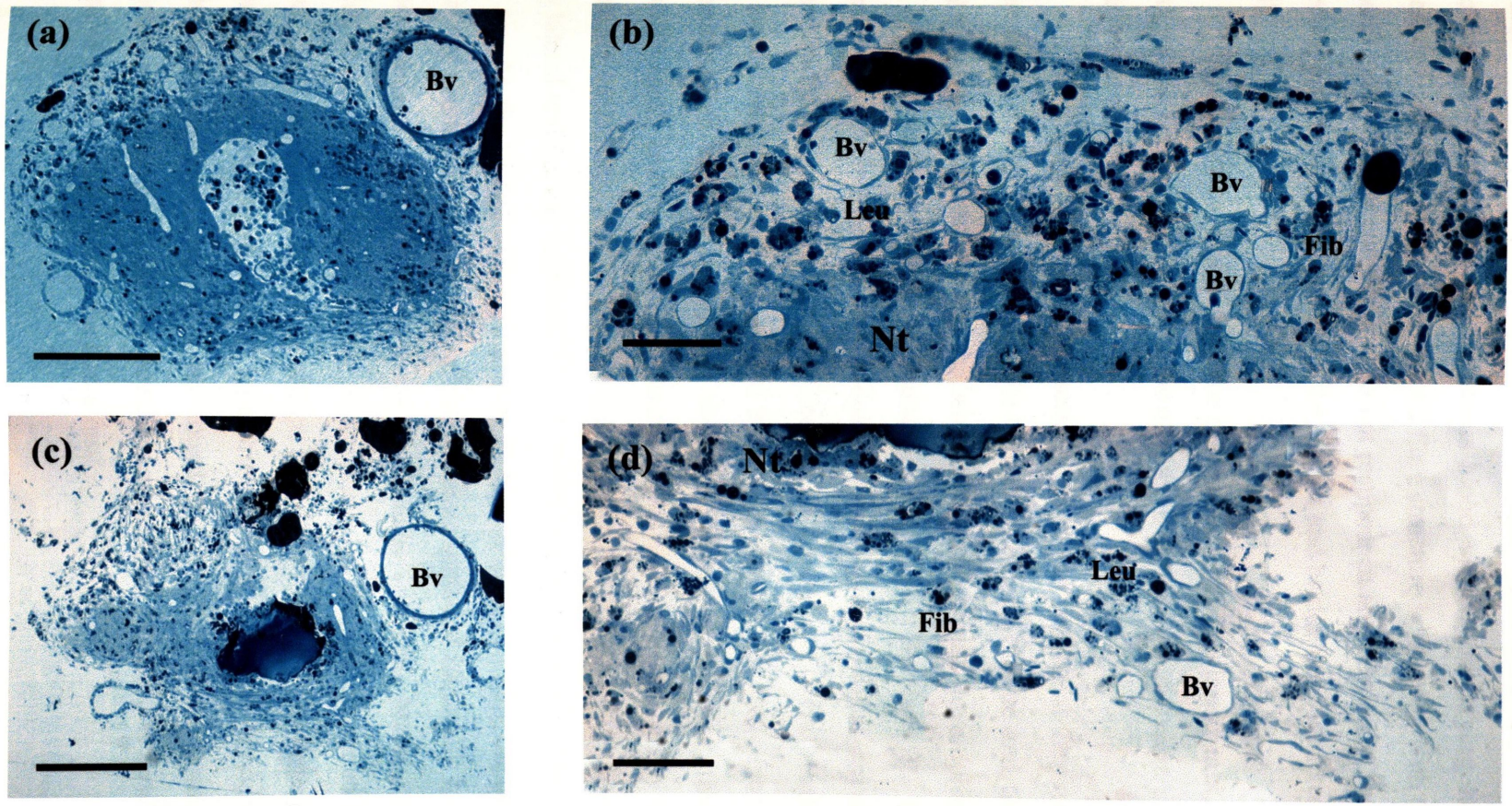


Figure 7.4a, b, c, d. Day 8. Fibroblasts aggregate to the periphery of the developing bridge in (a) and is seen at higher magnification in (b). Note the disorganised loose accumulation to the neural tissue (Nt). Within the lesion site (c), where a much more disorganised structure is present, note the similar cell-type within the clot (d) suggesting that the cells are of similar appearance. Bv = Blood vessel, Fib = Fibroblast, Leuc = Leucocytes. Scale bar (a) and (c) = 100 microns, (b) and (d) = 50 microns.

still loose arrangement of fibroblast-like cells and macrophages/monocytes is found (Fig. 7.4c, d). In regions of the stumps where the meninx remain, their constituents also change to a looser, almost lattice-like configuration, interspersed with monocytes/macrophages and numerous blood vessels of varying lumenal sizes. The breakdown of the collagen and elastic fibre structure is coupled with this reorganisation and in general these components do not reappear in any portion of the reorganising and developing meningeal structure in the stumps and bridge until later recovery stages (day 54).

Melanocytes, typified by the presence of dark melanosomes, do not appear to take part in the reorganisation of the meninx in the stumps and were always absent from the bridge region.

At 8 days following transection, an organised basal lamina of extracellular material is absent from the interface between the neural tissue and the loose fibroblast organisation in the stumps and the bridge and, instead, both developing tissues interface to produce an erratic cellular boundary (Fig. 7.5). By days 10 and 14, with the increasing development of the bridge, the meningeal-fibroblast covering is organised into a more compact structure, best seen on the ventral and lateral surfaces. An increase in thickness (cross sectional width) is also apparent at this stage (see Fig. 7.10). The meninx often appears to infiltrate the bridge structure; however, these ingrowths are usually small and local although, occasionally, as in one case at day 10 (see Fig. 7.6), they are extensive. Within the stumps, the meninx continues to thicken, particularly on the lateral and ventral surfaces.

As the bridge increases in size, as seen at days 14 to 20, the central canal opens dorsally producing two 'horns' of neural tissue bordered internally by ependymal cells (see chapter 8) and meningeal tissue on the outer surfaces. Meningeal outgrowth was often found on the dorsal surface of the horns but did not appear to infiltrate into the open canal region. Closer to the stumps (day 14) a meningeal covering extends over the canal region, producing a 'roof' type structure (Fig. 7.7), and occasionally, circular to elongate ependymal-type cells are found on the inner canal-facing surface. With closure of the central canal by day 20, a meningeal covering is evident on the dorsal surface of the bridge where the horns fuse.

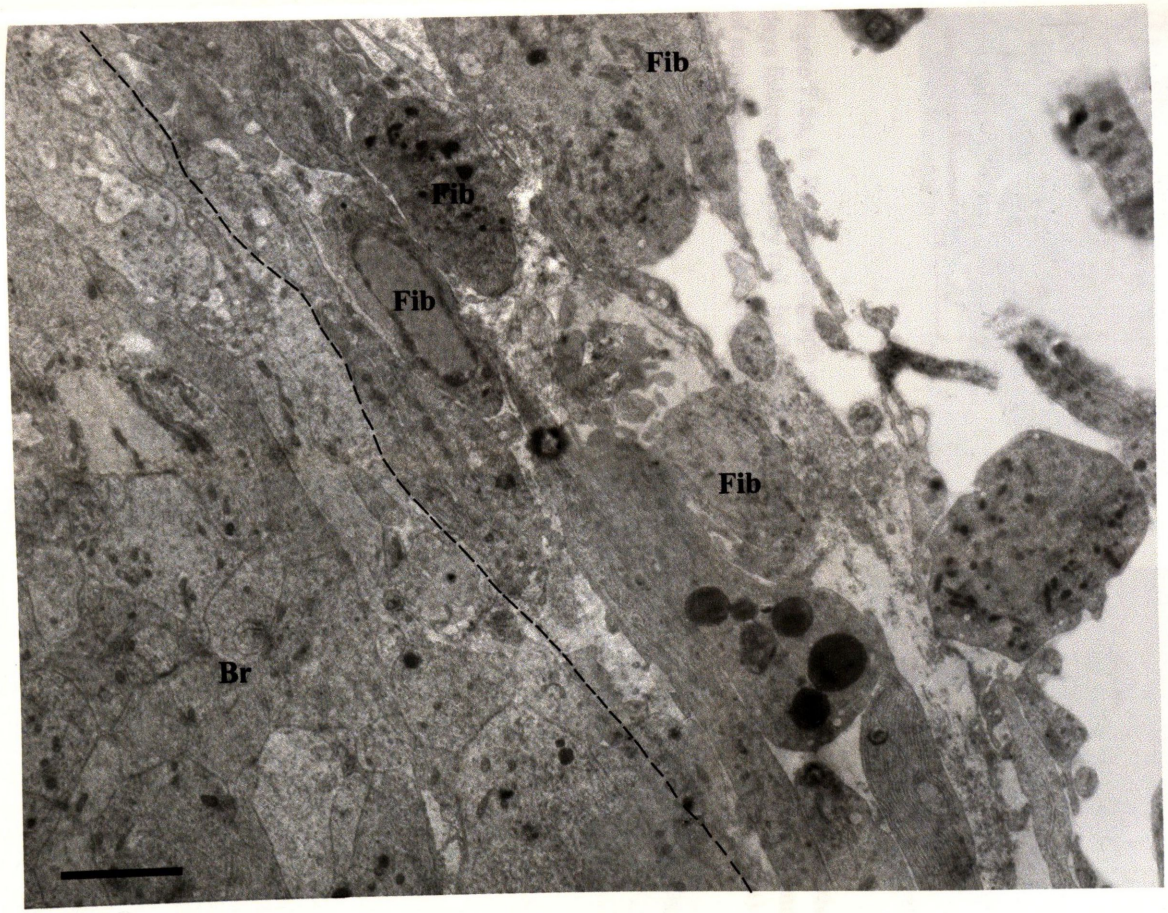


Figure 7.5. Day 8. Electron micrograph of the developing meninx at the perphery of the bridge (Br). Note the irregular interface between the two tissues (dotted line). Note also the loose layering of the fibroblast cells (Fib) and their irregular shape. Scale bar = 10 microns.

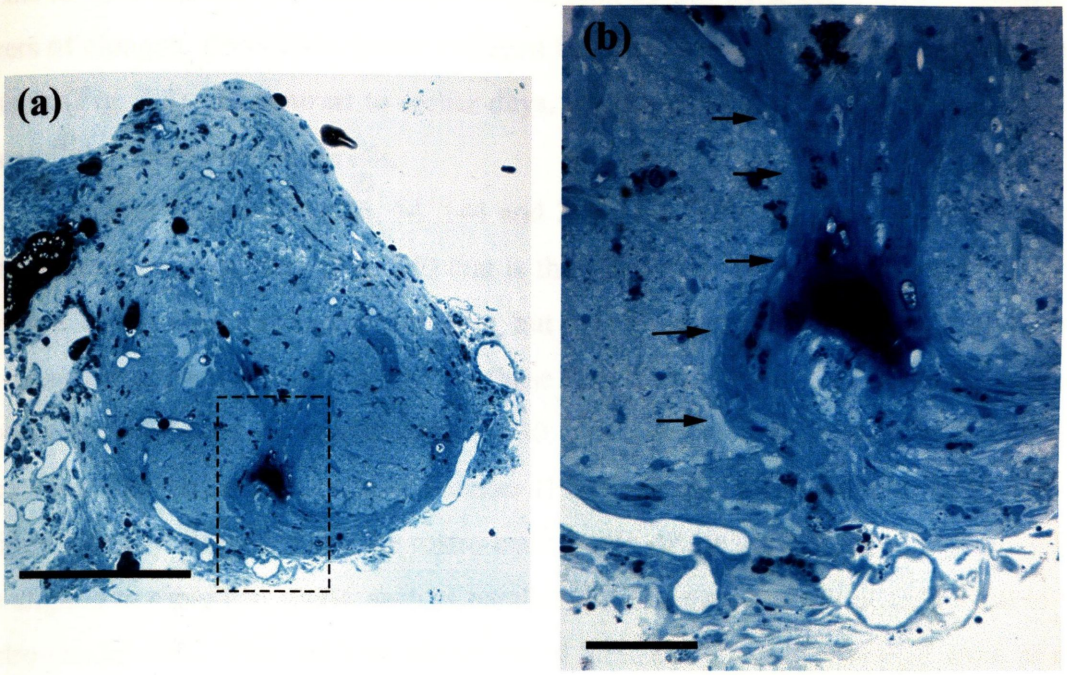


Figure 7.6a, b. Photomicrograph of the developing meninges at the periphery of the bridge 10 days following injury (a). In (b) note the thickening layers of meningeal tissue and the presence of meningeal tissue extending into the middle of the bridge (arrows). Scale bar (a) = 200 microns, (b) = 50 microns.

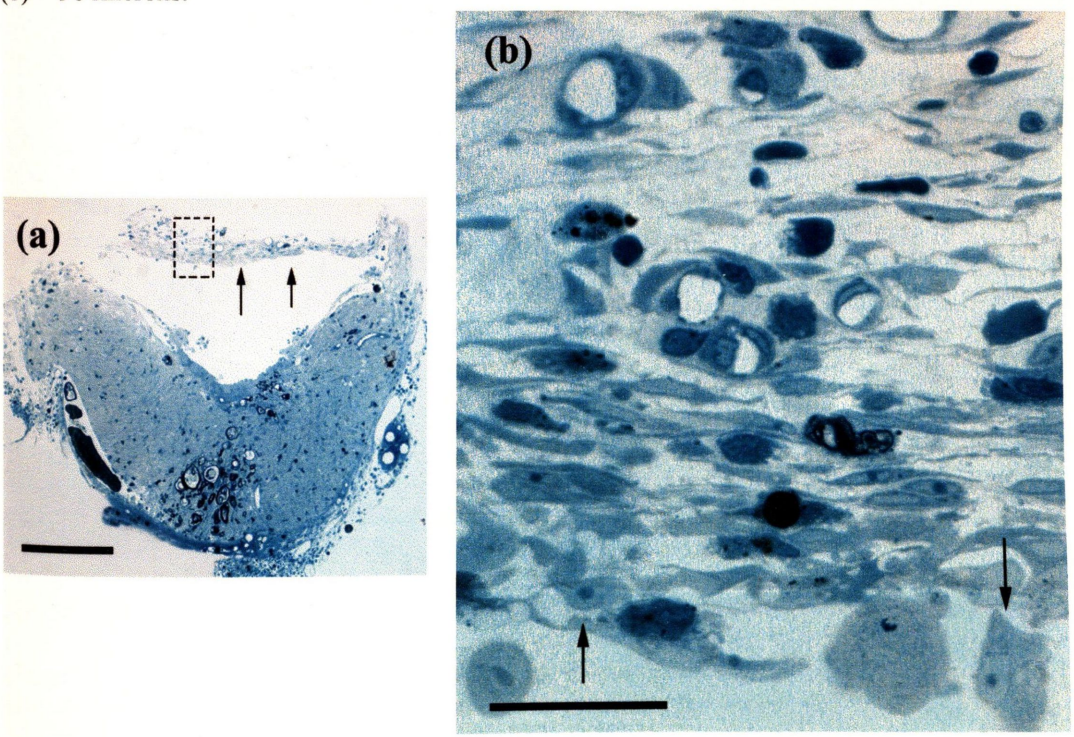


Figure 7.7a, b. Photomicrograph of a transverse section of the bridge at day 14 (a). Note the presence of a meningeal 'roof' that is forming over the canal (arrows) seen at higher magnification in (b) and note the presence of circular to ovoid type cells on the inner canal-facing surface (arrows) that are indicative of migrating ependymal cells.
Scale bar (a) = 200 microns, (b) = 20 microns.

At the level of the electron microscope, the meninx by day 20 is composed of numerous layers of elongate fibroblasts, sparse collagen fibres, monocytes/macrophages and blood vessels (Fig. 7.8). In contrast to earlier days, the organisation is compact with smaller intercellular spaces between cells.

At later stages (days 26, 54, 144 and 200), the bridge is completely enveloped with a meningeal covering (Fig. 7.9) that is thicker within the bridge region (Fig. 7.10) By days 144 to 200, this becomes thinner, but even by day 200 it is thicker than normal on all surfaces, particularly dorsally. At these later stages the meninx comprises several layers of fibroblasts (approximately 20-30 cell layers) and extracellular collagen organised into large inter-cellular bundles (Fig. 7.11a,b). The bundle orientation is unidirectionally aligned along the rostro-caudal axis of the cord. Few collagen bundles are aligned in other directions, such as parallel with the cord surface or tangential to the rostro-caudal axis. This uniform alignment of bundles was still prevalent even at day 144 (see Fig. 7.11b).

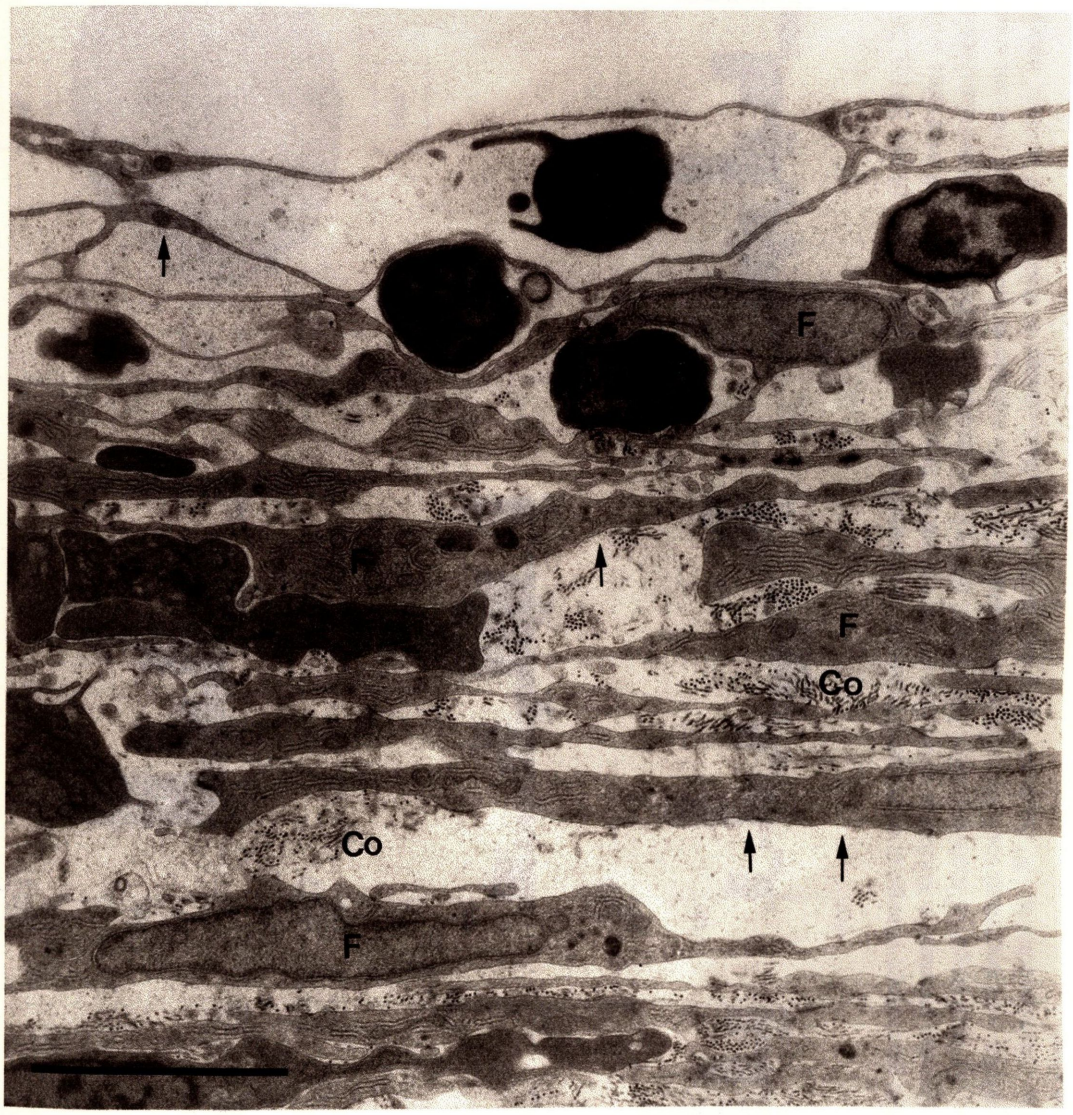


Fig.7.8. Electron micrograph of the meninges on the dorso-lateral surface in the middle of the bridge. Note the more organised array of cells that possess an elongate shape (arrows). Note the large amount of intercellular space that occurs between cells and which often contains macrophage/ monocyte cells but relatively little collagen. F = Fibroblasts, Co = Collagen, M = monocyte. Scale bar = 15 microns.

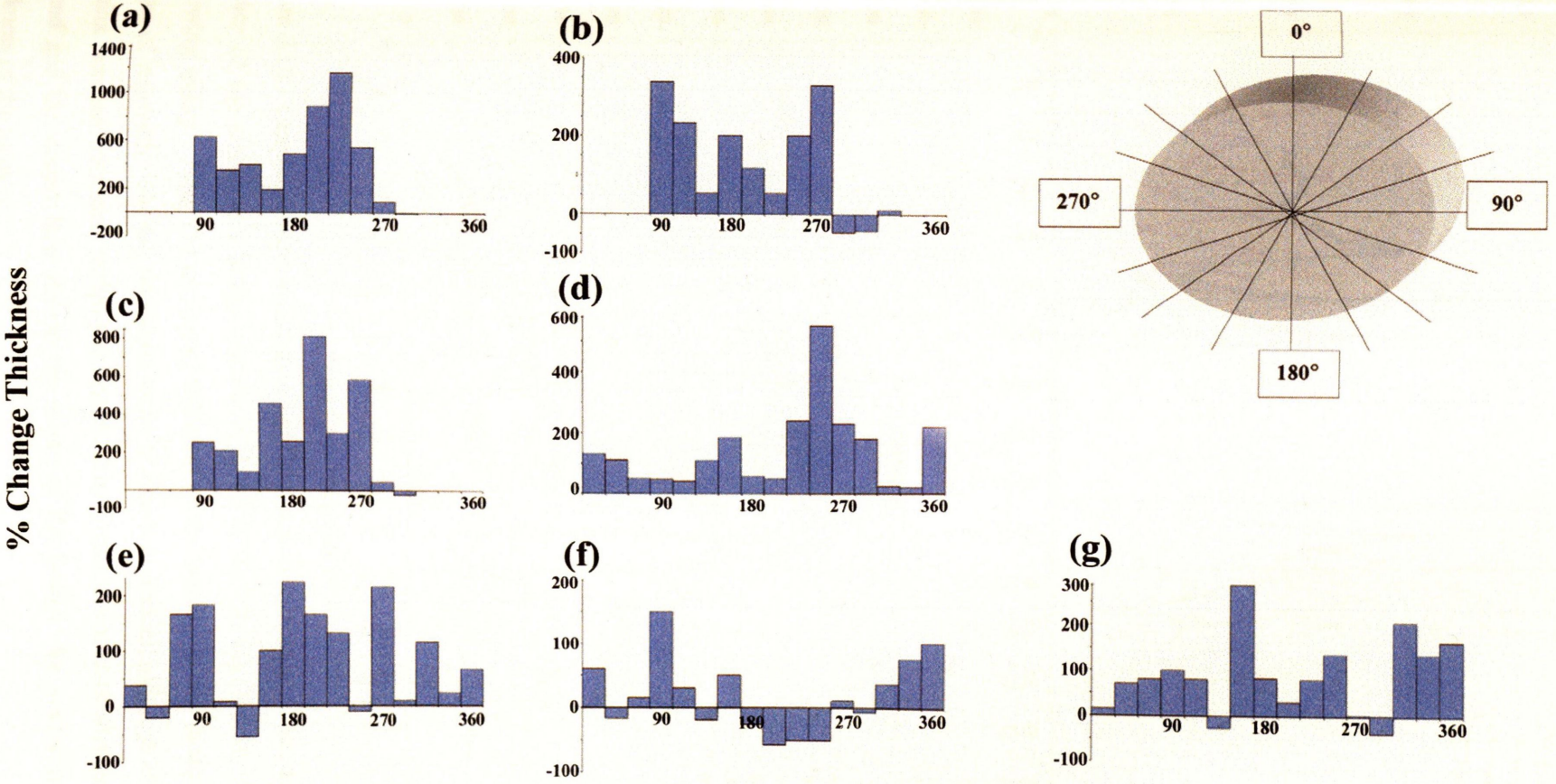


Figure 7.9. Graphical representation of the percentage change in meningeal thickness in the middle of the bridge at 10 (a), 14 (b), 20 (c), 26 (d), 54 (e), 144 (f) and 200 (g) days following injury. Note that the increase in thickness ccurs first on the ventral surface, which is accompanied over time with increases on the lateral and eventually, the dorsal surfaces. At later stages of recovery, days 144 (f) and 200 (g), the percentage difference between the thickness of the meninges in the bridge and the undamaged regions of the cord decreases such that it is often thinner. The x-axis represents the degrees of rotation around the cord with the dorso-medial equating to 0 degrees and the ventro-medial to 180 degrees. The y-axis is the percentage-change in thickness to 'normal' uninjured meninges aproximately 1mm from the bridge in each case.

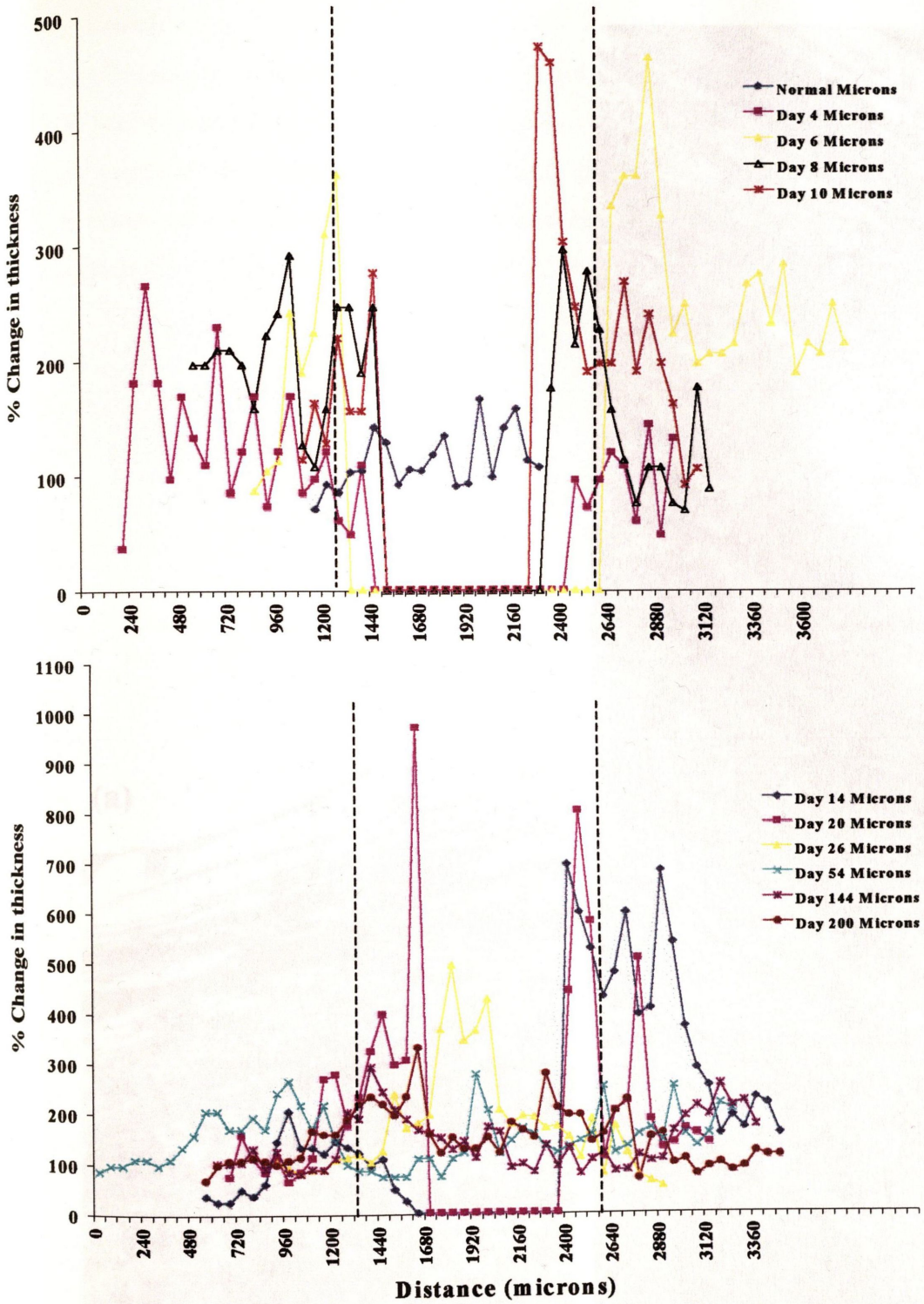


Figure 7.10. Graphical representation of the % change in thickness of the meninx on the dorsal surface of the stump and bridge regions at 4, 6, 8, 10, 14, 20, 26, 54, 144 and 200 days following injury. Note the increasing thickness of the meninx in the stumps during the early stages of regrowth. By day 54 values begin to return to normal, although even by day 200 the meninx remains thickened within the bridge. The x-axis is rostro-caudal distance through the wound and the dotted lines denote the extent of the bridge, the y-axis is the % change in thickness of the meninx.

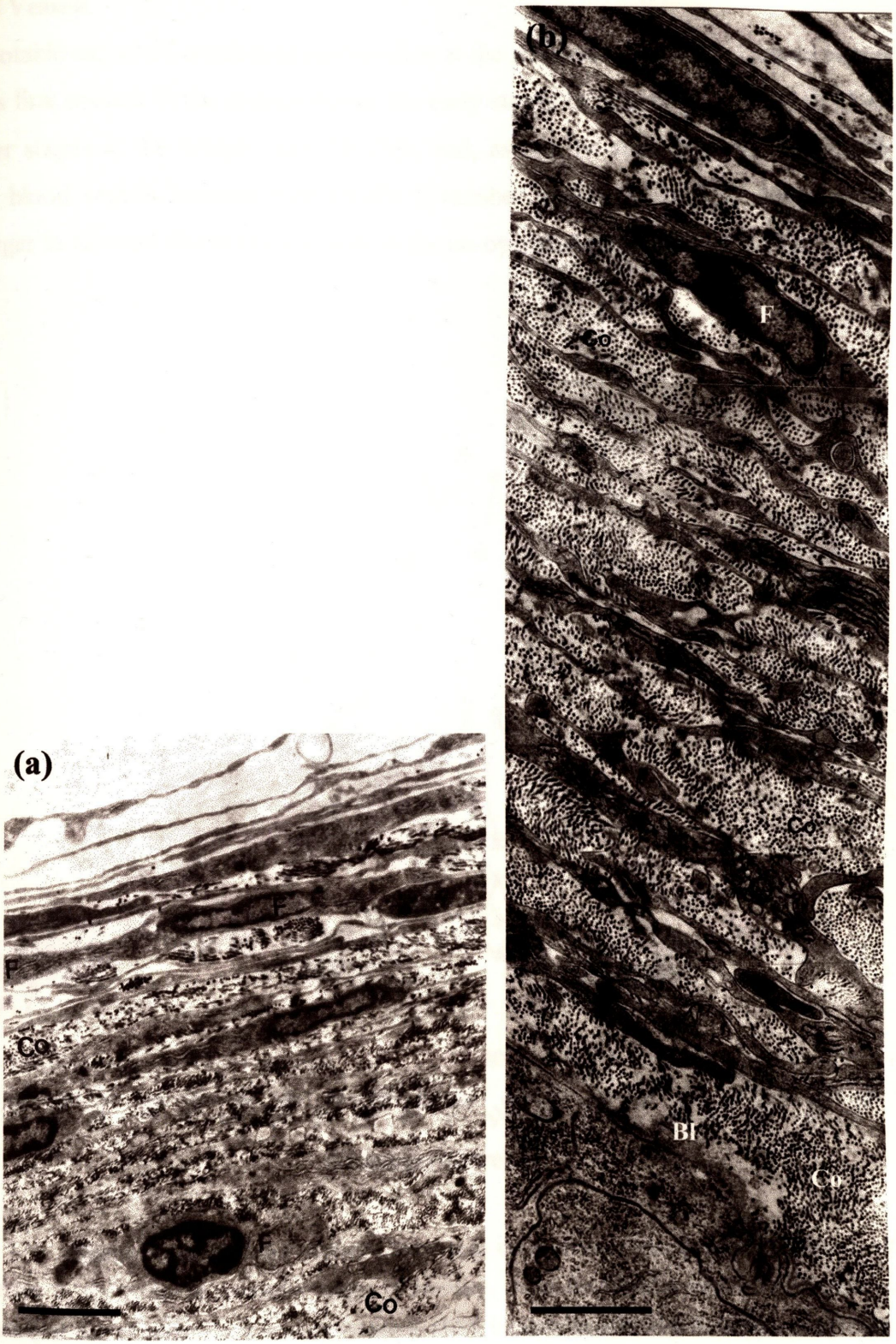


Figure 7.11a, b. In (a) and (b) which correspond to the dorsal meninx seen in transverse section at day 54 and the lateral meninx at day144 respectively, note the increased thickness of the tissue surrounding the bridge. Note the abundant collagen organised longitdinally along the rostro-caudal axis of the bridge (coll) and the spindle-shaped meningeal cells arrayed circular to the bridge. In contrast to earlier stages the meninx is more compactly organised but with numerous cell layers. Co = collagen, F = fibroblasts, Bl = basal lamina. Scale bar = 10 microns.

Blood Vessels

One notable aspect of meningeal regeneration is the richness of the blood vessel supply. This is first evident in the stumps during the early stages of regrowth (days 4, 6, 8) and at later stages in the bridge (days 10-200), and, as can be seen from the graph (Fig. 7.12), blood vessels increase substantially in number within the bridge. Most vessels are larger in lumenal diameter than those in the un-operated cord (see Fig 7.13).

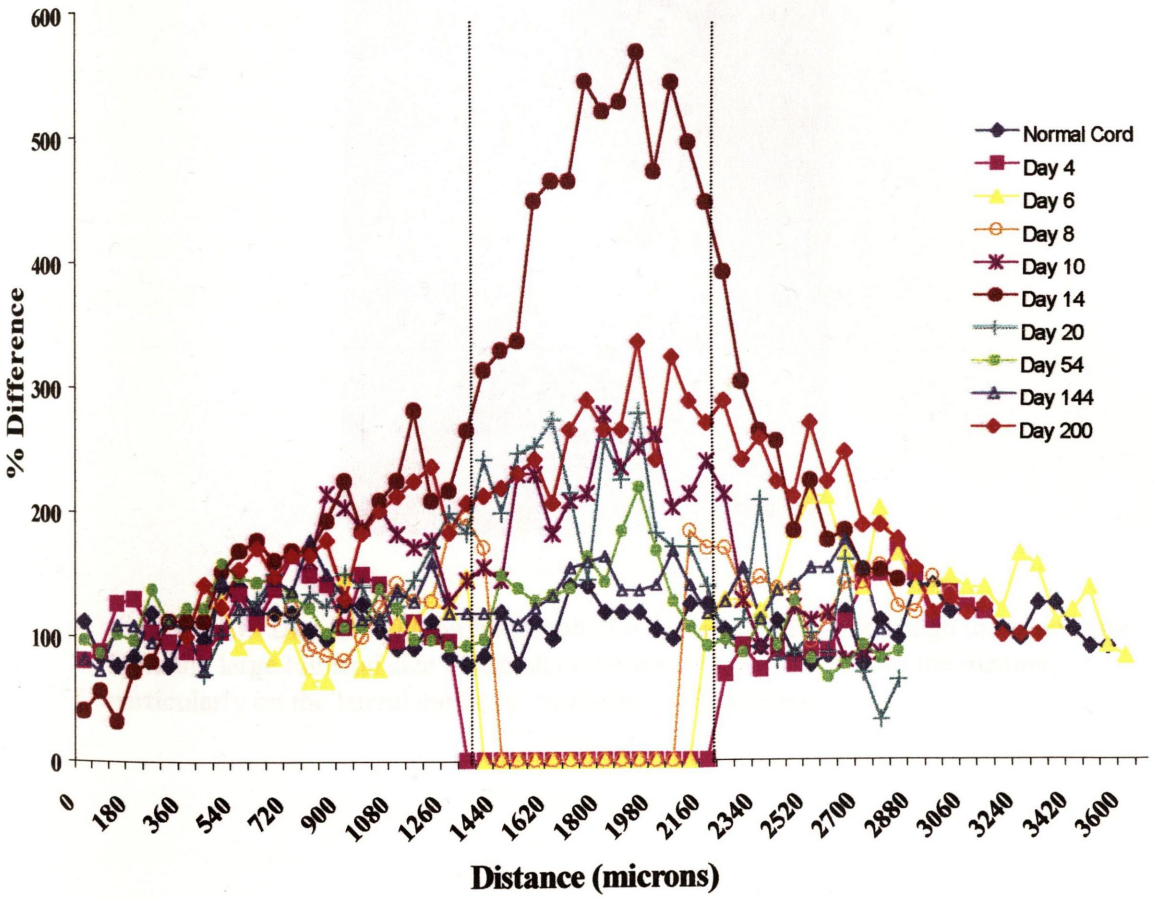


Figure 7.12. Graphical representation of the % increase in the number of blood vessels associated with the meninx in the bridge at successive stages of recovery. Note the elevated values for all days and particularly at day 14 where there is an approximate 600% increase compared with the unoperated cord. The x-axis is the rostro-caudal distance through the wound with the dotted lines representing the approximate area of the lesion site, the y-axis is the % difference in blood vessel number calculated from the difference between an average value for vessels in the regenerating and uninjured portions.

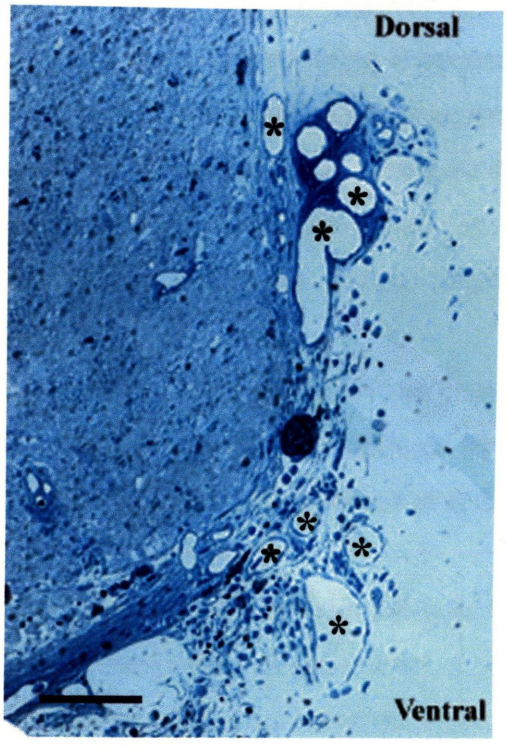


Figure 7.13. Day 14. Photomicrograph of a transverse section through the lesion site. Note the large lumenal size of the blood vessels (*) associated with the meninx, particularly on the lateral surfaces. Scale bar = 50 microns.

Impact of Meningeal Manipulation on Spinal Cord Regeneration

(a) Mechanical removal

The near complete removal of the meninx from around the cord immediately prior to its surgical transection does not affect its subsequent regenerative ability. Following removal, the organisation of the bridge at days 20 and 26 is similar to that found in non-manipulated cases by day 20. However, the central canal is already enclosed within the cord and a meningeal covering is present on the dorsal surface (see Fig. 7.14 a,b), in sharp contrast to non-manipulated regenerating cord, where the canal is still open at this time and lacks a meningeal covering on the dorsal surface (Fig. 7.14 c,d). At later stages (day 46) no differences could be distinguished between the mechanically manipulated material and the normal regenerate (day 54) (data not shown).

Within the spinal stumps, the removal of the meninx from the cord surface resulted in the 'extrusion' of neural material through the breach in the meningeal covering (Fig 7.15a, b). This was particularly obvious at at day 20.

(b) Mechanical removal combined with collagenase type VII application

If mechanical removal is combined with an application of collagenase the formation of the bridge appears to be accelerated, since a complete meningeal covering is present on the dorsal surface as early as day 16 (Fig. 7.16 b, d). This is in marked contrast to the non-manipulated situation, where at about the same time the meninx is confined to the ventral and lateral surfaces of the bridge (Fig. 7.16 a, c) which is dominated by the dorsal opening to the central canal. A similar meningeal thickness is found on the dorsal surface at later stages of recovery following collagenase treatment, days 20 and 26, with a thick meningeal covering on the dorsal surface (Fig 7.17).

(c) Mechanical removal combined with 6-hydroxydopamine (6-OHDA) application

Pulse application of 6-OHDA in conjunction with meningeal removal produced the greatest alteration in the structure of the regenerating spinal cord, as seen in the extensive dorsal movement of the regenerating tissue to produce large horn-like structures similar to those found in non-manipulated regenerating cord (see Fig. 7.18). A greatly enlarged central canal accompanies this dorsal projection. At days 20 and 26, a meningeal covering is present on the lateral and ventral surfaces of the bridge,

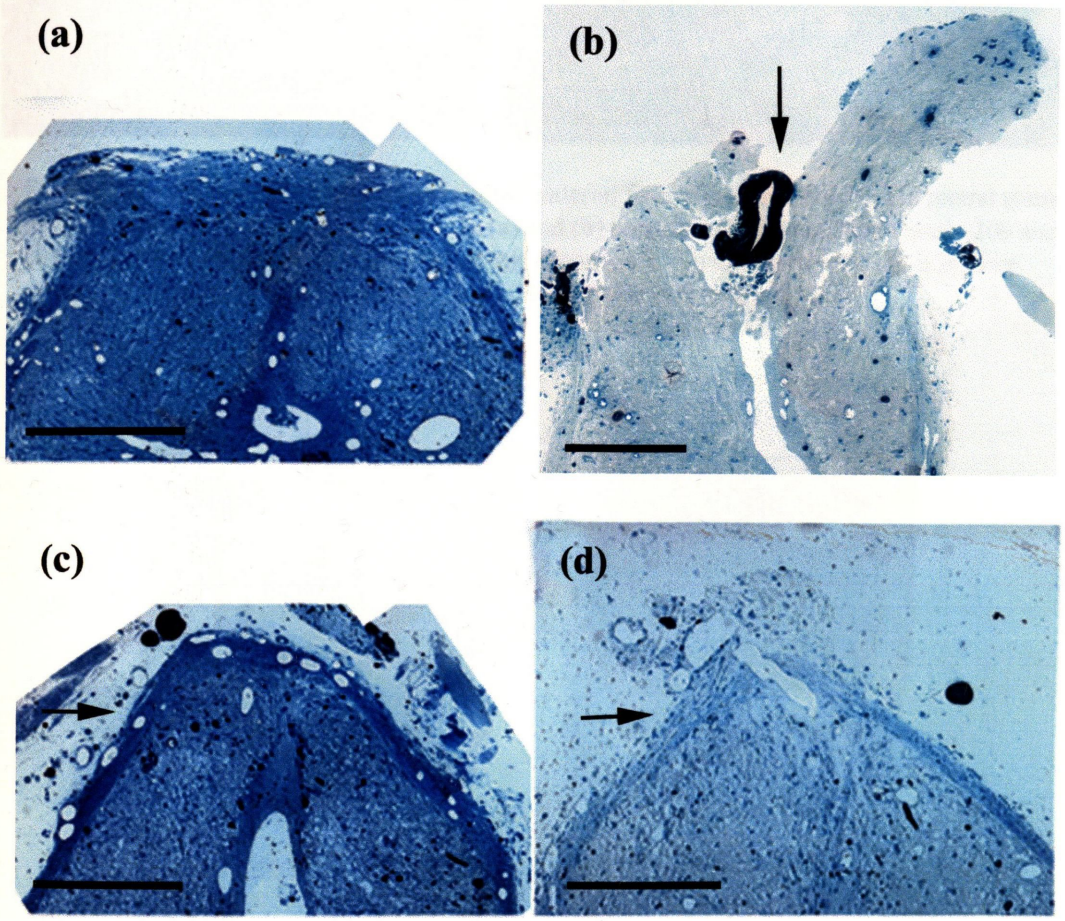


Figure 7.14a, b, c, d. Effects of mechanical removal of the meninx on the regenerating cord is seen at (a) day 20 and (c) day 25 while non-manipulated cord can be seen in (b) day 20 and (d) day 26. In (a) and (b) note that the central canal in the manipulated tissue is closed while in the untreated cord it remains open dorsally (arrows). In (c) and (d) note the similarity between both regenerates although the meninx is thicker on the treated animal (arrow). Scale bar = 200 microns.

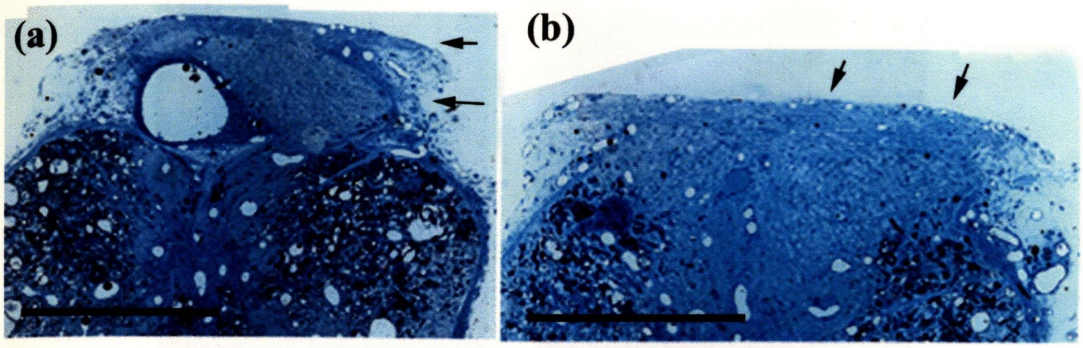


Figure 7.15a, b. Day 20. Extrusion of neural material from the spinal cord in the rostral stump through a breach in the dorsal meninx. In (a) and (b) corresponding to approximately 300 and 540 microns respectively from the bridge, this extrusion is obvious (arrows), but it is more extensive closer to the bridge, as seen in (a). Scale bar = 200 microns.

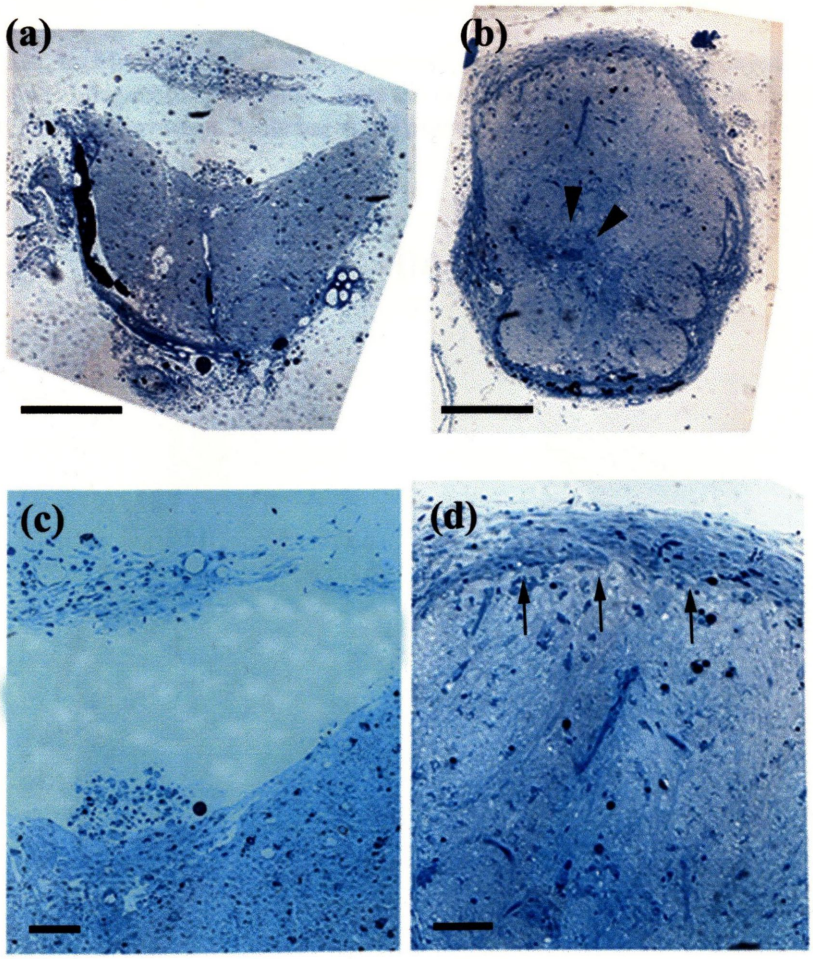


Figure 7.16a, b, c, d. (a) and (c) are non-manipulated cord 14 days following injury while (b) and (c) are collagenase-treated tissue at day 16. Note the presence of a meningeal covering in (b), seen at higher magnification in (d; arrows), compared to the absence of a meningeal covering and the presence of an open canal in (a) and (c). In (b) note the disorganised central canal area (arrowheads) in contrast to the greater organisation found in (b). Scale bar (a) and (b) = 200 microns, (c) and (d) = 50 microns.

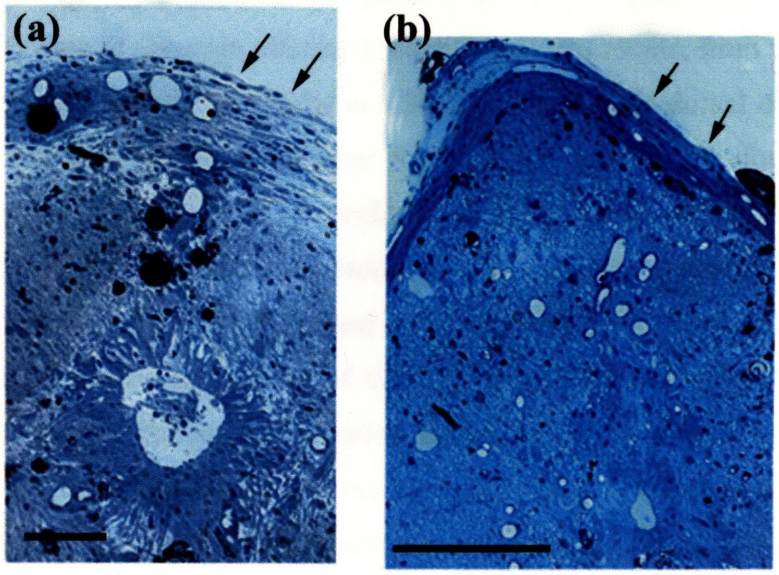


Figure 7.17a, b. Meningeal organisation on the dorsal surface of the cord days 20 (a) and 26 (b) following collagenase application. Note the thick meningeal covering on the lateral and the dorsal surfaces (arrows). Scale bar = 100 microns.

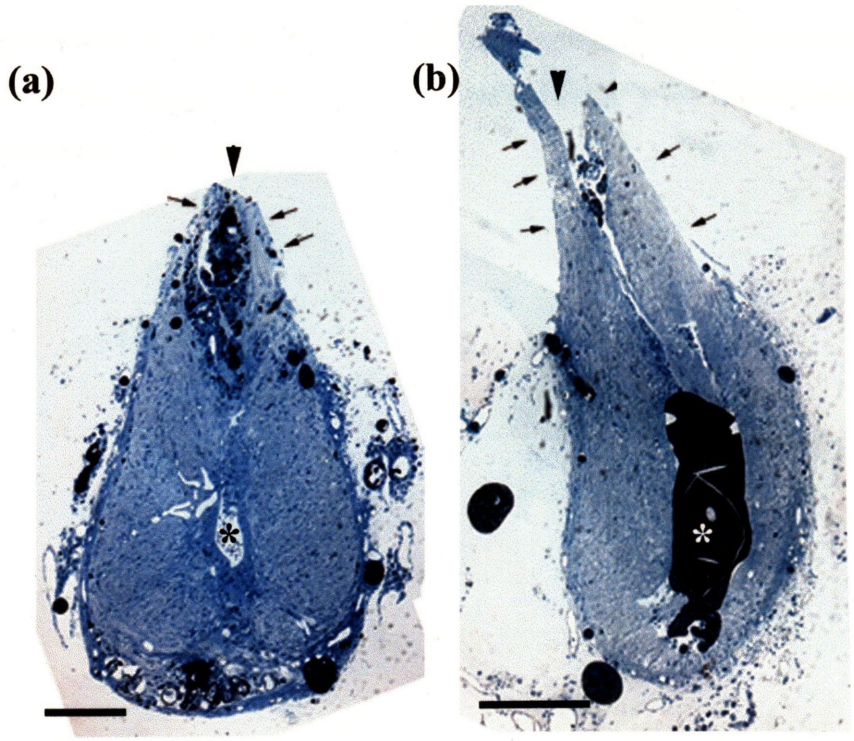


Figure 7.18a, b. Transverse sections of the bridge at day 19 (a, c) and day 26 (b, d) following 6-OHDA application. Note the extensive dorsal movement of regenerating tissue (arrowheads) and the enlarged central canal (*). A meningeal covering is present on the ventral and lateral surfaces of the bridge, however note its absence on the dorsal most region (arrows).
Scale bar = 200 microns.

although it is absent from more dorsal regions (Fig 7.18). Figure 7.19, and table 7.20, provide an overview of the main effects of the different treatments, from which it can be seen that treatment of 6-OHDA results in a 30-56% increase in dorsal displacement of regenerating material, while a smaller increase of 12-13% is found following collagenase type VII application. A negligible dorsal expansion was found after the meninx had only been removed mechanically. Collagenase treatment stimulates the earliest and greatest increase in meningeal thickness (see Figs. 7.21 , 7.22a), while no meninx forms on the dorsal surface of the bridge of 6-OHDA-treated material. In general, the pattern of meningeal formation is similar to that of normal regenerating cord (see Fig. 7.10a,b), with a progressive increase in thickness towards the middle of the bridge (Fig. 7.22). However, there are differences; cords that received just mechanical removal possessed the thickest meningeal covering by day 20; for collagenase-treated material a meninx was present at the centre of the bridge by day 16 that was approximately 700% thicker than normal, a value that changed little at later recovery times (days 20 and 26). 6-OHDA-treated material resembles normal regenerating material in that there is a considerable increase in thickness of the meninx on both sides of the bridge. However, this is less (250-350% for days 19 and 26) than in normal regenerates (600-900%, days 14-20)

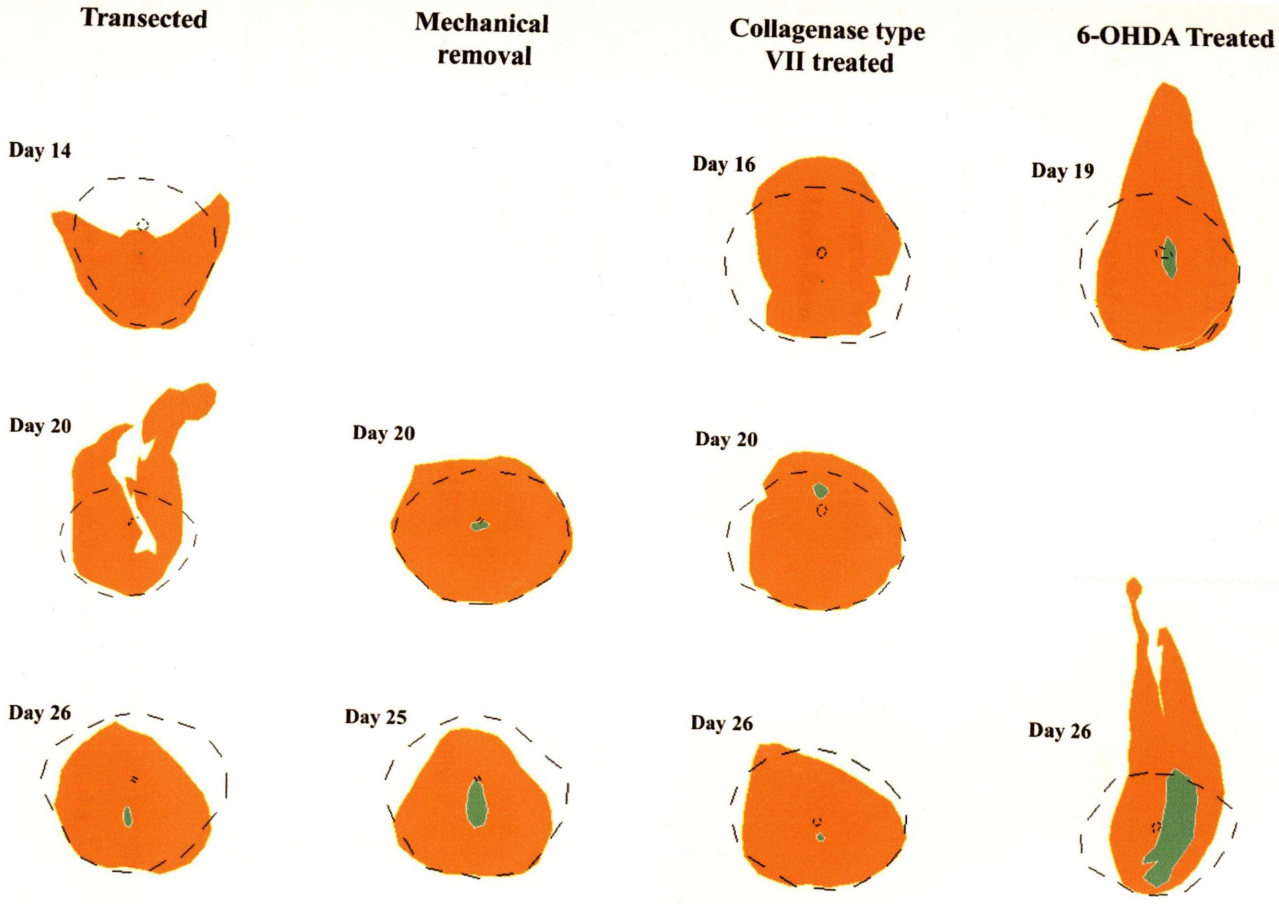


Figure 7.19. Diagrammatic representations of transverse sections from the middle of the bridge for (a) transected, (b) mechanical removal, (c) collagenase treated and (d) 6-OHDA treated cords. Note the differences in cross sectional area from bridge regions (coloured) compared to uninjured cord from outside the lesion site (dotted line).

Day	Experimental Procedure	(a) Changes in Cross Sectional Area of the Bridge (%)	(b) Dorsal Displacement (%)	*(c)* Dorso-Ventral Height
14	*Transected*	-13%	0%	.98
16	*Transected with Coll VII*	-11%	12%	1.23
19	*Transected with 6-OHDA*	+26%	30%	1.6
20	*Transected*	+43%	45%	2.24
20	*Transected with Coll VII*	+3%	13%	1.15
20	*Transected with Mech-Rem*	+13%	8%	1.06
25	*Transected with Mech-Rem*	-17%	0%	.78
26	*Transected*	-13%	0%	.92
26	*Transected withColl VII*	-8%	3%	1.075
26	*Transected with 6-OHDA*	+19%	56%	2.75

Key: Mech-Rem = Mechanical Removal; Transected = Non-Manipulated Regenerate; Coll VII = Collagenase Type VII application and 6-OHDA = 6-hydroxydopamine application.

Table 7.1. Quantification of the sections illustrated in Figure 7.18 for changes in (a) cross sectional area within the bridge and (b) cross sectional area of tissue displaced dorsally. Both are expressed as a percentage change from normal uninjured cord. In (c) the maximum dorsal extension of the neural tissue is expressed as a ratio to uninjured cord. Note the substantial increase by day 20 in the non-manipulated cord, and by days 19 and 26 in 6-OHDA-treated animals.

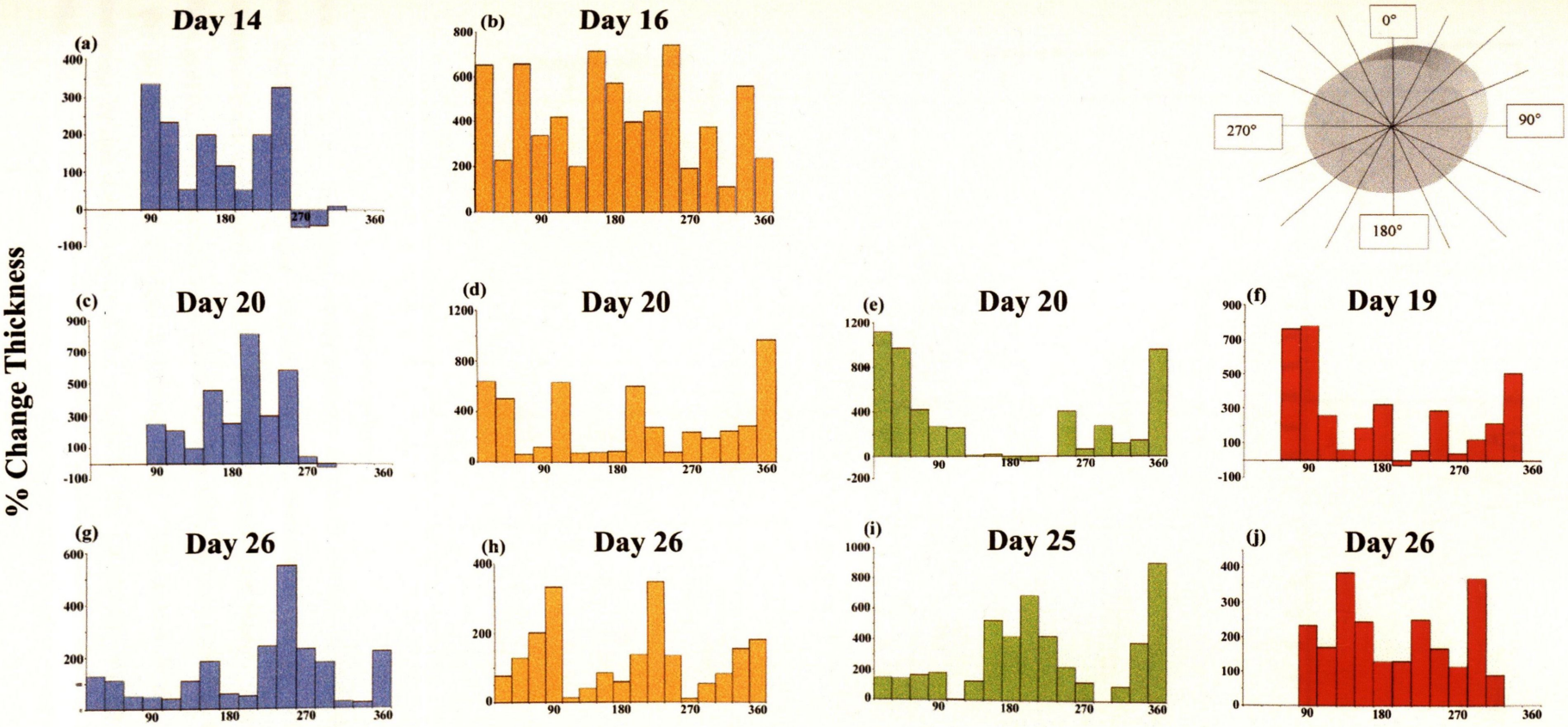


Figure 7.20. Graphical representations of the percentage increase, or decrease in meningeal thickness in the middle of the bridge. Note the presence of a thickened meninx in the bridge by day 16 (b) following collagenase treatment, that is also found at subsequent days, 20 (d) and 26 (h). Mechanical removal of the meninges resulted in the formation of a thickened meninx by day 20 (e), which is in contrast to non-manipulated (day 20; c) and 6-OHDA-treated animals (day 19; f), where it remained absent. At later stages, a meninx did eventually form on the dorsal surface of untreated regenerates (day 26; g), but it continued to be absent from the 6-OHDA-treated cord (day 26; j). The x-axis represents degrees of rotation around the cord with dorso-medial equating to 0 degrees and the ventro-medial to 180 degrees. The y-axis is the percentage change in thickness to 'normal' uninjured meningeal tissue placed 1mm from the bridge region in each case.

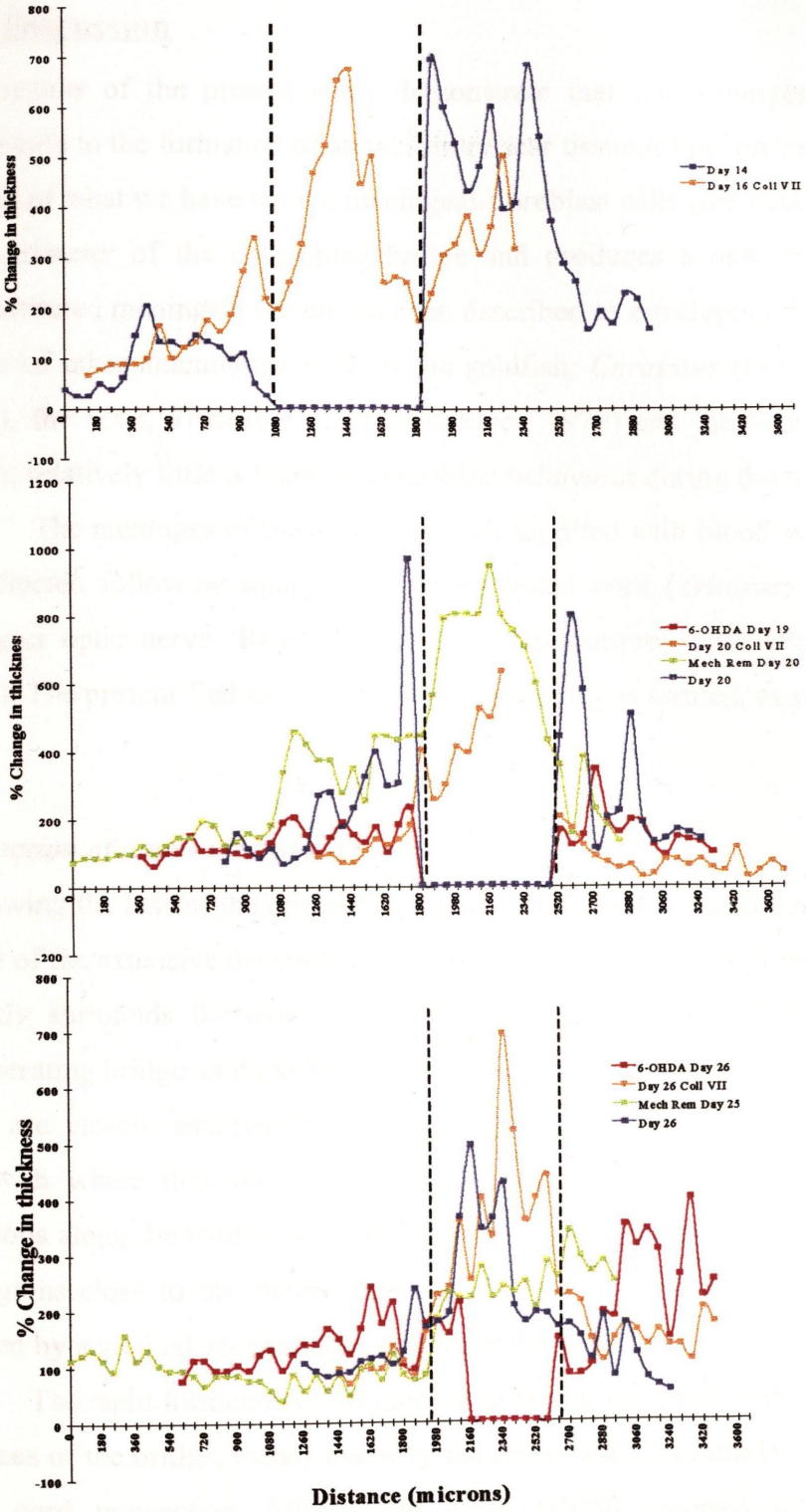


Figure 7.21a, b, c. Graphical representations of the % change in meningeal thickness on the dorsal surface of the bridge (dotted lines) and associated stumps for all experimentally manipulated cords compared to normal regenerating meningeal tissue. The results are presented as three graphs, each representing a particular time with (a) corresponding to approximately day 15, (b) 20 days and (c) 25 days following injury. The x-axis is the distance through the regenerating bridge (microns) and the y-axis in the percentage change in thickness of the meninx compared to undamaged tissue in the stumps.

7.4 Discussion

The results of the present study demonstrate that the meninges of the eel do not contribute to the formation of an inhibitory scar tissue following transection. Instead, a sheath of what we have termed meningeal-fibroblast cells (see next section) develops at the perimeter of the developing bridge and produces a new meninx. Although a reconstituted meningeal sheath has been described as enveloping the regenerated neural tissue of other anamniotes, such as the goldfish, *Carassius* (Bernstein and Bernstein, 1967), the newt, *Triturus* (Michel and Reier, 1979) and the lizard, *Anolis* (Simpson, 1983), relatively little is known of fibroblast behaviour during the regenerative event.

The meninges of the bridge are well supplied with blood vessels, a finding that is reflected following injury in the newt spinal cord (*Triturus*; Stensaas, 1983), in *Xenopus* optic nerve (Reier, 1979) and in the lamprey cord (*Petromyzon*, Hibbard, 1963). The present findings reveal how this covering is formed, as summarised in figure 7.23.

Formation of a new meningeal sheath

Following the loss of the original meningeal sheath from around the spinal stumps, as a result of the extensive degeneration seen at day 4, a population of meningeal-fibroblasts quickly surrounds the exposed neural tissue. They also subsequently envelop the regenerating bridge as it extends into the lesion site by days 6 and 8. At all times these cells are closely associated with the bridge, except at the leading front of neural regrowth where they are disorganised. Hence, a gradient of cellular organisation develops along the rostro-caudal axis of the bridge, with the tightest organisation being in regions close to the stumps (see Fig. 7.22). This indicates that a new meninx is formed by a gradual accumulation of cells at the perimeter of the developing bridge.

The rapid formation of the meningeal layers, especially on the ventral and lateral surfaces of the bridge, means that they are one of the first definite structures to regrow after cord transection. Michel and Reier (1979) reported a similar finding in regenerating juvenile *Triturus* spinal cord where complete reformation of the meninges also occurred. They further suggested the meninges might act as a barrier to regrowing ependymal cells and neurites, restraining them within a tubular sheath. In the eel, the meninges may also contain regrowing neural tissue because when they are absent, as on the dorsal surface, neural tissue extends beyond its normal form to produce the neural 'horns' (see chapters 4 and 5). With increasing recovery times, the newly formed

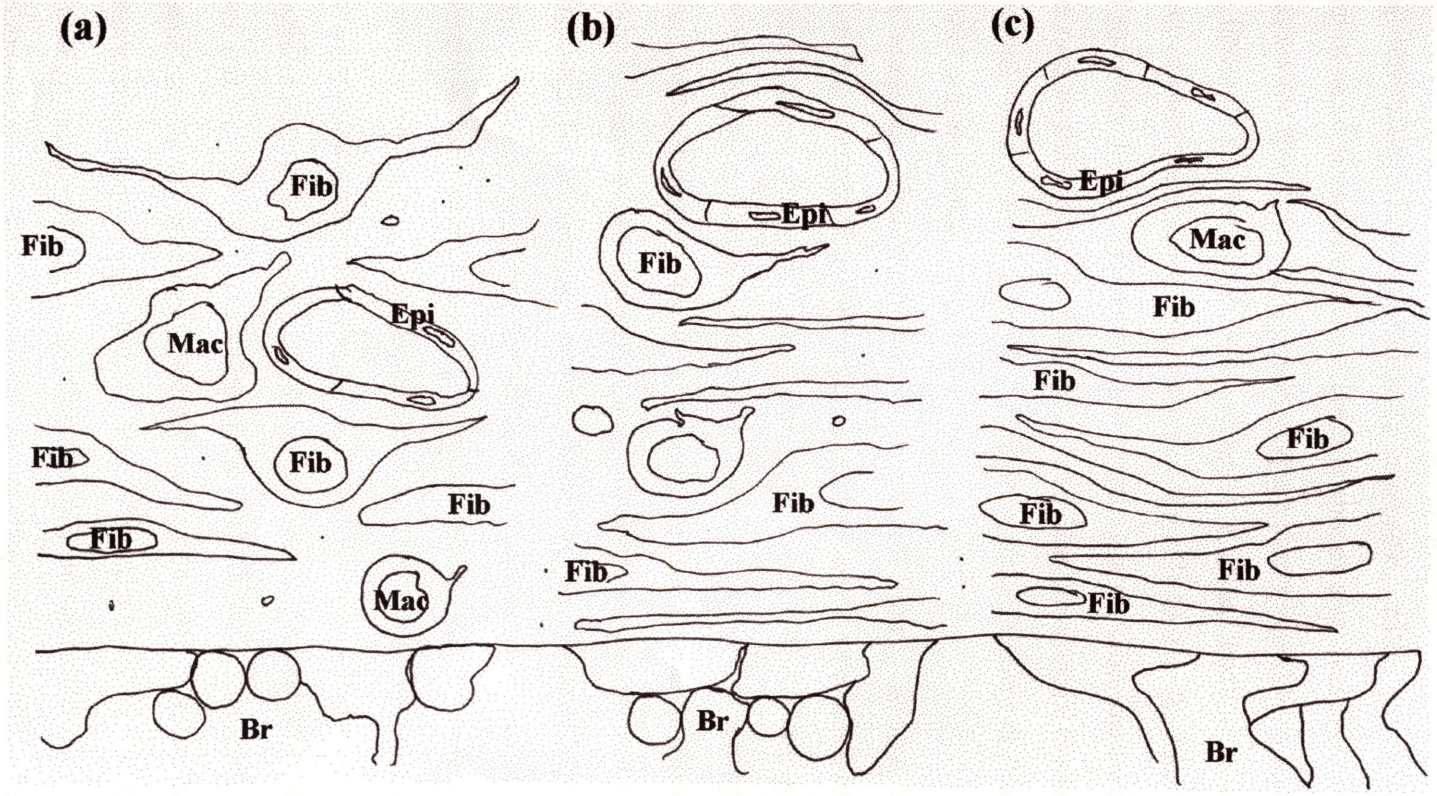


Figure 7.22. Diagrammatic representations that summarise the formation of a new meningeal sheath at the periphery of the developing neural bridge for days 8 (a), 20 (b) and 54 (c). Note the increased organisation of the meningeal layers with extended survival times. Epi = Epithelial cells, Fib = Fibroblasts, Mac = Macrophages, Br = Bridge.

meninx begins to reduce in cross sectional area from 500% by day 26 to 2-300% by days 54-200, a decrease in area that may reflect the loss of meningeal cells, possibly by apoptosis or by migration to other regions, such as the stumps. However, in view of the compact cellular organisation of this tissue seen by day 54 and later, this decrease may result from the reorganisation of the meningeal layers, and a change in the form of the meningeal-fibroblasts from globular to elongate, with increased formation and elongation of cellular processes. Intercellular spaces also decrease, such that by day 54 the cell layers are more closely apposed, and are interspersed with numerous bundles of collagen fibres. At the same time, there is a sharp reduction in the number of macrophage/monocytes interspersed between the cell layers. It would appear that with extended recovery times, the reconstituted meninges provide increased tensile strength and protection to the regenerated bridge. A similar connective tissue organisation has been reported during wound repair in other somatic tissues following injury (see, Martin, 1997; Clark, 1996).

In amniotes, following various types of injury, except compression and microlesion (e.g. Davies et al., 1996), cells of meningeal origin are known to infiltrate into the lesion site in the adult CNS (Pasterkamp et al., 1999; Wang et al., 1997; Li and David, 1996). Since in the eel we have also noted a purposeful meningeal accumulation around the developing neural tissue, it appears that there is an intentional movement of this cell type towards exposed neural tissue, possibly because vertebrate meningeal cells are predisposed to accumulate around neural tissue, recapitulating developmental events. The deliberate nature of the infiltration in the present study is suggestive of an instructive event that encourages meningeal-fibroblast cell accumulation. In view of this, it is interesting to note that 'soluble factors' released by meningeal cells can affect astrocytes by inducing intrinsic changes that render these cells less permissive for axon growth, whereas astrocyte growth medium can induce process formation in meningeal cells (Ness and David, 1997). Whether some type of factor, secreted by the regrowing neural tissue, or by the abundant macrophages/monocytes that are known to produce various stimulatory factors (see Merrill and Benveniste, 1996), is affecting fibroblast and presumably, meningeal cell migration can only be speculated.

Irrespective of this similarity in meningeal fibroblast accumulation, the meningeal cells of anamniotes and amniotes behave very differently in the injured spinal cord, for whereas in the eel they always accumulate and initiate ensheathment at the periphery of the developing bridge, in mammals meningeal infiltration contributes

to the formation of the scar that is thought to underlie regenerative failure (e.g. Reier et al., 1983; Matthews et al, 1979). Interaction with neural tissue, and more specifically with 'reactive' astrocytes, results in the production of an inappropriate glia limitans (e.g. Struckhoff, 1995; Carbonell and Boya, 1988), and basal lamina (e.g. Bernstein et al., 1985; Abnet et al., 1991).

In contrast, in foetal and neonatal amniotes, a fibroglial scar does not form after injury (e.g. Moore et al., 1987; Trimmer and Wunderlich, 1990), apparently because meningeal cells do not invade the wound. Instead, a sheath analogous to what we have found in the eel, forms over the lesion site. Therefore it would appear that the behaviour of meningeal cells in anamniotes is reflected in the regenerative potential of juvenile anamniotes before they are approximately 1 week old (Moore et al., 1987).

The components of the reforming meninx

Fibroblasts

There are several possible origins for the cells that contribute to the forming meninges, since cells can migrate into the often-extensive lesion site, from sources such as the injured overlying muscle and connective tissues, the ligaments and periosteum of the vertebrae (Bernstein and Bernstein, 1967). In mammals, this cellular infiltration into the lesion site contributes to the formation of the 'fibroglial' scar, the component cells of which have been considered to be of mesenchymal or fibroblast origin (e.g. Reier et al., 1983). However, it is now generally accepted that these cells are of meningeal origin (e.g. Pasterkamp et al., 1999; Wang et al., 1997; Li and David, 1996; Abnet et al., 1991) arising from the leptomeninges and dura. It must be emphasised, however, that many of these reports have utilised stab injury, which is a focal lesion that results in minimal disruption of the different tissue layers. In contrast, following spinal cord trauma where the fibroglial scar can be extensive (Fawcett and Asher, 1999), it has been suggested that fibroblast migration occurs from overlying tissues and not entirely from the meninges (Krikorian et al., 1981).

In the eel, we have found that the fibroblast-like cells in the clot, and the meningeal-fibroblasts surrounding the developing bridge, are indistinguishable, and appear to be identical in both structure and ultrastructure, having in general a globular to slightly elongate shape with occasional short lamellipoda, and with extensive cisterns of rough endoplasmic reticulum. As we are unable to distinguish between these cells, the new meningeal sheath may arise from cells of homogeneous or mixed origin. The

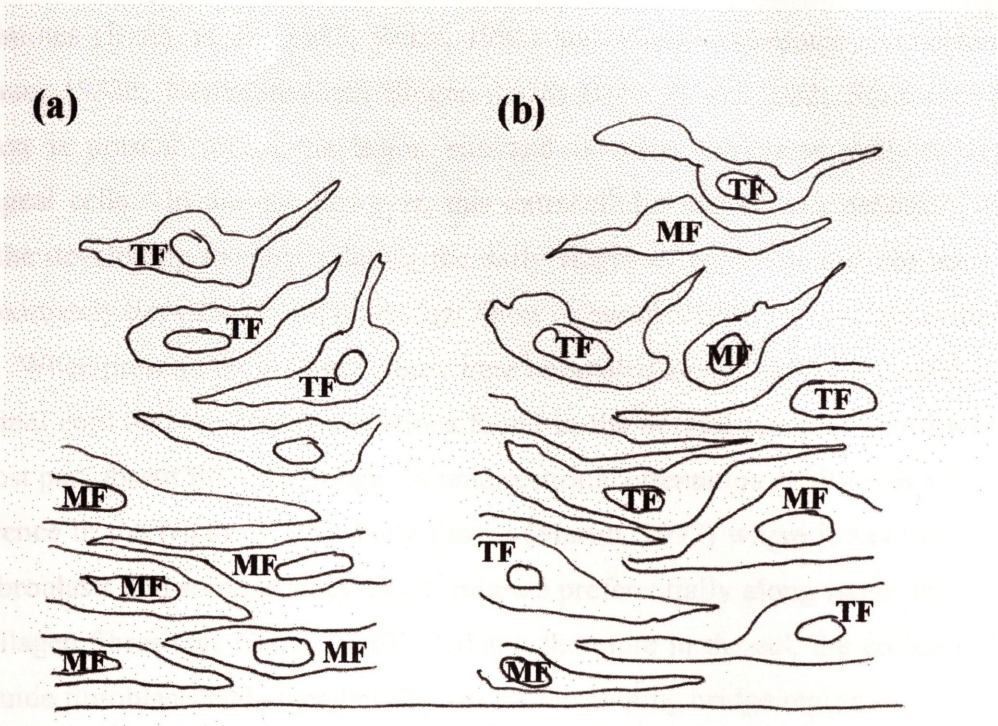


Figure 7.23. Diagrammatic representation of possible modes of development of the meninges at the lesion site. In (a) the clot is composed of fibroblasts from a variety of different tissues (tissue fibroblasts, TF) and meningeal-fibroblasts (MF). The new sheath, however, is composed of meningeal-derived cells that migrate with the regrowing neural tissue. Alternatively, as in (b), the tissue fibroblasts (TF) from a variety of regions may contribute to the formation of the reconstituted meninx, along with meningeal-fibroblasts (MF).

population of fibroblasts within the clot could be of meningeal origin, and form the new meningeal sheath (Fig. 7.23), or involve a mixed cell population of somatic and meningeal origin, as has been suggested by findings in some amniote (Krikorian et al., 1981) and anamniote (Egar and Singer, 1972; Bernstein and Bernstein, 1967; Hibbard et al., 1963) regenerates. Moreover reactive fibroblasts have been shown to be part of the normal response to injury in other body tissues and are an integral component to the reparative process, that includes extracellular matrix turnover (see Martin, 1997; Clark, 1996 for reviews) and wound closure (Desmoulière and Gabbiani, 1996). However, differences between meningeal fibroblasts and tissue-derived somatic fibroblasts have been shown when tissues are grown *in vitro* (Colombo et al., 1994).

The Extracellular Matrix - Collagen

In amniotes (Berry et al., 1983; Reier, 1986) and some anamniotes (Anderson and Waxman, 1983a; Nordlander and Singer, 1978; Bohn et al., 1982; Simpson, 1983) collagen is present within the lesion site and is often associated with infiltrating meningeal cells. In the eel, however, this extracellular matrix was generally absent from the developing meninges during the early stages of regrowth and not until later (approximately days 20-54) did individual fibres or bundles of fibres become evident.

When present, the collagen fibres were orientated along the rostro-caudal axis of the spinal cord and the other orientations found in the normal uninjured cord were for the most part absent from the bridge. A unidirectional orientation of fibres is a common occurrence in the repair of other body tissues (Martin, 1997) where it has been shown that fibroblasts and some leucocyte cells migrate preferentially along rather than across the collagen fibres (see Clark, 1996). Perhaps, therefore in the eel, the collagen fibres may guide fibroblasts and other cell types to the developing bridge region.

The gradual increase in the formation of collagen bundles over time (days 54-200) may provide for some increased tensile strength at the lesion site, compensating perhaps for the loss of the dorsal aspects of the vertebral column following laminectomy.

The Basal Lamina

It seems in the eel that the basal lamina provides some structural support to the normal spinal cord, for when breached, as in the experimentally manipulated cord, neural material is extruded. However, after cord transection a basal lamina was not seen at the interface between the regrowing meninges and the developing neural tissue during the early stages of bridge formation (days 4-20), although it was present later (first noted at day 54). Therefore, its presence appears not to be essential for the regrowth of axons, many of which have grown through the bridge by day 20. It would appear that basal lamina formation is initially prevented or is waiting for a 'cue' of some sort from other tissues. With a continually increasing perimeter, a certain degree of compliance is presumably required of the developing meninges in the bridge that might be hindered by an inflexible basal lamina.

In other studies of the regenerating anamniote CNS, it has been shown that when present, the basal lamina is a permissive substrate for axonal regrowth (Easter et al., 1984; Stensaas, 1983; Reier and Webster, 1974). Further to this, it has been

proposed that this structure may possibly act as a barrier that encloses axonal growth within the lesion site (Reier and Webster, 1974). Similarly, in regenerating amniote peripheral nerve, basal laminae are associated with Schwann cells as they proliferate and migrate to produce longitudinal arrays into which axons grow (e.g. Bunge, 1983; refs). However, this structure is not always supportive to axonal regrowth and in adult anamniotes, basal lamina formation in the lesion site has been suggested to be one of the contributing factors to the failure of axonal regrowth (see Stichel et al., 1999). Certain components of this structure, such as heparin sulphate proteoglycan and tenascin, have been identified among others to be potent inhibitors of axonal growth (see Fawcett, 1997; Fitch and Silver, 1997).

Macrophages/Monocytes

Macrophage accumulation is a common occurrence following injury to tissues such as the skin and it has been shown that locally released factors, such as fibronectin (Clark et al., 1982), TGF-β and PDGF (Elkabes et al., 1996) among others (Riches, 1997), are potent stimulators for the accumulation of this cell type. Macrophages are a noticeable feature of the regenerating spinal cord of the eel but even long after the removal of the clot from the lesion site, considerable numbers of cells of the macrophage and monocyte lineage are harboured in the meninges, interspersed between the layers, with greater numbers being associated with the blood vessels. Even by days 54-200, cells could be found close to blood vessels and, occasionally, interspersed between the meningeal-fibroblast layers.

In so far as we can ascertain, macrophages have not been described as part of the meningeal structure in other anamniote models, although they are evident in mammals where macrophage infiltration and accumulation in the meningeal tissue is readily invoked following the introduction of pro-inflammatory cytokines, such as interlukin-1 and TNF-α (Andersson et al., 1992b) or lipopolysaccharide (LPS) a potent pro-inflammatory antigen (Andersson et al., 1992a).

Are the meninges necessary for correct formation of the regenerating spinal cord?

Mechanical removal of the meninx in the region of the transection did not alter the regenerative ability of the bridge as a whole, or of the meninx, which was able to recover and grow across the denuded region and the bridge, and provide a fully formed

sheath by days 20 and 25. The organisation of the regenerated bridge was not affected but the meninx on the dorsal surface in these experiments was at times substantially thicker (by 1000%) than normal.

Pulse application of collagenase, which seems to disrupt the basal lamina (Halfter 1998; Halfter and Schurer, 1998), appeared to stimulate meningeal formation such that by day 16 the bridge and stumps were fully ensheathed in a covering of meningeal-fibroblasts. The application did not alter the structure of the bridge but the meninx was also substantially thicker than normal (by approximately 800%).

Following both these approaches there seems to be an increased infiltration of macrophages/monocytes, and a greater fibroblast proliferation and migration. The breaking down of the basal lamina in these regions may uncouple surviving meningeal cells from the basal lamina and induce an earlier reactive state. Application of 6-hydroxydopamine, however, in conjunction with mechanical removal seems to prevent the reformation of a meningeal covering even by day 26. At the same time, the neural tissue is displaced, such that by day 20, 30% and day 26, 56% of the bridge tissue was displaced dorsally. It is known that 6-OHDA selectively destroys meningeal cells in neonatal amniotes (Sievers et al., 1980; Sievers et al., 1985), and presumably in the eel, until its effect declines, meningeal cells surrounding the denuded stumps of the eel are selectively destroyed, and do not migrate into the denuded region. With time, 6-OHDA concentrations drop and meningeal cells are able to proliferate, migrate, and begin to colonise the surface of the bridge.

Despite the disruption of the meninx, axons continue to regrow but as they are no longer restrained, they displace further dorsally. This unrestrained movement of neural tissue is not found in normal, denuded or collagenase-treated cords. In the hamster (Sievers et al., 1994a) and rat (Sievers et al., 1994b) 6-OHDA application over the developing cerebellum and cortex results in developmental alteration of these structures. Since it is considered that a meningeal presence is necessary for the correct development of the amniote brain, and that meningeal cells possess the ability to organise the glia limitans and this has been shown both *in vivo* (Sievers et al., 1994b) and *in vitro* (Struckoff, 1995), we conclude from the present study that the meninges, or more specifically meningeal cells, are necessary for the correct development of the regenerating bridge in the eel.

Summary of main findings

- The meninges of the eel do not form scar tissue following transection; instead, this tissue develops at the periphery of the bridge.
- A gradient of development occurs along the rostro-caudal axis of the regenerating bridge with the least organisation found close to the leading elements of the bridge.
- With time, the meninges surrounding the bridge thickens considerably, but at later stages (~day 54) begins to reduce but the large number of cell layers remains, suggesting an increased tissue organisation.
- Fibroblasts are the major component of the developing meninges, but later large deposits of collagen are laid down between cells.
- Collagen fibres are laid down in a characteristic longitudinal orientation, indicating an increased tensile strength along the rostro-caudal axis of the bridge.
- Experimental manipulations indicate that meningeal tissue may be instrumental for correct development of the bridge.
- Meningeal fibroblasts, as suggested by 6-OHDA treatment, appear to be the integral component for this process.

Chapter 8

Organisation of radial astrocytes in the regenerating spinal cord

8.1 Introduction

The inability of the mammalian central nervous system to recover functionally following injury is thought to be due in part to the reaction of local astrocytes (reactive gliosis) to form a glial scar at the site of insult (see Malhotra et al., 1990 for review). Reactive astrocytes has been reported as a consequence of all types of injury, such as crush (Frank and Wolberg, 1996; Stoll and Mueller, 1988), contusion (Baldwin et al., 1998), laceration (Predy and Malhotra, 1989) and transection (Barrett et al., 1984) and results in the proliferation of cells that 'wall-off' the damaged portion from other uninjured regions of the CNS.

This astrocytic reaction has been extensively studied in both amniote and anamniote optic nerve and the spinal cord. A glial scar is found in the amniote optic nerve and spinal cord following all types of injury (see Reier, 1986; Malhotra and Shnitka, 1994 for reviews), but although a glial reaction also occurs in the anamniote CNS (e.g. Reier, 1979; Cohen et al., 1993; Blaugrund et al., 1993), it does not appear to inhibit the regrowth of axons through the wound region (e.g. Beazley et al., 1997). The optic nerve in fish, for example, is well known for its regenerative ability and can successfully recover from a variety of different types of injury, including crush and transection (Reier and Webster, 1974).

Following injury to the mammalian CNS, astrocytes associated with the wound region change from a normally supportive role to a reactive state. Typical of this event are alterations to the normal structure of the astrocyte both inter- and intracellularly. Cellular changes - an increase in cell size (hypertrophy), an increase in the number of cells (hyperplasia), and the number of cytoplasmic processes extending from the cell surface - combine to produce the scar tissue (Skoff 1975; Miller et al., 1985). These morphological changes are coupled with an intracellular alteration of the cytoskeletal structure and an upregulation of other elements, including growth factors, cytokines and recognition molecules (see Ridet et al., 1997 for review). Depending on the type of injury (e.g. transection, laceration or stab), where the damaged CNS is exposed to the surrounding non-neuronal milieu, an interactive reaction between astrocytes and invading meningeal cells and fibroblasts can also occur that further enhances the complexity of the scar tissue (e.g. Matthewson and Berry, 1985).

In the anamniote CNS, stellate astrocytes that are typical of the amniote CNS are absent and a number of astrocytic subtypes can be distinguished on the basis of their

radial architecture. In the fish optic nerve, for example, the predominant astroglial cell, the reticular astrocyte, is arranged spatially into a highly organised structure (Maggs and Scholes, 1990; Scholes, 1991) and it possesses a considerable regenerative ability being able to migrate with regrowing axons into the wound site (e.g. Blaugrund et al., 1993). The spinal cord of most anamniotes also possesses a specialised astroglial cell termed the radial astrocyte (see Chapter 2; Bodega et al., 1993; Lazzari et al., 1997) but numerous studies at the level of the light and electron microscope (e.g. Bernstein and Bernstein, 1967) and, more recently, immunohistochemically (Anderson et al., 1984), have not attributed a specific contributory role for the radial astrocyte in the regenerative event. It must be recognised, however, that most research in recent times has not concentrated on glial behaviour, but rather on the regrowth of axons (see chapter 9; Becker et al., 1997), and the role of the ependyma (see chapter 5; Benraiss et al., 1997; Chernoff, 1996). Moreover in some of the models used to study regeneration, such as amphibian and reptile tail regenerates (e.g. Singer et al., 1979; Simpson, 1968), the presence of a radial astrocytic organisation remains unclear. Consequently, this cell type in most regenerates has received little attention.

As part of the present study, we have documented the reactions of the radial astrocyte population following a transection injury to the spinal cord. The organisation of the radial astrocytic structure in the eel (see chapter 2), which is typical of other anamniote vertebrates (Bodega et al., 1994), comprises a single cell type that is radially oriented. This simple arrangement is in sharp contrast to the mammalian spinal cord where astrocytes are interspersed between the neuronal cell soma in the grey matter (protoplasmic astrocytes), and between myelinated tracts in the white matter (fibrous astrocytes), and produce a complex lattice-work of cells. In the eel, therefore, damage or alteration to the radial structure in the spinal cord, as a result of the injury can be easily identified and mapped, allowing a detailed examination of the cellular alterations to be made.

Although numerous molecular and immunohistochemical studies on the mammalian nervous system have documented the alteration in the levels of factors such as cytokines (e.g Interlukin-1, Takamiya et al., 1986; Interlukin-6), growth factors including NGF, bFGF, CNTF (Aubert et al., 1995; Szele et al., 1995), and recognition molecules (e.g. PSA-NCAM and APP, Ruttishauser and Landmesser, 1996), these molecules are not exclusive to reactive astrocytes and are expressed in others as well. The most common specific markers used in the detection of reactive astrocytes relate to

the changes in intermediate filament composition. Markers to the glial fibrillary acidic protein (GFAP) have long been the most commonly used (e.g. Sievers et al., 1995; Houle and Reier, 1988; Smith et al., 1986) and this intermediate filament is strongly upregulated following injury (Eng and Lee, 1995). Vimentin, a protein more commonly expressed in developing and immature astrocytes, is also associated with the wound site as a result of proliferating and immature cells (Schiffer et al., 1986). Finally, the S-100 protein, which is associated with intermediate filaments such as GFAP (Bianchi et al., 1993), is elevated in reactive astrocytes (Miyake et al., 1989) although it is less commonly used as a specific marker than GFAP. All three markers have previously been utilised and are proven to label specifically the glial response to injury in vertebrates, most notably in the optic nerve (e.g. Bignami and Dahl, 1985; Boyes et al., 1986).

As in chapters 2 and 5 we have combined here light and electron microscopy with an immunohistochemical study using antisera to GFAP, S-100 and vimentin in order to determine the astrocytic reaction to injury. In the past, many of the investigative approaches used in anamniotes have utilised only one method to determine the astrocytic reaction, for example immunohistochemistry (e.g. Cohen et al., 1993) or light and electron microscopy (e.g. Reier and Webster, 1974) and, as a result, combined studies are rare (but see Blaugrund et al., 1993). Our aim in the present study has been twofold: (a) to detect the role of the radial astrocyte in the colonisation of the newly forming bridge region, and (b) to determine if there is an alteration to the radial astrocyte structure in the spinal stumps as a result of the injury.

8.2 Materials and Methods

Animals

This study is based on 34 European eels, *Anguilla anguilla L.*, in a non migratory immature stage of their life cycle.

Surgery

For surgery, each eel was treated according to the operational procedures outlined in chapter 4. In brief each animal was anaesthetised by immersion in 0.3g/l MS-222 (Sigma) and further by a subcutaneous injection of 0.1ml alphaxalone ("Saffan" Pitman-Moore) subcutaneously. Cooling on ice provided additional anaesthesia. The spinal cord was exposed and transected using fine micro-scissors at the region of the 4th segment caudal to the anus. Following surgery, animals were placed in separate holding tanks.

Tissue Preparation

For histological investigation, each animal was treated according to the methods described in chapter 2. In brief, each animal was anaesthetised initially by immersion in 0.3mg/l MS-222 and further by a subcutaneous injection of 0.3ml alphaxalone ('Saffan' Pitman-Moore). To prevent blood clotting, 0.2ml heparin sodium (Leo Laboratories) was also given subcutaneously. The perfusion procedure consisted of a primary flush of Ringer's solution (with 0.1% procaine (Sigma) for further anaesthesia) through the heart followed by the fixative. Two fixative solutions were used (a) 4% paraformaldehyde in 0.1M phosphate buffer (PB) pH adjusted to 7.4, for immunohistochemical investigation and (b) 2% paraformaldehyde, 1.25% glutaraldehyde in 0.1M phosphate buffer (PB), pH adjusted to 7.4, for electron microscopy. Following perfusion, the region of the spinal cord containing the injury and portions immediately rostral and caudal, were dissected from the spinal column and post-fixed in the same fixative at 4^{o}C for a maximum of 3 hours.

Light Microscopy

Following postfixation, the spinal cords were prepared as described in chapter 2. However, tissue from 16 and 20 days post-transection were cryosectioned to produce 20μm thick transverse sections. For this the tissue was cryoprotected in 30% sucrose

solution overnight at 4°C prior to sectioning. All tissue was processed for rabbit anti-goldfish GFAP (generous gift from Dr. S. N. Nona), S-100 rabbit anti-bovine (Dako) and vimentin mouse monoclonal (Dako) antibody. For visualisation the avidin-biotin method (ABC kit, Vector) was used with (0.05%) 3,3'-diaminobenzidine (DAB, Sigma) as chromogen.

Electron Microscopy

The tissue was processed for electron microscopy according to the procedure described in chapter 2. Sections were cut both for light (1.5μm) and electron microscopy (~500Å). All images were downloaded, analysed and formatted on a Macintosh G3 computer using Adobe PhotoShop 5. Reconstructions from serial sections (60μm apart) of the regenerating spinal cord and central canal were produced according to the methods described in chapter 3.

8.3 Results

Light microscopy

Because of the extensive degeneration in the rostral and caudal stumps at day 4, radial astrocytes are absent from the stumps up to approximately 0.9 mm rostrally and 1 mm caudally. Furthermore, there is a notable absence of astrocytic soma structures and radial profiles (Fig. 8.1a) in these regions. Degenerative events extend even further into the stumps, but the radial astrocytic organisation was retained amidst other degenerating profiles, such as axons and their associated myelin sheaths, most notably in the ventral portions of the stumps (Fig. 8.1a, b). Further distal to the cut surfaces, radial profiles become predominant in all regions of the cord although they are frequently absent dorsally and laterally (fig. 8.1b). By approximately 0.9 mm from the cut surface, a full radial complement is present in both stumps (Fig. 8.1c). By days 6 (Fig. 8.2a) and 8 (Fig. 8.2b) the glial structure in the stumps continues to degenerate. In both figures it can be seen that the dorsal and lateral glial tracts become increasingly absent from large portions of the stumps while the best preserved are those of the ventral projecting glia that surround the large myelinated axonal tracts close to the ventral pial surface.

GFAP-labelling of the lesioned spinal cord at days 4 and 6 is enhanced and particularly pronounced indicates a pronounced close to the cut surface (Fig. 8.2c). A small number of longitudinally aligned immunopositive fibres was also found in this region. The gap produced by the retraction of the cord, filled with an extensive blood clot, was GFAP-ve for all days.

At day 8, GFAP+ve profiles are present in the wound close to the cut surface of the stumps, and consist of thin longitudinally orientated immunopositive fibres originating from the stumps and extending short distances into the developing bridge (Fig. 8.3a); those that extend the furthest are close to the periphery. In the stumps, GFAP+ve labelling is characterised by an intense staining on both sides of the central canal that correspond to the glial horns and radial processes. In conjunction with the increase in labelling, the normal radial organisation begins to disappear while longitudinally orientated profiles become prominent (Fig. 8.3b), although the radial organisation of GFAP+ve profiles are still evident in the stumps (see Fig 8.3c). By day 12 further infiltration of GFAP+ve processes continue and, as with those found at day 8, they are thin and elongate. The extension of processes appears to develop mainly from the central regions of the stumps as 'cone-shaped' projection that is most notable

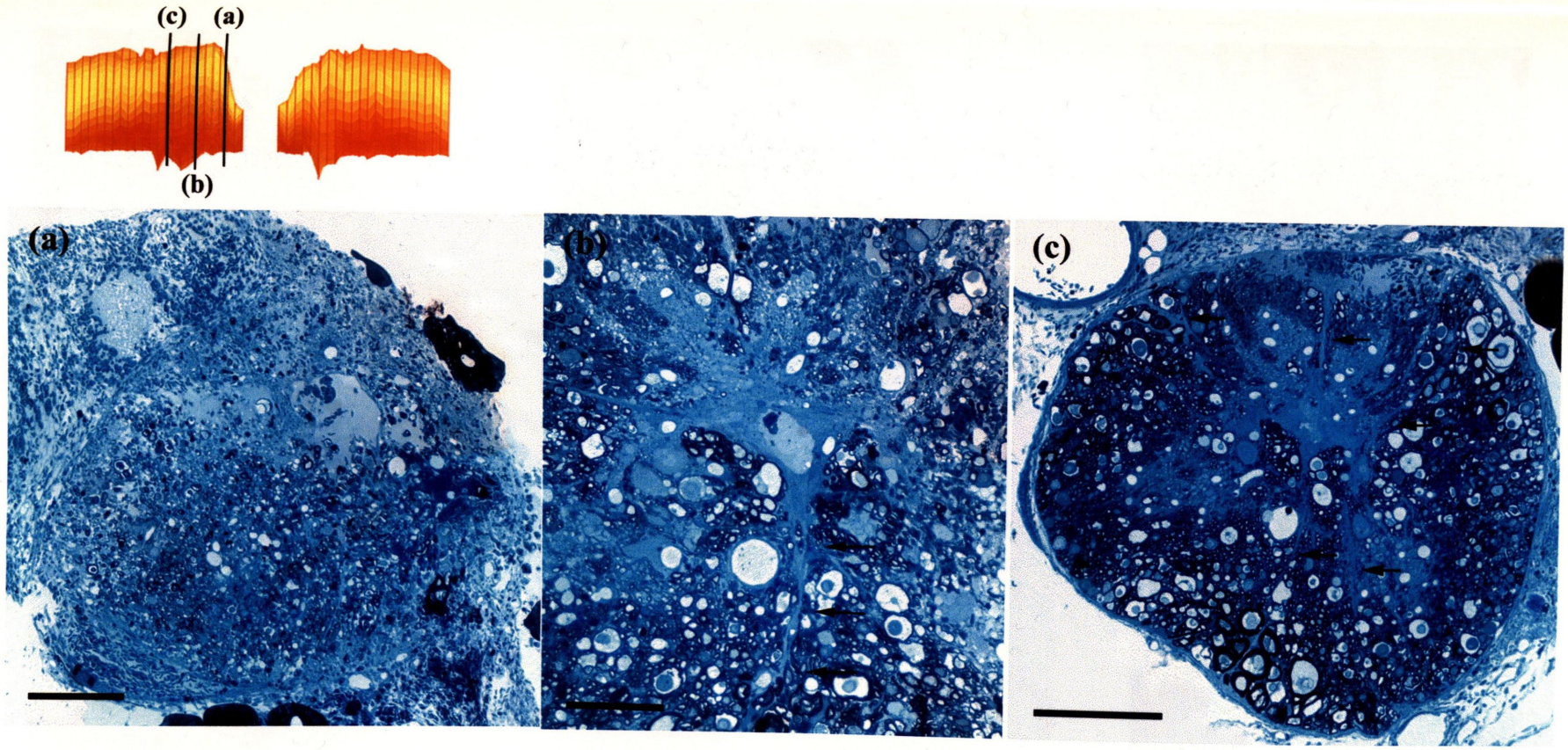


Figure 8.1a, b, c. Photomicrographs of the radial astrocyte organisation in the caudal stump 4 days (b) following injury. In regions of the stumps adjacent to the cut surface (a) the radial atrocytic structure is absent. In regions further away from the cut surface, portions of the astrocytic organisation are found most notably in ventral positions (arrows). Approximately 0.9 mm from the cut surface (c) a full complement of profiles similar to those in uninjured cord are found (arrows). Scale bar (a) and (c) = 200 microns, (b) = 100 microns.

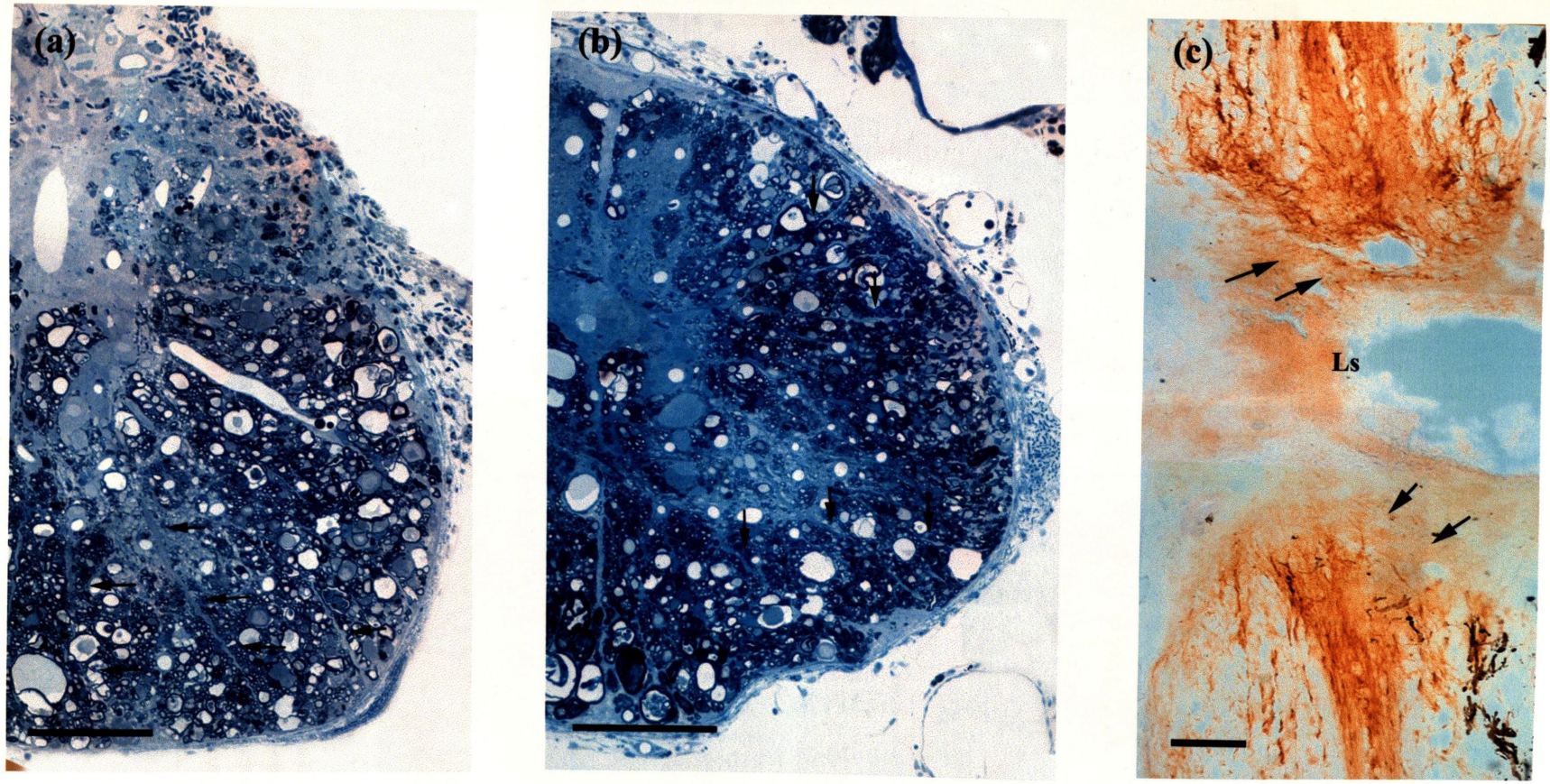


Figure 8.2a, b, c. Photomicrographs of the spinal stumps at days 6 (a) and 8 (b). In (a) note the extensive degeneration in the stump and the absence of radial astrocytes save for the ventral projecting processes (arrows). At day 8 (b), in the caudal stump 0.8 mm from the bridge note the absence of the ventro-lateral tract and the disorganised nature of the smaller profiles (arrows). In (c) labelling for the glial fibrillary acidic protein illustrates a strong labelling pattern in the spinal stumps at day 8 (arrows) particularly those regions close to the cut surface. Ls = lesion site. Scale bar = 100 microns .

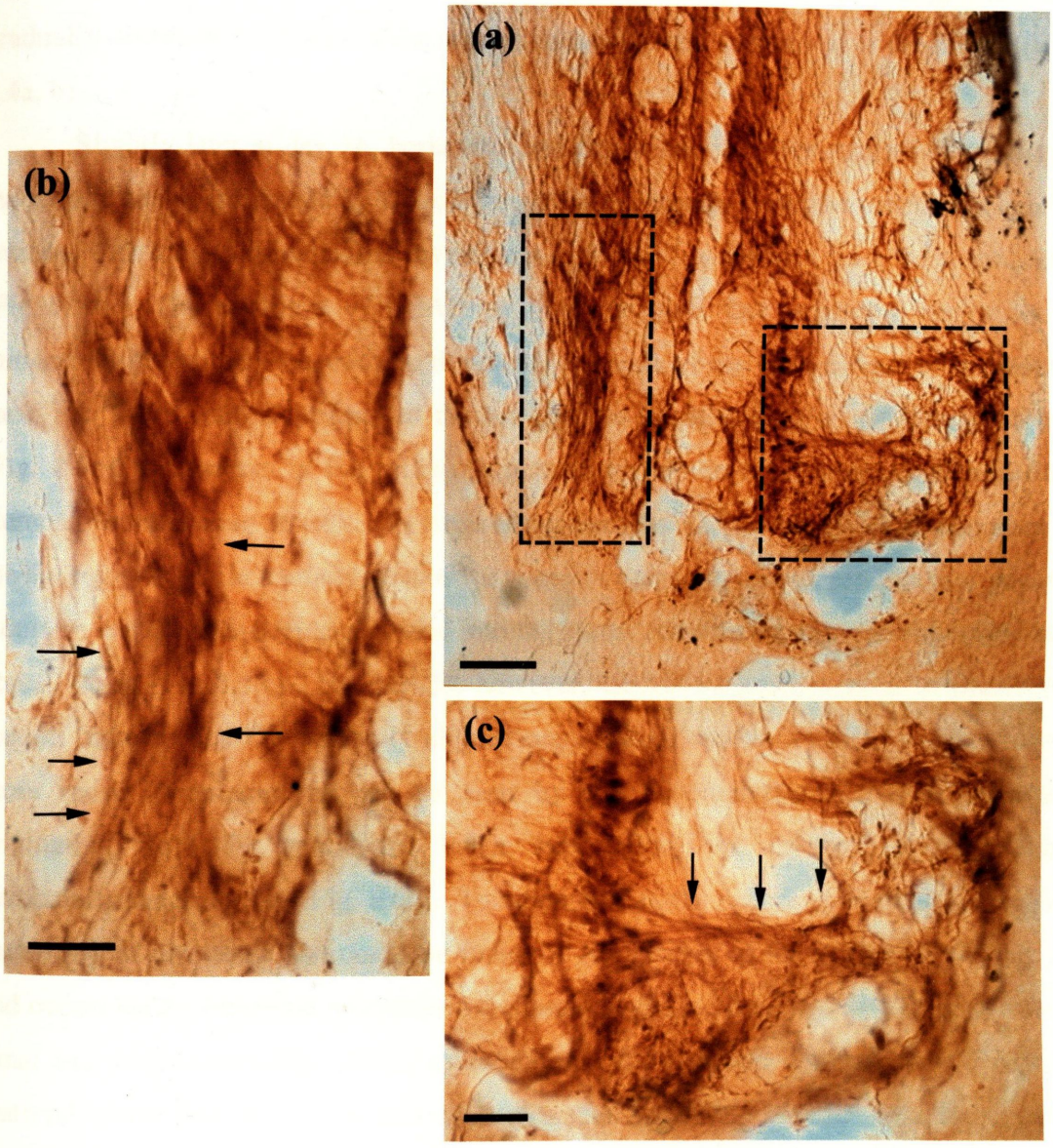


Figure 8.3a, b, c. Day 8. The photomicrograph of the rostral stump in (a) illustrates the different orientations of GFAP+ve processes that are found in the spinal stumps at this stage. Withgreater magnification in (b; from box in (a)) the immunopositive processes are aligned longitudinally (arrows) while in (c; from box in (a)) a radial organisation is still present, although disorganised (arrows). Scale bar (a) = 100 microns, (b) and (c) = 50 microns.

in the caudal stump (Fig. 8.4a, b). In the stumps, the radial organisation of GFAP+ve structures continues to change from the characteristic radial to a predominantly longitudinal orientation (Fig 8.4a, b). Similarly, a gradient of GFAP+ve labelling is evident in the stumps and the wound site with the strongest staining occurring in those regions close to the bridge, including those processes invading the wound site, and gradually decrease in regions of the stumps and uninjured cord distal to the bridge (Fig. 8.4a, b).

Slightly later at day 16, horizontal and transverse sections suggest that most of the wound site is infiltrated by GFAP+ve processes arising from the rostral and caudal stumps, with a trend for a greater investment of GFAP+ve profiles from the rostral cord (Fig 8.5a). The positions of GFAP+ve fibres suggest that a greater migration of immunopositive profiles occur into the dorsal portions of the bridge close to the central canal. In more ventral portions of the bridge, few immunopositive profiles are found (Fig. 8.5b). Processes in the bridge in general appear to be thinner to those in the stumps. In transverse section, an erratic organisation of GFAP+ve fibres is also seen in medial regions, while laterally, the bridge contains immunopositive profiles that possess a dorso-ventral orientation and extend into the horns, terminating close to the lateral and dorsal edges (Fig 8.5,c). By day 20, however, GFAP+ve profiles seen in transverse section indicate that the randomly aligned organisation has begun to be replaced by a more radial orientation as can be seen by the development of radial processes originating from the ependymal layers surrounding the enlarged central canal, particularly ventrally (see Fig. 8.6b). Toludine blue stained sections reveals a 'mosaic' patterning of processes that could be found in all portions of the bridge (Fig. 8.6c, d) and occasionally, tanycytic processes were found to extend from the developing central canal and project ventrally. In the spinal stumps, the semithin sections and GFAP+ve material show that the radial astrocytic structure continues to alter and the typical organisation found in uninjured cord is absent in progressively more distal stump regions.

By day 26 the reorganisation of immunopositive profiles continues in the bridge and stumps with many of the GFAP+ve processes now orientating into straight longitudinally directed paths with little deviation (Fig. 8.7). This was most notable

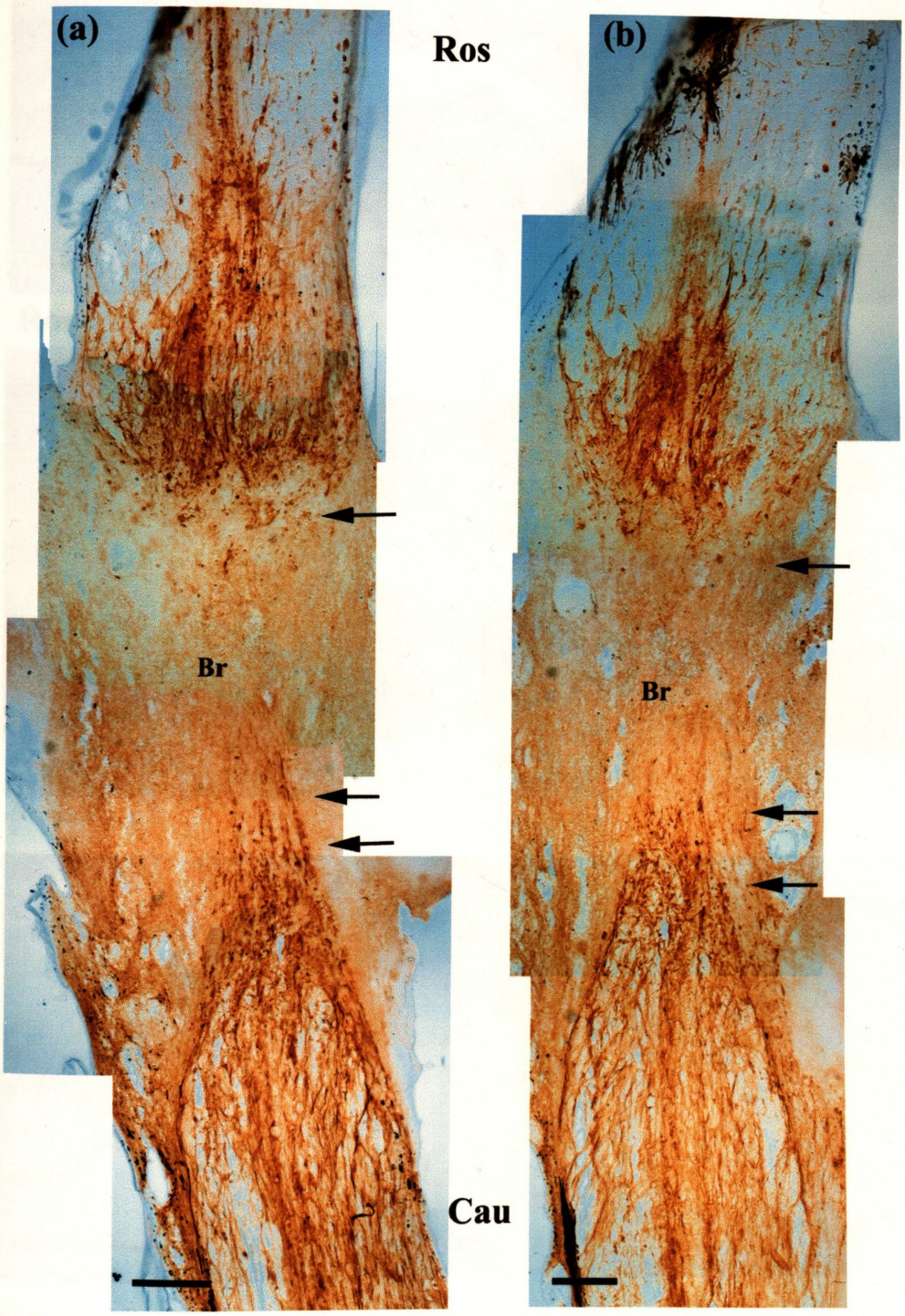


Figure 8.4a, b. GFAP+ve profiles extending into the bridge 12 days following injury. In regions placed more dorsally (a) a 'cone-shaped' extension of processes occurs (arrows) however in regions placed more ventrally (b) a greater influx of profiles can be seen (arrows). Br = bridge, Ros =rostral, Cau = caudal. Scale bar = 200 microns.

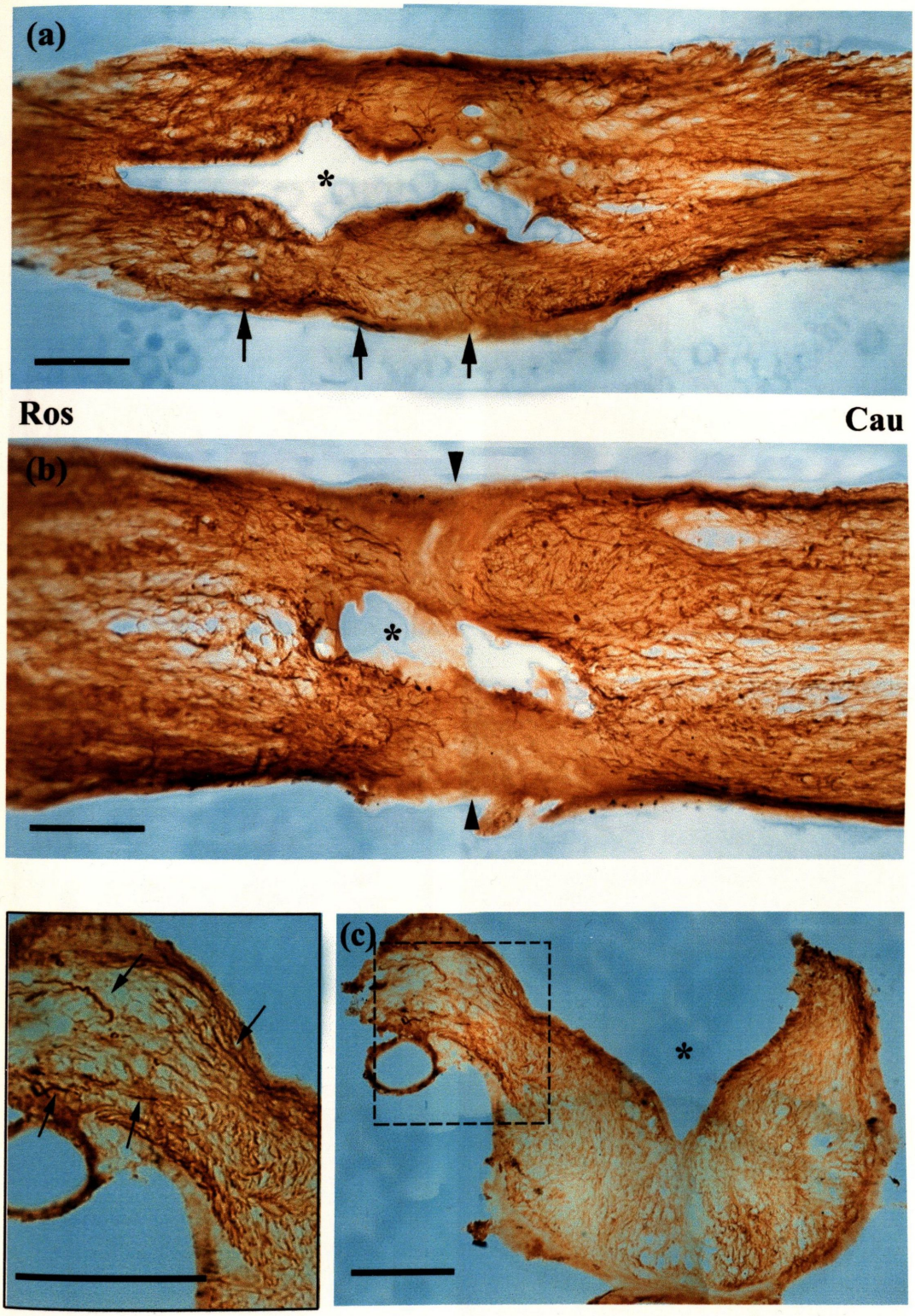


Figure 8.5a, b. GFAP+ve profiles in the bridge 16 days following injury. In (a) note the presence of immunopositive profiles in all regions of the bridge (arrows). In (b) corresponding to more ventral portions of the bridge, regions remain where no GFAP+ve profiles are found (arrowheads). In transverse section (c) immunopositive profiles are found throughout the bridge but note the greater labelling in more dorsal regions that show the extension of long processess into the developing neural horns (inset; arrows). Central canal = (*). Rostral = Ros, Caudal = Cau. Scale bar = 200 microns.

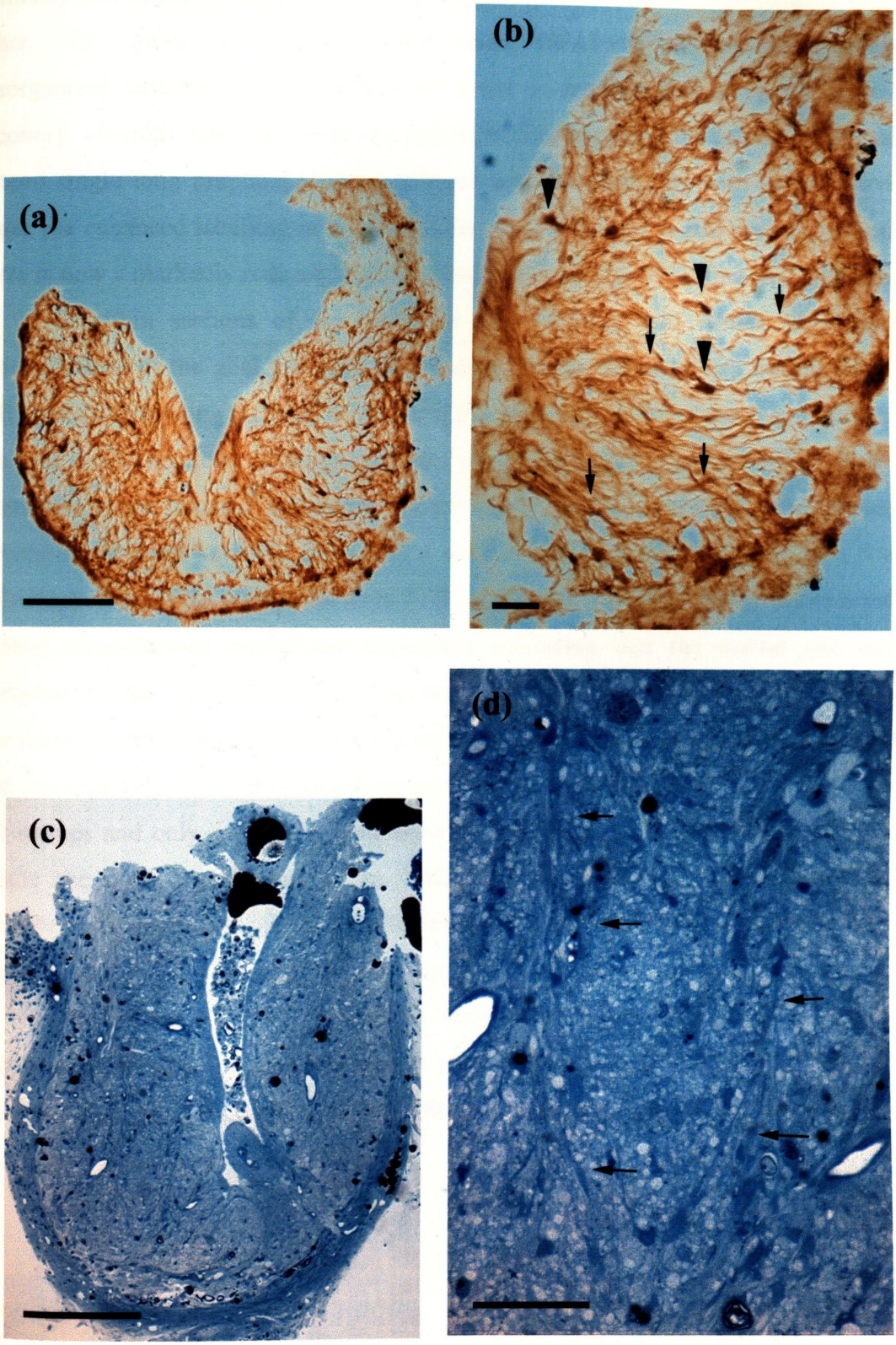


Figure 8.6a, b. Day 20. In transverse section GFAP labelling illustrates the reorganisation of the glial profiles to a more radial structure. At higher magnification (b) this can be seen (arrows) and also the presence of knots of intensely labelled profiles (arrowheads). In (c) toludine blue stained tissue, long cellular processes are also found in the bridge (d; arrows). Scale bar (a) an (c) = 200 microns, (b) and (d) = 50 microns.

ventrally and laterally where many of the immunopositive fibres align parallel to each other. In regions close to the central canal, GFAP+ve profiles still possess a disorganised structure, although, they are fewer in number than at earlier stages of recovery. Weakly labelled GFAP+ve radial profiles apposing the lumen of the canal extend single long immunopositive processes into the cord. As with earlier survival times the enhanced labelling in the rostral and caudal stumps is still present, although, there is now a markedly reduced level of GFAP+ve labelling of profiles in the bridge.

Semithin sections of the bridge at day 54 (Fig. 8.8) further illustrate the reorganisation of the glial processes as a predominantly radial pattern arising from the cell layers surrounding the central canal and extending towards the meningeal surface of the cord in all directions, although processes of undetermined origin are still present that contribute to the 'mosaic' patterning. In the spinal stumps, where the radial astrocytic structure had been severely disrupted, a similar radial reorganisation is also found. GFAP labelling of the stumps for days 70 (Fig. 8.9) and 175 (Fig. 8.10), shows a radial, central canal-derived orientation (tanycytes) indicating that the rostral and caudal portions of the stumps have undergone a glial reorganisation (Fig. 8.9, 8.10). Furthermore, many processes extend from this region into the bridge from both sides, and consequently, the normal radial astrocytic structure is absent from large portions of the stumps and only become evident in more distal regions of the cord (Fig. 8.11a,b). While the glial organisation in the bridge is dominated by the large number of GFAP+ve tanycytic processes, longitudinally aligned radial astrocytic processes are present and generally localised to the periphery of the bridge (Fig. 8.9, 8.10).

The intense GFAP+ve labelling in the bridge for days 70 and 175 is similar to that of day 26, with a weaker labelling of processes compared to the rostral and caudal stumps. The thin, longitudinal oriented fibres are more strongly labelled compared to the weaker labelled tanycytic processes.

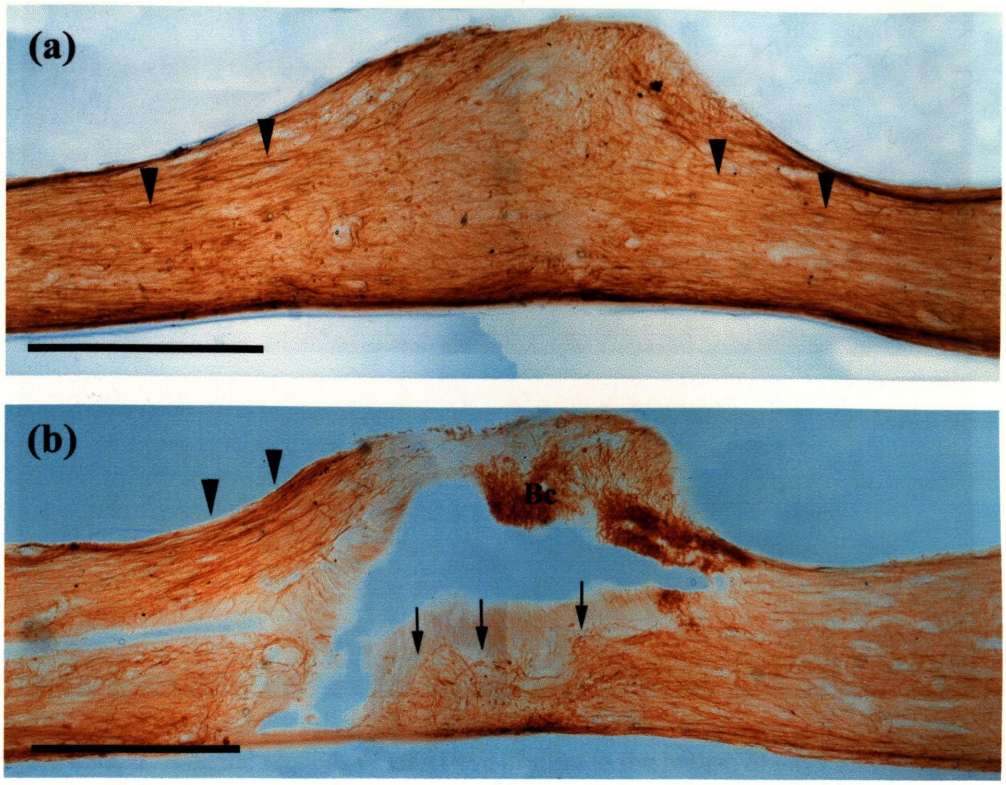


Figure 8.7. Day 26 saggital view. In both (a) and (b) note the presence of elongate immunopositive fibres that enter the bridge in parallel arrays. In (a) which is placed more lateral regions of the bridge note the extensive labeling of profiles that are primarily elongate in structure (arrowheads). In regions close to the enlarged central canal in (b) note the disorganised profiles (arrows) while at the periphery parallel elongate profiles predominate (arrowheads). Bc = Remnants of the blood clot. Scale bar = 100 microns.

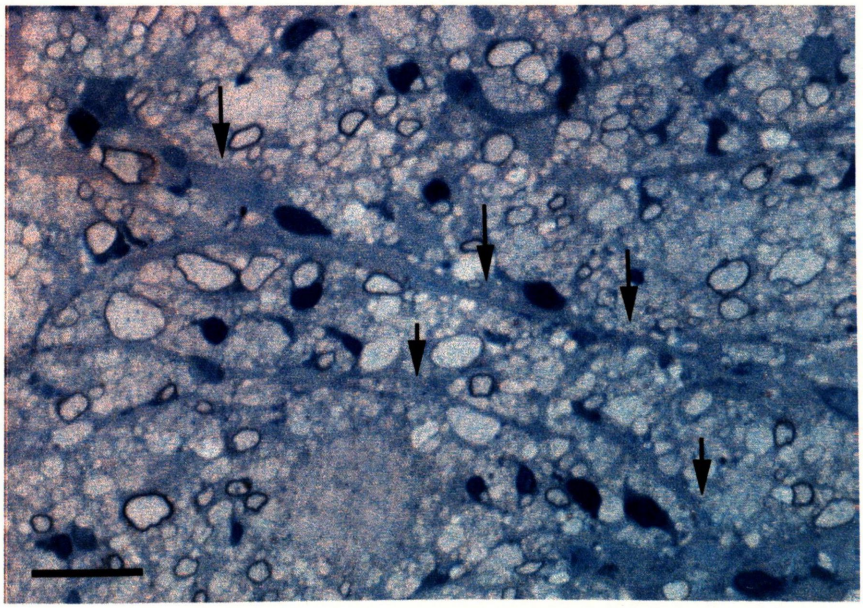


Figure 8.8. Toludine blue stained section of the bridge 54 days following injury. Note the long processes of undetermined origin in the bridge (arrows) that produce the 'mosaic' patterning found in the cord. Scale bar = 20 microns.

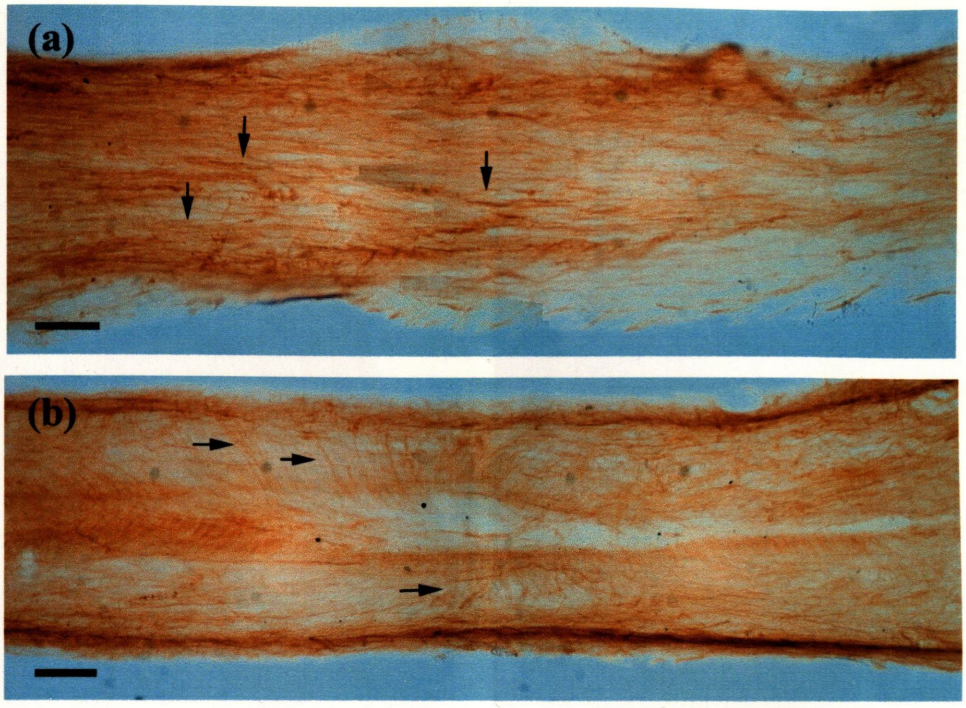


Figure 8.9a, b. Saggital sections of GFAP+ve profiles in the bridge 70 days following injury. In (a) close to the periphery, long immunopositive proflies are present (arrows). In (b) close to the central canal note the radial processes of tanycytes (arrows) and the sparse distribution of elongate profiles entering the bridge. Scale bar = 200 microns.



Figure 8.10a, b. Day 175. In (a) note the continual presence of the elongate profiles at the periphery (arrows). In (b) the increase in the number of tanycytic processses radiating from the central canal displace the radial astrocytic profiles. Scale bar = 200 microns.

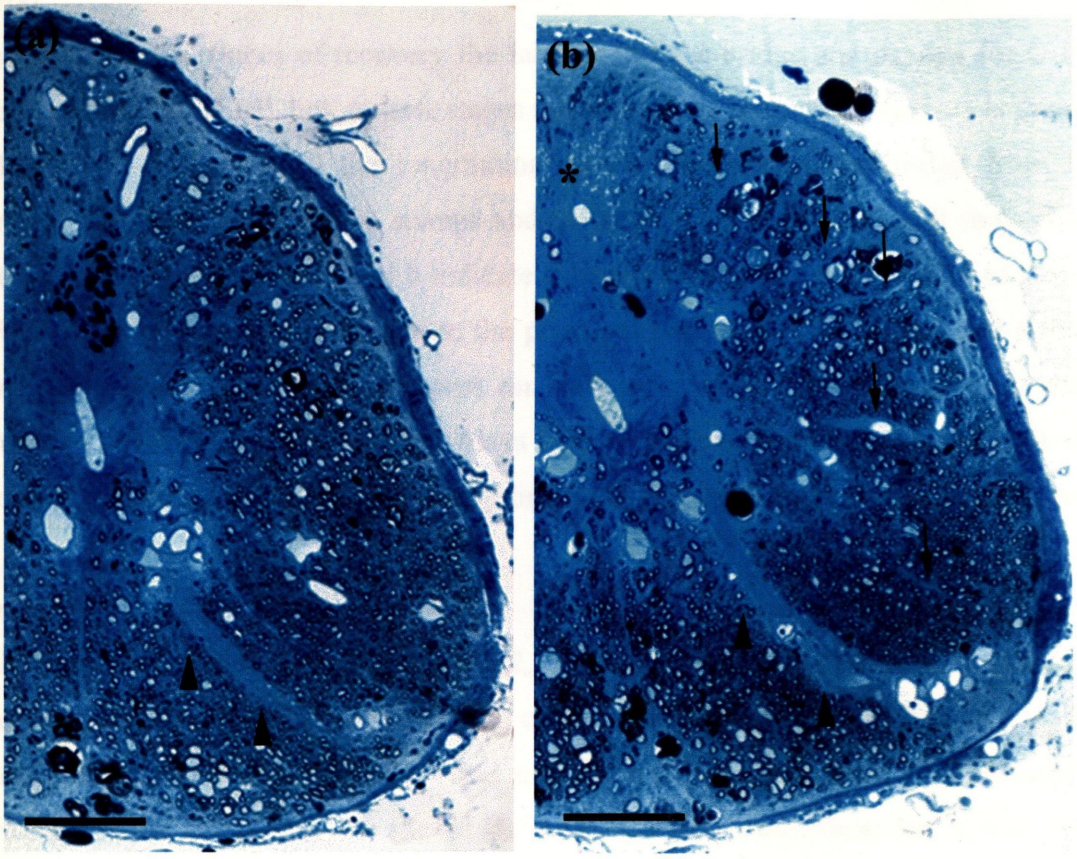


Figure 8.11a, b. Day 200. Toludine blue stained sections of the spinal stumps. In (a) corresponding to approximetely 0.95 mm from the centre of the bridge note the ventrolateral tracts (arrowheads) which are displaced from their normal position and the absence of many of the smaller radiating tracts. In (b) which is approximately 1.32 mm from the bridge centre note that the glial organisation is still disrupted particularly dorsally (*), but many radial processes are now present (arrows). Scale bar = 100 microns.

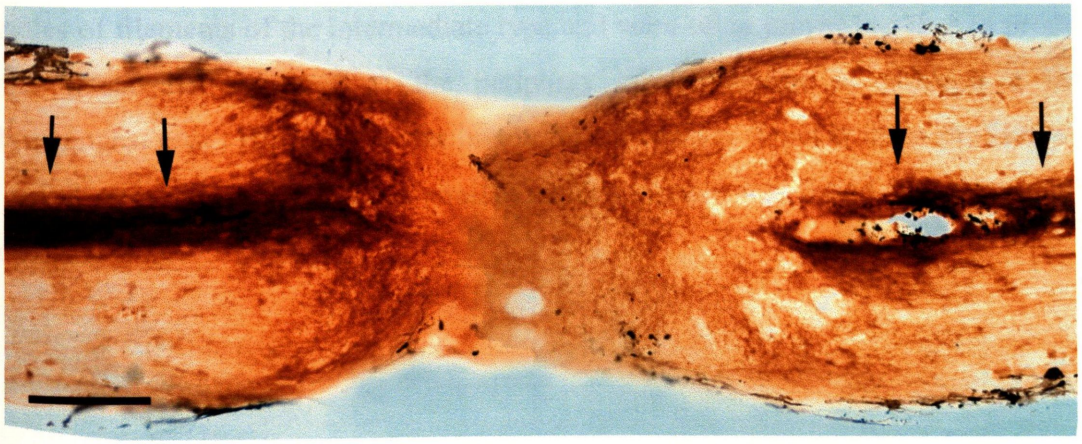


Figure 8.12. S-100 labelling in the rostral spinal stump 6 days following injury. Note the intense labelling in the spinal stumps, particularly those regions surrounding the central canal (arrows). Scale bar = 200 microns.

S-100

During the initial stages of recovery the labelling of the bridge and stumps for S-100 mirrored that for GFAP, but, at later stages staining of the astrocytic structure is greatly reduced and fails to label the longitudinal processes entering the bridge from the stumps. Labelling of the spinal stumps and the gap produced by the insult (now filled with a blood clot) by days 6 and 8 indicate a labelling regime that is similar to that of GFAP. At these short survival times, the proximal portions of the stumps and a thick band corresponding to the glial horns on both sides of the canal (Fig. 8.12) stain intensely. At later stages of recovery (days 14-20), however, labelling for this antibody decreases in the stumps and bridge, being limited to the ependyma and radial tanycytes.

Vimentin

Labelling for all days examined (8, 10, 12, and 26) with antisera to vimentin failed to stain astrocytic profiles in the stumps or the bridge (typified in Fig. 8.13) that correspond to radial astrocytic soma and associated cellular processes. The ependyma however, in the bridge and the stumps did label intensely, indicating that it was not a failure of the antiserum to recognise the protein in the regenerating tissue.

Electron microscopy

The electron micrographs showed that the bridge consisted of numerous processes that interweaved between the axonal profiles (Fig. 8.14) which in some instances, appeared to isolate the axons into discrete fasicles. Many of these processes contained numerous bundles of filaments of the intermediate type and were often joined together to produce larger tracts that extended to the periphery of the bridge to produce a large submeningeal area. However, it was impossible to confirm whether these profiles were of radial astrocytic origin since a similar staining pattern was found for the tanycytic processes.

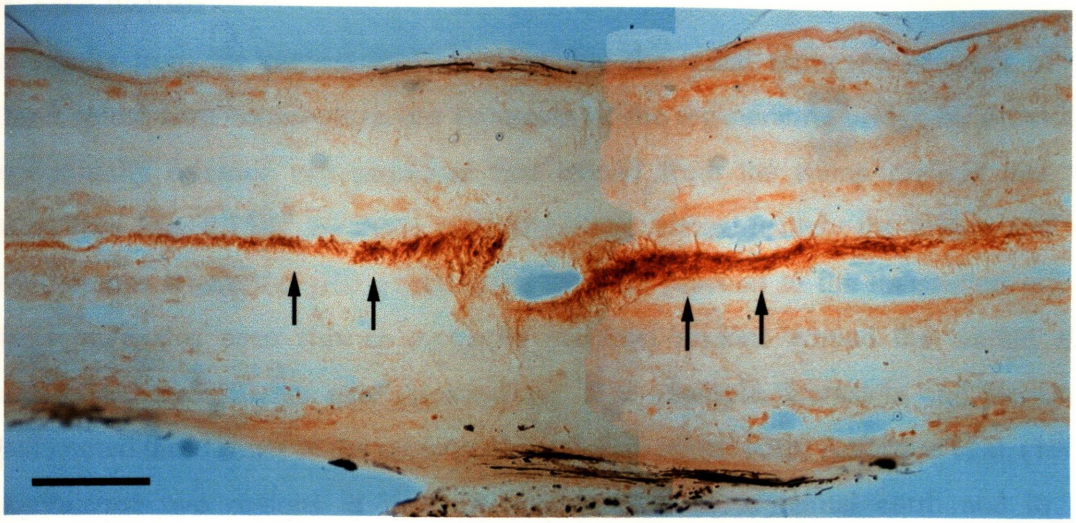


Figure 8.13. Vimentin labelling of the bridge 12 days fllowing injury. note the labelling that is specific to the epemdymal layers (arrows) with no other profiles outside this region being labelled. Scale bar = 200 microns.

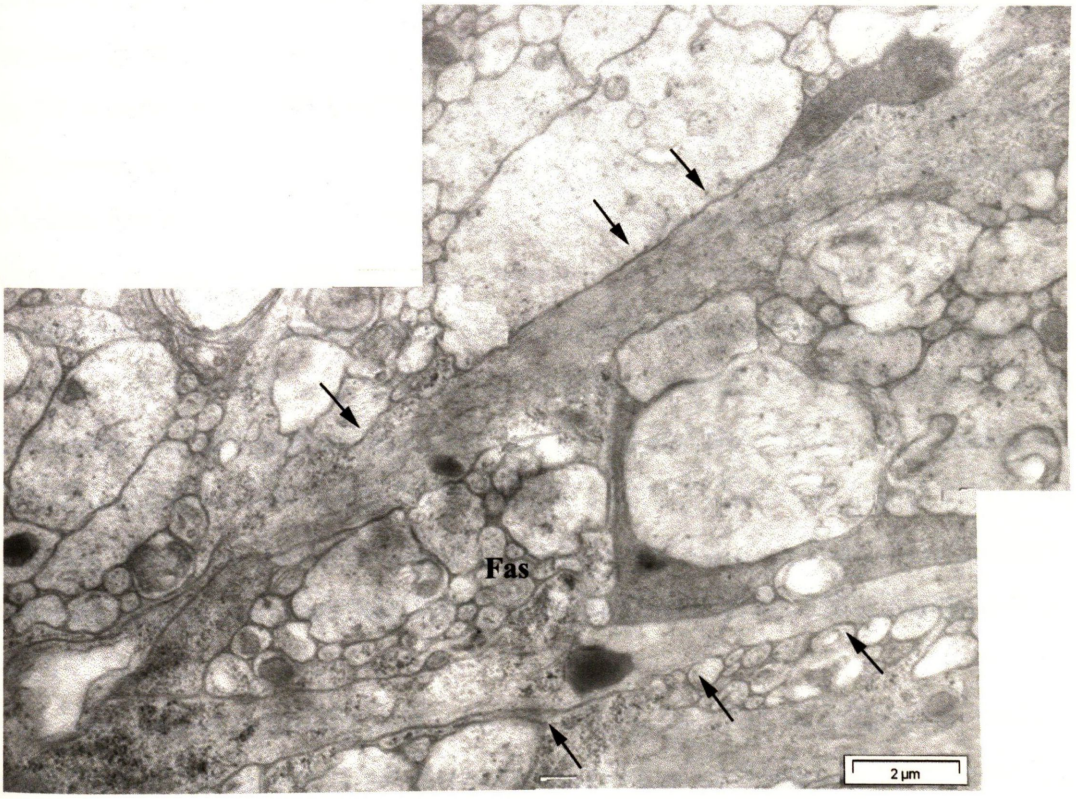


Figure 8.14. Electron micrograph of small glial tracts (arrows) in the spinal cord 54 days following injury. Note how both processes divide the surrounding axons into a small fasicle (Fas).

8.4 Discussion

The results from the present study suggest that the radial astrocytic network of the normal spinal cord contribute to the formation of the regenerating bridge by providing longitudinally oriented cell processes that extend from the stump regions into the wound (see Fig. 8.15). We have recognised two zones, namely the bridge and the spinal stumps where the glial organisation alters in reaction to the transection injury. Others have also been able to recognise different regions around the wound site, characterised by different glial organisation. For example, Bernstein and Bernstein (1967) noted three zones in the regenerating goldfish spinal cord; Anderson et al. (1984) distinguished two regions in the regenerating *Sternachus* spinal cord; and in the regenerating goldfish spinal cord, Bignami et al., (1974) separated the scar from a region of gliosis in both stumps.

The astrocytic contribution to the bridge

The macroglial contribution to the regeneration of anamniote CNS has previously been described in terms of ependymal (e.g. Simpson and Duffy, 1994) and ependymal-glial (e.g. Blaugrund et al., 1993) infiltration of the lesion site. In the amphibian and reptilian tail regenerates, the ependyma surrounding the enlarged central canal forms spaces in the lesion site before axons regrow, but in fish, ependymocytes and axons colonise the lesion site at approximately the same time (Anderson and Waxman, 1983a). In the present study, it was found that with time, the astrocytic structure becomes prominent in the bridge and forms what we have termed a 'mosaic' pattern. Such astrocytic inclusion in the lesion site, although noted for the lamprey (Wood and Cohen, 1981) and goldfish (Bernstein and Bernstein, 1967; 1969), has been most studied in the optic nerve, where regrowing axons in particular regions close to the regenerating nerve stumps are enveloped by glial processes (e.g. Reier, 1979; Blaugrund et al., 1993; Rungger-Brandle et al., 1995).

The mosaic patterning was found by day 20 and was considered to reflect the organisation of the mainly radial astrocytic profiles in the bridge as found with GFAP labelling. While this organisation remained prominent in the bridge at later stages, it also began to reorganise, from a random feltwork of processes, with some random orientations to principally longitudinally aligned pathways. A similar graded

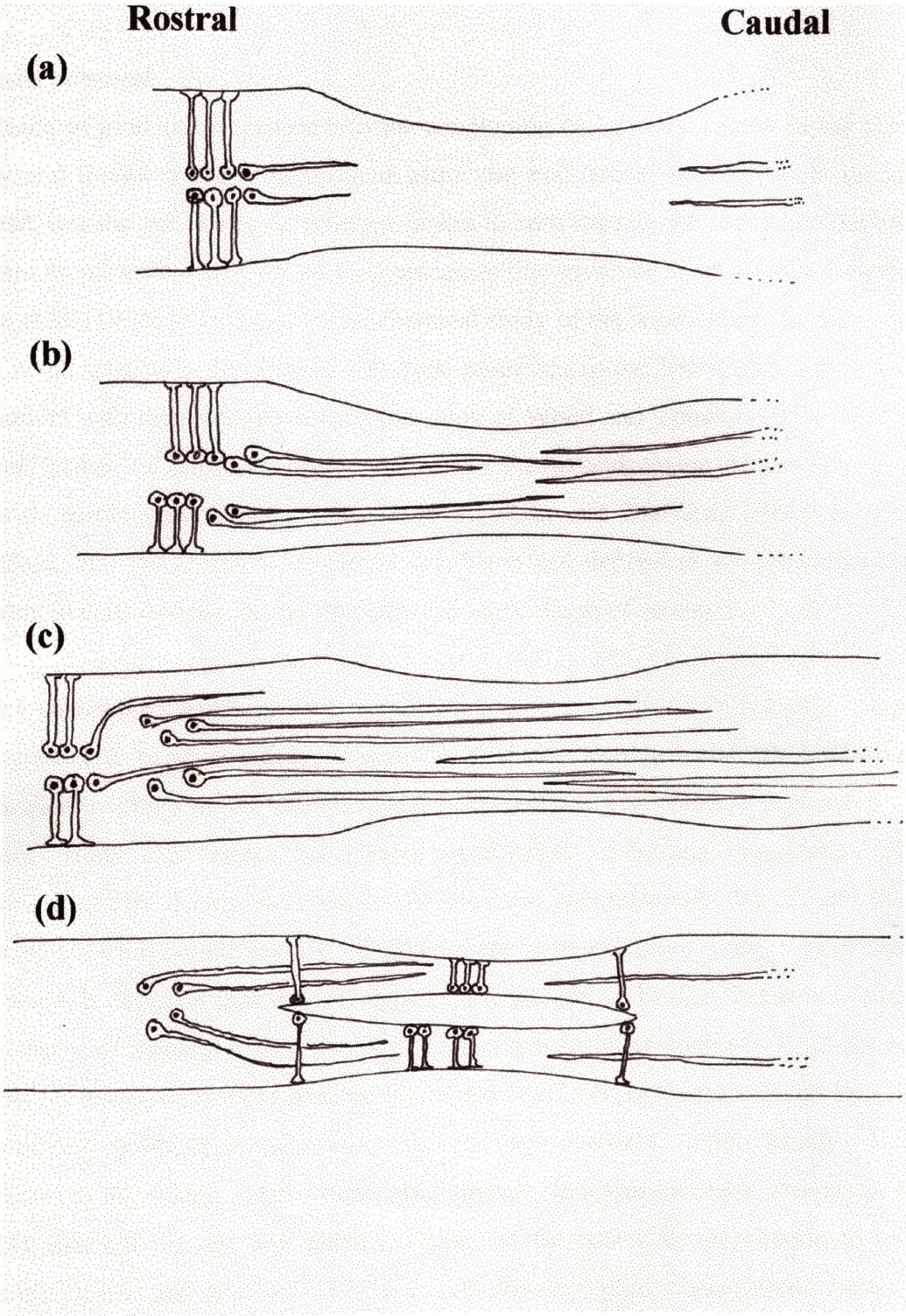


Figure 8.15. Diagrammatic representation of the radial astrocytic reaction following injury at days 8 (a), 16 (b), 26 (c) and 70 (d). Note the redirection of the astrocytic processes into the bridge. By day 70, radial astrocytic processes are superseded by tanycytes as the major glial component of the bridge.

organisation of astrocytes has been noted in the regenerating optic nerve (e.g. Bohn et al., 1982).

Do cells migrate?

Evidence of glial cell migration into the developing bridge was lacking in the present study and therefore the infiltration of astrocytic cell bodies probably fails to occur. Instead, it is the cell processes from astrocytes in both stumps that move into the bridge to form an intricate meshwork of glial processes that give rise to the mosaic patterning. Lurie et al. (1994) in an immunohistochemical study of the regenerating lamprey spinal cord noted longitudinally aligned astrocytic processes in the lesion site, and this is in agreement with the electron microscopic study of Wood and Cohen (1981). Similarly, no cell bodies of astrocytes were observed in the wound region of the regenerating goldfish spinal cord (Bignami et al., 1974; Nona and Stafford, 1995). It appears therefore, that the regrowth of axonal profiles is not dependent on the migration of macroglial cells into the lesion site during the early stages of recovery.

Which comes first; axons or astrocytes?

The question as to which cell type makes the 'first step' into the lesion site has intrigued researchers working on the various model systems where regeneration is possible. The present study illustrates that radial astrocytes, according to their GFAP immunoreactivity do not enter the lesion site until approximately day 12 and do not colonise the bridge until day 16. Since a bridge of regenerating material is present at this stage, it suggests that this cell type is not integral to bridge formation. Similar 'late' entry of astrocytic processes has been noted in other studies. Bignami et al. (1974) for example, did not observe the regrowth of astrocytes into the bridge of the regenerating goldfish spinal cord, although they observed longitudinally oriented processes in the bridge at later stages of recovery. In a similar study, Anderson et al. (1984) also did not see any initial reactions of the astrocytic population to injury. Recently Nona and Stafford (1995) found that the glial complement trailed the regrowing axonal profiles into the lesion site and Stensaas (1983) suggested that astrocytic processes lagged the regrowth of axons into the regenerating goldfish spinal cord.

The origin of pathways

From the combined light microscopical results of GFAP and toludine blue stained semithin sections we propose that an alteration of the radial astrocytic structure in the rostral and caudal stumps gives rise to the glial organisation in the bridge through the extension of long cytoplasmic processes into the bridge. Lurie and co-workers (1994) also documented the alteration of the radial glial structure into longitudinal profiles that extended into the lesion site in the regenerating lamprey cord.

The use of 50μm thick Vibratome sections in the present study allowed several astrocytic profiles to be mapped from the stumps into the bridge. With this said, it must be clarified that although immunopositive profiles could be traced in the stumps and bridge, the points of origin, namely the cell body, did not label. This in itself is not surprising as it is well known that glial fibrillary acidic protein frequently fails to label the cell soma (see chapter 5, Lindsay, 1986; Malhotra et al., 1990).

As longitudinal processes enter the bridge from the stumps, the radial organisation in more distal portions of the stumps begins to change orientation. Over extended survival times more and more radial profiles acquire a longitudinal orientation that is well characterised by day 26 (see Fig 8.7). The mechanism responsible for this changed orientation of the radial astrocytes in the stumps is unknown at the present time.

In mammals the astrocytic reaction is typified by activation of (a) astrocytes close to the wound region, termed proximal isomorphic astrocytes and (b) astrocytes in regions more distal to the lesion site, termed distal anisomorphic astrocytes, that are affected indirectly by the injury (e.g. Malhotra et al., 1993; Chauvet et al., 1997). But in comparison to mammals where both the proximal (close to or at the lesion site) and distal (some distance from the lesion site) reactions occur approximately at the same time, in the eel the alteration in structure in the spinal stumps is represented by a slow continuous retrograde alteration of the radial structure beginning in those regions close to the cut surface and then moving further into the stump. The loss of the glial horns and the radial processes in favour of an ependymal-derived radial tanycytic structure surrounding the enlarged central canal at extended recovery times typify this reaction. Therefore, the morphological changes in astrocytic structure occur not only following the initial insult, but also over extended periods. The upregulation of GFAP is a

characteristic feature of reactive astrocytes in mammals, but the intense labelling to this intermediate filament occurred in both normal and regenerating eel cord.

Hyperplasia of radial astrocytes in the regenerating cord?

Hyperplasia is a well-documented characteristic of reactive astrocytes in the mammalian CNS and the proliferating cells contribute to the resulting glial scar. In the anamniote regenerate, ependymal proliferation is well characterised and documented in the literature (Anderson and Waxman, 1983a; Simpson and Duffy, 1994). However, the proliferative ability of the radial astrocyte population, has not been well characterised following injury to the spinal cord. In the present study, it was found using the three markers to the common intermediate filament proteins, GFAP, vimentin and S-100, that there does not appear to be a significant hyperplasic event (if at all) in the bridge and spinal stumps. Although the glial fibrillary acidic protein is well characterised in astrocytes of all classes of vertebrate, it is well known that this protein is more commonly found in cytoplasmic processes and frequently fails to highlight the cell soma (the present study, chapter 5, Privat and Rataboul, 1986; Reier, 1986) and therefore is not a good marker for highlighting the cell body. The markers to the vimentin and S-100 proteins which are known to be upregulated in cells following injury can be localised to the cytoplasm of the cell body (Malhotra et al., 1990; Ridet et al., 1997). The labelling pattern for both markers in the present study failed to highlight somal structures in the bridge and the stump regions. The S-100 protein which labels the ependymal layers surrounding the central canal and glial horns (corresponding to the cell soma of radial astrocytes) in the normal cord failed to label structures that could be interpreted as cell bodies and although intense staining of the glial organisation of the spinal stumps occurred during the early stages of recovery, at later stages labelling for this protein decreased to such a level that only a weak labelling product could be detected in the ependymal layers surrounding the enlarged central canal. The labelling regime for vimentin followed a similar pattern, with no labelling of profiles in the stumps and the intense staining was isolated to the ependymal layers surrounding the enlarged central canal in the bridge. No cellular structures could be identified outside this intensely labelling region in the stumps or bridge. Although the labelling characteristics of the S-100 protein is capricious, particularly in mammals and can label other cell types such as oligodendroglia (Cocchia, 1981), the labelling pattern for vimentin protein in both mature and immature astrocytes is well characterised. Transient increased levels of this protein in mammalian astrocytes with a corresponding

low level of GFAP expression is characteristic of developing and immature cells (Pixley and de Vellis, 1984; Oudega and Marani, 1991; Elmquist et al., 1994) and reactive astrocytes in the lesion CNS. Takamiya et al. (1988) used a combined ^{3}H-thymidine, GFAP and vimentin study found that all three markers were expressed in reactive astrocytes, suggesting that the transient expression of vimentin is localised to, and only occurs in, astrocytes that proliferate in response to injury. Schiffer et al. (1986) noted an approximate 10% of proximal and distal astrocytes expressed vimentin suggesting that only a subset of cells proliferate in response to the injury, whether these cells are mature astrocytes that possess the ability to dedifferentiate (Malhotra and Shnitka, 1994), or are glial precursor cells similar to those found in the lateral ventricle of the rodent brain (Doetsch et al., 1997; Peretto et al., 1997) or even from undifferentiated stem cells that are known to be present in the rodent CNS (see Gage et al., 1995; Weiss et al., 1996b for reviews) remains to be verified. It is interesting to note that vimentin labelling is not detected following discrete axotomy induced injuries (Tetzlaff et al., 1988; Miyake et al., 1988) where it is known that astrocytes fail to proliferate (Davies et al., 1996) following the injury. Migrating reticular astrocytes in the regenerating optic nerve of the goldfish (Blaugrund et al., 1993) and the newt *Triturus* (Rungger-Brandle et al., 1995) also label intensely for this protein with a corresponding absence of GFAP labelling in the lesion site (Stafford et al., 1990; Nona et al., 1992). The upregulation of vimentin expression in the regenerating vertebrate CNS therefore is one possible indicator of proliferating cells. The consistent absence of vimentin labelling in the bridge and stumps of structures that could be interpreted as cell bodies, and the intense labelling for ependymal cells which are known to be proliferative and are migratory (see chapter 7, Benraiss et al., 1997), suggests that radial astrocytes may not proliferate following injury. Furthermore, these cells presumably fail to migrate from the stumps into the bridge. BrdU-labelling of nuclei as seen in chapter 5, showed that the majority of labelled profiles were confined to the lumen of the enlarged central canal, thus providing further evidence to our theory that this cell type fails to proliferate. Evidence form the literature further substantiates this hypothesis. For example, Giulian et al. (1985) in a study of optic tract glia following transection in the goldfish noted that the number of astroglial cells remained stable following injury and suggested that the outgrowth of astrocytic processes rather than the proliferation and migration of cells support regrowing axons. A similar finding was noted in the regenerating lamprey spinal cord from studies using ^{3}H-thymidine (Lurie et

al., 1994) and it was proposed that the astrocytic population fail to proliferate following transection.

It is prudent to acknowledge the fact that it is possible that astrocytes following injury do not utilise the vimentin or S-100 intermediate filament proteins as part of the cytoskeleton during the regenerative event. Since relatively little is known of this cell type both *in vivo* and *in vitro,* it is difficult to determine if the astrocytes express a different panel of intermediate proteins during the regenerative event. Cytokeratins, and in particular CK-8, CK-18 and CK-19 (Rungger-Brandle et al., 1995) are known to be preferentially upregulated in reticular astrocytes in the lesion site of the newt optic nerve following crush (Rungger-Brandle et al., 1995) while GFAP labelling is isolated to the stump regions of the nerve during regrowth (Stafford et al., 1990) and only at extended survival times are GFAP+ve fibres present in the bridge (e.g. Cohen et al., 1993).

Gliosis in the regenerating cord?

The literature concerning the activation of astrocytes to become reactive and undergo changes to form a glial scar at, or close to, the site of injury is somewhat perplexing. In the last five years the criteria used to classify the reactive astrocyte has undergone some change and this cell type is now considered to be 'reactive' and induce a gliosis, by the hypertrophy of the cell body and cellular processes, the upregulation of some intermediate proteins such as GFAP and 6.17 (Ridet et al., 1996), M-22 (Chauvet et al., 1997) and J1-31 (Malhotra et al., 1993) and of other factors such as cytokines, growth factors and recognition molecules (Ridet et al., 1997) while hyperplasia, once a criterion for gliosis, now appears not to be essential. Furthermore, the type and extent of the gliosis, that is dependent on the nature of the injury such as (e.g. contusion, crush or laceration) and the microenvironment of the CNS region that is injured and position in relation to the lesion site (Malhotra and Shnitka, 1994; Ridet et al., 1997). Indeed the astrocytic response to injury also appears to differ depending on the region of the CNS affected. For example, Alonso and Privat (1993) observed differences in the astrocytic response in the hypothalamus and forebrain following two types of surgical incision. The result is a heterogeneity of astrocytic activation that gives rise to a graded gliosis. Traumatic lesions such as transection and crush to X-ray irradiation and effects of neurotoxants (e.g. MPTP) and inflammatory demyelinating disorders (e.g. multiple sclerosis) frequently induce a strong astrocytic reaction that gives rise to often extensive

gliosis resulting in the formation of the astroglial scar tissue (Malhotra and Shnitka, 1994). In contrast, however, small discrete lesions in the CNS, such as axotomy of white matter tracts (e.g. Davies et al., 1996) fail to induce a typical astrocytic reaction, however axons still fail to cross the lesion site. Therefore, proliferation of astrocytes is not a necessary event for gliosis to develop and this reaction can be described in terms of the other criteria. In this light, the astrocytic reaction found in the present study can described as a gliotic event. Evidence to support such a hypothesis can be seen in the spinal stumps during the early stages of recovery. At the times studied (days 4-12) there is a progressive alteration of the GFAP+ve radial organisation to a longitudinal one, which is suggestive of hyperplasia. Furthermore, there is a marked increase in GFAP and S-100 labelling. In a similar vein the random orientation of immunopositive profiles and the dense aggregations in the proximal stumps during the initial stages (days 4-8) when profiles begin to make the transition from a radial to longitudinal orientation is suggestive of a gliosis in the stumps. In the bridge the patterning between days 14 and 26 of immunopositive fibres and the random orientation of the projecting fibres into the dorsal horns from the medial portions of the bridge suggest an aberrant organisation of astrocytic profiles. Thus, the reactions of the regenerating astrocytes initially are similar to the gliosis present in mammalian CNS, however it appears that this glial reorientation does not inhibit axonal regrowth. Instead, the GFAP+ve glial processes in the stumps and bridge either realign or regress, thus allowing an organised parallel array of profiles to develop. In a similar study of the regenerating spinal cord in goldfish, Bignami et al. (1974) noted the presence of a 'fibrous gliosis' in both stumps but not in the lesion site, however, in a later study (Nona and Stafford, 1995) a noticeable difference in labelling was not detected. In regenerating *Apternotous* spinal cord (Anderson et al., 1984), increased labelling for GFAP was noted in the transition zone between the undamaged cord and the lesion site. Immunohistochemical studies of the regenerating optic nerve suggest that a gliosis may also occur following crush injury (Levine, 1991) and is typified by an elevated GFAP expression and an increase in the number of astrocytic processes in the regenerating tissue. A gliotic event that results in the formation of an astrocytic scar can be induced in the goldfish spinal cord by the insertion of a Teflon block in the lesion site (Bernstein and Bernstein, 1967, 1969) which on removal impeded the regrowth of axons, resulting in their failure to traverse the lesion site. In order to induce the permanent glial scar the impeding block remained *in situ* for a considerable length of time (Bernstein and Bernstein, 1969). Taken

together, the results of the present study coupled with the few other studies of the glial reaction in the anamniote CNS suggest that the formation of a scar tissue by astrocytes is a difficult process, does not inhibit axonal growth and may even possess considerable regenerative powers.

Summary of main findings

- Following injury, GFAP labelling increased in the stumps close to the lesion site and remained elevated until approximately day 70. Thereafter labelling of profiles in the bridge and stumps became homogenous.
- S-100 labelling, apart from an initial increase in the spinal stumps, became negligible in both the stumps and the bridge for all times studied.
- Vimentin antisera did not label astrocytic structures and was confined to the ependymal layers surrounding the canal.
- Astrocytic processes begin to enter the bridge by day 12 but did not fully colonise it until approximately day 16.
- The astrocytic contribution to the bridge developed from cells within the spinal stumps, which reoriented their processes from radial to elongate that then projected into the bridge.
- While structures similar to the glial scar of mammals was found in the bridge in some cases, this reaction did not inhibit axonal growth.
- By day 26 the processes of radial astrocytes organise into parallel arrays longitudinally aligned along the rostro-caudal axis in the bridge.
- With time, the radial astrocytic contribution in the bridge is gradually displaced by the development of tanycytes that project their radial processes to the bridge periphery (see also chapter 5).

Chapter 9

Axon regrowth in the regenerating spinal cord

9.1 Introduction

It is well known that some components of the amniote nervous system, such as the peripheral nervous system (Bisby, 1995; Ide, 1996) and components of the olfactory nerve/system (Doucette, 1986; Munirathinam et al., 1997, Ramon-Cueto and Avila, 1998), are capable of encouraging and sustaining axonal regrowth following injury. However axons of the central nervous system (CNS), once injured, show a poor ability to regrow through the lesion site (Li and Raisman, 1997a; Fawcett and Asher, 1999). This inability to regrow can be attributed in part to the inhibitory environment that regenerating axons encounter; physically in the form of the fibroglial scar (Lindsay, 1986; Malhotra et al., 1990) and chemically by the presence of inhibitory molecules (Schwab, 1996). In contrast, injured axons of the anamniote CNS, such as in the optic nerve (e.g. Bohn et al., 1982; Beazley et al., 1997) and spinal cord (e.g. Sharma et al., 1993), have been shown to possess considerable regenerative capability even following different types of injury, such as crush (e.g. Stafford et al., 1990), amputation (Stensaas, 1968), ablation (Butler and Ward, 1965; Stensaas, 1983) and transection (Becker et al., 1997). Moreover, many of the axons that cross the lesion site are capable of reconnecting with their original targets and make functional synaptic contacts (McClellan, 1988; 1992). In the case of the lamprey it has been proposed that these reconnections allow for both functional and behavioural recovery (see Cohen et al., 1988).

The extent to which axons contribute to the formation of a bridge of regenerating material during the early stages of regrowth remains unclear. For example, following tail amputation in the newt *Triturus* (Egar and Singer, 1972; Singer et al., 1979) and the lizard *Anolis* (Simpson 1968), axons have been shown to trail behind a leading front of ependymal regrowth into the lesion site (Nordlander and Singer, 1978; Simpson, 1983), while evidence from other lesioning paradigms suggest that axons are among the first elements to form the bridge (Michel and Reier, 1979; Anderson and Waxman, 1983a). In exploring this question, we have determined the contribution made by regenerating axons to the formation of a new bridge. Furthermore, we have endeavoured to determine the time-scale for axonal regrowth through the bridge, the appearance of myelin-producing oligodendrocyte cells, and the onset of axon myelination in the bridge following injury.

Previous studies of axonal regrowth have utilised a variety of different investigative methods to determine axon regrowth, such as electron microscopy (e.g. Bohn et al., 1982; Michel and Reier, 1979), histochemistry (e.g. Bernstein and Bernstein, 1969), immunohistochemistry (e.g. Hall et al., 1997) and tracer analysis using horseradish peroxidase (HRP) (e.g. Wood and Cohen, 1981; Jacobs et al., 1997). However, many of these studies have employed qualitative analyses on select groups of axons. For example, anterograde tracer analysis with horseradish peroxidase (HRP), has been used to label selective groups of axons such as the Mauthner neuron, particularly in lamprey where this large neuron has been well documented (Lurie and Selzer, 1991; Lurie et al., 1994; Pijak et al., 1996). Retrograde studies have also employed HRP labelling (Bosch et al., 2000) as well as other markers (Becker et al., 1997) to label the nuclei of descending pathways from more rostral regions of the spinal cord and brain (Bosch, 1994; Becker et al., 1997). Relatively few studies have attempted to label axonal regrowth through the bridge *en masse*. One reason for this has been the lack of appropriate tracers that possess the ability label axons in large numbers. Recently it has been shown that a family of fluorescent carbocyanine tracers that include DiI and DiO, have the advantage of diffusing in an anterograde fashion over long distances through large numbers of axons in whole-mount fixed CNS tissue (Godement et al., 1987; Honig and Hume, 1989; Elberger and Honig, 1990; Von Bartheld et al., 1990). Use of these dyes has extensive and have been used to trace developing and adult neuronal tracts in amniote (e.g. Easter et al., 1993; Fritzsch and Nichols, 1993; Hilbig and Schierwagen, 1994) and anamniote (e.g. Wilson and Easter, 1991a; 1991b; Yoshida et al., 1995) CNS. In the present study, we have utilised DiI labelling to determine the extent of axonal recovery through the lesion site at set times following injury. In conjunction with this, we have also employed light and electron microscopy to determine axonal regrowth through the lesion site before the bridge has reconnected both stumps (days 6-8) and the developing bridge (days 10-200), at set times following injury.

9.2 Materials and Methods

Animals

This study is based on 20 eels, 9 prepared for light and electron microscopy, and 11 utilised for DiI tracing.

Histological Investigation

For histological investigation, each animal was treated according to the methodology described in the methods section in chapter 2. In brief, each animal was anaesthetised initially by immersion in 0.3mg/l MS-222 and further by a subcutaneous injection of 0.3ml alphaxalone (Saffan). To prevent blood clotting, 0.2 ml heparin sodium (Leo Laboratories) was also given subcutaneously. The perfusion procedure consisted of a primary flush of Ringer's solution (with 0.1% procaine for added anaesthesia) through the heart followed by the fixative, 2% paraformaldehyde and 1.25% gluteraldehyde in 0.1M phosphate buffer (PB), pH adjusted to 7.4. Two fixative solutions were used (a) 4% paraformaldehyde in 0.1M phosphate buffer (PB) pH adjusted to 7.4 for DiI tracing of axons and (b) 2% paraformaldehyde, 1.25% glutaraldehyde in 0.1M phosphate buffer (PB), pH adjusted to 7.4 for electron microscopy. Following perfusion, the spinal cord was immediately dissected from the spinal column and post-fixed in the same fixative for a maximum time of 3 hours at $4^{o}C$.

DiI tracing of axons

Labelling of axons was performed on perfusion fixed pieces of spinal cord (4% paraformaldehyde in 0.1M PB; see chapter 5 for more detail). In each case, approximately 40-50 mm of the cord, including the bridge, was dissected from the vertebral column as shown in figure 10.1a. Small crystals of DiI (1,1'–diotadecyl–3,3,3',3'-tetramethylindocarbocyanine perchlorate, Molecular Probes, Oregon) was applied to a small cut made in the rostral cord approximately 10 mm rostral to the bridge (Fig. 9.1b) and the dye allowed to diffuse through the cord.

In order to avoid leakage and external movement of the tracer along the cord surface, the whole length of the cord was sealed in 20% molten gelatin, which was then allowed to set. The sealed cords were then incubated in 4% paraformaldehyde in 0.1M PB at 35°C for up to 10 weeks to allow for diffusion of the tracer. Following incubation, all cords were sectioned in 0.1M PB at 50μm on a Vibratome (series 1000).

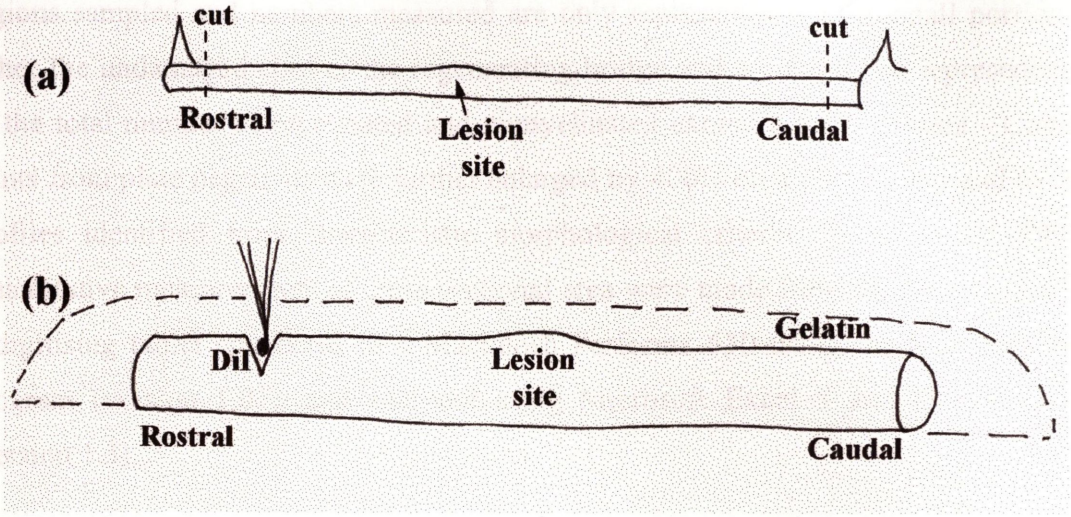


Figure 9.1. Dissection of the spinal cord from the vertebral column (a) and (b) the application of DiI crystals to a small incision in the rostral cord up to 10mm from the bridge.

Sections were mounted in Vectashield (Vector) and photographed immediately or stored in the dark at 4°C until used. Labelled axons were examined with a Nikon Optiphot 2 microscope with fluorescent attachment and using a rhodamine (556nm) filter set and photographed with a Polaroid DMC-1e digital camera. The resulting images were analysed with a Macintosh G3 computer using Adobe PhotoShop 5.

Electron Microscopy

The cord tissue was processed for electron microscopy according to the procedure described in chapter 2. Sections were cut for both light (1.5μm) and electron microscopy (500Å). All images were downloaded, analysed and formatted on a Macintosh G3 computer using Adobe PhotoShop 5. Qualitative and quantitative descriptions of regrowing axons were obtained for (a) the region at the cut surface of the rostral cord-lesion site border for days 6 and 8 and (b) the middle of the bridge, determined from reconstructions of the bridge from serial light microscopic sections, for days 8, 10, 20, 54, 144 and 200. For all cords, axonal profiles were surveyed from

random regions of the dorsal, lateral and ventral portions of the bridge in cross section and then photographed at varying magnifications from 6-40,000 for unmyelinated profiles and 1-10,000 for myelinated axons (see Fig. 9.2). It is worthy to note that the regions sampled and numbers measured are only representative of a small portion of either the undamaged cord or the regenerating bridge and are not a true representation of the total number of myelinated and unmyelinated axonal profiles present. Contact prints from plate negatives were further enlarged by 400% on a photocopier and axonal profiles identified from characteristic morphological criteria (Peters et al., 1991). Quantitative measurements of cross sectional area were made from the photocopies via a digitising tablet connected to a Macintosh Performa 630 using the MacStereology program (version 1.01), and analysed using Microsoft Excel 5 and Cricket Graph (version 1.3).

Analysis

In order to determine the rate and extent of myelination of axons in the bridge, we have utilised the G-ratio, first proposed by Rushton (1951), which has been shown to provide an accurate prediction of the optimal myelin thickness in the uninjured CNS (Waxman and Bennett, 1972). This value, which is the ratio of axon diameter to total diameter (axon and myelin sheath; see Fig. 9.3), is optimally 0.66 in the mammalian CNS. In the eel, the G-ratio was obtained for myelinated axons in the uninjured spinal cord, and for days 54, 144 and 200 following surgery.

Estimates of total axon number were obtained from randomly selected electron photomicrographs of the uninjured cord and the regenerating bridge for days 54, 144 and 200. For each time studied, an average axonal density per 1000μm^2 was calculated and a total axonal number estimated from the cross sectional area of neural material in the bridge.

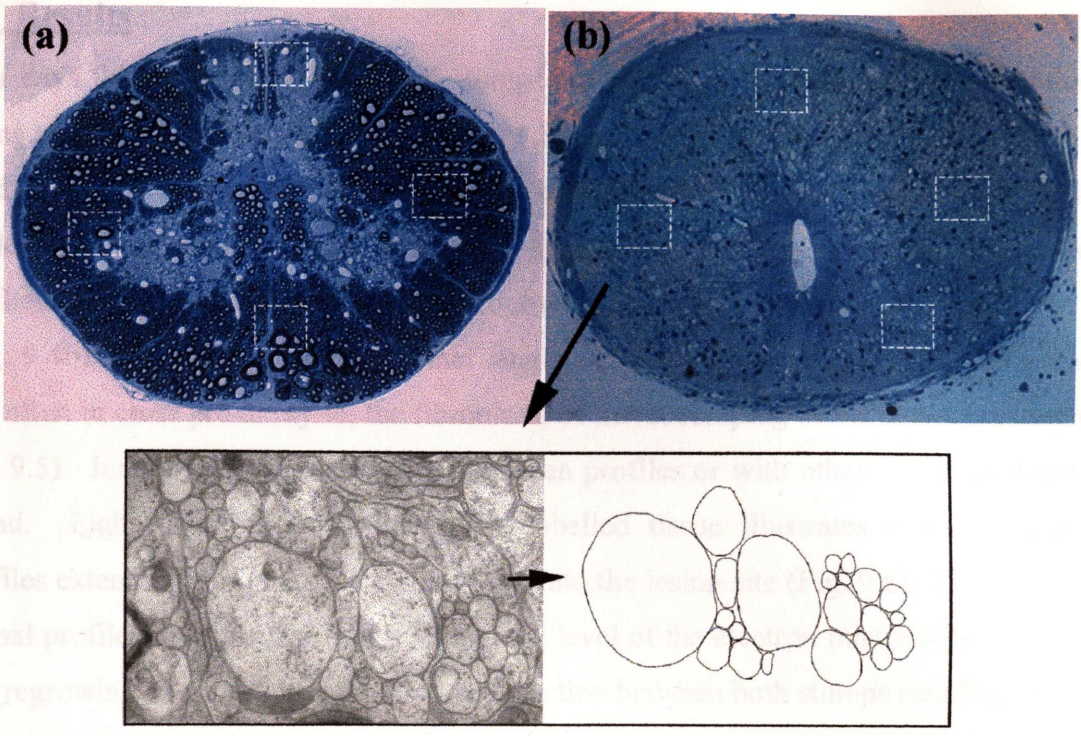


Figure 9.2a, b. Overview of the method used to measure myelinated and unmyelinated axons in (a) the uninjured spinal cord and (b) the regenerating bridge. The boxes denote that measurements were taken from all regions of the cord/bridge to account for the heterogeneity in axon size. The inset from (b) illustrates a typical group of axons encountered and the method of measurement using Macstereology.

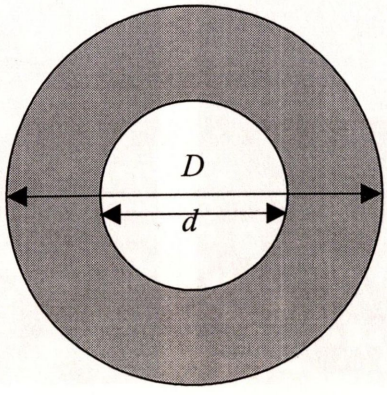


Figure 9.3. Determination of the G-ratio as proposed by Rushton (1951). This ratio is represented as the axon diameter (*d*) divided by the total fibre diameter (*D*).

9.3 Results

Four days following injury the spinal stumps are dominated by extensive degeneration of axons and myelin, extending up to at least 1.8 mm rostrally and 2mm caudally (Fig 9.4a); by day 6 it can be found up to 2.2mm into both stumps. Myelin debris was particularly evident in the ventral portions of the cord (Fig 9.4a). By day 6, unmyelinated axonal profiles are found in the more dorsal portions of the stumps extending into the lesion site (Fig. 9.4b), where they are found either singly or as small clusters, interspersed between and often in close proximity to, the fibroblasts of the developing blood clot/scar tissue (see Fig. 9.5). Junctional complexes, either between profiles or with other cell types, were not found. Eight days following injury, DiI-labelled tissue illustrates numerous labelled profiles extending from the rostral stump and into the lesion site (Fig. 9.6). The presence of axonal profiles in the bridge is also seen at the level of the electron microscope, suggesting that regrowing axons produce the first reconnection between both stumps (see Fig. 9.7).

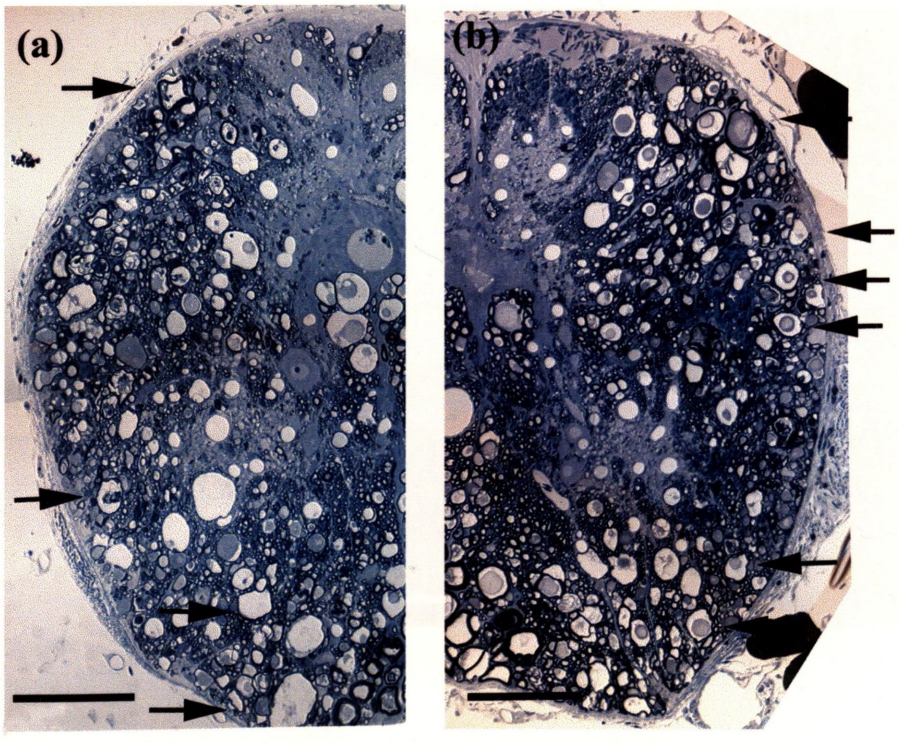


Fig. 9.4a, b. Degenerating axons and myelin sheath in the rostral stumps at days 4 (a) and 6 (b). Note the extensive degeneration in all aspects of the cord (arrows) at day 4 while by day 6 they are still present, particularly ventrally. Scale bar = 200 microns.

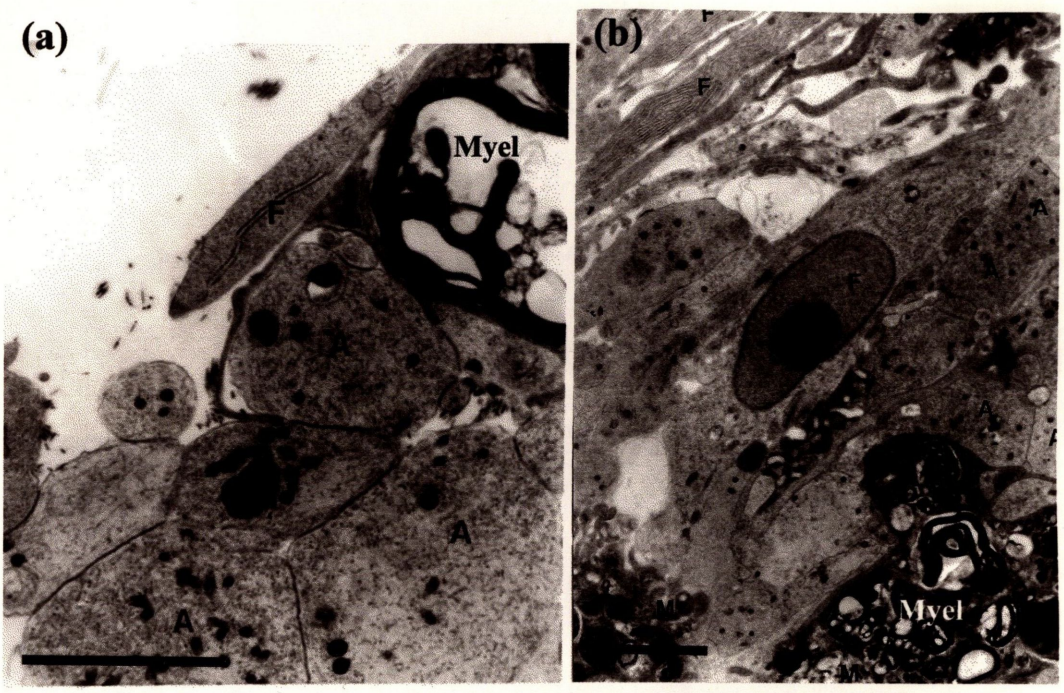


Figure 9.5a, b. Day 6. Electron micrographs of axonal profiles (A) interspersed between fibroblasts (F) and degenerating myelin (myel) at the transition zone between the degenerating stumps and the lesion site. M = Macrophages. Scale bar = 5 microns.

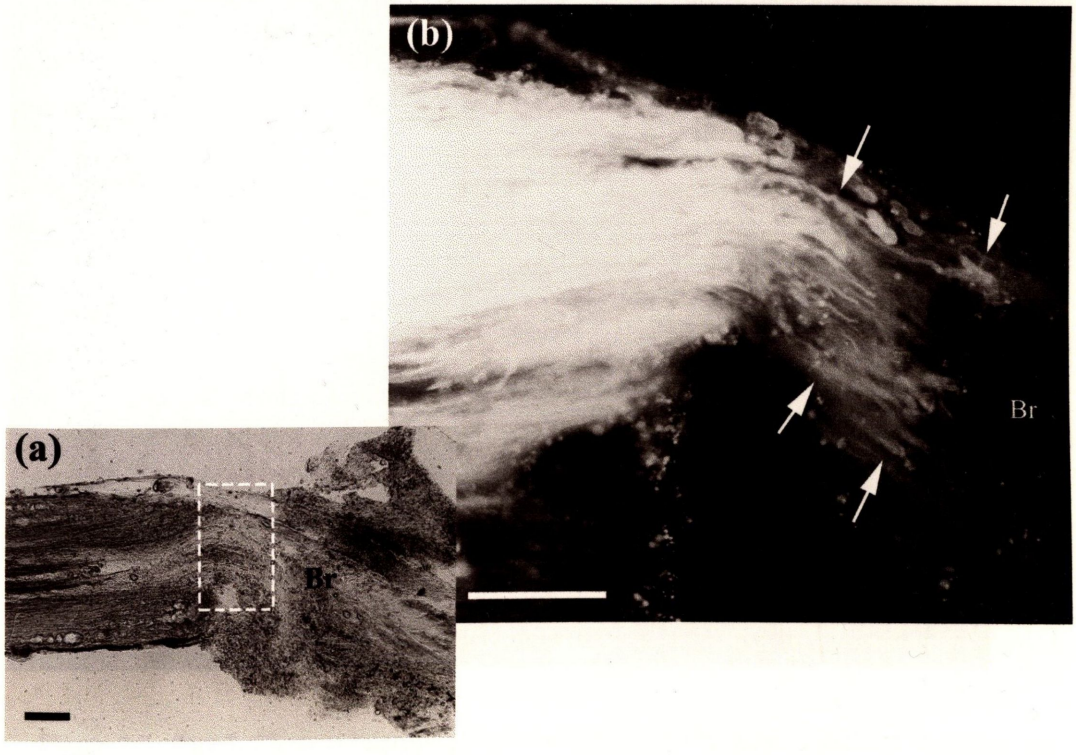


Figure 9.6a, b. Day 8. DiI labelling of axons (b, arrows) extending into the bridge. The extent of regrowth through the bridge can be seen in (a). Note that few growth cones are labelled in (b). Br = the developing bridge. Scale bar (a) = 200 microns, (b) = 50 microns.

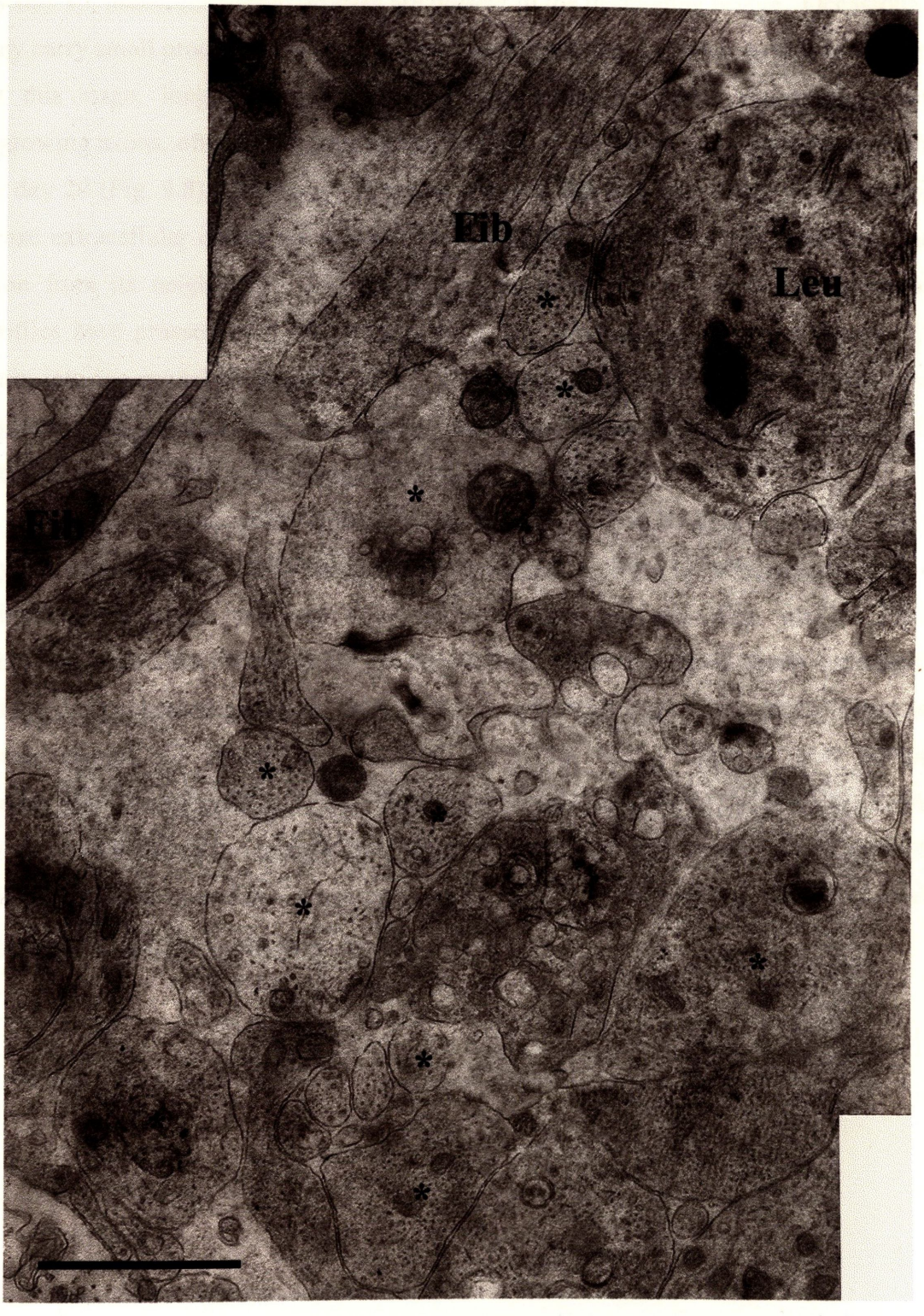


Figure 9.7. Day 8. Electron micrograph of axonal profiles (*) in the middle of the lesion site. Note their abundance and some of the different components of the blood clot such as fibroblasts = Fib, Leucocytes = Leu. Scale bar = 10 microns.

By day 10, numerous axonal profiles are present in the developing bridge. Occasionally they carry small projections that range from small bud-type swellings to thin extensions. At this stage, long thin cytoplasmic processes can be found surrounding some regrowing axons, often producing distinct bundles of profiles that are most recognisable by day 20 (Fig. 9.8). Noticeable between axons at this and later stages, is an electron dense extracellular matrix surrounding the unmyelinated axons, that demarcates each axon from its neighbours. DiI-labelling of axons at day 29 shows that numerous profiles have crossed the bridge at this stage and extended up to approximately 0.7-1mm into the caudal stumps (Fig. 9.9). These regrowing axons, however, extend into regions of the stump that still contain numerous degenerating axonal and myelin profiles, most notably in the large ventral tracts (see Fig. 9.10).

At later stages, axons begin to be myelinated, such that by day 54 thin bands of myelin can be found surrounding axons, in groups or more usually, singly, with an oligodendrocyte-type cell body often in close proximity (see Fig. 9.11). Tracer labelling around this time (day 75) shows that many of the numerous axons crossing the bridge have extended up to 1-2 mm caudally into the cord (Fig. 9.12). Both rostral and caudal stumps still contain large amounts of myelin debris, which is more obvious further into the stumps (Fig. 9.13). Myelination continues to occur in the bridge so that by days 144 and 200 a greater proportion of axons are ensheathed (see Fig. 9.14), although even at these late stages degenerating myelin can be still found amongst newly myelinated axons in the stumps (see Fig. 9.15).

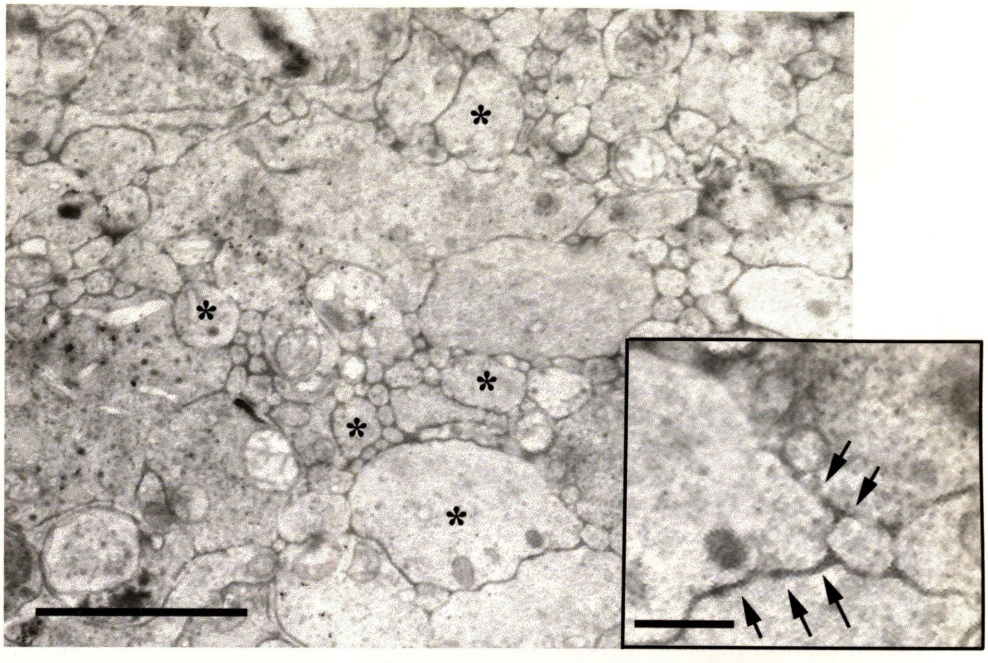


Figure 9.8. Day 20. Regrowing axons in the bridge (*) Note the presence of an electron dense extracellular matrix surrounding each axon (arrowheads; see inset). Noe the absence of oligodendrocytes and myelin at this stage. Scale bar = 5 microns, inset = 1 micron.

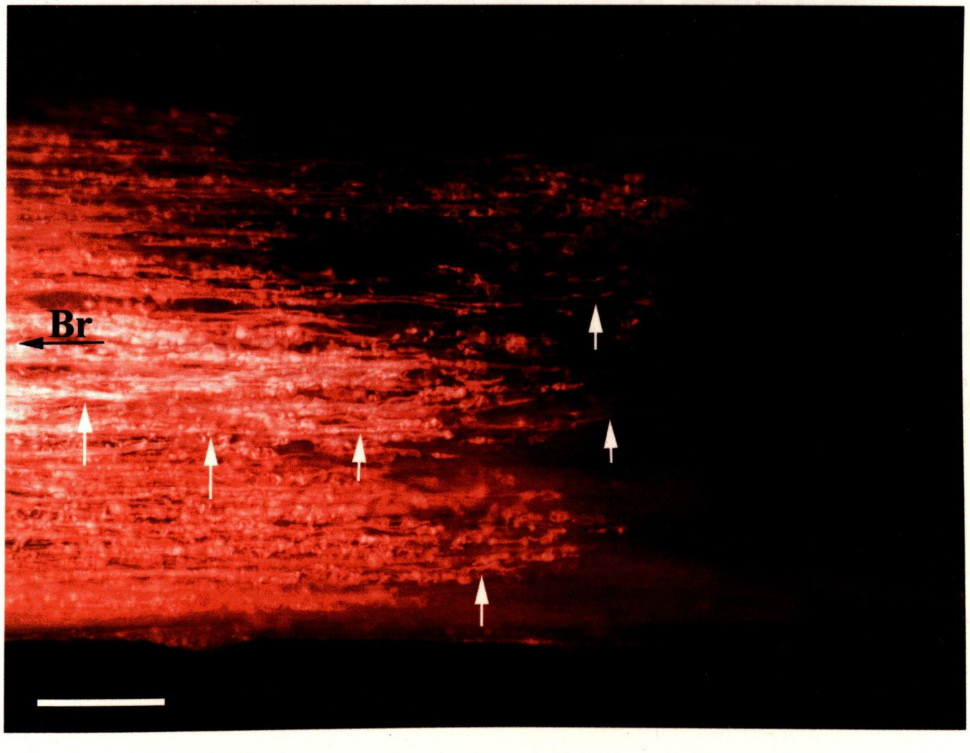


Figure 9.9. Day 29. DiI labelled axons (arrows) extending through the caudal cord. Note the straight parallel pathways taken by the labelled axons as they extend caudally into both the white and grey matter. Note the absence of erratic pathways. Br = denotes the position of the bridge. Scale bar = 200 microns.

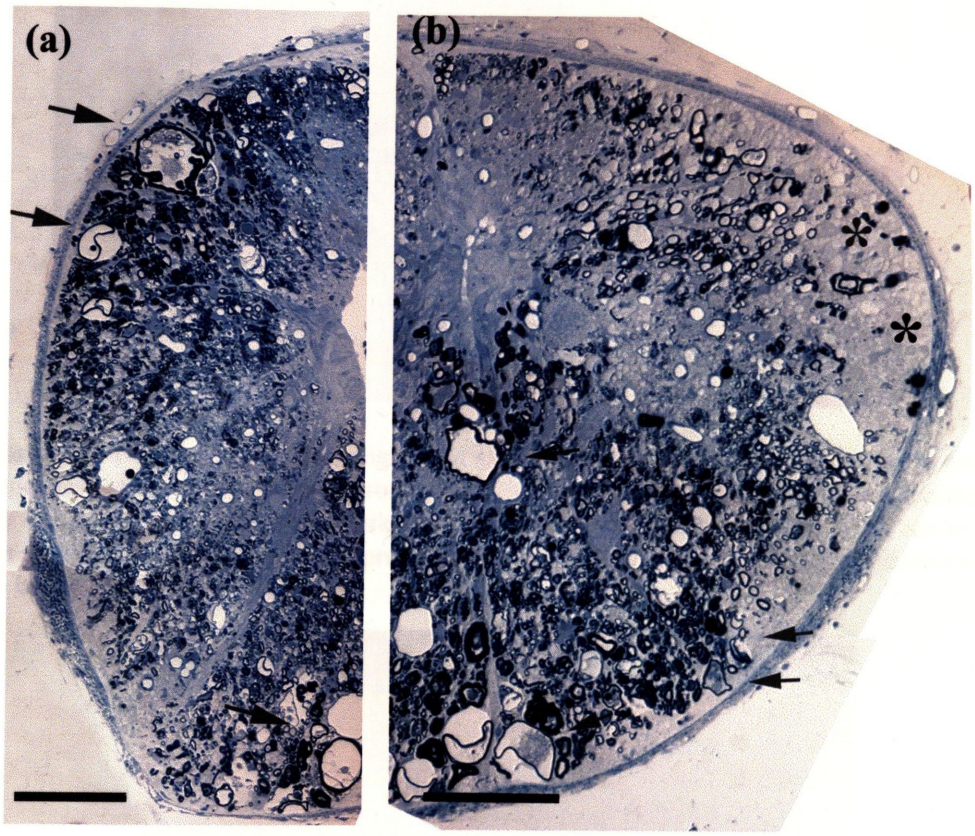


Figure 9.10. Degenerating myelin in the spinal stumps 20 days following injury. In (a) 0.85mm into the spinal cord from the bridge and (b) 1.8mm into the caudal cord note the extensive degeneration of myelinated axons (arrows) and regrowing regions in the caudal cord (*) that contain regenerating axons. Scale bar = 250 microns.

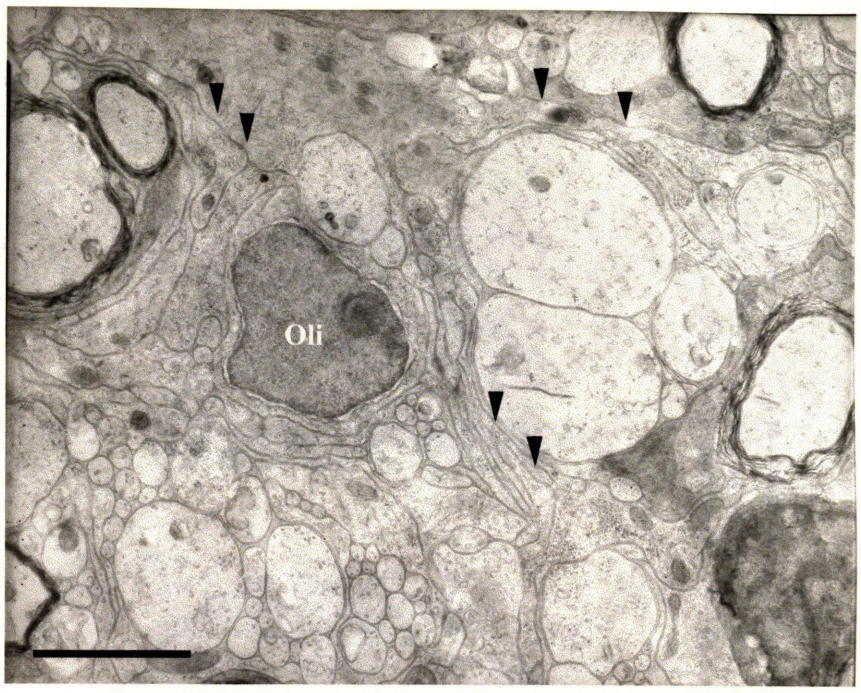


Figure 9.11. Day 54. Electron micrograph of axonal profiles in the bridge. Note the variation in thickness of the myelin sheath surrounding individual axons, with some profiles possessing very thin myelin. Electron dense perikarya, characteristic of oligodendrocytes (Oli), can be seen as well as the thin cytoplasmic processes (arrowheads) that continue to segregate axons into bundles. Scale bar = 3 microns.

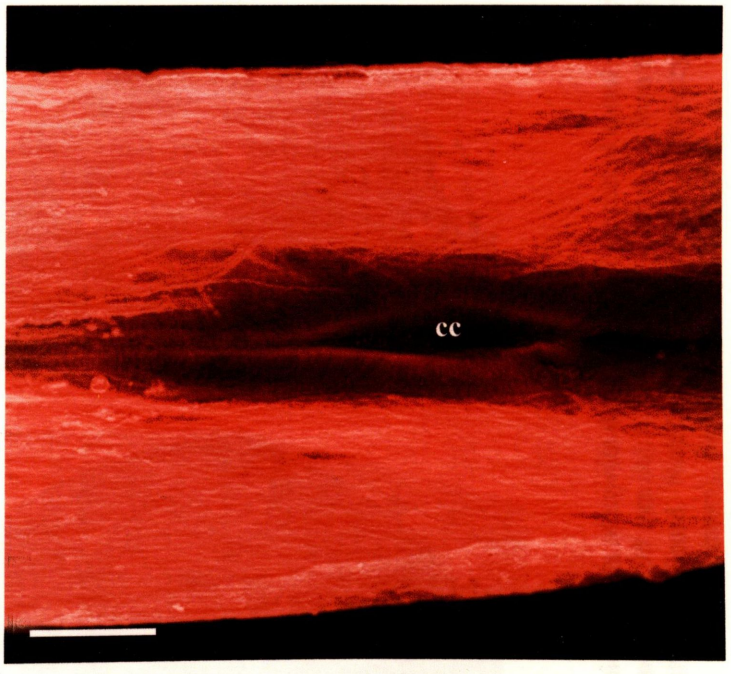


Figure 9.12. Day 77. DiI-labelled profiles traversing the bridge and extending into the caudal stump. Note the intense labelling of the bridge that indicate a large growth of axonal profiles through the bridge. Central canal = cc. Scale bar = 200 microns.

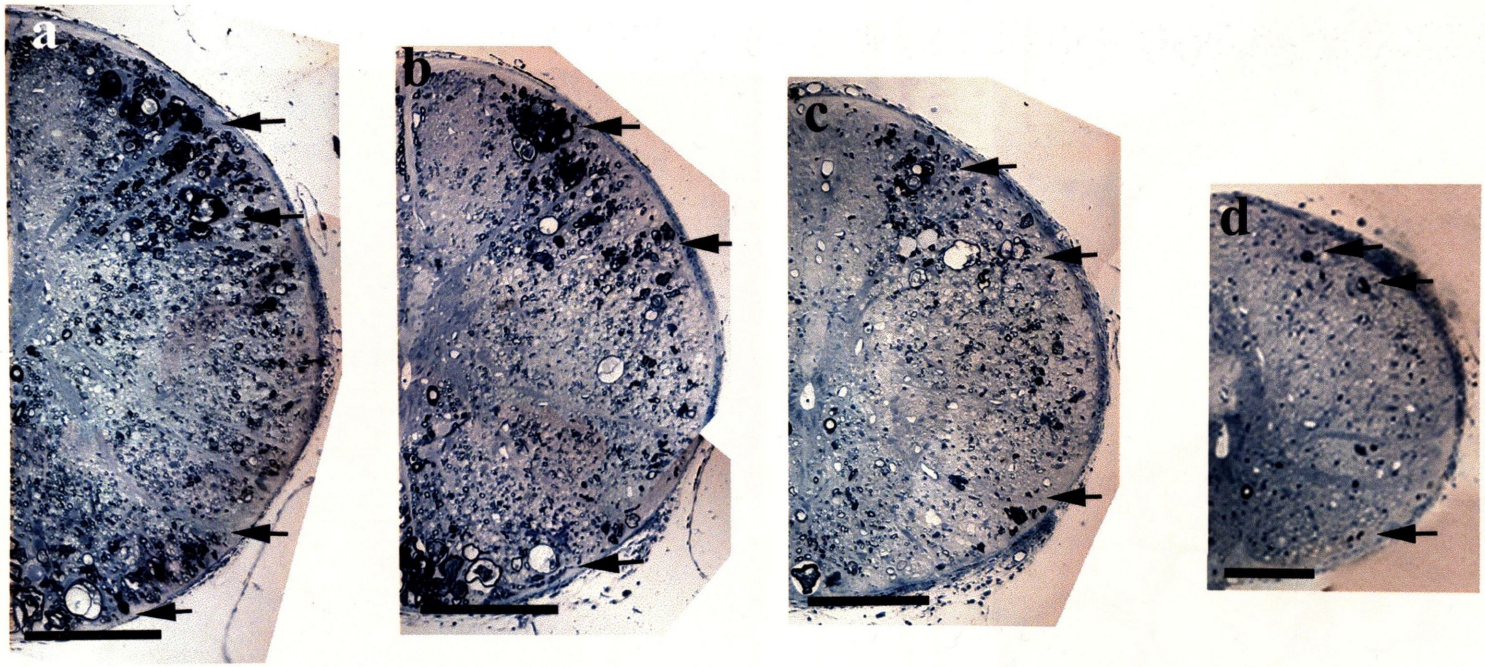


Figure 9.13. Photomicrographs of myelin degeneration in the rostral spinal stump 54 days following injury. Each photomicrograph represented corresponds to approximately 1.45 mm (a), 0.95 mm (b), 0.7 mm (c) and 0.4 mm (d) from the centre of the bridge. Although the rostral stump is represented here a similar situation is found in the caudal cord. Note that even at this stage of recovery when the spinal stumps contain large numbers of regrowing axons, myelin debris is prominent in many regions (arrows). Scale bar = 100 microns.

Quantitative analysis

During the early stages of recovery at days 6 and 8, and in the middle of the bridge at days 8, 10 and 20, large axonal profiles such as those seen in figure 9.7 are a prominent feature (see Fig. 9.16). We conclude that these profiles are most probably growth cones because of their relatively large sizes (Fig 9.17), with many having a cross sectional area greater than $5\mu m^2$. Electron microscopy however, did not illustrate any obvious intracellular differences between growth cones and axons. As can be seen from figure 9.17, there is a large variation in the size of these axonal profiles, particularly by day 8, both in the rostral cord entering the bridge, and in the middle of the bridge. Since these profiles appear in the bridge over a short period of time, namely between days 6 and 20, with the greatest influx centred around days 8 and 10, it appears that large numbers enter the bridge very quickly and are then followed by smaller numbers up to approximately day 54. By this time, relatively few large axonal-type profiles can be found in the bridge, with most unmyelinated axons occurring in the range of 1- $3\mu m^2$.

Comparisons between the estimates of the total number of axons in normal cord and in the bridge indicate a greater than normal number of axonal profiles are present for days 54, 144 and 200 (table 9.2). Furthermore, as the cross sectional area of the bridge increases with time, there is a corresponding decrease in axonal density, presumably because of the increased myelination in the bridge. In contrast to the uninjured cord, the decrease in standard deviation over time suggests that the axonal distribution is more uniform in the bridge.

Myelination of Axons

As seen from figure 9.11, axons in the process of myelination are found in the bridge at day 54, but the number of myelinated axons at this stage amounts to only 3% of the total number (Fig. 9.18). This value rises to approximately 28% and 21% by days 144 and 200. However, when divided into size class, it can be seen that myelination is taking place in the larger axons (see Fig. 9.19). At day 54, most axonal profiles above $10\mu m^2$ have been myelinated, with all of those above $20\mu m^2$ possessing a sheath. Later by days 144 and 200, all axonal profiles above $6\mu m^2$ have been myelinated. Although some of the smaller ones are also myelinated, values are lower than in the undamaged spinal cord, particularly those axons within the 1-$2\mu m^2$ range, with only 2-10% of axonal profiles ensheathed by days 144 and 200, compared to 50% in uninjured cord.

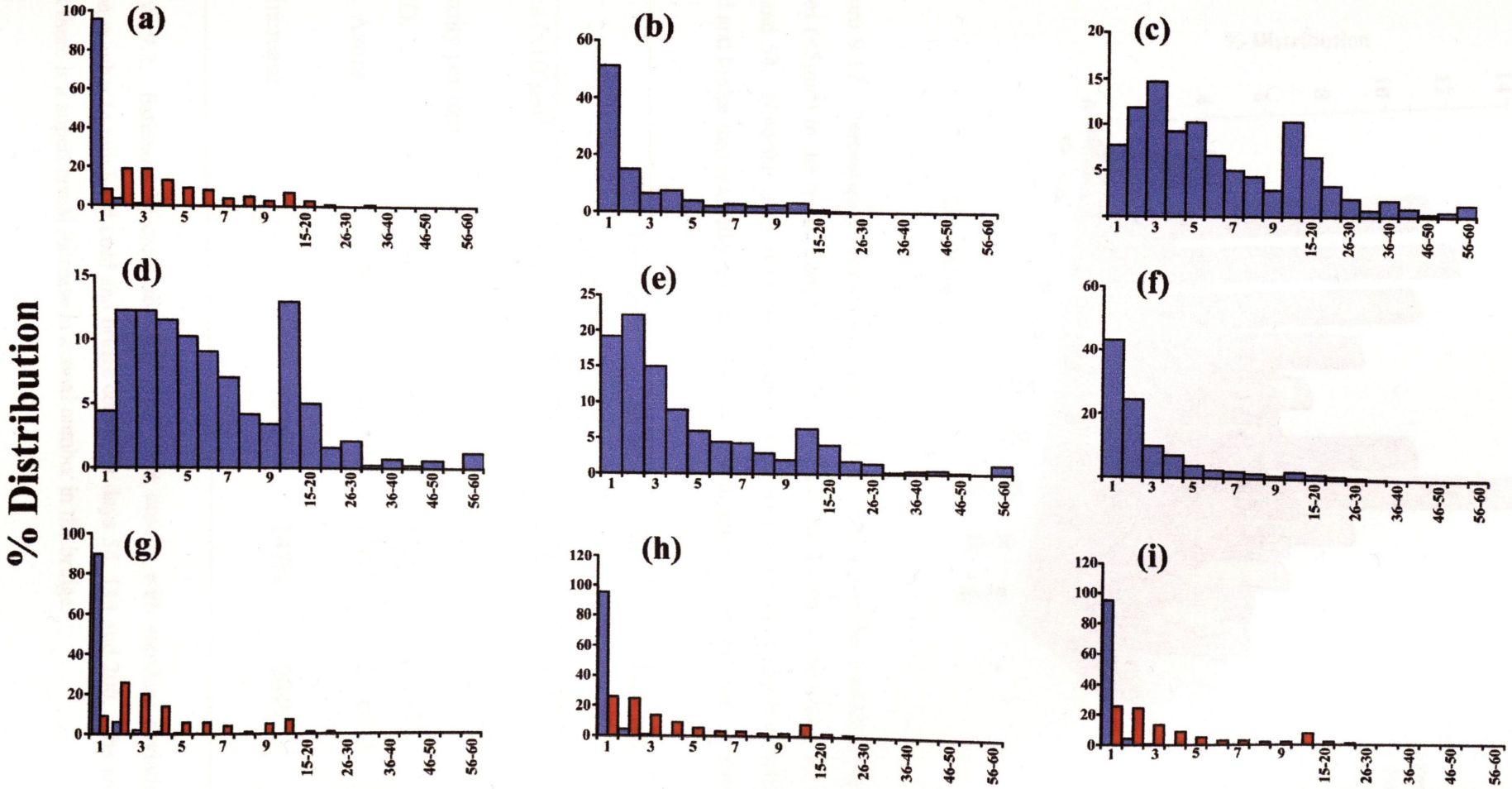


Figure 9.16. Distribution of unmyelinated (blue) and myelinated (red) axons and axonal profiles, represented as percentage distribution, in the normal spinal cord (a), the rostral stump/lesion site border for days 6 (b) and 8 (c) and the middle of the bridge for days 8 (d), 10 (e), 20 (f), 54 (g), 144 (h) and 200 (i). Note the increase in cross sectional area of unmyelinated axons entering the bridge at day 6, in the middle of the bridge by day 8 and day 20.Thereafter the size of profiles reduces (day 54; g) with area values for unmyelinated axons similar to those found in uninjured cord. The x-axis represents axonal cross sectional area (microns squared) divided into categories according to size.

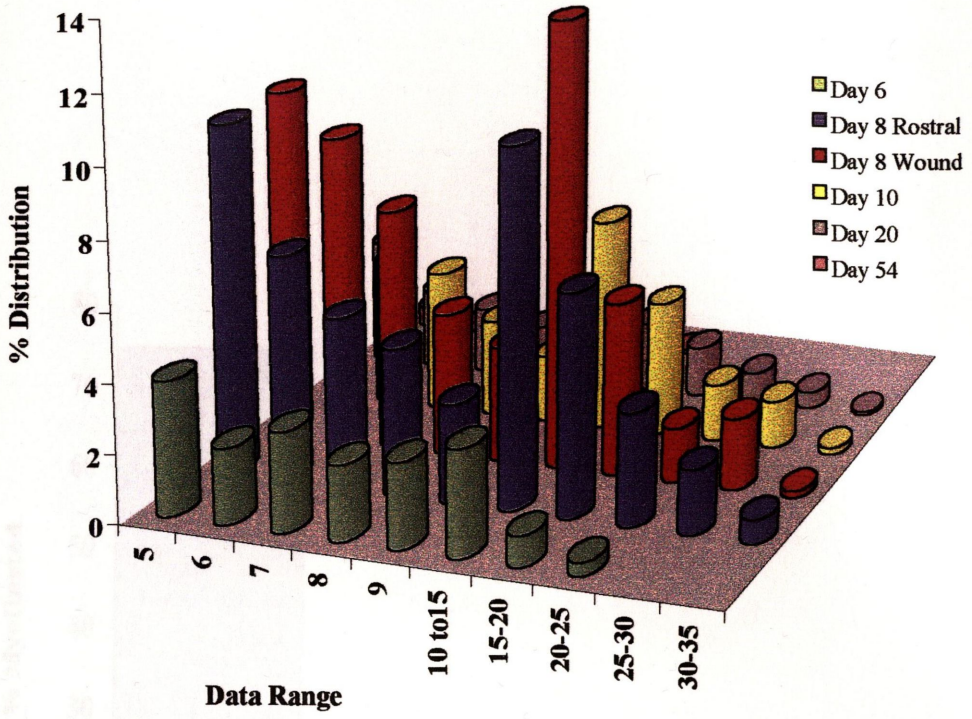


Figure 9.17. Percentage distribution of unmyelinated axonal profiles considered to be growth cones (<5μm^2) in the rostral cord for days 6 and 8 and the middle of the bridge for days 8, 10, 20 and 54. Note the large increases in size in cross sectional area at day 8 in both the rostral cord and bridge that gradually decreases by day 20 with few being above 5μm^2 by day 54.

	Uninjured Cord	Day 54	Day 144	Day 200
Area (x10^{3}μm^2)	400	137	215	311
Density per mm^2	222	751	514	685
± SD.	± 622	± 353	± 233	± 112
No. Axons	75,000	103,000	110,500	213,500
% Increase	-	137%	147%	284%

Table 9.2. Estimates of cross sectional area, axon density with standard deviation and total axon number in uninjured cord and bridge centre for days 54, 144 and 200. The values suggest that there is a supernormal increase in axonal number in the bridge.

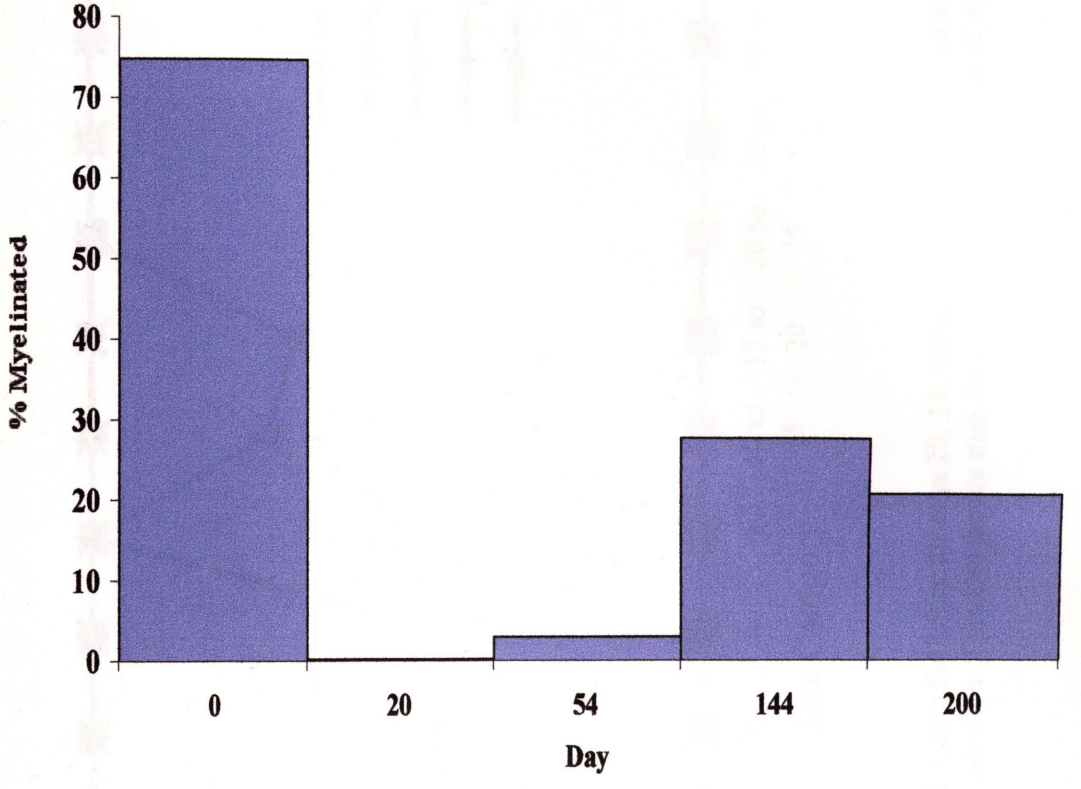


Figure 9.18. Proportion of myelinated axonal profiles in the bridge for the uninjured cord (denoted as 0) and for days 20, 54, 144 and 200. Note the absence of myelin in the bridge at day 20 and the small percentage of axons (3%) that are myelinated by day 54; this increases to approximately 28% and 21% by days 144 and 200.

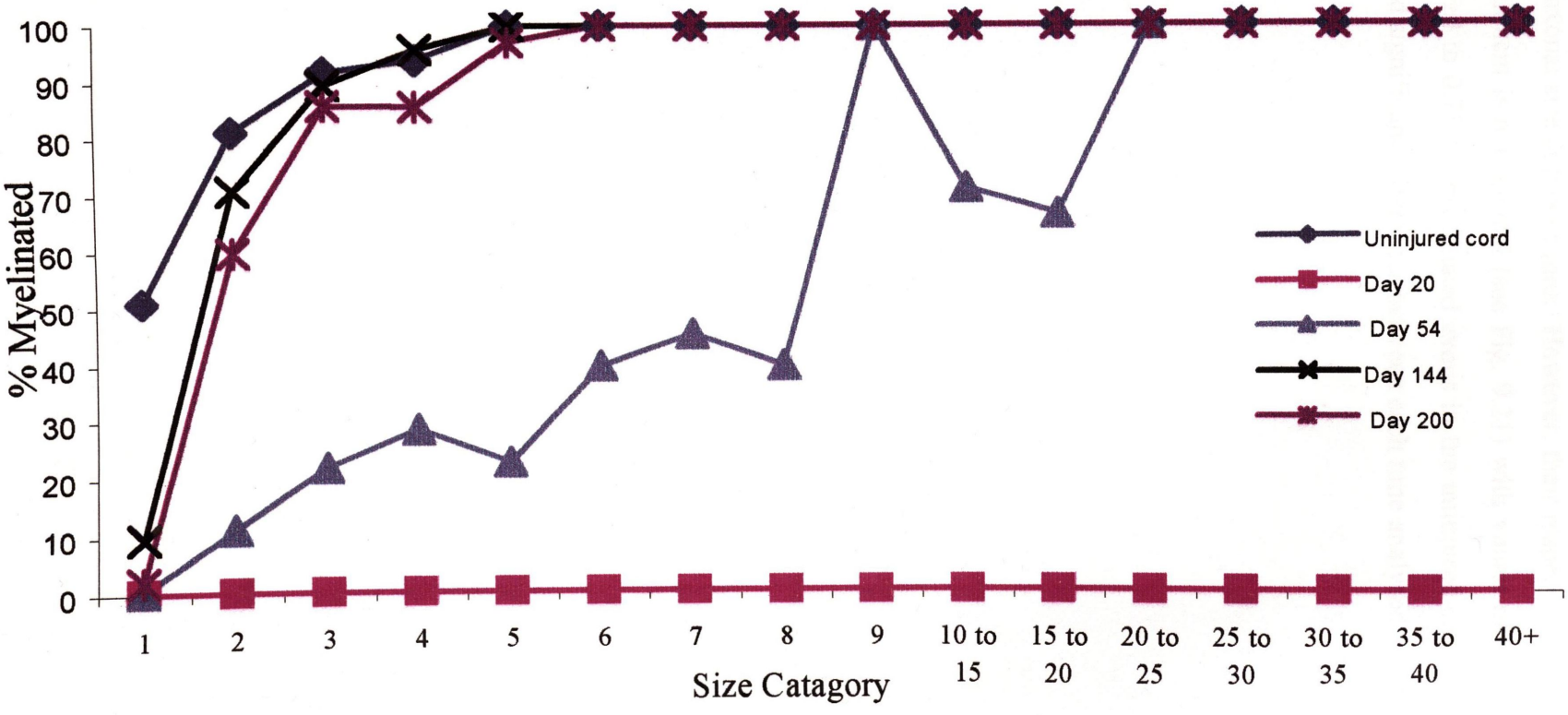


Figure 9.19. Axon size in relation to myelination in uninjured cord, and in the bridge for days 20, 54, 144 and 200. Note the presence of myelinated profiles in all size categories at day 54, and at later stages the complete myelination of profiles greater than 6μm^2; however, note the lack of myelination of axons with lower cross sectional area.

layer of myelin. At later stages, however, this ratio increases to 0.83 and 0.80 for days 144 and 200 respectively, suggesting that myelin thickness is more strongly predicted by the axonal size at these times. However, their respective G-values suggests that this ensheathment is not optimal (see Fig. 9.21) with values of 0.76 and 0.84 respectively compared to 0.71 for myelinated axons in the uninjured cord. T-tests of all G-values revealed significant differences between each time analysed ($p \leq 0.0001$).

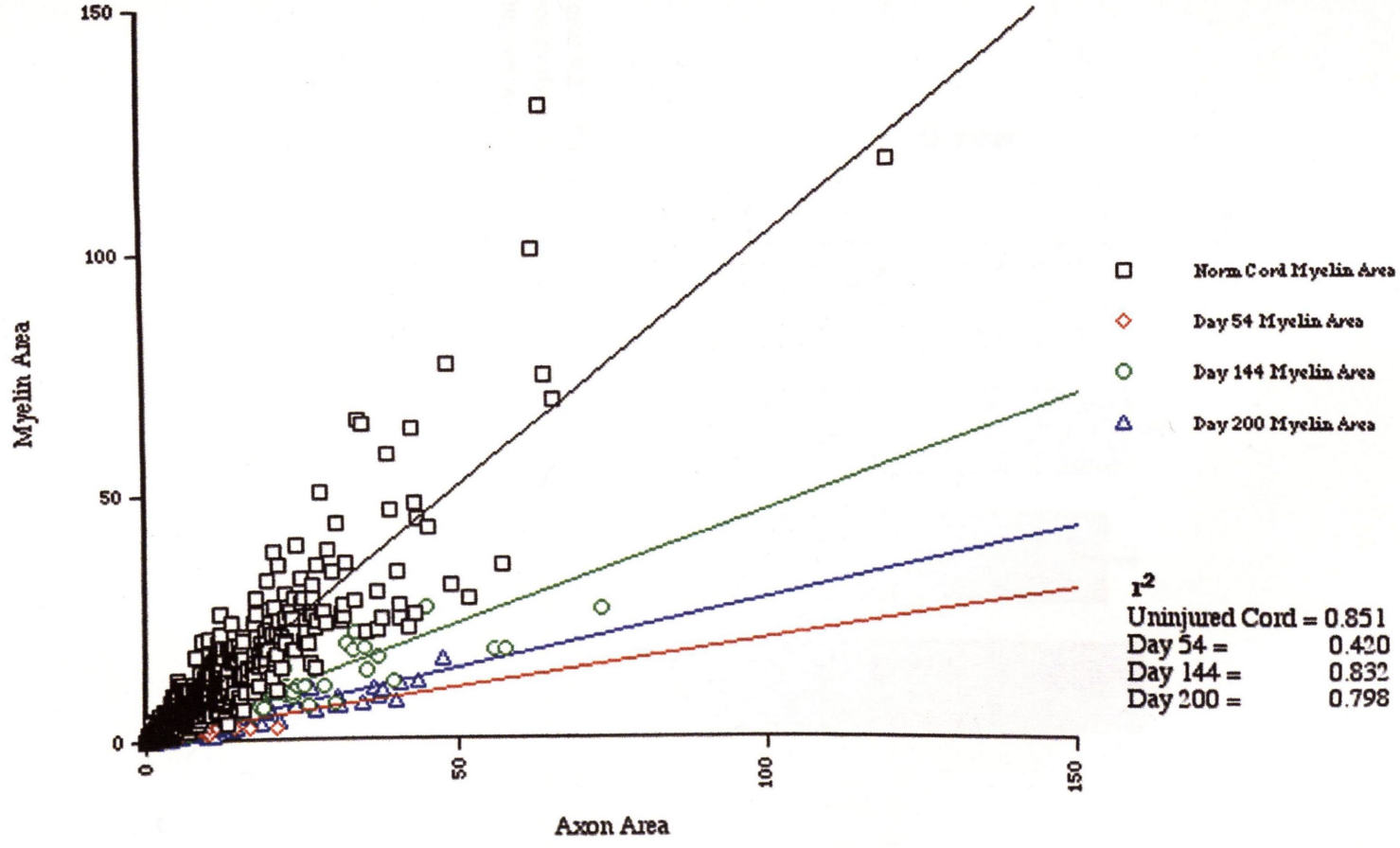


Figure 9.20. Correlatin of myelin and axonal area for uninjured cord and days 54, 144 and 200 with their corresponding r-squared values. Note the low value for day 54, while for days 144 and a 200 a stronger correlation is indicated.

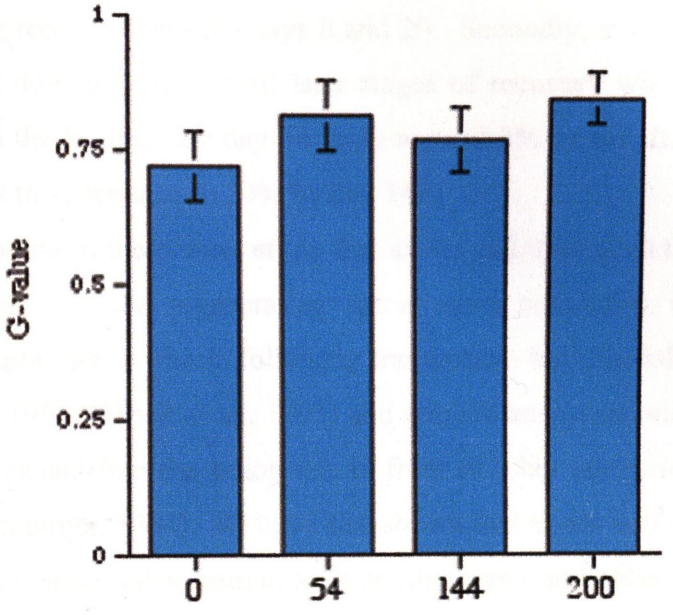


Figure 9.21. Plot of G-value ratio for uninjured cord (day 0) and days 54, 144 and 200. Note that even by days 144 and 200 the sheath thickness is lower compared to the myelin surrounding uninjured axons.

9.4 Discussion

The results of the present study demonstrate that following cord transection, axons and their growth cones are the first components to enter the lesion site and produce the first reconnections between the rostral and caudal stump. Furthermore, we have found that reestablishment of neuronal control of the caudal cord occurs in two steps (see figure 9.22). Firstly, axons and their growth cones migrate into the lesion site between days 6 and 54, in conjunction with non-neuronal cells, to produce the bridge, with maximal numbers being recorded between days 8 and 20. Secondly, myelination of axons takes place, but this does not begin until later stages of recovery when many of the axons have traversed the bridge. By day 54, only around 3% of the axons in the bridge are myelinated but this increases to 30% by day 144.

The finding in the present study that axons and their growth cones comprise the first components of the regenerating spinal cord resembles the situation in the regenerating optic nerve where, following transection, both in fish (*Carassius*, Strobel and Stuermer, 1994; Hirsch et al., 1995) and amphibians (*Xenopus,* Bohn et al., 1982), growth cones extend into the lesion site in front of other components such as the glia (Strobel and Stuermer, 1994). We have also shown that axons in the lesion site contact a variety of other, non-glial substrata, such as fibroblasts and collagen, and this has also been reported in the regenerating optic nerve (Hirsch et al., 1995). Following spinal cord injury, however, the timeframe for the entry of axons and their growth cones into the lesion site, relative to other regenerating elements such as ependyma and glia, is somewhat unclear in the literature. This is further complicated by the variable results obtained through the use of different lesioning paradigms, such as transection (*Carassius*, Coggeshall et al., 1982; Nona and Stafford, 1995) and amputation (*Anolis*, Simpson, 1968; *Trituris*, Nordlander and Singer, 1978; *Sternachus*, Anderson et al., 1983). In fish, following cord amputation, axons grow into a blastema of regenerating tissue in conjunction with ependymal and glial cells (*Sternachus*, Anderson et al., 1983: Anderson and Waxman, 1983a), whereas following transection in *Xenopus*, as in the present study, the leading elements are axons and their growth cones (e.g. Butler and Ward, 1965). Nona and Stafford (1995), in a primarily immunohistochemical study in goldfish, noted that labelled axons extended further into the lesion site following transection than labelled glia, while Butler and Ward (1965) noted that axons were the

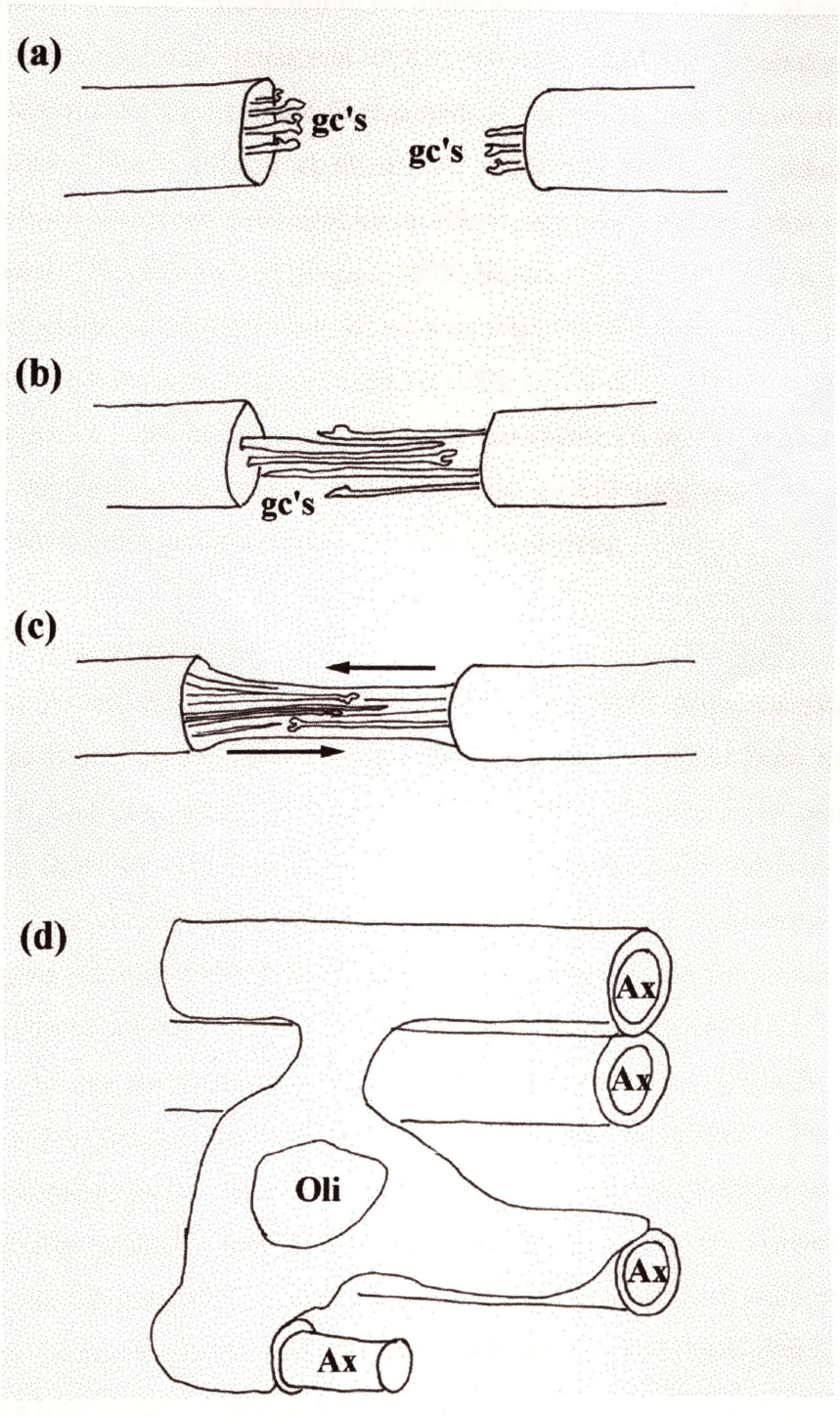


Figure 9.22. Diagrammatic representation of the reestablishment of neuronal continuity. The first stage is the extension of axons and their growth cones from the rostral cord by day 6 (a), through the lesion site to form the first components of the bridge (day 8) (b) and later by day 20 the colonisation of the bridge (c). The second stage occurs by day 54 and is the myelination of axons in the lesion site (d).

first components to cross the lesion site following cord ablation in *Xenopus* tadpoles. However, following spinal transection in the same animal, the emergence of axons from the cut ends of the cord was concurrent with ependymal outgrowth (Michel and Reier, 1979). Tail amputation results in a different type of outgrowth than follows transection and in the newt, *Triturus* (Singer et al., 1979), regrowing axons are guided through distinct predefined 'corridors' produced by proliferating ependymal cells that migrate in front of the axons (Nordlander and Singer., 1978; Singer et al., 1979). A similar type of glial-mediated guidance of regrowing axons was found in the regenerating tail of the lizard, *Anolis*, following amputation (Simpson, 1983; Duffy et al., 1992). In the present study glial processes and ependymal cells were not observed at the leading front of regrowth in the developing bridge, indicating that axonal outgrowth in the eel is independent of the other neural components of the spinal cord.

Timeframe for axonal regrowth

The timeframe for axonal entry into the lesion site in the present study indicates that at least some axons are capable of rapid regrowth and begin to project from the rostral cord by day 6 such that within two days small numbers of axons have reached the caudal cord to form the first elements of the bridge. Thereafter, the numbers increase dramatically. Comparisons to axonal growth in other animals are summarised in table 9.3. Although a variety of different types of lesioning paradigms are included in the table, the timeframe for the emergence of axons from regions adjacent to the lesion site are similar. As can be seen from the table, the time for the outgrowth of axons determined in the present study is similar to that found elsewhere. Differences, however, are apparent in the regenerating lamprey spinal cord where axons only extend into the lesion site by day 21 and enter the opposite stump by day 28. However, these studies (Lurie and Selzer, 1991; Lurie et al., 1994) were concentrated only on a small group of large descending tracts, that include the Muller and Mauthner axons, and they may not give a true picture of recovery.

Interestingly, in the amniote CNS when axon regrowth is possible, as in juvenile animals (Nicholls and Saunders 1996; Varga et al., 1996), or is encouraged through a conditioning lesion (Jacob and Croes, 1998), the time for the appearance of axonal profiles is also similar to that found in the different anamniote models (e.g. Reier and Webster, 1974; Lowenger and Levine, 1988; Michelle and Reier, 1979). The rapid reaction of axons in many animals to injury indicates that at least some are capable of

Animal	Tissue	Enter Wound (Day)	Reconnect (Day)	Reference
Eel	Spinal Cord	6	8	The present study
Goldfish	Optic Nerve	2-7	-	Levine, (1991)
Goldfish	Optic Nerve	-	8-12	Murray, (1982b); Lowenger and Levine, (1988); Paschke et al. (1992); Strobel and Stuermer, (1994)
Goldfish	Optic Nerve	-	14	Blaugrund et al. (1993)
Lamprey	Spinal cord[1]	21	28	Lurie and Selzer (1991); Lurie et al. (1994)
Xenopus	Optic nerve	5-7	-	Bohn et al. (1982)
Xenopus	Optic nerve	4-8	-	Reier and Webster (1974); Rungger-Brandle et al. (1995)
Xenopus	Spinal Cord	5-7		Michel and Reier (1979)
Triturus	Spinal Cord[2]	4	14	Stensaas (1983)
Opossum *Monodelphis*	Spinal Cord	3-5	-	Nicholls and Saunders (1996) Varga et al. (1996)
Rat	Spinal Cord[3]	4	-	Jacob and Croes (1998)

Table 9.3. Regrowth of axons into and through the bridge determined from several studies of anamniote and amniote optic nerve and spinal cord regeneration. [1] only a specific group of axons, the giant reticulospinal axons, were studied, [2] denotes that cord ablation was used and [3] a conditioning lesion to the adult spinal cord.

recovering from injury, develop growth cones (see next section), extending rapidly into the lesion site and presumably reach, or attempt to reach, their original targets. The finding of the present study supports this notion, as by day 8 the first elements of the bridge comprise a small group of axons and their growth cones. We have not attempted to determine the source of these axons and so it is unknown whether they arise from (a) local segmental neurons, (b) interneurons from other segments of the cord, or (c) some of the long descending tracts arising in the brain. No neuronal cell bodies were ever found in the bridge for all times studied. Nevertheless, it is likely that many of these first 'pioneer' axons arise from local sources, since many axons, particularly in the larger tracts, are still undergoing degeneration. In the regenerating lizard spinal cord, Duffy and colleagues (1992) found that axons from regions near the spinal injury had a high likelihood of growing into and through the lesion, but those from regions that are more distal were less likely to extend successfully through the lesion site. Furthermore, evidence from studies in rat spinal cord has shown that neurons which sustain injury closer to the cell body engage in a stronger axonal response to the injury compared to neurons which receive an injury more distal to the cell body (e.g. Richardson et al., 1984). In the eel it is most probable that the source of regrowing axons arise from neurons positioned in adjacent uninjured segments and that at least some, if not all of the component axons in the bridge at day 8 are of this origin. Bosch et al. (2000), in an HRP labelling study in the eel, found that local spinal interneurons contributed to the first wave of regrowing axons.

Why does a small group cross the bridge ahead of all the other regrowing axons? Aside from any differences in growth rates between different groups of axons, as shown from labelling studies of axons crossing the lesion site (zebra fish, Becker et al., 1997; eel, Bosch et al., 2000, Doyle et al., 2000), the initial outgrowth of axons from more local regions may act as pathfinders for other axons. Axons with such a function have been noted in the developing CNS of different vertebrates (see ten Donkelaar, 2000) and pioneer axons may pave the way for more substantial axon regrowth into the lesion site following injury. In the goldfish, Lowenger and Levine (1988) noted the passage of 'leader axons', singly or as groups, into the regenerating optic nerve that was then followed by a large outgrowth of regenerating axons. Bohn and colleagues (1982) also noted a graded entrance of axons into the distal cranial stump of regenerating *Xenopus* larvae and adults. Moreover, it has been shown that injured axons use other regrowing axons as preferable growth substrates (Easter et al., 1984; Strobel and Stuermer, 1994)

and that a molecule expressed by axons following injury mediates growth cone elongation along pre-existing axons (Giordano et al., 1993). These findings suggest that the small number of axons in the eel that traverse the lesion site by day 8 may be acting as pathfinders for the greater bulk of regrowth that occurs slightly later (days 10-20).

Growth cones

The evidence from DiI-labelling and the quantitative analysis of axonal profile size shows that in the bridge at days 6 and 8 growth cones are larger than regrowing axons. These large axonal-type profiles are seen in the bridge until approximately day 20, and few are present by day 54, as seen in figure 9.17, suggesting that many axons with prominent growth cones cross the bridge very early in the regenerative process.

Ultrastructurally, the growth cones contain numerous mitochondria, a common component of growth cones in many animals (e.g. Lurie et al., 1994), and vacuoles of varying size, many of which stain intensely. They also contain many neurofilaments, as is characteristic of axons and their growth cones in regenerating lamprey spinal cord (Lurie et al., 1994) and goldfish optic nerve (Easter et al., 1984; Strobel and Stuermer, 1994), although the rostro-caudal longitudinal organisation of neurofilaments we have found is absent in regenerating lamprey axons which contains filaments arranged randomly and in large whorls (Lurie et al., 1994). In goldfish, mRNA expression of the neurofilament ON-1 is increased during optic nerve regeneration (Tesser et al., 1986; Glasgow et al., 1994). Other components such as actin and myosin and microtubules (Jacobs et al., 1997), typical of growth cones in other animals (see general refs), were not identified in the growth cones of the regenerating axons in the present study.

The size and shape of the growth cones determined from DiI-labelling and electron micrographs are summarised in figure 9.23. In general, all labelled growth cones were larger than the parent axon and bulbous to irregular in shape. Similar shaped growth cones have been found in the developing fish CNS (e.g. Wilson and Easter, 1991b) and regenerating fish optic nerve (Strobel and Stuermer, 1994). It seems from figure 9.24 that small axons traverse the bridge at very early stages of recovery, although it is possible that some of these very small profiles are filopodia that extend from the surfaces of the growth cones, as have been observed in the developing fish CNS (Strobel and Stuermer, 1994). Our DiI-labelling, however, failed to reveal any such extensions. Moreover, studies using HRP labelling in the regenerating lamprey spinal cord also did not show lamellipoda and filopodia associated with growth cones

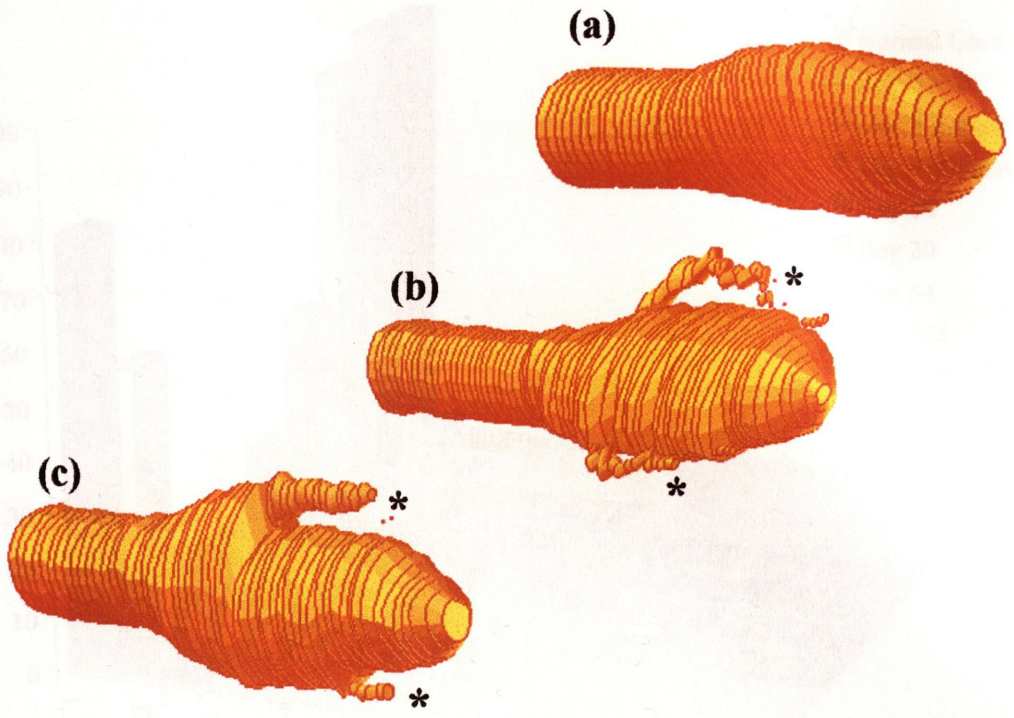


Figure 9.23. Diagrammatic representations of the different types of growth cone found in the regenerating bridge (a-c). In (a) note the simple elongate shape of the growth cone while in (b) and (c) other types, with more irregular shape, were also found. (*) denotes possible filopodial extensions from the growth cone.

(Lurie and Selzer, 1991) although in a later study (Lurie et al., 1994), in which regenerating giant reticulospinal axons had been iontophoretically filled with HRP, occasional small processes extending for short distances were observed. The growth cones in the regenerating optic nerve seem to resemble those of lamprey (Lanners and Grafstein, 1980), although Strobel and Stuermer (1994) in a HRP study noted the presence of filopodia on some regenerating retinal ganglion axons. In mammals, where recovery is abortive, injured axons develop growth cones that sport filopodia and lamellipoda similar to those found during CNS development (e.g. Li and Raisman, 1996; Davies et al., 1996) although simple growth cones with few lamellipoda and filopodia have been described in myelin-deficient rats (Gocht and Löhler, 1993), and in the late developing corticospinal tract of the rat (Gorgels, 1991). It has also been demonstrated that the growth cones of axons that follow predetermined pathways are

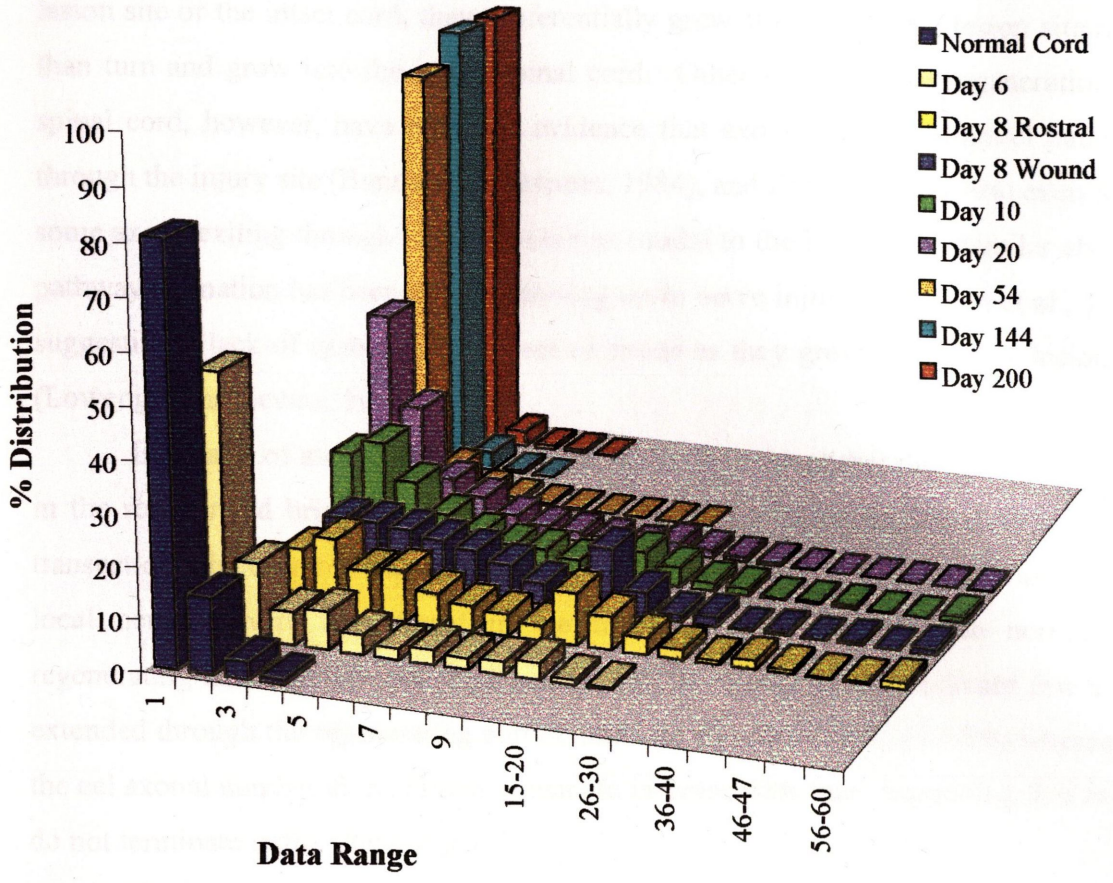


Figure 9.24. Graphical representation of all unmyelinated axonal profiles in normal cord, extending into the lesion site at days 6 and 8, and in the middle of the bridge at days 8, 10, 20, 54, 144 and 200.

relatively simple in shape, while those that leave pathways or come to decision regions, display more elaborate filopodial extensions (e.g. Nordlander and Singer, 1987; Kuwada et al., 1990). DiI has its limitations in revealing fine structural detail and it proved difficult in the present study to determine if the dye fully filled the growth cones and small projections, such as filopodia, completely. Possibly, different techniques such as intercellular dye filling could settle this issue.

The spatial organisation of regrowing axons in the bridge shown from our DiI -labelling suggests that very little deviation occurs in the pathways taken by axons as they traverse the bridge and enter the caudal cord. In the regenerating lamprey spinal cord (Wood and Cohen, 1981; Yin et al., 1984; Mackler et al., 1986) up to 96% of the regenerating axons also extend through the lesion site in relatively straight pathways (Lurie and Selzer, 1991). Interestingly, Lurie and Selzer (1991) noted that following

hemisection, where regrowing axons are offered a choice of pathway, either through the lesion site or the intact cord, they preferentially grew straight into the lesion site rather than turn and grow into the intact spinal cord. Other studies of the regenerating fish spinal cord, however, have provided evidence that axons can choose novel pathways through the injury site (Bunt and Fill-Moebs, 1984), and Zottoli et al. (1994) even found some axons exiting through ventral roots just caudal to the lesion site. Similar aberrant pathway formation has been noted following optic nerve injury (e.g. Bohn et al., 1982), suggesting a lack of spatial arrangement of axons as they grow through the lesion site (Lowenger and Levine, 1988).

Estimates of axon number in the present study suggest that there are more axons in the regenerated bridge than in the adjacent normal cord even 200 days after cord transection. Increases in the number of axons originating from both supraspinal and local neurons were also found in the transition zone between the normal and regenerating lizard spinal cord (Duffy et al., 1992). However, in the lizard few axons extended through the regenerating portion and into the caudal cord (4-56%) whereas in the eel axonal number in the bridge appears to increase with time, suggesting that axons do not terminate in the stump regions.

There are two explanations for the increased axon number: axon splitting, or novel projections into the caudal cord. Branching of regrowing axons is a common occurrence in regenerating systems. For example, in the regenerating lamprey spinal cord, axons have been shown with HRP labelling to bifurcate (Lurie et al., 1994) and sprout (Wood and Cohen, 1981; Lurie and Selzer, 1991). Sprouting has also been seen for regenerating axons in the optic nerve (Stuermer, 1988), and tectum (Schmidt et al., 1988). Our DiI-labelled material, however, provided no evidence of branching, but of course, the branch points may have been located rostral to the labelling site.

Duffy and co-workers (1990), in a study of the regenerating lizard spinal cord, noted that up to twice as many neurons projected axons into the regenerating compared to normal cord. Furthermore, Bosch and colleagues (2000) in a retrograde HRP labelling study of the regenerating eel spinal cord found that no new projections arise from supraspinal regions and project into the wound site. Taken together, these results, in conjunction with the present study, suggest that if new projections extend into the bridge it is likely that they arise from local and projecting interneurons.

Axon growth - Caudal Cord

As shown from DiI-labelling and electron microscopy, regrowing axons rapidly cross the lesion site and extend into the caudal cord where they presumably establish connections, perhaps with their original targets. As the axons do so, as seen in figures 9.4 and 9.10 corresponding to the rostral and caudal cord at days 6 and 20, by passing through regions where considerable degeneration is still taking place. Therefore, axons emerging from the bridge encounter a milieu that is atypical of the normal or developing CNS and at some stage, they will invariably encounter degenerating myelin debris. Becker and colleagues (1997) observed in the regenerating zebra fish spinal cord that many of the regenerating axons tended to pass through the grey matter, where there was relatively little myelin debris, and avoid white matter tracts rich in degenerating myelin profiles. We noted no such tendency in the regenerating eel cord, although we did find a predisposition for growth along the periphery of the cord close to the glia limitans and its associated basal lamina (see figure 9.10). These peripheral axons were often found to extend the furthest into the cord, indicating that this region perhaps supports axonal growth. Similar peripheral axonal regrowth has been noted in the regenerating optic nerve (e.g. Lowenger and Levine, 1988) and spinal cord (see Stensaas, 1983) while the attractive properties of the glia limitans and basal lamina to axonal growth are well recognised (see Powell et al., 1997). Moreover, in the regrowing mammalian PNS, axons selectively grow on basal lamina substrates (Reichardt and Tomaselli, 1991; see Bisby, 1995 for review).

Retinal ganglion cell (RGC's) axons in the regenerating optic nerve of the goldfish have been shown to contact various structures including degenerating myelin sheaths (Strobel and Stuermer, 1994) indicating that myelin in the fish CNS may not be inhibitory to regrowth. While this may be so *in vivo,* co-culture studies *in vitro* suggest that fish myelin does share some attributes of mammalian myelin which is known to be inhibitory to axonal growth. For example, low levels of immunoreactivity for the antibody IN-1, which specifically recognises one axon inhibitor, Nogo (Chen et al., 2000), in the mammalian CNS (Schwab et al., 1993), have been detected in the goldfish optic nerve (Wanner et al., 1995). Furthermore co-cultures of fish axons with rat oligodendrocytes and myelin have shown that fish axons are sensitive to the mammalian inhibitory molecules, and outgrowing neurites either collapse or actively avoid rat myelin, but they will grow across branched oligodendrocytes in the presence of IN-1 (Bastmeyer et al., 1991). Moreover, while it has been shown that fish myelin

allows for substantial fish and mammalian neurite outgrowth in culture (Bastmeyer et al., 1991; Wanner et al., 1995), application of IN-1 antibodies to co-cultures of fish RGC's and fish myelin appears to enhance neurite outgrowth (Sivron et al., 1994). This effect, however, was not found by Wanner and colleagues (1995) and remains a matter of debate (see Sivron and Schwartz, 1994; Sivron et al., 1994 and Wanner et al., 1995). However, Sivron and colleagues (1994) have shown that it may only be intact myelin in the uninjured fish CNS that is non-permissive to growth, whereas myelin disrupted as a result of CNS injury does not appear to be inhibitory. Bedi et al. (1992) noted that the myelin of uninjured rat sciatic nerve is not permissive to axonal growth but following injury becomes growth permissive to adult DRG neurons. In most cases, the components of the optic nerve, RGC's and their axons, have been studied while relatively little has been done with the spinal cord, which may exhibit differing levels of IN-1 immunoreactivity, as found in *Xenopus* (Lang et al., 1998). Therefore, it is possible that in fish spinal cord, injured myelin and associated debris may exhibit differing levels of inhibitory factors or none at all, since, as we have found in the eel, inhibition of axonal growth was not found.

With increasing time after transection, axons continue to extend further into the caudal stumps. DiI-labelling at these later stages (day 75; see figure 9.9) shows that regenerating axons project into the caudal cord with little pathway deviation. As the axons extend further into the caudal cord, they will begin to encounter regenerating ascending axons as well as increasing numbers of undamaged myelinated tracts belonging to the local segmental neuronal circuitry. If, as Sivron and colleagues (1994) suggest, intact myelin in the undamaged fish CNS does not permit growth, we might expect that axons in the eel would deviate to avoid these tracts; this, however, appears not to be the case. So, how are eel axons capable of growing long distances through regions containing undamaged myelin? A similar question can be asked about the fish optic nerve where the newly formed axons of retinal ganglion cells are capable of pathfinding and extending through regions of the optic nerve that already contain myelinated axons and into the tectum (Murray and Edwards, 1982b; Stuermer, 1988). In the regenerating eel spinal cord, complete regrowth of the supraspinal complement occurs over a 1 year period (Bosch et al., 2000), yet we know that myelination in underway by day 54, and so late-growing axons must enter and grow through the bridge and stumps when they contain newly myelinated axons. One possibility is that at these times the regrowing axons are desensitised to inhibitory stimuli from the local

environment. In a co-culture study Lang and co-workers (1998) showed that whereas rat dorsal root ganglion neurites and growth cones were inhibited when placed on myelin originating from the lizard *Gallotia*, lizard RGC axons grew successfully, suggesting that lizard axons were able to ignore the inhibitory signals.

The Bridge - Oligodendrocytes

Oligodendrocytes of mammals are considered to inhibit the regrowth of axons (e.g. Schwab, 1991; 1996) and it has been shown that *in vitro* they promote growth cone collapse and inhibit neurite outgrowth (Schnell and Schwab, 1990; Weibel et al., 1994; Meyenburg et al., 1998). In contrast, the oligodendrocytes of anamniote optic nerve, such as fish (Bastmeyer et al., 1991; Bastmeyer et al., 1993), amphibians (Lang et al., 1995) and reptiles (Lang et al., 1998), are able to support axon growth under these conditions.

The findings of the present study indicate that oligodendrocytes are absent from the bridge region during the early stages of recovery (~ days 6 to 50) but are present by day 54 when axons begin to be myelinated. Possibly this cell type is present in the bridge earlier, but in a quiescent form that does not engage in myelination. Their influx must occur some time after day 20 since then only ependymal cells and a few macrophages/monocytes are present in the bridge and representatives of the three different oligodendrocyte subtypes - light, medium and dark staining cells (see Peters et al., 1991) – were not found. Furthermore, Schwann cells which are capable of myelinating regenerating axons (following grafts e.g. Bunge, 1994; Brook et al., 1994; Guest et al., 1997) were not found in the bridge, although, interestingly, they do invade the lesion site in the fish optic nerve following crush (Nona et al., 1992) but not transection injury (Strobel and Stuermer, 1994).

The late appearance further implies that this cell type is not required for the initial formation of the bridge, as noted by Scott and Foote (1981) in the regenerating optic nerve of the frog *Rana* following transection. Therefore it seems that oligodendrocyte infiltration and their subsequent myelination of axons is one of the last processes to occur during the re-establishment of the structural integrity in the cord. One explanation for the absence of oligodendrocytes from the regenerating bridge until approximately day 54 is that they are possibly inhibitory to axon outgrowth. In *Xenopus*, for example, oligodendrocytes are refractive to axonal growth *in vitro* if from the spinal cord, but support growth if they are from the optic nerve (Lang et al., 1995).

In fish, optic nerve oligodendrocytes support axon outgrowth both *in vitro* (Bastmeyer et al., 1991; 1993) and *in vivo* (Strobel and Stuermer, 1994), but it is unknown whether their spinal cord oligodendrocytes behave similarly or are similar to *Xenopus* cord oligodendrocytes. If inhibitory to axonal growth, their initial absence would seem to be an appropriate adaptation.

Within the constraints of the present study, we have been unable to determine the sources of the bridge oligodendrocytes and a number of cellular origins are possible. For example, surviving oligodendrocytes within the spinal stumps may be able to dedifferentiate and become proliferative (see Fig. 9.25a). In the adult mammalian CNS it is debatable whether oligodendrocytes that survive the injury are viable (see Keirstead and Blakemore, 1997; Scolding and Lassman, 1996) but following injury to the PNS, Schwann cells quickly proliferate, surround the growth cones of peripheral nerves, and guide them through the lesion site (see Bisby, 1995). Olfactory ensheathing cells (OEC's) in the mammalian olfactory system possess similar properties (Ramon-Cueto and Avila, 1998).

An oligodendrocyte-specific precursor cell-type resident in the cord may be another source (see Fig. 9.25b). In mammals it has been shown that an extensive network of oligodendrocyte precursor cells, of the O2A lineage (Levine, 1994) are recruited to spinal cord lesion sites (Keirstead et al., 1998b) and although they do not express MAG or Nogo, the characteristic axonal inhibitory molecules of mature oligodendrocytes, they do express NG2-proteoglycan which has growth inhibitory properties (Dou and Levine, 1994). Therefore, these cells are considered another source of inhibition to the regeneration of the mammalian CNS (Fawcett and Asher, 1999). Whether this cell type is present in the CNS of fish is unknown.

Oligodendrocytes, or their precursors, may arise from multipotent progenitor cells from regions of the stumps close to the injury (see Fig. 9.25c). In the mammalian CNS, stem cells have been shown to arise from ventricular regions, such as the lateral ventricles and rostral migratory stream (see Peretto et al., 1999) and also the spinal cord following injury (Johansson et al., 1999). In the latter, it has been shown that ependymal cells proliferate to produce migratory cells that eventually differentiate as astrocytes and contribute to the formation of the inhibitory scar. In the brain, subependymal cells expressing the protein nestin differentiate into astrocytes following injury (Holmin et al., 1997). However, it is unknown whether all cells do this or whether a population of oligodendrocyte precursor cells is also produced. The context

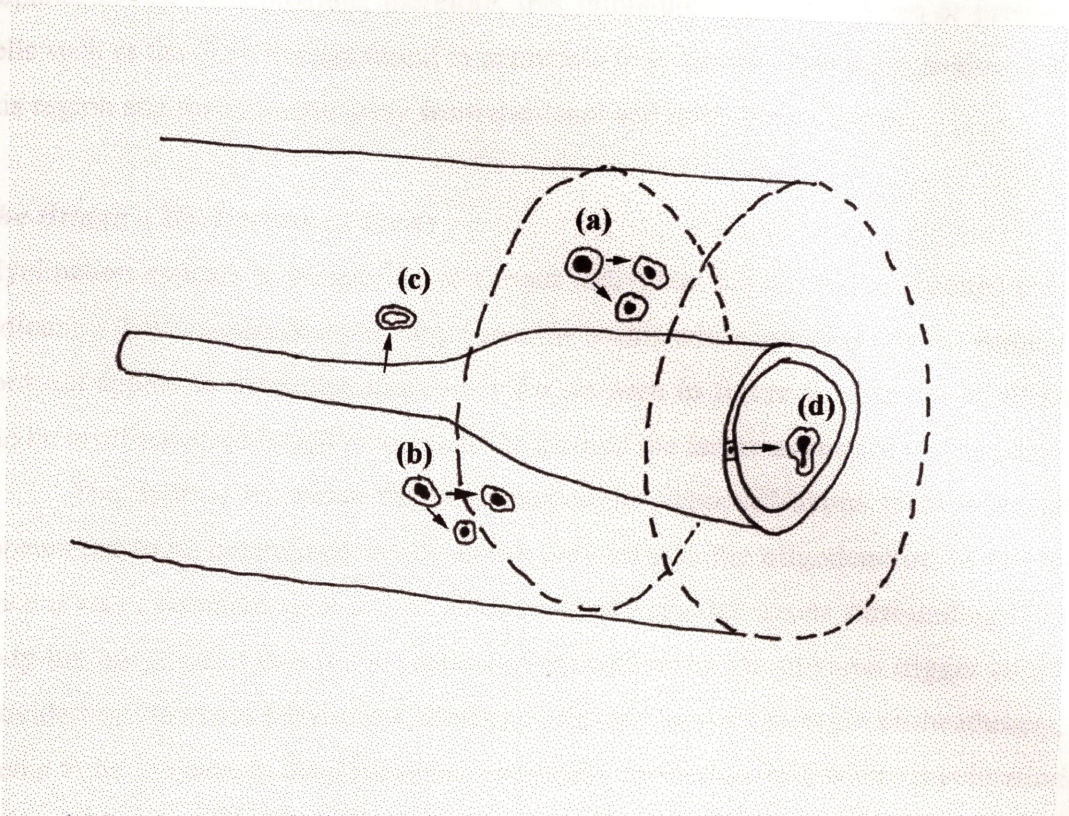


Figure 9.25. Graphical representation of the possible sources of oligodendrocytes in the regenerating bridge of the eel. In (a) oligodendrocytes arise from surviving cells in the stumps; in (b) from an existing precursor population similar to the O-2A cells of mammals; in (c) from precursor cells derived from stem cells in the stumps, and in (d) from stem cells derived the ependymal cells surrounding the newly formed central canal.

of the model used to study regenerative failure may be important, since there is little axonal regrowth through the scar in mammals there may be little use for oligodendrocytes, while there is a need for new astrocytes to form the characteristic astrocytic scar. In contrast, where axon regrowth is possible, as in fish, it is possible that there is need for more oligodendrocytes but fewer astrocytes, since a permanent scar does not form.

Another source of oligodendrocytes could be the newly formed central canal, which is composed of proliferative ependymal cells (see Fig. 9.25d). The ependyma of mammals have been shown to possess stem cell capability in normal and injured CNS (e.g. Johansson et al., 1999) and in fish it has been shown that the cells within this layer possess a high mitotic rate (Zupanc and Ott, 1999; Zupanc, 1999) and a long term

capability for postembryonic neurogenesis (Anderson and Waxman, 1991; Zupanc and Zupanc, 1992). It is possible, therefore, that immature oligodendrocytes or progenitor cells such as the O2A lineage found in mammals (e.g. Levine, 1994), are produced from this region and then migrate away from the canal and initiate myelination.

The Bridge – Myelination of axons

Myelination appears to be specific to certain individual axons or small groups (~1-3), indicating that oligodendrocytes target specific axons while ignoring others. Axon size does not appear to determine this choice for, as seen in figure 9.19, axons of all sizes can be myelinated, although proportionally more of the larger axons are ensheathed.

The method by which the oligodendrocytes "choose" axons to be myelinated appears not to be determined by the axon's proximity to the oligodendrocyte cell body since it was a common sight to find numerous unmyelinated axons surrounding the cell body but only one or two in the process of ensheathment. An obvious trigger could be provided by the axons themselves, directing oligodendrocytes to begin ensheathment, as seems to be the case in the developing peripheral nervous system where myelination is activated by axonally derived signals (Aguayo et al., 1976; Weinberg and Spencer, 1978). It is possible that those axons that have successfully made synaptic contact with appropriate targets are myelinated, while the unmyelinated axons have yet to establish correct connections with their targets in the caudal cord, or have made inappropriate ones.

The feedback mechanisms that encourage the axon to remain at its target and form strong synaptic contact may also induce other changes, such as modulation of the extracellular matrix, or release of trophic substances that attract and stimulate oligodendrocytes to engage in myelination. ECM modulation is a well-known factor in the regenerating amniote CNS. For example, in the adult amniote CNS, growth inhibitory factors such as chondroitin sulphate proteoglycan and tenascin are released by activated astrocytes close to the injury and inhibit axonal growth (see Fitch and Silver, 1997). In contrast, the extracellular matrix proteins that comprise basal lamina in the PNS encourage and support axonal regrowth (Hall, 1989; see Bisby, 1995). The presence of a distinctive electron dense ECM surrounding the regenerating axons in the present study by day 20 suggests that this structure may play a contributory role in supporting axonal growth and myelination.

With increasing recovery times, oligodendrocytes continue to ensheath axons such that 20-30% of all axons in the bridge at days 144 and 200 are myelinated. However, G-values for axons at these stages would indicate that this myelination is suboptimal as the ideal value of 0.6 proposed by Rushton (1951) has not yet been attained. But as the G-value is related to internode spacing, and this has not been determined in the present study, the axon performance may still be satisfactory.

Bosch et al., (2000) and Doyle et al. (2000) both note that the first functional recovery seen in the eel after cord transection is the cessation of spinal swimming, by approximately day 15, and the return of steady swimming movements between days 30 and 80. Since we have found that axons only become myelinated between days 20-50, it follows that, the first functional reconnections in the caudal cord must be made by unmyelinated axons.

Summary of main findings

- Axons comprise the first components of the regenerating bridge.
- Between days 6 and 54, axons possessing large growth cones enter and cross the bridge.
- The number of axons entering the bridge increases steadily with time such that by day 54 a supernormal number of axons are present.
- By day 20 a dark staining extracellular matrix is noticeable surrounding the regenerating axons.
- Oligodendrocytes are present in the bridge by approximately day 50.
- At this stage (day 54) approximately 3% of axons are myelinated in the bridge.
- Myelination of axons is not size specific, although larger axons tend to become myelinated more quickly.
- Most of the axons in the bridge are myelinated sub optimally as indicated by their respective G-ratios for days 54, 144 and 200, however all axons are myelinated to a certain degree that appears to be governed by the cross sectional area of the axon.
- Not all axons are myelinated by day 200.

Chapter 10

General Discussion

Studies carried out in parallel to this project on the locomotory performance of the transected eel have shown that the swimming performance is disrupted for a brief period but that it begins to return to normal after about 15 days and is well restored by 30 days (Doyle et al., 1999; 2000). This striking functional recovery is matched by an equally impressive morphological regeneration, in which regrowing neural tissue bridges the separated cord. The basis of this repair has been studied in this thesis, the primary aim of which has been to determine the sequence of different cellular events and the chronological order in which each of the different cell types involved in the regenerative event appear.

This is the first study, except for those on the rat, that presents a comprehensive view of the different cellular events that occur following injury to the vertebrate spinal cord in one experimental model. Previous investigations, through obvious experimental limitations, have provided detailed but limited studies on specific components of the regenerating cord such as the axons (e.g. McClellan, 1992; Lurie and Selzer, 1991; Duffy et al., 1992; Pijak et al., 1996) or some of the associated cell types; in the case of spinal cord this has generally been the ependymocytes (e.g. Nordlander and Singer, 1978; Anderson et al., 1983; Simpson, 1983; Chernoff, 1996). In many of these studies, the role of the ependyma has been explored in relation to axonal growth (e.g. Singer et al., 1979; Anderson and Waxman, 1983a) while relatively few studies have concentrated on aspects such as the astrocytic (Anderson et al., 1983; Nona and Stafford, 1995), and meningeal reaction (Michel and Reier, 1979) or the role of oligodendrocytes.

In contrast to the amniote CNS where axonal growth is inhibited by the formation of a complex scar at the site of injury (e.g. Fawcett and Asher, 1999), the injured anamniote CNS is capable of sustaining axonal regrowth through the injured portion and back to the original targets. In this thesis we have explored the different cellular events that surround the formation of a novel 'bridge' of spinal tissue that reconnects the rostral and caudal stumps. We have shown that for all times examined the organisation of the bridge is different from that of the uninjured spinal cord. Furthermore we have demonstrated that all of the different cell types common to the uninjured cord such as ependymocytes, liquor-contacting neurons (LCN's) and meningeal cells are found in the bridge, but their organisation and/or distribution within this newly formed spinal tissue is modified. The marked alterations include the formation of an enlarged central canal in the middle of the bridge and the envelopment

of the bridge on the outer surface by a thickened meninx (see Fig. 10.1). The regenerated neural material at all stages did not separate into the characteristic grey and white matter of uninjured cord and instead contains a homogeneous mixture of regenerating axons, oligodendrocytes, radial astrocytic and tanycyte processes. At all stages neuronal cell bodies were absent from the bridge.

The time scale for regrowth

The chronological organisation of the different events that take place in the formation of the bridge are charted in Fig. 10.1. As can be seen from the chart the graded appearance of the different cell types points to a certain degree of controlled organisation of the developing bridge, such that only particular cells become evident at certain stages in its development. The first event to occur in this process is the extravasation of blood from severed vessels in both the cord and meninges to form an extensive clot in the lesion site (chapter 4). We propose that the blood clot contributes positively to regeneration, and provides the first rudimentary bridge of material through which axons are capable of growing. Furthermore, the increase in the number of blood vessels of undetermined origin in this blood clot, particularly at day 8, indicates that angiogenesis is a significant component of the clot/scar development. At this time, neural tissue consisting of axons (chapter 9) and ependymal cells (chapter 5) grow into this blood clot/scar by days 8 and 10 respectively, indicating that axonal growth is not dependant on a pre-formed cellular scaffolding of neural origin as reported in other studies (Simpson, 1964; 1968; Egar and Singer, 1972; Nordlander and Singer, 1978; Singer et al., 1979; Simpson, 1983). The role of the ependymocytes in the present study (chapter 5) appears to be the re-establishment of a central canal in the bridge through the migration and settlement of cells to produce small aggregates that we have termed 'plates'. These small groupings were usually placed ventrally and served as the basis or template for further canal development. By approximately day 12, GFAP+ve processes of radial astrocytes (chapter 8) were found in the developing bridge and we have shown that these processes arise from undamaged cells in the stumps which re-align from their normal radial orientation to a longitudinal one and extend into the bridge. TH+ve and GABA+ve profiles of liquor contacting neurons (LCN's; chapter 6) were also found in the bridge by approximately day 12 as components of the enlarged central canal. Their function in the uninjured vertebrate CNS at present however, remains speculative, so possible functions following injury will also be conjectural. By day 14 the bridge has attained a

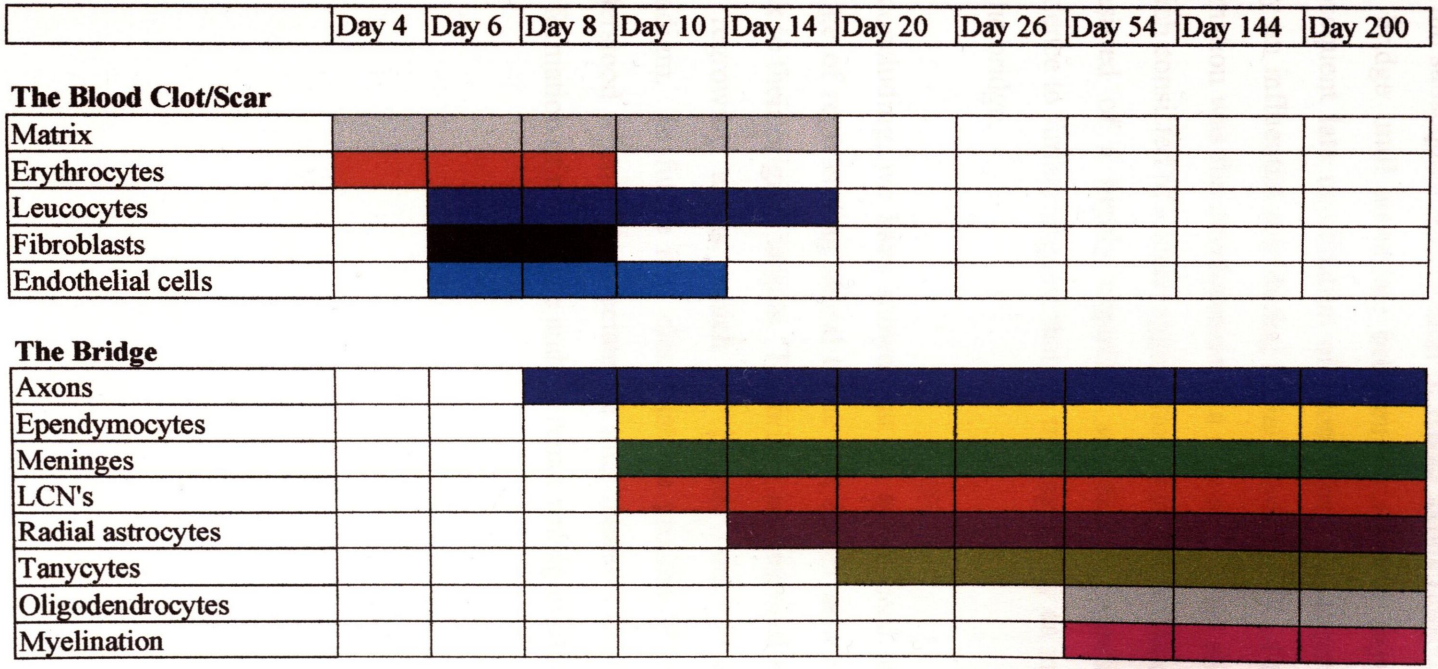


Figure 10.1. Summary of the different events that occur in (a) the lesion site and (b) the developing bridge following spinal cord transection. Note how the matrix and the associated clot/scar cells are completely removed by day 14. In the bridge axons are the first elements of the regenerating cord to enter the lesion site. Migrating ependymal cells and the formation of a meningeal covering at the periphery quickly follows this outgrowth.

cross sectional area of approximately 80% normal but two cells types do not appear until slightly later; the first, the ependymal derived tanycytes become evident in the bridge by day 16 (chapter 5) while the second cell type, oligodendrocytes, responsible for the subsequent myelination of naked axons (chapter 9), do not become apparent in the bridge until sometime between 30 and 50 days. This delayed entry and the subsequent late myelination of axonal profiles, suggest that oligodendrocytes do not play an influential role during initial development of the bridge. In parallel to bridge formation was the development of a new meningeal sheath at the periphery (chapter 7) which consisted of a loose aggregation of fibroblast-like cells by day 8 but by day 200 it consisted of a highly organised structure. Experimental manipulations provided evidence to further suggest that the meninges play an important role in the development of the bridge.

In concluding, we have shown that the spinal cord of the eel recovers to produce a bridge of regenerating neural tissue that serves as a conduit for the growth of axons back to their original targets. The bridge is composed mainly of 'new' tissue except for the regrowing axons, which are injured adult structures engaged in a regrowth paradigm. In future it is clear that the process of regeneration will most likely be understood when we appreciate the inter relations between developmental processes in the formation of new tissue and the repair strategies of adult structures.

Bibliography

Abnet, K., Fawcett, J. W. and Dunnett, S. B. (1991). Interactions between meningeal cells and astrocytes *in vivo* and *in vitro*. *Developmental Brain Research* **59**: 187-196.

Aguayo, A. J., Epps, J., Charron, L. and Bray, G. M. (1976). Multipotentiality of Schwann cells in cross-anastomised and grafted myelinated and unmyelinated nerves: Quantitative microscopy and autoradiography. *Brain Research* **104**: 1-20.

Alibardi, L. (1989). Differentiation of liquor contacting neurons in the regenerating spinal cord of the newt *Triturus*. *Biological and Structural Morphology* **2**: 3103-3109.

Alibardi, L. and Meyer-Rochow, V. B. (1990). Fine structure of regenerating caudal spinal cord in adult tuatara (*Sphenadon punctatus*). *Journal Hirnforschung* **31**: 5613-5621.

Alibardi, L., Gibbons, J. and Simpson, S. (1992). Fine structure of cells in the young regenerating cord of the lizard *Anolis carolinensis* after 3H-thymidine administration. *Biological and Structural Morphology* **4**: 245-252.

Alibardi, L., Gibbons, J. and Simpson, S. B. (1993). 3H-GABA administration during tail regeneration of lizards and autoradiographical localisation. *Journal Hirnforschung* **34**: 67-77.

Alibardi, L. (1994). 3H-thymidine labelled cerebrospinal fluid contacting cells in the regenerating caudal spinal cord of the lizard *Lampropholis*. *Anatomischer Anzaz* **176**: 4347-4357.

Alonso, G. and Privat, A. (1993). Reactive astrocytes involved in the formation of lesional scars differ in the mediobasal hypothalamus and in other forebrain regions. *Journal of Neuroscience Research* **34**: 523-538.

Anders, J. J. and Brightman, M. W. (1979). Assemblies of particles in the cell membranes of developing, mature and reactive astrocytes. *Journal of Neurocytology* **8**: 777-795.

Anderson, M. J. and Waxman, S. G. (1981). Morphology of regenerated spinal cord in *Sternachus albifrons*. *Cell and Tissue Research* **2219**: 1-8.

Anderson, M. J., Waxman, S. G. and Laufer, M. (1983). Fine structure of regenerated ependyma and spinal cord in *Sternachus albifrons*. *The Anatomical Record* **205**: 73-83.

Anderson, M. J. and Waxman, S. G. (1983a). Regeneration of spinal neurons in inframammalian vertebrates: Morphological and developmental aspects. *Journal Hirnforschung* **24**: 371-398.

Anderson, M. J. and Waxman, S. G. (1983b). Caudal spinal cord of the teleost *Sternachus albifrons* resembles regenerating cord. *The Anatomical Record* **205**: 85-92.

Anderson, M. J., Swanson, K. A., Waxman, S. G. and Eng, L. F. (1984). Glial fibrillary acidic protein in regenerating teleost spinal cord. *The Journal of Histochemistry and Cytochemistry* **31**: 1099-1106.

Anderson, M. J., Choy, C. Y. and Waxman, S. G. (1986). Selforganisation of ependyma in regenerating teleost spinal cord: evidence from serial section reconstructions. *Journal of Embryology and Experimental Morphology* **96**: 1-18.

Anderson, M. J. and Waxman, S. G. (1991). Neurogenesis in adult vertebrate spinal cord *in situ* and *in vitro*: a new model system. *Annals of the New York Academy of Sciences* **457**: 213-233.

Andersson, P. B., Perry, V. H. and Gordon, S. (1992a). The acute inflammatory response to lipopolysaccharide in CNS parenchyma differs from that in other body tissues. *Neuroscience* **48**: 169-186.

Andersson, P.-B., Perry, V. H. and Gordon, S. (1992b). Intracerebral injection of proinflammatory cytokines or leukocyte chemotaxins induces minimal myelomonocytic cell recruitment to the parenchyma of the central nervous system. *Journal of Experimental Medicine* **176**: 255-259.

Andrew, W. and Hickman, C. P. (1974). Histology of the vertebrates. London, The C.V. Mosby Company.

Arshavsky, Y. I., Deliagina, T. G. and Orlovsky, G. N. (1997). Pattern generation. *Current Opinion in Neurobiology* **7**: 781-789.

Asada, Y., Kawaguchi, S., Hayashi, H. and Nakamura, T. (1998). Neural repair of the injured spinal cord by grafting: comparison between peripheral nerve segments and embryonic homologous structures as a conduit of CNS axons. *Neuroscience Research* **31**: 241-249.

Aubert, I., Ridet, J. L. and Gage, F. H. (1995). Regeneration in the adult mammalian CNS: guided by development. *Current Opinion in Neurobiology* **5**: 625-635.

Avellino, A. M., Hart, D., Dailey, A. T., McKinnon, M., Ellegala, D. and Kliot, M. (1995). Differential macrophage responses in the peripheral and central nervous system during Wallerian degeneration of axons. *Experimental Neurology* **136**: 183-198.

Balasingam, V., Dickson, K., Brade, A. and Yong, V. W. (1996). Astrocyte activity in neonatal mice: apparent dependence on the presence of reactive microglia/macrophages. *Glia* **18**: 11-26.

Baldwin, S. A., Broderick, R., Blades, D. A. and Scheff, S. W. (1998). Alterations in temporal/spatial distribution of GFAP- and vimentin-positive astrocytes after spinal cord contusion with the New York University spinal cord injury device. *Journal of Neurotrauma* **15**: 1015-1026.

Ban, E. M. (1994). Interleukin-1 receptors in the brain: characterisation by quantitative *in situ* autoradiography. *Immunomethods* **5**: 31-40.

Barden, H. and Levine, S. (1983). Histochemical observations on rodent brain melanin. *Brain Research Bulletin* **10**: 847-851.

Barker, J. L., Behar, T., Liu, Y. X., Ma, W., Maric, D., Maric, I., Schaffner, A. E., Serafini, R., Smith, S. V., Somogyi, R., Vautrin, J. Y., Wen, X. L. and Xian, H. (1998). GABAergic cells and signals in CNS development. *Perspectives in Developmental Neurobiology* **5**: 305-322.

Barnett, C. P., Donati, E. J. and Guth, L. (1984). Differences between adult and neonatal rats in their astroglial response to spinal injury. *Experimental Neurology* **84**: 374-385.

Bartheld, S. S. V., Cunningham, D. E. and Rubel, E. W. (1990). Neuronal tracing with DiI: Decalcification, cryosectioning, and photoconversion for light and electron microscopical analysis. *The Journal of Histochemistry and Cytochemistry* **38**: 725-733.

Bastmeyer, M., Beckmann, M., Schwab, M. E. and Stuermer, C. A. O. (1991). Growth of regenerating goldfish axons is inhibited by rat oligodendrocytes and CNS myelin but not by goldfish optic nerve/tract oligodendrocyte-like cells and fish CNS myelin. *Journal of Neuroscience* **11**: 626-640.

Bastmeyer, M., Baehr, M. and Stuermer, C. A. (1993). Fish optic nerve oligodendrocytes support axonal regeneration of fish and mammalian retinal ganglion cells. *Glia* **8**: 1-11.

Battisti, W. P., Shinar, Y., Schwartz, M., Levitt, P. and Murray, M. (1992). Temporal and spatial patterns of expression of laminin, chondroitin sulphate proteoglycan and HK-1 immunoreactivity during regeneration in the goldfish optic nerve. *Journal of Neurocytology* **21**: 557-573.

Battisti, W. P., Wang, J., Bozek, K. and Murray, M. (1995). Macrophages, microglia, and astrocytes are rapidly activated after crush injury of the goldfish optic nerve: A light and electron microscopic analysis. *Journal of Comparative NeurologyNeurology* **354**: 306-320.

Beattie, M. S., Bresnahan, J. C., Komon, J., Tovar, C. A., Meter, M. V., Anderson, D. K., Faden, A. I., Hsu, C. Y., Noble, L. J., Salzman, S. and Young, W. (1997). Endogenous repair after spinal cord contusion injuries in the rat. *Experimental Neurology* **148**: 453-463.

Beazley, L. D., Sheard, P. W., Tennant, M., Starac, D. and Dunlop, S. A. (1997). Optic nerve regenerates but does not restore topographic projections in the lizard *Ctenophorus ornatus*. *Journal of Comparative Neurology* **377**: 105-120.

Becker, T., Willimann, M. F., Becker, C. G., Bernhardt, R. R. and Schachner, M. (1997). Axonal regrowth after spinal cord transection in adult zebrafish. *Journal of Comparative Neurology* **377**: 577-595.

Bedi, K. S., Winter, J., Berry, M. and Cohen, J. (1992). Adult rat dorsal root ganglion neurons extend neurites on predegenerated but not on normal peripheral nerves *in vitro*. *European Journal of Neuroscience* **4**: 193-200.

Bedi, K. S., Winter, J., Berry, M. and Cohen, J. (1992). Adult rat dorsal root ganglion neurons extend neurites on predegenerated but not on normal peripheral nerves in vitro. *European Journal of Neuroscience* **4**: 193-200.

Belhage, B., Hansen, G. H., Elster, L. and Schousboe, A. (1998). Effects of gamma-aminobutyric acid (GABA) on synaptogenesis and synaptic function. *Perspectives in Developmental Neurobiology* **5**: 235-246.

Benraiss, A., Arsanto, J. P., Coulon, J. and Y.Thouveny (1997). Neural crest-like cells originate from the spinal cord during tail regeneration in adult amphibian urodeles. *Developmental Dynamics* **209**: 15-28.

Bernhardt, R. R., Patel, C. K., Wilson, S. W. and Kuwada, J. Y. (1992). Axonal trajectories and distribution of GABAergic spinal neurons in wildtype and mutant zebrafish lacking floor plate cells. *Journal of Comparative Neurology* **326**: 2263-2272.

Bernhardt, R. R., Tongiorgi, E., Anzini, P. and Schachner, M. (1996). Increased expression of specific recognition molecules by retinal ganglion cells and by optic pathway glia accompanies the successful regeneration of retinal axons in adult zebrafish. *Journal of Comparative Neurology* **376**: 253-264.

Bernstein, J. J. and Bernstein, M. E. (1967). Effect of glial-ependymal scar and teflon arrest on the regenerative capacity of goldfish spinal cord. *Experimental Neurology* **19**: 25-32.

Bernstein, J. J. and Bernstein, M. E. (1969). Ultrastructure of normal regenerative capacity following teflon blockage in goldfish spinal cord. *Experimental Neurology* **24**: 538-557.

Bernstein, J. J., Getz, R., Jefferson, M. and Kelemen, M. (1985). Astrocytes secrete basal lamina after hemisection of rat spinal cord. *Brain Research* **327**: 135-141.

Bernstein, J. J. (1986). Ependyma formation in adult rat spinal cord after transplantation of fetal cerebral cortex homografts. *Journal of Neuroscience Research* **15**: 481-490.

Bianchi, R., Giambanco, I. and Donato, R. (1993). S-100 protein, but not calmodulin, binds to the glial fibrillary acidic protein and inhibits its polymerisation in a Ca^{+}-dependent manner. *The Journal of Biological Chemistry* **268**: 12669-12674.

Bignami, A., Forno, L. and Dahl, D. (1974). The neuroglial response to injury following spinal cord transection in the goldfish. *Experimental Neurology* **44**: 60-70.

Bignami, A., Raju, T. and Dahl, D. (1982). Localisation of Vimentin, the nonspecific intermediate filament protein, in embryonic glia and in early differentiating neurons. *Developmental Biology* **91**: 286-295.

Bisby, M. A. (1985). Enhancement of the conditioning lesion effect in rat sciatic motor axons after superimposition of conditioning and test lesions. *Experimental Neurology* **90**: 385-394.

Bisby, M. A. (1995). Regeneration of peripheral nervous system axons. The Axon - Structure, Function and Physiology. S. G. Waxman, J. D. Kocsis and P. K. Stys. Oxford, Oxford university Press.

Bittner, G. D. (1991). Long-term survival of anucleate axons and its implications for nerve regeneration. *Trends in Neurosciences* **14**: 188-193.

Blanc, A. C. L., Chen, H. Y., Autillo-Gambetti, L. and Gambetti, P. (1991). Differential APP gene expression in rat cerebral cortex, meninges, and primary astroglial, microglial and neuronal cultures. *FEBS Letters* **292**: 171-178.

Blaugrund, E., Sharma, S. and Schwartz, M. (1992). L1 immunoreactivity in the developing fish visual system. *Brain Research* **574**: 244-250.

Blaugrund, E., Lavie, V., Cohen, I., Solomon, A., and, D. J. Schreyer and Schwartz, M. (1993). Axonal regeneration is associated with glial migration: comparison between injured optic nerves of fish and rats. *Journal of Comparative Neurology* **330**: 105-112.

Bodega, G., Suarez, I. and Fernandez, B. (1990). Radial astrocytes and ependymocytes in the spinal cord of the adult toad (*Bufo bufo* L.). *Cell and Tissue Research* **260**: 307-314.

Bodega, G., Suarez, I., Rubio, M., Villalba, R. M. and Fernandez, B. (1993). Astroglial pattern in the spinal cord of the adult barbel (*Barbus comiza*). *Anatomy and Embryology* **187**: 385-395.

Bodega, G., Suarez, I., Rubio, M. and Fernandez, B. (1994). Ependyma: phylogenetic evolution of glial fibrillary acidic protein (GFAP) and vimentin expression in vertebrate spinal cord. *Histochemistry* **102**: 113-122.

Bohn, R. C., Reier, P. J. and Sourbeer, E. B. (1982). Axonal interactions with connective tissue and glial substrata during optic nerve regeneration in *Xenopus* larvae and adults. *The American Journal of Anatomy* **165**: 397-419.

Borgens, R. B., Roederer, E. and Cohen, M. J. (1981). Enhanced spinal cord regeneration in lamprey by applied electric fields. *Science* **213**: 611-617.

Bosch, T. (1994). Functional Organisation of the fish brainstem. Department of Experimental Zoology. Amsterdam, University of Amsterdam: 80-99.

Bosch, T. J. and Roberts, B. L. (1994). The size and number of neurons descending to the spinal cord in relation to body length in the European eel (*Anguilla anguilla*). *Brain Behaviour and Evolution* **44**: 50-60.

Bosch, T. J., Maslam, S. and Roberts, B. L. (Submitted). Regeneration and functional recovery following transection of the spinal cord in the eel (*Anguilla anguilla*).

Boyes, B. E., Kim, S. U., Lee, V. and Suong, S. C. (1986). Immunohistochemical co-localisation of S-100b and the glial fibrillary acidic protein in rat brain. *Neuroscience* **17**: 857-865.

Breathnach, T. (1988). Extracutaneous melanin. *Pigment Cell Research* **3**: 234-242.

Brook, G. A., Lawrence, J. M., Shah, B. and Raisman, G. (1994). Extrusion transplantation of Schwann cells into the adult rat thalamus induces directional host axon growth. *Experimental Neurology* **126**: 31-43.

Bruni, J. E. and Anderson, W. A. (1987). Ependyma of the rat fourth ventricle and central canal: response to injury. *Acta Anatomica* **128**: 265-273.

Bundgaard, M. and Cserr, H. F. (1991). Barrier membranes at the outer surface of the brain of an elasmobranch, *Raja erinacea*. *Cell and Tissue Research* **265**: 113-120.

Bunge, R. P. (1983). Aspects of Schwann cell and fibroblast function relating to central nervous system regeneration. Spinal Cord Reconstruction. C. C. Kao, R. P. Bunge and P. J. Reier. New York, Raven Press: 261-270.

Bunge, M. B. (1994). Transplantation of purified populations of Schwann cells into lesioned adult rat spinal cord. *Journal of Neurology* **242**: S36-39.

Bunt, S. M. and Moebs, P. F. (1984). Selection of pathways by regenerating spinal cord fibre tracts. *Brain Research* **318**: 307-311.

Butler, E. G. and Ward, M. B. (1965). Reconstitution of the spinal cord following ablation in Urodele larvae. *Journal of Experimental Zoology* **160**: 47-66.

Butler, E. G. and Ward, M. G. (1967). Reconstitution of the spinal cord after ablation in adult *Triturus*. *Developmental Biology* **15**: 464-486.

Butler, A. B. and Hodos, W. (1996). Comparative Neuroanatomy: evolution and adaptation. New York, Wiley-Liss.

Cai, D. and Filbin, M. T. (1999). Differences in cAMP levels in neurons can explain the switch in response to MAG from promotion to inhibition of axonal regeneration during development. *Journal of Neurochemistry* **73**: S126.

Cajal, S. R. Y. (1928). Degeneration and regeneration of the nervous system. London, Oxford University Press.

Campbell, L., Abraham, C. R., Masliah, E., Kemper, P., Inglis, J. D., Oldstone, M. B. and Mucke, L. (1993). Neurologic disease induced in transient mice by cerebral overexpression of interleukin 6. *Proceedings of the National Academy of Sciences USA* **90**: 10061-10065.

Carbonell, A. L. and Boya, J. (1988). Ultrastructural study on meningeal regeneration and meningo-glial relationships after cerebral stab wound in the adult CNS. *Brain Research* **439**: 337-344.

Card, J. P. and Rafols, J. A. (1978). Tanycytes of third ventricle of the neonatal rat: a Golgi study. *American Journal of Anatomy* **151**: 173-189.

Cardone, B. and Roots, B. I. (1990). Comparative immunohistochemcal study of glial filament proteins (glial fibrillary acidic protein and vimentin) in goldfish, octopus and snail. *Glia* **3**: 180-192.

Caruncho, H. J. and Anadon, R. (1990a). Endothelial cells of the meningeal capillaries in the rainbow trout: a freeze fracture study. *Journal of Morphology* **206**: 327-332.

Caruncho, H. J., Rodriguez-Moldes, I. and Anadon, R. (1990b). A freeze-fracture study of the soma membranes of monoaminergic neurons in the hypothalamic nucleus recessi posterioris of the rainbow trout (*salmo gairdneri* Rich.). *Journal Hirnforschung* **5**: 575-584.

Caruncho, H. J., Silva, P. P. D. and Anadon, R. (1993). The morphology of teleost meningocytes as revealed by freeze fracture. *Journal of Submicroscopy, Cytology and Pathology* **25**: 397-406.

Caruncho, H. J. and Silva, P. P. D. (1994). Alterations in the intermediate layer of goldfish meninges during adaptation to darkness. *Journal of Anatomy* **184**: 355-362.

Casper, D. (1996). Growth factors and dopaminergic neurons. CNS neurotransmitters and neuromodulators: dopamine. T. W. Stone, C. R. C. Press: 131-164.

Chauvet, N., Parmentier, M. L. and Alonso, G. (1995). Transected axons of adult hypothalamoneurohypophyseal neurons regenerate along tanycytic processes. *Journal of Neuroscience Research* **41**: 129-144.

Chauvet, N., Privat, A. and Alonso, G. (1996). Aged median eminence glial cell cultures promote survival and neuritic outgrowth of cocultured neurons. *Glia* **18**: 211-223.

Chauvet, N., Apert, C., Dumoulin, A., Epelbaum, J. and Alonso, G. (1997). Mab22V11 antibody to amyloid precursor protein recognises a protein associated with specific astroglial cells of the rat nervous system characterised by their capacity to support axonal outgrowth. *Journal of Comparative Neurology* **377**: 550-564.

Chauvet, N., Prieto, M. and Alonso, G. (1998). Tanycytes present in the adult rat mediobasal hypothalamus support the regeneration of monoaminergic axons. *Experimental Neurology* **151**: 1-13.

Chen, M. S., Huber, A. B., Haar, M. E. V. D., Frank, M., Schnell, L., Spillmann, A. A., Christ, F. and Schwab, M. E. (2000). Nogo-A is a myelin-associated neurite outgrowth inhibitor and an antigen for monoclonal antibody IN-1. *Nature* **403**: 434-439.

Chen, D. F., Jhaveri, S. and Schneider, G. E. (1995). Intrinsic changes in developing retinal neurons result in regenerative failure of their axons. *Proceedings of the National academy of Sciences USA* **92**: 7287-7291.

Cheng, H. and Olson, L. (1995). A new surgical technique that allows proximodistal regeneration of 5-HT fibres after complete transection of the rat spinal cord. *Experimental Neurology* **136**: 149-161.

Chernoff, E. A. G. (1996). Spinal cord regeneration: a phenomenon unique to urodeles? *International Journal of Developmental Biology* **40**: 823-831.

Cho, H. J., Kim, J. K., Park, H. C., Kim, J. K., Kim, D. S., Ha, S. O. and Hong, H. S. (1998). Changes in brain-derived neurotrophic factor immunoreactivity in rat dorsal root ganglia, spinal cord, and gracile nuclei following cut or crush injuries. *Experimental Neurology* **154**: 224-230.

Clark, R. A. F., Laningan, J. M., DellaPelle, P., Manseau, E., Dvorak, H. F. and Colvin, R. B. (1982). Fibronectin and fibrin provide a provisional matrix for epidermal cell migration during wound reepithelisation. *Journal of Investigative Dermatology* **70**: 264-269.

Clark, R. A. (1996). Wound Repair. Overview and general considerations. The Molecular and Cellular Biology of Wound Repair. R. A. F. Clark. New York, Plenum Press: 3-49.

Clarke, J. D., Holder, N., Soffe, S. R. and Storm-Mathisen, J. (1991). Neuroanatomical and functional analysis of neural tube formation in notochordless *Xenopus* embryos; laterality of the ventral spinal cord is lost. *Development* **112**: 2499-2516.

Cocchia, D. (1981). Immunocytochemical localisation of S-100 protein in the brain of adult rat. An ultrastructural study. *Cell and Tissue Research* **214**: 529-540.

Coggeshall, R. E., Birse, S. G. and Youngblood, C. S. (1982). Recovery from spinal transection in fish. *Neuroscience Letters* **32**: 259-264.

Cohen, A. A., Mackler, S. A. and Selzer, M. E. (1988). Behavioural recovery following spinal transection: functional regeneration in the lamprey CNS. *Trends in Neuroscience* **11**: 227-231.

Cohen, I., Shani, Y. and Schwartz, M. (1993). Cloning and characteristics of fish glial fibrillary acidic protein: implications for optic nerve regeneration. *Journal of Comparative Neurology* **334**: 431-443.

Colombo, J. A., Napp, M. I. and Puissant, V. (1994). Leptomeningeal and skin fibroblasts: two different cell types? *International Journal of Developmental Neuroscience* **12**: 57-61.

Currie, S. N. and Ayers, J. (1983). Regeneration of locomotor command systems in the sea lamprey. *Brain Research* **279**: 238-240.

Dahl, D., Crosby, C. J., Sethi, J. S. and Bignami, A. (1985). Glial fibrillary acidic (GFA) protein in vertebrates: immunofluorescence and immunoblotting study with monoclonal and polyclonal antibodies. *Journal of Comparative Neurology* **239**: 75-88.

Dale, N., Roberts, A., Ottersen, O. P. and Storm-Mathisen, J. (1987a). The morphology and distribution of 'Kolmer-Agduhr cells', a class of cerebrospinal-fluid-contacting neurons revealed in the frog embryo spinal cord by GABA immunocytocehmistry. *Proceedings of the Royal Society of London: B. Biological Science* **232**: 1267193-1267203.

Dale, N., Roberts, A., Ottersen, O. P. and Storm-Mathisen, J. (1987b). The development of a population of spinal neurons and their axonal projections revealed by GABA immunocytochemistry in frog embryos. *Proceedings of the Royal Society of London: B. Biological Science* **232**: 1267205-1267215.

Davies, S. J. A., Field, P. M. and Raisman, G. (1996). Regeneration of cut adult axons fails even in the presence of continuous aligned pathways. *Experimental Neurology* **142**: 203-216.

Davies, P., Anderton, B., Kirsch, J., Konnerth, A., Nitsch, R. and Sheetz, M. (1998). First one in, last one out: the role of GABAergic transmission in generation and degeneration. *Progress in Neurobiology* **55**: 651-658.

Davies, S. J. A., Goucher, D. R., Doller, C. and Silver, J. (1999). Robust regeneration of adult sensory axons in degenerating white matter of the adult rat spinal cord. *Journal of Neuroscience* **19**: 5810-5822.

Davis, B. M., Duffy, M. T. and Simpson, S. B. (1989). Bulbospinal and intraspinal connections in normal and regenerated salamander spinal cord. *Experimental Neurology* **103**: 41-51.

Davis, B. M., Ayers, J. L., Koran, L., Carlson, J., Anderson, M. C. and Simpson, S. B. (1990). Time course of salamander spinal cord regeneration and recovery of swimming: HRP retrograde pathway tracing and kinematic analysis. *Experimental Neurology* **108**: 198-213.

Davis, A. A. and Temple, A. (1994). A self-renewing multipotential stem cell in embryonic rat cerebral cortex. *Nature* **372**: 263-266.

De Graaf, F., Raamsdonk, W. V., Asselt, E. V. and Diegenbach, P. C. (1990). Identification of motoneurons in the spinal cord of the zebrafish (*Brachydanio rerio*), with special reference to motoneurons that innervate intermediate muscle fibres. *Anatomy and Embryology* **182**: 93-102.

Del Bigio, M. R. (1995). The ependyma: a protective barrier between brain and cerebrospinal fluid. *Glia* **14**: 1-13.

Dent, L. J. B., McCasland, J. S. and Stelzner, D. J. (1996). Attempts to facilitate dorsal column axonal regeneration in a neonatal spinal environment. *Journal of Comparative Neurology* **372**: 435-456.

Desmouliere, A. and Gabbiani, G. (1996). The role of the myofibroblast in wound healing and fibrocontractive diseases. The Molecular and Cellular Biology of Wound Repair. R. A. F. Clark. New York, Plenum Press**:** 391-423.

Deutch, A. Y. and Roth, R. H. (1999). Neurotransmitters. Fundamental Neuroscience. M. J. Zifmond, F. E. Bloom, S. C. Landis, J. L. Roberts and L. R. Squire, Academic Press**:** 193-234.

Dev, S., Adler, A. J. and Edwards, R. B. (1993). Adult rabbit brain synthesises retinoic acid. *Brain Research* **632**: 325-328.

Diepen, J. C. E. K. V, Lisdonk, M. H. M. V. D., Thiele, A. J. T., Van Kemenade, B. M. L. V. and Rombout, J. H. W. M. (1994). Characterisation of immunoglobulin-binding leucocytes in carp (*Cyprinus carpio* L.). *Developmental and Comparative Immunology* **18**: 45-56.

Doetsch, F., Garcia-Verdugo, J. M. and Alvarez-Buylla, A. (1997). Cellular composition and three dimensional organisation of the subventricular germinal zone in the adult mammalian forebrain. *The Journal of Neuroscience* **17**: 5046-5061.

Donkelaar, H. J. T. (2000). Development and regenerative capacity of descending supraspinal pathways in tetrapods: a comparative approach. *Advances in Anatomy, Embryology and Cell Biology* **154**: 1-145.

Doolittle, R. F. (1965). Differences in blood clotting of lamprey fibrinogen by lamprey and bovine thrombins. *Biochemical journal* **94**: 735-741.

Dou, C. L. and Levine, J. M. (1994). Inhibition of neurite growth by the ng2 chondroitin sulphate proteoglycan. *Journal of Neuroscience* **14**: 7616-7628.

Douarin, N. L. and Kalcheim, C. (1999). The Neural Crest. Cambridge, Cambridge University Press.

Doucette, J. R. (1986). Astrocytes in the olfactory bulb. Astrocytes. S. Federoff and A. Vernadakis. New York, Academic Press**:** 293-310.

Dowding, A. J., Maggs, A. and Scholes, J. (1991). Diversity amongst the microglia in growing and regenerating fish CNS: Immunohistochemical characterisation using FL.1. an antimacrophagal monoclonal antibody. *Glia*: 345-364.

Doyle, L. M. F., Stafford, P. P. and Roberts, B. L. (1999). The distribution of regrowing axons in relation to the restoration of locomotory performance after complete spinal cord transection in the eel. *Society for Neuroscience* **25**: 493.

Doyle, L. M. F., Stafford, P. P. and Roberts, B. L. (2000). Axonal regeneration and the recovery of locomotion after a complete spinal transection in the eel. *In Press*.

Dryer, J. K., Bourque, J. A. and Steeves, J. D. (1998). Regeneration of brainstem-spinal axons after lesion and immunological disruption of myelin in adult rat. *Experimental Neurology* **154**: 12-22.

Duffy, M. T., Simpson, S. B., Liebich, D. R. and Davis, B. M. (1990). Origin of spinal cord axons in the lizard regenerated tail: Projections from local spinal neurons. *Journal of Comparative Neurology* **293**: 208-222.

Duffy, M. T., Liebich, D. R., Garner, L. K., Hawrych, A., Simpson, S. B. and Davis, B. M. (1992). Axonal sprouting and frank regeneration in the lizard tail spinal cord: correlation between changes in synaptic circuitry and axonal growth. *Journal of Comparative Neurology* **316**: 363-374.

Easter, S. S., Bratton, B. and Scherer, S. S. (1984). Growth-related order of the retinal fibre layer in goldfish. *Journal of Neuroscience* **4**: 2173-2190.

Easter, S. S., Ross, L. S. and Frankfurter, A. (1993). Initial tract formation in the mouse brain. *The Journal of Neuroscience* **13**: 285-299.

Egar, M., Simpson, S. B. and Singer, M. (1970). The growth and differentiation of the regenerating spinal cord of the lizard, *Anolis carolinensis*. *Journal of Morphology* **131**: 131-152.

Egar, M. and Singer, M. (1972). The role of ependyma in spinal cord regeneration in the urodele, *Triturus*. *Experimental Neurology* **37**: 422-430.

Elberger, A. J. and Honig, M. G. (1990). Double-labelling of tissue containing the carbocyanine dye DiI for immunocytochemistry. *The Journal of Histochemistry and Cytochemistry* **38**: 735-739.

Elmquist, J. K., Swanson, J. L., Sakaguchi, D. S., Ross, L. R. and Jacobson, C. D. (1994). Developmental distribution of GFAP and vimentin in the Brazilian opossum brain. *Journal of Comparative Neurology* **344**: 283-296.

Eng, L. F., Vanderhaeghen, J. J., Bignami, A. and Gerstl, B. (1971). An acidic protein isolated from fibrous astrocytes. *Brain Research* **28**: 351-355.

Eng, L. F. (1980). The glial fibrillary acidic (GFA) protein. Proteins of the nervous system. R. A. Bradshaw and D. M. Schneider. New York, Raven Press: 85-117.

Eng, L. F. (1985). Glial fibrillary acidic protein (GFAP). The major protein of glial intermediate filaments in differentiated astrocytes. *Journal of Neuroimmunology* **8**: 203-214.

Eng, L. F. and Lee, Y. E. (1995). Intermediate filaments in astrocytes. Neuroglia. H. Kettenmann and B. R. Ransom. Oxford, Oxford University Press: 650-667.

Eriksson, P. S., Hansson, E. and Ronnback, L. (1992). Delta-opiate and kappa-opiate receptors in primary astroglial cultures. II. Receptor sets in cultures from various brain regions and interactions with beta-receptor activated cyclic-AMP. *Neurochemical Research* **17**: 545-551.

Evans, D. L. and Gratzek, J. B. (1989). Immune defence mechanisms in fish to protozoan helminth infections. *American Zoologist* **29**: 409-418.

Fairen, A., Alvarez-Bolado, G., DeDiego, I. and Smith-Fernandez, A. (1998). GABA-immunoreactive cells of the cortical primordium contribute to distinctly fated neuronal populations. *Perspectives in Developmental Neurobiology* **5**: 159-173.

Fawcett, J. W., Housden, E., Smith-Thomas, L. and Meyer, R. L. (1989). The growth of axons in three dimensional astrocyte cultures. *Developmental Biology* **135**: 449-458.

Fawcett, J. W. (1997). Astrocytic and neuronal factors affecting axon regeneration in the damaged central nervous system. *Cell and Tissue Research* **290**: 371-377.

Fawcett, J. W. and Asher, R. A. (1999). The glial scar and central nervous system repair. *Brain Research Bulletin* **49**: 377-391.

Fitch, M. T. and Silver, J. (1997). Glial cell extracellular matrix: Boundaries for axon growth in development and regeneration. *Cell and Tissue Research* **290**: 379-384.

Flament-Durand, J. and Brion, J. P. (1985). Tanycytes: morphology and functions: a review. *International Review of Cytology* **96**: 121-155.

Flight, W. G. F. and Verheijen, F. J. (1993). The 'neck-cut' (spinal transection): not a humane way to slaughter eel, *Anguilla anguilla* (L.). *Aquaculture and Fisheries Management* **24**: 523-528.

Frank, M. and Wolberg, H. (1996). Cellular reactions at the lesion site after crushing of the rat optic nerve. *Glia* **16**: 227-40.

Franklin, R. J. M., Crang, A. J. and Blakemore, W. F. (1992). The behaviour of meningeal cells following glial cell transplantation into chemically-induced areas of demyelination in the CNS. *Neuropathology and Applied Neurobiology* **18**: 189-200.

Frederickson, R. G. (1991). The subdural space interpreted as a cellular layer of meninges. *The Anatomical Record* **230**: 38-51.

Friede, R. L. and Beuche, W. (1993). Macrophage functional properties during myelin degradation. *Advances in Neurology* **59**: 327-336.

Fritzsch, B. and Nichols, D. H. (1993). DiI reveals a prenatal arrival of efferents at the differentiating otocyst of mice. *Hearing Research* **65**: 51-60.

Gage, F. H., Coates, P. W., Palmer, T. D., Kuhn, H. G., Fisher, L. J., Suhonen, J. O., Peterson, D. A., Suhr, S. T. and Ray, J. (1995). Survival and differentiation of adult neural progenitor cells transplanted to the adult brain. *Proceedings of the National Academy of Sciences USA* **92**: 11879-11883.

Gelderd, J. B. (1979). Quantitative anatomical and behavioural analyses of regeneration and collateral sprouting following spinal cord transection in the nurse shark (*Ginglymostoma cirratum*). *Acta Neurobiologica* **39**: 121-142.

Gelderen, C. V. (1926). Uber die Entwicklung der Hirnhaute bei telesotiern. *Anatomischer Anzeiger* **60**: 48-57.

Gilmore, S. A. and Leiting, J. E. (1980). Changes in central canal area of immature rats following spinal cord injury. *Brain Research* **201**: 185-189.

Giordano, S., Bastmeyer, A. Y., Loos, A. Y. and Stuermer, C. A. O. (1993). Expression of E 587antigen in embryonic zebrafish CNS and *in vitro* functional analysis. *Society for Neuroscience Abstracts* **19**: 1090.

Giulian, D. and Iwanij, V. (1985). The response of the optic tract glia during regeneration of the goldfish visual system. II. Tectal factors stimulate optic tract glia. *Brain Research* **339**: 97-104.

Giulian, D., Iwanij, V. and Stuckenbrok, H. (1985). The response of the optic tract glia during regeneration of the goldfish visual system. I. Biosynthetic activity within different glial populations after transection of retinal ganglion cell axons. *Brain Research* **339**: 87-96.

Glasgow, E., Druger, R. K., Fuchs, C., Levine, E. M., Giordano, S. and Schechter, N. (1994). Cloning of multiple forms of goldfish vimentin: differential expression in CNS. *Journal of Neurochemistry* **63**: 470-481.

Gocht, A. and Lohler, J. (1993). Microenvironmental changes during axonal regrowth in the optic nerve of the myelin deficient rat: immunocytochemical and ultrastructural observations. *Journal of Neurocytology* **22**: 461-479.

Godement, P., Vaneslow, J., Thanos, S. and Bonhoeffer, F. (1987). A study in developing visual systems with a new method of staining neurones and their processes in fixed tissue. *Development* **101**: 697-713.

Goldgeier, M. H., Klein, L. E., Klein-Angerer, S., Moellmann, G. and Nordlund, J. J. (1984). The distribution of melanocytes in the leptomeninges of the human brain. *Journal of Investigative Dermatology* **82**: 235-238.

Goodlett, C. R., Leo, J. T., O'Callaghan, J. P., Mahoney, J. C. and West, J. R. (1993). Transient cortical astrogliosis induced by alcohol exposure during the neonatal brain growth spurts in rats. *Brain Research and Developmental Brain Research* **72**: 85-97.

Gorgels, T. G. (1991). Outgrowth of the pyramidal tract in the rat cervical spinal cord: growth cone ultrastructure and guidance. *Journal of Comparative Neurology* **306**: 95-116.

Gotow, T. and Hashimoto, P. H. (1984). Plasma membrane organisation of astrocytes in elasmobranchs with special reference to the brain barrier system. *Journal of Neurocytology* **13**: 727-742.

Grafstein, B. (1980). Cellular mechanisms for recovery from nervous system injury. *Surgical Neurology* **13**: 363-365.

GrandPre, T., Nakamura, F., Vartanian, T. and Strittmatter, S. M. (2000). Identification of the NOGO inhibitor of axon regeneration as a Reticulon protein. *Science* **403**: 439-443.

Grillner, S., Deliagina, T., Ekeberg, M., Manira, A. E., Hill, R. H., Lansner, A., Orlovsky, G. N., Wallen., P. (1995). Neural networks that co-ordinate locomotion and body orientation in lamprey. *Trends in Neurosciences* **18**: 270-279.

Gruberg, E. R. and Stirling, V. (1974). An autoradiographic study of changes in the frog tectum after cutting the optic nerve. *Brain Research* **76**: 359-362.

Guest, J. D., Rao, A., Olson, L., Bunge, M. B. and Bunge, R. P. (1997). The ability of human Schwann cell grafts to promote regeneration in the transected nude rat spinal cord. *Experimental Neurology* **148**: 502-522.

Haines, D. E. (1991). On the question of a subdural space. *The Anatomical Record* **230**: 3-21.

Halfter, W. and Schurer, B. (1998). Disruption of the pial basal lamina during the early avian embryonic development inhibits histogenesis and axonal pathfinding in the optic tectum. *Journal of Comparative Neurology* **397**: 105-117.

Halfter, W. (1998). Disruption of the retinal basal lamina during early embryonic development leads to a retraction of vitreal end feet, an increased number of ganglion cells, and aberrant axonal outgrowth. *Journal of Comparative Neurology* **397**: 89-104.

Hall, G. F., Poulos, A. and Cohen, M. J. (1989). Sprouts emerging from the dendrites of axotomised lamprey central neurons have an axon-like ultrastructure. *Journal of Neuroscience* **9**: 588-599.

Hall, G. F., Yao, J., Selzer, M. E. and Kosik, K. S. (1997). Cytoskeletal changes correlated with the loss of neuronal polarity in axotomised lamprey central neurons. *Journal of Neurocytology* **26**: 733-753.

Harel, A., Fainaro, M., Schafer, Z., Hernanadez, M. and Schwartz, M. (1989). Optic nerve regeneration in adult fish and apolipoprotein A-1. *Journal of Neurochemistry* **52**: 1218-1228.

Hassan, S. J., Keirstead, H. K., Muir, G. D. and Steeves, J. D. (1993). Axonal regeneration contributes to repair of injured brainstem-spinal neurons in embryonic chick. *The Journal of Neuroscience* **13**: 492-507.

Healey, E. G. (1967). Experimental evidence for the regeneration of nerve fibres controlling colour change after anterior spinal section in the minnow (*Phoxinus phonixus* L.). *Proceedings Royal of London Series B: Biology* **168**: 57-81.

Heine, U. I., Munoz, E. F., Flanders, K. C., Ellingsworth, L. R., Lam, H. Y., Thompson, N. L., Roberts, A. B. and Sporn, M. B. (1987). Role of transforming growth factor-Beta in the development of the mouse embryo. *Journal of Cell Biology* **105**: 2861-2876.

Hibbard, E. (1963). Regeneration in the severed spinal cord of the chordate larvae of *Petromyzon marinus*. *Experimental Neurology* **7**: 175-185.

Hilbig, H. and Schierwagen, A. (1994). Interlayer neurones in the rat superior colliculus: a tracer study using DiI/Di-ASP. *NeuroReport* **5**: 477-480.

Hildebrand, M. (1995). Analysis of vertebrate structure. New York, John Wiley and Sons.Inc.

Hill, D. J. and Rowley, A. F. (1998). Are integrins involved in the aggregatory and phagocytic behaviour of fish haemostatic cells? *The Journal of Experimental Biology* **201**: 599-608.

Hirsch, S., Cahill, M. A. and Stuermer, C. A. O. (1995). Fibroblasts at the transection site of the injured goldfish optic nerve and their potential role during retinal axonal regeneration. *Journal of Comparative Neurology* **360**: 599-611.

Hoffmann, W. (1992). Goldfish ependymins: cerebrospinal fluid proteins of meningeal origin. *Progress in Brain Research* **91**: 13-17.

Hoffmann, W. and Schwarz, H. (1996). Ependymins: meningeal-derived extracellular matrix proteins at the blood-brain barrier. *International Review of Cytology* **165**: 121-158.

Holmin, S., Almqvist, P., Lendahl, U. and Mathiesen, T. (1997). Adult nestin-expressing subependymal cells differentiate to astrocytes in response to brain injury. *European Journal of Neuroscience* **9**: 65-75.

Honig, M. G. and Hume, R. I. (1989). DiI and DiO: versatile fluorescent dyes for neuronal labelling and pathway tracing. *Trends in Neurosciences* **12**: 333-341.

Hooker, D. (1932). Spinal cord regeneration in the young rainbow fish, *Lebistes reticulatus*. *Journal of Comparative Neurology* **56**: 277-295.

Houle, J. D. and Reier, P. J. (1988). Transplantation of fetal spinal cord tissue into the chronically injured rat spinal cord. *Journal of Comparative Neurology* **269**: 535-547.

Howland, D. R., Bregman, B. S., Tessler, A. and Goldberger, M. E. (1995). Transplants enhance locomotion in neonatal kittens whose spinal cords are transected: a behavioural and anatomical study. *Experimental Neurology* **135**: 123-145.

Huang, C. J., Lee, M. S., Huang, F. L. and Chang, G. D. (1995). A protease inhibitor of the serpin family is a major protein in carp perimeningeal fluid: II. cDNA cloning, sequence analysis, and *Eschericha coli* expression. *Journal of Neurochemistry* **64**: 1721-1727.

Huang, S. and Sato, S. (1998). Progenitor cells in the adult zebrafish nervous system express a Brn-1-related POU gene, tai-ji. *Mechanisms of Development* **71**: 23-35.

Ide, C. (1996). Peripheral nerve regeneration. *Neuroscience Research* **25**: 101-121.

Ide, C., Tohyama, K., Tajima, K., Endoh, K., Sano, K., Tamura, M., Mizoguchi, A., Kitada, M., Morihara, T. and Shirasu, M. (1998). Local acellular nerve transplants for allogenic grafting and the effects of basic fibroblast growth factor on the growth of regenerating axons in dogs: a preliminary report. *Experimental Neurology* **154**: 99-112.

Ishikawa, K., Kabeya, K., Shinoda, M., Katakai, K., Mori, M. and Tatemoto, K. (1995). Meninges play a neurotrophic role in the regeneration of vasopressin nerves after hypophysectomy. *Brain Research* **677**: 20-28.

Jacob, J. M. and Croes, S. A. (1998). Acceleration of axonal outgrowth in motor axons from mature and old F344 rats after a conditioning lesion. *Experimental Neurology* **152**: 231-237.

Jacobs, A. J., Swain, G. P., Snedeker, J. A., Pijak, D. S., Gladstone, L. J. and Selzer, M. E. (1997). Recovery of neurofilament expression selectivity in regenerating reticulospinal neurons. *The Journal of Neuroscience* **17**: 5206-5220.

Johansson, C. B., Momma, S., Clarke, D. L., Risling, M., Lendahl, U. and Frisen, J. (1999). Identification of a neural stem cell in the adult mammalian central nervous system. *Cell* **96**: 25-34.

Keefe, J. R. (1973a). An analysis of urodelian retinal regeneration. III. Degeneration of extruded melanin granules in *Notophthalmus viridescens*. *Journal of Experimental Zoology* **184**: 233-238.

Keefe, J. R. (1973b). An analysis of urodelian retinal regeneration. IV. Studies of the cellular source of retinal regeneration in *Triturus cristatus carnifex* using 3H-thymidine. *Journal of Experimental Zoology* **184**: 239-258.

Keirstead, H. S. and Blakemore, W. F. (1997). Identification of post-mitotic oligodendrocytes incapable of remyelination within the demyelinated adult spinal cord. *Journal of Neuropathology and Experimental Neurology* **56**: 1191-1201.

Keirstead, H. S., Hughes, H. C. and Blakemore, W. F. (1998a). A quantitative model of axonal regeneration in the demyelinated adult rat spinal cord. *Experimental Neurology* **151**: 303-313.

Keirstead, H. S., Levine, J. M. and Blakemore, W. F. (1998b). Response of the oligodendrocyte progenitor cell population (defined by NG2 labelling) to demyelination of the adult spinal cord. *Glia* **22**: 161-170.

Kemnitz, C. P. (1997). Dopaminergic modulation of spinal neurons and synaptic potentials in the lamprey spinal cord. *Journal of Neurophysiology* **77**: 289-298.

Kern, C., Meutz, D. S. and Bernards, C. M. (1995). Epinephrine is metabolised by the spinal meninges of monkeys and pigs. *Anaesthesiology* **83**: 1078-1081.

Kestner, R. (1987). Comparative studies on the astrocytic reaction in the lesioned central nervous system of different vertebrates. *Journal Hirnforschung* **28**: 221-232.

Kettenmann, H. and Ransom, B. R. (1995). Neuroglia. Oxford, Oxford university Press.

Kimmel, C. B. (1982). Reticulospinal and vestibulospinal neurons in the young larva of a teleost fish. *Brachydanio rerio. Progress in Brain Research* **57**: 1-23.

Kirsche, W. (1951). Die regenerativen vorgange am rukenmark erwachsener telesotier nach operativer kontinuitatstrennung. *Zeitschrift vor Mikroskopische und Anatomische Forschung* **56**: 190-265.

Klika, E. and Zajikova, A. (1975). The ultrastructure of the leptomeninx in fish. *Folia Morphologica (Praha)* **23**: 380-389.

Konigstorfer, A., Sterrer, S. and Hoffmann, W. (1990). Ependymins are expressed in the meninx of goldfish brain. *Cell and Tissue Research* **261**: 59-64.

Koppanyi, T. and Weiss, P. (1922). Funktionelle regeneration des ruckenmarks bei anamniern. *Anzaz Akadamie Wissenshaften Wienna* **59**: 206.

Krenz, N. R. and Weaver, L. C. (1998). Sprouting of primary afferent fibres after spinal cord transection in the rat. *Neuroscience* **85**: 443-458.

Krikorian, J. G., Guth, L. and Donati, E. J. (1981). Origin of the connective tissue scar in the transacted rat spinal cord. *Experimental Neurology* **72**: 698-707.

Krisch, B., Leonhardt, H. and Oksche, H. (1983). The meningeal compartments of the median eminence and the cortex. *Cell and Tissue Research* **228**: 597-650.

Kruger, L. and Maxwell, D. S. (1967). Comparative fine structure of vertebrate neuroglia: teleosts and reptiles. *Journal of Comparative Neurology* **129**: 115-142.

Kruger, S., Sievers, J., Hansen, C., Sadler, M. and Berry, M. (1986). Three morphologically distinct types of interface develop between adult host and fetal brain transplants: Implications for scar formation in the adult central nervous system. *Journal of Comparative Neurology* **249**: 103-116.

Krum, J. M. and Rosenstein, J. M. (1988). Patterns of angiogenesis in neural transplant models: II. Fetal neocortical transplants. *Journal of Comparative Neurology* **271**: 331-345.

Krum, J. M. and Rosenstein, J. M. (1998). VEGF mRNA and its receptor *flt-1* are expressed in reactive astrocytes following neural grafting and tumour cell implantation in the adult CNS. *Experimental Neurology* **154**: 57-65.

Krushel, L. A., Sporns, O., Cunningham, B. A. and Crossin, K. L. (1995). Neural cell adhesion molecule (N-CAM) inhibits astrocyte proliferation after injury to different regions of the adult brain. *Proceedings of the National Academy of Sciences USA* **92**: 4323-4327.

Kuan, C. Y., Roth, K. A., Flavell, R. A. and Rakic, P. (2000). Mechanisms of programmed cell death in the developing brain. *Trends in Neurosciences* **23**: 291-297.

Kuwada, J. Y., Bernhardt, R. R. and Nguyen, N. (1990). Development of spinal neurons and tracts in the zebrafish embryo. *Journal of Comparative Neurology* **302**: 617-628.

Laabich, A., Graff, M. N., Dunel-Erb, S., Sensenbrenner, M. and Delaunoy, J. P. (1991). A study of *in vitro* and *in vivo* morphological changes of ependymal cells induced by galactocerebrosides. *Glia* **4**: 504-513.

Laabich, A., Delaunoy, J. P., Cremel, G. and Staedel, C. (1992). Modifications of ependymal cell membranes by galactocerebrosides in cell culture. *Neuroscience Letters* **142**: 196-199.

Lamas, J., Santos, Y., Bruno, D. W., Toranzo, A. E. and Anadon, R. (1994). Non-specific cellular responses of rainbow trout to *Vibrio anguillarum* and its extracellular products (ECPs). *Journal of Fish Biology* **45**: 839-854.

Landis, D. M. D. and Reese, T. S. (1982). Regional organisation of astrocytic membranes in cerebellar cortex. *Neuroscience* **7**: 937-950.

Lang, D., Rubin, B. P., Schwab, M. E. and Stuermer, C. A. O. (1995). CNS myelin and oligodendrocytes of the *Xenopus* spinal cord - but not optic nerve - are nonpermissive for axon growth. *Journal of Neuroscience* **15**: 99-109.

Lang, D. M., Monzon-Mayor, M., Brandtlow, C. E. and Stuermer, C. A. O. (1998). Retinal axon regeneration in the lizard *Gallotia gallotti* in the presence of CNS myelin and oligodendrocytes. *Glia* **23**: 61-74.

Lanners, H. N. and Grafstein, B. (1980). Early stages of axonal regeneration in the goldfish optic tract: An electron microscopic study. *Journal of Neurocytology* **9**: 733-751.

Laudano, A. P. and Doolittle, R. F. (1980). Studies on synthetic peptides that bind fibrinogen and prevent fibrin polymerisation. Structural requirements, number of binding sites, and species differences. *Biochemistry* **19**: 1013-1019.

Lauder, J. M., Liu, J., Devaud, L. and Morrow, A. L. (1998). GABA as a trophic factor for developing monoamine neurons. *Perspectives in Developmental Neurobiology* **5**: 247-259.

Lawson, L. J., Frost, L., Risbridger, J., Fearn, S. and Perry, V. H. (1994). Quantification of the mononuclear phagocyte response to Wallerian degeneration of the optic nerve. *Journal of Neurocytology* **23**: 729-744.

Lazarov-Spiegler, O., Solomon, A. S., Zeev-Brann, A. B., Hirschberg, D. L., Lavie, V. and Schwartz, M. (1996). Transplantation of activated macrophages overcomes central nervous system regrowth failure. *FASEB Journal* **10**: 1296-1302.

Lazzari, M., Franceshini, V. and Ciani, F. (1997). Glial fibrillary acidic protein and vimentin in the radial glia of *Ambystoma mexicanum* and *Triturus carnifex*: an immunocytochemical study. *Journal of Brain Research* **38**: 187-194.

Leary, J. H., Evans, D. L. and Jaso-Friedmann, L. (1994). Partial amino acid sequence of a novel protozoan parasite antigen that inhibits non-specific cytotoxic cell activity. *Scandinavian Journal of Immunology* **40**: 158.

Levine, R. L. (1989). Organisation of astrocytes in the visual pathways of the goldfish: an immunohistochemical study. *Journal of Comparative Neurology* **285**: 231-245.

Levine, R. L. (1991). Gliosis during optic nerve fibre regeneration in the goldfish: an immunohistochemical study. *Journal of Comparative Neurology* **312**: 549-560.

Levine, J. M. (1994). Increased expression of the NG2 chondroitin-sulphate proteoglycan after brain injury. *The Journal of Neuroscience* **14**: 4716-4730.

Levitt, P. and Rakic, P. (1980). Immunoperoxidase localisation of glial fibrillary acidic protein in radial glial cells and astrocytes of the developing Rhesus monkey brain. *Journal of Comparative Neurology* **193**: 815-840.

Li, M. S. and David, S. (1996). Topical glucocorticoids modulate the lesion interface after cerebral cortical stab wounds in adult rats. *Glia* **18**: 306-318.

Lindsay, R. M. (1986). Reactive Astrocytes. Astrocytes. S. Federoff and A. Vernadkis. London, Academic Press. **3:** 231-262.

Lotan, M. and Schwartz, M. (1994). Cross talk between the immune system and the nervous system in response to injury: implications for regeneration. *FASEB Journal* **8**: 1026-1033.

Lowenger, E. and Levine, R. L. (1988). Studies of the early stages of optic axon regeneration in the goldfish. *Journal of Comparative Neurology* **271**: 319-330.

Lurie, D. I. and Selzer, M. E. (1991). Preferential regeneration of spinal axons through the scar in hemisected lamprey spinal cord. *Journal of Comparative Neurology* **313**: 669-679.

Lurie, D. I., Pijak, D. S. and Selzer, M. E. (1994). Structure of reticulospinal axon growth cones and their cellular environment during regeneration in the lamprey spinal cord. *Journal of Comparative Neurology* **344**: 559-580.

Madri, J. A., Sankar, S. and Romanic, A. M. (1996). Angiogenesis. Molecular and cellular biology of wound repair , R. A. F. Clark, Plenum Press, London, 355-371.

Mackler, S. A., Yin, H. S. and Selzer, M. E. (1986). Determinants of directional specificity in the regeneration of lamprey spinal axons. *Journal of Neuroscience* **6**: 1814-1821.

Mackler, S. A. and Selzer, M. E. (1987). Specificity of synaptic regeneration in the spinal cord of the larval sea lamprey. *Journal of Physiology* **388**: 183-198.

Maggs, A. and Scholes, J. (1990). Reticular astrocytes in the fish optic nerve: Macroglia with epithelial characteristics form an axially repeated lacework pattern, to which nodes of Ranvier are apposed. *The Journal of Neuroscience* **10**: 1600-1614.

Malhotra, S. K., Shnitka, T. K. and Elbrink, J. (1990). Reactive astrocytes - a review. *Cytobios* **61**: 133-160.

Malhotra, S. K., Svensson, M., Aldskogius, H., Bhatnagar, R., Das, G. D. and Shnitka, T. K. (1993). Diversity among reactive astrocytes: proximal reactive astrocytes in lacerated spinal cord preferentially react with monoclonal antibody J1-31. *Brain Research Bulletin* **30**: 395-404.

Malhotra, S. K. and Shnitka, T. K. (1994). Adaptive plasticity and diversity among reactive astrocytes in central nervous system lesions. *Biomedical Letters* **49**: 273-302.

Margotta, V., Lauro, G. M., Lorenzo, N. D., Grossi, M., Scorsini, D., Grifone, N. and Palladini, G. (1989). Central axon regeneration and autoimmunity in adult birds. *Journal Hirnforschung* **30**: 595-602.

Maron, K. (1963). Regeneration of the spinal cord in shark embryos (*Scyliorhinus canicula*). *Folia Biologia (Krakow)* **11**: 269-275.

Martin, P. (1997). Wound healing-aiming for perfect skin regeneration. *Science* **276**: 75-81.

Martin, S. C., Heinreisch, G. and Sandell, J. H. (1998). Sequence and expression of glutamic acid decarboxylase isoforms in the developing zebrafish. *Journal of Comparative Neurology* **396**: 2253-2266.

Matthews, M. A., Onge, M. F. S. and Faciane, C. L. (1979). An electron microscopic analysis of abnormal ependymal cell proliferation and envelopment of sprouting axons following spinal cord transection in the rat. *Acta Neuropathologica* **45**: 27-36.

Matthewson, A. J. and Berry, M. (1985). Observations on the astrocyte response to a cerebral stab wound in adult rats. *Brain Research* **327**: 61-69.

Maxwell, W. L., Felows, R., Ashhurst, D. E. and Berry, M. (1990). The response of the cerebral hemisphere of the rat to injury. II. The neonatal rat. *Philosophical Transactions of the Royal Society of London B. Biological Science* **328**: 501-513.

Mayenburg, J. V., Brosamle, C., Metz, G. A. S. and Schwab, M. E. (1998). Regenerating and sprouting of chronically injured corticospinal tract fibers in adult rats promoted by NT-3 and the mAb IN-1, which neutralises myelin-associated neurite growth inhibitors. *Experimental Neurology* **154**: 583-594.

McClellan, A. D. (1988). Functional regeneration of descending brainstem command pathways for locomotion demonstrated in the *in vitro* lamprey CNS. *Brain Research* **448**: 339-345.

McClellan, A. D. (1990). Locomotor recovery in spinal-transected lamprey-regenerated spinal coordinating neurons and mechanosensory inputs couple locomotor-activity across a spinal lesion. *Neuroscience* **35**: 675-685.

McClellan, A. D. (1992). Functional regeneration and recovery of locomotor activity in spinally transected lamprey. *The Journal of Experimental Zoology* **261**: 274-287

McKeon, R. J., Schreiber, R. C., Rudge, J. S. and Silver, J. (1991). Reduction of neurite outgrowth in a model of glial scarring following CNS injury is correlated with the expression of inhibitory molecules on reactive astrocytes. *Journal of Neuroscience* **11**: 3398-3411.

Menei, P., Montero-Menei, C., Whittemore, S. R., Bunge, R. P. and Bunge, M. B. (1998). Schwann cells genetically modified to secrete human BDNF promote enhanced axonal regrowth across transected adult rat spinal cord. *European Journal of Neuroscience* **10**: 607-621.

Merrill, J. E. and Benveniste, E. N. (1996). Cytokines in inflammatory brain lesions: helpful and harmful. *Trends in Neurosciences* **19**: 331-338.

Meyenburg, J. V., Bromsamle, C., Metz, G. A. S. and Schwab, M. E. (1998). Regenerating and sprouting of chronically injured corticospinal tract fibres in adult rats promoted by NT-3 and the mAB IN-1, which neutralises myelin-associated neurite growth inhibitors. *Experimental Neurology* **154**: 583-594.

Michel, M. E. and Reier, P. J. (1979). Axonal-ependymal associations during early regeneration of the transected spinal cord in *Xenopus laevis* tadpoles. *Journal of Neurocytology* **8**: 529-548.

Miller, R. H., David, S., Patel, R., Abney, E. R. and Raff, M. C. (1985). A quantitative immunohistochemical study of macroglial cell development in the rat optic nerve: *in vivo* evidence for two distinct astrocyte lineages. *Developmental Biology* **111**: 35-41.

Miller, R. H. and Liuzzi, F. J. (1986). Regional specialisation of the radial glial cells of the adult frog spinal cord. *Journal of Neurocytology* **15**: 187-196.

Millhouse, O. E. (1972). Light and electron microscopic studies of the ventricular wall. *Zeitschrift fur Zellforschung und Mikroskopische Anatomie* **127**: 149-174.

Miyake, T., Hattori, T., Eukuda, M. and Kitamura, T. (1989). Reactions of the S-100-positive glia after injury of mouse cerebral cortex. *Brain Research* **489**: 31-40.

Momma, S., Johansson, C. B. and Frisen, J. (2000). Get to know your stem cells. *Current Opinion in Neurobiology* **10**: 45-49.

Momose, Y., Kohno, K. and Ito, R. (1988). Ultrastructural study on the meninx of the goldfish brain. *Journal of Comparative Neurology* **270**: 327-336.

Monzon-Mayor, M., Yanes, C., Ghandour, M. S., Barry, J. D. and Gombos, G. (1990). Glial fibrillary acidic protein and vimentin immunohistochemistry in the developing and adult midbrain of the lizard *Gallotia gallotii*. *Journal of Comparative Neurology* **295**: 569-579.

Moore, I. E., Buontempo, J. M. and Weller, R. O. (1987). Response of fetal and neonatal rat brain to injury. *Neuropathology and Applied Neurobiology* **13**: 219-228.

Morse, D. E. and Low, F. N. (1972). The fine structure of the pia mater of the rat. *American Journal of Anatomy* **133**: 349-368.

Morshead, C. M., Reynolds, B. A., Craig, C. G., McBurney, M. W., Staines, W. A., Morassutti, D., Weiss, S. and Kooy, D. V. D. (1994). Neural stem cells in the adult mammalian forebrain: a relatively quiescent subpopulation of subependymal cells. *Neuron* **13**: 1071-1082.

Mugnaini, E. and Walberg, F. (1965). The fine structure of the capillaries and their surroundings in the cerebral hemispheres of *Myoxine glutinosa* (L.). *Zeitschrift fur Zellforschung* **66**: 333-351.

Muller, K. J., McGlade-McCulloh, E. and Mason, A. (1987). Tinkering with successful synapse regeneration in the leech: adding insult to injury. *Journal of Experimental Biology* **132**: 207-221.

Muller-Schmid, A., Gans, B., Gorr, T. and Hoffmann, W. (1993). Molecular analysis of ependymins from the cerebrospinal fluid of the orders Clupiformes and Salmoniformes: No indication for the existence of an euteleost infradivision. *Journal of Molecular Evolution* **36**: 578-585.

Munirathinam, S., Rao, M. S., Mohan, Y. R. and Raju, T. R. (1997). Regeneration of the olfactory tract following neonatal lesion in rats. *Experimental Neurology* **144**: 174-182.

Murphy, K., Borich, S. M., Boyce, A., Doyle, L. and Roberts, B. L. (2000). Immunohistochemical detection of the number and distribution of GAP-43-positive neurons in the brain of the spinal transected European eel, *Anguilla anguilla*. *Experimental Neurology* **163**: 292.

Murray, M. (1982). A quantitative study of regenerative sprouting by optic axons in goldfish. *Journal of Comparative Neurology* **209**: 352-362.

Murray, M. and Edwards, M. A. (1982). A quantitative study of the reinnervation of the goldfish optic tectum following optic nerve crush. *Journal of Comparative Neurology* **209**: 363-373.

Nakao, T. (1979). Electron microscopic studies on the lamprey meninges. *Journal of Comparative Neurology* **183**: 429-454.

Naujoks-Manteuffel, C. (1992). Glial cells in salamander brains before and after lesions. Development and Regeneration of the Nervous System. S. Nona, J. Cronly-Dillon, M. Ferguson and C. Stafford. Cambridge, Cambridge University Press: 267-269.

Nelson, T. J. and Alkon, D. L. (1989). Specific protein changes during memory acquisition and storage. *Bioessays* **10**: 75-79.

Ness, R. and David, S. (1997). Leptomeningeal cells modulate the neurite growth promoting properties of astrocytes *in vitro*. *Glia* **19**: 47-57.

Neumann, S. and Woolf, C. J. (1999). Regeneration of dorsal column fibres into and beyond the lesion site following adult spinal cord injury. *Neuron* **23**: 83-91.

Nichols, J. and Saunders, N. (1996). Regeneration of immature mammalian spinal cord after injury. *Trends in Neurosciences* **19**: 229-234.

Noll, E. and Miller, R. H. (1993). Oligodendrocyte precursors originate at the ventral ventricular zone dorsal to the ventral midline region in the embryonic spinal cord. *Development* **118**: 563-573.

Nona, S. N., Shehab, S. A. S., Stafford, C. A. and Cronley-Dillon, J. R. (1989). Glial fibrillary acidic protein (GFAP) from goldfish: its localisation in visual pathway. *Glia* **2**: 189-200.

Nona, S. N., Stafford, C. A., Shehab, S. A. S. and Cronly-Dillon, J. R. (1992). GFAP as a marker for astrocytes in normal and regenerating goldfish visual system. Development and Regeneration of the Nervous System. S. Nona, J. Cronly-Dillon, M. Ferguson and C. Stafford. Cambridge, Cambridge University Press**:** 97-108.

Nona, S. N., Stafford, C. A., Duncan, A., Cronly-Dillon, J. R. and Scholes, J. (1994). Myelin repair by Schwann cells in the regenerating goldfish visual pathway - regional patterns revealed by X-irradiation. *Journal of Neurocytology* **23**: 400-409.

Nona, S. N. and Stafford, C. A. (1995). Glial repair at the lesion site in regenerating spinal cord: an immunohistochemical study using species-specific antibodies. *Journal of Neuroscience Research* **42**: 350-356.

Nordlander, R. H. and Singer, M. (1978). The role of ependyma in regeneration of the spinal cord in the urodele amphibian tail. *Journal of Comparative Neurology* **180**: 349-374.

Nordlander, R. H. and Singer, M. (1982). Spaces precede axons in *Xenopus* embryonic spinal cord. *Experimental Neurology* **75**: 221-228.

Nordlander, R. H. and Singer, M. (1987). Axonal growth cones in the developing amphibian spinal cord. *Journal of Comparative Neurology* **263**: 485-496.

Nordlander, R. H. and Liu, S. (1996). Axons of *Xenopus* neural tube respond to reversals of neural tube orientation. *Journal of Neurobiology* **29**: 4490-4502.

O'Hara, C. M., Egar, M. W. and Chernoff, E. A. G. (1992). Reorganisation of the ependyma during axolotl spinal cord regeneration: changes in intermediate filament and fibronectin expression. *Developmental Dynamics* **193**: 103-115.

O'Hara, C. M. and Chernoff, E. A. G. (1994). Growth factor modulation of injury-reactive ependymal cell proliferation and migration. *Tissue and Cell* **26**: 599-611.

Ohe, Y., Ishikawa, K., Itoh, Z. and Tatemoto, K. (1996). Cultured leptomeningeal cells secrete cerebrospinal fluid proteins. *Journal of Neurochemistry* **67**: 964-971.

Onteniente, B., Kimura, H. and Maeda, T. (1983). Comparative study of the glial fibrillary acidic protein in vertebrates by PAP immunohistochemistry. *Journal of Comparative Neurology* **215**: 427-436.

Oudega, M. and Marani, E. (1991). Expression of vimentin and glial fibrillary acidic protein in the developing rat spinal cord: an immunocytochemical study of the spinal cord glial system. *Journal of Anatomy* **179**: 97-114.

Pablo, F. D. and Rossa, E. J. D. L. (1995). The developing CNS: A scenario for the action of proinsulin, insulin and insulin-like growth factors. *Trends in Neurosciences* **18**: 143-150.

Palay, S. L., McGree-Russell, S. M., Gordon, S. and Grillo, M. A. (1962). Fixation of neural tissues for electron microscopy by perfusion with solutions of osmium tetroxide. *Journal of Cell Biology* **12**: 385-410.

Palay, S. L. (1961). The histology of the meninges of the toad (*Bufo*). *The Anatomical Record* **132**: 257-269.

Park, D. L., Girod, D. A. and Durham, D. (1998). Evidence for loss and recovery of chick brainstem auditory neurons during gentamicin-induced cochlear damage and regeneration. *Hearing Research* **126**: 84-98.

Pashke, K. A., Lottspeich, F. and Stuermer, C. A. (1992). Neurolin, a cell surface glycoprotein on growing retinal axons in the goldfish visual system, is reexpressed during retinal axon regeneration. *Journal of Cell Biology* **117**: 863-875.

Pasterkamp, R. J., Giger, R. J., Ruitenberg, M.-J., Holtman, A. J. G. D., Wit, J. D., Winter, F. D. and Verhaagen, J. (1999). Expression of the gene encoding the chemorepellent semaphorin III is induced in the fibroblast component of neural scar tissue formed following injuries of adult but not neonatal CNS. *Molecular and Cellular Neuroscience* **13**: 143-166.

Pearcy, J. F. and Koppanyi, T. (1924-1925). A further note on regeneration of the cut spinal cord in fish. *Proceedings of the Society for Experimental Biology and Medicine* **22**: 17-19.

Pehlemann, F. W., Sievers, J. and Berry, M. (1985). Meningeal cells are involved in foliation, lamination, neurogenesis of the cerebellum: evidence from 6-hydroxydopamine induced destruction of meningeal cells. *Developmental Biology* **110**: 136-146.

Peretto, P., Merighi, A., and, A. F. and Bonfanti, L. (1997). Glial tubes in the rostral migratory stream of the adult rat. *Brain Research Bulletin* **42**: 9-21.

Peretto, P., Merighi, A., Fasolo, A. and Bonfanti, L. (1999). The subependymal layer in rodents: A site of structural plasticity and cell migration in the adult mammalian brain. *Brain Research Bulletin* **49**: 221-243.

Perry, V. H., Bell, M. D., Brown, H. C. and Matyszak, M. K. (1995). Inflammation in the nervous system. *Current Opinion in Neurobiology* **5**: 636-641.

Pesheva, P. and Probstmeier, R. (2000). The yin and yang of tenascin-R in CNS development and pathology. *Progress in Neurobiology* **61**: 465-493.

Peters, A., Palay, S. L. and Webster, H. D. F. (1991). The fine structure of the nervous system. New York, Oxford University Press.

Philips, L. L. and Turner, J. E. (1991). Biphasic cellular response to transection in the newt optic nerve: glial reactivity precedes axonal degeneration. *Journal of Neurocytology* **20**: 51-64.

Pietsch, P. (1993). Retinoic acid treatment inhibits mitosis in the pre-existing spinal cord during tail regeneration of the axolotl larva, *Ambystoma mexicanum*. *Cytobios* **76**: 3047.

Pijak, D. S., Hall, G. F., Tenicki, P. J., Boulos, A. S., Lurie, D. I. and Selzer, M. E. (1996). Neurofilament spacing, phosphorylation, and axon diameter in regenerating and uninjured lamprey axons. *Journal of Comparative Neurology* **368**: 569-581.

Pinal, C. S. and Tobin, A. J. (1998). Uniqueness and redundancy in GABA production. *Perspectives in Developmental Biology* **5**: 109-118.

Pixley, S. P. and Vellis, J. D. (1984). Transition between immature radial glia and mature astrocytes studied with a monoclonal antibody to vimentin. *Developmental Brain Research* **15**: 201-209.

Pokay, M. A. (1993). Tanycytes in the sunfish brain: NADPH-diasphorase histochemistry and regional distribution. *Journal of Comparative Neurology* **336**: 77-95.

Popovich, P. P., Wei, P. and Stokes, B. T. (1997). Cellular inflammatory response after spinal cord injury in Sprague-Dawley and Lewis rats. *Journal of Comparative Neurology* **377**: 443-464.

Powell, E. M., Meiners, S., DiProspero, N. and Geller, H. M. (1997). Mechanisms of astrocyte-directed neurite guidance. *Cell and Tissue Research* **290**: 385-393.

Predy, R., Malhotra, S. K. and Das, G. D. (1988). Enhanced expression of a protein antigen (J1-31 antigen, 30 kilodaltons) by reactive astrocytes in lacerated spinal cord. *Journal of Neuroscience Research* **19**: 397-404.

Predy, R. and Malhotra, S. K. (1989). Reactive astrocytes in lesioned rat spinal cord: effect of embryonic transplants. *Brain Research Bulletin* **22**: 81-87.

Privat, A. and Leblond, C. P. (1972). The subependymal layer and neighbouring region in the brain of the young rat. *Journal of Comparative Neurology* **146**: 277-302.

Privat, A. and Rataboul, P. (1986). Fibrous and protoplasmic astrocytes. Astrocytes. S. Federoff and Vernadakis. London, Academic Press. **1:** 105-129.

Prota, G. (1992). Melanins and melanogenesis. London, Academic Press.

Raamsdonk, W. V., Mos, W., Onel, M. J. S. and Laarse, W. L. V. (1983a). The development of the spinal motor column in relation to the myotomal muscle fibres in the zebrafish (*Brachydanio rerio*). *Anatomy and Embryology* **167**: 125-139.

Raamsdonk, W. V., Heyting, C., Pool, C. W., Onel, M. J. S. and Groen, J. L. (1984). Differentiation of neurons and radial glia in the spinal cord of the teleost *Brachydanio rerio* (the zebrafish): An immunocytochemical study. *International Journal of Developmental Neuroscience* **2**: 471-481.

Raamsdonk, W. V., Onel, M. J. S. and Diegenbach, P. C. (1993b). Metabolic profiles of white and red-intermediate spinal motoneurons in the zebrafish. *Acta Histochemica (Jena)* **95**: 129-138.

Rafols, J. A. and Goshgarian, H. G. (1985). Spinal tanycytes in the adult rat: A correlative Golgi toning study. *The Anatomical Record* **211**: 75-86.

Rafols, J. A. (1986). Ependymal tanycytes of the ventricular system in vertebrates. Astrocytes. S. Federoff and A. Vernadakis. London, Academic Press. **1:** 131-148.

Raivich, G., Bohatschek, M., Kloss, U. A., Werner, A., Jones, L. L. and Kreutzberg, G. W. (1999). Neuroglial activation repertoire in the injured brain: graded response, molecular mechanisms and cues to physiological function. *Brain Research Reviews* **30**: 77-105.

Ramon-Cueto, A. and Avila, J. (1998). Olfactory ensheathing glia: properties and function. *Brain Research Bulletin* **46**: 175-187.

Reichardt, L. F. and Tomaselli, K. J. (1991). Extracellular matrix molecules and their receptors: Functions in neural development. *Annual Reviews of Neuroscience* **14**: 531-570.

Reichenbach, A. and Robinson, S. R. (1995). Ependymoglia and ependymoglia-like cells. Neuroglia. H. Kettenmann and B. R. Ransom. Oxford, Oxford Univeristy Press.

Reier, P. J. and Webster, H. D. F. (1974). Regeneration and remyelination of *Xenopus* tadpole optic nerve fibres following transection or crush. *Journal of Neurocytology* **3**: 591-618.

Reier, P. J. (1979). Penetration of grafted astrocytic scars by regenerating optic nerve axons in *Xenopus* tadpoles. *Brain Research* **164**: 61-68.

Reier, P. J., Stensaas, L. J. and Guth, L. (1983). The astrocytic scar as an impediment to regeneration in the central nervous system. Spinal Cord Reconstruction. C. C. Kao, R. P. Bunge and P. J. Reier. New York, Raven Press**:** 163-195.

Reier, P. J. (1986). Gliosis following CNS injury: the anatomy of astrocytic scars and their influences on axonal elongation. Astrocytes. S. Federoff and A. Vernadakis. London, Academic Press. **3:** 263-324.

Richardson, P. M., Issa, V. M. K. and Aguayo, J. (1984). Regeneration of long spinal axons in the rat. *Journal of Neurocytology* **13**: 165-182.

Ridet, J. L., Alonso, G., Chauvet, N., Chapron, J., Keonig, J. and Privat, A. (1996). Immunocytochemical characterisation of a new marker of fibrous and reactive astrocytes. *Cell and Tissue Research* **283**: 39-49.

Ridet, J. L., Malhotra, S. K., Privat, A. and Gage, F. H. (1997). Reactive astrocytes: cellular and molecular cues to biological function. *Trends in Neurosciences* **20**: 570-577.

Risling, M., Fried, K., Linda, H., Carlstedt, T. and Cullheim, S. (1993). Regrowth of motor axons following spinal cord lesions: distribution of laminin and collagen in the CNS scar tissue. *Brain Research Bulletin* **30**: 405-414.

Riva-Depaty, I., Fardeau, C., Mariani, J., Bouchaud, C. and Delhaye-Bouchaud, N. (1994). Contribution of peripheral macrophages and microglia to the cellular reaction after mechanical or neurotoxin-induced lesions of the rat brain. *Experimental Neurology* **128**: 77-87.

Roberts, B. L. and Meredith, G. E. (1987). Immunohistochemical study of a dopaminergic system in the spinal cord of the ray, *Raja radiata*. *Brain Research* **437**: 171-175.

Roberts, B. L., Meredith, G. E. and Maslam, S. (1989). Immunocytochemical analysis of the dopamine system in the brain and spinal cord of the European eel, *Anguilla anguilla*. *Anatomy and Embryology* **180**: 401-412.

Roberts, B. L., Maslam, S., Scholten, G. and Smit, W. (1995). Dopaminergic and GABAergic cerebrospinal fluid-contacting neurons along the central canal of the spinal cord of the eel and trout. *Journal of Comparative Neurology* **354**: 423-437.

Rodriguez, E. M., Gonzalez, C. B. and Delannoy, L. (1979). Cellular Organisation of the lateral and postinfundibular regions of the median eminence in the rat. *Cell and Tissue Research* **201**: 377-408.

Rogers, S. L., Letourneau, P. C., Palm, S. L., McCarthy, J. and Furcht, L. T. (1983). Neurite extension by peripheral and central nervous system neurons in response to substratum-bound fibronectin and laminin. *Developmental Biology* **98**: 212-220.

Rombout, J. H. W. M., Wal, J. W. V. D., Companjen, A., Taverne, N. and Taverne-Thiele, J. J. (1997). Characterisation of a T cell marker in carp (*Cyprinus carpio* L.). *Developmental and Comparative Immunology* **21**: 35-46.

Roots, B. I. (1986). Phylogenetic development of astrocytes. Astrocytes. S. Federoff and A. Vernadakis. London, Academic Press. pp1-33.

Rosenstein, J. M. (1996). Permeability of the blood brain barrier to protein and (3H) GABA in intraparenchymal fetal CNS tissue grafts. *Experimental Neurology* **142**: 66-79.

Rovainen, C. M. (1970). Glucose production by lamprey meninges. *Science* **167**: 889-890.

Rovainen, C. M., Lemcoe, G. E. and Peterson, A. (1971). Structure and chemistry of glucose-producing cells in meningeal tissue of the lamprey. *Brain Research* **30**: 99-118.

Rowley, A. F., Hunt, T. C., Page, M. and Mainwaring, G. (1988). Fish. Vertebrate Blood Cells. A. F. Rowley and N. A. Rathcliffe. Cambridge, Cambridge University Press. **19-127**.

Rubio, M., Suarez, I., Bodega, G. and Fernandez, B. (1992). Glial fibrillary acidic protein and vimentin immunohistochemistry in the posterior rhombencephalon of the Iberian barb (*Barbus comiza*). *Neuroscience Letters* **134**: 203-206.

Rungger-Brandle, E., Achtstatter, T. and Franke, W. W. (1989). An epithelium-type cytoskeleton in a glial cell: astrocytes of amphibian optic nerves contain cytokeratin filaments and are connected by desmosomes. *The Journal of Cell Biology* **109**: 705-716.

Rungger-Brandle, E., Alliod, C., Fouquet, B. and Messerli, M. M. (1995). Behaviour of macroglial cells, as identified by their intermediate filament complement, during optic nerve regeneration of *Xenopus* tadpole. *Glia* **13**: 255-271.

Rushton, W. A. H. (1951). A theory of the effects of fibre size in medullated nerve. *Journal of Physiology* **151**: 101-152.

Rutishauser, U. and Landmesser, L. (1996). Polysialic acid in the vertebrate nervous system: a promoter of plasticity in cell-cell interactions. *Trends in Neurosciences* **19**: 422-427.

Rutka, J. T., Giblin, J., Dougherty, D. V., McCulloch, J. R., DeArmond, S. J. and Rosenblum, M. L. (1986). An ultrastructural and immunocytochemical analysis of leptomeningeal and meningioma cultures. *Journal of Neuropathology and Experimental Neurology* **45**: 285-303.

Sankhla, S. K., Lynch, P. G. and Davis, C. H. (1996). Spinal meningeal melanocytoma: a case report and review of the literature. *British Journal of Neurosurgery* **10**: 205-209.

Sarnat, H. B., Campa, J. F. and Lloyd, J. M. (1975). Inverse prominence of ependyma and capillaries in the spinal cord of vertebrates: a comparative histochemical study. *American Journal of Anatomy* **143**: 439-450.

Sasaki, H. and Mannen, H. (1981). Morphological analysis of astrocytes in the bullfrog (*Rana catesbeiana*) spinal cord with special reference to the site of attachment of their processes. *Journal of Comparative Neurology* **198**: 13-35.

Schauwecker, P. E. and Stewart, O. (1997). Genetic influences on cellular reactions to brain injury: activation of microglia in denervated neuropil in mice carrying a mutation (Wld^S) that causes delayed Wallerian degeneration. *Journal of Comparative Neurology* **380**: 82-94.

Schiffer, D., Giordano, M. T., Mighelli, A., Giaccone, G., Pezzotta, S. and Mauro, A. (1986). Glial fibrillary acidic protein and vimentin in the experimental glial reaction of the rat brain. *Brain Research* **374**: 110-118.

Schmidt, J. T. and Shashoua, V. E. (1988). Antibodies to ependymin block the sharpening of the regenerating retinotectal projection in the goldfish. *Brain Research* **446**: 269-284.

Schmidt, J. T. (1998). Up-regulation of protein kinase C in regenerating optic nerve fibers of goldfish: Immunohistochemistry and kinase activity assay. *Journal of Neurobiology* **36**: 315-324.

Schnell, L. and Schwab, M. E. (1990). Axonal regeneration in the rat spinal cord produced by an antibody against myelin-associated neurite growth inhibitors. *Nature* **343**: 269-272.

Schnell, L. R., Schneider, R., Kolbeck, R., Barde, Y. A. and Schwab, M. E. (1994). Neurotrophin-3 enhances sprouting of corticospinal tract during development and after spinal cord lesion. *Nature* **367**: 170-173.

Schnitzer, J., Franke, W. W. and Schanchner, M. (1981). Immunocytochemical demonstration of vimentin in astrocytes and ependymal cells of developing and adult mouse nervous system. *Journal of Cell biology* **90**: 435-447.

Scholes, J. (1991). The design of the optic nerve in fish. *Visual Neuroscience* **7**: 129-139.

Schonbach, C. (1969). The neuroglia in the spinal cord of the newt, *Triturus viridescens*. *Journal of Comparative Neurology* **135**: 93-120.

Schwab, M. E. (1991). Nerve fibre regeneration after traumatic lesions of the CNS: progress and problems. *Philosophical Transactions of the Royal Society of London* **331**: 303-306.

Schwab, M. E., Kapfhammer, J. and Brandtlow, C. E. (1993). Inhibitors of neurite growth. *Annual Reviews of Neuroscience* **16**: 565-595.

Schwab, M. E. (1996). Structural plasticity of the adult CNS. Negative control by neurite growth inhibitory signals. *International Journal of Developmental Neuroscience* **14**: 379-385.

Schwarz, H., Muller-Schmid, A. and Hoffmann, W. (1993). Ultrastructural localisation of ependymins in the endomeninx of the brain of the rainbow trout: possible association with collagen fibrils of the extracellular matrix. *Cell and Tissue Research* **273**: 417-425.

Scolding, N. and Lassmann, H. (1996). Demyelination and remyelination. *Trends in Neurosciences* **19**: 1-2.

Scott, T. M. and Foote, J. (1981). A study of degeneration, scar formation and regeneration after section of the optic nerve in the frog, *Rana pipiens*. *Journal of Anatomy* **133**: 213-225.

Seitz, R., Lohler, L. and Schwendemann, G. (1981). Ependyma and meninges of the spinal cord of the mouse. *Cell and Tissue Research* **220**: 61-72.

Sharma, S. C., Jadhao, A. G. and Rao, P. D. P. (1993). Regeneration of supraspinal projection neurons in the adult goldfish. *Brain Research* **620**: 221-228.

Shashoua, V. E. (1981). Extracellular fluid proteins of goldfish brain: Studies of concentration and labelling patterns. *Neurochemical Research* **6**: 1129-1147.

Shashoua, V. E. (1991). Ependymin, a brain extracellular protein, and CNS plasticity. *Annals of the New York Academy of Science* **627**: 94-114.

Shehab, S. A. S., Stafford, C. A., Nona, S. N. and Cronly-Dillon, J. R. (1989). Anti-goldfish glial fibrillary acidic protein (GFAP) recognises astrocytes from rat CNS. *Brain Research* **504**: 343-346.

Shen, Y. J., DeBellard, M. E., Salzer, J. L., Roder, J. and Filbin, M. T. (1998). Myelin-associated glycoprotein in myelin and expressed by Schwann cells inhibits axonal regeneration and branching. *Molecular and Cellular Neuroscience* **12**: 79-91.

Shimizu, Y. (1983). Transplantation of cultured cerebellar autografts into the spinal cords of chronic paraplegic dogs. Spinal Cord Reconstruction. C. C. Kao, R. P. Bunge and P. J. Reier. New York, Raven Press: 359-366.

Sievers, J., Klemm, H. P., Jenner, S., Baumgarten, H. G. and Berry, M. (1980). Neuronal and extraneuronal effects of intracisternally administered 6-hydroxydopamine on the developing rat brain. *Journal of Neurochemistry* **34**: 765-771.

Sievers, J., Pehlemann, F. W., Baumgarten, H. G. and Berry, M. (1985). Selective destruction of meningeal cells by 6-hydroxydopamine: a tool to study meningeal-neuroepithelial interaction in brain development. *Developmental Biology* **110**: 127-135.

Sievers, J., Pehlemann, F. W., Gude, S. and Berry, M. (1994a). Meningeal cells organise the superficial glia limitans of the cerebellum and produce components of both the interstitial matrix and the basement membrane. *Journal of Neurocytology* **23**: 135-149.

Sievers, J., Pehlemann, F. W., Gude, S. and Berry, M. (1994b). A time course study of the alterations in the development of the hamster cerebellar cortex after destruction of the overlying meningeal cells with 6-hydroxydopamine on the day of birth. *Journal of Neurocytology* **23**: 117-134.

Sievers, J., Bamberger, C., Debus, O. M. and Lucius, R. (1995). Regeneration in the optic nerve of adult rats: influences of cultured astrocytes and optic nerve grafts of different ontogenetic stages. *Journal of Neurocytology* **24**: 783-793.

Silver, R., Witkovsky, P., Hovarth, P., Alones, V., Barnstable, C. J. and Lehman, M. N. (1988). Coepression of opsin- and VIP-like-immunoreactivity in CSF-contacting neurons of the avian brain. *Cell and Tissue Research* **253**: 189-198.

Simpson, S. B. (1964). Analysis of tail regeneration in the lizard *Lygosoma laterale*.L. Initiation of regeneration and cartilage differentiation: The role of ependyma. *Journal of Morphology* **114**: 425-436.

Simpson, S. B. (1968). Morphology of the regenerated spinal cord in the lizard, *Anolis carolinensis*. *Journal of Comparative Neurology* **134**: 193-210.

Simpson, S. B. (1970). Studies on regeneration of the lizard's tail. *American Zoology* **10**: 157-165.

Simpson, S. B. (1983). Fasciculation and guidance of regenerating central axons by the ependyma. Spinal Cord Reconstruction. C. C. Kao, R. P. Bunge and P. J. Reier. New York, Raven Press**:** 151-162.

Simpson, S. J. B. and Duffy, M. T. (1994). The lizard spinal cord: a model system for the study of spinal cord injury and repair. *Progress in Brain Research* **103**: 229-241.

Singer, M., Nordlander, R. H. and Egar, M. (1979). Axonal guidance during embryogenesis and regeneration in the spinal cord of the newt: the blueprint hypothesis of neuronal pathway finding. *Journal of Comparative Neurology* **185**: 1-22.

Sivron, T., Schwab, M. E. and Schwartz, M. (1994). Presence of growth inhibitors in fish optic nerve myelin: Postinjury changes. *Journal of Comparative Neurology* **343**: 237-246.

Sivron, T. and Schwartz, M. (1994). The enigma of myelin-associated growth inhibitors in spontaneously regenerating nervous systems. *Trends in Neurosciences* **17**: 277-281.

Skene, J. H. P. and Willard, M. (1981). Changes in axonally transported proteins during axon regeneration in toad retinal ganglion cells. *The Journal of Cell Biology* **89**: 86-95.

Skoff, R. P. (1975). The fine structure of pulse-labelled (3H) thymidine cells in degenerating rat optic nerve. *Journal of Comparative Neurology* **161**: 595-612.

Smit, W. A., Roberts, B. L. and Velzing, E. H. (1991). Changes in size and number of spinal motoneurons in relation to growth of the musculature of the eel, *Anguilla*. *Developmental Brain Research* **58**: 73-80.

Smith, G. M., Miller, R. H. and Silver, J. (1986). Changing role of forebrain astrocytes during development, regenerative failure, and induced regeneration upon transplantation. *Journal of Comparative Neurology* **251**: 23-43.

Smith, P. J., Shepherd, D. and Edwards, J. S. (1991). Neural repair and glial proliferation: parallels. *Bioessays* **13**: 65-72.

Soriano, E., Alvardo-Mallart, R. M., Dumesnil, N., Rio, J. A. D. and Sotelo, C. (1997). Cajal-Retzius cells regulate the radial glia phenotype in the adult and developing cerebellum and alter granule cell migration. *Neuron* **18**: 563-577.

Stafford, C. A., Shehab, S. A. S., Nona, S. N. and Dillon, J. R. C. (1990). Expression of glial fibrillary acidic protein (GFAP) in goldfish optic nerve following injury. *Glia* **3**: 33-42.

Stensaas, L. J. and Stensaas, S. (1968). Astrocytic neuroglial cells, oligodendrocytes and microgliocytes in the spinal cord of the toad. II Electron microscopy. *Zeitschrift fur Zellforschung* **86**: 184-213.

Stensaas, L. J. (1983). Regeneration in the spinal cord of the newt *Notophthalmus (Triturus) Pyrrhogaster*. Spinal Cord Reconstruction. C. C. Kao, R. P. Bunge and P. J. Reier. New York, Raven Press: 121-149.

Sterzi, G. (1901). Ricerche intorno all' anatomia comparata ed all' ontongenesi delle meningi e considerazioni sulla filogenesi. *Arti R. Ist. veneto di sci., lett. ed arti* **60**: 1101-1372.

Sterzi, G. (1902). Recherches sur l'anatomie comparee et sur l'ontogenese des meninges. *Archivio Italiano Biologico* **37**: 257-269.

Stevenson, J. A. and Yoon, M. G. (1982). Morphology of radial glia, ependymal cells, and periventricular neurons in the optic tectum of the goldfish (*Carassius auratus*). *Journal of Comparative Neurology* **205**: 128-138.

Stichel, C. C., Niermann, H., D'Urso, D., Lausberg, F., Hermanns, S. and Muller, H. W. (1999). Basal membrane-depleted scar in lesioned CNS: Characteristics and relationships with regenerating axons. *Neuroscience* **93**: 321-333.

Stoll, G. and Mueller, H. W. (1988). Lesion induced changes of astrocyte morphology and protein expression in rat optic nerve. *Annals of the New York Academy of Sciences* **540**: 461-462.

Strobel, G. and Stuermer, C. A. O. (1994). Growth cones of regenerating retinal axons contact a variety of cellular profiles in the transected goldfish optic nerve. *Journal of Comparative Neurology* **346**: 435-448.

Struckhoff, G. (1995). Cocultures of meningeal and astrocytic cells - a model for the formation of the glial-limiting membrane. *International Journal of Developmental Neuroscience* **13**: 595-606.

Struckoff, G. and Turzynski, A. (1995). Demonstration of parathyroid hormone-related protein in meninges and its receptor in astrocytes: evidence for a paracrine meningo-astrocytic loop. *Brain Research* **676**: 1-9.

Stuermer, C. A. O. (1988). Trajectories of regenerated retinal axons in the goldfish tectum: II. Exploratory branches and growth cones on axons at early regeneration stages. *Journal of Comparative Neurology* **267**: 69-91.

Stuermer, C. A. O. (1988). Trajectories of regenerating axons in the goldfish tectum: I. A comparison of normal and regenerating axons early regeneration stages. *Journal of Comparative Neurology* **267**: 69-91.

Sunderland, S. (1980). The anatomy of the invertebral foramen and the mechanisms of compression and stretch of nerve roots. Modern developments in the Principals and Practice of Chiropractics. S. Haldeman. New York, Appleton-Century-Crofts: 45-64.

Suzuki, M. and Raisman, G. (1992). The glial framework of central white matter tracts: segmental rows of contiguous interfasicular oligodendrocytes and solitary astrocytes give rise to a continuous meshwork of transverse and longitudinal processes in the adult rat fimbria. *Glia* **6**: 222-235.

Suzuki, M. and Raisman, G. (1994). Multifocal pattern of postnatal development of the macroglial framework of the rat fimbria. *Glia* **12**: 294-308.

Szele, F. G., Alexander, C. and Chesselt, M. F. (1995). Expression of molecules associated with neuronal plasticity in the striatum after aspiration and thermocoagulatory lesions of the cerebral cortex in adult rats. *Journal of Neuroscience* **15**: 4429-4448.

Takamiya, S., Kohsaka, S., Toya, S., Otani, M., Mikoshiba, K. and Tsukada, Y. (1986). Possible association of platelet-derived growth factor (PDGF) with the appearance of reactive astrocytes following brain injury *in situ*. *Brain Research* **383**: 305-309.

Takamiya, Y., Kohsaka, S., Toya, S., Otani, M. and Tsukada, Y. (1988). Immunohistochemical studies on the proliferation of reactive astrocytes and the expression of cytoskeletal proteins following brain injury in rats. *Developmental Brain Research* **38**: 201-210.

Takano, Y., Kubo, Y., Shimizu, K., Mise, K., Okuno, T. and Furusawa, I. (1995). Structural analysis of PKS1, a polyketide synthase gene involved in melanin biosynthesis in *Colletotrichum lagenarium*. *Molecular and General Genetics* **15**: 162-167.

Temple, S. and Alvarez-Buylla, A. (1999). Stem cells in the adult mammalian central nervous system. *Current Opinion in Neurobiology* **9**: 135-141.

Tencer, A. F., Allen, B. L. and Fergusen, R. L. (1985). A biomechanical study of thoracacolumnar spine fractures with bone in the canal. Part III. Mechanical properties of the dura and its tethering ligaments. *Spine* **110**: 741-747.

Tennyson, V. M. and Pappas, G. D. (1964). Fine structure of the developing telencephalic and myencephalic choroid plexus in the rabbit. *Journal of Comparative Neurology* **123**: 379-412.

Tesser, P., Jones, P. S. and Schechter, N. (1986). Elevated levels of retinal neurofilament mRNA accompany optic nerve regeneration. *Journal of Neurochemistry* **47**: 1235-1243.

Tetzlaff, W., Graeber, M. B., Bisby, M. A. and Kreutzberg, G. W. (1988). Increased glial fibrillary acidic protein synthesis in astrocytes during retrograde reaction of the rat facial nucleus. *Glia* **1**: 90-95.

Thormodsson, F. R., Antonian, E. and Graftstein, B. (1992). Extracellular glycoproteins of goldfish optic tectum labelled by intraocular injection of 3H-proline. *Experimental Neurology* **117**: 260-268.

Torigoe, K. and Lundborg, G. (1998). Selective inhibition of early axonal regeneration by myelin-associated glycoprotein. *Experimental Neurology* **150**: 254-262.

Trimmer, P. A. and Wunderlich, R. E. (1990). Changes in astroglial scar formation in rat optic nerve as a function of development. *Journal of Comparative Neurology* **296**: 359-378.

Uematsu, K., Shirasaki, M. and Storm-Mathisen, J. (1993). GABA- and glycine-immunoreactive neurons in the spinal cord of the carp *Cyprinus carpio*. *Journal of comparative Neurology* **332**: 59-68.

Ungez, G. A. and Zakon, H. H. (1997). Role of innervation in the maintenance of phenotypic properties of the myogenically-derived electric organ in the weakly electric fish *Sternopygus macrurus*. *Society for Neuroscience Abstracts* **23**: 1728.

Urade, Y., Kitahama, K., Ohishi, K., Kaneko, T., Mizuno, N. and Hyaishi, O. (1993). Dominant expression of mRNA for prostaglandin D synthase in leptomeninges, choroid plexus, and oligodendrocytes of the adult brain. *Proceedings of the National Academy of Sciences USA* **90**: 9070-9074.

Vandenabeele, F., Creemers, J. and Lamberts, I. (1996). Ultrastructure of the human arachnoid mater and dura mater. *The Journal of Anatomy* **189**: 417-430.

Varga, Z. M., Schwab, M. E. and Nicholls, J. G. (1995). Myelin-associated neurite growth-inhibitory proteins and suppression of regeneration of immature mammalian spinal cord in culture. *Proceedings of the National Academy of Sciences USA* **92**: 10959-10963.

Varga, Z. M., Fernandez, J., Blackshaw, S., Martin, A. R., Muller, K. J., Adams, W. B. and Nichols, J. G. (1996). Neurite outgrowth through lesions of neonatal opossum spinal cord in culture. *Journal of Comparative Neurology* **366**: 600-612.

Vaudano, E., Campbell, G., Anderson, P. N., Davies, A. P., Woolhead, C., Schreyer, D. J. and Lieberman, A. R. (1995). The effects of a lesion or a peripheral nerve graft on GAP-43 upregulation in the adult rat brain: An *in situ* hybridisation and immunocytochemical study. *The Journal of Neuroscience* **15**: 3594-3611.

Vigh-Teichmann, I., Vigh, B. and Aros, B. (1973). CSF contacting axons and synapses in the lumen of the pineal organ. *Zeitschrift fur Zellforschung* **144**: 139-152.

Vitry, F. D., Picoret, R., Jacque, C. and Tixier-Vidal, A. (1981). Glial fibrillary acidic protein: a cellular marker of tanycytes in the mouse hypothalamus. *Developmental Neuroscience* **4**: 457-460.

Voigt, T. (1989). The development of glial cells in the cerebral wall of ferrets: direct tracing to their transformation from radial glia into astrocytes. *Journal of Comparative Neurology* **289**: 74-88.

Waagepetersen, H. S., Sonnewald, U. and Schousboe, A. (1999). The GABA paradox: multiple roles as metabolite, neurotransmitter, and neurodifferentiative agent. *Journal of Neurochemistry* **73**: 1335-1342.

Wang, J., Murray, M. and Grafstein, B. (1995). Cranial meninges of goldfish: Age-related changes in morphology of meningeal cells and accumulation of surfactant-like multilamellar bodies. *Cell and Tissue Research* **281**: 349-358.

Wang, X. M., Terman, J. R. and Martin, G. F. (1996). Evidence for growth of supraspinal axons through the lesion after transection of the thoracic spinal cord in the developing opossum *Didelphis virginiana*. *Journal of Comparative Neurology* **371**: 104-115.

Wang, X., Messing, A. and David, S. (1997). Axonal and noneuronal cell responses to spinal cord injury in mice lacking glial fibrillary acidic protein. *Experimental Neurology* **148**: 568-576.

Wang, X. M., Basso, D. M., Terman, J. R., Bresnahan, J. C. and Martin, G. F. (1998a). Adult opossums (*Didelphis virgiana*) demonstrate near normal locomotion after spinal cord transection as neonates. *Experimental Neurology* **151**: 50-69.

Wang, X. M., Terman, J. R. and Martin, G. F. (1998b). Regeneration of supraspinal axons after transection of the thoracic spinal cord in the developing opossum (*Didelphis virginiana*). *Journal of Comparative Neurology* **398**: 83-97.

Wanner, M., Lang, D. M., Brandtlow, C. E., Schwab, M. E., Bastmeyer, M. and Stuermer, C. A. (1995). Reevaluation of the growth permissive substrate properties of goldfish optic nerve myelin and myelin proteins. *Journal of Neuroscience* **15**: 7500-7508.

Wasowicz, M., Pierre, J., Reperant, J., Ward, R., Vesselkin, N. P. and Versaux-Botteri, C. (1994). Immunoreactivity to glial fibrillary acidic protein (GFAP) in the brain and spinal cord of the lamprey (*Lampetra fluviatilis*). *Journal of Brain Research* **35**: 71-78.

Waxman, S. G. and Bennett, M. V. L. (1972). Relative conducting velocities of small myelinated and non-myelinated fibres in the CNS. *Nature New Biology* **238**: 217-219.

Waxman, S. G. and Anderson, M. J. (1986). Regeneration of central nervous system structures. *Apteronotus* spinal cord as a model system. Electroreception. T. H. Bullock and W. Heiligenberg. New York, Wiley**:** 183-208.

Weibel, D., Cadelli, D. and Schwab, M. E. (1994). Regeneration of lesioned rat optic nerve fibres is improved after neutralisation of myelin-associated neurite growth inhibitors. *Brain Research* **642**: 259-266.

Weinberg, J. H. and Spencer, P. S. (1978). The fate of Schwann cells isolated from axonal contact. *Journal of Neurocytology* **7**: 555-569.

Weiss, S., Dunne, C., Hewson, J., Wohl, C., Wheatley, M., Peterson, A. C. and Reynolds, B. R. (1996). Multipotent CNS stem cells are present in the adult mammalian spinal cord and ventricular neuroaxis. *Journal of Neuroscience* **16**: 7599-7609.

Weiss, S., Reynolds, B. A., Vescovi, A. L., Morshead, C., Craig, C. G. and Kooy, D. V. D. (1996). Is there a neural stem cell in the mammalian forebrain. *Trends in Neurosciences* **19**: 387-393.

Wicht, H., Derouche, A. and Korf, H. W. (1994). An immunohistochemical investigation of glial morphology in the pacific hagfish: radial and astrocyte-like glia have the same phylogenetic age. *Journal of Neurocytology* **23**: 565-576.

Wilson, S. W. and Easter, S. S. (1991a). A pioneering growth cone in the embryonic zebrafish brain. *Proceedings of the National Academy of Sciences USA* **88**: 2293-2296.

Wilson, S. W. and Easter, S. S. (1991b). Stereotyped pathway selection by growth cones of early epiphysial neurons in the embryonic zebrafish. *Development* **112**: 723-746.

Wood, R. M. and Cohen, M. J. (1981). Synaptic regeneration and glial reactions in transected spinal cord of the lamprey. *Journal of Neurocytology* **10**: 57-79.

Yamada, K. M. and Clark, R. A. F. (1996). Provisional Matrix. The Molecular and Cellular Biology of Wound Repair. R. A. F. Clark. New York, Plenum Press**:** 51-93.

Yanes, C., Monzon-Mayor, M., Ghandour, M. S., Barry, J. D. and Gombos, G. (1990). Radial glia and astrocytes in developing and adult telencephalon of the lizard *Gallotia gallotti* as revealed by immunohistochemistry with anti-GFAP and anti-vimentin antibodies. *Journal of Comparative Neurology* **295**: 559-568.

Yin, H. S., Mackler, S. A. and Selzer, M. E. (1984). Directional specificity in the regeneration of lamprey spinal axons. *Science* **224**: 894-896.

Yoshida, M. (1997). Oligodendrocyte maturation in *Xenopus laevis*. *Journal of Neuroscience Research* **50**: 169-176.

Yoshida, M., Tomoda, H. and Uematsu, K. (1995). Spinal and parachordal neurons in the eel leptocephali, *Anguilla japonica* revealed by labelling with a fluorescent dye. *Neuroscience Letters* **195**: 206-208.

Zerlin, M. and Goldman, J. E. (1997). Interactions between glial progenitors and blood vessels during early postnatal corticogenesis: blood vessel contact represents an early stage of astrocyte differentiation. *Journal of Comparative Neurology* **387**: 537-546.

Zottoli, S. J., Bentley, A. P., Feiner, D. G., Hering, J. R., Prendergast, B. J. and Rieff, H. I. (1994). Spinal cord regeneration in adult goldfish: Implications for functional recovery in vertebrates. *Progress in Brain Research* **103**: 219-228.

Zupanc, G. K. H. and Zupanc, M. M. (1992). Birth and migration of neurons in the central posterior/prepacemaker nucleus during adulthood in weakly electric knifefish. *Proceedings of the National Academy of Sciences USA* **89**: 9539-9543.

Zupanc, G. K. H., Kompass, K. S., Horschke, I., Ott, R. and Schwartz, H. (1998). Apoptosis after injuries in the cerebellum of adult teleost fish. *Experimental Neurology* **152**: 221-230.

Zupanc, G. K. (1999). Neurogenesis, cell death and regeneration in the adult gymnotiform brain. *Journal of Experimental Biology* **202**: 1435-1446.

Zupanc, G. K. and Ott, R. (1999). Cell proliferation after lesions in the cerebellum of adult teleost fish: time course, origin, and type of new cells produced. *Experimental Neurology* **160**: 178-187.

Zupanc, G. K. H. (1999). Up-regulation of somatostatin after lesions in the cerebellum of the teleost fish *Apteronotus leptorhynchus*. *Neuroscience Letters* **268**: 135-138.